

9th EFRC Conference

September 11-12, 2014

Hofburg, Vienna



EUROPEAN FORUM
for RECIPROCATING
COMPRESSORS



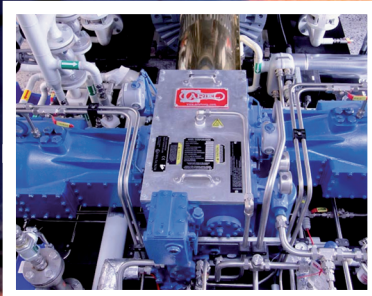
CONFERENCE SPONSORS

9th Conference of the EFRC
September 11th / 12th, 2014, Vienna



EUROPEAN FORUM
for RECIPROCATING
COMPRESSORS

The Sky is the Limit.



- » Planning, Engineering, Construction and Maintenance
- » Cutting Edge Technologies combined with ARIEL-Compressors
- » Customized Solutions for all Applications
- » Quality Service and Parts, in a Fraction of Time and Cost

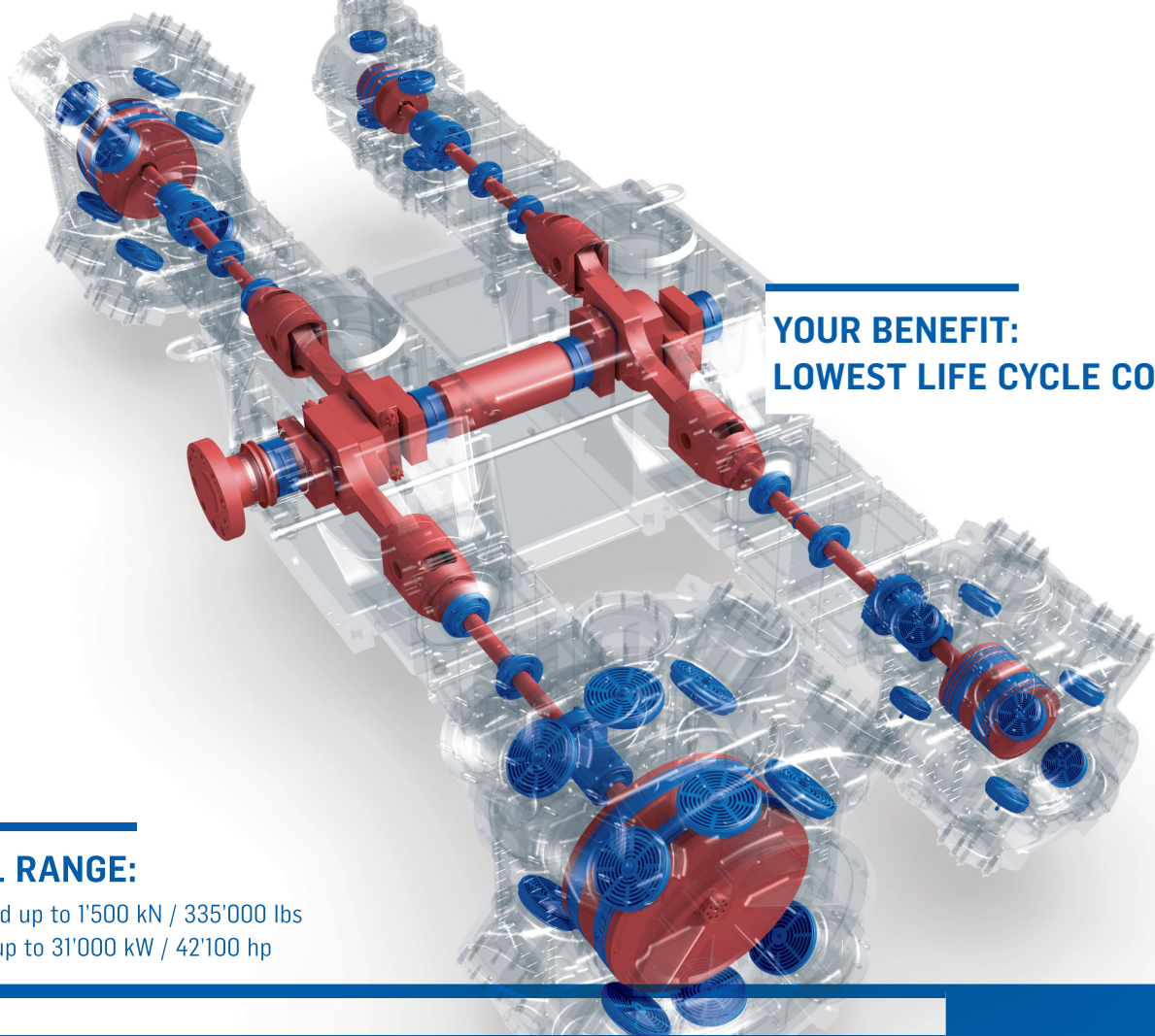
Excellence through Diversification.

PSE Engineering GmbH » Compression Systems

Ahrensburger Strasse 1
D-30659 Hannover

Fon +49.(0)511.261420-0
Fax +49.(0)511.261420-11
info@pse-eng.de

» www.pse-eng.de



**YOUR BENEFIT:
LOWEST LIFE CYCLE COSTS**

FULL RANGE:

Rod load up to 1'500 kN / 335'000 lbs
Power up to 31'000 kW / 42'100 hp

API 618

RELIABLE SWISS QUALITY

**YOU GET MORE THAN JUST A
PROCESS GAS COMPRESSOR**

Lubricated up to 1'000 bara,
non-lubricated up to 300 bara

For highest availability: We recommend our own designed, in-house engineered compressor valves and key compressor components

Designed for easy maintenance

We are the competent partner with the full range of services – worldwide

→ www.recip.com/api618

Compressors for a Lifetime



9th Conference of the EFRC

September 11th / 12th, 2014, Vienna

CONTROLS

- Comparison of Operation Experiences of Capacity Controls** -17-
by: R. Stocker, E. Glück, R. Aigner, Burckhardt Compression AG
- Compressor Innovations Bring Improvements to Gas Storage Operations** -26-
by: Oliver Friedlaender, Siegfried Müssig, RAG Rohöl-Aufsuchungs Gesellschaft

MONITORING

- Successful Detections of Loosened Parts on a Reciprocating Compressor** -37
by: César Luis Fernandez Valdez, Cesar Marín García Repsol Refinery Cartagena
- Condition Monitoring and Simulated Start Up Sequences Successfully Supported the Commissioning of a New Reciprocating Compressor Unit** -43-
by: Patrick Ferrage, TOTAL

SEALING / WEAR 1

- Genuine New Concept for a Zero-Emission Packing for Reciprocating Compressors** -59-
by: Tino Lindner-Silwester, Christian Hold, HOERBIGER
- Eliminating Gas Leakage with a Novel Rod Sealing Solution** -65-
by Johan Klinga, Öresundskraft AB
- Best Practice for Efficiency and Emissions Upgrades of a Gas Gathering Compressor** -70-
by: Robbert Pol, Nederlandse Aardolie Maatschappij B.V.



EUROPEAN FORUM
for RECIPROCATING
COMPRESSORS

9th Conference of the EFRC

September 11th / 12th, 2014, Vienna

CALCULATION 1

- 79- **A Comparative Analysis of Numerical Simulation Approaches for Ring Valve Dynamics**
by: Carsten Möhl, Technische Universität Dresden
- 86- **Method for Evaluating the Pass / Fail Criterion for the Fatigue Design Margin & Life Estimation for Reciprocating Compressors** *by: Ani Ketkar, Federico Pamio, Mark Patterson, GE Oil & Gas*
- 92- **Improvement of the Cooling Performance of a Reciprocating Compressor Cylinder by a Conjugate Heat Transfer and Deformation Analysis** *by: Francesco Balduzzi, Giovanni Ferrara, University of Florence; Riccardo Maleci, Alberto Babbini GE Oil & Gas*

PULSATION 1

- 105- **Root Cause Analysis of the Fatigue Failures of the Pulsation Dampers of a large Underground Gas Storage (UGS) System** *by: A. Eijk & D. de Lange TNO; J. Maljaars TNO, & Eindhoven University of Technology; A. Tenbrock-Ingenhorst & A. Gottmer, RWE*
- 116- **Vibrations in the Environment - Remedial Actions at a New Compressor Foundation**
by: Jan Steinhausen, KÖTTER; Poul Christian Larsen, DONG Energy
- 127- **Optimized Robust Compressor Station Design Methodology**
by: Benjamin A. White, Barron J. Bichon, David L. Ransom, Eugene L. Broerman, SwRI®

CALCULATION 2

- 143- **Systematic Calculation / Design of the Piston Rod Unit**
by: Vasillaq Kacani, LMF



EUROPEAN FORUM
for RECIPROCATING
COMPRESSORS

9th Conference of the EFRC

September 11th / 12th, 2014, Vienna

CALCULATION 2

An Advanced Model for Journal Paths in Reciprocating Compressors including Deformation, Cavitation and Crosshead Bearings by: *I.A.M. van der Kroon, P.N. Duineveld, Howden Thomassen Compressors BV* -150-

Thermodynamic Calculation of Reciprocating Compressor Plants by: *Ullrich Hesse, Gotthard Will, Technische Universität Dresden* -158-

EFRC

Feasibility Investigation of Non-Metallic and Light Weight Metallic Materials for Light Weight Compressor Pistons by: *C.M. Wentzel & O.K. Bergsma, TU Delft NL, Faculty of Aerospace Engineering; A. Eijk, TNO;* -173-

EFRC Guidelines on how to avoid Liquid Problems in Reciprocating Compressor Systems by: *P. Shoeibi Omrani & A. Eijk, TNO* -187-

8th EFRC workshop for students “Reciprocating Compressors” by: *Gunther Machu, Chairman of the EFRC Student Excursion* -197-

DESIGN

Capacity Control System Applications and Developments by: *A.Raggi, A.Giampà, COZZANI; M.Grassi, INEOS* -205-

Revamp of an Existing Reciprocating-Compressor Unit by: *Andreas Hahn, Klaus Hoff and Gerhard Knop, NEUMAN & ESSER* -217-

Challenges of Oxygen Reciprocating Piston Compressors by: *Wolfgang Grillhofer, Air Liquide* -227-



EUROPEAN FORUM
for RECIPROCATING
COMPRESSORS

CONTENTS

9th Conference of the EFRC

September 11th / 12th, 2014, Vienna

SEALING / WEAR 2

- 239- **Performance Improvement of Dry-Running Sealing Systems by Optimization of Wear Compensation** *by: Norbert Feistel, Burckhardt Compression AG*
- 248- **Scientific Research Methods to Analyse Compressor Wear Parts and Lubricants** *by: Thomas Heumesser, LMF*

LUBRICATION

- 259- **Eliminating Excessive Lubrication** *by: Alexander, Lee, CPI*
- 265- **New Approach for a Smart Compressor Lubrication System** *by: Matthias Kornfeld, Bernhard Spiegl, Bernhard Fritz, HOERBIGER*

PULSATION 2

- 277- **Case Study: Community Noise Annoyance Mitigation with Intake / Exhaust Silencer Redesign** *by: Eugene L. Broerman, Ray G. Durke, Richard M. Baldwin; SwRI®*
- 284- **Integrity Evaluation of Small Bore Connections (Branch Connections)** *by: Chris B. Harper, Beta Machinery Analysis*

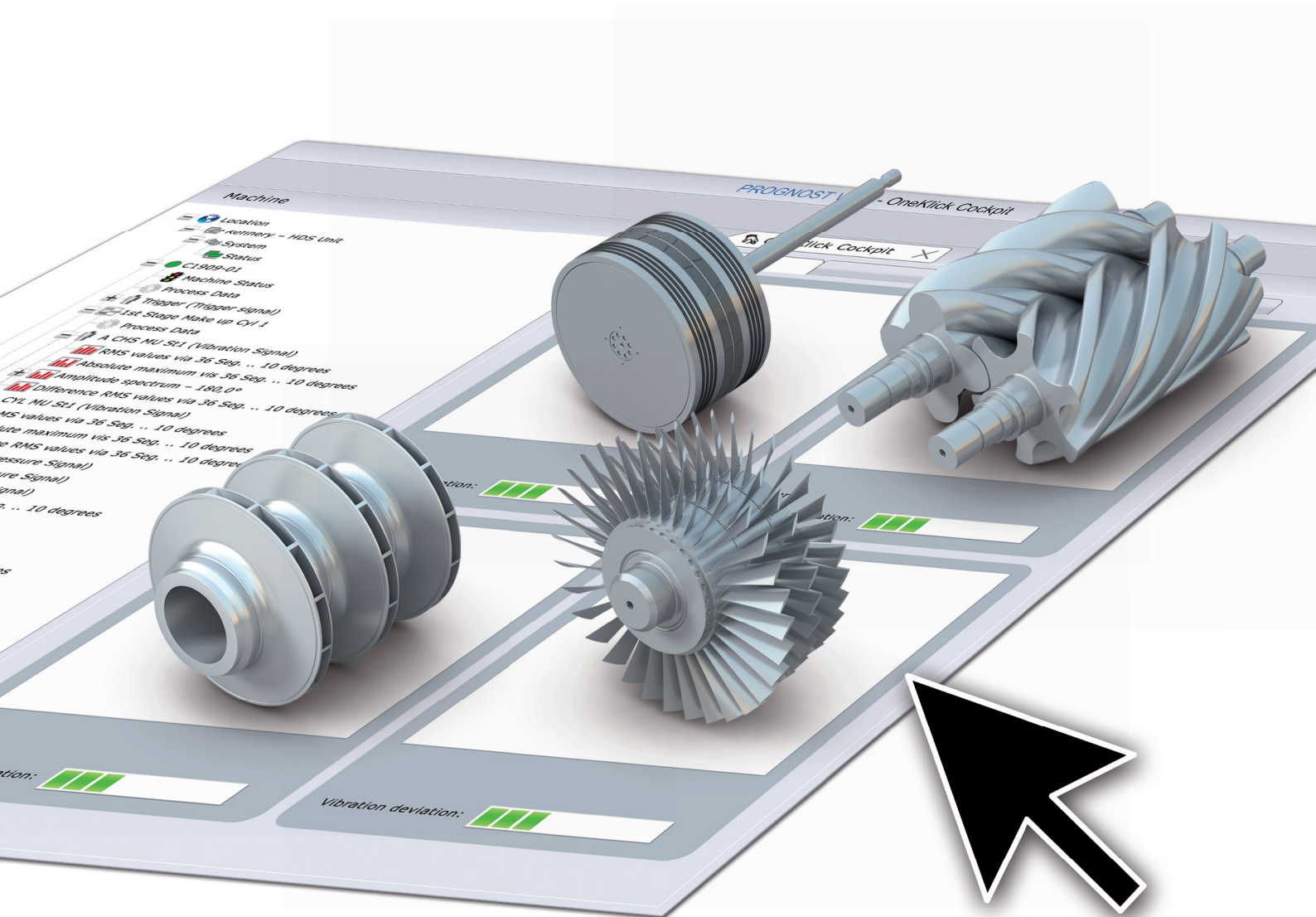
APPLICATION

- 299- **Gas-to-Liquids Technology and the Use of Reciprocating Compressors** *by: Benjamin F. Williams, Ariel Corporation*
- 305- **Managing Start-Up Conditions of Hyper Compressors** *by: Marcello Agostini, Cosimo Carcasci, Alessio Cristofani, Compression Service Technology*



EUROPEAN FORUM
for RECIPROCATING
COMPRESSORS

Trust the #1 online monitoring system for mission-critical equipment



Machinery uptime is at your fingertips

Which monitoring system gives you the most time to respond?
Maximize lead times with PROGNOST® – the #1 system in early failure detection.
You get the early warnings you need to make well-informed decisions and
cut maintenance costs.

reply@prognost.com www.prognost.com

 **PROGNOST**
Intelligence on Duty

9th Conference of the EFRC

September 11th / 12th, 2014, Vienna

AIR LIQUIDE

- 227- **Challenges of Oxygen Reciprocating Piston Compressors**
by: Wolfgang Grillhofer, Air Liquide

ARIEL CORPORATION

- 299- **Gas-to-Liquids Technology and the Use of Reciprocating Compressors**
by: Benjamin F. Williams, Ariel Corporation

BETA MACHINERY ANALYSIS

- 284- **Integrity Evaluation of Small Bore Connections (Branch Connections)**
by: Chris B. Harper, Beta Machinery Analysis

BURCKHARDT COMPRESSION

- 17- **Comparison of Operation Experiences of Capacity Controls**
by: R. Stocker, E. Glück, R. Aigner, Burckhardt Compression AG
- 239- **Performance Improvement of Dry-Running Sealing Systems by Optimization of Wear Compensation** *by: Norbert Feistel, Burckhardt Compression AG*

COMPRESSION SERVICE TECHNOLOGY

- 305- **Managing Start-Up Conditions of Hyper Compressors**
by: Marcello Agostini, Cosimo Carcasci, Alessio Cristofani, C.S.T.

COZZANI

- 205- **Capacity Control System Applications and Developments**
by: A.Raggi, A.Giampà, COZZANI; M.Grassi, INEOS

COMPRESSOR PRODUCTS INTERNATIONAL

- 259- **Eliminating Excessive Lubrication**
by: Alexander, Lee, CPI

EFRC

- 173- **Feasibility Investigation of Non-Metallic and Light Weight Metallic Materials for Light Weight Compressor Pistons** *by: C.M. Wentzel & O.K. Bergsma, TU Delft NL, Faculty of Aerospace Engineering; A. Eijk, TNO;*
- 187- **EFRC Guidelines on how to avoid Liquid Problems in Reciprocating Compressor Systems** *by: P. Shoeibi Omrani & A. Eijk, TNO*
- 197- **8th EFRC workshop for students “Reciprocating Compressors”**
by: Gunther Machu, Chairman of the EFRC Student Excursion

CONTENTS BY CONTRIBUTOR

9th Conference of the EFRC

September 11th / 12th, 2014, Vienna

GE OIL & GAS

- Method for Evaluating the Pass / Fail Criterion for the Fatigue Design Margin & Life Estimation for Reciprocating Compressors** -86-
by: Ani Ketkar, Federico Pamio, Mark Patterson, GE Oil & Gas
- Improvement of the Cooling Performance of a Reciprocating Compressor Cylinder by a Conjugate Heat Transfer and Deformation Analysis** -92-
by: Francesco Balduzzi, Giovanni Ferrara, University of Florence; Riccardo Maleci, Alberto Babbini GE Oil & Gas – Nuovo Pignone

HOERBIGER

- Genuine New Concept for a Zero-Emission Packing for Reciprocating Compressors** -59-
by: Tino Lindner-Silwester, Christian Hold, HOERBIGER
- New Approach for a Smart Compressor Lubrication System** -265-
by: Matthias Kornfeld, Bernhard Spiegl, Bernhard Fritz, HOERBIGER

HOWDEN THOMASSEN COMPRESSORS

- An Advanced Model for Journal Paths in Reciprocating Compressors including Deformation, Cavitation and Crosshead Bearings** -150-
by: I.A.M. van der Kroon, P.N. Duineveld, Howden

KÖTTER

- Vibrations in the Environment - Remedial Actions at a New Compressor Foundation** -116-
by: Jan Steinhausen, KÖTTER; Poul Christian Larsen, DONG Energy

LEOBERSDORFER MASCHINENFABRIK

- Systematic Calculation / Design of the Piston Rod Unit** -143-
by: Vasillaq Kacani, LMF
- Scientific Research Methods to Analyse Compressor Wear Parts and Lubricants** -248-
by: Thomas Heumesser, LMF

NEUMAN & ESSER

- Revamp of an Existing Reciprocating-Compressor Unit** -217-
by: Andreas Hahn, Klaus Hoff and Gerhard Knop, NEUMAN & ESSER

ÖRESUNDSKRAFT

- Eliminating Gas Leakage with a Novel Rod Sealing Solution** -65-
by Johan Klinga, Öresundskraft AB

CONTENTS BY CONTRIBUTOR

9th Conference of the EFRC

September 11th / 12th, 2014, Vienna

RAG ROHÖL-AUFSUCHUNGS GESELLSCHAFT

- 26- **Compressor Innovations Bring Improvements to Gas Storage Operations**
by: Oliver Friedlaender, Siegfried Müssig, RAG

REPSOL REFINERY CARTAGENA

- 37- **Successful Detections of Loosened Parts on a Reciprocating Compressor**
by: César Luis Fernandez Valdez, Cesar Marin Garcia Repsol Refinery Cartagena

SHELL / NAM

- 70- **Best Practice for Efficiency and Emissions Upgrades of a Gas Gathering Compressor**
by: Robbert Pol, Nederlandse Aardolie Maatschappij B.V.

SOUTHWEST RESEARCH INSTITUTE®

- 127- **Optimized Robust Compressor Station Design Methodology**
by: Benjamin A. White, Barron J. Bichon, David L. Ransom, Eugene L. Broerman, SwRI®
- 277- **Case Study: Community Noise Annoyance Mitigation with Intake/Exhaust Silencer Redesign**
by: Eugene L. Broerman, Ray G. Durke, Richard M. Baldwin; SwRI®

TNO

- 105- **Root Cause Analysis of the Fatigue Failures of the Pulsation Dampers of a large Underground Gas Storage (UGS) System** *by: A. Eijk & D. de Lange TNO; J. Maljaars TNO, & Eindhoven University of Technology; A. Tenbroek-Ingenhorst & A. Gottmer, RWE*

TOTAL - REFINING & CHEMICALS

- 43- **Condition Monitoring and Simulated Start Up Sequences Successfully Supported the Commissioning of a New Reciprocating Compressor Unit** *by: Patrick Ferrage, TOTAL*

TU DRESDEN, GERMANY

- 79- **A Comparative Analysis of Numerical Simulation Approaches for Ring Valve Dynamics**
by: Carsten Möhl, Technische Universität Dresden
- 158- **Thermodynamic Calculation of Reciprocating Compressor Plants**
by: Ullrich Hesse, Gotthard Will, Technische Universität Dresden

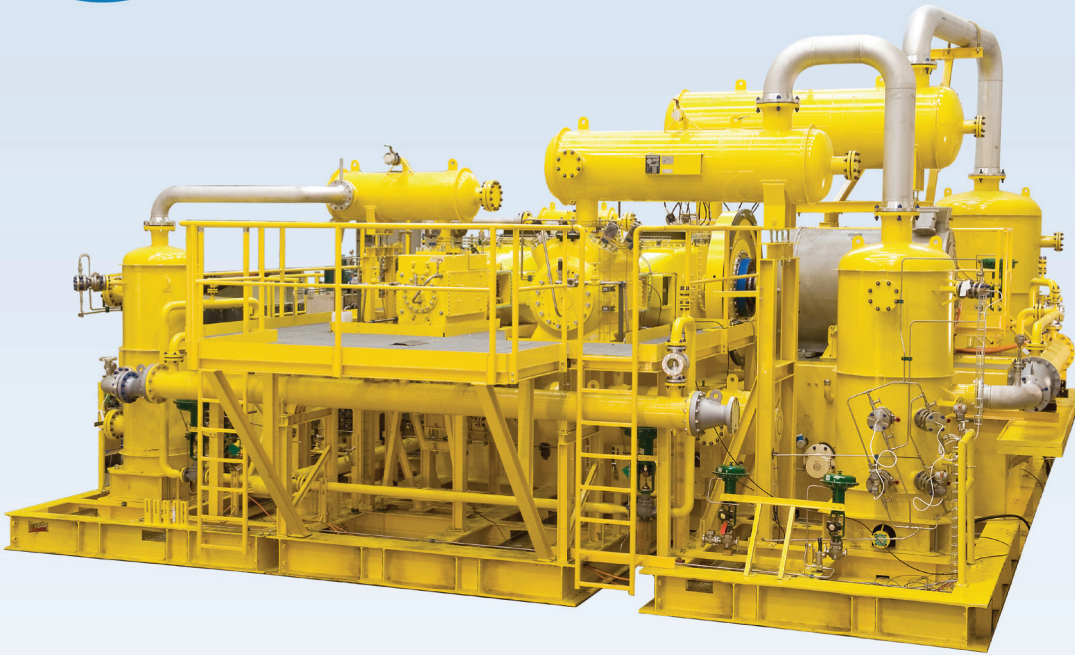


EUROPEAN FORUM
for RECIPROCATING
COMPRESSORS

CONTENTS BY CONTRIBUTOR



worldwide compressor technology made in austria



LMF, the leading Austrian manufacturer with over 60 years experience in the compressor business, produces high pressure piston compressor systems for air, natural gases, technical and industrial gases (process gases) with power rates of up to 6,200 kW (8,300 hp) and pressure rates of up to 700 bar (10,150 psi).

LMF's high pressure systems are designed according to international standards, using standard design principles. As a single source LMF offers design, engineering, production, testing under full load, erection, start-up and related services.



MOBILE SYSTEMS



INDUSTRIAL COMPRESSOR SYSTEMS



RECIPROCATING COMPRESSORS AC. TO API618, API 11P



www.lmf.at



Visit us at our booth **Nr.21**

your high pressure solution

9th Conference of the EFRC September 11th / 12th, 2014, Vienna

Comparison of Operation Experiences of Capacity Controls
by: R. Stocker, E. Glück, R. Aigner, Burckhardt Compression AG

-17-

Compressor Innovations Bring Improvements to Gas Storage Operations
by: Oliver Friedlaender, Siegfried Müssig, RAG Rohöl-Aufsuchungs Gesellschaft

-26-

SESSION CONTROLS



EFRC
EUROPEAN FORUM
for RECIPROCATING
COMPRESSORS



Comparison of Operation Experiences of Capacity Controls

by:

R. Stocker, E. Glück, R. Aigner

Burckhardt Compression AG

Winterthur, Switzerland

roland.stocker@burckhardtcompression.com

9th Conference of the EFRC

September 11th / 12th 2014, Vienna

Abstract

Capacity control has been around for years, but the implementation is still challenging for certain compressors and application areas. The goal of this paper is to show the benefits and challenges of different capacity controls. Operation experiences show the importance of design, sizing and further development for both new systems and conventional valve unloaders. In addition, new technologies, improvements in simulation and calculation, and the combination of capacity control systems allow not only a wide range of flow rates, but also an increase in system reliability and durability.

Comparison of Operation Experiences of Capacity Controls

by: R. Stocker, E. Glück, R. Aigner, Burckhardt Compression AG

Introduction

Capacity control of reciprocating compressors is required to adjust mass flow and/or to ensure certain interstage and discharge pressures. There are a wide range of control strategies available but all of them influence both the operation and the auxiliaries of a compressor. The decision on which capacity control should be implemented is based not only on the technical requirements, but also on the investment cost, operation expenses, and reliability.

There are two major groups of capacity controls that can change mass flow in a reciprocating compressor. The first contains the valve unloading, clearance pocket, and start-and-stop controls where the mass flow can only be changed gradually (stepped control). The second contains various methods such as bypass lines, reverse flow controls and speed controls, to adjust mass flow continuously (stepless control). A combination of capacity control strategies is also possible. All capacity controls influence the compressor's operation and process; however, depending on the control strategy, the influence can be quite different.

Design and sizing are essential not only for compressors, but also for capacity control equipment. Even established capacity controls have room for improvement, as shown by operation experiences with conventional valve unloaders with a focus on failure evaluation (Chapter 2). With correct design and sizing, the flow control range can be enlarged. For example, the flow rate of a reciprocating compressor can be decreased from 100% to 33% just by speed control. With a combination of different capacity controls, this can be expanded to deliver a flow range from 100% to 16%. Combining different capacity controls brings together the benefits of each individual control system, but can also lead to some unfavourable effects, both of which are detailed in the next sections.

1 Capacity Controls of Reciprocating Compressors

1.1 Control Descriptions

This section contains short summaries of relevant capacity control methods. More detailed descriptions can be found in references [1] and [2].

Bypass Lines: In this control method, discharge gas is fully or partially routed back to the suction side of the compressor in order to regulate mass flow. The two types of bypass discussed in this paper are detailed below.

Bypass First Stage: A bypass from the first stage discharge line to the first stage suction line is

implemented, which results in the shaft power decreasing with a higher bypass flow due to the reduced flow through the following stage(s). The advantages are energy savings, the implementation is very simple, and it is even safe for oxygen applications. The disadvantages are the limited capacity range, interstage pressure changes and temperature variations throughout the compressor (which may result in undesirable rod loads or compressor wear).

Bypass All Stages: A bypass from the last stage discharge line to the first stage suction line is implemented, which effectively allows a full control range (100% to 0%) while not changing the operation point of the compressor. It does not, however, provide energy savings. In addition, a bypass cooler might be necessary to avoid condensation of the gas.

Suction Valve Unloading: Using this control method requires that the suction valve is kept open by means of an unloading device. Therefore, the gas in the compression chamber cannot be regularly compressed during the compression phase, but instead is pushed back through the open suction valve and into the suction line. For this strategy to work, the force of the actuator onto the unloading device must be higher than the sum of the opposing forces, namely from the valve springs, static pressure difference, and streaming force from the gas over the valve sealing element. The streaming force depends mainly on the gas, gas condition (temperature, pressure, etc.), gas velocity and valve geometry. The gas velocity depends on factors such as the compressor design (compression chambers, number of valves, etc.), and the compressor speed.

There are different suction valve unloading systems on the market. The common advantage they offer is energy savings from the reduced mass flow, which requires less compression work. There are two common disadvantages. First, the gas temperature rises in the unloaded compression chamber and associated suction line due to the gas circulation. Second, the suction valve life time may decline due to the impact of the unloader finger on the sealing element. Similar to first stage bypass control, temperatures and pressures may vary in the compressor, possibly creating undesirable rod loads, pulsations, etc. The three types of suction valve unloading discussed in this paper are detailed below.

Conventional Valve Unloading: The compression chamber is unloaded for a long period. Different capacities are available based on the number of unloaded compression chambers per stage. Therefore, the regulation range is limited. However, the impact on the compressor is small and the efficiency is higher than with reverse flow control. With this method, the

Comparison of Operation Experiences of Capacity Controls

by: R. Stocker, E. Glück, R. Aigner, Burckhardt Compression AG

load on each stage must be similar to minimise the change of the interstage pressure.

Intermittent Flow Control (IFC): The compression chamber is alternatively unloaded and loaded. The chamber can be unloaded during one or more crank shaft revolutions. Mass flow rates vary depending on the number of consecutive unloaded revolutions. The gas temperature is less influenced at low mass flow compared to reverse flow controls, but this strategy may cause increased low frequency pulsations for high capacities. A special case of the IFC method is extended valve unloading, i.e. when the valve is unloaded for a long period (see conventional valve unloading).

Reverse Flow Control (RFC): The compression chamber is partially loaded with each crank shaft revolution by holding the suction valves open during part of the compression stroke. This allows a portion of the gas back into the suction line before compressing the rest. The major advantage of this method is the wide stepless capacity range, but it is limited by the increase of the suction temperature caused by the valve losses and the behaviour of the discharge valve. It is an energy efficient method of control and it is easy to retrofit the system on existing compressors. In addition, it is possible to adjust the interstage pressure by setting the mass flow of each stage. The life time of the valves can be higher, if the impact velocities between the unloader and the valve sealing element are small (soft landing [3]).

Different actuators to perform RFC are available, namely electromagnetic, hydraulic and pneumatic activated actuators. The pneumatic actuators are only used in a small application area and will not be discussed further. The main advantage of electromagnetic actuators compared to a hydraulic system is their low maintenance costs.

One system available which is capable of not only RFC but also IFC is an electromagnetic actuator. The major advantages of such a system are stepless flow control over a wide range, increased efficiency by switching to IFC at certain loads (e.g. 75%, 50% and 25% with fully unloaded compression chambers) and possibly increased life time of the suction and discharge valves due to the reduced partly loaded cycles with IFC.

Speed Control: This control strategy works by changing the speed of the compressor. A frequency converter is the most common way to achieve this. Speed control is one of the most energy efficient solutions of all capacity control methods. Additionally, the interstage pressures, the pressure ratios and the temperatures remain nearly constant. One of the major drawbacks of speed control is higher preliminary expenditure on plant design to

check for critical resonance frequencies. Vibration, pulsation, and torsion analyses provide information on critical speed ranges which must be avoided during operation. The rod reversal and combined rod loads produced by the analyses have to be verified for the entire speed range. In addition, when changing the speed of the compressor, the valves do not work on the design point anymore. Furthermore, an external lube oil system might be necessary for low speeds.

Start-and-Stop Control: With this method, the compressor will start and stop on demand. This does not have any influence on operating points of the compressor, but there is a limitation of possible start and stop cycles without reducing the life time of the plant components.

1.2 Capacity Control Comparison

In Table 1.1 seven capacity controls are rated by process relevant properties and expenses on a scale from one (worst) to three (best) and zero (not possible). The rating of the process relevant properties is a summary based on the previous capacity control descriptions, [4], [2] and internal experiences. Particular applications may vary from this general rating. The following points have been evaluated:

Capacity Range: includes the capacity range or the amount of capacity steps.

Reliability: rates the failure safety of the capacity control system and components including valves. This rating is based on failure records.

Pulsations: rates the increased pulsations.

Pressure Consistency: refers to the changing interstage pressures.

Temperature Consistency: includes the stability of the gas temperature.

Investment Cost: compares the investment cost of the implementation of the capacity control systems without an additional system (e.g. bypass). The investment costs of the capacity control systems for three different compressor sizes in terms of motor power have been compared.

Maintenance Cost: compares the average cost of capacity control system-relevant parts, valves and outage costs during 12 years of operation.

Energy Savings: refers to the potential energy savings of the motor. The theoretical possible energy savings of the capacity control systems for three different compressor sizes have been compared.

Comparison of Operation Experiences of Capacity Controls

by: R. Stocker, E. Glück, R. Aigner, Burckhardt Compression AG

Capacity Control Method	Capacity Range	Reliability	Pulsations	Pressure Consistency	Temperature Consistency	Investment Cost	Maintenance Cost	Energy Savings
Bypass (all)	●●●	●●●	●●●	●●●	●●	●●	●●●	○
Bypass (1 st)	●	●●●	●●	●	●	●●	●●	●
Unloaders	●●	●●	●●	●●	●	●●	●●	●●
RFC and IFC electromagnetic	●●●	●●	●●	●●●	●●	●●	●●	●●●
RFC hydraulic	●●●	●	●	●●	●●	●●	●	●●
Speed Control	●●	●●	●●	●●●	●●●	●	●●	●●●
Start-and-Stop	●	●●●	●●●	●●●	●●●	●●●	●●●	●●●

Table 1.1: Comparison of capacity controls concerning process properties and expenses

2 Experiences with Conventional Unloaders

Conventional unloaders have been used extensively, but in exceptional circumstances the unloaders may have difficulties fulfilling their purpose. The following three examples highlight challenges for conventional unloading systems in terms of installation, commissioning, design, and sizing.

Unloading Process and Forces

In the following cases the force to unload the valve is provided by a double acting gas pressured actuator. The design control pressure describes the required pressure which is necessary to generate the force to unload the valve properly. During the unloading process the following forces arise: spring force of the unloader, valve spring force, as well as the gas streaming forces on the valve rings and on the unloader (Figure 2.1). The streaming force acts in two directions. During the suction cycle it acts in the direction of the compression chamber, which results in a minimal change in the required actuation force. During the compression cycle it acts in the direction of the suction line, which results in a large change to the required actuation force.

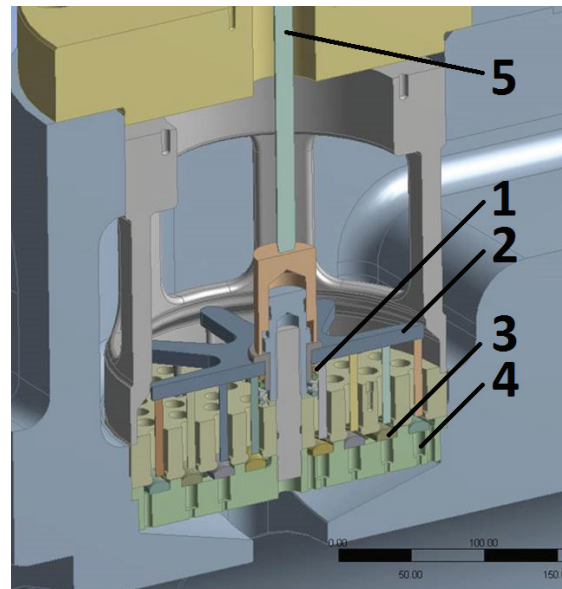


Figure 2.1: Forces acting on the unloader: 1) Spring force unloader, 2) Gas forces on unloader, 3) Gas forces on valve rings, 4) Valve spring force, 5) Actuator force

2.1 Control Pressure of Conventional Unloaders

In this section two operation experiences concerning the control pressure of valve unloaders are described. Case 1 (Figure 2.2) shows a ring valve with an unloader which failed during operation. Snapped off unloader pins and deep marks on the valve rings are extensive. The unloader was activated by a gas pressured actuator.

Comparison of Operation Experiences of Capacity Controls

by: R. Stocker, E. Glück, R. Aigner, Burckhardt Compression AG

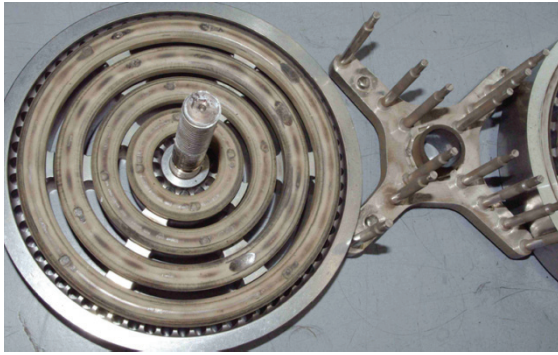


Figure 2.2: Case 1: Damage from excessively high control pressure

At first glance, the valve damage looks similar in case 2 (Figure 2.3) compared to the one described above. However the damage on the valve sealing elements has reached a more advanced stage.



Figure 2.3: Case 2: Damage with too little control pressure

Evaluation

A failure evaluation for damage case 1 and 2 was carried out. The gas pressured actuator in case 1 was designed for a target control pressure of 6.5 bar. During the investigation, the actual control pressure was determined to be 9 bar. The pressure deviation results in an almost 40% higher force pushing the unloader on to the valve sealing. To evaluate the effects of the high actuation force a static analysis of the valve unloader device was conducted. The static analysis detailed in Figure 2.4 shows that:

- The equivalent stress at the unloader pin's end is very high, which leads to deformation.
- The equivalent stress at the conjunction between the pins and base is moderate with a maximum of 145 MPa with a tensile yield of 155 MPa and a tensile ultimate of 250 MPa.

- Due to the flexibility of the arms of the unloading device, the pins in the inner circle are more stressed than the outer pins.

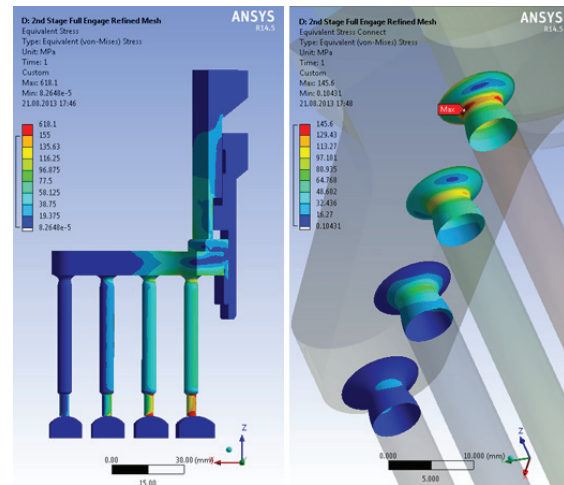


Figure 2.4: Static analysis, overloaded unloader

In case 2, the result of the failure evaluation was a pressure deviation of 60% of the design control pressure. Therefore, only 40% of the design actuator force was acting on the unloader.

Solution

Due to the higher actuation force in case 1, the unloader pins and the valve sealing elements experienced very high stress (Figure 2.4). This resulted in deformation of the inner unloader pin's end. The deformation triggered a chain reaction in which the stress on the pins was too high and successively snapped off the pins. After reducing the control pressure to the original calculated pressure the issue was not repeated.

Due to the resulting small actuation force in case 2, the actuator was unable to properly unload the valve during the compression cycle. During each compression stroke the valve rings fluttered between the unloader pins and the valve guard, which led to wear and damage of the valve rings. In addition, the unloader has fluttered against the valve seat, which caused the broken pins. After increasing the control pressure to the designed pressure, the unloader did not encounter the issue again.

As a conclusion it can be said that proper control pressure is fundamental for the successful operation of a valve unloading system. Whether excessively high or low control pressure, both led to similar unloader and valve sealing damage.

2.2 Spring of Conventional Unloader

A valve unloader on a ring valve had broken pins after a short running period. Additionally, the valve rings showed deep marks from the pins and the valve seat

Comparison of Operation Experiences of Capacity Controls

by: R. Stocker, E. Glück, R. Aigner, Burckhardt Compression AG

had a damaged sealing profile. In this case the gas force on the ring was up to 6800 N during unloading.

Evaluation

The investigation of the damage and the unloading system showed there are two points to consider for a reliable unloading system in this application.

First, during the investigation of the streaming forces (Figure 2.5) it was shown that the spring force of the unloading device was not sufficient to properly resist the suction force. Therefore, the inactive unloader was drawn in and fluttered against the valve seat, which was the main cause of the damage to the unloader.

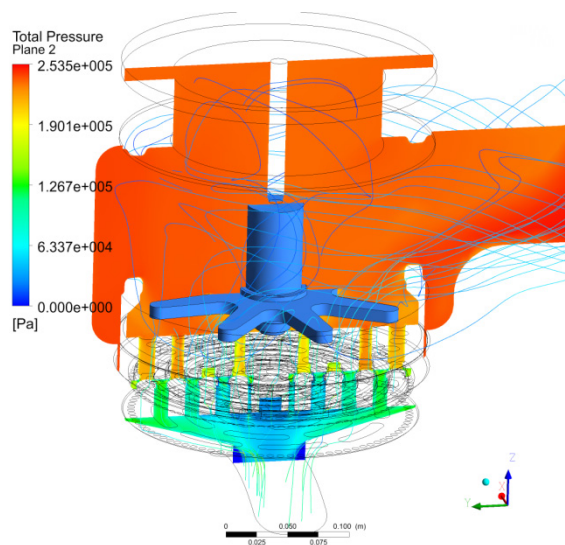


Figure 2.5: Evaluation of the streaming force on the unloading device by means of a Computational-Fluid-Dynamics calculation

Second, due to the piping of the actuator not being installed in accordance with the drawings, the control pressure was measured and revealed as unstable. Therefore the unloader might have not been able to correctly unload the valve.

Solution

Following changes of the unloading system resolved the problems:

- The unloader spring was exchanged in accordance with the resulting streaming force.
- The control pressure was stabilised by exchanging the piping with a bigger diameter.

3 SFCS Replacing Frequency Converter

In a refrigeration application five similar compressors are parallel linked and will start and stop on demand

(Figure 3.1). The first compressor in the row was fitted with a frequency converter to control the mass flow. The mass flow range of 50% to 100% of this compressor was used to adjust the mass flow precisely whereas the other compressors produce the main flow. The mass flow rate of the other four compressors can each be switched between 100% and 50% by means of valve unloaders.

The three process relevant values are constant refrigeration temperature of -30°C , constant gas temperature in the suction accumulator and constant pressure in the receiver.

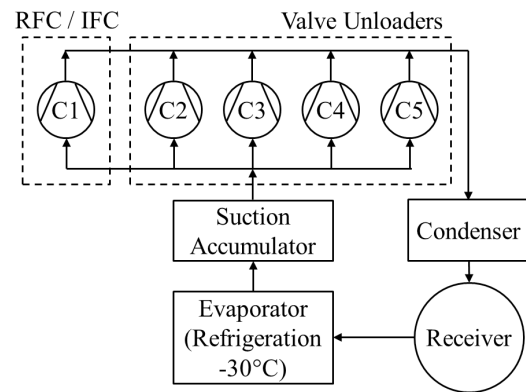


Figure 3.1: Schematic diagram of the application with parallel operating compressors

Customer demands

Vibration difficulties occurred when operating the compressor with speed control. At certain frequencies the vibrations and the pulsations exceed the specified limits. Therefore the frequency converter was taken out of operation. A compressor with valve unloading (100%, 50%) had temporarily taken over the capacity control. Due to the missing control capabilities of this compressor the refrigeration temperature was not stable and the additional compressors switched on and off more often. Therefore a replacement had to be found. Experiences have shown that capacity control capable of 100% to 50% mass flow reduce the start and stop cycles of the other compressors. Due to the easy retrofitting and the capacity control range a RFC-system was an alternative to the frequency converter. A reverse flow control system as presented in [3] and [4] with electromagnetic actuators was installed.

Operation

At this plant, a prototype of the previously mentioned RFC-IFC-system has been in operation since October 2011. The two stage compressor is fitted with two actuators, one at each stage. A combination of RFC and IFC strategy [5] is used to provide the requested mass flow. A stepless mass

Comparison of Operation Experiences of Capacity Controls

by: R. Stocker, E. Glück, R. Aigner, Burckhardt Compression AG

flow is delivered between a capacity of 100% and 60%. At 50% mass flow the IFC is used (special case of the IFC: full unloading of the compression chamber). A mass flow between 60% and 50% is not provided, in order to keep the influence on the discharge valves small [3].

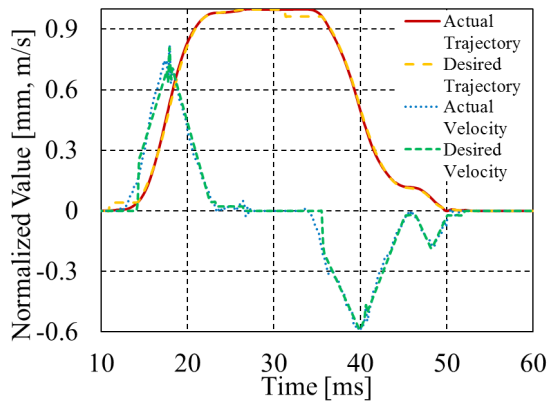


Figure 3.2: Data of the valve control

Figure 3.2 shows the position and velocity of the unloader during RFC. The impact velocities of the unloader can be kept low due to the soft landing on the valve sealing element. Therefore the life time of the suction valve is not decreased. Combining the RFC and IFC strategies increases not only the efficiency of the compressor at a capacity of 50% but also the life time of the discharge valve. In addition, pulsation and gas temperature changes are minimised.

Improvement

No vibration limitation exceeds have been reported by the customer after the RFC-IFC-system was installed. In addition, the reverse flow control works as expected throughout the full capacity range. The start and stop cycles of the additional compressors at the plant have been reduced considerably compared to the 50% valve unloading system.

Figure 3.3 shows a chart comparing the recorded start and stop cycles of the compressors at the plant as well as temperature and pressure fluctuation in the process. During an ordinary 12 day production period, with similar mass flow request, an average reduction of start and stop cycles to 34% was achieved. Moreover, in particular production cases the cycles are reduced to 3%, which highly extends the durability of the compressor components.

In addition, the process is stabilized. The temperature fluctuation in the suction accumulator has been reduced by 77% and the pressure fluctuation in the receiver by 60%.

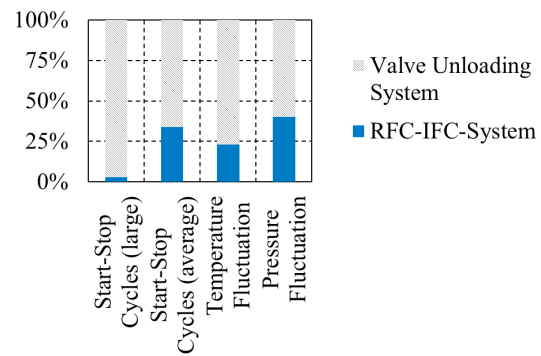


Figure 3.3: Improvement with RFC-IFC-system

In this application with small compressors the aim was to provide a stable operation of the compressor within the regulation range and increased process stability. This was achieved by the implementation of the RFC-IFC strategy which also increases durability of the other compressor's auxiliaries due to the significantly reduced start and stop cycles.

4 Control Range of Frequency Converters

A compressor with variable speed for capacity control was required. The capacity should range from 500 to 1500 kg/h (33% to 100%) mass flow. In addition the suction pressure varies between 14 and 20 bar.

Solution

A new flywheel and motor were designed bearing in mind the natural frequencies as well as the stress and torque, both static and dynamic, to achieve the desired flow conditions. It turned out that an external bearing was necessary to hold the crank shaft in place. In addition a flexible coupling must be used. The benefits of a flexible coupling are the dampening of torsion vibrations and the simplification of the installation.

The resulting resonance frequency could be avoided throughout the designed speed range of 175 to 495 rpm. The calculation showed that only the 4th, 5th and 6th harmonic orders are within the desired speed range. However, the static torque of the corresponding compressor excitation harmonic remains almost unchanged. Therefore, there is no frequency range to avoid. Figure 4.1 shows the function of excitation torque and response torque of the coupling at nominal speed. The static and dynamic stresses of the shaft system are below the admissible limits for all operation cases. The rotational irregularity (cycle irregularity [4]) of the motor, which arises at low speed, needed to be dampened with the frequency converter, in order to avoid a negative influence on power supply.

Comparison of Operation Experiences of Capacity Controls

by: R. Stocker, E. Glück, R. Aigner, Burckhardt Compression AG

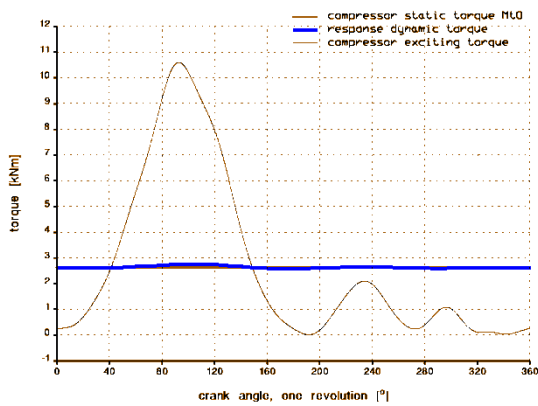


Figure 4.1: Vibratory torque of the shaft system

Regulation range

The advantages of this system are a wide regulation range of 100% to 33% of mass flow coupled with almost perfectly linear shaft power to flow rate ratio (Figure 4.2). This linear ratio is likely to save on cost in terms of power consumption compared to other capacity control systems. Furthermore, the maintenance costs for the speed control system are low.

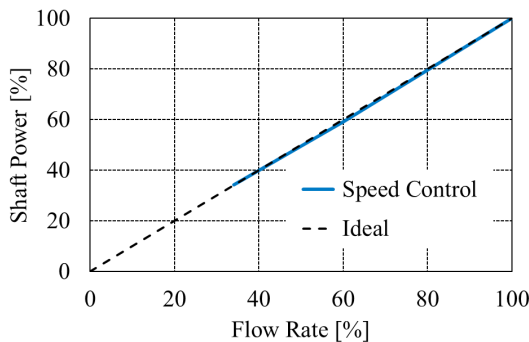


Figure 4.2: Power consumption of the compressor depending on flow rate

It is not completely without drawbacks, however, as both an external lube oil system is required and the valves are more loaded during low speed operation. As such, more wear on valves may result in increased valve maintenance costs.

5 Combination of Different Capacity Controls

In this case a compressor should deliver a mass flow of 1560 kg/h to a minimal flow of 250 kg/h (100% to 16%).

Boundary Conditions

The mechanical properties of the compressor, the equipment, and also the costs set the boundary

conditions of the regulation range for a speed control. In this example the following limitations due to the compressor, motor and the frequency converter are given:

- Rotational irregularity can be up to 1/40 due to the absorption with the frequency converter.
- Motor operating range considering torque is from 265 to 520 rpm.

Taking into account the resonance frequency, harmonic orders and torsion analysis, a flywheel and coupling was sized to operate the compressor between 285 and 500 rpm.

Control Strategy

The control strategy includes a combination of three capacity control methods in a total of four ranges (Figure 5.1). The first range is a speed control for a stepless capacity control from 100% to 64% of mass flow. The second is coupled valve unloading and bypass control, which results in a capacity reduction from approximately 64% to 54%. The third range is a combination of valve unloading and speed control to provide a step-less range from 54% to 32%. Fourth and finally, a bypass line is able to control from 32% to 16% of the mass flow. Note that when the unloaders are activated for 50% mass flow, the motor speed must be increased to 500 rpm to maintain the same shaft load and mass flow of the compressor.

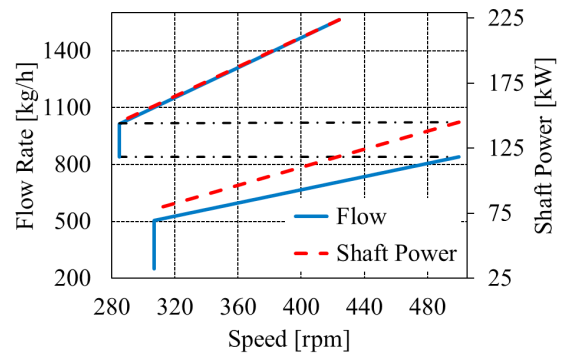


Figure 5.1: Regulation Range of speed control with valve unloading and bypass

The major benefits of this combined capacity control are the wide control range and the high efficiency. In Figure 5.2 the shaft power versus the flow rate is shown. The shaft power behaves ideally in the first range while reducing the mass flow from 100% to 64% by speed control. During the second range when valve unloading and bypass are used, the efficiency is at most 11% off from the ideal curve. As the mass flow request decreases further in the third range of valve unloading and speed control, the efficiency rises again. As soon as the minimal speed

Comparison of Operation Experiences of Capacity Controls

by: R. Stocker, E. Glück, R. Aigner, Burckhardt Compression AG

is reached, the fourth range starts and as only the bypass is remaining to reduce the mass flow there are no more power savings.

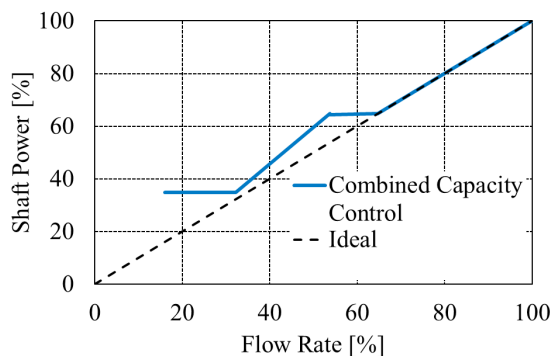


Figure 5.2: Power consumption of the compressor depending on flow rate

Due to the valve unloading a very small flow rate can be achieved without reducing the compressor speed below 50% of the nominal speed. Because the speed is maintained above this limit, an external lube oil system is not needed during operation. Drawbacks of this system are the high investment costs and valve wear may increase at low speed operation.

6 Summary

A variety of capacity controls are available on the market. Some of them have been established for years, such as conventional valve unloaders. Nevertheless, development efforts are still necessary to extend the application area. In applications with both high streaming forces and large valves, streamlined and rotationally locked unloading devices are essential. This is necessary not only to ensure a proper function in terms of operating forces, but also to ensure a long life time of the equipment. Even the approved valve unloading systems might present challenges if the designed operating conditions are not fulfilled.

Capacity controls using combinations of reverse flow control and intermittent flow control, are versatile in use because of their wide regulation ranges, controllable interstage pressures, energy efficiency and easy retrofitting. For larger compressors power savings of such a system are significant. For small compressors the main target is process optimisation. The drawback is the high investment cost.

Frequency converters also have a high investment cost, but it is offset overtime due to their high efficiency. When a custom designed flywheel and coupling is used, it is possible to have no resonance frequencies occur in the desired speed range. Therefore, no speed ranges have to be avoided and a full range of capacity control can be achieved. The drawbacks are higher

loaded valves while not working on the valve design points and the need for an additional lube oil system during low speed.

The technical capabilities of the capacity control range may be limited by the process or the properties of the compressor but a combination of capacity controls can nevertheless provide a wide capacity control range. For example, the resonance frequency of a speed controlled compressor allows only a certain speed range, which limits the possible mass flow range, but with additional valve unloaders and a bypass line the resonance frequencies can be avoided and the target mass flow range can be achieved. However, the drawbacks are the high investment cost and higher maintenance cost due to the complexity of the system.

Overall, the decision for a capacity control system is not only based on technical possibilities, but also on the investment and maintenance cost, as well as on energy savings, reliability and other customer needs. Therefore an optimal solution for each individual application has to be devised on a case-by-case basis.

References

- 1 Aigner, R. (2013): Erfahrungen mit stufenlosen Massenstromregelungssystemen (Workshop Kötter 2013)
- 2 Workshop documentation of the 5th EFRC-Conference (2007): Capacity Control.
- 3 Aigner, R., Voser, A., Allenspach, A. (2010): Development of a Stepless Flow Control System. 7. EFRC-Konferenz Tagungsband, 169-178.
- 4 Aigner, R., Sasse, L., Glück, E., Allenspach, A. (2012): Experience with Electromagnetic Stepless Flow Control Systems. 8. EFRC-Konferenz Tagungsband, 182-191.
- 5 Patent: Method for Controlling Delivery Quantity, and Reciprocating Compressor having Delivery Quantity Control, Publication no.: WO 2011/009879 A1



Compressor Innovations Bring Improvements to Gas Storage Operations

by:

Oliver Friedlaender, Siegfried Müssig

RAG Rohöl-Aufsuchungs Gesellschaft

Vienna, Austria

oliver.friedlaender@rag-austria.at

**9th Conference of the EFRC
September 11th / 12th, 2014, Vienna**

Abstract:

RAG Rohöl-Aufsuchungs Aktiengesellschaft is Austria's oldest oil and gas exploration and production company. RAG operates besides the typical oils and gas production facilities a number of underground storages for natural gas, including the Haidach storage with 2.6 billion m³ working gas near Salzburg.

The gas flows of Haidach vary greatly over timescales of hours, weeks and months in both directions during injection and production of the gas. During cold winter periods gas peak demand can exceed 1 million m³/h. Correspondingly very high volumes of gas need to be compressed and delivered to the market. The reliable delivery of the gas demand creates a technical challenge for the operating flexibility of the compressors.

The Haidach compression site consists of four reciprocating compressors fitted with reverse flow stepless capacity control. With the existing compressor valves this allows an operating range of 20–100% of nominal flow rate, and gives corresponding energy savings. New high-performance compressor valves have extended the lower flowrate limit down to 10%, thus increasing the flexibility of the capacity control system. This paper describes the successful application of an innovative fully electric capacity control system. Compared to the traditional hydraulic system it offers identical operational performance, but with much simpler installation and easier maintenance, and thus better economics for small compressors.

The state-of-the-art condition monitoring system used in Haidach is designed specifically for reciprocating compressors. It allows to align maintenance schedules concurrent with periods of low compressor demand, as well as quick and reliable shutdown possibilities in the event of an unexpected compressor malfunction.

Compressor Innovations Bring Improvements to Gas Storage Operations

by: *Oliver Friedlaender, Siegfried Müssig, RAG Rohöl-Aufsuchungs Gesellschaft*

1 Introduction

The compressors used by gas storage operator's face challenging requirements in terms of operating flexibility, reliability and energy efficiency. Although reciprocating compressors are increasingly hard to match the performance of turbocompressors, they are competitive in some aspects of gas storage service when equipped with the latest control systems and components.

Gas storage operations are characterised by frequent changes in suction and discharge pressure. This necessitates rapid changes to the operating point of the compressor. On reciprocating compressors, stepless capacity control via suction valve unloading is essential to accommodate this variation without wasting energy.

Capacity control of this type is traditionally accomplished through hydraulic valve actuators. This paper describes the use of a new all-electric capacity control system at the Haidach gas facility in Austria. Benefits include plug-and-play installation, easier commissioning, low maintenance costs thanks to the ability to replace components easily, and user-friendly operation. Operating performance is identical to that of a traditional hydraulic capacity control system.

Although reverse-flow capacity control is energy-efficient over its rated range, temperature rise in the suction chamber generally limits the turndown to 20% of the nominal load. As demonstrated at Haidach, new high-efficiency valve technology allows the minimum safe flowrate to be reduced to 10% and so considerably increases the operating flexibility of the compressor.

Experience at the plant has also shown the value of state-of-the-art condition monitoring of reciprocating compressors. Maintenance operations that require a compressor shutdown should ideally be timed for periods when the demand for compression is low, such as during the winter when gas is being withdrawn from the reservoir. The condition monitoring system used at Haidach provides detailed information that allows maintenance intervals to be planned accurately, as well as enabling quick and reliable shutdown in the event of a serious fault.

2 The need for gas storage

Storage facilities play a key role in meeting the varying demand and securing and balancing the natural gas network.

Natural gas production is often constant from hour

to hour and month to month. Gas consumption of the industry, power stations and households, on the other hand, varies greatly according to the season and the time of day. Not surprisingly, much more gas is used on winter days than summer nights.

This variability is essential to be able to store large quantities of gas for use in periods of peak demand. High-pressure gas pipelines provide some of the necessary capacity, with underground storage accounting for the rest.

As a fuel for power generation, gas emits considerably less carbon dioxide than coal does. With the ever-growing need to reduce greenhouse gas emissions, therefore, the use of gas is set to increase in the long term. Along with increasing European gas imports and the continuing need to maintain energy security, this can only boost the future demand for gas storage.

3 The Haidach Site

3.1 About RAG

RAG is Austria's oldest exploration and production company, with a history dating back to 1935. Its core businesses are oil and gas exploration and production and gas storage. The company employs some 400 people, with annual sales of around 600 million m³ of natural gas and 140,000 t of crude oil. RAG operates mainly in Austria, Germany and Hungary.

With a total gas storage volume of approximately 5.7 billion m³, RAG is one of Europe's leading storage providers and plays an important role in securing gas supply not just in Austria but also in Central Europe. The company's experience of natural gas storage goes back over 30 years.

RAG is characterised by a culture of forward thinking and innovation, and the company is never afraid to be an early adopter of promising new technology.

3.2 Huge volumes and high flows

With a Turn Over Volume of 2.6 billion m³ Haidach is the second-largest gas storage facility in Central Europe. This is about one-third of Austria's annual gas demand.

RAG discovered the porous sandstone reservoir Haidach in 1997 located 25 km north-east of Salzburg. With a total Gas-in Place of 4.3 billion m³, it was one of the largest gas finds in Austria.

The gas bearing reservoir rock in Haidach is extraordinary thick – over 100 m in some places – and extends over an area of 17.5 km².

Compressor Innovations Bring Improvements to Gas Storage Operations

by: Oliver Friedlaender, Siegfried Müssig, RAG Rohöl-Aufsuchungs Gesellschaft

A tight cap of clay marl seals the gas in place at a depth of 1,600 m.

Once the original gas had been produced, the reservoir was re-used as a storage facility. The first stage of construction was finished in 2007, giving a capacity of 1.2 billion m³. A pipeline 900 mm in diameter and 39 km long links the facility to the Austro-German gas hub in Burghausen/Überackern.

A further expansion began in 2009 and was completed in 2011. Additional storage wells were drilled and two additional compressors with their associated gas dehydration units were installed.

RAG collaborated on the expansion with German Gas Company WINGAS and Russia's Gazprom. The three companies have invested a total of €300 million in the expansion, and each company holds a third of the total 2.6 billion m³ storage capacity. RAG operates the facility on behalf of its partners.

The high permeability of the reservoir rock at Haidach allows very high injection and withdrawal rates – more than 1 million m³/h. Across Europe there are only a few gas reservoirs that can match this performance.

A typical winter day sees gas withdrawal rates of approximately 800,000 m³/h. The current record was set on 8 February 2012, a particularly cold day on which the withdrawal rate peaked at 1.85 million m³/h. Even then the reservoir's utilisation was only 80%, so Haidach could have sustained the same withdrawal rate for at least another eight weeks.



Figure 1: Overview of the Haidach storage facilities (UGS Haidach)

3.3 Compressors are the key

The reservoir pressure at Haidach varies from a maximum of 157 bar down to around 60 bar. Since the supply pipeline operates at 40–60 bar, compression is always required to charge the reservoir.

The picture is slightly more complex when gas is being withdrawn. When the reservoir pressure is above 90 bar the gas flows by gas expansion; control valves further reduce the pressure to the export pipeline pressure. When the reservoir pressure drops further, compressors are required to maintain the export

pressure in the range 55–98 bar.

The compressed gas is cooled on its way into and out of the underground store. Because the stored gas contains moisture, the recovery plant also has silica beds to dehydrate the gas.

On the site there are four main turbocompressors. With its full power of 14.6 MW, each one is designed to compress 225,000 Nm³/h gas from 46 to max. 182 bar. Capacity control is provided by four variable-frequency electric drives which allow the compressors to run at 40–105% of their 13,700 rpm rated speed.

These giant turbomachines are not the only compressors at Haidach, however. Also essential to operate the Haidach site are four reciprocating compressors.

RGV1, RGV2 and RGV3 are “residual gas compressors”, fairly small two-cylinder machines connected directly to wells drilled outside the normal storage operations. They are designed to extract the remaining original gas from the reservoir and compress it to around 30 bar for injection into the export pipeline. Hence, these reciprocating compressors are assigned to the conventional production rather than to the Haidach station.

The fourth reciprocating compressor, RGV4, is a larger four-cylinder machine which operates as part of the so-called UGS Aigelsbrunn and UGS H5 gas storage system. Its purpose is to shift gas between the pipeline and the underground reservoir at flowrates below the lower operating limit of the turbocompressors.



Figure 2: Overview of the Haidach production and storage facilities (UGS Aigelsbrunn and UGS H5)

4 Capacity control

4.1 The traditional approach

All the compressors at Haidach rely on capacity control to handle the varying demands of the gas storage and production operation with the minimum use of energy. In the case of the four reciprocating compressors this is achieved by using hydraulic actuators to hold the suction valves open during the first part of each compression stroke, so that only the required quantity of gas is compressed.

Compressor Innovations Bring Improvements to Gas Storage Operations

by: Oliver Friedlaender, Siegfried Müssig, RAG Rohöl-Aufsuchungs Gesellschaft

The electrohydraulic capacity control system used in Haidach has been proven in more than 1,000 successful installations worldwide. Actuator forces of up to 8,000 N, response times down to a few milliseconds, stepless control over the turndown range between 100% and 20% and excellent reliability make this an excellent choice for the Haidach compressors. Concerning the reliability it is worth mentioning that the electrohydraulic system was installed in 2004 and is running flawlessly since then.

Because the back-and-forth flow path through the suction valve is short, energy losses are low. As a result, the suction valve unloading system gives a merely linear relationship between capacity and compressor energy consumption.

4.2 Advantages of Electric Actuators

Capacity control via suction valve unloading reaches back to the 1930s. The original concept was based on electric actuators, but with the electrical technology of that time it was difficult to provide the required combination of high actuator forces and short response times. As a result, reverse-flow controllers relied on pneumatic actuators until the 1990s, when the change to a combination of electronics and hydraulics improved both performance and reliability.

Current electro-hydraulic capacity control systems work well for compressors of all sizes, but their comparative complexity makes their economics better suited to compressors at the medium-to-large size of the range. Specifically, the use of a central hydraulic unit makes the system less competitive for compressors with only a small number of valves.

If an all-electric actuator could be developed with the same performance as the electro-hydraulic version, it could bring more economic capacity control to small compressors. At the same time, the promise of greater simplicity in installation and operation would make the all-electric system equally attractive for larger machines.

RAG therefore used the opportunity to a field test of a new-all electric capacity control system on the RGV3 residual gas compressor at Haidach.

4.2.1 Design constraints

The main design requirements for the new system were set to:

- compressor speeds up to 1,500 rpm
- maximum actuator force 8,000 N, with load spikes up to 14,000 N

- valve closing time < 4 ms
- full control of unloader motion to keep unloader speed within defined limits independent of compressor speed and load
- no external cooling
- able to handle sealing element wear and thermal expansion totalling ± 5 mm
- 48,000 hours of service-free operation
- no mechanical adjustments on actuator
- completely oil-free design
- one actuator fits all applications
- easy installation and service
- compliance to explosion protection requirements (ATEX Zone 1)

From the many types of electric actuator available, the designers chose a hybrid solenoid, optimised to provide the best force/distance relationship over the appropriate stroke length. They also mastered the challenging task of designing a control system to deliver high operating speeds yet also limit the impact force at the end of the stroke, which could otherwise damage the valve. Careful thermal design ensured that the new actuator did not require external cooling.

In the final design, a main interface unit located in a safe area is connected to the main plant control system. The main interface unit communicates with a smaller control unit mounted in the compressor house. This in turn supplies power and control signals to each actuator via a single cable, thus simplifying installation and minimising cabling costs.

4.2.2 System characteristics

The main characteristics of the new system are:

- retrofitting to an existing compressor requires only a brief shutdown;
- plug and play connections;
- 100% oil-free;
- friction-free drive unit results in long maintenance intervals;
- controlled closing promotes long valve life;
- no external cooling required;
- no adjustments needed following valve service or actuator reassembly, thanks to automatic compensation of clearance between actuator and unloader rod;
- one interface unit can handle up to 48 actuators;
- maximum standardisation for simple spares management;

Compressor Innovations Bring Improvements to Gas Storage Operations

by: Oliver Friedlaender, Siegfried Müssig, RAG Rohöl-Aufsuchungs Gesellschaft

- suitable for corrosive atmospheres and non-lubricated applications;
- ATEX and IECEx certification for hazardous atmospheres.

The new system matches the original electro-hydraulic version in terms of actuator force and response speed, but has several advantages in terms of cost and usability. Although it can be used on compressors of any size, its relative simplicity makes the new system cost-effective for compressors of 400–1,000 kW – the first time that suction valve unloading has been economic in this size range. Payback time is typically less than 12 months.

Positive past experience with electro-hydraulic capacity control, plus a company culture of staying at the forefront of technical developments, meant that RAG did not hesitate to host the first field application of the new all-electric system.

The new system was installed on a single cylinder of the RGV3 residual gas compressor at Haidach (see Figure 4) in April 2012. Installation was straightforward and it was clear from the start that the new system would be considerably easier to retrofit than the older type, thanks to the simpler wiring and the absence of hydraulic lines.

Since then it has run for more than 10,000 hours with no problems. In fact, performance has been indistinguishable from that of the electro-hydraulic capacity control systems elsewhere on the site, see Figure 3.

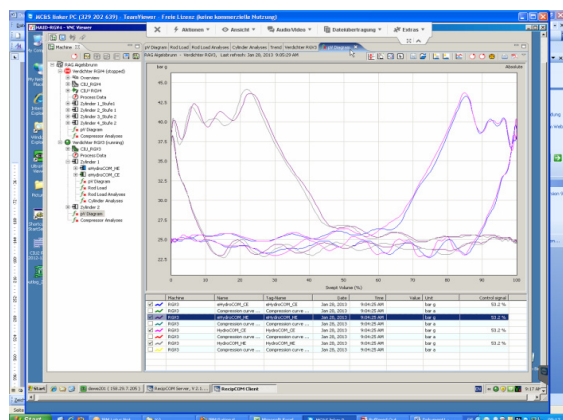


Figure 3: Indistinguishable P-V diagrams of the electrohydraulic vs. electrical reverse flow capacity control system installed on opposing cylinders of the same compression stage.

After this successful operating experience, RAG now plans to fit the all-electric system as a technology of choice in the future and not only just to small

compressors: All the results yielded that the new system provides a user-friendly and cost-effective replacement for electro-hydraulic capacity control on machines of all sizes.

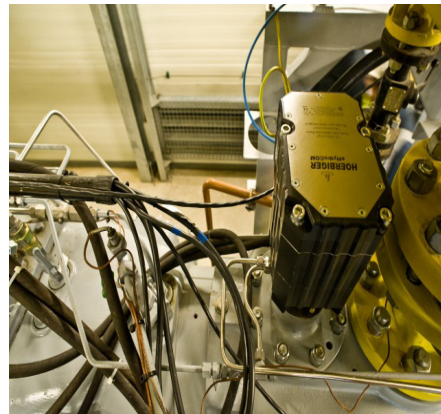


Figure 4: Picture of actuator of the electrical reverse flow control system

5. High efficiency valves

Stepless capacity controlled suction valves allow an operating range from 100% capacity “practically” down to zero (idle running). In practice, however, flow losses across the suction valve set a lower limit to the turndown. The lost energy generates heat, which creates an unacceptably large temperature rise below a certain limiting gas throughput (see Table 1, overleaf).

With the standard suction valves currently used on the Haidach compressors, the lower limit of turndown is around 20%. Valves with lower losses could reduce this limit and so improve the ability of the plant to follow wide load swings, see Figure 5 with a comparison of the valve efficiency of different valve types.

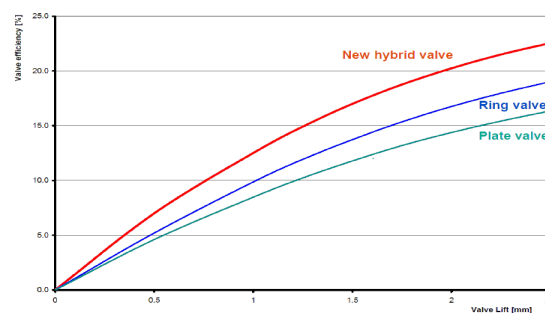


Figure 5: Valve efficiency over valve lift

RAG was provided the opportunity for field testing

Compressor Innovations Bring Improvements to Gas Storage Operations

by: Oliver Friedlaender, Siegfried Müssig, RAG Rohöl-Aufsuchungs Gesellschaft

of a new high-efficiency valve. The new valve plate based on a special polymer is a hybrid between a profiled plate and a ring valve, and combines the advantages of both. In September 2012 the new valve was fitted to the cylinders of RGV4, the largest of the four reciprocating compressors at Haidach.

The lower flow losses offered by this valve reduce heating and so allow the minimum turndown to be reduced to less than 10%. This is an advantage for RAG in the gas storage and production business, where demand fluctuates from day to day and throughout the year. Table 1 shows the improvements achieved with the new high efficiency suction valves:

	Standard suction valve	High Efficiency suction valve
Lowest possible flow	12000 Nm ³ /h	4000 Nm ³ /h
Suction valve temperature at lowest possible flow	62.5 °C	57 °C

Table 1: Comparison of minimal possible flow rate with standard and high efficiency valve

After this result, RAG is ready to fit the new valves to all its reciprocating compressors equipped with suction valve unloaders.

6. Planning Maintenance

RAG believes that state-of-the-art monitoring is a worthwhile investment on any reciprocating compressor that requires a high level of reliability.

One important function of such a system is to trip the compressor in the event of a serious malfunction. The best modern protection systems can bring the compressor to a complete stop within two or three revolutions, considerably reducing the secondary damage that will result from, say, a broken piston rod if the machine continues to run.

Just as important, however, is the ability of such a system to track the status of vital components – such as valves, bearings, and crosshead pins – and report any deterioration before it becomes a problem.

The seasonal demand pattern found in the gas storage industry often makes it possible to carry out planned compressor maintenance without any loss of service. When demand is low, one compressor can be shut down while another takes up the slack. Conversely, planned maintenance during the winter peak period is normally impossible.

Such a strict timing in maintenance operations, of course, requires an excellent knowledge of the internal state of the compressors – which is where condition monitoring comes in.

The monitoring system used by RAG is purpose-designed for recips. As with the analogous systems used on turbocompressors, it measures vibration levels, temperatures and pressures (see Figure 7). Unlike other systems, however, it uses vibration alarm thresholds that are not constant but vary with crank angle. During “noisy” events such as valves closing, the alarm threshold is high and so the system avoids spurious trips. Quieter parts of the cycle have lower alarm thresholds, allowing the system to detect abnormal behaviour with a high degree of confidence, as indicated in Figure 6.

RAG uses this monitoring system on reciprocating compressors and we are convinced of its benefits in allowing us to plan maintenance for periods of low demand. The confidence that compressors will shut down quickly in the event of a serious problem is also very welcome.

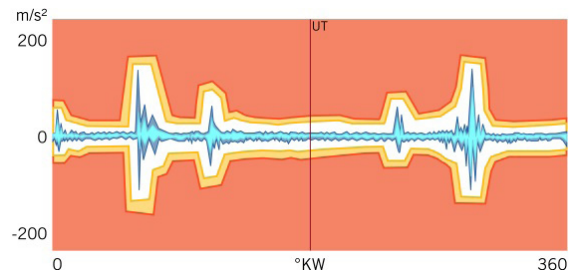


Figure 6: Vibration alarm levels as a function of degree crank angle

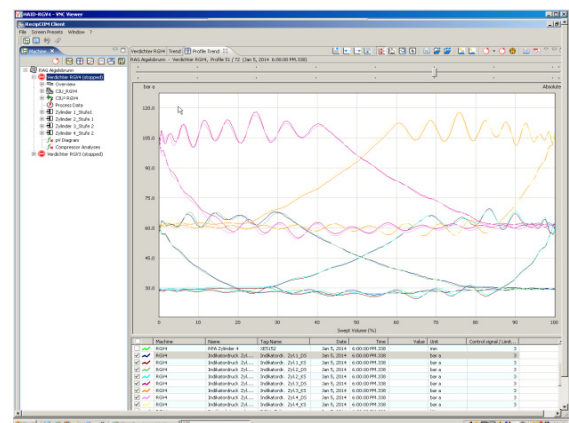


Figure 7: Monitoring of cylinder pressure at RGV4 compressor

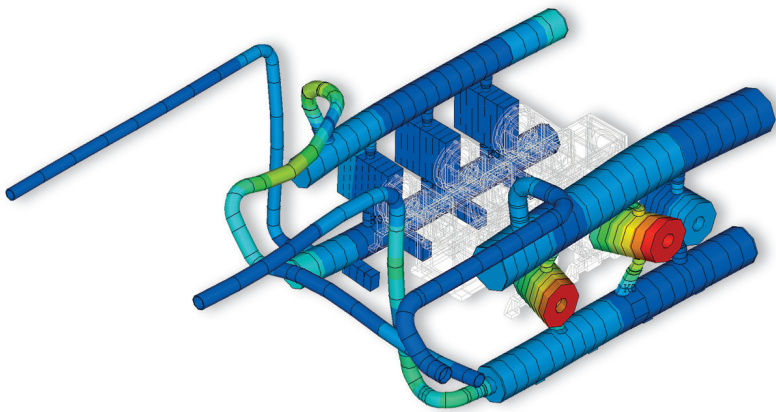
Compressor Innovations Bring Improvements to Gas Storage Operations

by: Oliver Friedlaender, Siegfried Müssig, RAG Rohöl-Aufsuchungs Gesellschaft

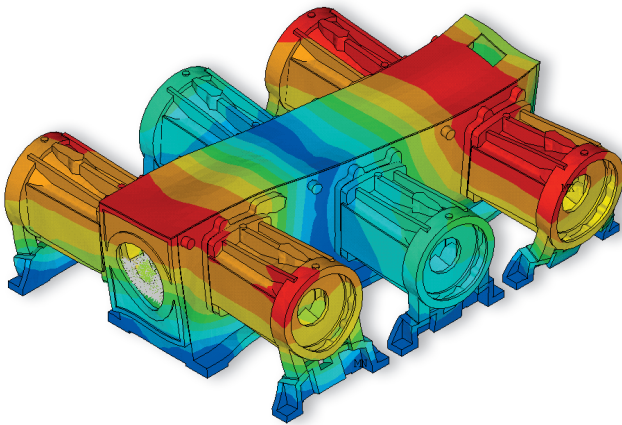
7. Summary

With rising demand of gas as energy source the role and importance of gas storage rises continuously. Reciprocating compressors are optimally suited for the challenging demands of the unsteady and varying operating conditions of gas storage. Hence, latest innovations for reciprocating compressors which increase the flexibility, efficiency and safety of the compressors are perfectly in line with the need of gas storage operators.

GOODBYE VIBRATIONS



Mode shape of a reciprocating compressor manifold system



FE model of a reciprocating compressor

CONSULTANCY PROJECTS

- Pulsation and vibration analysis according to API 618, API 674 and API 619
- Flow-induced, anti-surge control and transient analysis for turbo compressors

ROOT CAUSE ANALYSIS

Trouble shooting of flow dynamic, noise and vibration problems

INNOVATIVE RESEARCH PROJECTS

Active surge control, high frequency dynamics and fluid structure interaction analysis for turbo compressors

SOFTWARE DEVELOPMENT

PulsimSuite® software which integrates the different steps in an API analysis

TNO innovation
for life

**Please meet us at
EFRC 2014 at booth 24**

CONTACT

André Eijk
Senior Mechanical Consultant Oil & Gas
E andre.eijk@tno.nl
P +31 88 866 63 54
M +31 6 519 830 52

TNO.NL/HTFD



9th Conference of the EFRC September 11th / 12th, 2014, Vienna

Successful Detections of Loosened Parts on a Reciprocating Compressor -37-
by: César Luis Fernandez Valdez, Cesar Marín García Repsol Refinery Cartagena

Condition Monitoring and Simulated Start Up Sequences Successfully Supported the Commissioning of a New Reciprocating Compressor Unit -43-
by: Patrick Ferrage, TOTAL



EFRC
EUROPEAN FORUM
for RECIPROCATING
COMPRESSORS

SESSION MONITORING



Successful Detections of Loosened Parts on a Reciprocating Compressor

by:

César Luis Fernandez Valdez, Cesar Marín García
Repsol Refinery Cartagena
30350 Cartagena Murcia, Spain

9th EFRC Conference
September, 11th / 12th, 2014, Vienna

Abstract

This paper describes case studies about the detection, root cause analyses and lessons learned of incidents with loosened components on a piston inside a reciprocating compressor.

During the commissioning of a new reciprocating compressor the machine was automatically shut-down by the protection system installed due to high vibration on the crosshead slide. The detailed root cause analyses of all available monitoring data revealed that the piston nut was not sufficiently fixed so that the piston could move on the piston rod.

In another incident, a piston loosened its blind bolt during normal compressor operation. This damaged the piston, the rider bands, and the piston rings. Due to alarms that came from the protection system, based on high crosshead slide vibration and a high vertical movement of the piston rod, the reliability teams was able to determine the root cause.

The presentation illustrates the failure analysis process and explains why the incidents caused the observed changes to the monitored parameters such as crosshead vibration, rod position, and dynamic cylinder pressure.

Successful Detections of Loosened Parts on a Reciprocating Compressor

by: César Luis Fernandez Valdez, Cesar Marín García Repsol Refinery Cartagena

Introduction

Repsol Petroleo owns and manages five industrial complexes in Spain located in Cartagena, La Coruña, Bilbao, Puertollano and Tarragona, with a total distilling capacity of 896,000 barrels of oil/day.

Repsol's refineries processed 37 million tonnes of crude oil in 2012 and nearly 60% of Spain's conversion capacity.

The Cartagena refinery, after the expansion, is now at the forefront of industrial complexes with the greatest conversion capacity in Europe, measured using the FCC equivalent ratio (% of conversion per million barrels processed per day).

The complex includes distillation units with a capacity of 220.000 barrels/day, a Coker unit with 3.000 kt./year and a Hydrocracker unit with 2.500 kt./year.

The expansion of the Cartagena refinery has made the Escombreras valley an energy and industrial hub in the Region of Murcia. The impact of the modernized facilities, which entailed the largest industrial investment in Spain's history, has created wealth and employment in the area. ¹⁾

In course of the refinery expansion project, emphasis was put on having modern machine monitoring systems (MMS) and machine protection systems (MPS) on all critical reciprocating compressors. The scope of the MPS and MMS systems was based on the experiences made in other plants.

Detection of a loose piston nut based on high vibration on the crosshead slide

A compressor was prepared for its initial start-up with gas load. During this start-up run, the MPS and MMS were already activated for automatic safety shutdown.

The machine at site:

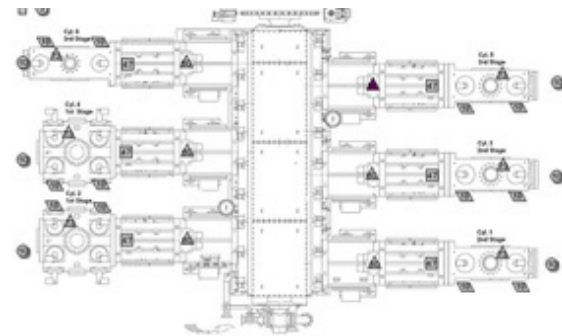


Figure 1: Machine design

Cylinders: 6
Service: Make Up Hydrogen
Stages: 3

C2/C4 1st STG: 22/53 kg/cm²a
C1/C3 2nd STG: 52/107 kg/cm²a
C5/C6 3rd STG: 106/199 kg/cm²a

The MPS and MMS are using the following sensors:

- Trigger for phase reference
- Accelerometers on all crosshead slides and cylinders
- Vertical piston rod position sensors
- Dynamic pressure sensors on cylinder headend (HE) and crankend (CE) side

During the first loaded compressor run, all safety limit settings (Alert, Shutdown) for all vibration analyses (crosshead slide, cylinder) and displacement analyses (rod position) were set at factory default level. The alert and shutdown limits for the dynamic pressure analyses were adjusted, based on the compressor OEM's re-recommendations.

Sequence of events

On October 6, 2011, the new compressor was started with 30% load for the first time. The machine ran smoothly for the first 2,5 hours and all vibration levels were below the limit of 62,5m/s² RMS. Without any advanced warning, the vibration of CHS 5, 3rd stage increased. At its maximum, the level reached almost 75m/s².

Based on the pre-set safety limits, the protection system automatically shut the compressor down.

Successful Detections of Loosened Parts on a Reciprocating Compressor

by: César Luis Fernandez Valdez, Cesar Marín García Repsol Refinery Cartagena

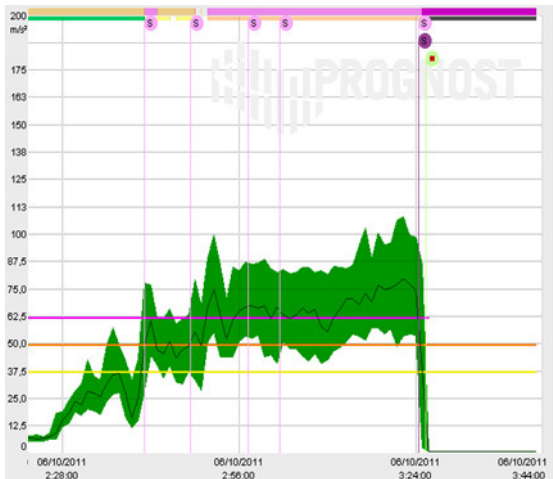


Figure 2: Increase of the vibration on crosshead slide on cylinder 5 (3rd stage).

The dark green line in the above graph is the trended RMS vibration of the segment 21 referring to 200–210 degree crank angle after BDC, while the green shadow indicates the minimum and maximum values. The two lower lines are warning thresholds for early failure detection, the pink line is the pre-set safety limit.

The vibration increased over a period of approx. 1 hour starting around 02:20 hrs, causing a first safety limit violation at 02:40 hrs and ending with the automatic trip at 03:24 hrs.

The logbook shows in detail the sequence of safety limit violations. Alarms have only been caused by high vibration in segments 20 and 21 related to 10 to 30 degree crank angle after the bottom dead center.

Date	Message
06/10/2011 11:49:25	Safety Alarm reset!
06/10/2011 3:24:21	Safety Alarm dead center activated!
06/10/2011 3:24:21	Safety Alert: Safety limits violated in the following segments: 20
06/10/2011 3:02:25	Safety Alert: Safety limits violated in the following segments: 21
06/10/2011 3:02:24	Safety Alert for safety limit segment canceled
06/10/2011 3:02:23	Safety Alert: Safety limits violated in the following segments: 21
06/10/2011 2:57:20	Safety Alert: Safety limits violated in the following segments: 21
06/10/2011 2:50:15	Safety Alert: Safety limits violated in the following segments: 21
06/10/2011 2:48:59	Safety Alert for safety limit segment canceled
06/10/2011 2:48:13	Safety Alert: Safety limits violated in the following segments: 21
06/10/2011 2:40:54	Safety Alert: Safety limits violated in the following segments: 21

Figure 3: Logbook of cylinder 5, 3rd stage, crosshead slide vibration (read from bottom to top).

Data analyses

Usually, the diagnostic data analyses are conducted by the reliability team of Repsol Cartagena. In cases when no clear root cause can be determined, external analysts are contacted to remotely access the MMS data and to confirm the findings and to obtain an additional opinion from another diagnostic specialist.

This MMS acquires and diagnoses machine vibrations for each revolution and then segments signals into crank angle-related portions. This allows harmless but sometimes erratic machine behavior to be rightly identified as a “good condition” – thereby avoiding false alarms.

As a first step of the analyses, the RMS values of the different segments (36 per crankshaft revolution) were examined in the recorded trend. This revealed a very high vibration in segment 21. Each line in the above picture represents one of the 36 segments per revolution. The highest vibration (green line) that is recorded is from segment 21 and shows a very high deviation.

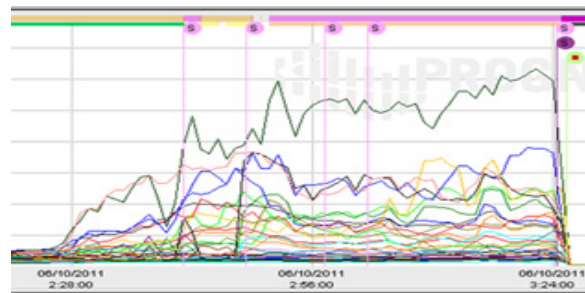


Figure 4: Development of vibration increase CHS 5, 3rd stage

In combination with the data from the pV diagram it was obvious that at segments 20/21 the rod reversal period takes place. High vibration readings at the time of the piston rod load reversal are caused by the change from tensile to pressure forces causing all parts, from crosshead pin to piston, to move within existing bearing or bolting clearances.

Machine analyses

The maintenance team first checked the crosshead connections, because they can be accessed most easily. However, they could not detect any damage of the crosshead pin or on other parts of the compressor. No looseness of the bolting was detected.

Based on the trended vibration increase, it was obvious that looseness had to be somewhere in the loaded components. With all other checks completed, only the connections of the piston inside the cylinder had not been verified. Hence the cylinder was opened and the piston removed. The inspection revealed that the piston nut had loosened and allowed the piston to move on the piston rod creating the high vibration levels during the rod reversal period.

SESSION MONITORING

Successful Detections of Loosened Parts on a Reciprocating Compressor

by: César Luis Fernandez Valdez, Cesar Marín García Repsol Refinery Cartagena

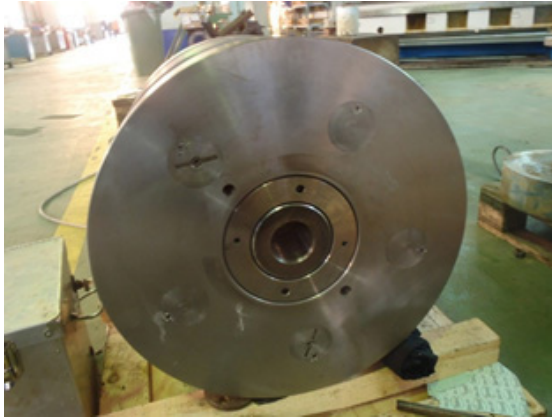


Figure 5: Piston with loosened piston nut of cylinder 5

Another incident occurred on another compressor of the same model and in the same hydrogen service. The MMS detected a loosened blind bolt on the piston.

Sequence of events

On a Friday night at 22:00 hrs, the control room called the maintenance department due to high vibration readings on the compressor that had caused alarms. Because the stand-by compressor was on maintenance and this compressor unit could not be stopped, the MPS safety trip was on bypass.

Data analyses

To determine the root cause of the alarms, we reviewed the trended CHS vibration data as shown in Fig. 6. The red line is the RMS value of CHS on cylinder 4. The data showed a high vibration level on crosshead slide 4. The flags mark the various alarms.



Figure 6: Trend view of the vibration RMS analyses of all six crosshead slides of the compressor

To get more information about the time when the increase started, we opened another view of this specific CHS 4 shown in Fig. 7.

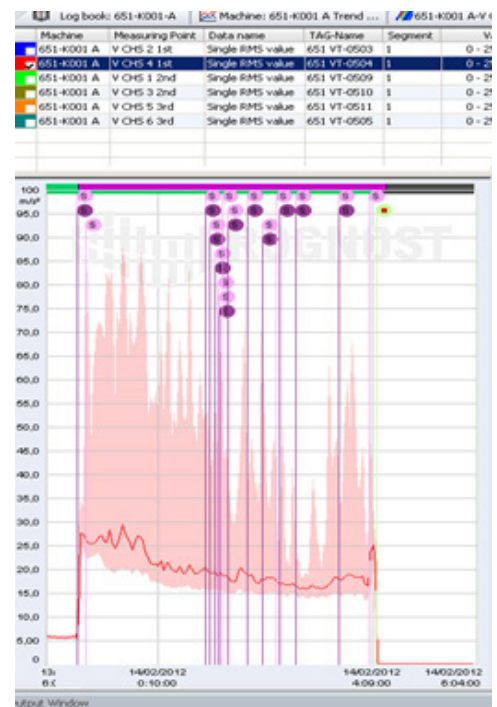


Figure 7: Four hours trend of CHS 4 vibration beginning at 23:00 hrs

Successful Detections of Loosened Parts on a Reciprocating Compressor

by: César Luis Fernandez Valdez, Cesar Marín García Repsol Refinery Cartagena

This trend view displays a time frame of four hours; beginning at 23:00 hrs. The shadow shows the minimum and maximum values of the vibration level. The “S” marks stand for “Alert” (light violet) and “Shutdown” (dark violet) alarms.

We analyzed the segmented vibration signal of the CHS in cylinder 4 and revealed a high vibration around the TDC area at segments 1 and 2 which are at 10° and 20° of the crank angle.

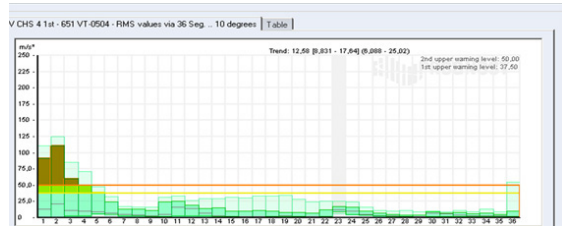


Figure 8: The segmented vibration analysis showed safety violation in segments 1 and 2

The comparison between the vibration levels on both 1st stage cylinders 2 and 4 with a 3D plot of trended segmented vibration (see Fig. 9), showed that only cylinder 4 was experiencing high vibrations and that peaks were mainly in the TDC area. After two hours we were convinced that cylinder 4 had a problem.

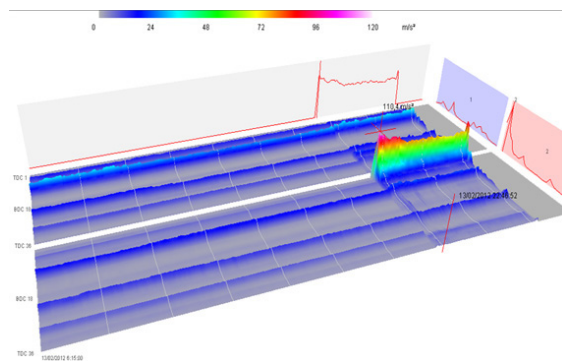


Figure 9: 3D diagram of CHS vibration on cyl. 2 (back) and cyl. 4 (front)

To find out the root cause, we checked the 3D trend of the piston rod position and compared it to the CHS vibration (see. Fig. 10). It showed that both signals had increased at the same time. This confirmed that some problem was inside the cylinder at the piston.

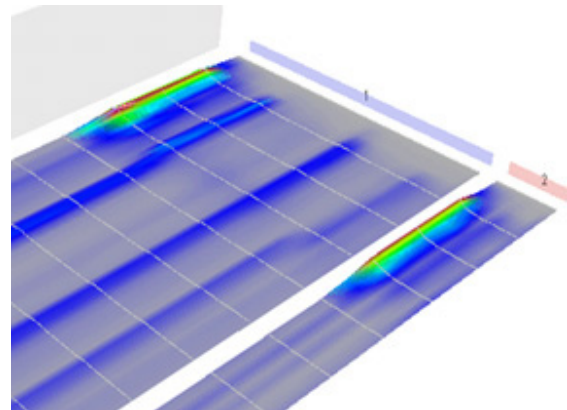


Figure 10: 3D diagram of CHS vibration (back) and piston rod position (front) on cyl. 4

Although the automatic shutdown for safety protection was on bypass, a transient ring buffer had been automatically started recording with each single alarm. Using these uncompressed time wave form signals, we looked at the online signals of the CHS vibration and the vertical piston rod position (see. Fig. 11). The vertical piston rod position sensor in some revolutions had gone out of range.

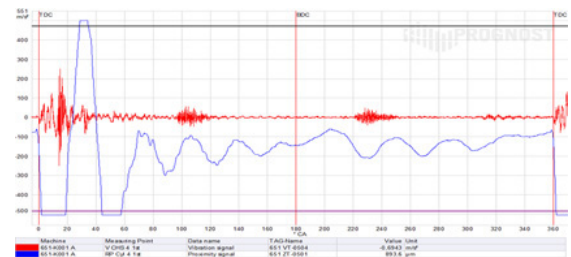


Figure 11: Online signal of the CHS vibration (red) and piston rod position (blue) of cylinder 4 over one revolution

The following three screens (Fig. 12-14) of the ring buffer show the same revolution.

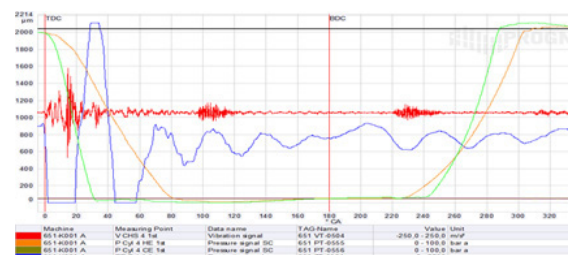


Figure 12: This plot shows the pressure signal in good condition (green) two days before the failure and the pressure signal (orange) in bad condition during the failure. During the failure (orange pressure signal) the compression and the re-expansion took longer time

SESSION MONITORING

Successful Detections of Loosened Parts on a Reciprocating Compressor

by: César Luis Fernandez Valdez, Cesar Marín García Repsol Refinery Cartagena

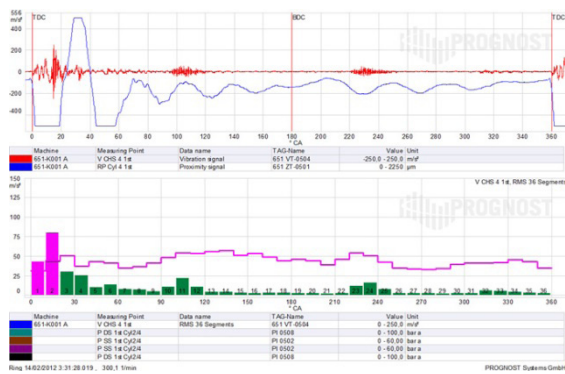


Figure 13: Online signal of the crosshead slide vibration and piston rod position of cylinder 4 with safety violations of the RMS value over 36 segments

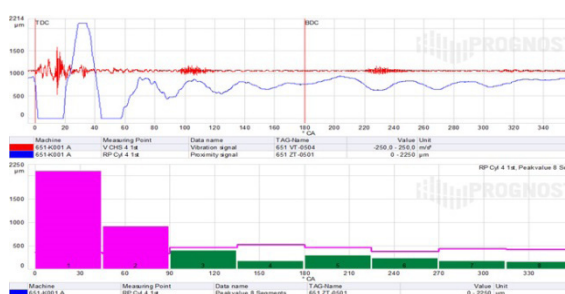


Figure 14: Online signals CHS and piston rod position of cylinder 4 with safety violation of rod position Peak-to-Peak over 8 segments

Findings

After we had executed a full analysis of the available monitoring data until the stop of the machine, we concluded that some part on the head end side of the cylinder had loosened. The vibration peaks occurring at the TDC area and the increase in piston rod position at the same time were pointing to an object at the head end side of the piston that might have been stuck below the piston.

Our recommendation was to open the head end side of cylinder 4 for inspection.



Figures 15: Photo of the piston after inspection

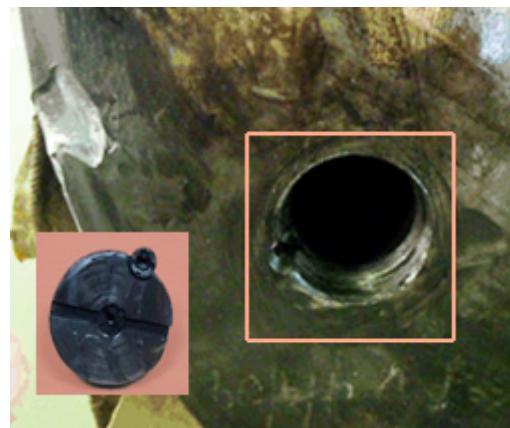


Figure 16: Close up photo of the loose blind bolt

The inspection revealed that a blind bolt of the piston had been falling into the compression chamber. The piston, the liner, the rider bands and the piston rings were damaged.

Such a loose blind bolt can further cause damage not only to the piston, piston rings and rider bands. In another case, an open piston (no correct sealing action) filled up with high explosive gas composition and probably the piston was ripped off by the highly flammable gas mixture apart.

Published on 17th Kötter Workshop 2013: Broken Piston on compressor GB-7302 A (BP Europe SE)

Abbreviations:

1st STG	-	1st stage
BDC	-	bottom dead center
CE	-	crank end
CHS	-	crosshead slide
C2	-	cylinder 2
HE	-	head end
RMS	-	root mean square
TDC	-	top dead center

Table 1: Abbreviations of shown data plots

Source:

¹⁾ Repsol Webpage



Condition Monitoring and Simulated Start Up Sequences Successfully Supported the Commissioning of a New Reciprocating Compressor Unit

by:

Patrick Ferrage

Senior Rotating Machinery Engineer

TOTAL - Refining & Chemicals - Pôle Technique de Lyon

69792 Saint-Priest Cedex, France

patrick.ferrage@total.com

**9th Conference of the EFRC
September 11th / 12th, 2014, Vienna**

Abstract:

The commissioning and smooth start up of a new reciprocating compressor is always a challenge. To avoid delays and a “start up – engineering” in the field, the compressor OEM simulated the start up sequence upfront for three operating start up cases. Because of the large capacity (20 000 m³/h at suction, 4 stages) a basic start up was impossible without disturbing the upstream unit or reaching process trip set points.

The paper describes the simulation and the implementation of control parameters into the DCS, which ensured a reliable start up for process and machinery using specific loading sequences instead of bypassing trip set points. In addition, special crank angle based diagnostics of vibration monitoring, in combination with dynamic pressure-, piston rod position- and temperature monitoring provided essential information to evaluate the condition of the reciprocating compressor as a base for operation decisions during the start up phase and normal operation. Several examples are presented. Even, the unusual e-motor shaft movement with eddy current sensors provided valuable information, e.g. the rubbing on the shaft due to the corroded and blocked e-motor end shield shaft sealing.

1 Introduction

1.1 Plant overview

TOTAL Normandy Platform is a Refinery and Petrochemicals Site based in Gonfreville nearby Le Havre in France, see Figure 1.



Figure 1: Location of TOTAL Normandy Platform

The Petrochemicals part of the Normandy Platform includes Naphtha Steam Cracker, PE, PP, PS units and one Styrene Monomer Unit (SMU) where the compressor tagged 12 K 4001, which this presentation deals with, has been installed.

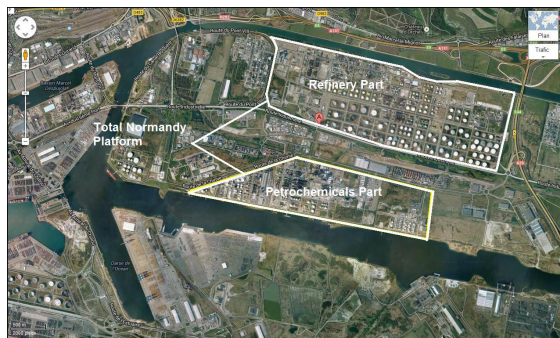


Figure 2: Overview of industrial area, Total Normandy Platform with its petrochemicals and refinery parts.

The refinery part of Total Normandy Platform has insufficient hydrogen for operation.

The Tail Gas of Styrene Monomer Unit is rich in hydrogen (90% mol, average MW is 6.5). Previously this tail gas was sent to a fuel gas network to supply boilers.

To improve the global efficiency of both sites, it was decided to purify Styrene Monomer Unit Tail Gas to extract hydrogen and send it to the refinery.

This project was the first one dealing with synergy between petrochemicals and refining activities, following the merger of refining and petrochemicals branches of TOTAL group. The scope was as follows:

- One non lubricated reciprocating compressor tagged 12 K 4001, in charge of tail gas compression to supply PSA (Pressure Swing Absorber Unit), and send pure hydrogen to refinery. Compressor shall be non lubricated since PSA does not withstand any trace of oil.

- One PSA unit (Pressure Swing Absorber unit) to purify Styrene Monomer Unit (SMU) Tail Gas and extract hydrogen.

- One hydrogen pipeline between petrochemicals site and refinery parts.

The compressor 12 K 4001 is located downstream of three tail gas compressors, non lubricated screw type, suction under vacuum and discharge pressure is suction pressure of the studied reciprocating compressor.

1.2 Reciprocating Compressor

The suction capacity is about 20 000m³/h or 6000kg/h, while the suction pressure is 1.2 bara at 40°C and discharge pressure is 35 bara. An additional side stream of pure hydrogen is coming from the steam cracker unit and injected between 3rd and 4th stage.

The compression is achieved in four stages with inter-stage coolers and separators.

The reciprocating compressor has six throws and is equipped with Free Floating Pistons (non-lubricated), 320mm stroke and five cylinders: two DA cylinders with 990mm bores for the first stage, One DA cylinder with 940mm bore for the 2nd stage, one DA cylinder with 620mm bore for the 3rd stage and one DA cylinder with 450mm bore for the 4th stage. The average linear speed is 4.00 m/s. The maximum power achievable with this crankcase is 11.5 MW at 370 rpm. The maximum allowable rod load is 825 kN (C&T). The machine is driven by a 4.2MW single bearing electrical motor at 370rpm.

The Capacity control is achieved with clearance pockets, unloading of compression chambers and bypass. Capacity steps are 50%, 70%, 76%, 80%, 87%, 93% and 100% plus two additional steps dedicated to start up sequences. Additional Step 1: 1st stage 0% all other stages 50%; Additional Step 2: 1st stage 25% all other stages 50%. The compressor includes 56 suction and discharge valves.

The main challenge with Styrene Monomer Unit Tail Gas is to avoid liquid and polymer build up (tail gas includes styrene, benzene, water, CO₂).

Condition Monitoring and Simulated Start Up Sequences Successfully Supported the Commissioning of a New Reciprocating Compressor Unit by: Patrick Ferrage, TOTAL

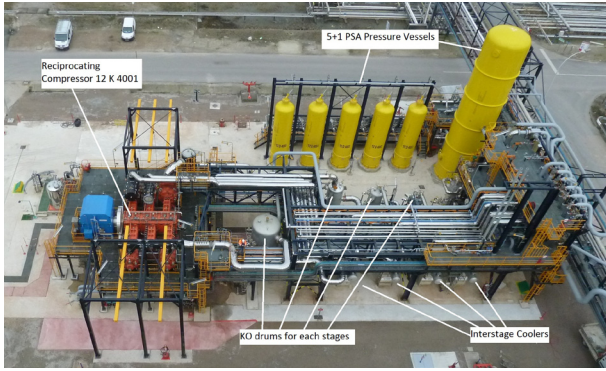


Figure 3: Compressor in operation, 5+1 PSA pressure vessels at top right hand.

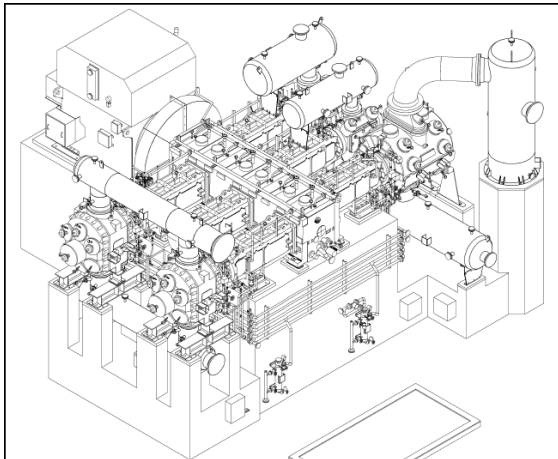
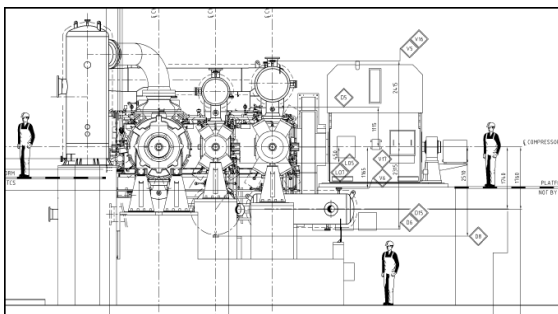


Figure 4a&b: Elevation view and 3d view of the compressor

1.3 Lay out and technical choice overview:

Project team decided to install only one compressor of 100% capacity to minimize CAPEX, and commits itself for 11 months per year availability.

With such lay out, the estimated Return On Investment has been evaluated after two years.

Implemented solutions:

The compressor is erected at the highest point of the unit to avoid/minimize any liquid ingestion and to enhance the self-draining capacity of suction piping. This leads to a high foundation and civil works. All suction pipes and suction pulsation dampeners are steam traced and insulated.

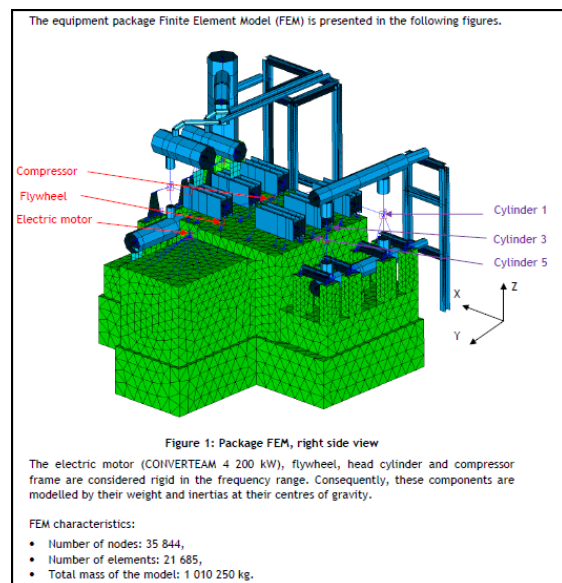
The machine is huge and no stand by spare compressor is installed, which leads to a very high level of condition monitoring. Online performance measurements and accurate diagnosis are implemented to protect the machine but also to prepare maintenance work for shutdowns to minimize down times.

1.4 Challenges during studies and commissioning:

Because of the quite high civil works (the shaft centre line is four meters above the ground level) and the soft ground (sea shore and Seine River), it was decided to implement a dynamic study to make sure that vibration levels of foundation and compressor were correct. The goal was to avoid any problems of foundation resonances.

Following ground samples, the mechanical ground characteristics have been analyzed and foundations optimized, since the first piles arrangement (11 piles of 600mm diameter) couldn't comply with the vibration target. Indeed the first resonance mode of foundations plus compressor was excited by the compressor rotation.

After the modification of diameter, quantity and location of piles (16 piles of 900mm diameter), the vibrations levels have been reduced in accordance with the EFRC document "Guidelines for Vibrations in Reciprocating Compressor Systems".



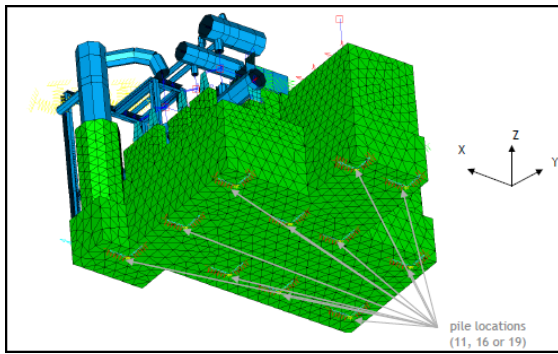


Figure 5 a&b: Extract of FEA and dynamic study to minimize foundations and compressor vibrations in operation.

The machine start up sequence was also a challenge for the following reasons:

The Styrene Monomer Unit is a quite stable unit but its most sensitive point is the discharge pressure of its tail gas compressors, which is also the suction pressure of 12 K 4001. For that reason, 12 K4001 shall be able to start without disturbing the tail gas compressors, by means of a minimum impact on suction pressure.

The compressor shall also be able to start up in a closed loop mode, running on its bypass.

Because of the high inter-stage volumes (coolers and KO drums), the Settle Out Pressure (SOP) is quite high (6.8 bara) compared with the normal inter-stage pressure. SOP defines the inter-stage pressure relief valve setting of the first interstage.

The pressure profile is as follows: 1.2 bara at suction, 3.9 bara at inter-stage 1-2, 8.5 bara at inter-stage 2-3, 18 bara at inter-stage 3-4 and 35 bara at discharge.

At last, the compressor shall be operated under nitrogen for commissioning, but also after maintenance for the following purposes:

- remove air and oxygen from compression loop before working under process
- nitrogen test run to verify if maintenance activities have been implemented correctly, before the compressor is coming back to process (easy reworks if any, since machine hasn't seen any hazardous components, no need of gas masks to perform maintenance reworks).

2 Start up Simulation

When TOTAL asked the compressor OEM for a start-up simulation, they reacted quite surprised.

After several clarification meetings with TOTAL process and operation departments to define start up sequences and cases, everybody was convinced that a start up simulation was not a “nice to have” option, but a key point to achieve a successful and smooth start up.

The first part of the challenge was how to get a smooth start up with 20.000 m³/h capacity at suction, very small hold up on suction network and upstream tail gas compressors, which don't accept any pressure increase at their discharge.

The second part of challenge was how to ensure a reliable start up under SOP without any inter-stage pressure relief valve pop up and with a more elegant manner than bypassing PSHH and or PSLI at inter-stage for a while, during first start up.

The aim was to avoid field modifications, implemented on DCS or safety PLC set points and logics during the commissioning. In many cases, these adjustments are always done in hurry and with no or minimum engineering input. Firstly for safety reasons; but also to minimize start up timeline and commissioning period.

The development of such start up sequences in DCS was also a good tool to save time during machine restart after trip or shutdown. In addition it is a comfortable and confidential instrument for operators.

Indeed, problems or failures of large machines mainly happen during transient. The automatic start up sequence is reproducible since all draining, loading sequences and safe start up conditions will be respected, whatever operation shift in charge of machine.

2.1 Start-up sequence:

All logics have been developed to enable a quick change and fine tuning of set points and time delay if any modification was required during commissioning. The operation interface is simple; operators have just to select the start up mode on DCS: “H2 under SOP”, “H2 under suction pressure” or “N2 mode”.

Each start up mode has got its own loading logic, time delay and alarm and trip set points. At the end of each start up sequence (duration is about 1200 seconds) the compressor will reach 50% load on its bypass.

After the start up sequence has been completed, operators are able to operate the machine as needed and can continue to start up the whole PSA unit.

Condition Monitoring and Simulated Start Up Sequences Successfully Supported the Commissioning of a New Reciprocating Compressor Unit by: Patrick Ferrage, TOTAL

2.1.1 Start up under SOP of 6.8 bara.

The target was to establish the normal pressure profile at all inter-stages with no PSHH and TSHH at discharge of each stage and to avoid inter-stage pressure relief valve pop up.

The loading sequence is as follows and includes six phases:

Phase 1: The first stage is fully unloaded and second, third and fourth are 50% loaded on crank end compression chambers. Bypass is 100% open. Duration is 150 seconds.

Phase 2: The bypass is closing slowly until one discharge temperature reaches 120°C (duration about 200 seconds), then the bypass remains in same position for 150 seconds to reach steady state.

Phase 3: One throw of first stage is loaded (crank end) and bypass is still in the same position. This phase lasts 150 seconds to reach steady state condition.

Phase 4: The closing of bypass is restarted, till one discharge temperature reaches 120°C, it lasts 250 seconds including 150 seconds to achieve steady state after bypass stops closing.

Phase 5: A second throw of first stage is loaded (all cylinders are 50% loaded), the bypass is still in the same position, and it lasts 150 seconds to reach steady state. The compressor runs at 50% load on its closed loop.

Phase 6: Operators have to make sure that feed line is open, than the downstream unit is ready and switches the compressor in suction pressure control mode.

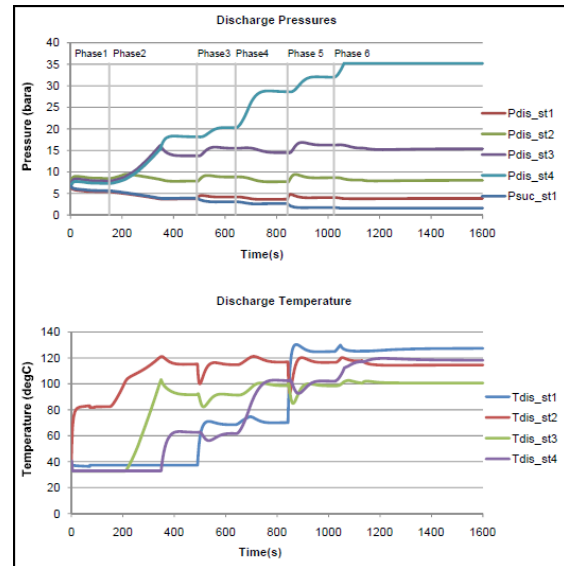


Figure 6: Calculated pressures and temperatures versus time during start up under SOP

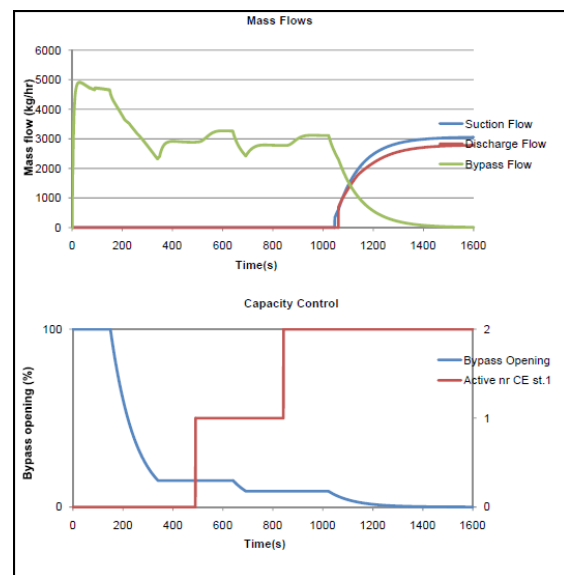


Figure 7: Calculated bypass mass flow and capacity control profile versus time during start up under SOP

2.1.2 Start up under suction pressure 1.6 bara:

During this condition, the target is to establish the normal pressure profile at all inter-stages with no PSLI at suction or TSHH at discharge of each stage. The goal is to minimize and control the process gas flow to build up a pressure profile at inter-stage since a feed flow of 1000 kg/h has a minimum impact on the tail gas compressors and doesn't disturb the Styrene Monomer Unit.

SESSION MONITORING

Condition Monitoring and Simulated Start Up Sequences Successfully Supported the Commissioning of a New Reciprocating Compressor Unit by: Patrick Ferrage, TOTAL

The loading sequence is as follows and includes six phases:

Phase 1: The first stage is 25% loaded (only one throws) and the second, third and fourth stages are 50% loaded on crank end. The bypass is 50% open and remains at 50% for all phase 1. Duration time is 150 seconds.

Phase 2: Bypass is closing slowly until one discharge temperature of 2nd, 3rd or 4th stage reaches 120°C (duration about 270 seconds), then the bypass remains in same position for 150 seconds to reach steady state.

Phase 3: A second throw of the first stage is loaded (crank end) and the bypass remains in the same position. This phase lasts 300 seconds to reach steady state.

Phase 4: The closing procedure of the bypass is restarted until the normal discharge pressure of 35 bara is reached, then the bypass remains in same position. This phase lasts for 180 seconds.

Phase 5: Steady operation with limited suction flow of 1000kg/h, with bypass in the same position.

Phase 6: Transition to operation on full suction flow. The bypass closing is restarted as soon as full feed process flow is available. When bypass is fully closed, the compressor operates at 50%.

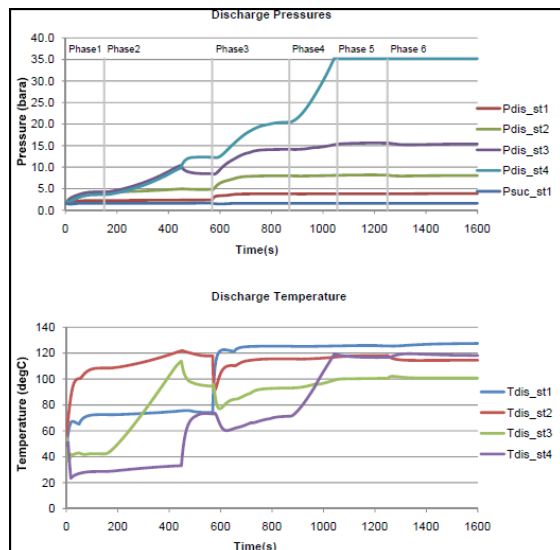


Figure 8: Calculated pressures and temperatures versus time during start up under Suction Pressure

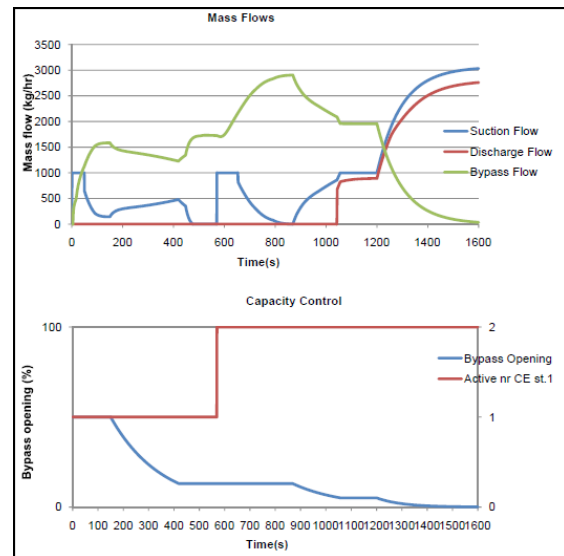


Figure 9: Calculated bypass mass flow and capacity control profile versus time during start up under Suction Pressure

2.1.3 Start up under nitrogen (SOP =4.6 bara):

The nitrogen case is different from process cases since discharge pressure is limited to 23.7 bara to limit discharge temperatures and pulsations. The start up with nitrogen is made on a closed loop mode under settle out pressure of 4.6 bara. Loop pressurization is obtained with site nitrogen network, while the machine is at standstill.

The target is to establish the normal pressure profile at all inter-stage with no PSHH at either inter-stage or TSHH at discharge of each stage and with no inter-stage pressure relief valve pop up.

The loading sequence is simple:

The compressor operates in a closed loop mode and the bypass position is open at 100%, SOP = 4.6 bara in all cylinders and loop. The start up is 100% unloaded and bypass 100% open. The loading is in accordance to N2 mode: All throws are loaded except one throw on first stage. The bypass remains 100% open and a pressure drop is achieved with 100% open valve because of the higher molecular weight of nitrogen.

Condition Monitoring and Simulated Start Up Sequences Successfully Supported the Commissioning of a New Reciprocating Compressor Unit by: Patrick Ferrage, TOTAL

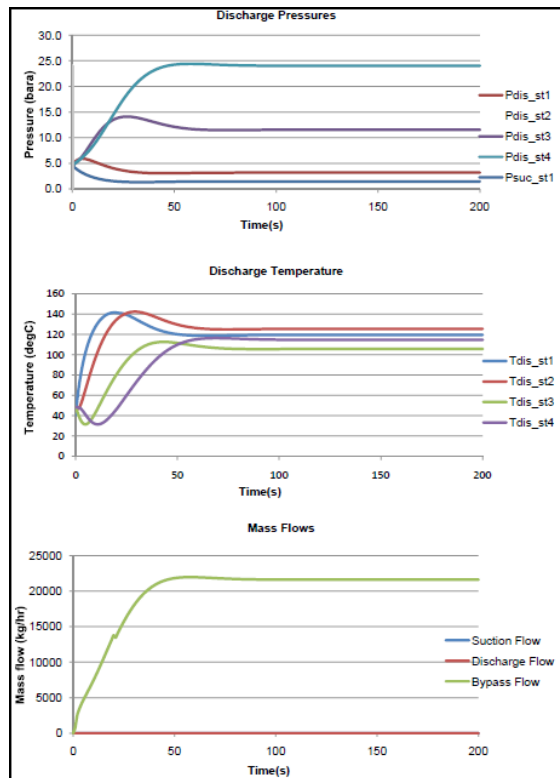


Figure 10: Calculated pressures, temperatures and mass flow versus time during start up under Nitrogen

2.1.4 Transition from nitrogen to hydrogen:

We developed a transition case, which enables operation to switch from nitrogen to process. This transition mode doesn't require complicated sequences. Alarm and trip set points in nitrogen mode shall move to set points of process mode after confirming that compressed gas contains 100% process gas (the mixture of nitrogen and process gas is sent to the flare network).

The transition from hydrogen to nitrogen was not implemented because of the limited nitrogen flow supply and complicated bypass valve control. The nitrogen purging will be done while machine is stopped, as agreed with operation team.

3 Results during commissioning:

All process parameters have been recorded during all start up phases with DCS but also with display software. It appeared that process parameters (pressures and temperatures versus time) perfectly match theoretical calculation. We noticed only one slight deviation regarding settle out pressure which was 0.3 bara lower than calculated one. This deviation

didn't affect start up sequences which didn't require any modification.

Operation team appreciates automatic start up sequences and highlighted that machine was running smooth, with very low level of vibrations at foundation, casing, cylinders and piping (thanks to dynamic study of foundation and optimized pulsation study / mechanical response). Noise level is also lower than expected during detailed engineering (due to Free Floating Piston and pipes/pulsation dampener insulation (tracing) designed with an additional "acoustical layer").

4 Online Condition Monitoring¹.

4.1 Reasons to install an Online Condition Monitoring System

TOTAL Petrochemicals committed to deliver hydrogen to the refinery network, which is located in the same industrial area. In an informal agreement, the availability of 47 weeks per year was guaranteed. Without having a spare compressor in place, this challenging goal is only achievable, when data on the machine's health is permanently collected and evaluated.

The reciprocating compressor is monitored by a continuous operational condition monitoring system. Data from vibration, dynamic pressures and temperatures are constantly collected and analysed with hard- and software thresholds to provide automated and detailed information of machine's condition. In addition special rules provide clear text messages and maintenance recommendations.

Condition based maintenance requires a detailed knowledge of machines behaviour. The health of each throw is monitored by vibration-, rod position- and temperatures measurements. Sealing elements like valves, rings and packings are assessed by the dynamic pressure measurement for each compression chamber. If leaks occur, valve cover temperature measurements and leak gas temperatures of the packing pinpoint to the exact leaking component. This enables to make precise maintenance decisions, to exchange the failed parts, only. In this case, the compressor has 56 valves. Considering the weight of the valves of about 20 kg and the mounting position, special maintenance devices are needed. Every part of the cylinder is too heavy to lift by hand. Special tools and fixtures are needed to maintain the valves. For a complete replacement of all valves, four motivated mechanics are needed, which work in two shifts for four days.

SESSION MONITORING

Condition Monitoring and Simulated Start Up Sequences Successfully Supported the Commissioning of a New Reciprocating Compressor Unit by: *Patrick Ferrage, TOTAL*

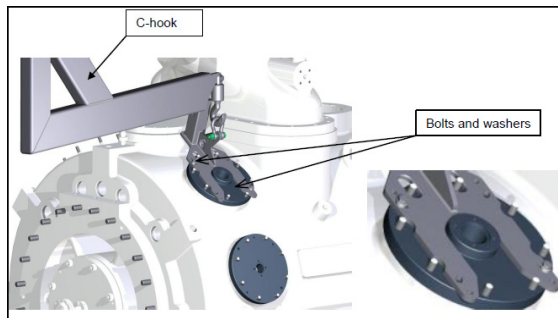


Figure 11: Lifting device for suction valves covers

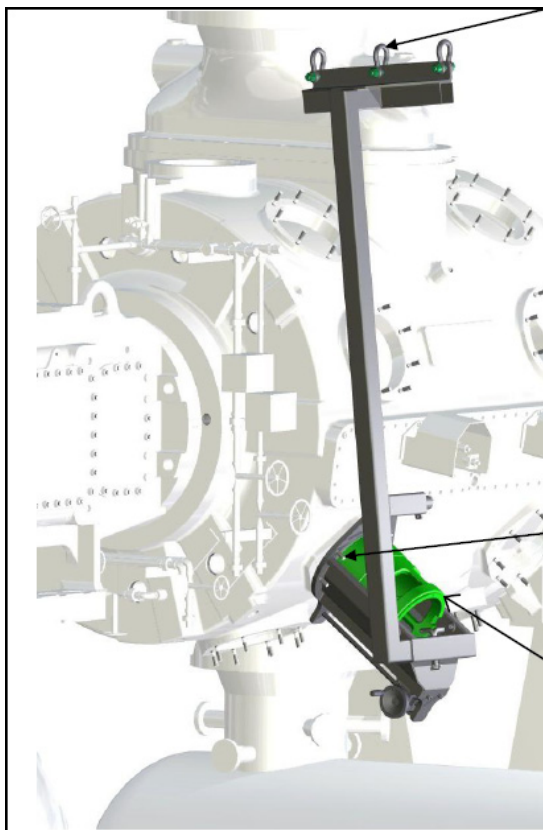


Figure 12: Device to fit the discharge valve and cage (about 50kg) lifted by a crane.

To improve reliability, availability, and safety, TOTAL Petrochemicals decided to install an online condition monitoring system to

- Protect health (of workers) and the machine and to avoid mechanical damages which result in unscheduled machinery shutdowns.
- Implement a condition based maintenance program to perform precise maintenance and component replacement to minimize downtime instead of overhauling the whole compressor
- Detect gas leaking components and failures in the running gear in an early stage

- Get information of the running behaviour of the newly installed unit to share with the compressor manufacturer and to measure that the guaranteed performance is available
- Not to operate the compressor blind during the commissioning. Visualize measured dynamic pressures and vibration, to receive detailed information about the performance
- Ensure a smooth start up and rely on measured data to implement optimizations
- Guarantee the delivery of hydrogen to the refinery.
- Increase MTBM.

4.1 Description of the Installation ¹⁾

4.1.1 Running Gear Health Monitoring

Accelerometers are mounted on the top of each crosshead slide to monitor the mechanical safety of the six throws. They detect machinery problems due to impact-type events such as loose running gear components, liquid ingestion into the cylinder, or excessive clearance in the crosshead pin bushing. Placing accelerometers over each crosshead guide provides the best method to detect machinery problems due to impact-type events.

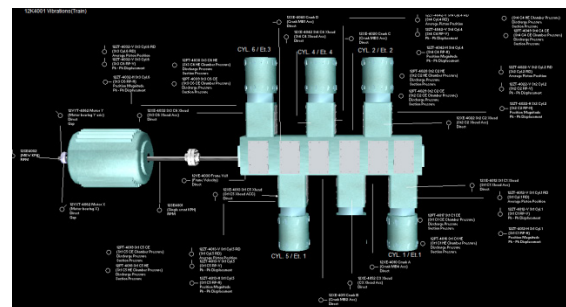


Figure 13: Overview of installed measurements

The online condition monitoring system synchronizes the vibration signals with crankshaft rotation to associate vibration peaks to the piston position along the stroke. Dynamic bands e.g. in the rod reversal area monitor the impulses continuously and therefore provide detailed information of the condition of the running gear components for each throw.

Condition Monitoring and Simulated Start Up Sequences Successfully Supported the Commissioning of a New Reciprocating Compressor Unit by: Patrick Ferrage, TOTAL

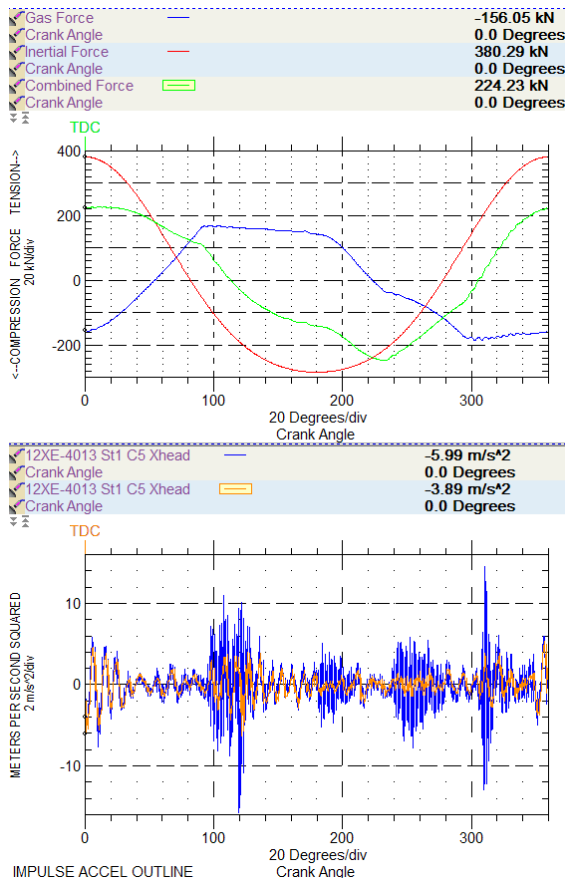


Figure 14: Forces and Crosshead acceleration over one revolution

Two Frame velocity measurements on the side of the frame monitor the response of the oscillating system to the main forces and moments that are occurring on the balanced-opposed compressors. Velocity measurements are ideal for detecting machinery problems on reciprocating compressors where rotation-related vibration is transmitted to the compressor frame

An increase in frame vibration can indicate problems such as imbalance due to unusual pressure differential or inertial unbalance, looseness in the foundation attachment (such as deteriorating grout or shims) and high moments caused by excessive rod load.

The forces are transmitted through the bearing to the frame, resulting in frame vibration at one or two times machine running speed and all whole multiples of running speed due to gas forces.

Excessive amplitudes at these frequencies indicate mechanical or operational problems and will result in alarming from the condition monitoring system in an early stage.

4.1.2 Sealing Element Health Monitoring

The most effective way of determining the overall health of a reciprocating gas compressor is by measuring the cylinder pressure profile. Online access to the internal pressure for each compressor cylinder chamber enables continuous monitoring of cylinder pressures, compression ratios, peak rod loads, and rod reversal. This provides valuable information on the condition of suction valves, discharge valves, piston rings and packing glands. With the help of the PV diagram analysis, the condition / functionality of capacity control devices, such as suction valve unloaders, clearance pockets and stepless unloaders can be assessed.

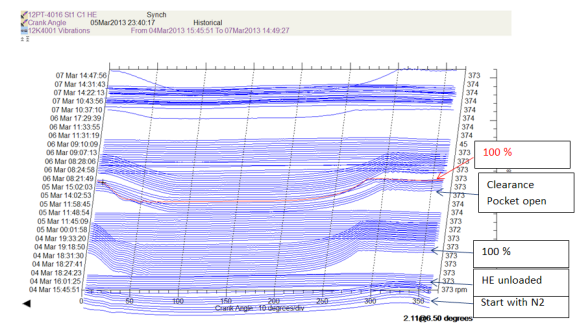


Figure 15: Waterfall diagram of stage 1 head end compression chamber during several load steps

Suction and discharge valves typically represent the most significant element of the overall maintenance costs. Faulty valves reduce the efficiency of the compressor. By recompressing the same gas, a leaky valve becomes hotter than normal, causing the valve cover plate temperature to increase.

Leaking piston rings will cause the temperature of the entire cylinder to increase through the reworking of gas between each side of the piston. Therefore, detecting changes in absolute valve temperature is also important. If a temperature increase for all valves in the same cylinder is not due to a process change or lubrication problem, it is most likely due to piston ring leakage. Both intake and discharge valves at the head end and crank end will show an increase in temperature due to piston ring leakage.

In addition to the dynamic pressure measurement for each compression chamber, the suction- and discharge valve cover temperature are measured and monitored to pinpoint to a particular valve in distress. Equipped with 56 valves, the added value becomes visible.

Continuous monitoring of rod packing temperature provides useful information on developing problems related to the packing, including excessive wear, insufficient cooling, and inadequate lubrication.

SESSION MONITORING

Condition Monitoring and Simulated Start Up Sequences Successfully Supported the Commissioning of a New Reciprocating Compressor Unit by: Patrick Ferrage, TOTAL

Combined (inertia and gas) rod loads (refer to Figure 14) calculated at the crosshead provide information about the lubrication condition of the crosshead pin. Insufficient reversal or excessive rod load can be identified and corrected before costly running gear damage occurs.

4.1.3 Piston Rod Health Monitoring

Horizontal and vertical proximity probes, mounted in an orthogonal arrangement, observe the piston rod and provide information on rod bow and rider band wear for each throw. Continuous monitoring gives maximum magnitude and direction of rod movement along with the crank angle at which the maximum occurs. Because rod motion is bounded by mechanical clearances between crosshead / crosshead guide and rider bands / cylinder bore – excessive motion can indicate worn components as rider bands, piston rings, packing rings, crosshead slipper. The source of movement can be identified, enabling the proactive scheduling of maintenance for rider band replacement or crosshead repair.

4.1.4 Temperature Monitoring

Measuring temperatures and correlating them with other process variables can assist in determining the overall condition of the compressor. They indicate problems related to fluid film bearings, including overload, bearing fatigue, or insufficient lubrication. At this reciprocating compressor, the main bearings temperatures and crosshead shoe temperatures are measured by thermocouples. In addition, the big end- and small end bearing temperatures of the connecting rod are captured by a radar-based wireless system.

4.1.5 Timing / Keyphasor® reference

For reciprocating compressor diagnostics it is essential to know the exact crank angle position of each piston along the stroke. This is provided by a proximity probe observing a multi-toothed wheel on the crankshaft. Synchronization every 30 degrees of rotation in addition to a once-per turn reference allows measurements such as rod position, crosshead acceleration and cylinder pressure to be correlated with crank angle measurement with extra accuracy.

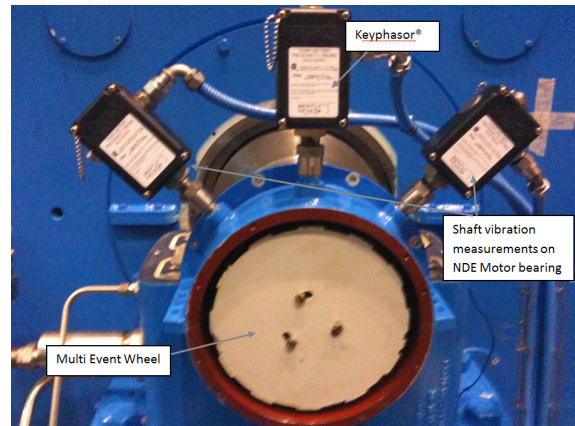


Figure 16: Multi Event Wheel mounted on the NDE shaft of the motor

4.2 Cases during start up

During the first start up with nitrogen, the unit was tripped automatically due to high discharge gas temperatures at both cylinders of the 1st stage head end compression chambers.

However, the nitrogen operating condition was also part of the simulation, doubts came up. During the start-up sequence, both head end compression chambers are unloaded by suction valve unloaders on each of the three suction valves per compression chamber.

A closer look to the dynamic pressure measurements delivered the reasons. Even when the head end compression chamber is unloaded and the gas is usually recirculating, pressure was build up from 0,4 bar g to 1,6 bar g (discharge pressure at 1,9 barg), refer to figure 17.

In addition a vertical peak to peak movement of 2200 μm of the Free Floating Piston was recognized. It seems that the operation of the Free Floating Piston is directly linked to the delta pressure of both compression chambers.

Condition Monitoring and Simulated Start Up Sequences Successfully Supported the Commissioning of a New Reciprocating Compressor Unit by: Patrick Ferrage, TOTAL

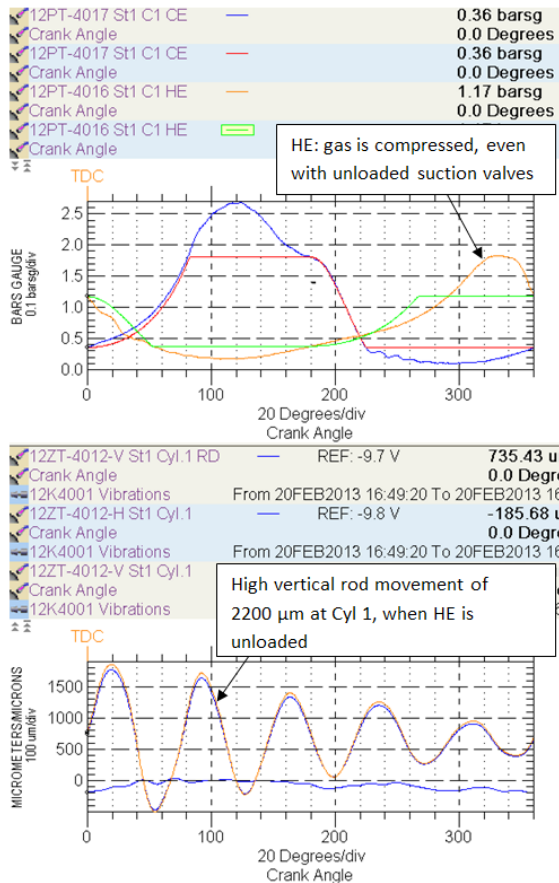


Figure 17: Crank angle based signals of dynamic pressures and piston rod movement of cylinder 1

To proceed with the test run, the decision was made to dismantle two suction valves on that head end compression chamber to avoid overheating of the unloaded suction valves during operation under nitrogen. Since the valves have been designed for hydrogen service the high overshooting of 0,9 bar g during discharge and high discharge valve losses are remarkable during nitrogen operation.

The results are visible in the next figure:

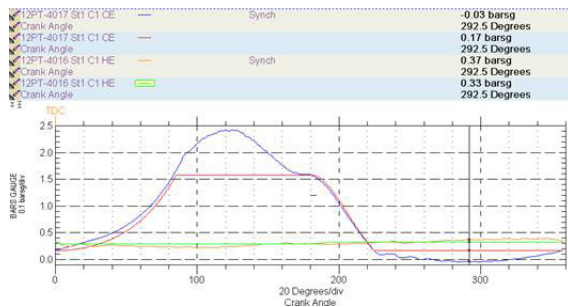


Figure 18: Crank angle based signals of dynamic pressures after two suction valves were removed

It was also noticed, that the correct unloading had an impact on the vertical piston movement. It operated

in a normal way of approx. 500 µm peak to peak.

In the meantime, the suction valve unloading system was inspected. It was recognized, that one stem of the unloader was too short, that means it was not able to unload the suction valve completely, when unloading was requested. In consequence, the length of the stem was adjusted.

Also during the next run with Nitrogen, the compressor unit was tripped. At that time, high shaft vibration, on the NDE motor bearing appeared 10 minutes after starting up.

Two orthogonal installed eddy current probes measure the radial shaft vibration to monitor the relative shaft movement inside the clearance of the motor NDE bearing. This is a well-known analysis for high speed centrifugal compressors, but a quite unusual measurement for reciprocating compressors.

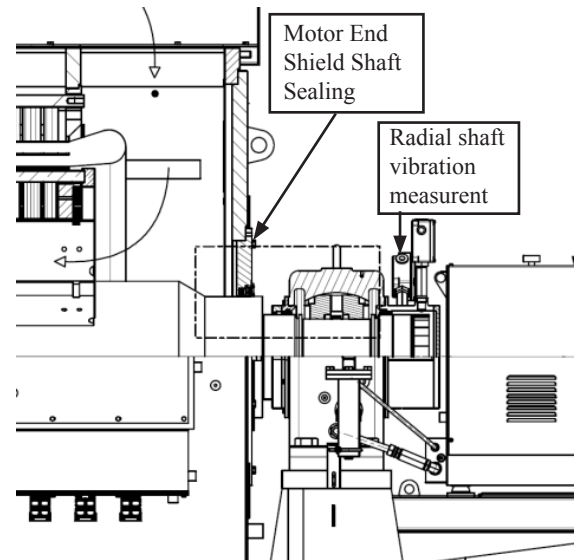


Figure 19: Sectional drawing displaying area of NDE motor bearing

The motor sealing assembly was removed and found in a corroded condition. The three sealing rings were blocked with rust and grease. Radial scratches on the motor shaft indicated a glancing with the rings, which caused shaft vibration up to 140 µm peak to peak, refer to Figure 20.

The rubbing of the motor shaft sealing caused a hotspot and true 1X unbalance vibration components.

To prove the cause, the Commissioning Engineers decided a non-hazardous test run with nitrogen and without the sealing element. A direct vibration level below 30 µm peak to peak confirmed the problem, as displayed in the trend at 16:00h.

SESSION MONITORING

Condition Monitoring and Simulated Start Up Sequences Successfully Supported the Commissioning of a New Reciprocating Compressor Unit by: *Patrick Ferrage, TOTAL*

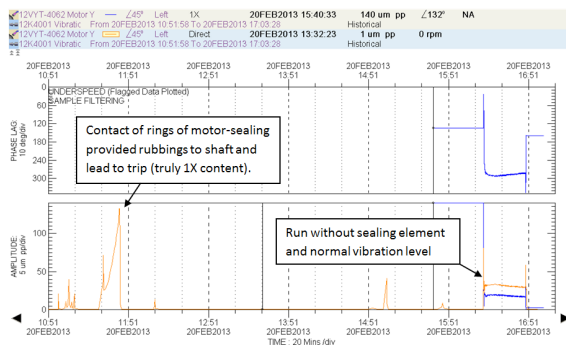


Figure 20: Rubbing of e-motor shaft sealing caused imbalance, detected by radial shaft vibration measurements on NDE Motor bearing, confirmation by running without sealing

The rings of the sealing and the bore were cleaned and smoothed with glass paper to avoid any constraint of the rings at operation. During assembly, it was found out, that the pin, which holds the stack of carbon rings in place to avoid rotation, was missing. In consequence, the whole stack was rotating.



Figure 21: Rusty ring of motor end shaft sealing was found

After fixing the initial problems, the compressor was ready for the first hydrogen run at low capacity. The vibration and piston rod movement were on a low level without attracting attention, but the discharge temperatures and valve losses were recognized higher than predicted.

The valve plate lifting clearances were checked at the spare valves from stock and compared with the drawings. It was found out, that the drawings were correct, but the valves not. The valves have been machined in accordance to the previous revision of the drawing.

The valve manufacturer collected the spare valves to increase the lift by adding a shim, to be in accordance with the drawings and engineering. With correct lift, performance was as predicted.

12PT-4039 St3 C6 CE

Discharge Volumetric Efficiency	50.5 %
Suction Volumetric Efficiency	85.4 %
Indicated Horse Power	320 kW
Adiabatic Discharge Temp	96.0 deg C
Discharge Capacity	12245 m ³ /h
Suction Capacity	12324 m ³ /h
Median Capacity	12284 m ³ /h
Adiabatic Median Capacity	12351 m ³ /h
Flow Balance	1.01
Adiabatic Flow Balance	1.00
Power / Median Capacity Ratio	26.0 w/m ³ /h
Indicated Clearance Volume	21.0
Discharge Power Loss	10.3 kW
Suction Power Loss	6.06 kW
Suction Temperature	22.0 deg C
Discharge Temperature	100 deg C
Suction Pressure	6.15 barg
Discharge Pressure	14.2 barg

Figure 22: Performance variables from pressure measurements are monitored and help to optimize the efficiency of the machine.

5 Conclusion

Since the commissioning of the reciprocating compressor, the project department received excellent feedback of the running behaviour and comfortable start-up procedure.

The operation team is happy with their new compressor, which is already a success from engineering point of view.

The simulated start up procedure ensured the save and fast commissioning of the unit since field modifications on DCS and safety PLC, which are usually implemented in a hurry and mostly with minor engineering have been avoided.

The development of the start up sequences was also a good instrument to improve availability and minimize down time with laborious and tricky start up procedures.

During commissioning, the online condition monitoring system helped to detect and fix problems quickly and will support to anticipate optimized maintenance turnaround schedules.

For more than 8000 h, data from vibration, dynamic pressures and temperatures are continuously collected and analysed with hard and software thresholds to guarantee safe operation and to provide automated and detailed information of machine's condition.

Condition Monitoring and Simulated Start Up Sequences Successfully Supported the Commissioning of a New Reciprocating Compressor Unit *by: Patrick Ferrage, TOTAL*

The next step is to implement a remote connection for TOTAL's technical centre and for the monitoring system OEM.

To summarize, the key points of this successful project were:

- Open minded people and discussion between technical people (OEM, project and operation) within a short communication network.
- Capability to listen to each other and understand the constraints of each others.
- Willingness of OEM to learn and understand the process to get perfect machine integration into process.
- Willingness of TOTAL operation and process team to learn and understand the operation of the reciprocating compressor and to adapt the process to compressor's constraints and to optimize operation.

TOTAL would like to thank again the compressor and monitoring system OEM for their collaboration to realize this successful project, which included the opportunity to learn from all participants.

References

¹ According to GE Bently Nevada Best Practices for API 618 reciprocating compressors.

9th Conference of the EFRC September 11th / 12th, 2014, Vienna

**Genuine New Concept for a Zero-Emission Packing
for Reciprocating Compressors** -59-
by: Tino Lindner-Silwester, Christian Hold, HOERBIGER

Eliminating Gas Leakage with a Novel Rod Sealing Solution -65-
by Johan Klinga, Öresundskraft AB

**Best Practice for Efficiency and Emissions Upgrades of a
Gas Gathering Compressor** -70-
by: Robbert Pol, Nederlandse Aardolie Maatschappij B.V.



EUROPEAN FORUM
for RECIPROCATING
COMPRESSORS

SESSION SEALING / WEAR 1



Genuine New Concept for a Zero-Emission Packing for Reciprocating Compressors

by:

Tino Lindner-Silwester, Christian Hold
Research & Development, Global Product Manager R&P
HOERBIGER Ventilwerke GmbH & Co KG
Vienna, Austria

tino.lindner-silwester@hoerbiger.com, christian.hold@hoerbiger.com

9th Conference of the EFRC
September 11th / 12th, 2014, Vienna

Abstract:

The piston rod sealing system is one of the key factors determining the efficiency and reliability of a reciprocating compressor. In a conventional compressor packing, no matter how elaborate its design, there will always be a certain amount of leakage. The magnitude of this leakage is affected by a variety of different factors such as ring design, ring material and manufacturing tolerances, and under certain conditions – such as high ring wear or pressurized standstill – it may exceed tolerable limits.

Especially in applications with low leakage requirements, efforts made to prevent any loss of gas to the atmosphere may be significant; they include purged distance pieces, pressurized crank cases, gas recovery equipment and additional static seals. A leak-free packing would be of great benefit in such applications, and as greenhouse gas emissions have gained public attention in recent years the demand for such a solution has grown.

This paper presents an entirely new piston rod sealing concept that is inherently leak-free under both dynamic and static conditions. Besides ensuring zero leakage, this system offers additional advantages. It does not require a packing cooling system, and it allows packing condition to be monitored continuously. The system has demonstrated high performance not only in the lab but also in the field. This technology has the potential to eliminate one of the major sources of emissions from compressor stations and to keep reciprocating compressors the top choice for flexible, environmentally sound, and efficient compression.

1 Introduction

The reciprocating compressor is a workhorse of the energy industry, with decades of proven reliability. However, the trend towards high standards of efficiency and environmental friendliness poses a challenge to the performance-determining components of reciprocating compressors, particularly the piston rod sealing system.

Despite recent progress in the sealing efficiency of pressure packings (e.g. [1]), a certain amount of process gas leakage past the packing sealing elements is inevitable. Additional efforts thus have to be made to reduce process gas emissions to the atmosphere. In applications where the gas is kept pressurized while the compressor is stopped, an additional static sealing system, usually pneumatically activated, is needed.

All these efforts required to ensure environmental friendliness (greenhouse gas emissions, hazardous gases) and economic operation (cost of lost process gas, cost of purge gas) could be avoided if the piston rod sealing system were leakage-free. This paper presents a genuinely new leakage-free sealing system that is already successfully running in the field.

2 The new leak-free packing principle

The basic idea behind the new packing system is simple. A pressurized volume of oil, referred to henceforth as the oil barrier, surrounds the reciprocating rod and is sealed by specially designed oil seal rings “1” and “2” (Figure 1). This barrier prevents pressurized process gas from leaking along the rod as long as the oil pressure $p_{oilbarrier}$ exceeds the process gas pressure p_{gas} .

At first sight this approach closely resembles the concept of purging a conventional pressure packing. There is a significant difference, however, which arises from the much higher dynamic viscosity of oil as compared to gases. The new leak-free packing takes advantage of this difference.

2.1 Difference in sealing characteristics between oil and gases

Suppose a gas, say nitrogen, were used as the barrier medium instead of oil in Figure 1. In this case there would also be no leakage of process gas past this “gas barrier”. However, the amount of barrier gas leaking into both the cylinder and the distance piece would be orders of magnitude higher than the corresponding amount of oil.

This difference is partly due to the much higher

resistance of oil compared to gases when flowing through narrow gaps. There is also, however, another effect which occurs only with oil and not with gases: the reciprocating motion of the rod makes it possible to “pump” oil, after it has leaked out of the barrier, back into the barrier against the counteracting pressure gradient, i.e. from lower (p_{gas} or $p_{ambient}$) to higher pressure ($p_{oilbarrier}$).¹

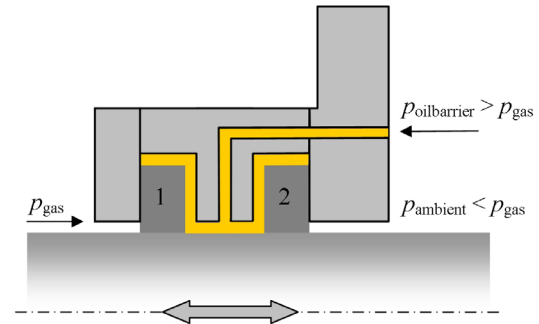


Figure 1: The new packing design relies on a pressurized volume of oil held between two sealing rings.

2.2 Oil film dynamics

The flow of fluids, be they gases or liquids, is governed by the Navier-Stokes equation. This equation expresses the balance between inertia, pressure forces, and viscous forces. For the case of interest here, i.e. the flow of oil through a narrow gap, the thin-film approximation applies. The high viscosity of the oil allows us to neglect the inertia terms, so that the Navier-Stokes equation reduces to a linear balance between pressure and viscous forces².

Under such conditions, any lubrication flow can then be regarded as a combination of three fundamental cases [2]: a) shear flow between two plane parallel surfaces in relative tangential motion; b) pressure-driven flow between stationary parallel surfaces; and c) the flow resulting from parallel surfaces approaching each other with no tangential motion (Figure 2). The continuity equation, together with the appropriate boundary conditions, then determines how these three fundamental flow cases can be combined to describe any particular local flow in a narrow gap bounded by non-parallel walls.

¹ This effect [3] is well known and is made use of by hydraulic seals. Elastomeric hydraulic seals, however, are subject to far lower load collectives (“ $p\nu$ ” load where p and ν stand for the (differential) pressure to be sealed and the mean rod speed, respectively), so that hydraulic seals cannot be used for the system presented in this paper. Besides, for hydraulic seals to operate satisfactorily, the rod has to be guided very precisely since these seals are not of the “free-floating” type.

² This limiting case is governed by an equation referred to as the Reynolds equation in honour of O. Reynolds.

Genuine New Concept for a Zero-Emission Packing for Reciprocating Compressors

by: Tino Lindner-Silwester, Christian Hold, HOERBIGER

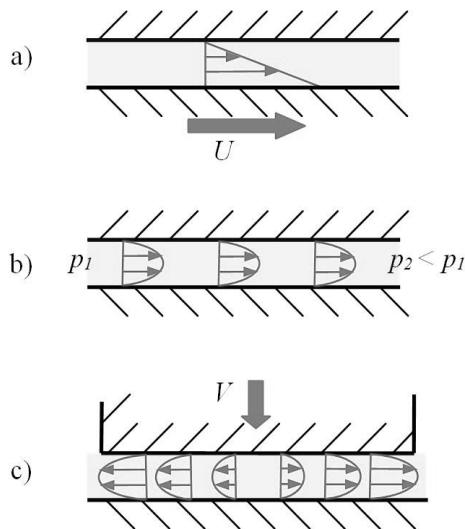


Figure 2: Fundamental lubrication flow cases: a) Couette shear flow, b) pressure-driven Poiseuille flow, c) squeezing flow.

A classic example showing the combined effects of a) and b) is when a lubricant is pulled by a moving surface into a narrowing, stationary, wedge-shaped space (Figure 3). Continuity dictates that the mean flow velocity u_{mean} (i.e. the velocity averaged over the local film height) has to increase in the x -direction. Such an increase is brought about by a build-up of hydrodynamic pressure $p(x)$. Upstream of the pressure maximum, u_{mean} is smaller than $U/2$; downstream of the maximum, u_{mean} is higher than $U/2$. At the pressure maximum the local pressure gradient vanishes and the velocity profile is of the Couette type, so that $u_{\text{mean}} = U/2$.

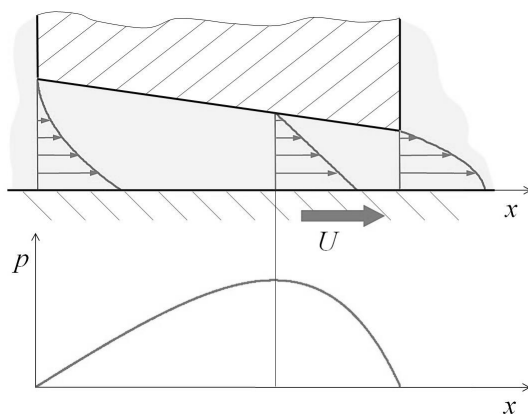


Figure 3: Build-up of hydrodynamic pressure $p(x)$ (bottom) arising as a surface moving at velocity U pulls oil into a convergent gap (top).

1.1 Elastohydrodynamic effects

The lubricating effect described above is closely related to the potential to establish a build-up of hydro-

dynamic pressure when oil is forced into a narrowing gap by a moving surface. This pressure build-up may be large enough to deform the surrounding solid components, depending on the stiffness of the materials concerned.

As long as any deformations have no noticeable effect on the hydrodynamic pressure distribution, we can regard the containing surfaces as rigid. But if elastic deformations significantly affect the film dynamics, elastohydrodynamic effects come into play. In this case we have to solve not only the Reynolds equation but also simultaneously for the elastic response of the solids to the hydrodynamic pressure distribution.³

These elastohydrodynamic effects make it possible to recover oil lost during the outstroke when the rod drags oil out of the oil barrier. To show how this comes about we will consider a simplified model in which the rod speed stays constant during both the outstroke and the instroke, so that unsteady squeezing effects can be disregarded⁴.

The left-hand side of Figure 4 shows what is going on during the outstroke in the lubrication gap formed between the piston rod and the oil seal ring (we are looking at the ring that seals the oil barrier against atmosphere, i.e. ring “2” in Figure 1). The oil film pressure first rises from the barrier pressure level at $x = 0$ to a certain peak pressure at $x = x_{\text{out}}^*$. This pressure increase arises from the existence of a convergent gap during the outstroke; this convergent gap is in turn created by the hydrodynamic pressure build-up, both effects being mutually dependent in a way that is determined by the geometry and material of the seal ring. Downstream of the location x_{out}^* , the pressure drops until it reaches the oil vapour pressure and cavitation sets in. The flow velocity profile is of the Couette type at the location of the peak pressure $x = x_{\text{out}}^*$, so the volumetric leakage rate per unit circumference during the outstroke is given by $(U/2)h_{\text{out}}^*$, where h_{out}^* denotes the film thickness at the location of the peak pressure.

³ The deformations caused by the shear stresses are usually negligible, and the viscous normal stresses are in any case small compared to the pressure forces in the thin-film limit.

⁴ These squeezing effects dominate at bottom and top dead centre, where the rod reverses direction, and vanish when the rod is at its maximum speed, i.e. when the acceleration of the rod is zero. A complete analysis of the problem needs to take this variability into account [3].

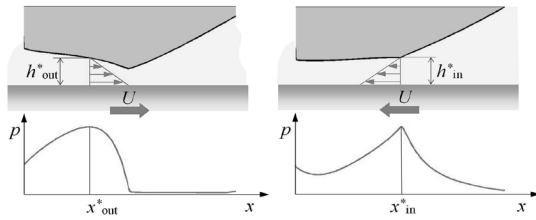


Figure 4: Velocity profile in the sealing gap between the oil seal ring and the piston rod, and the corresponding pressure distribution, during the outstroke (left) and instroke (right), respectively.

Oil therefore leaks out during the outstroke, and at the end of the stroke the piston rod is covered with a thin film of oil downstream of the seal ring. As the right-hand side of Figure 4 shows, however, there is also a pressure build-up during the instroke; the peak pressure is of the same order of magnitude as during the outstroke, and the film thickness h_{in}^* is virtually the same as h_{out}^* . As a result, virtually all (>99%) of the oil that leaks out during the outstroke is dragged back into the oil barrier during the instroke. This effect not only keeps oil losses to an absolute minimum, but also allows the oil seal rings to operate virtually without wear.

3 System layout and configuration

3.1 Packing case

The system comprises in essence a packing case (Figure 5) equipped with several sealing elements, and a hydraulic unit (Figure 6) supplying pressurized oil to establish the oil barrier. The packing closely resembles a conventional pressure packing, consisting of a series (usually two or three) of conventional single-acting packing rings (1), a buffer volume (2), oil seal rings (3a), (3b), (3c), and a wiper ring (4). All rings are floating, i.e. they are free to move with lateral movements of the piston rod.

The conventional packing rings (1) ensure that while the compressor is operating the gas in the buffer volume (2) remains at suction pressure p_s . These rings need only a modest leakage performance to effectively damp the dynamic pressure component $p_{cyl} - p_s$ (p_{cyl} denotes the varying cylinder pressure). Even considerably worn rings will not give rise to noticeable pressure fluctuations in the buffer volume. Any small rise in buffer volume pressure above the suction pressure, induced by blow-by leakage past the rings (1) during the compression stroke, immediately falls back to zero during the suction stroke owing to the single-acting nature of the rings. Besides, the larger the buffer volume, the smaller the pressure increase caused by a certain amount of gas leaking into it.

The combination of ring set (1) and buffer volume (2) thus allows the oil barrier pressure to be set lower than it would be if these components were not used. Instead of having to keep the barrier pressure above the discharge pressure, it is sufficient to stay above the suction pressure. This in turn reduces the mechanical loading on the oil seal rings.

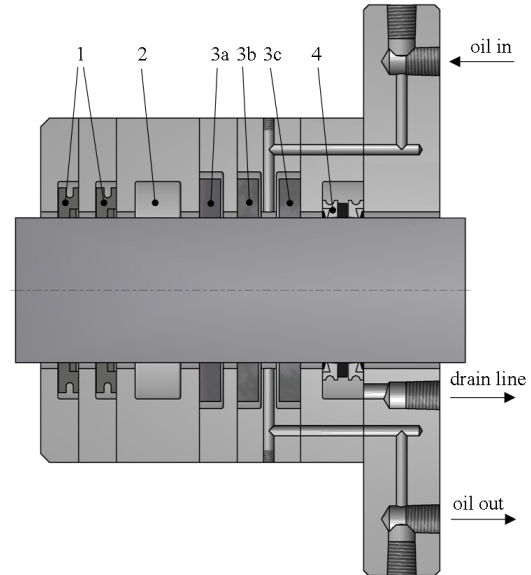


Figure 5: Section through a zero-emission packing.

The oil barrier is sealed by the oil seal rings (3b) and (3c). Any remaining oil leaking past the oil seal ring (3c) in the crankcase direction is wiped off the rod by the oil wiper (4) and recovered via a drain line connected back to the tank. The specific wiper arrangement depends on the compressor configuration, such as whether a distance piece is used. An additional oil seal ring (3a) helps to minimize oil leakage into the cylinder over the whole lifetime of the seal rings.

3.2 Hydraulic oil supply unit

A specially designed hydraulic unit supplies oil at a defined flowrate and pressure (Figure 6). The oil circulates through the channels in the oil barrier, where it picks up the frictional heat released by the oil seal rings. Oil returning to the hydraulic unit is cooled by an integral heat exchanger, so no additional packing cooling is required.

Depending on rod size, speed, and process gas pressure, one hydraulic unit can supply up to six packing cases. Great emphasis has been placed on reliability in the design and construction of the hydraulic unit. The entire system is approved for explosive environments.

Genuine New Concept for a Zero-Emission Packing for Reciprocating Compressors

by: Tino Lindner-Silwester, Christian Hold, HOERBIGER



Figure 6: Hydraulic oil supply unit.

Apart from this basic functionality, the hydraulic unit offers additional optional features such as the possibility to switch to a higher oil pressure during operation. This feature can be important in applications where the compressor is kept pressurized during standstill periods. In such cases, leaking discharge valves can allow cylinder pressures to rise until they reach the full discharge pressure, so the inevitable leakage past the seal rings (1) will eventually raise the buffer volume pressure up to the cylinder pressure. This scenario can be managed by automatically switching to a higher oil pressure during periods of pressurized standstill. The increased oil pressure stops any gas passing the oil barrier, while the resulting increased load on the oil seal rings is of no relevance when the piston rod is stationary.

3.3 Malfunction mode

The rate of oil loss is continuously monitored. If it exceeds tolerable limits, or if there is a sudden loss of hydraulic pressure (for instance from a pump failure or power blackout), the system switches automatically into malfunction mode (Figure 7, lower part), which needs no external power supply. In malfunction mode, there is no longer an oil barrier and the oil supply line acts as a vent line. The buffer volume is at vent pressure, and oil seal ring 3c acts as a vent seal. The process gas is entirely sealed by the conventional packing rings (1), with any leakage directed to the vent line. Thus the whole system acts in this case as a conventional vented pressure packing. For applications involving hazardous gases, where a purge system would be used in conjunction with conventional pressure packings, it is possible to purge the system automatically when (and only when) it enters malfunction mode.

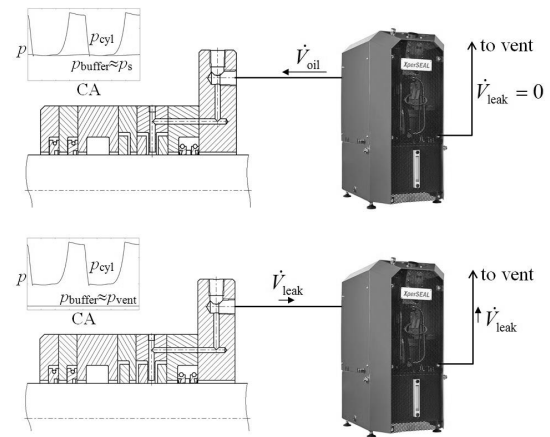


Figure 7: Normal operation (top) and malfunction mode (bottom). In malfunction mode the system operates as a conventional vented packing.

4 Test results and field experience

The system performance is determined mainly by the performance of the oil seal rings. The requirements to be met by these rings (and of course the complete system) were defined at the beginning of the development phase:

- oil loss rate of system no higher than lube rate of conventional packing;
- stable operation under huge variety of different operating conditions (pressure level, temperature level, rod size, speed) including multiple start/stops;
- lifetime of at least 8000 hours.

Even at the earliest stages of development it became clear that these requirements could only be fulfilled by using a high-performance tribological polymer grade. To derive the optimum ring geometry, a comprehensive simulation model was developed to determine the effects of ring geometry and operating conditions on the behaviour of the lubrication film. The theoretical findings were checked on a specially designed test rig and long-term tests were conducted on both this test rig and an in-house test compressor. After thousands of hours of successful operation in the lab, the field test phase began.

4.1 CNG refilling station

The first system was installed in the field in February 2012 at a CNG bus refilling station operated by Öresundskraft in Helsingborg, Sweden. In this application, natural gas is compressed in four stages (the second and third of which are sealed by a pressure packing) from 4 bar to 250 bar.

Genuine New Concept for a Zero-Emission Packing for Reciprocating Compressors

by: Tino Lindner-Silwester, Christian Hold, HOERBIGER

The compressor speed is 1400 rpm, with a 3-inch stroke and a rod diameter of 1½ inch. Depending on the demand, the compressor is started and stopped several times a day. The compressor is lubricated, yet bus engines have severe problems with oil-contaminated gas. Annual gas leakage reports are mandatory. The compressor operator therefore had two aims: to cut overall oil consumption and to eliminate vent gas leakage.

The system has lived up to its promise, to the utmost satisfaction of the customer. The system has been running successfully since start-up without any issues, and an inspection after one year of operation showed it to be in good condition.

4.2 Offshore gas compression

The new sealing system has also been installed on a gas compression unit at NAM, Den Helder. The two-stage/two-cylinder machine compresses gas supplied from a source offshore from 13 bar to 62 bar. The compressor speed is 510 rpm, with a stroke of 125 mm and a rod diameter of 60 mm. The primary reason for equipping this compressor with the new seal system is to eliminate vent gas leakage; this reduces operating costs and improves the environmental performance of the process by eliminating benzene emissions. The system is working as expected.

4.3 Propane service

The third field application, on a propane refrigeration compressor in Egypt, is characterized by the high cost of lost gas. The compressor has a high leakage rate (26 tonnes per year), propane is a valuable product, and the remote location in the Western Desert means that transport costs are high. The propane is compressed in two stages from 4 bar to 18 bar. The compressor speed is 750 rpm, the stroke is 5 inch and the rod diameter is 2¼ inch. The customer is very impressed with the system which reduces operating costs by more than US\$100,000 a year.

5 Conclusions

The growing energy hunger of the world calls for environmentally friendly solutions. Natural gas, as a clean fuel that can be found almost everywhere, will play an important role in the future as an attractive alternative to oil. However, with more than 20 times the global warming potential of carbon dioxide, fugitive emissions of natural gas from compression equipment have to be kept to an absolute minimum.

Of course, the need to prevent fugitive emissions from compression equipment is not restricted to natural gas. Hazardous process gases, and the need to li-

mit the cost of environmental compliance or the value of lost gas, are other common reasons to require low leakage. With roughly a third of the fugitive emissions from reciprocating compressors originating from piston rod seals, recent years have seen a growing demand for leak-free pressure packings.

This paper has set out a new approach to a completely leak-free packing solution. The system is based on a pressurized oil barrier which prevents any process gas leakage. In sealing this oil barrier, use is made of elasto-hydrodynamic effects. The special design of the oil seal rings which contain the oil barrier exploits the elasto-hydrodynamic performance to the maximum and allows the system to operate with minimum wear and oil losses.

Apart from being leakage-free, the new system offers additional advantages over conventional pressure packings. These include:

- no need for a separate packing cooling system;
- no need for an additional static sealing system in applications where the compressor is kept pressurized during standstill;
- ability to incorporate condition monitoring of the sealing system; and
- no purge gas consumption.

The system has been exhaustively tested in the lab and has proved its great potential in several field installations.

6 References

- ¹ Lindner-Silwester, T. and Hold, C.: "The BCD packing ring – a new high performance design". 7th EFRC conference (2010), 112–119.
- ² Reynolds, O.: "On the theory of lubrication". *Philosophical Transactions of the Royal Society of London* (1886), 157–234.
- ³ Kotesovec, B. and Steinrück, H.: "Zero Leakage Sealings for Reciprocating Compressors". *Proc. Appl. Math. Mech.*, 10 (2010): 375–376. doi: 10.1002/pamm.201010180



Eliminating Gas Leakage with a Novel Rod Sealing Solution

by

Johan Klinga

Öresundskraft AB

251 06 Helsingborg, Sweden

johan.klinga@oresundskraft.se

9th EFRC Conference

September 11th/12th, 2014, Vienna

Abstract

Öresundskraft, a Swedish power company, operates a natural gas compression plant which serves a fleet of buses in the city of Helsingborg. The company takes its environmental responsibilities very seriously.

In this case Öresundskraft wanted primarily to reduce natural gas leakage to the atmosphere from the compressor plant at the bus station. A secondary motivation was to reduce the amount of oil lost in the compressed gas; if not carefully controlled downstream, this oil can cause serious problems for the bus engines.

Trials on a single compressor with a new completely leak-free sealing system of novel design have proved highly successful. The most important achievement in terms of the company's environmental commitments is that gas emissions from the compressor station have been eliminated. The system has been running for more than a year with no problems.

The new sealing system also seems to have practically eliminated oil consumption, though this is still to be confirmed. If successful, the oil saving should amount to around €3,200/year.

Öresundskraft now plans to fit the new sealing system to the remaining two compressors at the bus station.

Eliminating Gas Leakage with a Novel Rod Sealing Solution

by Johan Klinga, Öresundskraft AB

1 Introduction

Öresundskraft, an energy company in Helsingborg, Sweden, saw an opportunity to reduce oil and gas leakage from high-speed reciprocating compressors used to supply a mixture of natural gas and biogas to the city's bus fleet. Environmental performance is high on Öresundskraft's list of priorities, and the benefit would be primarily to lower greenhouse gas emissions. Cost savings in terms of reduced gas and oil losses would provide a secondary benefit.

Accordingly, the company decided to become an early adopter of a highly innovative compressor sealing system. This uses pressurised oil, rather than the conventional solid packings, to contain the pressurised gas, creating a wear-free system with almost perfect sealing properties.

2 About Öresundskraft

Öresundskraft is the municipal energy company serving Helsingborg, a city of around 100,000 inhabitants at the southern tip of Sweden, and nearby communities. A complete regional energy player, Öresundskraft supplies electricity, gas, district heating and cooling, and a wide range of other energy services and solutions.

Öresundskraft is wholly owned by the city of Helsingborg, and has around 400 employees and 260,000 customers. It supplies around 4 TWh/year of energy, mainly in the form of electricity and district heating. The Västhamnsverket and Filbornaverket plants in Helsingborg, and the Åkerlundsverket plant in Ängelholm, produce heat and power from biofuels and municipal waste. The portfolio also includes wind power and biogas.

Öresundskraft operates two public filling stations for gas-fuelled vehicles, supplying a 50/50 mix of biogas and natural gas. Compared with petrol or diesel this cuts carbon dioxide emissions by around 60%, as well as reducing particulates.

The company takes its responsibilities to the environment and the local community seriously, and is always seeking to lower its greenhouse gas emissions – including methane as well as carbon dioxide and nitrogen oxides.

3 Bus fleet runs on gas

Öresundskraft supplies a 50/50 mixture of natural gas and biogas to run Helsingborg's fleet of around 150 buses. Gas-fuelled buses are common in Sweden,

giving better fuel economy than diesel as well as lower emissions. A private company operates the Helsingborg buses under a regional contract (Figure 1).



Figure 1: The Helsingborg bus fleet runs on a mix of natural gas and biogas.

The CNG station at the bus depot is owned by Öresundskraft and was built in 2005–2006. It takes gas from the main at 4 bar and raises its pressure to 250 bar.

The plant has three identical Ariel JGQ/2 compressors (Figure 2), which are a popular choice for CNG applications. Each is rated at 1,000 Nm³/h, and the total daily demand is 16,000–22,000 Nm³. Two of the compressors generally run at any one time, with the third as a standby. A typical compressor run during a busy period might be from 6 pm on Thursday to noon on Saturday, but the demand pattern varies considerably.



Figure 2: One of the three natural gas compressors at the Helsingborg bus station.

Each compressor has two cylinders and four stages. The speed is 1400 rpm, with a 3-inch (76 mm) stroke and a rod diameter of 1.125 inch (28.6 mm). The compressors are fully lubricated, with the second and third stages sealed by pressure packings.

Eliminating Gas Leakage with a Novel Rod Sealing Solution

by Johan Klinga, Öresundskraft AB

4 Seeking continuous improvement

Although CNG is widely considered an environment-friendly fuel, gas leakage from CNG compressors is a significant issue – though one that is not often talked about outside the compressor industry.

Gas losses at the Helsingborg plant were previously measured at around 300 l/h per compressor during normal operation, and occasionally up to 11,000 l/h as the packing rings approached the end of their lives. This is a significant amount of gas in terms of both cost and environmental performance.

Öresundskraft is always seeking to reduce or eliminate greenhouse gas emissions, including natural gas and biogas, so the idea of a truly leak-free compressor sealing system was very attractive.

A secondary reason for choosing the new sealing system was a promise of reduced oil use and lower levels of oil carryover in the compressed gas. At present, each compressor uses around 0.75 l/day of oil to lubricate the packings, and all of this oil ends up in the compressed gas.

Oil carryover is bad news for engines because it clogs their injectors. At the moment the bus operator does not report any issues, in part because the engines are fitted with protective filters, but there have been some oil-related problems in the past with a previous bus company.

Problems with oil carryover can be hard to pin down, because it is difficult to distinguish compressor oil from the buses' own crankcase oil. It is therefore good business practice for the CNG supplier to take care to avoid oil carryover, so as not to get into commercial arguments. Öresundskraft has considered moving to oil-free or semi-oil-free compression for this reason.

Oil contamination can potentially clog positive displacement gas meters. Really serious oil carryover can also reduce the fuel capacity of the buses as it takes up space in their CNG tanks. Neither of these issues has been a problem for Öresundskraft, however.

5 New way to eliminate leakage

Current pressure packings, properly chosen and maintained, perform well for extended intervals. However, they often leak significant amounts of gas – for small CNG compressors, 300 l/h per packing is typical – and use significant amounts of oil – up to 1 l/day per packing. The use of a purge gas can control the routing of process gas losses but not their quantity, and adds to both installation and running costs.

A radically different approach to piston rod sealing is to surround the rod with pressurised oil to form a barrier. In turn, two oil seal rings keep the oil in place (Figure 3).

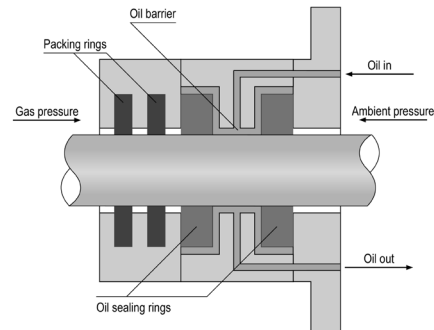


Figure 3: Pressurised oil surrounds the shaft to eliminate any leakage of gas. The oil is kept in place between two sealing rings.

At first glance, the use of sealing rings to contain the oil is similar to the use of conventional packings to contain gas. However, there are two important differences.

First, oil is hundreds of times more viscous than gas. This in itself greatly limits the amount of oil that is lost through the narrow gap between piston rod and sealing ring. It also allows the rod surface to maintain a thin film of oil at all times, so that the rings never touch the rod and the system is essentially wear-free.

The second important difference is that oil transport is not a one-way process. With every forward stroke, the rod drags a thin film of oil past the corresponding seal ring. The clever part, however, is that on the return stroke the same oil is “pumped” back into the oil barrier with almost perfect efficiency, even against the prevailing gas pressure gradient. The result is a system that provides perfect gas containment with very low oil consumption.

This pumping effect is well-known in hydraulic seals, but is much harder to replicate in piston packings. It requires the seal ring to have the correct profile to generate the necessary hydrodynamic forces, and the free-floating motion of the compressor rod adds complexity.

A buffer volume and a pair of conventional packing rings work together to stabilise the pressure inside the packing box, allowing the oil supply pressure to be set well below the cylinder discharge pressure and so reducing the mechanical loads on the system.

Eliminating Gas Leakage with a Novel Rod Sealing Solution

by Johan Klinga, Öresundskraft AB

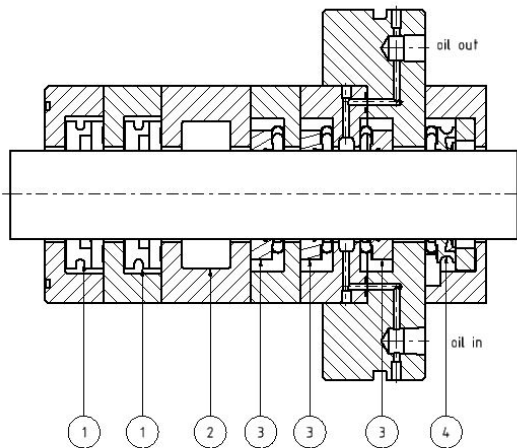


Figure 4: The complete packing system comprises a set of conventional packing rings (1), a buffer volume (2), the new oil seal rings (3), and a wiper ring (4).

A specially designed oil supply unit supplies up to six packing boxes with oil at a defined flowrate and pressure. The oil flow removes heat from the packing, eliminating the need for separate cooling. The self-contained nature of the system makes it easy to retrofit.

Control functions built into the oil supply unit monitor oil temperature, pressure, tank level and consumption rate. In the event of a power failure or loss of oil pressure, the system automatically enters a failsafe mode in which it operates as a standard vented (or purged) pressure packing.



Figure 5: The central oil supply unit also provides important control and monitoring functions.

A further key advantage is the system’s ability to maintain an effective seal when the compressor is shut down but the system remains pressurised. Leakage from conventional packings during pressurised

standstill can be very high, and may require the use of separate static seals that are actuated on compressor shutdown. The system described here achieves equivalent or better performance with less complexity.

6 Installation and operation

The leak-free sealing system was installed on a single compressor in February 2012. Installation was straightforward, barring a few plant layout issues attributable to the fact that this was the first field test of the new sealing system, which was not yet in serial production.

The new system has fully lived up to its promise. Since start-up it has run with very few issues, and the compressor is now essentially 100% gas-tight. Leakage is now undetectable by the flowmeter installed for this purpose, compared to the previous leakage of 300 l/h or more.

The compressor also seems to run more smoothly, thanks to the absence of mechanical contact and friction from conventional sealing rings. The sound made by the machine when it is running is smoother and quieter than before.

The oil supply pressure is 70 bar, the temperature of the oil return line is around 58°C, and the temperature of the oil tank in the main oil supply unit is around 46°C.

Since this is a test unit it has to be switched on and off manually, rather than being interlocked with the compressor. On one occasion the system was not switched on when the compressor started up. It immediately went into failsafe mode and continued to operate in this way – equivalent to a standard vented pressure packing – for a month. There was no damage to the equipment, and no gas or oil losses beyond what would be expected from a standard packing.

Inspection of the level in the oil tank shows that oil consumption has been negligible since the system was installed. To the resulting projected saving of 0.75 l/day of oil per compressor could be added a corresponding reduction in the cost of buying and disposing of oil filters.

7 Longer-term experience

An inspection after one year in operation showed that the oil seal rings were still in good condition, and the performance of the complete sealing system was unchanged.

Eliminating Gas Leakage with a Novel Rod Sealing Solution

by Johan Klinga, Öresundskraft AB

By this time the design of the oil sealing rings had been modified based on experience gained in other installations. The new-style rings were fitted when the packing box was reassembled, and have since performed as well as the original ones.

When the piston rods were inspected after 8,000 running hours, the oil pressure applied by the new sealing system was found to have deformed the rod surfaces. After replacement rods suffered the same damage, hardened rods were fitted. This was not an expensive operation, and would not be an issue for compressors that use hardened rods as standard. Performance since then has been entirely satisfactory.

The leak-free sealing system has been running successfully since February 2012. Öresundskraft now plans to fit the new sealing system to the other two compressors, hopefully during 2014.



NAM Nederlandse Aardolie Maatschappij B.V.

Best Practice for Efficiency and Emissions Upgrades of a Gas Gathering Compressor

by

Robbert Pol,

Nederlandse Aardolie Maatschappij B.V.

Assen, Netherlands

Robbert.pol@shell.com

9th EFRC Conference

September 11th / 12th, 2014, Vienna

Abstract

This paper demonstrates significant improvements achieved by installing a new “real” zero-emission packing and the latest valve technology on two compressors at a natural gas gathering and treatment plant operated by Nederlandse Aardolie Maatschappij BV (“NAM”) in the Netherlands.

Natural gas operators face cost pressures, stringent safety requirements and the need to comply with tightening environmental legislation. Continuous improvement of equipment is key to success. Two important issues for reciprocating compressors are packing leakage and poor valve performance.

Gas lost from leaky rod packings often has significant financial costs, contributes to greenhouse gas emissions, and attracts extra attention from environmental regulators when it contains toxic components such as benzene. If purged packing boxes are used, consumption of nitrogen is an important extra cost.

At the plant in question, gas leakage has been virtually eliminated from the compressor fitted with the new sealing system, with consequent benefits for environmental and safety performance. This was only the second field installation of the new sealing system, and technical development has continued through the trial period.

Compressor valves, meanwhile, are frequently a major cause of both downtime and energy losses, especially when they are not optimally matched to the compressor duty.

Fitting new valves of proven design to a second compressor has reduced valve losses by almost 50%, yielding significant energy savings and rapid payback. Valve life has increased from as little as two months to around a year, and a service-free life of two years is targeted. This will significantly improve compressor reliability and reduce life cycle costs.

Best Practice for Efficiency and Emissions Upgrades of a Gas Gathering Compressor

by: *Robbert Pol, Nederlandse Aardolie Maatschappij B.V.*

1 Introduction

This paper describes how NAM has installed and tested two new technologies to improve reciprocating compressor performance at a natural gas gathering and processing plant in the Netherlands.

The first innovation was a revolutionary sealing system which uses a continuous flow of pressurised oil to eliminate gas leakage, while reducing oil consumption compared to conventional packings.

The new sealing system has been entirely successful in terms of stopping fugitive gas emissions. As first installed, it was less successful at reducing oil usage. Since then it has developed further, and recent progress has been promising. Compressor reliability has not been compromised at any stage.

The second development was a new type of compressor valve which combines high efficiency with robustness. The new valves have cut valve losses by around 50%, leading to significant energy savings and rapid payback. Their increased durability has allowed them to operate for at least a year without servicing or replacement, compared to as little as two months for the original valves, and a lifetime of two years is targeted.

2 Den Helder gas treatment plant**2.1 Introduction**

The compressors in question are located at the Den Helder gas gathering and processing facility in the Netherlands, 60 km north of Amsterdam (Figure 1).



*Figure 1: source NAM
The Den Helder gas treatment plant*

The plant is operated by Nederlandse Aardolie Maatschappij (NAM), the leading producer of natural gas

in the Netherlands. NAM is owned 50/50 by Shell Nederland B.V. and ExxonMobilNAM is a separate company but the Shell UI Operating model has been implemented in NAM..

Three pipelines collect gas from North Sea platforms and bring it ashore at Den Helder. Here it is processed in three separate plants, the first of which dates from 1976.

Before the gas leaves the offshore platforms, liquids are removed and the gas is cleaned and dried. The dry gas is then compressed by centrifugal or reciprocating compressors, and the condensate is re-injected before the compressed gas enters the pipelines for transport to shore.

The condensate-rich gas enters the gas treatment facility at a pressure of 68–80 bar. Here a slugcatcher removes the condensate once more. The gas goes on to further treatment, starting with the low temperature separator (LTS) plant. The liquids are processed separately.

Altogether there are eight reciprocating compressors on the Den Helder site. The largest is the main booster compressor, a 6-cylinder, single-stage machine rated at 6 MW and dating from the 1990s.

Each of the two projects described here – leak-free sealing and high-performance valves – was tested on one of a group of smaller reciprocating compressors which handle offgas from the various downstream processes.

2.2 Gas leakage from conventional packings

NAM is always looking for affordable ways to reduce gas emissions as a way to improve economics, safety and environmental performance in the face of tightening regulations. The company identified improved sealing of the piston rods as a route to reduce:

- gas leakage to the atmosphere;
- potential gas leakage into the crankcase; and
- oil consumption.

At present, all the compressors are fitted with conventional oil-lubricated rod packings. These leak significant quantities of gas, which is collected and vented through the roofs of the compressor houses. Typical packing leakage rates are in the range 300 litres/hour per packing, so the total leakage across the whole site is potentially of the order of 20 tons/year, and the value of the lost gas could be more than €10,000 a

year for this location alone. Within Shell Upstream International Operated more than 50 reciprocating compressors are operated, so the total eventual saving could be large.

A particular concern is benzene, which commonly occurs in natural gas – including that from the North Sea – and so is an issue for many producers. At present the site's benzene emissions are acceptable, but from 2015 the Dutch agencies responsible for gas safety and environmental emissions (the Staatstoezicht op de Mijnen (SODM) and the Rijkswaterstaat, or Ministry of Infrastructure and Environment) will reduce the legal limits for benzene. The applicable legislation is the Nederlandse Emissie Richtlijn Lucht (NeR), which controls levels of volatile organic compounds (VOCs) in air.

A further issue concerns gas leakage into the crankcase. The newer compressors on the site, including the one used in this trial, are of the dual-compartment type (API 618, 6.12.1.5), with a vented distance piece between the cylinder and the crankcase. Many of the older machines, however, are of single-compartment design (API 618, 6.12.1.3 type B), with a direct gas leakage path between cylinders and crankcase.

Dissolved gas can lower the flashpoint of the crankcase oil and so increase the fire hazard in the event of an accident. NAM regularly checks the crankcase oil for the presence of gas, but eliminating any chance of leaks would make the older compressors inherently safer.

The new leak-free packing promised a way to eliminate gas emissions from packings and so to help the site improve its environmental performance at relatively low cost. A secondary bonus would be a reduction in oil consumption (see below).

3 Zero-emissions packing

3.1 Principle of operation

A radically new concept for piston rod sealing promised NAM the chance to eliminate packing leakage completely, rather than simply reducing it, as previous low-emission packings have done.

The principle behind the “zero-emission packing” is the use of oil, rather than a solid material, as the sealing medium. A volume of pressurised oil surrounds the piston rod and is kept in place by two specially-designed oil seal rings (Figure 2).

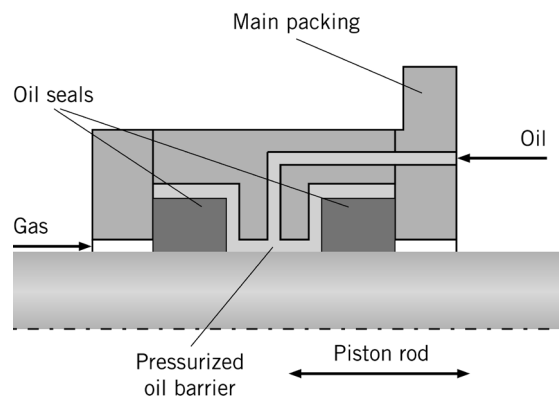


Figure 2: The new packing design relies on a pressurised volume of oil held between two sealing rings.

Oil can leak past these seal rings, of course, just as gas leaks past the rings of the conventional pressure packing. The difference is that the leakage of oil is extremely slow compared to the corresponding situation for gas.

In part this is because of the much higher viscosity of oil compared to gas, but there is another important reason: the reciprocating motion of the rod “pumps” oil back into the sealing barrier against the prevailing pressure gradient. This effect is well-known in hydraulic seals, but has never before been applied to compressor seals – a much more challenging application. Because the rod is always covered with a film of oil, the oil seal rings operate virtually without wear.

As well as the oil space and the two oil wiper rings, the packing box also contains a set of conventional single-acting packing rings, a buffer volume, and a wiper ring. The presence of the buffer volume allows the oil pressure to be held just above the suction pressure, rather than requiring the full discharge pressure (Figure 3).

Best Practice for Efficiency and Emissions Upgrades of a Gas Gathering Compressor

by: Robbert Pol, Nederlandse Aardolie Maatschappij B.V.

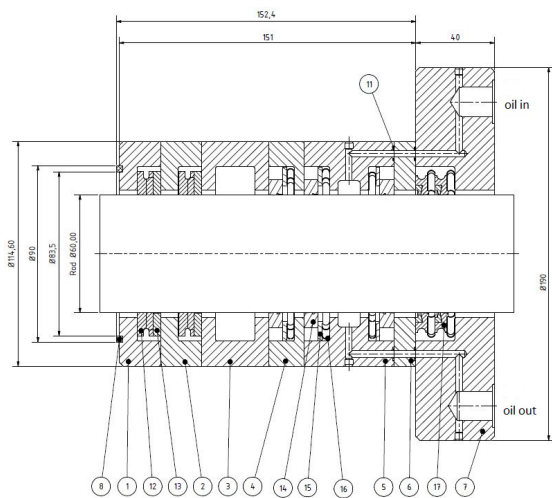


Figure 3: Section through a zero-emission packing.

A central oil supply unit (Figure 4) circulates oil through the packing box, removing heat and eliminating the need for a separate packing cooling circuit. The central unit can supply up to six packing boxes and incorporates all the necessary control functions, allowing the system to be retrofitted easily in place of conventional packings.



Figure 4: Source Hoerbiger Central oil supply unit.

Systems that remain pressurised when the compressor is shut down typically require an additional static sealing system to prevent excessive leakage. With the new ceiling system, simply maintaining the oil pressure at all times ensures an effective static seal.

In the event of a power failure or a rapid loss of oil, the system also automatically enters a failsafe mode

in which it behaves as a conventional vented packing, with a purge system if necessary.

3.2 Gas leakage eliminated

The new sealing system was installed on a single compressor in April 2013. This two-stage, two-cylinder machine (Figure 5) takes gas recovered from the condensate stabiliser feed vessel and re-compresses it to feed back into the sales gas line.



Figure 5: Source HTC Zero-leakage sealing system installed on a compressor at Den Helder.

The inlet pressure is around 15 bar and the discharge around 62 bar. A variable-speed drive operates the compressor at 510–990 rpm, with a stroke of 125 mm and a rod diameter of 60 mm. Capacity is 210,000 Nm³/day, with a recycle system to provide turndown in steps of 25%.

A second compressor provides redundancy. Each machine can handle 100% of the process demand, so normally only one of the pair runs at once.

Installation of the new sealing system was straightforward, with no drilling of the cylinders or other structural modifications required. The main oil supply unit supplies oil to the packings at 55 bar.

The system is in operation since May 2013 including modifications and periods of operation in failsafe mode (see below).

From the start, the new sealing system has been a complete success in terms of its most important benefit: eliminating leakage. The gas leakage rate is now almost zero, as calculated from measurements of methane and benzene concentrations around the compressor.

3.3 Experience with oil consumption

The amount of oil used by the existing conventional packings is not really a problem for NAM. Current consumption is in the region of 1.5 litres/day per packing, and oil carryover does not cause any problems for downstream gas quality.

However, all this oil does have to be removed from the gas stream and disposed of. As a result, the forecast that the new leak-free packing would cut oil use significantly, to 0.5–1.0 litre/day per packing, was attractive. The potential saving at Den Helder could be around 6,000 litres/year of oil which would not have to be bought or disposed of.

So far, unfortunately, oil consumption has mostly been higher than forecast, though generally no higher than with conventional packings.

For a short period after the original start-up, oil consumption was as planned: 0.5–0.6 litre/day per packing. It soon increased, however, and after 840 hours' runtime the system was shut down because oil use had risen to 1 litre/day per packing. Oil usage is measured by monitoring the level in the oil circulation tank. The system displays an alarm and goes into failsafe mode if oil consumption exceeds a threshold value that can be set according to the individual application.

Design modifications now in place (see below) should get around all these problems, though success has yet to be confirmed on the plant.

3.4 The design evolves

The NAM installation was only the second field test of this pioneering leak-free compressor sealing system. As a result of the experience gained here and elsewhere, the system has in the meantime undergone engineering modifications.

After an initially successful start up, high oil consumption was found to be related to the design of the oil sealing rings. The scraping edge of the lead ring was deforming under load, leading to premature ring failure and also lessening the effectiveness of the pumping action that keeps the oil in place.

In October 2013 the system was re-started with a modified ring design. This second test proceeded in a very promising way, with low oil consumption recorded, until high temperatures in the oil circuit tripped the system into failsafe mode.

At the time of writing it seems that an extended previous period of operation in failsafe mode had allowed dirt from the gas stream to block one of the oil

circulation channels as well as a filter in the main oil supply unit. The filter was bypassed and the system was started up again; oil use this time was a little higher than before, but still below the rate expected from a standard lubricated packing.

This incident also confirms the success of the system's built-in safety function in switching automatically to failsafe mode when the blockage was detected. The temperature at which a malfunction is signalled can be set to suit the individual demands of the application.

The design of the system has now been modified to prevent a repeat of this incident, but at the time of writing the standby compressor is not in service, so it has not been possible to check the actual state of the sealing system and apply the modifications. Once the standby compressor is back in use NAM hopes to confirm both the blockage diagnosis and the effectiveness of the modified design.

4 New valves improve performance

4.1 Issues with existing valves

NAM's second set of concerns lay with the compressor valves, specifically the potential to reduce flow-related losses and to improve valve life.

The ring valves widely used at the Den Helder site typically need frequent replacement, sometimes after as little as two months. Work to find valves that would last longer began back in 2004.

The main issue is the presence of condensate droplets which damage the valves. The compressor operating procedures are designed to maintain gas temperatures high enough to avoid condensation, but sometimes this is not possible.

Condensate droplets can cause valve flutter and spring breakage, which in turn creates metal fragments which can soon wreck the valve. In addition, selection of the ideal valve is complicated by the fact that every well has a different gas quality.

NAM believed that a more modern valve design could improve both efficiency and service life.

4.2 New valve design performs well

NAM selected one compressor – a different one from the one used for the new sealing system – to test the new valves.

The new valves owe their durability and high efficiency to their aerodynamic design and use of injection-

Best Practice for Efficiency and Emissions Upgrades of a Gas Gathering Compressor

by: *Robbert Pol, Nederlandse Aardolie Maatschappij B.V.*

moulded thermoplastic reinforced with carbon fibre as the material of construction. The manufacturer claims that the profiled plate design gives energy savings of up to 9% over competitive products.



Figure 6: Hoerbiger High-performance profiled plate valve.

The plastic construction, meanwhile, contributes durability and reduces the risk of damage from metal fragments. Specially developed springs ensure maximum dynamic safety, and an integrated anti-rotation element guarantees reliable gripper actuation, even with frequent compressor load changes.

The new valves are available in diameters of 79–212 mm. An operating temperature range from -200 to +210°C at a maximum pressure of 50 bar and a differential pressure of 30 bar allow their use in liquefaction systems for LNG, ethylene and other hydrocarbons.

The new valves have performed well. The current indication is that they will have an operating life of at least a year; the target lifetime is two years. Valve losses have been reduced by almost 50%, giving significant energy savings with a short payback.

Conclusions and future plans

The leak-free sealing system has been successful in its main objective of virtually eliminating emissions from the compressor under test.

The expected reduction in oil use has been harder to achieve. It is likely that the re-design of the oil sealing rings and other modifications have corrected the previous problems, but it is a little too early to say.

Certainly NAM believes that this is a very promising technology for reducing gas leakage from reciprocating compressors. With any necessary further development it has the potential to become an effective and widely used solution.

Assuming that further tests continue to be successful, NAM will certainly consider adopting the new sealing system more widely across its reciprocating compressor fleet.

The new valves have met all expectations for both efficiency and service life.

9th Conference of the EFRC September 11th / 12th, 2014, Vienna

**A Comparative Analysis of Numerical Simulation Approaches
for Ring Valve Dynamics**

-79-

by: Carsten Möhl, Technische Universität Dresden

**Method for Evaluating the Pass / Fail Criterion for the Fatigue Design Margin
& Life Estimation for Reciprocating Compressors**

-86-

by: Ani Ketkar, Federico Pamio, Mark Patterson, GE Oil & Gas

**Improvement of the Cooling Performance of a Reciprocating Compressor
Cylinder by a Conjugate Heat Transfer and Deformation Analysis**

-92-

by: Francesco Balduzzi, Giovanni Ferrara, University of Florence; Riccardo Maleci, Alberto Babbini GE Oil & Gas – Nuovo Pignone



**EUROPEAN FORUM
for RECIPROCATING
COMPRESSORS**

SESSION CALCULATION 1

A Comparative Analysis of Numerical Simulation Approaches for Ring Valve Dynamics

by:

Carsten Möhl

**Institute of Power Engineering Bitzer Chair of Refrigeration,
Cryogenics and Compressor Technology
Technische Universität Dresden
Dresden, Germany
carsten.moehl@tu-dresden.de**

**9th Conference of the EFRC
September 11th / 12th, 2014, Vienna**

Abstract:

In this work fluid structure interaction (FSI) simulation was introduced to solve the plate valve dynamics considering movement, fluid dynamics and heat transfer. With these obtained results, shape optimization studies considering lifetime can be started.

1 Introduction

Compressor valves are closely linked to performance and reliability. Therefore they are one of the most critical components of reciprocating compressors. Valve defects were identified as primary cause for most of the unscheduled maintenance effects¹. Consequently, the industry has to consider improvements in valves. Advances in materials sciences as well as an increased understanding of underlying fluid dynamics lead to design improvements prolonging maintenance intervals and thus lifetime.

As a result of broad availability of high-performance computers plus the development of commercial codes the computational simulation found its way into the iterative process of optimization

This paper presents the current status within the 3D simulation of fluid and structural dynamics of plate valves.

2 Motivation & Modeling

2.1 Piston movement

State of the art computational simulations typically neglect the piston movement. Instead they often use a mass flow based on piston area, mean velocity and intake density. This simplification reduces the computational complexity and thus time and expenses. In contrast to this common approach the movement of the piston will be the driving force for changes of working chamber volume within this work.

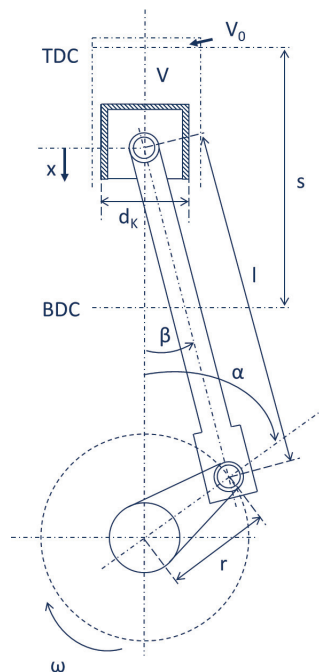


Figure 1: Single acting reciprocating compressor

Figure 1 shows a schematic depiction of a reciprocating compressor. To ensure reproducibility to conducted measurements as well as technical literature it is reasonable to contemplate the piston movement as crank angle dependent.

$$x(\alpha) = r \cdot (1 - \cos \alpha + 1/\lambda (1 - \sqrt{1 - \lambda^2 \sin^2 \alpha})) \quad (1)$$

This enables to view the change of states and masses within an indicator diagram (Figure 2). The whole process takes place in one revolution of the crankshaft. When the piston moves downwards from the top dead center (TDC), the remaining gas in the clearance volume (V_0) expands. When the pressure of the gas remaining inside the working chamber drops to below the suction pressure, the suction valve opens and suction gas is sucked in from the suction chamber adjacent the cylinder. At the BDC the suction valve closes and compression starts. When the gas is compressed to just above the discharge pressure, the discharge valve opens. The expulsion ends at the TDC.

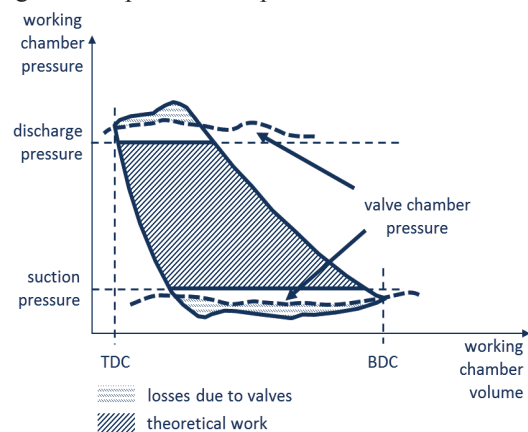


Figure 2: Indicator diagram

The efficiency of a reciprocating compressor strongly depends on the performance of its suction and discharge valves. In modern units, valve performance is worsened further by the increased frequency leading to more valve impacts at higher impact velocities. In general the compression cycle is affected directly by valve losses which lower the theoretical work as depicted in Figure 2.

2.2 Valve plate movement

Process gas compressors consist of at least one pair of suction and discharge valves. To reduce the complexity and following the computation time, within this paper the focus will primarily be on the suction valve. Additionally Georg Flade² provides in his doctoral thesis an in-depth analysis of the opening phase. On this ground the present work will emphasize on the closing. In relation to Figure 3 the period modeled starts at approximately 360°.

A Comparative Analysis of Numerical Simulation Approaches for Ring Valve Dynamics

by: Carsten Möhl, Technische Universität Dresden

Although details of valve design may differ considerably, the basic principle of operation is similar. To setup the fluid-structure-interaction (FSI) that induces the valve plate movement fundamentals of valve theory are necessary. Figure 4 depicts the functional components of a compressor valve. Most of the valve theories consider the moving parts as a mass-spring-damper-system³.

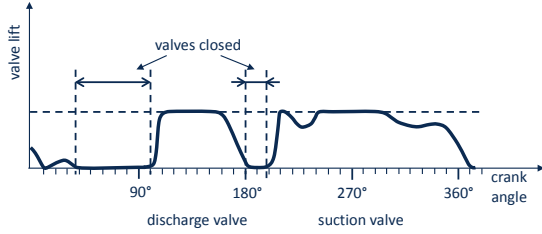


Figure 3: Valve opening time in a real cycle⁴

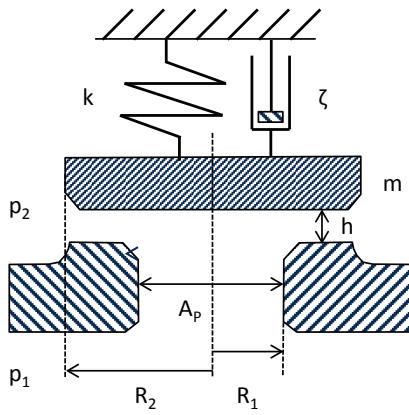


Figure 4: Schematic representation of functional components of a compressor valve

$$m \frac{d^2 h}{dt^2} + \zeta \frac{dh}{dt} + k(h + h_{pl}) = c_g A_p \Delta p \quad (2)$$

The term on the right hand side of equation (2) represents the gas force acting on the valve plate. The semi-empirical coefficient can be determined, within the limits of viscous flow according to equation (3). For larger valve lifts or inviscid flow equation (4) applies³.

$$c_g = \left(\frac{R_2^2}{R_1^2} - 1 \right) \left[\ln \left(\frac{R_2^2}{R_1^2} \right) \right]^{-1} \quad (3)$$

$$c_g \approx 1 + 8 \left(\frac{h}{R_1} \right) \quad (4)$$

Computational simulations considering mesh displacement in combination with FSI tend to diverge; typically ending in errors like not matching interfaces or negative volume elements. The latter

error generally occurs when the gradient of applied load relative to the prior time step gets too steep. Thus double-checking implemented conditions is mandatory.

Considering the valve plate movement, the differential equation (2) can be analyzed using classical Runge-Kutta method. By application of parameters listed in Table 1 the trends of valve lift and velocity as depicted in Figure 5 can be obtained. The rapid displacement of this model plate shows that the time step sizing needs special attention to ensure that there will not be any sudden jumps in force calculation. Furthermore valve lift limiting is essential to prohibit structural interaction of valve plate and a fixed wall. The exchange of kinetic energy while bouncing will not be modelled.

Table 1: Mechanical parameters of model valve

Parameter	Value
plate mass	35.2 g
damping coefficient	1.45 Ns/m
spring stiffness	3000 N/m
port area	1.02E-03 m ²
preload distance	0 mm

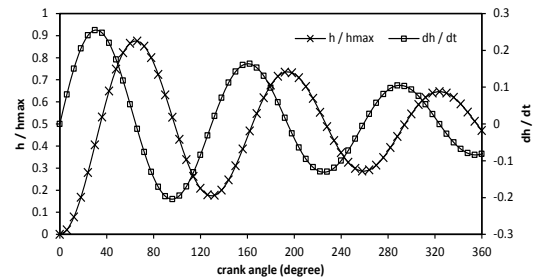


Figure 5: Relative valve lift and velocity for a model valve

Since the working fluid will be free of oil no additional stick-on-effect has to be modeled. To ensure sealing, the port area will be represented by a General Grid Interface (GGI). By using Boolean conditions this kind of interface gets either interpreted as a wall or as an opening letting fluid pass. It enables direct coupling of thermodynamic state and streaming through the valve. One possible condition can be pressure dependent. As the valve plate movement is already linked to a pressure condition, the usage of valve plate displacement seems more commendable.

2.3 Geometry & Meshing

Figure 6 shows the first geometry used. It depicts the simplified version of a 2-quadrant-model. The piston surface (7) moves according to equation (1) as the crank angle is derived from computation time steps.

SESSION CALCULATION 1

A Comparative Analysis of Numerical Simulation Approaches for Ring Valve Dynamics

by: Carsten Möhl, Technische Universität Dresden

Thus the volume of the working chamber (5) changes as well as pressure and temperature. The valve plate (4) movement is directly linked to the pressure difference and a force induced by spring stiffness via “CFX Expression Language” (CEL) expressions. This enables direct access to the valve lift. For computational stability and convergence reasons the preclusion of domain interference, e.g. the collision of valve plate and guard, is recommended.

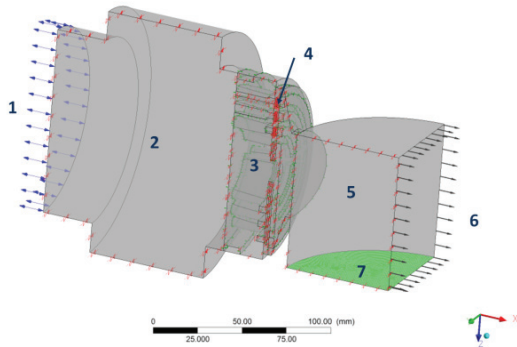


Figure 6: First geometry used - (1) Inlet; (2) Suction chamber; (3) Valve; (4) Valve plate; (5) Working chamber; (6) Outlet; (7) Piston surface

Considering the piston movement induced mesh displacement it should be noted, that this translation needs to be scaled onto the whole working chamber in correlation to the initial mesh. Using a CEL expression this can be achieved by

$$\frac{\maxVal(Initial X)@domain - Initial X}{\maxVal(Initial X)@domain - \minVal(Initial X)@domain} \quad (5)$$

This scaling should only be applied for meshes consisting primarily of hex elements or small displacements. Figure 7 shows an appearing gap while the piston moves towards its BDC. Such defects cast doubts on every computational simulation.

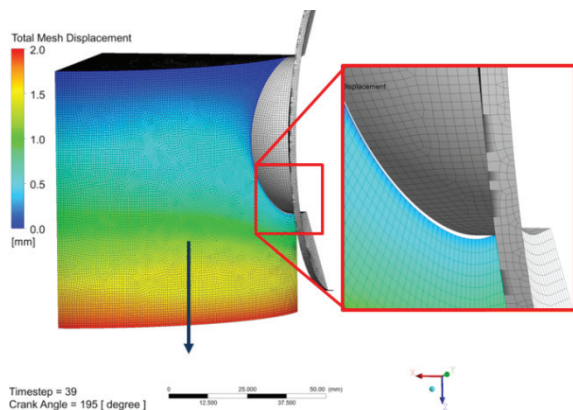


Figure 7: Mesh displacement error

Figure 8 provides a more generalized view on possible FSI issues⁵. It depicts an arbitrarily chosen and discretized geometry that is being deformed at a specific time step concluding in mesh displacement. Thus it appears that each node moves differently in relation to a space fixed reference system. Therefore high quality meshing for domains with deformation or displacement is a necessity. Furthermore if the scaling of movement is not applied in relation to the initial mesh, the translation can shift towards any kind of motion.

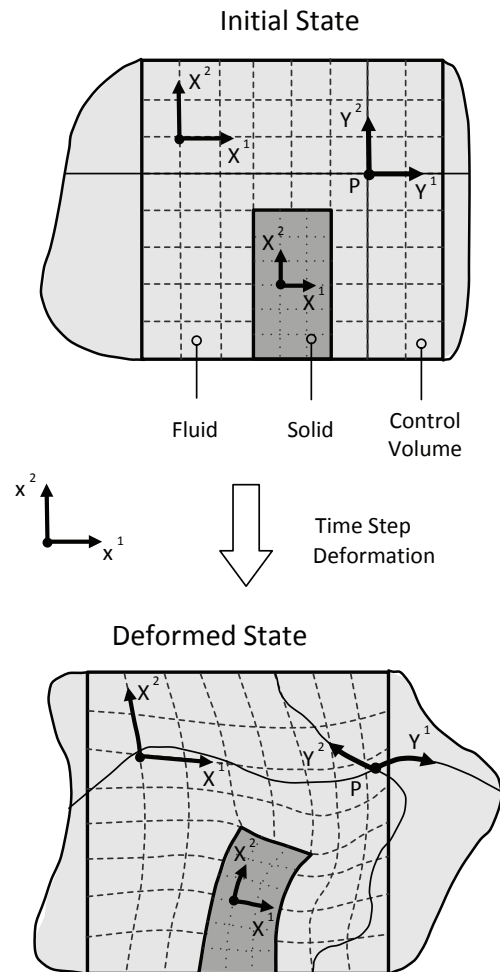


Figure 8: Schematic representation of FSI; X – material reference system; x – space-fixed reference system; Y – reference system of point P

A Comparative Analysis of Numerical Simulation Approaches for Ring Valve Dynamics

by: Carsten Möhl, Technische Universität Dresden

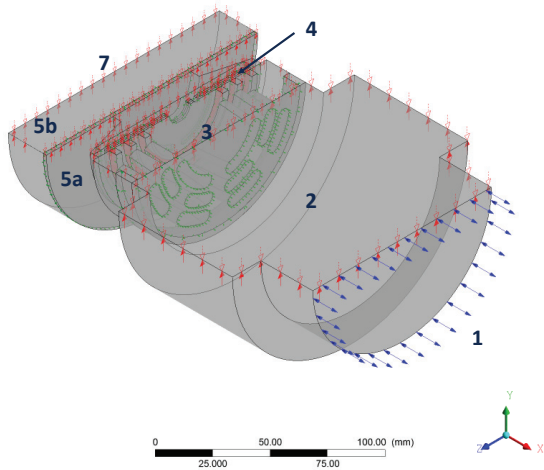


Figure 9: Second geometry used - (1) Inlet; (2) Suction chamber; (3) Valve; (4) Valve plate; (5a) Stationary part of working chamber; (5b) Moving part of working chamber; (7) Piston surface

To surpass the mesh displacement induced gap buildup depicted in Figure 7 a second geometry was setup (Figure 9). The working chamber was relocated and a stationary part (Figure 9 – 5a) introduced. The latter ensures a non-displaced division, hence stabilizing the numerical simulation. To look at this newly introduced region technically, it represents the dead volume and its size is conform to the original setup.

The following table lists the simulation parameters used as well as mesh data.

Table 2: Basic simulation data

Parameter	Value
working fluid	Air Ideal Gas
suction pressure	1 bar
piston diameter	130 mm
piston stroke	40 mm
mesh nodes	1.3191e6
mesh elements	1.9268e6

Numerical data

The following section presents the results of the transient computation. To clarify visualization planes depicting pressure as well as flow velocity distribution or mesh displacements Figure 10 shows the three planes that are going to be used. While (1) and (2) match coordinate planes, (3) is rotated by 25 ° about the x-coordinate axis. This is due to the fact that this particular angle enables the cutaway view through all

valve bores.

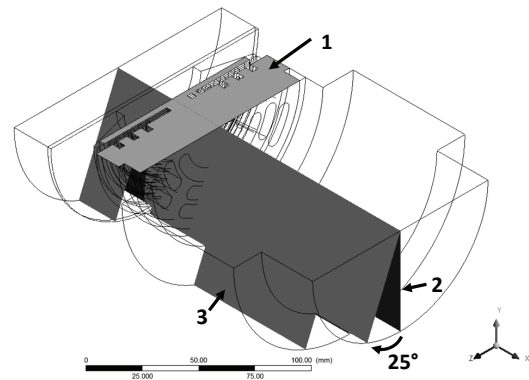


Figure 10: Declaration of visualization planes: (1) Valve symmetry plane; (2) x-y-plane; (3) Plane used for contour plots

Computational limitations, such as there should not be negative volume elements restrict the valve lift. Figure 11 shows three deformed mesh element rows representing the minimum gap. Therefore a relative valve lift of zero cannot be computed. The correlation between valve lift and piston stroke is depicted in Figure 12. The marked point at 80° pictures the BDC of the piston and the end of its downward movement. Irrespective of the valve lift induced by the pressure difference across the plate, an additional accelerating effect arises in the latter time steps. Thus the pressure and velocity distribution within the gaps has to be analyzed further. The corresponding time steps are marked in Figure 12. The large phase shift between the BDC and the closed state of the valve is caused by two central issues. On the one hand the unfavorable working point and on the other hand the feedback of the applied forces. Due to the application of 1-Way-FSI, which reduces the computational time drastically, there is an offset between computed displacement and applied forces within a time step. Minimization of the step size is recommended for compensation, but cannot be used to cancel out the mentioned effects.

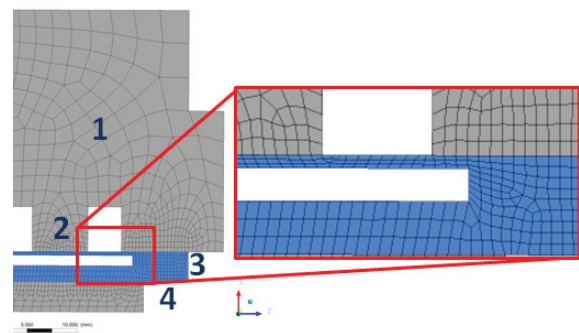


Figure 11: Detail view of maximum valve lift mesh displacement (1) Seat; (2) Plate; (3) Gas portion around plate; (4) Guard

SESSION CALCULATION 1

A Comparative Analysis of Numerical Simulation Approaches for Ring Valve Dynamics

by: Carsten Möhl, Technische Universität Dresden

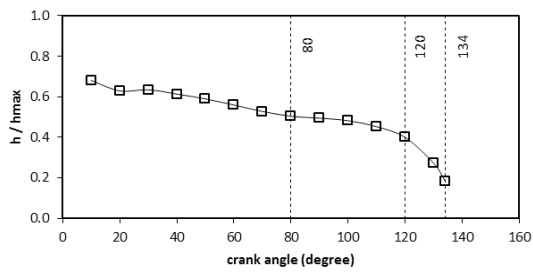


Figure 12: Valve lift; 80 ° marks the BDC of the piston

The following six figures show the streaming velocities and pressure distributions at two different time steps within the compression phase. The latter represents the minimum valve lift computed. While comparing the velocities in the gap between valve plate and seat of Figure 13 and Figure 16 the larger vortex shapes in all bores should be noted as well as the overall higher specific amounts. This leads to a local drop shown in Figure 17. As a result the pressure difference rises, accelerating the valve plate and therefore the closing process additionally. For deeper insight 3D representations of the fluid surrounding the valve plate are depicted in Figure 15 and Figure 18.

4 Conclusion

This paper presented the application of 3D computational fluid dynamics on ring plate valves using FSI. The model included, in relation to the original compressor, realistic volumes and shapes. Main objective was the usage of the piston movement as a function of the crank angle as driving force for changes of the pressure distribution, leading to forces acting on the valve plate and concluding in a displacement.

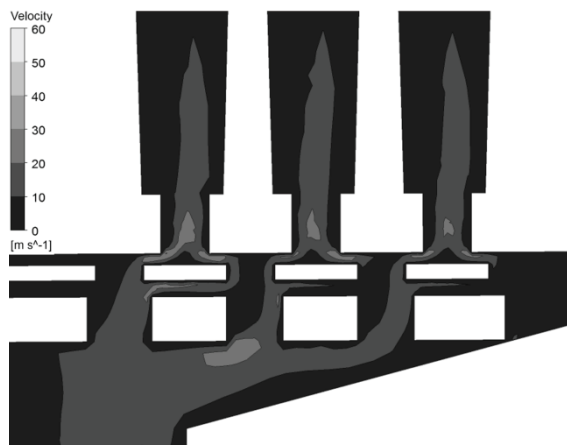


Figure 13: Flow velocity at 120 °

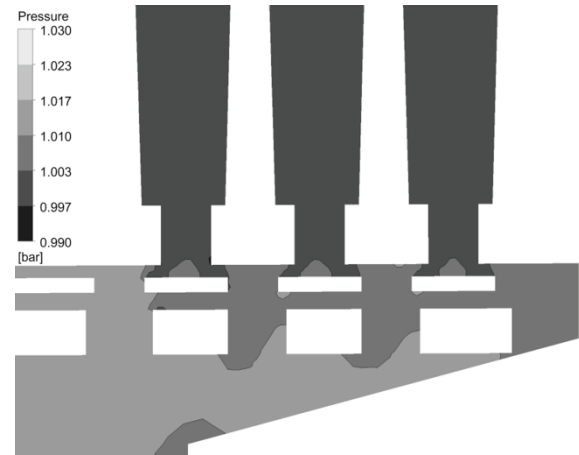


Figure 14: Pressure distribution at 120 °

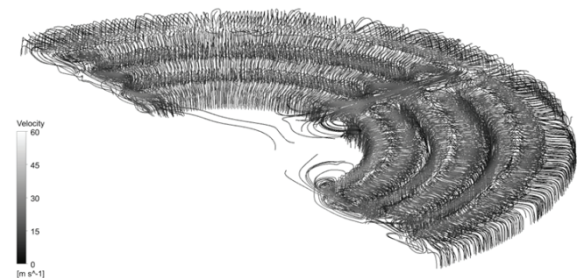


Figure 15: 3D-Flow velocity at 120 °

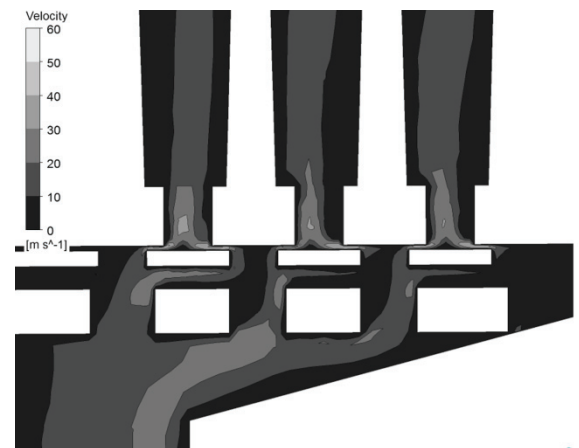


Figure 16: Flow velocity at 124 °

A Comparative Analysis of Numerical Simulation Approaches for Ring Valve Dynamics

by: Carsten Möhl, Technische Universität Dresden

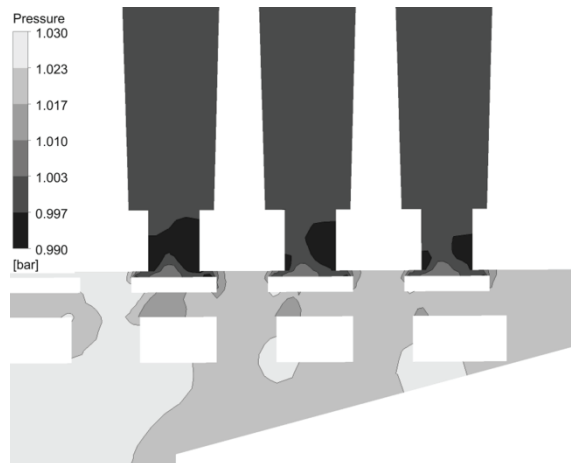


Figure 17: Pressure distribution at 124 °s

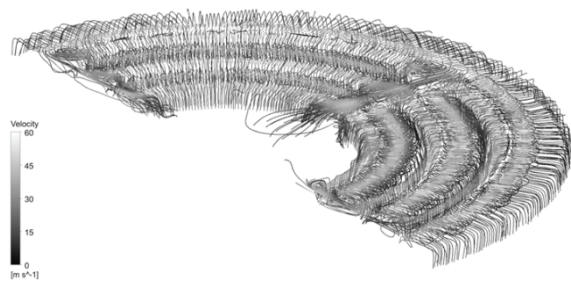


Figure 18: 3D-Flow velocity at 124 °s

The presented analysis covers only a part of the complete operation cycle. Therefore further studies have to be conducted. Additionally the influence of suction chamber pressure fluctuations should be analyzed.

For further studies the author recommends the usage of multiple configurations for ensuring mesh quality through all time steps.

5 Acknowledgements

I would like to thank Prof. G. Will for his support. The computations were performed on a PC-Farm at the Center for Information Services and High Performance Computing (ZIH) at TU Dresden.

References

- ¹ Foreman, S. (2002): Compressor Valves and Unloaders for Reciprocating Compressors - An OEM's Perspective, <http://www.dresser-rand.com/techpapers/tp015.pdf>
- ² Flade, G. (2006): Weiterentwicklung der Berechnungsmethoden für Kolbenverdichterventile auf der Basis zweidimensionaler Strömungssimulation, Thesis, Technische Universität Dresden
- ³ Habing, R. A. (2005): Flow and Plate Motion in Compressor Valves, Thesis University of Twente, Enschede
- ⁴ Touber, S. (1976): A Contribution to the improvement of compressor valve design, Thesis University of Technology, Delft
- ⁵ Möhl, C., Langebach, R., Hesse, U. (2013): Numerische Simulation eines Hubkolben-verdichters unter Berücksichtigung der Ventilbewegung



GE Oil & Gas
Downstream Technology
Solutions

Method for Evaluating the Pass / Fail Criterion for the Fatigue Design Margin & Life Estimation for Reciprocating Compressors

by:

Ani Ketkar, Federico Pamio, Mark Patterson

New Product Development

GE Oil & Gas

Houston, TX, USA

aniruddha.ketkar@ge.com

**9th Conference of the EFRC
September 11th / 12th, 2014, Vienna**

Abstract:

In a competitive business environment, products should be designed to meet regulations, while maximizing reliability and end user satisfaction. In order to attain this goal, a procedure to evaluate the Pass / Fail criterion for the Fatigue Design Margin for products, is proposed in this study. The procedure is applied to evaluate the design margin criterion for a reciprocating compressor cylinder, which requires high reliability for safe operation. The Z score corresponding to the required reliability was scaled using the coefficients of variation, in order to evaluate the design margin criterion. The coefficients of variation include the variations due to material properties, material imperfections, load variations, load excursions, stress variations, stress analysis techniques etc. The coefficients of variation were evaluated based on actual data measured on a statistically significant sample size. The resulting design margins helped achieve a reliable product, while preventing the product from being over designed. While this paper describes the application of the method to a Reciprocating Compressor cylinder, the method may be applied to evaluate the design margin criterion for every component of the reciprocating compressor and in general, to any mechanical part subjected to fatigue loads. In addition to the Fatigue Design Margins, the Life Estimation methods quantify the life of product designs, in order to improve reliability and enhance product safety. This paper describes the application of a life estimation method to a Reciprocating Compressor cylinder.

1 Introduction

One of the primary failure modes for Reciprocating Compressors is a structural failure. Structural failures may adversely impact either a single component or a sub-system. Structural failures may be classified primarily into static failures and fatigue failures. Majority of the structural failures occur as a result of fatigue. Product designs should at the minimum be analytically validated to ensure that the cyclic loads resulting from normal operation do not lead to a fatigue failure. Section 4.0 of this paper, includes the procedure for conducting structural fatigue analyses on Reciprocating Compressors. The resulting Fatigue Design Margin should be equal to or greater than the pass / fail criterion determined for the component as per section 6.0 of this paper. This technical paper identifies a method for evaluating the Pass / Fail criterion for the Fatigue Design Margins for Reciprocating Compressors. When components are designed to last for a number of load cycles that are greater than the total number of load cycles that the component will be subjected to for its entire planned useful life, the result is a well-designed product. Section 7.0 of this technical paper identifies a method for estimating the life of Reciprocating Compressors.

2 Background

According to the Goodman Fatigue Locus, when ferrous components are designed such that the Fatigue Design Margin equals to 1, the components are expected to have an “infinite life”. However, in reality, components have part to part variation in structural properties, due to the factors outlined in Section 5.0. Hence components must be designed such that the Fatigue Design Margin is greater than 1, in order to ensure that the entire population of components has a Fatigue Design Margin greater than or equal to 1. Components designed to a Fatigue Design Margin lower than 1, are not expected to have an “infinite life”. Refer to *Figure 1*.

While a lower Fatigue Design Margin increases the risk of failure, a redundantly high Fatigue Design Margin results in over designed components. Over designed components are often priced to an uncompetitive piece part cost, as well as lower profit margins. Refer to *Figure 2*.

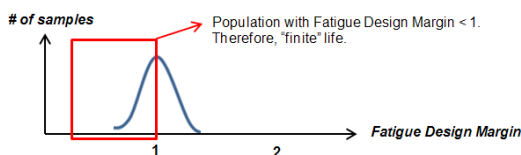


Figure 1: Fatigue Design Margin = 1

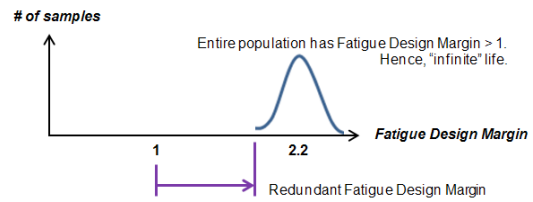


Figure 2: Redundant Fatigue Design Margin

3 Scope

The method proposed in this paper applies to all components of Reciprocating Compressors. This paper applies the proposed method to a ductile iron cylinder (Figure 3) as an example, in order to illustrate the method. This paper describes only the method and does not reveal information such as the stresses generated, the level of reliability for components and the product lifing strategy. Lifing a product refers to designing the product to last a certain number of load cycles. The method proposed in this paper applies, as long as the fatigue analyses are conducted as outlined in section 4.0.

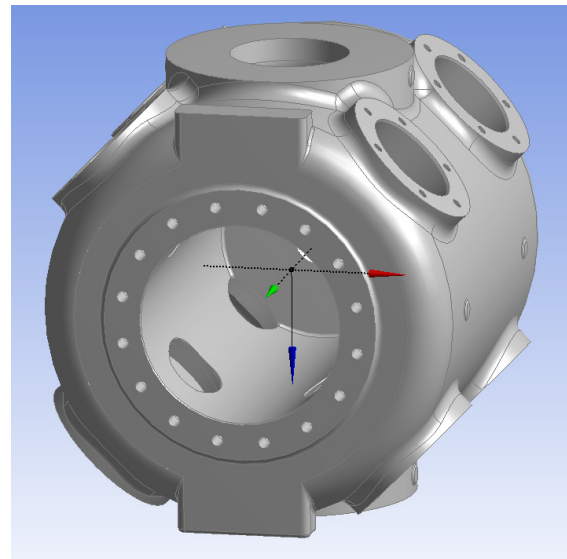


Figure 3: Typical Ductile Iron Cylinder

4 Fatigue Analysis Procedure

The validation plan for the product depends on several factors such as the failure modes, severity of failure, effects of failure, production volumes, required reliability and the overall product strategy. Product designs are often refined using relatively

SESSION CALCULATION 1

Method for Evaluating the Pass / Fail Criterion for the Fatigue Design Margin & Life Estimation for Reciprocating Compressors by: Ani Ketkar, Federico Pamio, Mark Patterson, GE Oil & Gas

inexpensive analytical validation, followed by physical tests. The analytical validation must entail structural fatigue analyses, in order to evaluate the component's Fatigue Design Margin. The structural fatigue analysis shall be conducted in the order listed in the following sections.

1. Identify the typical operating range or the duty cycle of the component. In addition, evaluate the load excursions if any, the magnitude of the excursion and the frequency. Using this data, evaluate the maximum load, the intermediate load steps and the minimum load acting on the component during its planned useful design life.

2. Conduct a static structural analysis, using the maximum load, the intermediate load steps and the minimum load acting on the component. Calculate the Maximum Principal Stress for each load step. The static structural analysis may be conducted using a commercially available Finite Element code or using handbook calculations. When a component is subjected to cyclic loads, cracks may initiate and propagate along the grain boundaries¹. Cracks propagate due to cyclic tensile stresses. Cyclic compressive stresses do not contribute to crack propagation. Hence the Maximum Principal Stresses should be evaluated and considered as inputs for step 3 below.

3. Using the maximum Principal Stresses, evaluate the Mean Stress and the Alternating Stress².

4. Evaluate the Endurance Limit for Steels and Ductile Irons. Evaluate the Fatigue Strength at 10¹⁰ cycles for Grey Cast Iron and non-Ferrous metals. The Endurance Limit or the Fatigue Strength at 10¹⁰ cycles may either be leveraged from in house fatigue test data or estimated by scaling the Ultimate Tensile Strength of the material using the Endurance limit modification factors².

5. Calculate the Fatigue Design Margin using either the Modified Goodman Diagram or the Modified Goodman formula².

6. The Fatigue Design Margin shall be equal to or greater than the Pass / Fail criterion determined for the component.

5 Sources of Acceptable Variation

Standard quality inspections are conducted on production parts, in order to ensure that the product conforms to the drawing, before being shipped to the customer. However, conforming material displays part to part variations, within the acceptable specification limits. The factors contributing to the

part to part variations in the structural integrity of the components are listed below:

1. Variations in the ultimate tensile strengths due to,
 - I. Variations in the chemical composition and microstructure and,
 - II. Material defects and casting imperfections such as porosity, inclusions, shrinkages and voids.
2. Variations in the Geometry due to part-to-part variations within the tolerance zone.
3. Variations in the applied loads due to,
 - I. Load excursions and,
 - II. Variations in the delivery system, metering and control.
4. Variations in the actual stress generated during operation relative to the predicted analytical stress due to,
 - I. Estimations involved with conducting the stress analyses such as, FEA Mesh Sensitivity, simplified boundary conditions, use of empirical coefficients etc.
 - II. Potential casting defects such as porosity, inclusions, shrinkages and voids, which are typically not accounted for as a part of the stress analysis.
5. Variation due to the difference in the applied stress state to the allowable strength. The margin for error increases, when the failure theory compares a dissimilar applied stress state, to an allowable strength.

6 Method to evaluate the Pass / Fail Criterion

The method for evaluating the Pass / Fail criterion for the Fatigue Design Margin, follows "Appendix C – Factor of Safety as a Design Variable" from "The Mechanical Design Process" by David Ullman³, which derives the formula in Figure 8, based on physical and statistical interactions between the material strengths and the stresses generated.

The Pass / Fail criterion must be evaluated as per the steps listed below³:

1. Evaluate the Reliability required for the product in order to meet the safety, reliability and the end-user requirements.

$$\text{Reliability required} = \frac{\text{Failures Allowed}}{\text{Million Opportunities}}$$

The required Reliability must take into consideration the Effects of a Failure. For safety related components, the Probability of Failure shall be extremely low to none. Since Reliability is 1 minus

Method for Evaluating the Pass / Fail Criterion for the Fatigue Design Margin & Life Estimation for Reciprocating Compressors by: Ani Ketkar, Federico Pamio, Mark Patterson, GE Oil & Gas

the Probability of Failure, the Reliability for safety related components shall be very high. The short term process performance is quantified by the short term Z score ($t_{z=0}$). Evaluate the Z score for the Reliability required, using the corresponding defects per million opportunities, as per step 2 below. The required Reliability for all components, should meet the technical objectives and the product strategy of the organization as well as the applicable regulations.

2. Evaluate the Z score corresponding to the required Reliability, from a standard normal distribution table. For example, the cylinder is a safety related component. Hence the required Reliability shall be very high. For example, a Reliability of 0.9998 indicates that 2 out of 10,000 cylinders may not have infinite life. The corresponding Z - score is 3.49, as illustrated in Figure 4.

z	.00	.01	.02	.03	.04	.05	.06	.07	.08	.09
3.4	.9997	.9997	.9997	.9997	.9997	.9997	.9997	.9997	.9997	.9998

Figure 4: Standard normal distribution table

3. Evaluate the Allowable Strength Coefficient of Variation by conducting tensile tests on a statistically significant sample size. Data from archived material certifications may be leveraged, as long as the supplier and the manufacturing processes stay unchanged. For example, if statistically significant samples for ductile iron cylinders have a measured mean ultimate tensile strength of 69640 psi, with a standard deviation of 3544 psi, the Allowable Strength Coefficient of Variation is 0.0509, calculated using the formula below.

$$\text{Allowable Strength COV} = \frac{\text{Standard Deviation}}{\text{Mean Strength}}$$

4. Evaluate the Geometry Coefficient of Variation at the critical location(s) on the component, using the nominal dimension and the tolerance specification. For example, if the nominal dimension at the critical location is 0.375 inches with a tolerance zone of 0.01 inches, the Geometry Coefficient of Variation is 0.0089, calculated using the formula below.

$$\text{Geometry COV} = \frac{\text{Tolerance zone}}{\text{Nominal dimension}}$$

5. Evaluate the Applied Load Coefficient of Variation, taking into consideration, the potential load excursions and variations in the delivery system, metering and control. For example, if the maximum allowable working pressure (MAWP) for a cylinder is 10% greater than the maximum working pressure (MWP), the Most Likely Load is 100%, the Pessimistic Load is 110% and the Optimistic Load is

95%. The Applied Load Coefficient of Variation is calculated to be 0.0248, using the formulae listed in Figure 6³. Please note that the MWP is the maximum gas discharge pressure during normal operation and the MAWP is the pressure excursion at which the pressure relief valves ruptures.

$$\begin{aligned} \bar{m} &= \frac{1}{6}(o + 4m + p) \\ \rho &= \frac{1}{6}(p - o) \\ \frac{\rho}{\bar{m}} &= \frac{p - o}{o + 4m + p} \end{aligned}$$

Where,
 “o” is the optimistic estimate
 “m” is the most likely estimate
 “p” is the pessimistic estimate
 “m” is the mean
 “ρ” is the standard deviation

Figure 5: Applied Load COV

6. Evaluate the Stress Analysis Coefficient of Variation, taking into consideration the potential variation in actual stress generated during operation, with respect to the predicted analytical stress. The analytical stress may vary from the actual stress, due to certain approximations and limitations involved with conducting stress analyses. Few examples of these limitations are the assumed homogenous material in the FE model free of material defects, a perfectly refined FE mesh, perfectly realistic boundary conditions etc. The Stress Analysis Coefficient of Variation must account for potential increase in actual stress generated due to potential material imperfections such as porosity, inclusions, shrinkage and voids for castings and inclusions inside forgings. The porosity and voids inside the wall membrane create stress concentrations, which are detrimental to the life of the component. For example, if the cylinder has an analytically predicted stress (Most Likely Stress) of 100%, potentially an actual operating stress (Pessimistic Stress) of 170% and an Optimistic Stress of 95%, the calculated Stress Analysis Coefficient of Variation is 0.1128, calculated using the formulae listed in Figure 5³.

7. Evaluate the Failure Analysis Technique Coefficient of Variation, due to the difference in the applied stress state relative to the allowable strength. The margin for error increases, when the failure theory compares a dissimilar applied stress state to an allowable strength. Values for the Failure Analysis Technique Coefficient of Variation are recommended in Figure 6³. For example, if a cylinder is analytically validated as per the procedure outlined in section 4.0, the Failure Analysis Technique Coefficient of Variation is 0.1.

Method for Evaluating the Pass / Fail Criterion for the Fatigue Design Margin & Life Estimation for Reciprocating Compressors by: Ani Ketkar, Federico Pamio, Mark Patterson, GE Oil & Gas

The formula in Figure 11 is determined from a linear approximation of constant life diagrams, as shown in Figure 12⁴.

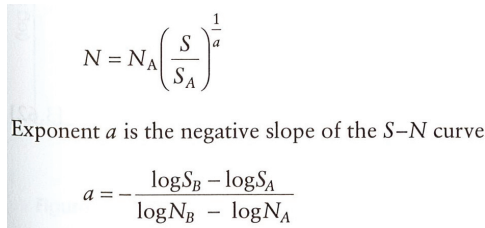


Figure 12: Constant life stress correlation

3. Evaluate the life in years, by dividing the cycles to failure by the cycle expected per year, based on the duty cycle of the machine. For the example cylinder from steps 2 & 3, the life in years is 1.27E6 years, based on a maximum speed of 1500RPM and assuming continuous operation of the reciprocating compressor.

Figure 13 indicates a relationship between the Fatigue Design Margin and the Life of a component in Years, for Fatigue Design Margins between 1 and 2.

Figure 14 plots the alternating stress as a function of cycles, using the expression in Figure 10, modified for an $N_B = 10^7$.

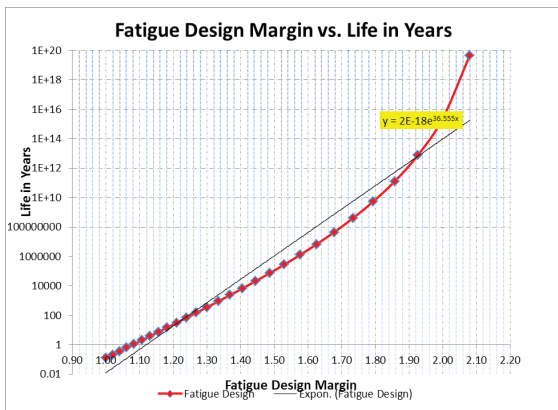


Figure 13: FDM & Life correlation

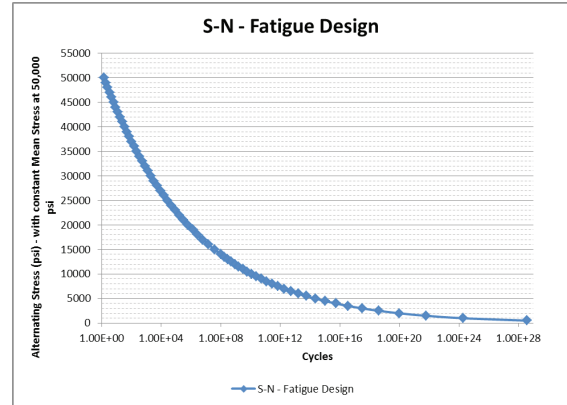


Figure 14: Stress Life estimation

8 Conclusion

The Pass/Fail criterion for assessing the Design Margin of a product should be evaluated by measuring and statistically quantifying the part to part variations, as well as evaluating the cumulative effects of variation. The method outlined in this report, lists the sources of variation, identifies a method to statistically quantify the variations and identifies a method to evaluate the cumulative effects of variation, in order to evaluate the Pass / Fail criterion. The Pass / Fail criterion and the Lifting criterion must take into consideration the effects of failure, the applicable regulations and the overall product line strategy, in order to strike an optimal balance between reliability, cost and end user satisfaction.

References

1. Callister, W. D. (2001). Fundamentals of Material Science and Engineering. New York, NY.
2. Shigley, J. E. (2001). Mechanical Engineering Design. New York, NY.
3. Ullman, D. G. (2003). The Mechanical Design Process. New York, NY.
4. Zahavi, E. (1996). Life Expectancy of Machine Parts. Boca Raton, FL.

Improvement of the Cooling Performance of a Reciprocating Compressor Cylinder by a Conjugate Heat Transfer and Deformation Analysis

by:

Francesco Balduzzi, Giovanni Ferrara

Research Fellow, Assistant Professor

University of Florence, Italy

balduzzi@vega.de.unifi.it, ferrara@vega.de.unifi.it

Riccardo Maleci, Alberto Babbini

Lead Engineer / Technologist

GE Oil & Gas – Nuovo Pignone

Florence, Italy

riccardo.maleci@ge.com, alberto.babbini@ge.com

**9th Conference of the EFRC
September 11th / 12th, 2014, Vienna**

Abstract:

The cooling system of a reciprocating compressor has a big impact on the total cost of the unit, depending on the total head and the capacity of the system. Considering that current regulations API618 for reciprocating compressor impose the refrigeration of the cylinder, cooling water passages inside cylinder shall be designed to limit as much as possible thermal dilatation and to avoid hot spots, while lowering down capacity and pressure losses.

In this paper, a conjugate heat transfer (CHT) analysis on a double-acting water-cooled reciprocating compressor cylinder is presented. The aim of the study was the simulation of simultaneous heat transfer in both the solid metal and the water circuit, where the conduction in the solid and the convection in the fluid are analysed concurrently. A detailed overview on some critical issues for the assessment of the proper boundary conditions for the metal body is given.

Two different geometrical configurations of the refrigerating system were studied in order to improve the cooling performance. Moreover, a thermal deformation analysis to check the induced dilatations was carried out. Finally, the most suitable geometrical layout was assessed and a sensitivity analysis was performed on the influence of the mass flow rate on the cooling efficiency.

1 Introduction

The presence of a cooling system in a reciprocating compressor cylinder has several advantages: avoids the presence of cold spots (that could cause condensation of gas); reduces the fresh gas heating due to hot cylinder body, improving volumetric efficiency; limits the thermal expansion of the metal parts and therefore the thermal stresses on the cylinder. Together with these advantages, there are also negative aspects: needs a cooling console, that increasing plant and lifecycle costs; its complex shape complicates casting and increases its cost; reduces space available for gas chambers.

Traditional shape of the water jacket comprises an annular chamber all around the hole for rod packing with the aim of cooling the packing itself. The use of piston rod packing with an integrated cooling system is increasing in the past years, and it is nowadays feasible and convenient for most of the applications. The annular chamber in the water jacket has therefore lost its primary scope.

This work shows one of the first applications of the investigation method realized by the authors and described in detail in a separate paper¹.

The analysis was focused on the evaluation of the effects of the removal of the annular chamber on the water jacket in terms of heat exchange, metal temperatures and thermal deformation of the cylinder.

2 CHT model

2.1 Simulation approach

Three-dimensional numerical simulations were carried out for a double-acting water-cooled reciprocating compressor cylinder. The heat transfer process was modelled by means of a steady-state *conjugate heat transfer* (CHT) approach, i.e. a combined simulation of the water-circuit flow field and the thermal conduction inside the solid metal. Figure 1 shows in detail both the water and metal parts of the analysed geometry. The different regions of the water body are also highlighted, as well as the inlet and outlet sections.

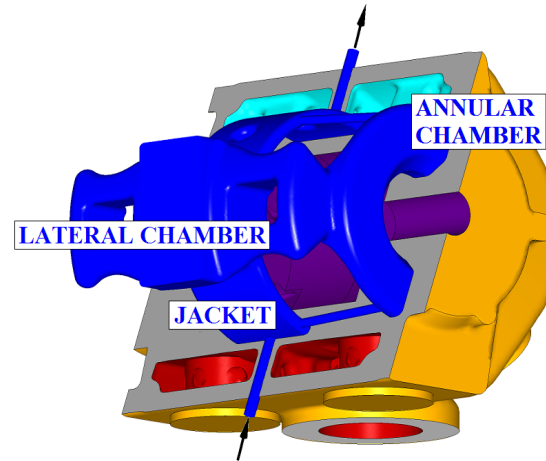


Figure 1: Water body (blue) and half section of the metal body – Surfaces in orange (external), violet (compression chamber), red (discharge ducts) and light blue (suction ducts)

The coupling between the two separate simulation domains was performed by the introduction of a *fluid-solid interface*, which ensured the conservation of the heat flux between the water body and the metal body.

Thermal boundary conditions were imposed for all other metal surfaces, in order to account for the various heat transfer phenomena responsible of the heat generation/removal inside the machine:

- Forced convection inside suction and discharge gas ducts;
- Natural convection on the external surface;
- Forced convection and heat generated by friction inside the compression chamber.

In the matter of heat transfer related to friction between piston and liner, the heat flux q through the boundary surfaces was known from experimental data.

Regarding the heat transfer related to a generic convective process, the situation is more complex. The metal temperature can be calculated by evaluating the heat flux q through the boundary surfaces, defined by Eq. 1:

$$q = HTC \cdot (T_w - T_{bulk}) \quad (1)$$

where T_w is the unknown metal temperature at the wall surface, HTC is the convective heat transfer coefficient between fluid and metal and T_{bulk} is the undisturbed fluid temperature. The values of HTC and T_{bulk} to be imposed as boundary conditions for the surfaces of the metal body, were evaluated through a proper modelling of all the convection processes.

For the external natural convection, the heat transfer

SESSION CALCULATION 1

Improvement of the Cooling Performance of a Reciprocating Compressor Cylinder by a Conjugate Heat Transfer and Deformation Analysis *by: F. Balduzzi, G. Ferrara, UniFI; R. Maleci, A. Babbini GE Oil & Gas*

coefficients were determined with a simplified method, thanks to the availability in literature of several empirical correlations relative to heat transfer for basic geometries. McAdams correlations² were used, which provide the Nusselt-number (Nu) as a function of the Rayleigh-number (Ra) for vertical plates (Eq. 2) and horizontal plates, upper surface hot (Eq. 3) and lower surface hot (Eq. 4).

$$Nu = 0.13 \cdot Ra^{1/3} \quad (2)$$

$$Nu = 0.15 \cdot Ra^{1/3} \quad (3)$$

$$Nu = 0.27 \cdot Ra^{1/4} \quad (4)$$

In a first approximation, this simplification can be considered suitable since the amount of heat transfer with the ambient represents roughly 5-7% of the total heat exchange.

Concerning the convection inside the compression chamber, Fagotti³ showed that best results are provided by Annand correlation⁴ for the Nusselt-number, expressed as a function of the average piston speed (U_p) and the piston bore (B) as shown in Eq. 5:

$$Nu = A \cdot \left(\frac{\rho U_p B}{\mu} \right)^b \quad (5)$$

Therefore, the correlation was used inside a specific 0-D numerical model of the compression cycle in order to obtain a representative trend of in-cylinder HTC and temperature as a function of the displacement (Figure 2). In the paper, the values of HTC and temperature are reported in a dimensionless form, i.e. as a function of the maximum in-cylinder value ($HTC^* \equiv HTC/HTC_{max}$) and the gas discharge temperature ($T^* \equiv T/T_d$) respectively. An average effective value of both HTC^* and T^* was computed from the time-dependent functions to be adopted for the steady-state CHT simulations.

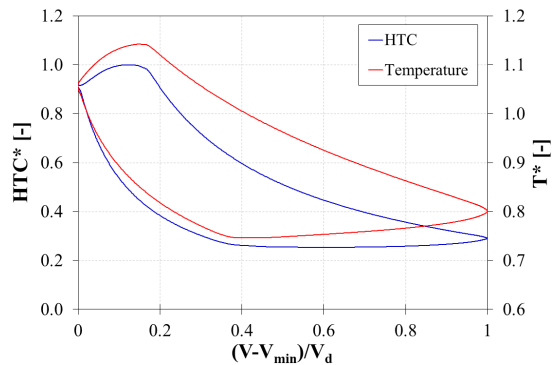


Figure 2: Output of the 0-D model – Trends of HTC and temperature

In case of internal forced convection inside suction and discharge gas ducts, specific 3-D CFD simulations

were carried out in order to guarantee a more accurate estimation of the actual distributions of HTC and T_{bulk} . Figure 3 shows an example of the results of a steady-state simulation of the gas flow inside the suction geometry: the resulting HTC field has to be patched as a boundary condition for the CHT simulation. The assessment and validation of the numerical settings for the 3-D CFD simulations of the working gas is not here discussed. All the details for the sensitivity analysis on the simulation parameters can be found in the authors' recent works^{5,6,7}.

Globally, the proposed approach is summarized in Figure 4, where all the boundary conditions for the simulation of the conjugate heat transfer between the solid cylinder body and the fluid cooling circuit are indicated.

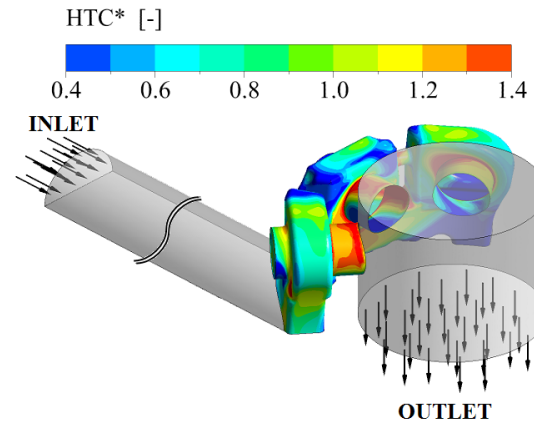


Figure 3: Results of the 3-D CFD simulation of the suction duct – Distribution of the Heat Transfer Coefficient on the walls

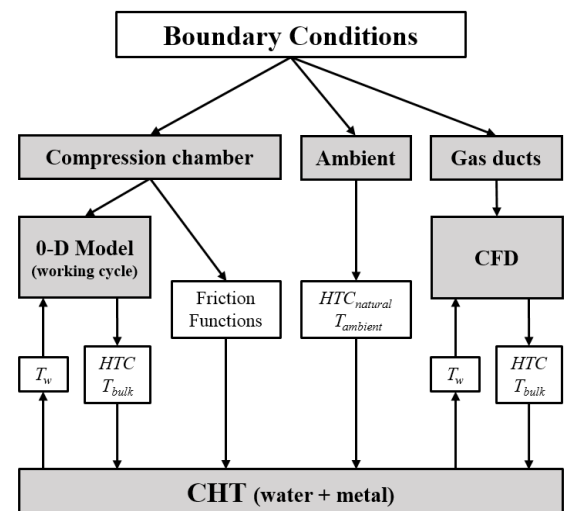


Figure 4: Conceptual scheme for the determination of the boundary conditions for the Conjugate Heat Transfer simulation

2.2 Numerical setup

The commercial software ANSYS CFX was used in performing the 3-D steady-state RANS (*Reynolds-Averaged Navier-Stokes*) simulations. The standard $k-\omega$ closure model was adopted to predict the complex turbulent structure of the confined flow, along with the automatic treatment in the near-wall region. The effect of gravity was accounted for by activating the buoyancy model since the low fluid velocity and the large volumes are responsible of the instauration of free convection.

Velocity-inlet and pressure-outlet boundary conditions were supplied for the simulation of the water flow. The water inlet temperature (T^*) was set to 80.4% of the gas discharge temperature (T_d). HTC and T_{bulk} distributions were imposed on all the surfaces of the solid region, except for the walls in contact with the moving piston and rod, where an additional heat source was imposed accounting for friction heating.

A tetrahedral unstructured grid was generated for the computational mesh of both the metal and the water body. In addition, in the latter case, an extrusion of 16 prism layers was placed adjacent to the viscous wall in order to resolve the thermal boundary layer. The first cell at any surface point was sized such that $y^+ \sim 1$ (scaled normal distance from the wall) whereas grids away from it were expanded at a rate of 10%.

2.3 Study cases

The investigated geometry for the CHT analysis included the water circuit and all the solid components of a double-acting cast iron cylinder with a bore of 770 mm. The main characteristics of the studied compressor are resumed in Table 1.

Table 1: Compressor specifications – Geometry and operating conditions

Parameter	Units	Value
Bore	[mm]	770
# Suction Valves	[-]	3 + 3
# Discharge Valves	[-]	3 + 3
Suction Temperature (T^*)	[-]	77.95%
Suction Pressure	[Pa]	1200000
Discharge Pressure	[Pa]	2700000

The domain is oriented such as the water enters from an inlet pipe located on the bottom part of the cylinder, which is the side where the pressurized hot gas is discharged. At the end of the inlet duct, the water flows into the water jacket surrounding the

cylinder walls; two lateral horizontal chambers are then addressed to the isolation of the hot side of the cylinder from the cold side.

In the *original* configuration, both the jacket and the lateral chambers are connected to an annular chamber, on the crank-end side, for the cooling of the connecting rod packing. A *modified* version was also analysed, which is analogous to the *original*, except for the absence of the annular chamber. Figure 5 shows the simulation domain for both configurations.

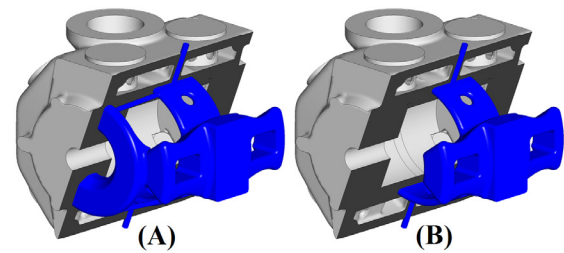


Figure 5: Simulation domains for the original (A) and modified (B) configurations

In order to evaluate the effect of the reduction of the water volume on the heat removed by the cooling circuit, the two configurations were tested under the same nominal mass flow rate. Afterwards, a specific sensitivity analysis on the effect of the flow conditions was carried out on the *modified* configuration: three additional regimes were studied by varying the imposed mass flow rate. In particular, the three cases were obtained by multiplying the nominal inlet velocity by the factors 0.5, 2 and 4.

3 Results

3.1 Geometry modification

In this section, the numerical results of CFD simulations are analysed and compared considering the water temperature variation (ΔT) and the amount of heat exchange (Q). The numbered planes highlighted in Figure 6 refer to the sampling cross-sections where the water temperature values are calculated in order to split the contributions of the various parts of the cooling circuit:

- Section 0-1: inlet duct;
- Section 1-2: water jacket on the discharge side (left path);
- Section 1-3: water jacket on the discharge side (right path);
- Section 2-4: lateral chamber (left path);
- Section 3-5: lateral chamber (right path);
- Section 4-6: water jacket on the suction side (left path);
- Section 5-6: water jacket on the suction side (right path).

SESSION CALCULATION 1

Improvement of the Cooling Performance of a Reciprocating Compressor Cylinder by a Conjugate Heat Transfer and Deformation Analysis *by: F. Balduzzi, G. Ferrara, UniFI; R. Maleci, A. Babbini GE Oil & Gas*

Water temperature variation and heat are reported in a dimensionless form, i.e. as a function of the global values for the original configuration: $\Delta T^* \equiv \Delta T / \Delta T_{0,orig}$ and $Q^* \equiv Q / Q_{T,orig}$.

Upon examination of Figure 7, where the water ΔT^* is reported as a function of the sampling cross-sections for both geometrical layouts (*original* and *modified*), some useful indications can be provided. The overall raise in the water temperature is reduced by 2.5% in the *modified* case, due to the reduction of the extent of the metal-water interface. Notwithstanding this, the ΔT^* in sections 1-2 and 1-3 is higher in the *modified* case, since a higher amount of water is flowing through the water jacket, as shown in Figure 8. In particular, an increase of 9% in the velocity of the water flowing through the right path is observed, while no significant variations are shown in the left path.

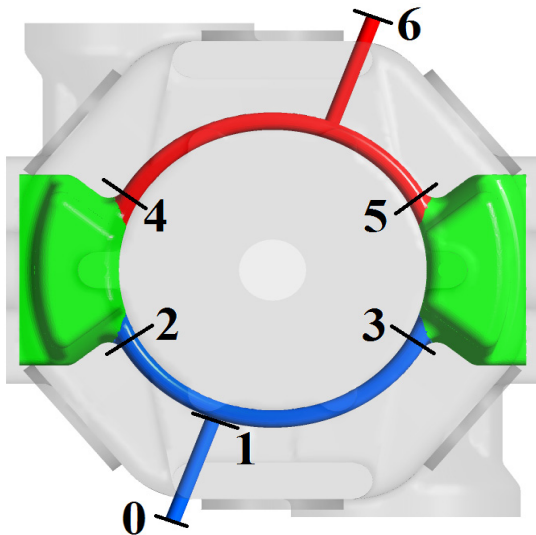


Figure 6: Location of the sampling cross-sections for the evaluation of relevant quantities in the water domain

As a result, the heat exchange in the water jacket is markedly intensified (Figure 9), thanks to the higher velocities, which determine a more efficient cooling of the cylinder liner walls. Moreover, it can be noticed that the jacket is responsible of the greatest contribution to the global heat transfer, in the *original* case, while the annular chamber has a minor impact.

In light of the above consideration, the global heat transfer is slightly lower (-2.5%) for the *modified* version, as reported in Figure 10, despite a large reduction in the occupancy volume (-24%).

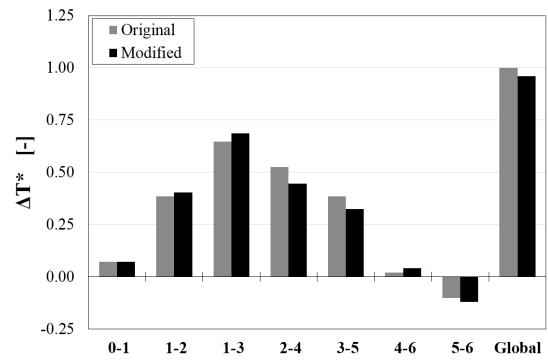


Figure 7: Water temperature variation as a function of the sampling cross-sections for both geometrical configurations

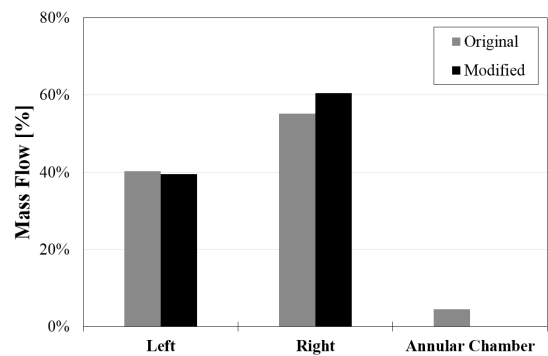


Figure 8: Mass flow rate sharing between left path, right path and annular chamber

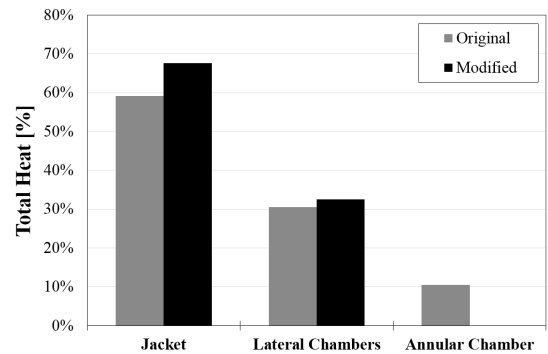


Figure 9: Heat transfer sharing between the surfaces of the water circuit

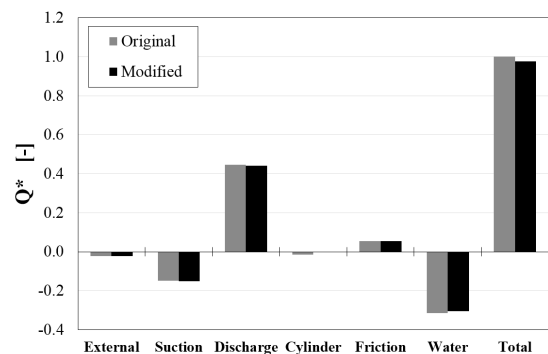


Figure 10: Contribution of each metal boundary with respect to the overall heat transfer

Improvement of the Cooling Performance of a Reciprocating Compressor Cylinder by a Conjugate Heat Transfer and Deformation Analysis *by: F. Balduzzi, G. Ferrara, UniFI; R. Maleci, A. Babbini GE Oil & Gas*

Therefore, the *modified* version is designed to better exploit the volume at disposal since the heat flux q (heat per unit surface) for the water body surfaces is 26.3% greater. In addition, it is worth pointing out that no significant changes were observed in the behaviour of the metal surfaces, from a global point of view.

The system responses were also compared from a local point of view: Figure 11 reports the metal temperature field over an oblique section for both geometries.

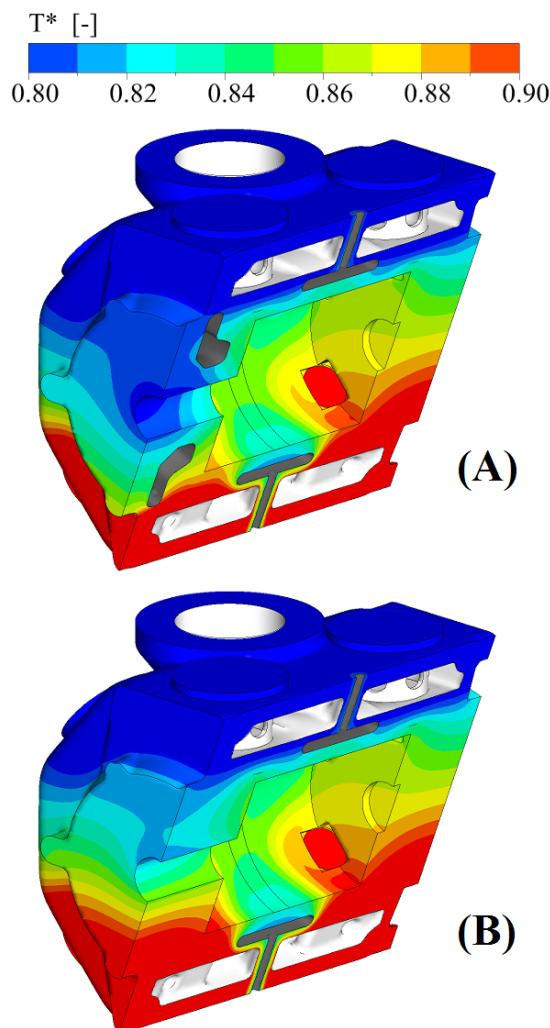


Figure 11: Temperature fields for the original (A) and modified (B) metal bodies

Although in the region of the connecting rod packing, lower temperatures can be found in the *original* configuration (the peak value on the packing surface is 11% lower), no significant differences can be appreciated in the rest of the domain. Moreover, highest temperature are located in the discharge side of the head-end, i.e. on the opposite side of the connecting rod. Globally, the volume of metal at a temperature (T^*) higher than 0.9 is increased by only 2.7%.

Upon examination of Figure 12, which shows a volume rendering of the water temperature field, some additional considerations can be made: the temperature reached by the water inside the annular chamber is almost 50% higher than the outlet temperature. The presence of a stagnation region inside the chamber does not permit an efficient use of all the volume at disposal of the cooling system. Indeed, only 5% of the overall mass flows through the annular chamber.

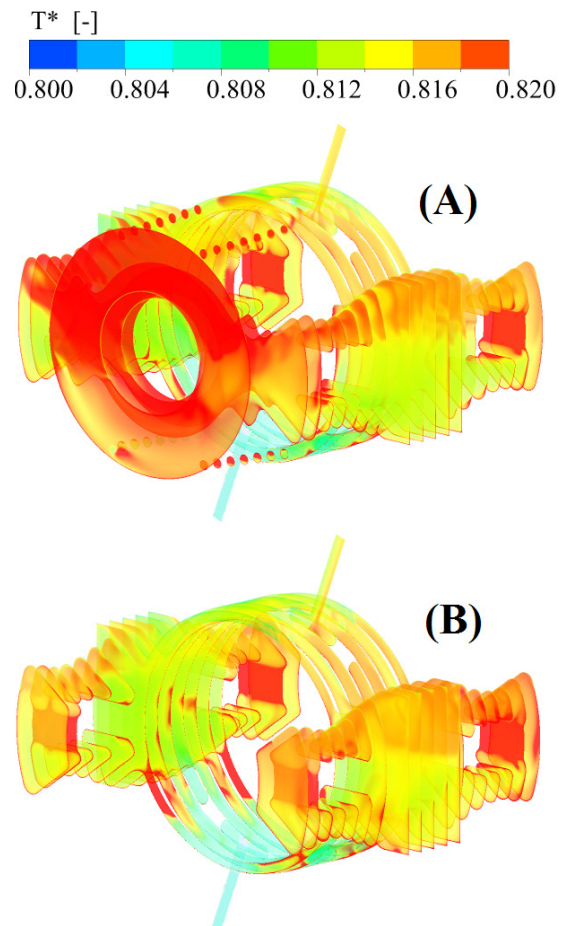


Figure 12: Temperature fields for the original (A) and modified (B) water circuits

The analysis was accomplished by performing a static structural analysis in order to evaluate the deformation of the metal due to the non-uniform temperature distribution.

The cylinder is constrained by a fixed support on the crank-end side and is sustained by a support on the bottom part of the head-end side, allowing only a displacement in the horizontal direction (Z).

Figure 13 shows the resulting deformation along the Z-axis for both configurations in a dimensionless form, i.e. as a function of the maximum displacement of the *original* case. As predictable, a variation of

the induced dilatations can be observed: in fact, even if in both cases the structure is subject to a bending strain, due to an expansion of the hot part five times bigger than the cold part, the largest displacement for the *modified* case was increased by 5%. Such a modification can be tolerated, also because low stresses are associated to these thermal loads.

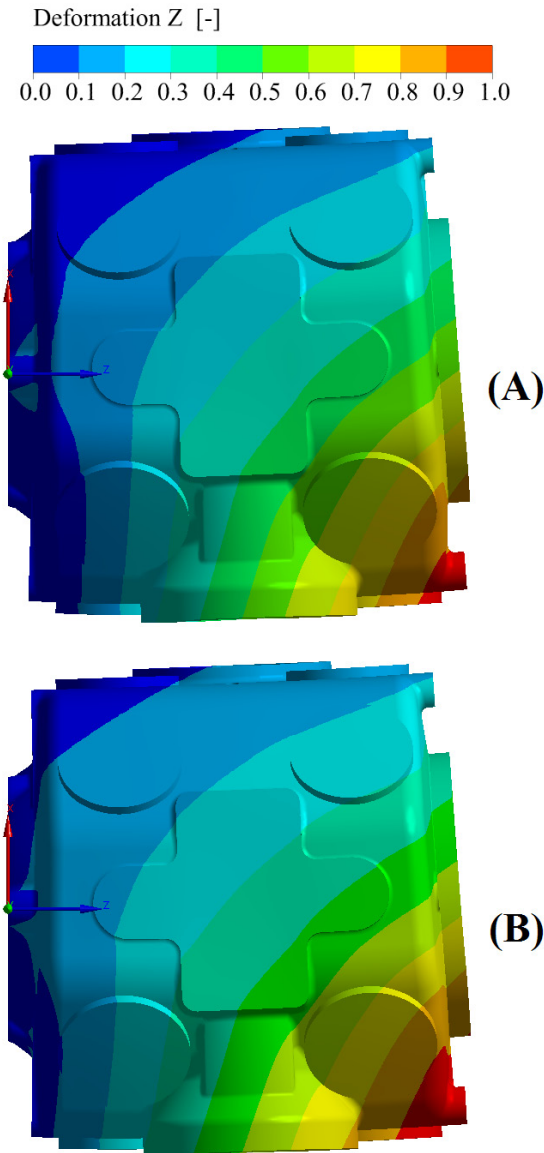


Figure 13: Metal displacement in the horizontal direction for the original (A) and modified (B) layouts

3.2 Mass flow rate

The main results of the analysis on the effects of the mass flow rate for the *modified* layout are summarised in Figure 14 and Figure 15. Water inlet temperature was kept constant throughout all the simulation cases. As expected, the raise in the water temperature is remarkably higher for the case at lowest mass flow rates, while the ΔT^* tends toward zero as the capacity is progressively doubled. It is worth noticing that the decrease is not linear and shows the same law in all

the considered sections: a doubled mass flow rate does not translate into a halved ΔT^* . As a result, the cooling potential of the circuit is reduced as the velocity is increased. This trend is also confirmed by Figure 16, where the heat absorbed by the water per unit mass flow rate is reported as a function of the mass flow rate itself in a dimensionless form, i.e. as a function of the reference value of the *original* configuration. An increase of the capacity directly translates into a decrease of the “efficiency”.

In more detail, comparing the two extreme cases, the enhancement in the heat absorbed by water is roughly 70% greater while the flow rate increase is 800%. This variation is substantially due only to an intensification in the heat transfer of the discharge gas ducts, while no significant influence can be observed in the response of the external surface, the compression chamber and the suction duct.

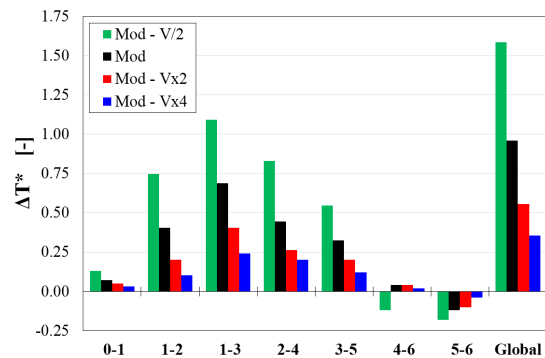


Figure 14: Water temperature variation as a function of the sampling cross-sections for different mass flow rates

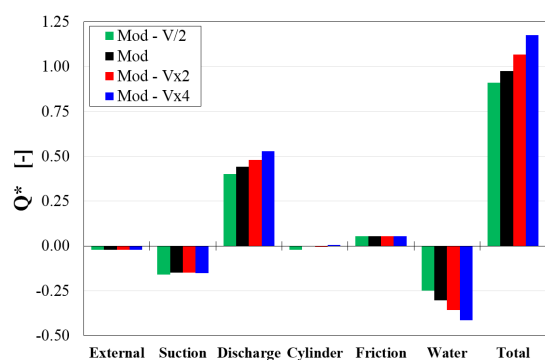


Figure 15: Contribution of each metal boundary with respect to the overall heat transfer for different mass flow rates

Improvement of the Cooling Performance of a Reciprocating Compressor Cylinder by a Conjugate Heat Transfer and Deformation Analysis by: F. Balduzzi, G. Ferrara, UniFI; R. Maleci, A. Babbini GE Oil & Gas

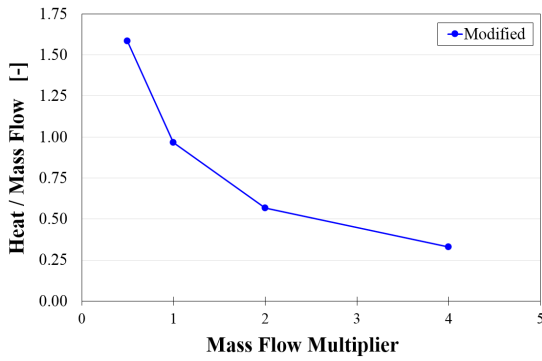
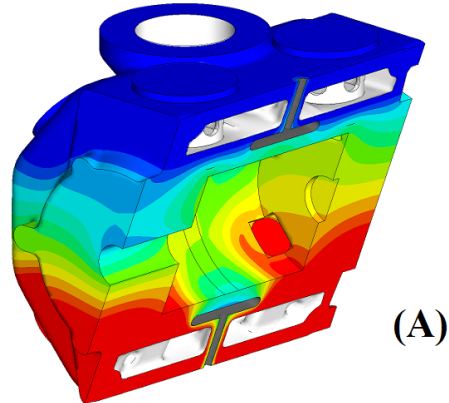
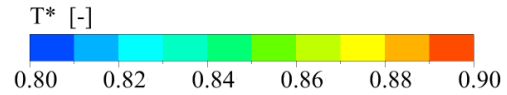


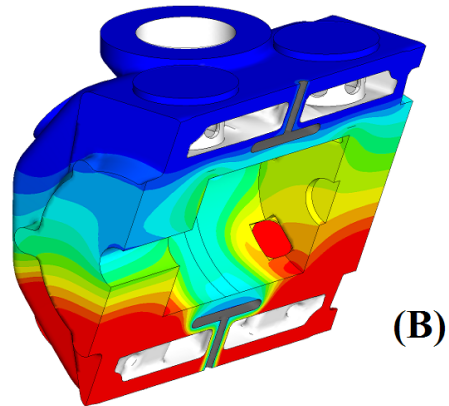
Figure 16: Heat absorbed by water per unit mass flow rate as a function of the cooling capacity

Focusing the attention on these two operating conditions (lowest and highest mass flow rate), Figure 17 and Figure 18 lead to some interesting considerations. The metal temperature field is reported over two different oblique sections, the first one aligned with the water inlet and outlet ducts, the second one orthogonal in order to show a section of the lateral chambers. Temperatures are notably decreased on the hot side of the cylinder and on the compression chamber surface as the mass flow rate is increased. As a matter of facts, the volume of metal at a temperature (T^*) higher than 0.9 decreases by roughly 10%. On the other hand, the cold side is not significantly affected since the variation of the average temperature of the suction duct surface is below 0.5%. As a consequence, the volumetric efficiency would remain approximately constant.

Lastly, it is worth pointing out that the peak value of the metal temperature does not change as the water flow rate increases. This consideration implies that the cooling water does not have an influence on the temperature of the hot spots.

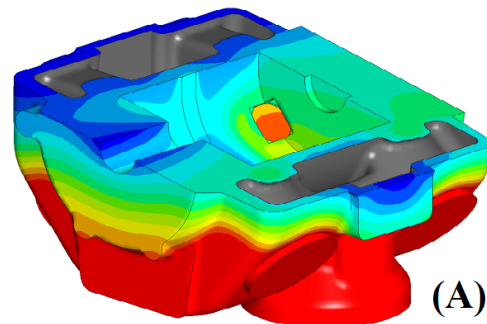


(A)

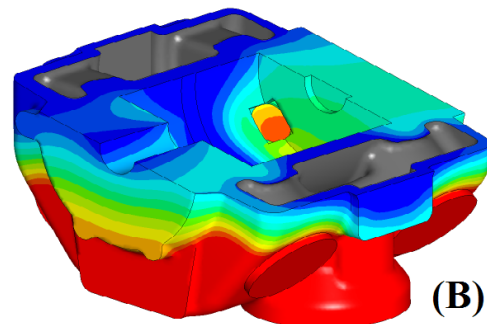


(B)

Figure 17: Temperature fields of the metal body for the lowest (A) and highest (B) mass flow rates



(A)



(B)

Figure 18: Temperature fields of the metal body for the lowest (A) and highest (B) mass flow rates

4 Conclusions

An in-depth analysis was carried out to evaluate the thermal state of a double-acting water-cooled reciprocating compressor cylinder. With this goal in mind, the first step of the analysis consisted in the assessment of the numerical approach for the conjugate heat transfer (CHT) analysis to characterize simultaneously the flow field of the cooling system and the heat conduction in the metal. As a second step, a modification of the water circuit geometry was proposed and the thermal response of both geometrical configurations (*original* and *modified*) was investigated. Finally, the *modified* version was studied under different flow conditions in a comparative analysis to optimize the refrigerating capacity.

The analysis showed that the elimination of the annular chamber surrounding the rod packing represents a profitable solution: indeed, the total heat removed by the water was almost unaltered while the complexity and the occupancy volume of the cooling system were greatly reduced (-24%). Therefore, higher efficiency was achieved thanks to this solution, with a higher heat absorbed per unit area (+26.3%). Furthermore, on the basis of a static structural analysis, the thermal expansion was checked and an increase of only 5% in the maximum displacement was found.

Focusing on the *modified* solution, the results at four different mass flow rates highlighted the opportunity of lowering as much as possible the capacity of the system, compatibly with the subsequent thermal expansion, since the increase of the heat absorbed by water is not proportional to the mass flow rate growth.

5 Acknowledgements

The authors wish to thank Prof. E. A. Carnevale for his guidance during this research and GE Oil & Gas for permission to publish the information reported in this paper.

References

- ¹ Balduzzi, F; Ferrara, G; Babbini, A; Maleci, R. (2014): Reciprocating compressor cylinder's cooling: a numerical approach using CFD with Conjugate Heat Transfer. Draft paper submitted in ASME PVP Conference, Anaheim.
- ² McAdams, W.H. (1954): Heat Transmission, 3rd Ed. McGraw-Hill, New York.
- ³ Fagotti, F; Todescat, M.L; Ferreira, R.T.S; Prata, A.T. (1994): Heat transfer modeling in a reciprocating compressor. Int. Compressor Eng. Conference at Purdue, West Lafayette, USA, paper ID 1043.
- ⁴ Annand, W.J.D. (1963): Heat Transfer in the Cylinders of Reciprocating Internal Combustion Engines. Proc. J. Mech. Engrs., 117(36), 973-996.
- ⁵ Balduzzi, F; Ferrara, G; Maleci, R; Babbini, A; Pratelli, G. (2014): A Parametric CFD Analysis of the Valve Pocket Losses in Reciprocating Compressors. Paper accepted for publication in J. of Pressure Vessel Technology.
- ⁶ Pratelli, G; Babbini, A; Balduzzi, F; Ferrara, G; Maleci, R; Romani, L. (2012) CFD Evaluation of Pressure Losses on Reciprocating Compressor Components. Proc. of the 8th Conference of the EFRC, Dusseldorf.
- ⁷ Balduzzi, F; Ferrara, G; Babbini, A; Pratelli, G. (2012): CFD evaluation of the pressure losses in a reciprocating compressor: a flexible approach. Proc. of the ASME 11th ESDA Conference, Nantes.

THINK GERMAN, ACT LOCAL.

DO YOU WANT TO GET MORE OUT OF YOUR RECIPI?



COMPRESSOR
SYSTEMS

REVAMP: THE BEST ECONOMICAL CHOICE TO GET MORE.

Process adaptation or optimisation? Bringing your recip compressor back to state of the art? Whichever parameter needs to be changed, trust NEA and NEAC Compressor Service when it comes to revamp or modernization of your machine. We have references on hand in all kind of applications with tailor-made solutions. NEA can apply its revamp experience to its 11 legacy and any other brands including risk assessment acc. to CE and ATEX directives. Revamp with "as-new guarantee".

Authorized OEM supplier for
reciprocating compressor lines:



Linde Demag HALBERG

Borsig
(recips built in Berlin
up to the end of 1995)



NEUMAN & ESSER
NEAC Compressor Service
www.neuman-esser.com

Contact me for requests world-wide:
Andreas Hahn
Product Manager Revamp & Modernization
Andreas.hahn@neuman-esser.de
Direct Phone: +49 2451 481-182



9th Conference of the EFRC

September 11th / 12th, 2014, Vienna

Root Cause Analysis of the Fatigue Failures of the Pulsation Dampers of a large Underground Gas Storage (UGS) System -105-

by: A. Eijk & D. de Lange TNO; J. Maljaars TNO, & Eindhoven University of Technology; A. Tenbrock-Ingenhorst & A. Gottmer, RWE

Vibrations in the Environment - Remedial Actions at a New Compressor Foundation -116-

by: Jan Steinhausen, KÖTTER; Poul Christian Larsen, DONG Energy

Optimized Robust Compressor Station Design Methodology -127-

by: Benjamin A. White, Barron J. Bichon, David L. Ransom, Eugene L. Broerman, Southwest Research Institute®



EUROPEAN FORUM
for RECIPROCATING
COMPRESSORS

SESSION PULSATION 1



Root Cause Analysis of the Fatigue Failures of the Pulsation Dampers of a large Underground Gas Storage (UGS) System

by:

A. Eijk & D. de Lange

TNO, Delft, NL

andre.eijk@tno.nl, dorus.delange@tno.nl

J. Maljaars

TNO, Delft, & Eindhoven University of Technology, NL

johan.maljaars@tno.nl

A. Tenbrock-Ingenhorst & A. Gottmer

RWE Gasspeicher GmbH, EPE Germany

Tenbrock-Ingenhorst@rwe.com, Andreas.Gottmer@rwe.com

**9th Conference of the EFRC
September 11th / 12th, 2014, Vienna**

Abstract

Two large identical 6-cylinder Ariel JGB/6 reciprocating compressors each of 7.5 MW, are used for an underground gas storage system (UGS) plant of RWE Gasspeicher GmbH located in Epe, Germany. The system is in operation since 2005. In 2011 several internal parts (baffle plates and baffle choke tubes) of the pulsation dampers were broken.

TNO has carried out a Root Cause Analysis (RCA) and it was shown that the failures were caused by a combination of bad manufactured welds, too high thermal (cyclic) stresses caused by heating up and cooling down the system several times a day and by too high dynamic stresses caused by vibrations.

The paper will give a detailed overview of the RCA and the proposed measures to avoid these failures.

1 Introduction

This chapter provides an overall introduction to the system, the acoustic dampers, the observed failures and finally the performed root cause analysis.

1.1 System description

Two large identical 6-cylinder Ariel JGB/6 reciprocating compressors each of 7.5 MW, are used for an underground gas storage system (UGS) plant located in Epe, Germany.

The compressors run at a variable speed range from 400 till 750 RPM. The three cylinders of each stage have a common suction and discharge damper. The compressors can be operated at a wide range of operating conditions, such as variable suction and discharge pressures, 2-stage mode during gas storage, 1-stage mode during gas withdrawal, capacity control by speed variation and valve lifters on the head end of the 1st stage cylinders.. The suction pressure varies between approximately 40 and 70 Bara, while the discharge pressure can vary between approximately 90 and 220 Bara. Besides the normal two-stage mode during gas storage, the compressors can also be operated in a one-stage mode (during gas withdrawal). The capacity of the compressors is controlled by speed variation and by valve lifters on the head end side of the 1st stage cylinders. Plant operations are done based on seasonal- as well as day-to-day basis following the gas demands or trading opportunities. Therefore, an excellent flexibility, availability and reliability of the plant is obliged. A photo of the 1st stage side of the reciprocating compressor is shown in Figure 3.

1.2 Damper description

One of the most important parts in the design of the compressor system to keep the vibration and cyclic stress levels within acceptable levels, is the design (volume, location of nozzles etc.) of the pulsation dampers. From the acoustic analysis it was concluded that an acoustic filter consisting of a vessel with internal baffles and baffle choke tubes, was the most optimum design. This design mitigates the pulsation levels and pulsation-induced shaking forces over the damper to acceptable levels according to the API Standard 618¹². All pulsation dampers have a similar layout.

A sketch of the suction 1st stage and discharge 2nd stage dampers is shown in respectively Figure 1 and Figure 2. A photo showing respectively the suction 1st stage and discharge 2nd stage damper is shown in respectively Figure 3 and Figure 4.

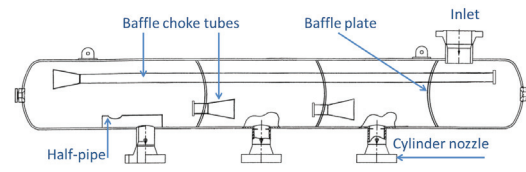


Figure 1 Sketch of the original 1st stage suction damper

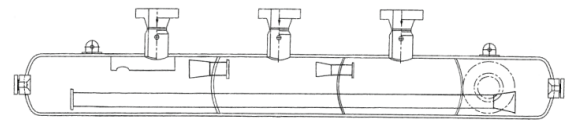


Figure 2 Sketch of the original 2nd stage discharge damper



Figure 3 Photo of the suction 1st stage damper



Figure 4 Photo of the discharge 2nd stage damper

1.3 Observed failures

The system was put into operation in 2005 and has been operated satisfactory up to 2011. Since 2011 a knocking noise was observed at certain process and compressor operating conditions. It was obvious that the knocking noise was originating from the

Root Cause Analysis of the Fatigue Failures of the Pulsation Dampers of a large Underground Gas Storage (UGS) System by: A. Eijk & D. de Lange TNO; J. Maljaars TNO, & TU/e; A. Tenbrock-Ingenhorst & A. Gottmer, RWE

discharge pulsation dampers. The pulsation dampers were inspected and it was found that several parts of the internal components of mainly the discharge 1st and 2nd stage were broken.

The photo in Figure 5 shows the failure of the baffle plate of the discharge 1st stage damper located at the outlet side of the damper. It can be seen clear that the complete baffle plate was broken and the plate was found on bottom of the damper. Figure 6 shows the broken baffle choke tube of discharge 1st stage damper located at the inlet side. The complete baffle plate was broken and was found on the bottom of the damper.

The photos in figure 7 show the broken brace of the baffle choke tube of the discharge 1st stage damper located at the inlet side. The complete bracing was broken off from the choke tube and damper wall. From visual inspection it was concluded that the quality of the weld was also very poor.

All broken parts were inspected and it was clear that all failures were caused by fatigue.

The discharge damper 2nd stage had similar failures. The inspection of the suction pulsation dampers showed cracks in the welds of the bracings of the baffle choke tubes for both stages.



Figure 5 Failure of the baffle plate of the discharge 1st stage damper (outlet side)



Figure 6 Broken baffle choke tube of discharge 1st stage damper (inlet side)



Figure 7 Broken brace of the baffle choke tube of the discharge 1st stage damper (inlet side)

1.4 Summary of the paper

A root cause analysis (RCA) was carried out by TNO to investigate the cause of the failures. For that purpose a detailed finite element model has been set up consisting of 3D solid elements, including detailed modelling of all welds.

All possible loads that could have caused the fatigue failures have been analysed. These loads were thermal loads due to heating up and cooling down the system several times a day, pulsation-induced shaking forces acting on the internal parts of the pulsation dampers, and mechanically induced vibrations of the compressor cylinders.

In order to accurately account for the combined effect of the two very different types of stress cycles, a fracture mechanics analysis was carried out to evaluate the stresses instead of using the S-N curves as provided in the applicable standards.

The paper summarizes the root-cause analysis performed by TNO, consisting of:

- Applied fatigue assessment method.
- Description of the used finite element models, focussing on modelling of the welds.
- Applied stress calculation method and allowable stresses.
- Results and conclusions.
- Recommendations to avoid fatigue failures.

2 Fatigue strength

This chapter discusses the fatigue strength assessment method used for the root cause analysis.

2.1 S-N curves

The S-N curve provides the fatigue strength of a specific type of detail. It provides a relationship between the logarithm of the stress range – $\log(\Delta\sigma_r)$ – and the number of cycles to failure – $\log(N)$. The stress range is the peak-to-peak value of a stress cycle. The S-N curves are determined experimentally and involve significant scatter. The design SN-curves in standards are often given as two standard deviations away from the average, corresponding to 97.7% probability of survival.

Different S-N curves are put forward in standards such as PD 5500:2006 for different types of (welded) joints. The typical inverse slope of the S-N curves of welded joints plotted on double logarithmic scale is $m_1 =$ approximately 3 for relatively large stress ranges, as indicated in Figure 8. At the so called ‘knee-point’ of the S-N curve, the inverse slope of the curve changes from m_1 to m_2 . The inverse slope m_2 depends on the type of spectrum. In PD5500:2006¹, as well as in most other standards with emphasis on welded joints, a slope $m_2 = m_1 + 2$ is assumed in case of a variable amplitude load. This is an approximation, in reality the slope m_2 depends on the type of spectrum.

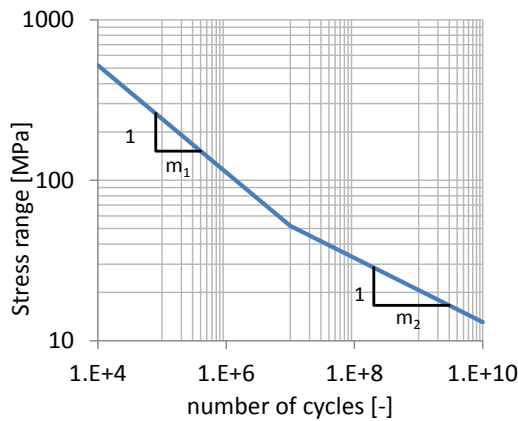


Figure 8 S-N curve with the definitions of the slopes m_1 and m_2 .

The slope $m_2 = m_1 + 2$ is generally considered a reasonable assumption for welded joints in case of a ‘complete’ stress range histogram, where all stress ranges are present with more or less increasing numbers for decreasing ranges as indicated with ‘spectrum A’ in Figure 9. For the stress range histogram of the pulsation dampers of the investigated system, however, this is a very conservative approximation. For the dampers, a large number of stress ranges occur that are far below the stress range at the knee-point of the curve (referred to as type II stress ranges, caused by mechanical vibrations) and a significantly smaller number of cycles occur above the stress range at the knee-point (type I stress ranges, caused by heating up and cooling down). The number of cycles with these stress ranges are referred to as n_{II} and n_I , respectively. There is no load case in between these two extremes. This is indicated with ‘spectrum B’ in Figure 9. According to the theory of fracture mechanics, the cycles with a stress range below the knee-point are unable to initiate a crack. They can only contribute to crack growth once the large stress cycles have resulted in a relatively large crack. In such a case, the resulting inverse slope of the S-N curve is generally larger than $m_2 = m_1 + 2$.

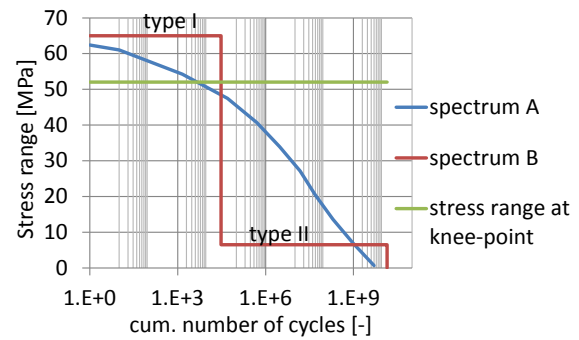


Figure 9 Two types of stress histograms

In principal, it is possible to use the conservative approximation of $m_2 = m_1 + 2$ for the design of a structure. However, in a root cause study, the actual response should be simulated as accurately as possible. For this reason, a more accurate fatigue life calculation is carried out using fracture mechanics for the critical details in this structure.

2.2 Fatigue life based on fracture mechanics

The fatigue life is determined using the TNO’s in-house developed software Fafam, which is based on the fracture mechanics standard BS 7910:2005⁷. The procedures and material properties used in the calculations are also adopted from this standard.

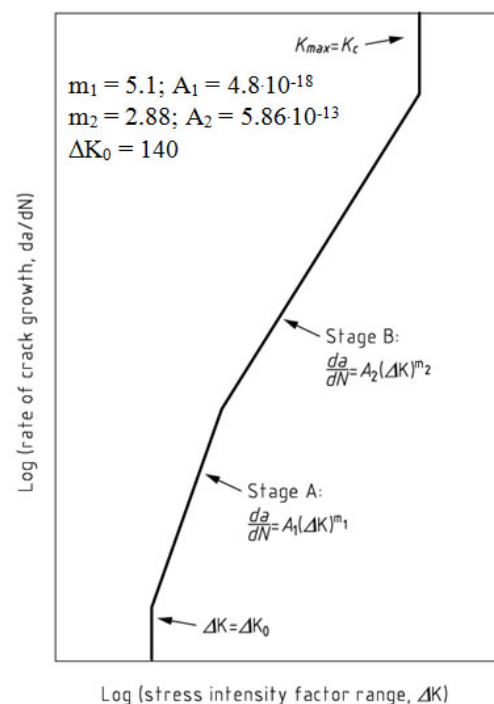


Figure 10 Average crack growth law (units N, mm)

The fracture mechanics method is based on a relationship between the crack increment per cycle increment, da/dN , as a function of the stress intensity range, ΔK . This relationship is based on tests, and is presented in Figure 10. The average relationship is used here because the study is a root case study.

The stress intensity range, ΔK , has an analytical background and can be considered as a measure for the stress state in the vicinity of the crack front. It is a function of the geometry of the joint, the crack size, the type of loading (membrane or bending stress), and the magnitude of the far field stress. In this paper, the expressions for ΔK have been used of a semi-elliptical surface crack according to Newman and Raju¹³ with a correction for the weld toe according to Maddox and Andrews¹⁴. The number of cycles N required for a crack to grow from an initial defect with depth a_0 , to a final crack with depth a_p is obtained by numerical integration of the following function:

$$N = \int_{a_0}^{a_f} \frac{da}{f(\Delta K(a))} \quad (1)$$

$$f(\Delta K(a)) = \begin{cases} 0 & \text{if } \Delta K \leq \Delta K_0 \\ A_1(\Delta K(a))^{m_1} & \text{if } \Delta K_0 < \Delta K \leq \left(\frac{A_2}{A_1}\right)^{\frac{1}{m_2-m_1}} \\ A_2(\Delta K(a))^{m_2} & \text{if } \Delta K > \left(\frac{A_2}{A_1}\right)^{\frac{1}{m_2-m_1}} \end{cases}$$

where A_1 , A_2 , m_1 , m_2 and ΔK_0 are material parameters provided in Figure 10. The initial crack considered is a semi-circular crack with depth $a_0 = 0.15$ mm. This is a representative defect for an as welded structure⁷. The final crack depth, a_p , considered here is taken equal to the plate thickness. In the calculation, the stress ranges type I are assumed to be completely mixed with the stress ranges type II, so that a stress cycle type I occurs after n_{II}/n_I stress cycles type II. The numbers of cycles n_I and n_{II} have been determined based on the operating condition of the system (are not given due to confidentially reasons). Using a numerical procedure, it is now possible to determine the combinations of stress ranges $\Delta\sigma_I$ and $\Delta\sigma_{II}$ for which failure is expected after $(n_I + n_{II})$ cycles. These are the combinations for which $n_I + n_{II} = N$, with N according to Equation (1).

The results of the calculations are provided in Figure 11. The vertical axis represents the acceptable stress range $\Delta\sigma_I$ based on the number of start-stops of the system n_I as a result of the thermal loading during heating up and cooling down of the system. The horizontal axis represents the accompanying acceptable stress range $\Delta\sigma_{II}$ based on the maximum number of expected cycles of the pulsation-induced shaking forces and cylinder vibrations n_{II} . The curves

in the figure represent a probability of survival of 50% (average crack growth curves). The curves are valid for full penetration welds, starting at the weld toe. The acceptable levels depend on the thickness and node length of the material as shown in Figure 11. Figure 11 provides results for membrane stress ranges. In case of bending, the acceptable stress range combinations are larger than those in Figure 11.

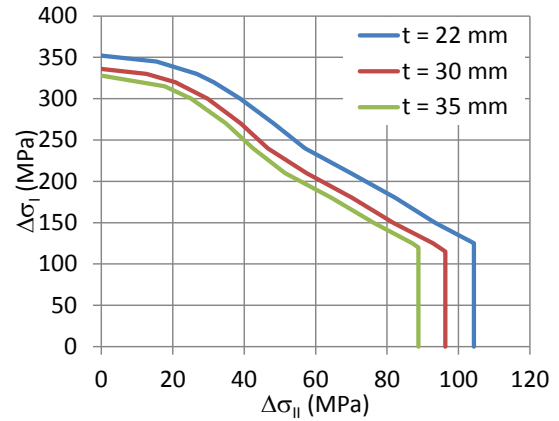


Figure 11 Example of curves indicating the combinations of membrane stress ranges for a 50% probability of survival, valid for the specific combination of n_I and n_{II}

3 Root cause analysis

This chapter discusses the different steps of the Root Cause Analysis (RCA). The different steps will be discussed more into detail of only the discharge 1st stage pulsation damper in the next sections.

3.1 Models

Detailed finite element models have been generated of all pulsation dampers. An example of the discharge 1st stage is shown in Figure 12. All weld details have been modelled into detail of which some examples are shown in Figure 13 and Figure 14. The geometrical boundary conditions as summarized in the next section have been included where applicable.

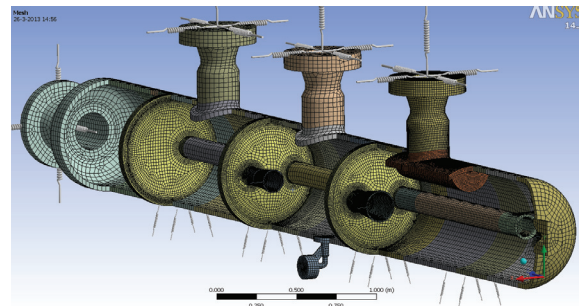


Figure 12 Finite element model of the complete discharge damper 1st stage

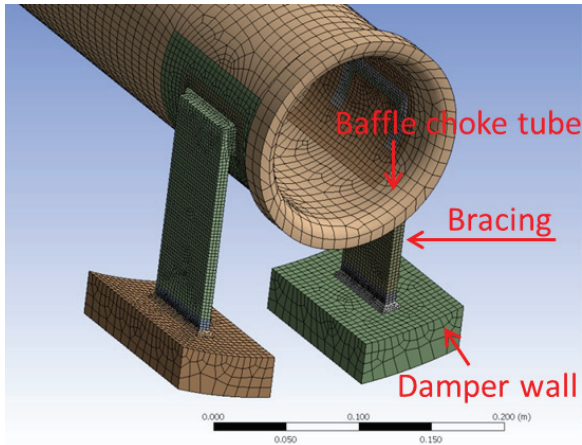


Figure 13 Detail of the choke tube bracing

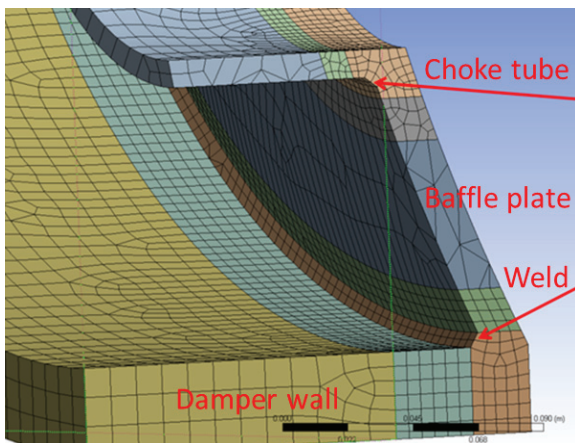


Figure 14 Detail of one of the baffle chock tubes

3.2 Geometrical boundary conditions

The cylinder nozzles of the pulsation dampers which are mounted to the compressor cylinders will deform when the compressor is heating up. The expansion of the compressor (frame, crosshead guide, distance piece and cylinders) can have a large effect on the thermal stresses of the pulsation dampers.

Correct calculation of the thermal expansion of the cylinders is essential for an accurate prediction of stresses. TNO has carried out a detailed compressor manifold analysis according to the API Standard 618⁸ during the design stage of the project. In this analysis the vibration levels of the compressor and pipe system are calculated caused by pulsation-induced shaking forces, cylinder stretch and mechanical unbalanced loads. The detailed finite element model of the compressor and pipe system has been used in this project to calculate the thermal displacements at the cylinders and line nozzle flanges. These values have been incorporated in the analysis of the pulsation dampers to achieve accurate results.

3.3 Load cases

The pulsation dampers have been subjected to the following loads which could have caused the failures of the dampers:

1. Static pressure.
2. Transient thermal loads to the rapid start-up.
3. Steady state thermal loads.
4. Dynamic loads such as pulsation-induced shaking forces acting on damper internals and cylinder vibrations (at resonance conditions).

Only the 2nd and 4th load case will be discussed more into detail in this paper.

3.3.1. Thermal loads

As a consequence of hot gas rapidly flowing through the dampers when the compressor is started, temperature differences will occur in the system which results in stresses. The maximum stress range that occurs at welds are caused by:

- Difference in stress in a weld between the two steady states of the system: compressor turned on and turned off. The temperature of the dampers is higher than that of the compressor which will generate thermal stresses.
- As a consequence of the high flow velocity, high gas temperature, high gas pressure and low mass of the internal parts of the dampers such as the baffle choke tubes heat up more rapidly than the damper itself. This results in temperature gradients and consequently in thermally induced stresses.

3.3.2 Mechanical vibrations

Pulsation-induced shaking forces are generated at locations where the pulsations “couple” to the mechanical structure of the pulsation dampers, such as baffle plates, end caps, reducers, etc. The pulsation-induced forces vary with pressure, unloading conditions of the cylinders and compressor speed. The maximum pulsation-induced shaking forces for all possible operating conditions have been calculated to find the maximum cyclic stresses. It should be noted that this is a rather worst-case assumption due to the fact that the compressor will not operate all the time under these conditions.

Another source of vibrations are the mechanical vibrations of the compressor cylinders which can cause unacceptable stresses, especially in case of resonance conditions. The maximum cyclic stresses as calculated in the compressor manifold vibration analysis⁸ occur in the cylinder nozzles. These stress ranges have been used and combined with the thermal stress ranges, according to the procedure as described in chapter 2 to check if fatigue failure is to be expected.

3.4 Determination of the stress ranges

The hot-spot stress method (also called geometrical stress method) is suitable for the assessment of toe cracking of welded joints. The method consists of a linear extrapolation of the stresses to the weld toe, from the stresses determined at two distances from the weld toe. The distances used in this paper are $a=0.5$ and $b=1.5$ times the plate thickness away from the weld toe, refer to Figure 15.

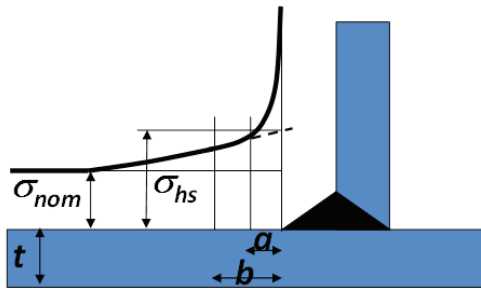


Figure 15 Definition of the hot-spot stress at a weld toe.

The hot spot stress applies to cracks growing from the weld toe. The hot-spot stress method is not suitable for assessing stress components parallel to the weld. In principle, it is not possible to check weld root cracks (cracks inside the weld) with the hot-spot stress method.

The hot-spot method requires more modelling effort for the structural (finite element) model as compared to the nominal stress approach. The required mesh is denser, and in building the model, the modeller should already take notice of the points where the stresses should be read. The method is provided in many standards dealing with fatigue ^{1, 2, 3, 4, 5}

4 Results

The fatigue assessment calculations have been carried out for the thermal loads and for the vibration loads described in the previous chapter. In this chapter a summary will be given of the results caused by the described loads for the discharge 1st stage pulsation damper. The conclusions for other dampers are similar.

4.1 Cyclic stresses caused by thermal loads

The maximum stress in several welds, especially those of the choke tube and choke tube bracings, caused by heating up of the system is a function of the relative displacement between the choke tube and damper wall. The first step in the calculations is therefore to find the time at which the maximum relative displacement will occur. For that reason a transient thermal stress calculation has been carried out. In

Figure 16 the difference in temperature between the choke tube and the damper wall of the discharge 1st stage damper is shown. From this picture it can be concluded that the maximum relative displacement and consequently also the maximum stress will occur 55 seconds after start-up of the compressor. For other welds the maximum stress can occur at other times. This means that the hot spot stress method has been carried out at different times in order to find the maximum stresses for all welds.

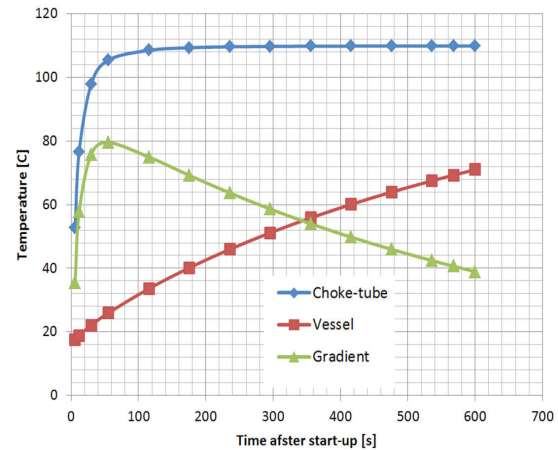


Figure 16 Example of the difference in temperatures between choke tube and vessel wall during start-up of the system.

Figure 17 and Figure 18 show respectively the temperature profile and deformation in longitudinal direction of the damper 55 seconds after start-up of the compressor. It can clearly be seen that the choke tube has a much higher temperature than the damper wall.

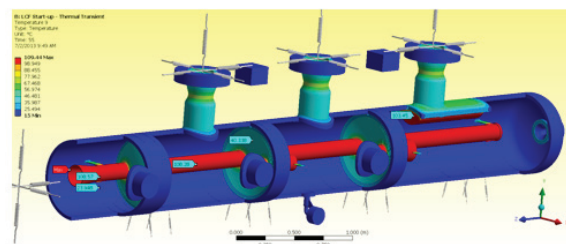


Figure 17 Example of temperature profile 55 seconds after start-up

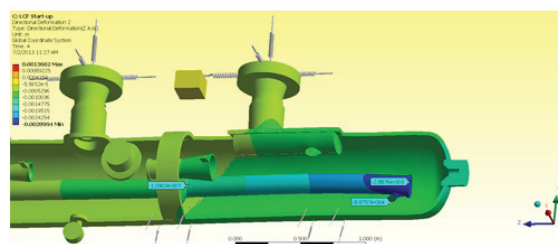


Figure 18 Deformation in the longitudinal (Z) direction 55 seconds after start-up

SESSION PULSATION 1

Root Cause Analysis of the Fatigue Failures of the Pulsation Dampers of a large Underground Gas Storage (UGS) System by: A. Eijk & D. de Lange TNO; J. Maljaars TNO, & TU/e; A. Tenbrock-Ingenhorst & A. Gottmer, RWE

Figure 19 shows the steady-state deformation (internal parts and the damper wall have the same temperature) in the longitudinal direction, clearly showing the thermal expansion and bending of the nozzles.

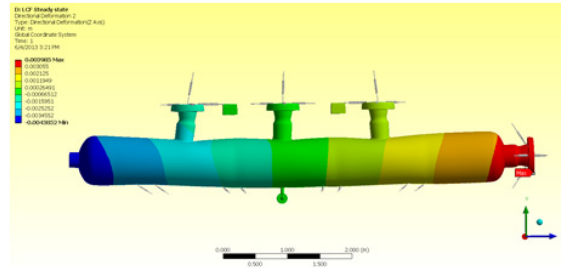


Figure 19 Steadystate deformation in the longitudinal (Z) direction.

An example of the resulting stresses in the choke tube bracing as a result of the inner pressure and temperature difference 55 seconds after start-up are shown in Figure 20 and Figure 21. The maximum calculated stress is extremely high. In a linear elastic analysis, it is in the order of several Giga Pascal. This is caused by a difference of elongation of the choke tube and the damper wall of approximately 1.7 mm. Although the stresses are overestimated in a linear elastic analysis, it is clear that the thermal load results in unacceptable strains and stress ranges, which causes low cycle fatigue. It can be concluded that the bracing has probably failed in a very early stage after start-up of the system due to thermal expansion. The photo in Figure 7 shows similarity between the location of failure and the location of maximum stress in the model.

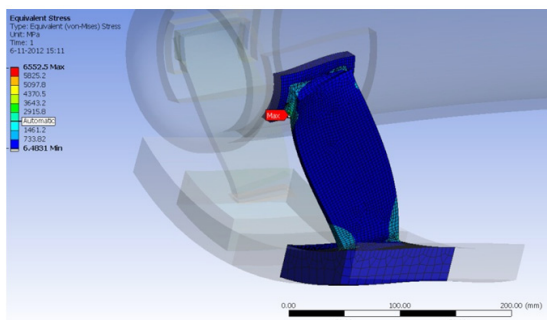


Figure 20 Stress at 55 seconds after start-up in the choke tube brace

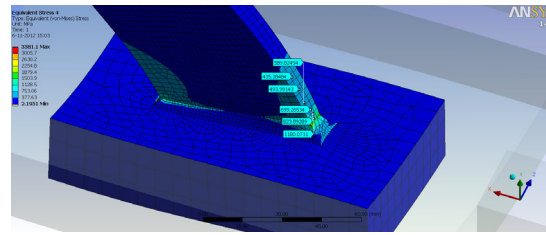


Figure 21 Stress at 55 seconds after start-up in the choke tube brace

4.2 Cyclic stresses caused by mechanical vibrations

If the frequency of the maximum calculated pulsation-induced forces coincides or is close to a mechanical natural frequency (MNF) of an internal part of the pulsation damper, e.g. baffle plate, high dynamic stresses can occur. For that reason a mechanical natural frequency calculation has been carried out first. For those MNF's which coincide or are close to the frequency of the pulsation forces, a harmonic response calculation has been carried out to find the maximum cyclic stress levels. The maximum amplitudes, phases and frequencies of the pulsation-induced forces have been calculated with a pulsation study⁸ and have been applied to the model. The calculation of the MNF's showed that the frequency of the excitation forces do not coincide or are not close to any excitation frequency of the pulsation forces for the as built layout.

However, as explained before the bracings of the choke tube had failed probably in a very early stage of the project. This means that the boundary conditions of the choke tube have changed and the consequence is that the MNF's will be much lower. The lowest MNF with broken bracings is 36.0 Hz of which the mode shape is shown in Figure 22.

It is well known that the frequencies of the cylinder vibrations do not occur only at one and two times the compressor speed but also at higher harmonics.

Looking to the mode shape of the MNF at 36 Hz, it can be concluded that this mode can easily be excited by mechanical vibrations of the cylinders in the horizontal direction.

Due to the fact that the cylinder vibrations occur at frequencies of multiples of the compressor speed, the MNF of 36 Hz can be excited at different compressor speeds in the range from 400-750 rpm (e.g. at a frequency of 4 times the compressor speed of 540 rpm, 3 times the compressor speed of 750 rpm etc.). In that situation high cyclic stresses will occur at the welds of the choke tube/baffle plate connection.

Another important observation revealed by visual inspection was that the welds of the structure, especially those of the bracings, were of exceptionally bad quality. Large craters and total lack of fusion were observed in the welds. Such welds are unacceptable, especially in a fatigue loaded structure. The fatigue

Root Cause Analysis of the Fatigue Failures of the Pulsation Dampers of a large Underground Gas Storage (UGS) System by: A. Eijk & D. de Lange TNO; J. Maljaars TNO, & TU/e; A. Tenbrock-Ingenhorst & A. Gottmer, RWE

strength of such welds is close to nothing.

The general conclusion is therefore that the choke tube bracings have probably failed in a very early stage after start-up of the system caused by too high thermal stresses. Subsequently, fatigue failures occurred in the choke tube/baffle plates welds caused by the excitation of a MNF of the choke tube.

The system under consideration will be subjected to a relatively large number of start-stops. In order to indicate the influence of this, Figure 23 provides the average and the design fatigue failure curves for the design number of starts and stops and the design curve for an arbitrary chosen number of starts and stops of 5000. The average curves are determined with the average crack growth parameters listed in section 2.2. The design curves are determined with the average + 2 times standard deviation crack growth parameters provided in BS 7910⁷. In both cases, the as-welded initial defect was assumed as a semi-circular crack with a radius of 0.15 mm. The significant differences between the design curves in Figure 23 for the arbitrary chosen number of cycles $n_1 = 5000$ and the actual number of cycles n_1 indicate that the number of starts and stops should be taken into account in the detailed design of vessels such as pulsation dampers and separators. This is especially the case for compressors installed on UGS systems due to the fact that they will normally be started and stopped more frequently than other systems.

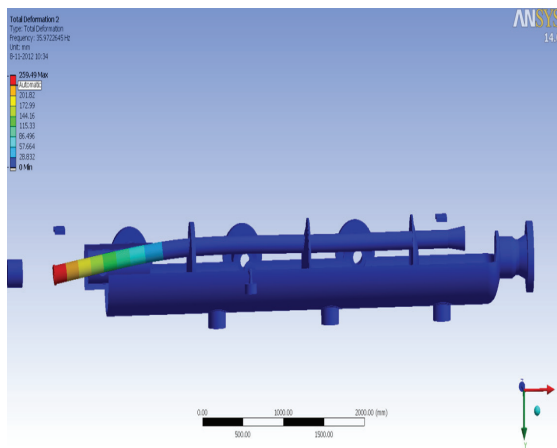


Figure 22 Mode shape of the MNF of the choke tube at 36.0 Hz

As explained before, the cylinder vibrations can cause unacceptable stresses in internal parts of the pulsation dampers if one or more MNF's are excited. Besides that, the cylinder vibrations can also cause unacceptable cyclic stresses in the cylinder nozzles, especially at cylinder resonance conditions. The maximum calculated cylinder vibrations have been applied to the model for that reason.

4.3 Results summary

The maximum calculated stress range combinations for most of the critical welds are indicated with dots

in Figure 23. From this plot it can be concluded that the assessed stress ranges exceeded the fatigue failure curves (dots above drawn lines) for many welds – not only in case of the design curves, but also for the average curves and for the design curve with the arbitrary chosen number of starts and stops of 5000. This indicates that the structure is not acceptable even for a lower number of start-stops and for normal quality welds.

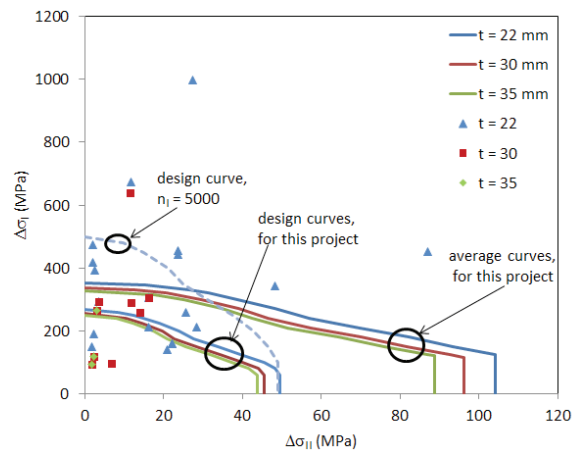


Figure 23 Fatigue strength curves and maximum calculated stress range combinations

5 Conclusions

1. From the root cause analysis it was concluded that the choke tube bracings has probably failed in a very early stage after start-up of the system due to a too high thermal stress. After that several fatigue failures occurred at the welds of the choke tube/baffle plate connection caused by the excitation of a MNF of the choke tube by cylinder vibrations.
2. The quality of several welds, especially those of the choke tube bracings, were very poor. This means that the fatigue strength was reduced considerably. Had the design been adequate, fatigue failure would still have been expected with such poor execution quality. It is advised to take good care of the quality of welds especially in structures subjected to fluctuating loads.
3. The maximum number of starts and stops of a compressor system installed at an UGS system is in general much larger than that of a compressor installed on e.g. a refinery. The consequence is that the acceptable stress range is reduced considerably e.g. by a factor of 2-3 depending on the maximum number of starts and stops. For that reason this effect should always be considered in the design of vessels and other parts of the system e.g. the piping.
4. All possible loads such as start-up and shut down, pulsation-induced forces and cylinder vibrations, should be considered in the pulsation

damper design. For an existing system it is advised to take into account the maximum measured cylinder vibrations levels, if available. For the design stage the maximum calculated cylinder vibration levels, which are calculated with a compressor manifold vibration analysis according to the API Standard 618¹², should be taken into account.

6 Recommendations

Several modifications have been investigated for each damper in such a way that the maximum stress range combinations do not exceed the design fatigue strength curves.

One of the most important challenges was to improve the design of the baffle choke tube & bracings. To avoid that MNF's of the choke tube will be excited, a so-called half pipe design has been recommended. A half-pipe design consists of a part of a pipe cut through over the length of the pipe and welded to the wall of the pipe. An example is shown in Figure 24. The advantage is that this design is much stiffer than a choke tube which is normally supported with braces to the wall of the damper. Fatigue failures caused by pulsation-induced shaking forces and cylinder vibrations are avoided with this design. However, one should be careful in applying a half-pipe design due to the fact that one part of the damper wall will be heated up more quickly than the other side. The damper will deform as shown in Figure 25 and too large deformations can lead to unacceptable stresses e.g. in the cylinder nozzles. The location of the half-pipe, either on the bottom or side, can have an important effect on the deformation and stresses so this should also be considered in the design. The half pipe has been designed such that the original acoustical properties of the entire system (length, area etc.) were kept the same.

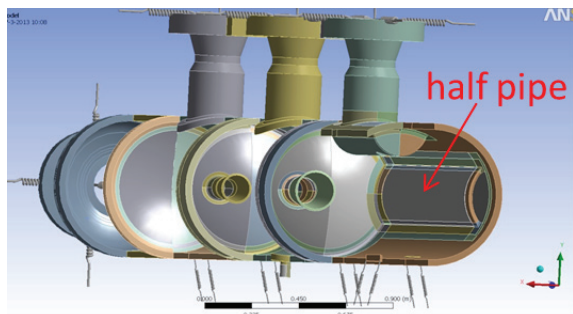


Figure 24 Example of a half pipe design

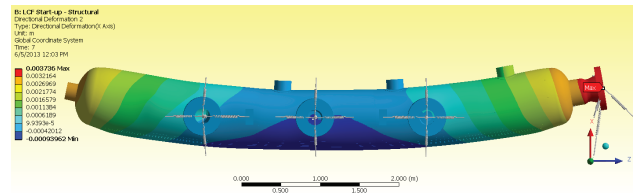


Figure 25 Example of the deformation of a half pipe design

Further on the following modifications are carried out to achieve acceptable stress ranges:

- Increased thickness of some small choke tubes and some baffle plates in order to reduce stress ranges.
- Additional bracing of the 2nd stage cylinder nozzles, see example in Figure 26.
- Long welding neck nozzles of one damper (LWN flanges do not have but welds).
- Changed design of the bracing of the suction damper choke tubes, see example in Figure 27.
- Other types of welds, avoiding fatigue cracks starting from the root.
- As a final possibility, if other actions prove unsatisfactory, post weld treatment¹¹ techniques could be considered for welds which are subjected to cyclic stresses (improving geometry to get smooth transitions, introducing compressive residual stresses etc.).

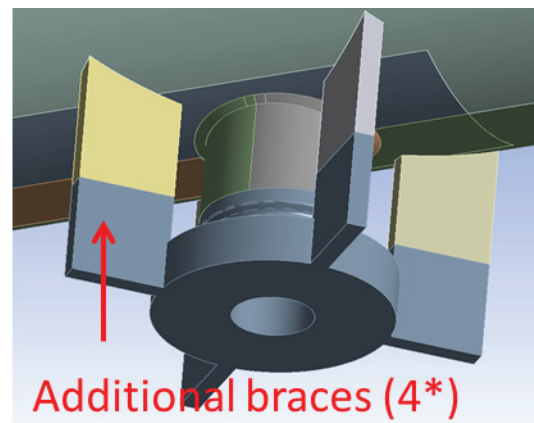


Figure 26 Additional cylinder nozzle bracings at the discharge side

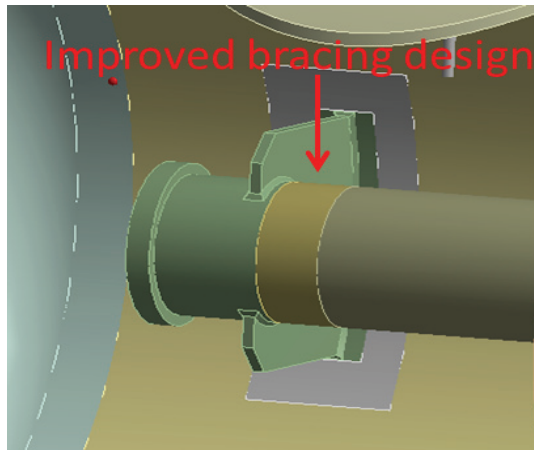


Figure 27 Improved bracing design of the choke tubes of the suction dampers

7 Acknowledgements

The authors would like to thank RWE Gasspeicher GmbH, especially Mr. Tenbrock and Mr. Gottmer, for their contribution to the paper and for the permission to publish the results of this project.

References

- ¹ PD 5500:2006: “PD5500 Pressure vessel – Specification for unfired fusion welded pressure vessels”
- ² DNV RP C203, 2012: “Fatigue Design of Offshore Steel Structures”
- ³ IIW recommendations XIII-1965-03 / XV-1127-03, “Recommendations for fatigue design of welded joints and components”
- ⁴ Eurocode 3 (EN 1993-1-9:2006): “Design of steel structures - Part 1-9: Fatigue” & “Design of structures with tension components” (EN 1993-1-11:2007)
- ⁵ FKM Richtlinie Rechnerischer Festigkeitsnachweis für Maschinenbauteile
- ⁶ Barsom and Rolfe, 1999 “Fracture and fatigue control in structures: Applications of fracture mechanics”
- ⁷ BS 7910:2005, “Guide to methods for assessing the acceptability of flaws in metallic structures
- ⁸ “Extensive Optimization Analyses of the Piping of two large Underground Gas Storage Ariel compressors” 5th EFRC Conference, March 22-23, 2007 Prague, Czech Republic, A. Eijk and H. Korst TNO Science & Industry Delft, The Netherlands, G. Ploumen Plant Manager Essent Epe, Germany, D. Heyer HGC Hamburg, Germany
- ⁹ NEN 6786, “Voorschriften voor het ontwerpen van beweegbare bruggen (VOBB)”
- ¹⁰ Haibach, E. (2006), “Betriebsfestigkeit – Verfahren und Daten zur Bauteilberechnung”, Springer Verlag, Berlin
- ¹¹ Kirkhop et al. Marine Structures 1999
- ¹² API Standard 618, 5th edition 2007, “Reciprocating Compressors for Petroleum, Chemical, and Gas Industry Services”
- ¹³ J.C. Newman and I.S. Raju. Stress intensity factor equations for cracks in three-dimensional finite bodies subjected to tension and bending loads. NASA Technical Memorandum 85793.
- ¹⁴ S.J. Maddox and R.M. Andrews. Stress intensity factors for weld toe cracks. In: Proc. 1st int. conf. on computer-aided assessment and control of localized damage, Portsmouth, UK, June 26–28 1990.

Vibrations in the Environment - Remedial Actions at a New Compressor Foundation

Field Investigation and Redesign by FEM-Calculations

by

Jan Steinhausen

KÖTTER Consulting Engineers GmbH & Co. KG

Rheine, Germany

steinhausen@koetter-consulting.com

Poul Christian Larsen

DONG Energy A/S

Nyrup, Denmark

poucl@dongenergy.dk

**9th Conference of the EFRC
September 11th / 12th, 2014, Vienna**

Abstract

After installation of an additional 4 MW reciprocating compressor at an underground gas storage in Denmark very disagreeable vibrations occurred in the administration building nearby and in the private home of a neighbour, a bit more far away. Comprehensive field measurements were carried out in order to detect the mechanism of the vibration transmission. The results of the investigation revealed a resonance mode shape of the complete compressor foundation (rocking mode at approx. 13 Hz). The foundation was mainly excited by the free mass forces and moments of the compressor at the 2nd order of the operating speed. After discussion of the results the operator decided to reduce the vibrations at the source. Hence, the complete compressor foundation was built up in a FEM-model including the soil-structure-interaction. Challenging was that any measure at the foundation was restricted by the space available within the existing compressor hall. With the model the effect of a horizontal extension by a concrete slab at each side of the original concrete block was investigated. This article also deals with the particularities of FEM regarding the infinite extent of the soil.

Vibrations in the Environment - Remedial Actions at a New Compressor Foundation

by: Jan Steinhausen, KÖTTER; Poul Christian Larsen, DONG Energy

1 Introduction

The Stenlille underground natural gas storage is located in Seeland, Denmark and operated by a Danish energy utility. Originally, the storage was projected to supply peak loads and on the other hand to balance the lack between gas production and demand in summer and winter. Today, the facility is a more commercial storage and the gas is owned by the customers. Depending on their requests – forced by the situation on the gas market – the gas has to be stored or withdrawn as fast as possible.

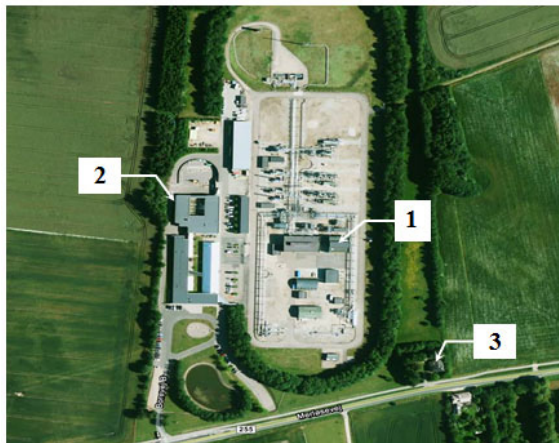


Figure 1: Aerial photo of the gas storage facility with building for engineering services and administration; 1: Machine hall for compressor K-24, 2: Administration of-fices, 3: Residential building.

The natural gas is stored in a groundwater reservoir (aquifer) at a depth of 1,500 m. The aquifer below Stenlille offers a capacity of approx. $2 \cdot 10^9 \text{ m}^3$ at a pressure of 150 bar.

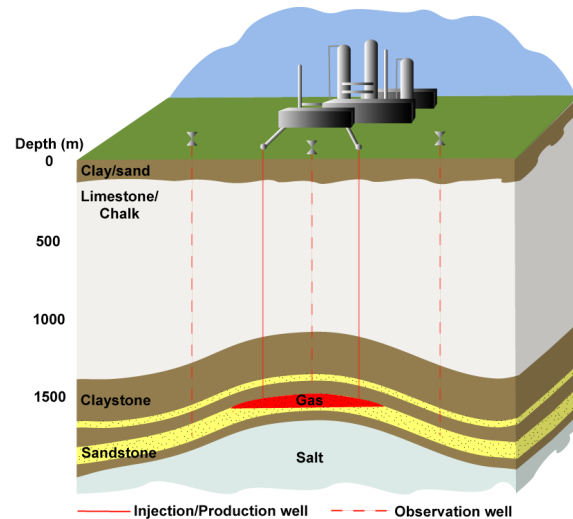


Figure 2: Geological configuration of the underground gas storage.

Up to the year 2007 three reciprocating compressor units produced a volume flow of approx. $100,000 \text{ Sm}^3/\text{h}$. For doubling the capacity a new compressor was projected by the operating company and set into operation in July 2009. The new compressor was designed as 1-stage, 2-crank, flat-type case, running with constant speed at 375 1/min (6.25 Hz rotational frequency), power consumption: 4 MW. The volume flow is controlled by stepped suction valve unloaders.

In summer 2009 the mean line pressure of the suction piping was higher than expected and the new compressor K-24 could store 20 % more gas as predicted. However, several members of the staff in the administration building complained about vibrating desks, computer screens etc. when the new compressor was running. Hence, the vibrations could be traced back to compressor K-24. Thus, the question arose, whether the vibration level at the compressor foundation was harmful for the machine itself.

First measurements were conducted by the Danish engineering company, who had supported the energy utility in this project so far. It turned out that the vibrations were dominated by the frequency of 12.5 Hz, i.e. the double rotational frequency (6.25 Hz) of compressor K-24. The compressor manufacturer stated that the measured vibration level at the machine foundation was not harmful for long-term operation of the compressor.

However, in summer 2010 the neighbour outside the storage facility – distance 160 m from the K-24 compressor foundation - complained about vibration inside the house, see figure 1, position no. 3. For example, the central-heating boiler was making an annoying noise that was strongly inconvenient for sleep during the night.

The operating company took seriously the disturbances for the staff and the neighbour due to the compressor operation. At that time, it should be clarified, whether there was a mistake in the basic design of the compressor installation causing the vibration problem. Therefore, as a next step a detailed root cause analysis was performed.

2 Root cause analysis

2.1 Operational vibration measurements

For the design of mitigation measures to improve the vibration situation the picture that could be drawn from the first measurements was unsatisfactory. In particular, it was not clear if the compressor was running at a speed that excites a natural frequency of the complete compressor foundation, i.e. the concrete block with the machine set on the top.

A rough estimation of the lower natural frequencies of the foundation embedded in the soil turned out that a resonance at 12.5 Hz, i.e. twice the rotational frequency, could not be excluded.

Thus, in order to detect the vibration behaviour in detail, extensive measurements during operation of the compressor were performed on site. Figure 3 shows the compressor K-24 inside the hall. The essential measuring positions at the concrete foundation are depicted in figure 4. During operation of the compressor the maximum vibration velocities arose at positions v02 and v05 in z-direction. These positions were located on the foundation area for the (vertical) supports of the compressor cylinders, see figure 5.



Figure 3: Compressor K-24 in the machine hall.

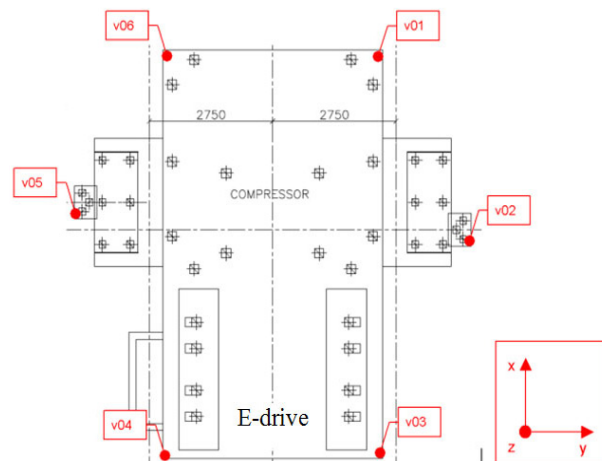


Figure 4: Denomination and location of the main measuring positions at the compressor foundation.

Vibrations in the Environment - Remedial Actions at a New Compressor Foundation

by: Jan Steinhausen, KÖTTER; Poul Christian Larsen, DONG Energy

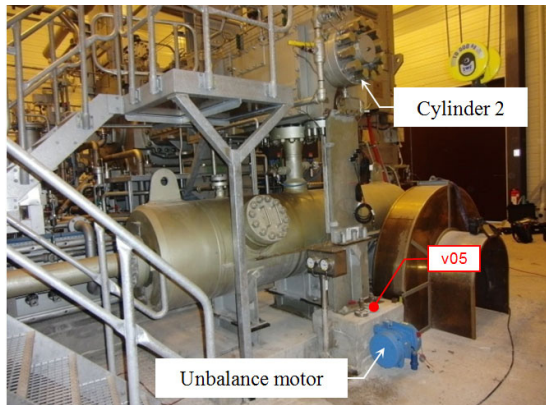


Figure 5: Support of cylinder 2, mounted unbalance motor (blue) at the foundation.

During the first 3 minutes after run up of the compressor (from approx. 18:00 h, see figure 6) the load, i. e. the volume flow, was increased stepwise by means of suction valve unloaders. The vibration level at the foundation (v05z) achieved a maximum of approx. 2.7 mm/s RMS at 100 % load, figure 6. In comparison to other compressors at similar installations this level is not unusually high. According to ISO 10816 – 8 [1] respectively EFRC guidelines [2] a vibration level up to 3 mm/s RMS is allowable for long-term operation of the compressor. Hence, this result mainly implied that regarding the dynamic behaviour a fundamental deficiency of the compressor foundation was not existent.

Nevertheless, on the floor slab in the office (see figure 1, no. 2, air-line distance approx. 150 m) and in the residential building outside of the facility area (see figure 1, no. 3, distance approx. 160 m) the vibration level achieved not more than approx. 0.05 mm/s RMS. This level is even below the defined sensitive threshold of 0.1 mm/s RMS. Anyhow, annoying secondary effects for the staff and the residents appeared like for example vibrating computer screens, noise emission at the heating system like “buzzing / growling” etc.

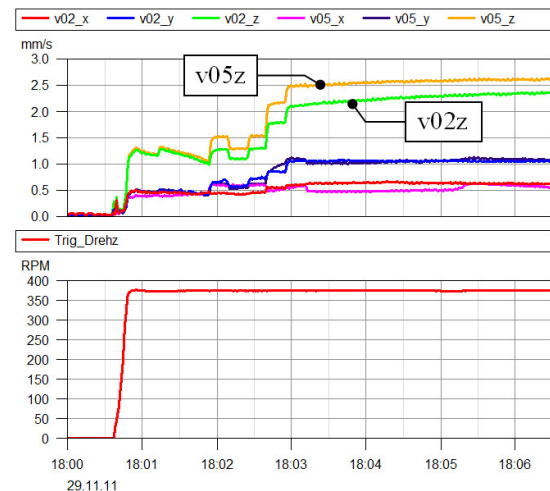


Figure 6: Top: Measured vibration velocity as RMS-values at the machine foundation during start-up of the compressor, below: compressor rotational speed.

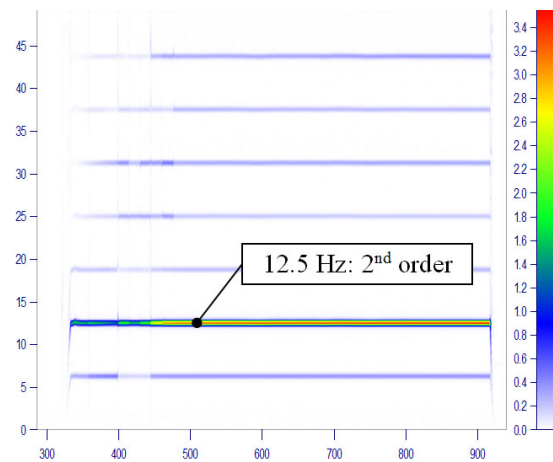


Figure 7: Time-frequency-spectrum of the vibration at the measuring position v05z during start-up of the compressor, cf. figure 6.

The time-frequency-spectrum in figure 7, which corresponds to the run up of the compressor in figure 6, reveals that the 12.5 Hz frequency was the dominating component of the foundation vibration for all load cases.

Regarding the phase shift relationship between the measured signals at different positions of the foundation it turned out that the foundation was rocking around the x-axis (rocking mode). The vibration mode shape of the complete compressor foundation (compressor, e-drive, concrete foundation) is depicted in figure 8.

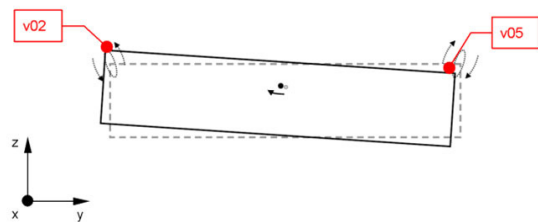


Figure 8: *Vibration mode shape of the foundation with compressor; in the sketch there is only the block foundation depicted, „rocking“ with 12.5 Hz.*

2.2 Excitation with unbalance motor

Since the compressor is running at a constant speed with 375 rpm, the resonance frequencies of the foundation cannot be determined by the results of the operational vibration measurements. Hence, an unbalance exciter (e-drive) with variable speed (controlled by a frequency converter) was used for the excitation of the foundation. The unbalance exciter was mounted with anchor bolts directly at the concrete foundation. Figure 5 shows the position of the exciter below the cylinder no. 2. With the known quantity of the exciting force the measured response of the foundation can be used to determine the transfer functions as shown exemplarily in figure 9. The transfer functions show obviously the resonance amplification at the frequency range around 13 Hz.

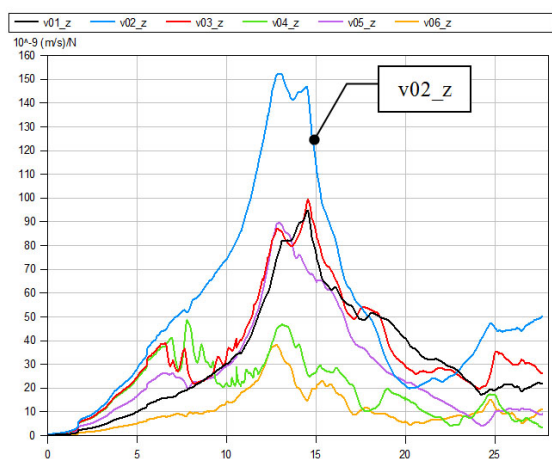


Figure 9: *Transfer function (frequency response) at different measuring positions (ratio: vibration velocity in z-direction / exciting force), excitation by unbalance motor up to 28 Hz.*

These results revealed that the 2nd order of the compressor speed at 12.5 Hz, i. e. two times of the rotational frequency (6.25 Hz), lay actually close to the “rocking mode” resonance of the foundation.

2.3 Possible mitigation measures

Although in this case the main goal was the reduction of the vibration level in the environment of the compressor and not the reduction of the foundation vibration itself, possible solutions had the focus initially on measures at the foundation itself. With regard to the results of the field measurements the detuning of the resonance frequency of the rocking mode, i. e. the ratio between exciting and natural frequency, can be considered as favourable solution. In the following some essential approaches for achieving this aim are presented:

- M1 Decreasing (M1.a) or increasing (M1.b) the natural frequency (rocking mode shape) of the complete machine foundation (concrete block including compressor and drive).
- M2 Decreasing or increasing the excitation frequency, i. e. change of the (constant) compressor speed.
- M3 Reduction of the resonance vibration at foundation by means of tuned additional oscillating masses (vibration absorber) mounted at the foundation.
- M4 Decreasing or increasing the (1st) natural frequency of the concrete floor slab in the office.
- M5 Reduction of the resonance vibration at floor slab in the office by means of tuned additional oscillating masses (vibration absorber) mounted below the floor slab.
- M6 Reduction of the vibration transmission in the soil by means of underground construction measures, for example diaphragm walls etc.

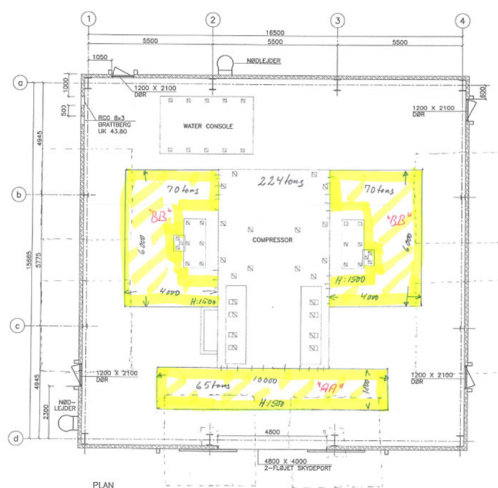


Figure 10: *First draft for the extension (yellow) of the compressor foundation.*

Vibrations in the Environment - Remedial Actions at a New Compressor Foundation

by: Jan Steinhausen, KÖTTER; Poul Christian Larsen, DONG Energy

It is obvious that passive measures in the office (M4 or M5) do not have any impact on the situation at the residential building. After discussion with the operator it was decided to pursue the approach M1.b: shifting upwards the natural frequency of the machine foundation.

With regard to the discovered rocking mode shape the first idea for the redesign of the foundation was a horizontal extension of the concrete block. But the available space for this measure was quite restricted. Figure 10 shows the first design of the foundation extension with two “wings” on the left and the right side of the existing concrete block and an additional stripe in front of the e-drive.

3 Computations for redesign of the foundation

3.1 Modelling and adjustment

The goal of the structural dynamic calculations was an estimation whether the redesign of the foundation with the new horizontal extensions achieves a sufficient reduction of the vibration level in the administration building as well as in the neighbouring residential building.

At first, a FEM-model was built up for the reciprocating compressor with the e-drive and the concrete foundation embedded in the soil for the original situation as examined during the field measurements. With utilisation of the symmetry characteristics, which arise from the rocking mode of the foundation, and in consideration of the mainly concentric propagation of the soil vibrations from the source, an initial model with a quite rough meshing was generated, see figure 11. For this model the soil was considered as homogenous for the complete model extent.

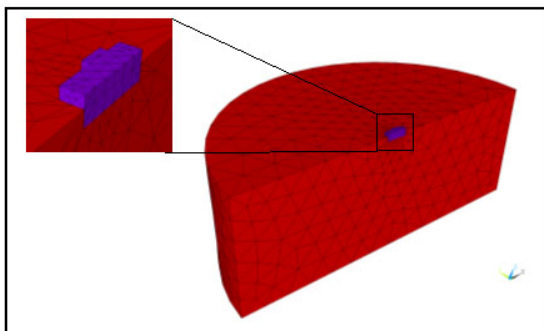


Figure 11: First FEM-model of the compressor foundation (purple) with soil bedding (red), radius: 150 m, depth: 54 m.

At this point it has to be remarked that FEM-modelling of infinite structures – in this case: the soil – leads by implication to artificial mode shapes of the model. The model dimensions and the parameters have to be chosen properly that the artefacts are minimized and do not overlap the frequency range of interest.

For excitation of the model the dynamic load reactions of the compressor were used as documented by the compressor manufacturer. The results of the first calculations did not show the rocking movement of the foundation. Further calculations revealed that for the appearance of this shape of movement an unbalanced inertia moment around the (crank) shaft axis was necessary, which was not indicated yet. It turned out that the reaction forces due to the inertia forces at the cross-head guides were mainly responsible for the sought load on the foundation and subsequently for the excitation of the rocking movement.

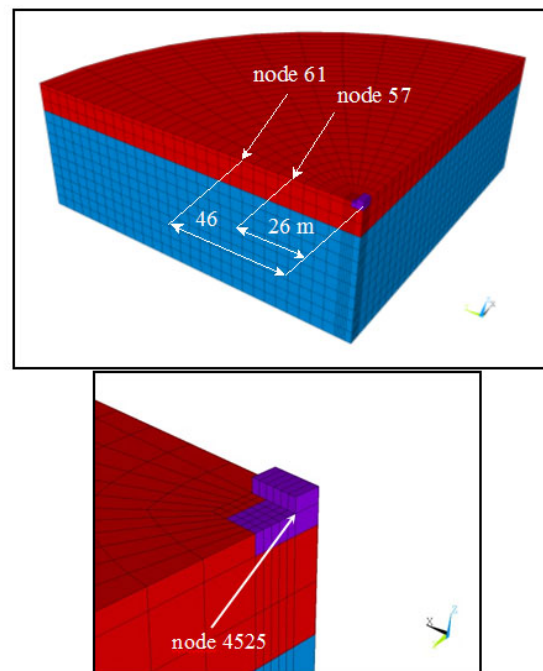


Figure 12: Tuned FEM-model of the compressor foundation with 2-layer soil model.

With this knowledge, i. e. the completed model, a first assessment of the planned foundation retrofit could be carried out. The results for the original design of the foundation were compared to the results of the retrofitted foundation. The results show that a reduction of the vibration level can be expected of at least 50 % at the foundation itself. However, the natural frequency of the rocking mode shape was shifted not more than 3 Hz upwards.

Further results of extended calculations revealed that the quite slim concrete stripe at the position in front of the e-drive had only a weak effect on improving the situation. Hence, this part of the retrofit was abandoned.

3.2 Optimisation of the foundation extension

In the next step, for improving the validity of the model – for areas far from the compressor (> approx. 25 m) - a structured (mapped) and finer mesh was generated for the soil. Meanwhile, the soil properties had been determined more in detail. The results were used to build a layered model of the soil with two layers. Additionally, further properties of symmetry were used which finally led to a “quarter pie” model, see figure 12.

The improved modelling of the soil succeeded in a better adaptation of the computed rocking mode frequency to the measured result. Nevertheless, with the available soil parameters the computed rocking mode frequency (approx. 20 Hz) was still above the measured frequency on site. At this time an improving of the model was not pursued furthermore. Thus, the assessment of design measures at the foundation was (mainly) carried out by comparing the results of the models for the state with and without the extension.

The results with the improved modelling showed now for the extended foundation that a reduction down to 30 % (in relation to the original situation) could be achieved. In the far field (administration and residential building) the model showed a reduction of about 50 %. In figures 13 and 14 the results are exemplarily presented for selected node positions as depicted in figure 12 (note: different scales are used in the charts).

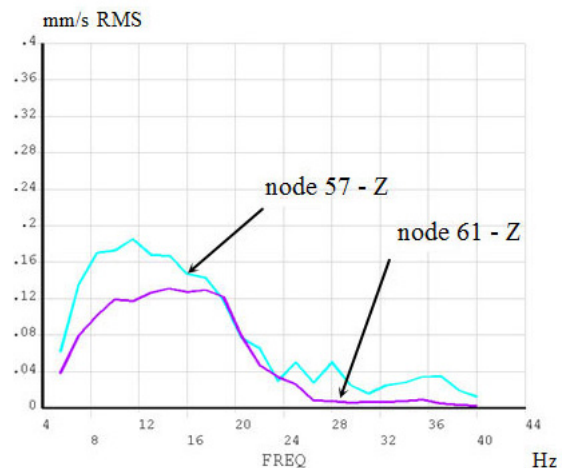
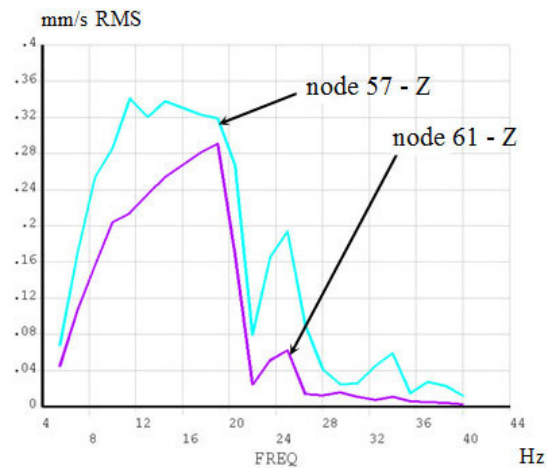
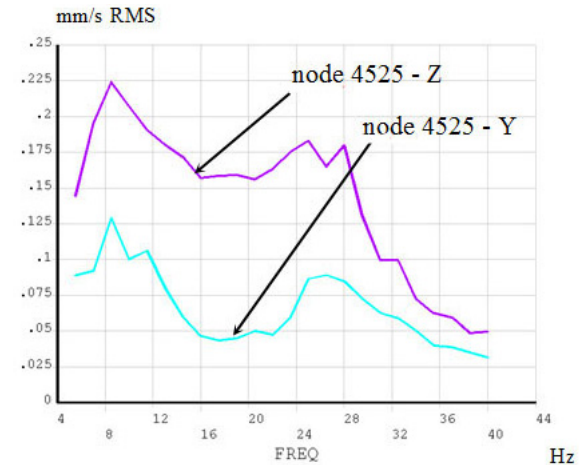
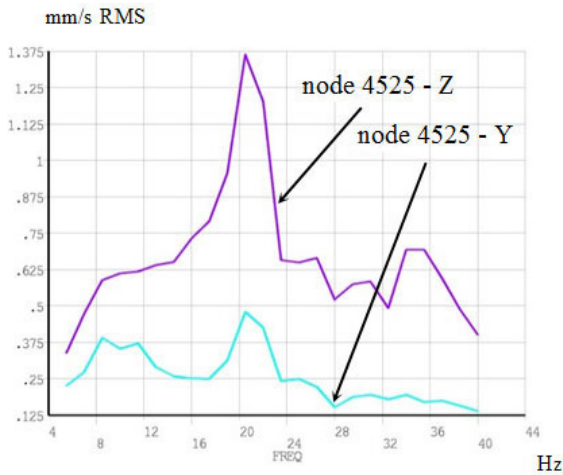


Figure 13: Frequency response of vibration velocity, foundation in original state, top: at the foundation, below: in the surrounding, see figure 12 for positions of nodes.

Figure 14: Frequency response of vibration velocity, foundation with extension, top: at the foundation, below: in the surrounding, see figure 12 for positions of nodes.

Vibrations in the Environment - Remedial Actions at a New Compressor Foundation

by: Jan Steinhausen, KÖTTER; Poul Christian Larsen, DONG Energy

But the results for the “wings”-extension still showed a natural frequency for the “rocking” of the foundation which was not more than 2 – 3 Hz above that of the original foundation. Hence, the expected new “rocking” frequency was still close to the 2nd order excitation of the compressor. Therefore, in order to shift this frequency up, the effect of additional piles supporting the foundation “wings” was investigated in the next step. As an initial design 4 piles were placed below each wing, altogether 8 piles, see figure 15. The pile length was set to 14 m since they should penetrate sufficiently the stiffer lower layer. The pile diameter was set to 0.5 m.

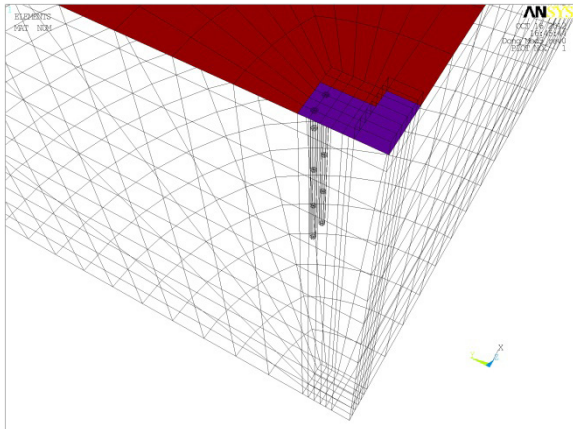


Figure 15: FEM-model for the foundation with extension and additionally 4 x 2 concrete piles below the foundation extension.

The results with the additional pile foundation revealed that this measure can shift the rocking mode frequency at least 6 Hz up compared to the original situation, see figure 16. Using 16 piles instead of 8 could shift up the frequency additionally 3 Hz.

After discussion with the operator and the supporting civil engineering experts the final design for the extension of the foundation was configured with overall 12 piles, 6 piles below each slab, see figure 17.

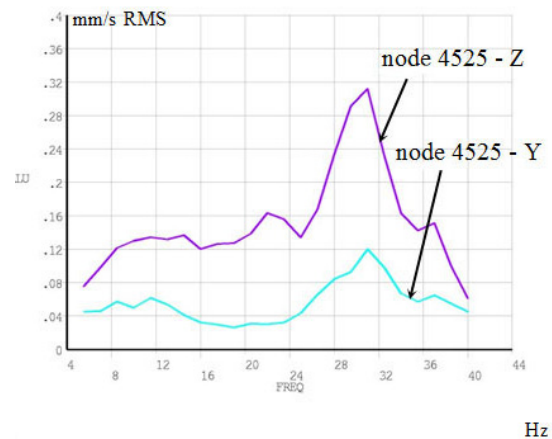


Figure 16: Frequency response of vibration velocity, foundation with extension and 8 piles, see figure 12 for positions of nodes.

In order to ensure the function of the extended foundation, it was absolutely necessary to accomplish as high stiffness as possible at the connection to the existing concrete block, although the dynamic load reactions are quite low at the interfaces. In the same way the connection between the concrete slabs (of the extension) and the pile heads had to be executed.

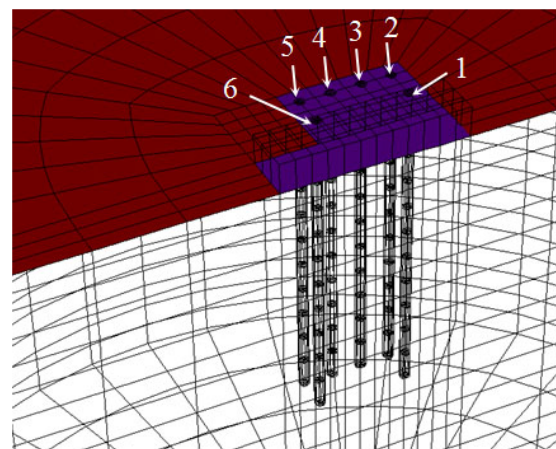


Figure 17: FEM-model with numeration of piles for the final design of the foundation extension with 2 x 6 concrete piles.

4 Realisation of retrofit

Between November 2012 and end of March 2013 the civil engineering of the retrofit was planned and executed, see figure 18. For the construction of the piles with on site mixed concrete it was necessary to ditch the ground around the compressor foundation inside the existing hall. Afterwards, the bore holes for the piles were drilled with a depth of 14 m, in which the baskets for reinforcement were put in.

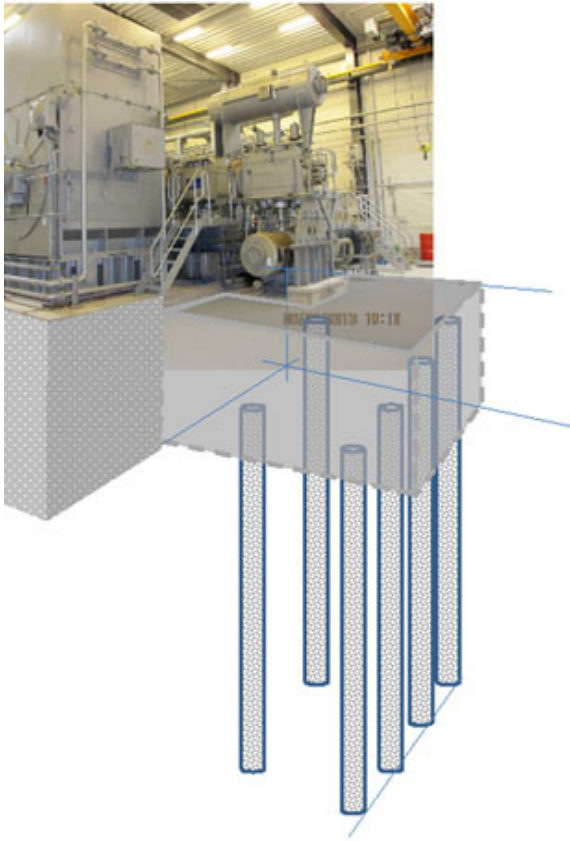


Figure 18: Sketch of the planned foundation extension in the machine hall.



Figure 19: View on one side of the foundation after completion of the concrete piles.



Figure 20: Reinforcement of the foundation extension.

Figure 19 shows the ends of the core wiring of the baskets which protrude from the pile heads for the monolithic connection with the extended slab (“wing”), see also figure 20.

5 Check measurements after retrofit

After recommissioning of the compressor in April 2013 the actual vibration situation was checked by measurements on site again at 100 % load. The results showed that the vibration level at the foundation was decreased to approx. 10 % compared to situation before the retrofit – from 2.7 mm/s RMS to 0.3 mm/s RMS. As predicted by the computations the diminution of the vibration level depended on the direction of the vibration. The vibration level in x-direction was reduced only down to approx. 40 % - 50 % compared to the original state, see figure 21.

In the office of the administration building a reduction of at least 50 % in any direction was achieved, although the natural frequency (13 Hz) of the floor slab was not modified. In vertical direction the vibration level lies at 44 % of the level before the retrofit, see figure 22.

Slightly different is the picture at the residential building. Here, the highest reduction was achieved – as intended – in horizontal x-direction, see figure 23. The vibrations generated by the compressor K-24 could be reduced to approx. 30 % of the level without the extension of the foundation. In the vertical direction the vibrations were very low already before the retrofit.

Vibrations in the Environment - Remedial Actions at a New Compressor Foundation

by: Jan Steinhausen, KÖTTER; Poul Christian Larsen, DONG Energy

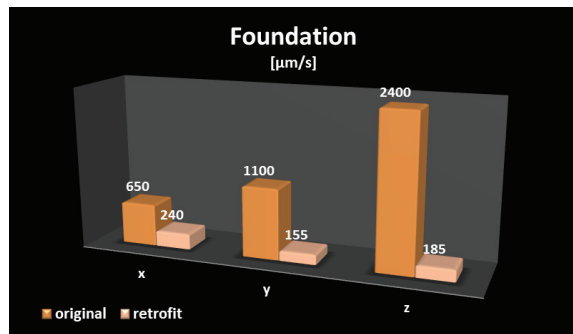


Figure 21: Comparison of vibration velocity level at the foundation (position v02) before and after retrofit.

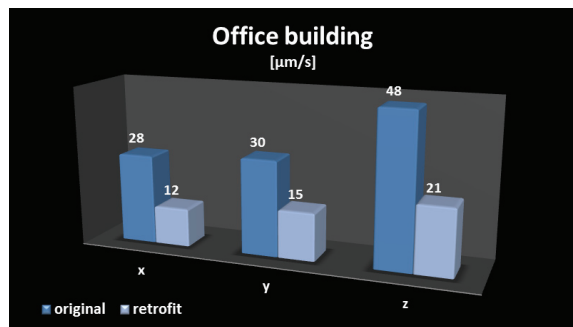


Figure 22: Comparison of vibration velocity level in the office building before and after retrofit.

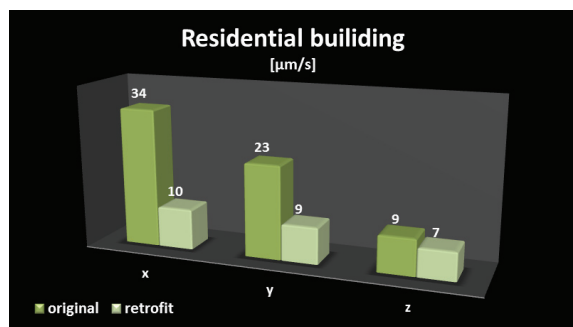


Figure 23: Comparison of vibration velocity level in the residential building before and after retrofit.

6 Conclusion

After recommissioning of a new reciprocating compressor at the Stenlille underground storage in Denmark inconveniently high vibrations arose in the administration building inside the facility and in a residential building close to the facility.

A comprehensive metrological investigation during operation of the compressor revealed that no exceeding vibrations occurred at the foundation itself. Nevertheless, the rocking mode resonance of the complete installation at approx. 13 Hz was excited by 2nd order of the compressor (12.5 Hz).

As a first step - due to the results of the measurements - an extension of the foundation was designed in order to improve the vibration situation in the neighbouring buildings. Finite-element calculations including the soil-structure interaction showed that additionally a pile foundation below the extended concrete slabs was necessary.

After the retrofit of the foundation a metrological check of the actual situation during operation of compressor K-24 was performed. The results could prove a successful reduction of the vibration level in the offices and in the neighbouring residential building, which give no reason for complaints anymore.

The presented case study in this paper shows that for the foundation design of reciprocating compressor installations possible vibration emissions in the environment, like neighbouring buildings close or far from the compressor, should be taken into account. At least it should be checked by calculations whether the lower resonance frequencies of the foundation might be close to the main excitation frequencies due to the free inertia forces and moments of the compressor. Even if the arising resonance vibrations are not harmful for the compressor, the vibration emission in the environment could be too strong.

7 Bibliography

- [1] ISO/DIS 10816 – 8 (2012): Mechanical vibration – Evaluation of machine vibration by measurements on non-rotating parts – Part 8: Reciprocating compressor systems
- [2] EFRC Guidelines (2009): Guidelines for Vibrations in Reciprocating Compressor Systems, 1st edition

- [3] Steinhausen, J. (2009): Schwingungstechnische Planung der Aufstellung von Kolbenmaschinen auf einer Offshore-Plattform, 3. VDI Fachtagung Baudynamik, VDI-Berichte 2063, pp. 337 - 349, ISBN 978-3-18-092063-4, VDI Verlag, Düsseldorf

- [4] Steinhausen, J.; D. Stoll (2010): Erfolgreiche Reduktion fundamentinduzierter Schwingungen am Beispiel einer Neuinstallation eines Sekundärkompressors K10, Tagungsband 14. Workshop Kolbenverdichter, pp. 107 – 124, KÖTTER Consulting Engineers, Rheine

- [5] Studer, J.; Ziegler, A. (2007): Bodendynamik, 3. Auflage, Springer-Verlag, Berlin / Heidelberg

- [6] Flesch, R. (1997): Baudynamik - Band 1, Bauverlag, Wiesbaden / Berlin

- [7] Haupt, W. (1986): Bodendynamik, Friedrich Vieweg & Sohn

SOUTHWEST RESEARCH INSTITUTE®

Optimized Robust Compressor Station Design Methodology

by

**Benjamin A. White, Barron J. Bichon, David L. Ransom,
Eugene L. Broerman
Research & Development
Southwest Research Institute®
Texas, USA**

benjamin.white@swri.org, barron.bichon@swri.org,
david.ransom@swri.org, eugene.broerman@swri.org

**9th Conference of the EFRC
September 11th / 12th, 2014, Vienna**

Abstract

In the process of designing a gas compression facility, it is important to ensure the mechanical reliability of the system through proper analysis of the fluid (flow) and structural systems. Pulsation models of the reciprocating compressor systems are developed to study the dynamic pressure and flow characteristics for the planned operating conditions. Similarly, mechanical models are developed for the study of the structural dynamic characteristics. Predicted pulsations and loading from the reciprocating compressor components are added to the simulation to predict the forced response of the mechanical system. These predictions are then used to identify potential problems and design modifications are studied to eliminate the problems. However, design iterations can be time consuming, so system optimization is often limited to a small number of variables.

This paper presents recent research on the subject of optimizing the design and robustness of pulsation and vibration control techniques of reciprocating compressors using Southwest Research Institute® (SwRI®) developed probabilistic analysis software. Efforts are being made in the following areas:

- Bottle size (cost & weight) optimization versus pulsation and vibration amplitudes
- Improving design robustness to be less sensitive to installation variables
- Identifying key piping restraint locations that are most critical to successful operation
- Rapidly evaluating multiple load steps and operating conditions to determine worst cases

Optimized Robust Compressor Station Design Methodology

by: Benjamin A. White, Barron J. Bichon, David L. Ransom, Eugene L. Broerman, Southwest Research Institute®

1. INTRODUCTION AND BACKGROUND

This paper presents results on the subject of optimizing the design and robustness of pulsation and vibration control techniques of reciprocating compressors from a recent research project. The goal was to develop a design practice that better incorporates the characteristics of the fluid and structural systems and efficiently determines the preferred robust, least sensitive compressor pulsation filter bottle and piping system design.

In the process of designing a gas compression facility, typically for pipeline applications, it is important to ensure the mechanical reliability of the system through proper analysis of the fluid (flow) and structural systems. Pulsation models of the reciprocating compressor systems are developed to study the dynamic pressure and flow characteristics for the planned operating conditions. This analysis is performed using a transient 1-dimensional pulsation modeling software code. Similarly, mechanical models of the structures involved (e.g., compressor frame, pulsation filter bottles, adjacent piping, etc.) are developed in a commercially-available finite element software package for the study of the structural dynamic characteristics. Predicted pulsations and loading from the reciprocating compressor components are added to the simulation to predict the forced response of the mechanical system. These predictions are then used to identify potential problems and design modifications are studied to eliminate the problems. In the analysis phase, each design iteration can be time consuming (expensive) due to the nature of the work, so design optimization is sometimes limited to a small number of variables.

The objectives of this project included:

- Development of an optimization methodology for the design of gas compression stations to maximize station reliability and efficiency.
- Development of a robust design methodology to minimize design sensitivity to typical operational variability, installation inaccuracies/variability, and degradation of mechanical systems, such as piping restraints, over time.

Figure 1 shows a typical reciprocating compressor manifold system. Figure 2 shows a flow chart for a typical pulsation and structural analysis.

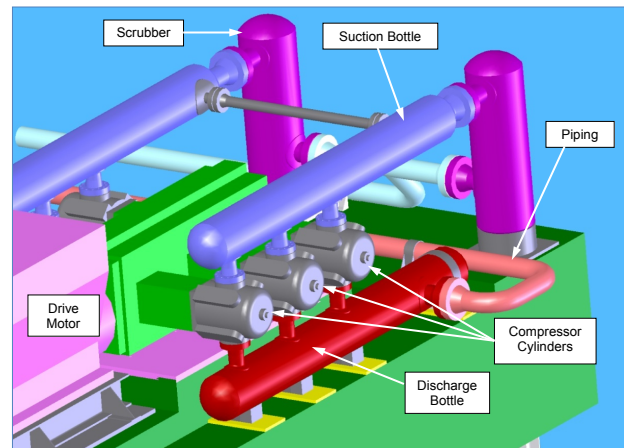


Figure 1. Typical 6-Cylinder Gas Compressor Manifold System

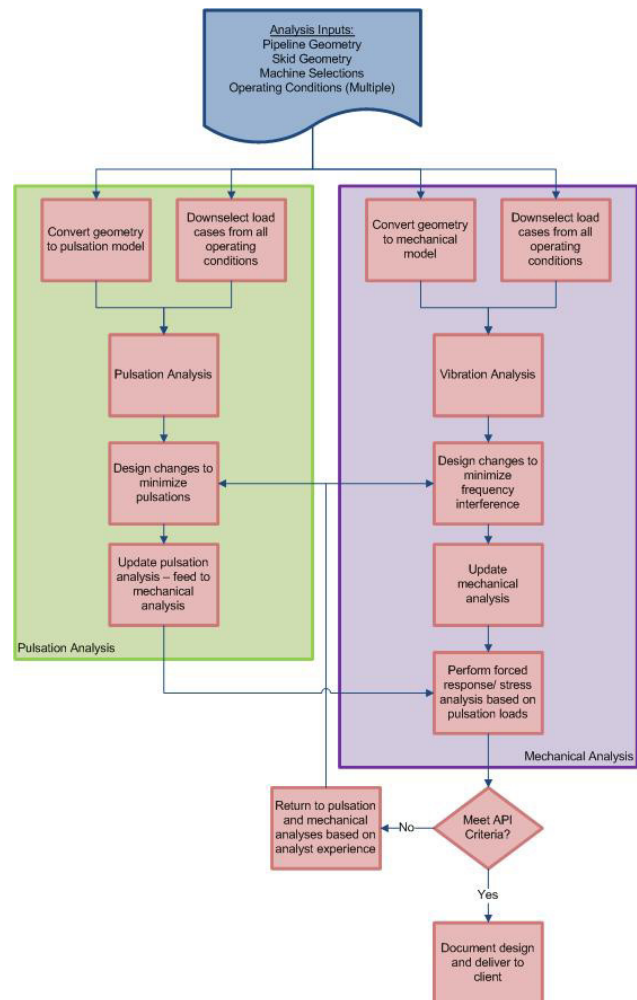


Figure 2. Flow Chart of Typical Pulsation and Structural Analysis

Optimized Robust Compressor Station Design Methodology

by: Benjamin A. White, Barron J. Bichon, David L. Ransom, Eugene L. Broerman, Southwest Research Institute®

2. RESULTS

2.1 Test Model

Prior to beginning the research phase of the project, it was necessary to develop a relatively simple test model for the optimization process. A simple model allows for faster process development by reducing solution and post-processing times and allows engineers to have a better intuitive understanding of the physical behavior of the system. The design process can then be applied to more complex models.

The developed test model consists of a single gas compressor cylinder, an empty suction bottle and a simple piping system. The structural version of the model is shown in Figure 3. A corresponding pulsation model and one-dimensional type drawing were developed (not shown). Operating conditions were selected based on typical similar machines. The structural model was initially tuned to produce a mechanical natural frequency near the first order running speed (16.67 Hz at 1,000 rpm) to simulate a problem. See Figure 4. The pulsation model was initially tuned to produce an acoustic lateral length response near the same frequency.

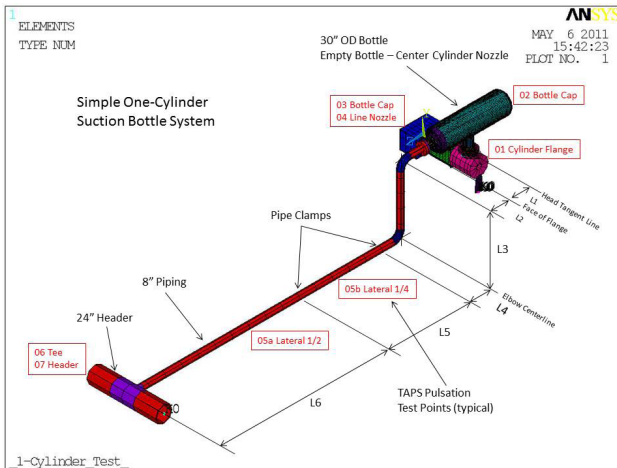


Figure 3. One-Cylinder Test Model

A set of 20+ load steps was developed for the one-cylinder pulsation test model. All 20+ load cases can be simultaneously solved on a computer cluster in parallel allowing all load cases to be analyzed in approximately the same amount of time as an analysis of a single load step. Post-processing of the results will allow engineers to quickly determine the worst-case load on the system.

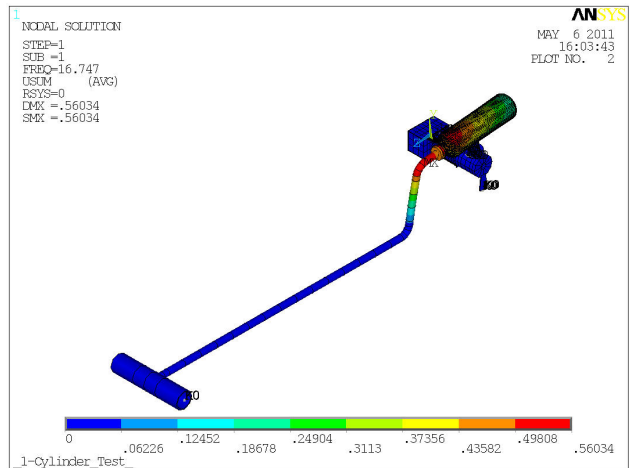


Figure 4. Lowest Structural Mode of One-Cylinder Test Model

The structural model is setup to directly import magnitude and phase output data from the pulsation model into the structural model on a case consistent basis for each unique frequency step of each important running speed order. The structural model is also setup to allow the simultaneous application of compressor rod loads and pressure pulsation forces, but only pulsation loads are applied in this particular exercise. Finally, the structural model is setup to take into account certain orders when the orders begin to “overlap”. For example, excitation at 67 Hz could be generated at the 4th order of compressor running speed at 1,000 rpm or at the 5th order at 800 rpm. The structural model will evaluate the pulsation loads at each order and automatically determine the worst case, with respect to dynamic loads imposed on the mechanical system.

An example plot of predicted stress output from a structural analysis is presented in Figure 5.

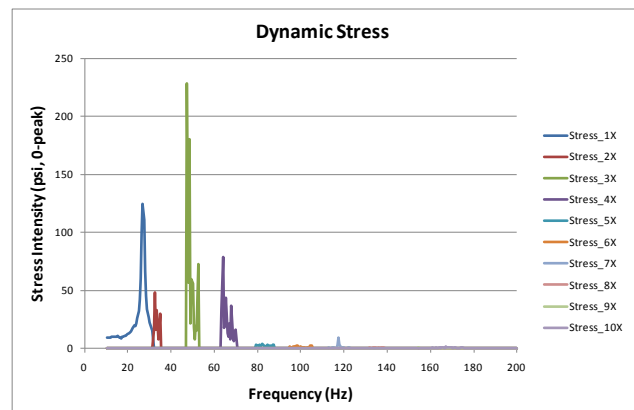


Figure 5. Example Stress Plot from Structural Analysis Output Data

Optimized Robust Compressor Station Design Methodology

by: Benjamin A. White, Barron J. Bichon, David L. Ransom, Eugene L. Broerman, Southwest Research Institute®

2.2 Normalization Criteria

When a forced response vibration analysis is run on a structural finite element model (FEM) of a reciprocating compressor, the predicted vibration and dynamic stress amplitudes are reviewed for acceptability. However, even a very simple structural model can produce vast quantities of output data. Vibration and stress data are generated for each of the several thousand node locations and over a wide frequency range. It is necessary to develop several key parameters for use in evaluating and optimizing the structural design.

To optimize the structural system, the peak vibration velocity at any point in the system was primarily used for this project. However, any weighted combination of peak stress, peak vibration velocity, average stress or average vibration velocity can be used. Stress is in units of „stress intensity, psi, 0-peak“ and vibration velocity is „inches/sec (ips), 0-peak“. The predicted stress and vibration levels are normalized by factors of 3,000 psi and 1.0 ips (based on SwRI’s standard design criteria).

The structural analysis normalization criterion has several purposes. First, it allows the optimization logic to focus on reducing the highest amplitude structural responses to lower both peak and overall values for vibration and stress. Second, it provides a method for the engineer reviewing the results of the optimization to quickly measure how successful the optimization process was. For example, by looking at the final value of peak stress or vibration, if the value is less than 1.0, then the optimization reached a solution that would be acceptable for stress or vibration levels based on SwRI’s standard design criteria. Third, it provides a method for the optimizer to weigh the importance of each factor.

Similar to the structural analysis results, the pulsation simulation can produce predicted pulsation amplitudes at many different locations and at many different frequencies. Therefore, it is also necessary to develop criteria by which the pulsation amplitudes are evaluated and optimized.

For this optimization project, the pulsation evaluation criteria are as follows:

- At each of the eight test points in the one-cylinder pulsation model, a pressure wave as a function of time is produced and a FFT performed.
- An integral of the peak-hold pulsation data up to 10X is summed at select test points as a measure of the pulsation “energy”.
- The goal of the optimization is typically to minimize pulsation levels as much as

possible by minimizing the sum of the four above-noted integrals.

- The pulsation model is initially run at all load cases to determine pressure loss and pulsation amplitudes for each compressor load case. The optimization is typically only run on select cases (such as the highest pulsation case and/or the highest pressure drop case).
- After the optimal solution is determined, all load cases are re-checked to verify if the highest pulsation load case or the highest pressure drop load case have changed.

The pulsation measurement approach just described provides a useful metric for comparing designs. However, the resulting measure of pulsation energy is a unitless number and does not provide the engineer with a measure that is easily compared to typical physical measurements. Therefore, efforts were made to develop a pulsation normalization criterion.

- Normalize pulsation results based on API 618 allowable levels for piping.
- API 618 allowables are a function of pipe diameter, compressor order (frequency), static pressure in the piping and process fluid speed of sound.

For each order of each node of interest, calculate the ratio of predicted pulsation to the API 618 allowable level. See Figure 6.

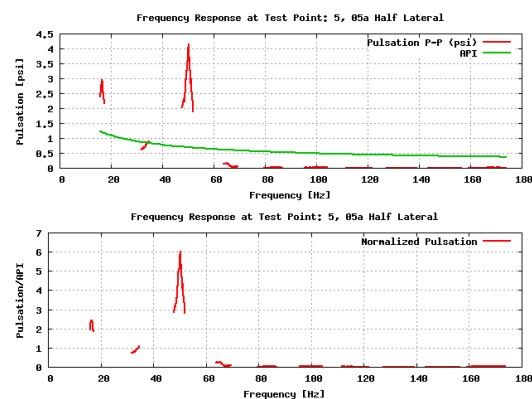


Figure 6. Pulsation Data Before and After Normalization to API 618 Criteria

Although this pulsation normalization criteria was initially developed and implemented, it is not included in the later optimization results since those runs optimized the system based on structural responses only.

Optimized Robust Compressor Station Design Methodology

by: Benjamin A. White, Barron J. Bichon, David L. Ransom, Eugene L. Broerman, Southwest Research Institute®

2.3 Load Case Evaluation

It is well known that reciprocating compressors generally generate the highest even-order pulsations (i.e., pulsations at even multiples of compressor running speed) when the compressor cylinders are operating in a double-acting mode. It is also well known that fully deactivating one end, either the Head End (HE) or Crank End (CE), of a double-acting compressor cylinder will result in the highest odd-order pulsations that can be generated by that particular cylinder. Other possible cylinder end loading scenarios include the addition of fixed- or variable-volume pockets on either the HE or CE, or HE and CE of the cylinder. In addition to cylinder load steps, the general fluid energy levels can be altered by changing operating conditions. Higher pulsation energy is typically associated with higher flow rates. Lower flow rates typically mean the energy content is reduced, but the lower flow system will also have less damping due to reduced pressure losses.

When trying to determine the worst-case scenario for pulsation/acoustic modeling purposes, the following cases are often critical:

- The highest flow case
- The highest flow, single-acting case
- The lowest flow, single-acting case

However, while these are often the most critical load cases to evaluate, there is no guarantee that they will always be the worst case for every system.

Table 1 illustrates an example load case evaluation analysis that was performed. Pulsation amplitudes were predicted for each of the 20+ load cases. The peak pulsation levels are noted in red (integral of 1X-10X, psi peak-to-peak). Depending on the test point selected, there are three potential worst-case load cases.

Table 1. Example Pulsation Amplitudes for Various Load Cases

2.4 Deterministic Orifice Evaluation

Figure 7 illustrates a deterministic evaluation that was run for orifice location optimization. This particular graph is for one load case and shows the variations in pulsation amplitudes versus orifice location. The orifice is located in the lateral piping. The horizontal axis of the graph indicates the location of the orifice as a percentage of total lateral length. Positions of 0% and 100% represent the orifice at the header tee and pulsation filter bottle inlet, respectively.

From the graph below it can be seen that the orifice is most effective in reducing pulsation amplitudes when it is located near either extreme end of the lateral piping. It becomes less effective near the middle of the piping run. This is consistent with practical experience as the orifice location varies compared with the pattern of the acoustic standing wave.

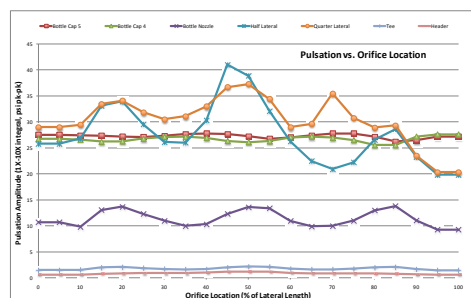


Figure 7. Example Pulsation Amplitudes for Various Orifice Positions

Optimized Robust Compressor Station Design Methodology

by: Benjamin A. White, Barron J. Bichon, David L. Ransom, Eugene L. Broerman, Southwest Research Institute®

2.5 Orifice Optimization

For this task, the objective was to investigate methods to optimize the design of the previously developed one-cylinder test model by varying the flow restriction orifice size and location. Two key criteria were selected for orifice optimization. The first criterion was the integral of pulsation amplitudes up to 10X (i.e., 10 times the compressor running speed). This value will capture changes in pulsation amplitudes at any of the first ten running orders of the compressor. The second criterion was the amplitude of just 1X pulsation. An overly restrictive orifice can reduce pulsation amplitudes at higher orders while increasing 1X pulsation amplitudes.

For this task, the pulsation design and the structural design are considered separately. First, we seek to optimize the pulsation design, where we have simplified the “design” to specifying the location (L) and beta ratio (β) of a single orifice. The goal is to minimize the pulsation in the system without overly affecting throughput, which we formulate as:

$$\begin{aligned} &\text{minimize} && \text{pulsation}(\beta,L) \\ &\text{subject to} && \text{pressure_drop}(\beta,L) \leq 0.25\% \\ & && 0 < \beta < 1 \\ & && 0 < L < 100 \end{aligned}$$

Before the optimization was attempted, a parameter study was run to visualize the functional relationship between the inputs (beta ratio and location) and the outputs (pulsation and percent pressure drop). Figures 8 and 9 show the results of these studies.

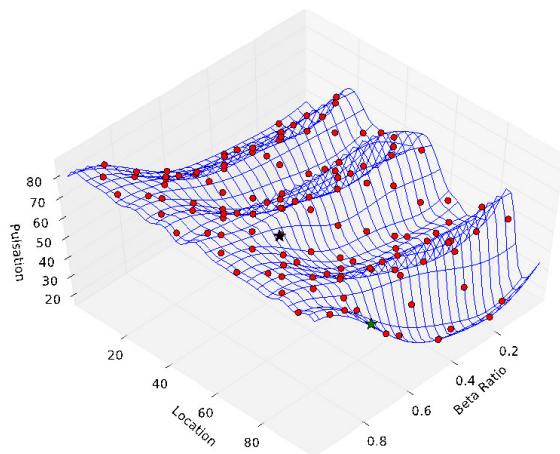


Figure 8. Pulsation as a Function of Orifice Location and Beta Ratio

Note: The red dots indicate measured data; the blue surface is a Gaussian process interpolation fit to those data. Note the nonlinearity of the surface and the „valleys“ that could cause trouble for gradient-based optimizers.

Two types of optimizers were applied to this problem. First, a gradient-based optimizer starting at the center ($\beta = 0.5, L = 50\%$) was used. The result is shown as a black star in Figures 8 and 9. The second attempt employed the Efficient Global Optimization method. The result of this method is shown as a green star in Figures 8 and 9. Note that the gradient-based optimizer converged to a greater (worse) pulsation than the global optimizer because it was unable to “escape” the valley in the pulsation output.

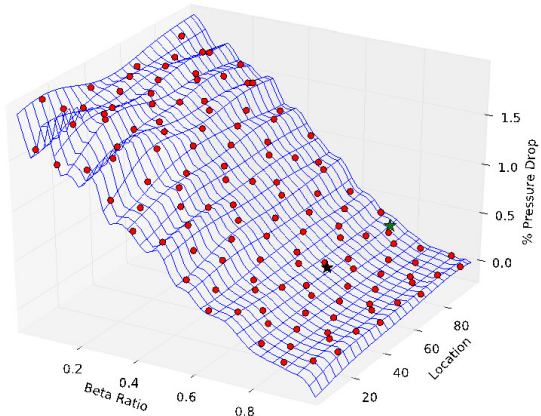


Figure 9. Percent Pressure Drop as a Function of Orifice Location and Beta Ratio

Note: The red dots indicate measured data; the blue surface is a Gaussian process interpolation fit to those data. The pressure drop is clearly more dependent on beta ratio than location.

2.6 Clamp Sensitivity Evaluation Task

From experience, it is known that it is unlikely that a compressor system is constructed exactly as it is represented in the design documents and in the analyses. This task investigates how deviations in the installation of the clamps can impact the station performance. It is theorized that the actual clamp location could deviate from the design in a manner that follows a normal distribution with a zero mean and an 8” standard deviation (so +/- 24” would cover > 99% of the total deviation). In addition, the clamp could be installed in such a manner as to make the stiffness as much as twice and as little as 10% of the expected stiffness in the design.

Beginning at the nominal (not optimal) design with clamp locations $c_1 = 30$ ” and $c_2 = 150$ ”, a three-level full factorial study was performed. Note that because c_1 was constrained at a minimum of 13.1”, a maximum negative deviation of only -16.9” was possible (before the clamp interferes with the weld seam of the elbow). The results of this study are shown in Table 2. The maximum stress, average stress, maximum vibration, average vibration, and a

Optimized Robust Compressor Station Design Methodology

by: Benjamin A. White, Barron J. Bichon, David L. Ransom, Eugene L. Broerman, Southwest Research Institute®

“score” that is a weighted sum of these are included. Note that these are listed as a ratio to the nominal case (at the bottom of the table) and are colored by the direction and magnitude of the change – red indicates an increase and blue a decrease.

Table 2. Results of Clamp Sensitivity Study

Loc. 1	Loc. 2	Stiffness Factor 1	Stiffness Factor 2	Ratio to Nominal		Ratio to Nominal		Score
				Max. σ	Avg. σ	Max. v	Avg. v	
-16.9	-24.0	0.11	0.11	1.20	1.15	0.73	1.13	0.86
-16.9	-24.0	1.90	0.11	3.86	2.55	2.32	1.82	2.69
-16.9	24.0	0.11	0.11	1.18	1.16	0.75	1.13	0.87
24.0	-24.0	0.11	0.11	1.20	1.30	0.72	1.06	0.86
24.0	24.0	0.11	0.11	1.19	1.28	0.74	1.09	0.87
24.0	-24.0	1.90	0.11	1.07	1.02	0.90	1.17	0.95
-16.9	24.0	1.90	0.11	3.86	2.55	2.34	1.83	2.71
24.0	24.0	1.90	0.11	1.07	1.02	0.90	1.17	0.95
-16.9	-24.0	0.11	1.90	1.21	1.21	0.72	1.08	0.86
-16.9	-24.0	1.90	1.90	3.68	2.56	2.34	1.82	2.67
-16.9	24.0	0.11	1.90	1.04	1.21	0.92	1.13	0.96
24.0	-24.0	0.11	1.90	1.21	1.29	0.72	1.09	0.86
24.0	24.0	0.11	1.90	1.06	1.28	0.89	1.14	0.95
24.0	-24.0	1.90	1.90	1.08	1.05	0.89	1.02	0.94
-16.9	24.0	1.90	1.90	3.85	2.60	2.56	1.88	2.87
24.0	24.0	1.90	1.90	1.08	1.06	0.88	1.01	0.94
-16.9	0.0	1.00	1.00	1.58	1.43	1.39	1.30	1.43
24.0	0.0	1.00	1.00	1.11	1.12	0.85	1.04	0.92
0.0	-24.0	1.00	1.00	1.01	0.99	0.99	1.06	1.00
0.0	24.0	1.00	1.00	1.01	1.00	1.00	0.99	1.00
0.0	0.0	0.11	1.00	1.04	1.27	0.92	1.18	0.96
0.0	0.0	1.90	1.00	0.95	1.07	2.12	1.33	1.79
0.0	0.0	1.00	0.11	1.01	1.00	0.99	1.04	1.00
70.0	0.0	1.00	1.90	1.02	1.00	0.99	0.99	0.99
0.0	0.0	1.00	1.00	1.00	1.00	1.00	1.00	1.00

In the worst case, if the first clamp moved closer to the bottle and was 1.9x stiffer, while the second clamp moved away from the bottle (so the two clamps were farther apart) and was also stiffer, the maximum stress increased by a factor of 3.86 (the average stress and the measures of vibration also increased).

In general, all cases that placed the first clamp closer to the bottle *and* increased the stiffness of this clamp greatly increased the maximum stress. All cases that moved the second clamp closer to the first *and* decreased the stiffness of this clamp, lead to a decrease in the maximum vibration. These cases are indicated by the red and blue shading in the list of inputs.

It should be noted that the peak stress and vibration in the system used for this particular clamp sensitivity evaluation were primarily due to a mechanical response of the elevated suction bottle and the modification of the grade elevation clamps would not typically be the most effective way to reduce this high stress and vibration.

2.7 Two-Variable Bottle Sizing Optimization Task

The basic objective of the task was to take the one-cylinder test model and to vary the length and diameter of the pulsation suppression bottle attached to the compressor cylinder such that the weight of the bottle could be minimized while still providing acceptable pulsation and vibration characteristics for the piping system. The objective of minimizing

weight was because the weight of the bottle is typically proportional to the fabrication cost of the bottle (a smaller bottle costs less to build).

Previous optimization tasks have, for the most part, treated the fluid and structural systems independently. Although forcing function loads from the pulsation analysis are applied to the structural model, they are typically only done so after the optimization is run on the fluid system (since it has fewer computational limitations). For the bottle optimization task, the approach is different in that variations in bottle diameter and length have a significant impact on both the fluid and structural models. Therefore, the approach was to run one pulsation analysis and then apply those results to one structural solution, followed by iterations on the process.

The specific goals of the bottle optimization task are outlined below and in Table 3.

- Optimize: Weight (minimize weight & cost).
- Vary bottle diameter and length.
- Pulsation – not optimized directly.
- Normalized Peak Vibration < 0.75.
- Normalized Peak Stress < 0.75.
- Keep constant cylinder nozzle acoustic length and always center-feed bottle.
- Calculate bottle wall thickness in structural modal based on bottle diameter.
- Calculate bottle weight in structural modal.

Table 3. Variable Ranges for Bottle Optimization Task

	Outside Diameter (OD) (inches)	Wall Thickness (WT) (inches)	Inside Diameter (ID) (inches)	Acoustic Bottle Half Length (feet)	Total Bottle Length (t-t, in)
Min. Value	19.28	0.643	18	1.22'	20"
Current Value	30.00	1.000	28	4.22'	92"
Max. Value	36.40	1.214	34	4.22'	92"
Step Size	NA	NA	2	1/12'	2"
# of Steps	NA	NA	9	37	37

For this task, the orifice details and clamp locations were fixed while we sought to optimize the size of the bottle.

$$\min \text{weight}(ID, Len)$$

$$\text{s.t. } \sigma_{\max}(ID, Len) / 3000 < 0.75$$

$$v_{\max}(ID, Len) / 1 < 0.75$$

$$18" < ID < 34" \text{ (in 2" increments)}$$

$$20" < Len < 92" \text{ (in 2" increments)}$$

Optimized Robust Compressor Station Design Methodology

by: Benjamin A. White, Barron J. Bichon, David L. Ransom, Eugene L. Broerman, Southwest Research Institute®

where ID was the inner diameter of the bottle and Len was the length of the bottle. For each potential combination of ID and Len , both a pulsation and a structural analysis were required (the weight of the bottle was calculated in the structural analysis). This optimization problem was solved using a constrained Efficient Global Optimization (EGO) solver. The following Table 4, Table 5 and Table 6 contain the details of the original bottle design, the outcome from a re-analysis performed using typical sizing guidelines, and finally, the results of the optimization study.

Table 4. Details of the Original Bottle Design

Input Details		Output Details	
ID	28"	$weight$	2,723 lbs
Len	92"	$v_{max}/1$	2.59
		$s_{max}/3,000$	1.46

Table 5. Results using Typical Bottle Sizing Guidelines

Input Details		Output Details	
ID	22"	$weight$	723 lbs
Len	32"	$v_{max}/1$	0.703
		$s_{max}/3,000$	0.243

Table 6. Results of the Bottle Optimization

Input Details		Output Details	
ID	22"	$weight$	658.1 lbs
Len	28"	$v_{max}/1$	0.638
		$s_{max}/3,000$	0.250

Note that the original design was infeasible. The maximum vibration was more than three times the allowable value and the maximum stress was approximately two times the allowable. By manually refining this, a full ton of steel was removed from the bottle, and the solution was found to be feasible - all stress and vibration constraints were met. The optimization method was able to investigate a larger number of potential solutions (because it required no manual intervention), and, thus, was able to identify a slightly better solution. It was ~9% lighter than the manual refinement, while still meeting the stress and vibration requirements.

2.8 Six-Variable System Optimization Task

Expanding on all the previous tasks, now we combine the optimization of the bottle, orifice, and the clamp locations together into a single problem to find the

optimal settings for all of these simultaneously. The goal is to minimize the $weight$ of the bottle (and therefore, the cost of this system) while ensuring that constraints on maximum vibration, v_{max} , and pressure drop, P_{drop} , are not violated. The design variables included the inner diameter of the bottle (ID), the length of the bottle (Len), the beta ratio (β) of an orifice to be placed at a specified location (Loc), and the locations of two clamps (c_1 and c_2).

Previous optimizations were formulated with all functions (objective and constraints) explicitly dependent on all design variables. However, it is easy to see that this is not the case in reality (obviously, the bottle weight does not depend upon the clamp locations, for instance), and it was observed that formulating the problem in this way was detrimental to the performance of the optimizer. To avoid this issue, the problem was formulated as:

$$\begin{aligned}
 & \min \text{weight}(ID, Len) \\
 & \text{s.t. } v_{max}(ID, Len, \beta, Loc, c_1, c_2) < 0.75 \\
 & P_{drop}(ID, Len, \beta, Loc) < 1\% \\
 & 18" < ID < 34" \text{ (in 2" increments)} \\
 & 20" < Len < 92" \text{ (in 2" increments)} \\
 & 0 < \beta < 1 \\
 & 0 < Loc < 100 \\
 & 14" < c_1 < 212" \\
 & 212" < c_2 < 378"
 \end{aligned}$$

where each function is now dependent only on the variables that directly impact it.

This problem is solved using a constrained EGO solver. This solver performs an initial Latin hypercube study over this 6-variable space using a small number of samples (28 in this case) and then uses these data to construct Gaussian process (GP) models of the objective function and each of the constraints. Note that while the total design space is 6-dimensional, as described in the problem formulation, the implementation of EGO been modified so that each function is only built over the subset of variables upon which it depends. EGO then uses a standard augmented Lagrangian penalty scheme to determine where to add additional data to iteratively update and improve these models while simultaneously seeking out the global optimum. The underlying concept is that in any region of the space, the models only need to be accurate enough to determine if they could be the global optimum. Because GP models provide an estimate of the uncertainty in their predictions, it can be clear that for some regions of the design space, even if the true value of the models at a point is not known,

Optimized Robust Compressor Station Design Methodology

by: Benjamin A. White, Barron J. Bichon, David L. Ransom, Eugene L. Broerman, Southwest Research Institute®

there is little chance of that unknown value providing a “good” design. Using this logic, the sampling data is focused only in the interesting regions within which it is useful to search for the optimum, making the method highly efficient. Reducing model evaluations is important for a problem like this, where evaluating a single point requires a great deal of computational time.

By default, EGO identifies only a single new point to be added to the GP models at each iteration. This is the single point at which, given the current state of knowledge, the algorithm computes the largest expectation of finding an improved solution to the optimization problem. Recognizing that the available computational resources would allow for the solution of multiple points simultaneously, a modification was made to the algorithm to find several potentially good points at each iteration instead of just the single best.

The results of this optimization study are shown in Table 7.

Table 7. Results of Six-Variable System Optimization

Design Details		Output Details	
<i>ID</i>	18”	<i>weight</i>	355.9 lbs
<i>Len</i>	20”	v_{max}	0.531
<i>b</i>	0.61	P_{drop}	0.756%
<i>Loc</i>	68%		
c_1	14”		
c_2	229”		

There are a few important things to note in this solution. The minimum possible bottle size (and, therefore, the minimum weight) has been selected, so there is no additional room for improvement in the objective function. Both constraints are satisfied; the peak vibration is less than 0.75 ips (inches per second) and the pressure drop is less than 1%. Also, the first clamp, c_1 , at 14 inches, is placed as close as possible to the bottle, which is in line with where it would likely be placed if this design was performed manually rather than algorithmically, lending some credibility to the solution.

By including the orifice details and the clamp locations in the analysis, we located lighter solutions than were possible when these were fixed and only the bottle was optimized in the previous section. Note that c_1 was set at the lower bound. This was as close to the bottle as a clamp could be placed, which we know is a critical location to place a clamp, so it was good to see the optimizer deduce this as well.

2.9 Sensitivity Study

The optimization considered six design variables, but not all of these have the potential to vary from their specified value when the system is constructed. The bottle dimensions (inner diameter and length) are expected to be exact, as is the beta ratio of the orifice. It is possible to see some slight variation in the location of the orifice, but previous analyses have shown the performance of the system to be almost completely insensitive to small changes in the orifice location. The remaining variables are the clamp locations and stiffness.

Figure 10 through Figure 13 show the changes in the peak vibration as the locations and stiffness of each clamp are varied. Note that stiffness is varied using a factor on the nominal stiffness for the clamp and is applied to all translation and rotation modes. For each plot, only the indicated variable is being perturbed; all other variables remain at the values determined by the optimization and listed in Table 7.

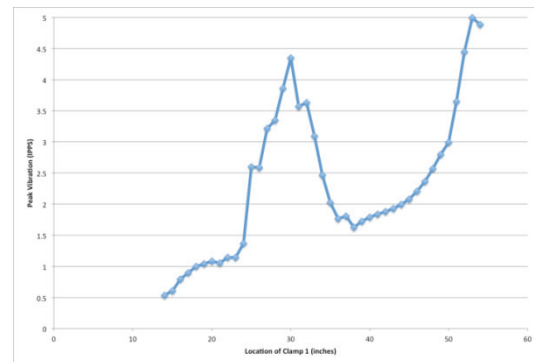


Figure 10. Change in the Peak Vibration as Clamp 1 Moves from the Design Location

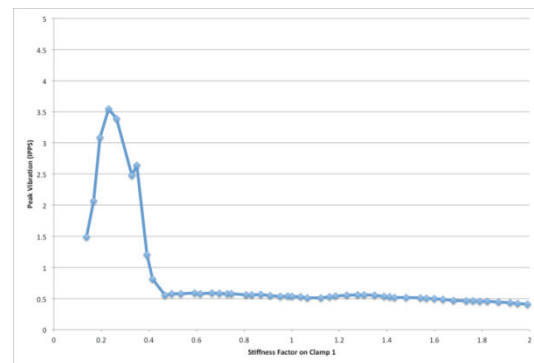


Figure 11. Change in Peak Vibration as the Stiffness of Clamp 1 Varies from Nominal

Optimized Robust Compressor Station Design Methodology

by: Benjamin A. White, Barron J. Bichon, David L. Ransom, Eugene L. Broerman, Southwest Research Institute®

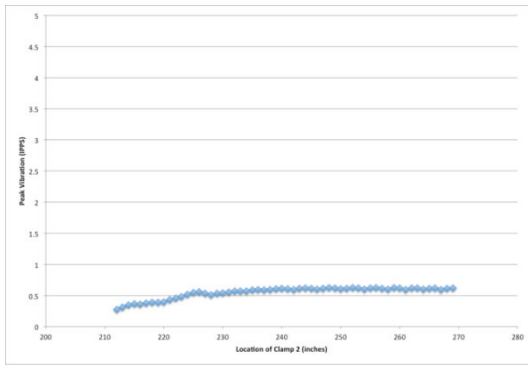


Figure 12. Changes in Peak Vibration as Clamp 2 Moves from the Design Location

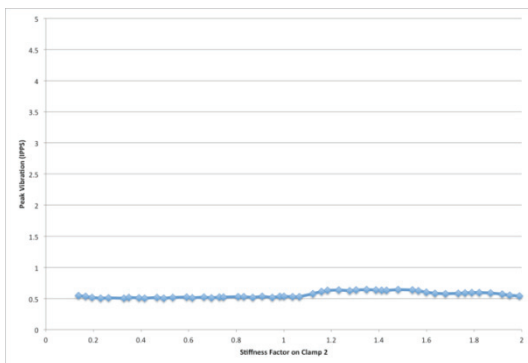


Figure 13. Change in Peak Vibration as the Stiffness of Clamp 2 Varies from Nominal

It is clear that the peak vibration is much more sensitive to variations in the first clamp (the one placed immediately adjacent to the bottle) than the second. Moreover, this sensitivity is such that the first clamp needs to move only five inches away from the bottle for the peak vibration to increase to unacceptable levels ($v_{max} > 1$). In addition, the peak vibration also becomes excessive when the stiffness of the first clamp is reduced below 40% of its nominal value.

Further, it is logically assumed that the installed location and stiffness of the clamp are independent, so there is nothing precluding them from varying simultaneously. It is, therefore, important to investigate the sensitivity of the design to the combined variation of stiffness and location in the first clamp. Figure 14 shows a contour map of this analysis. The areas shaded green are regions where the peak vibration is acceptable ($v_{max} < 1$).

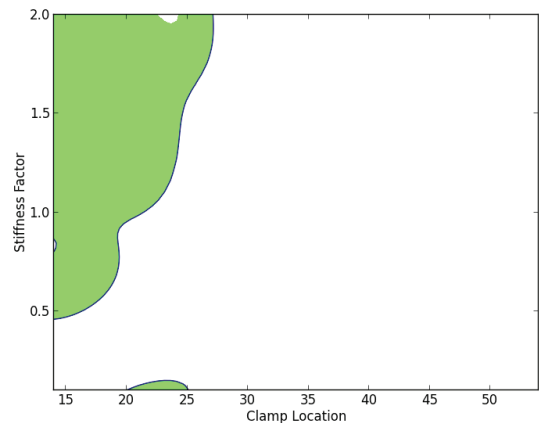


Figure 14. Filled Contour Plot Showing the Region Where, as the Location and Stiffness of Clamp 1 are Varied, the Peak Vibration Remains Below 1 ips (Shown in Green)

This analysis has shown that while the optimal design is a feasible solution, it is possible for perturbations from that design that could occur during its implementation could lead to unacceptable performance. The remaining question is then to determine how likely this poor performance is to occur given expected variations in the construction of the system. To quantify this, a reliability analysis is performed.

2.10 Reliability Analysis

The goal of the reliability analysis is to compute the probability that the peak vibration, v_{max} , which depends on design variables $\mathbf{d}=[ID,Len,\beta,Loc,c_1,c_2]$ (set at the previously determined optimal values) and random variables $\mathbf{x}=[dc,dk]$ (deviations in the location and stiffness of the first clamp from its design value), exceeds the maximum allowable vibration of 1 ips, or:

$$P[v_{max}(\mathbf{d},\mathbf{x}) > 1]$$

The stiffness deviation is modeled as a factor applied to the nominal condition (so a value of $dk = 1$ recovers the nominal stiffness), and is assumed to follow a lognormal distribution with a mean value of 0.8 and a standard deviation of 0.3. A graphical depiction of this distribution is shown in Figure 15.

Optimized Robust Compressor Station Design Methodology

by: Benjamin A. White, Barron J. Bichon, David L. Ransom, Eugene L. Broerman, Southwest Research Institute®

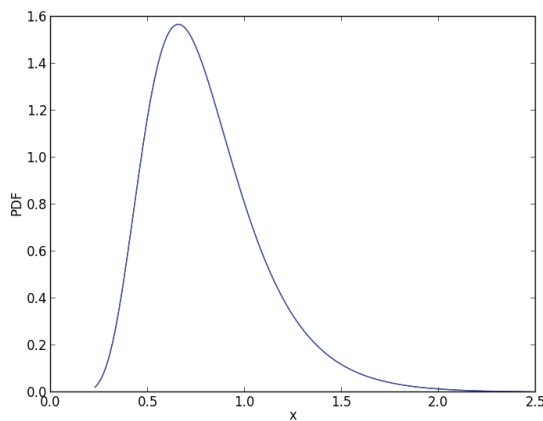


Figure 15. Probability Density Function for the Clamp Stiffness Factor

The location deviation is modeled as an additive shift from the nominal condition (so a value of $dc = 0$ recovers the nominal condition), but the bounds of the location must be kept in mind so that the clamp is only placed (in the model) in locations that are physically possible. The distribution of dc is assumed to follow a normal distribution with a mean of 0 and a standard deviation of 8 inches, truncated so that $c+dc$ has a lower bound of 14 and an upper bound of 378.

To reduce the computational expense of performing this analysis, the Efficient Global Reliability Analysis (EGRA) method was used. This method (much like the EGO optimizer, hence the similar name) constructs a Gaussian process model using a small number of samples and then iteratively adds new samples to improve the model by targeting these only near the boundary that separates the success and failure regions (i.e., the contour depicted in Figure 14). In this way, an accurate surrogate model is constructed with a minimal number of function evaluations.

The results of this analysis show that the probability of failure for the optimal design is 52.9%, meaning that even though the nominal design produces a peak vibration of 0.531 ips, when the design is implemented, there is a greater than 50% chance that the actual peak vibration will exceed 1 ips. This is clearly problematic. One way to overcome this is to directly include a constraint on this probability of failure into the optimization process through reliability-based design optimization (as discussed in the following section).

Some of the predicted vibration levels in the design space were as high as approximately 10 ips (increasing from a nominal value of 0.531 ips). To verify the validity of the reliability solution, the results of several potential solutions with very high vibration levels were reviewed in detail.

The cause of the sharp increase in predicted vibration was primarily due to a mechanical response of the vertical pipe run near the bottle. As the location of the clamp nearest the vertical pipe run is shifted, the lowest mechanical response frequency of the vertical pipe run drops down from above the operating speed range into the frequency range where it is excited. In the nominal case, the peak vibration occurs in the pipe span between clamps, where the excitation doesn't couple very well into the structural system. The vertical pipe run doesn't exhibit any significant vibration peaks since its lowest mechanical response is above 2X running speed. In the higher vibration cases (with the clamps moved), the response frequency of the vertical pipe run drops from 36 Hz (nominal case) down to the range of 21-28 Hz, and the vibration increases greatly. See Figure 16 and Figure 17.

In summary, it was determined that the reliability solution was accurate and the system is very sensitive to the first clamp location and stiffness. For this particular nominal optimized solution, the system is designed with a very small bottle (less pulsation control) and relies on carefully placing the mechanical response frequencies, which are more susceptible to clamp variability.

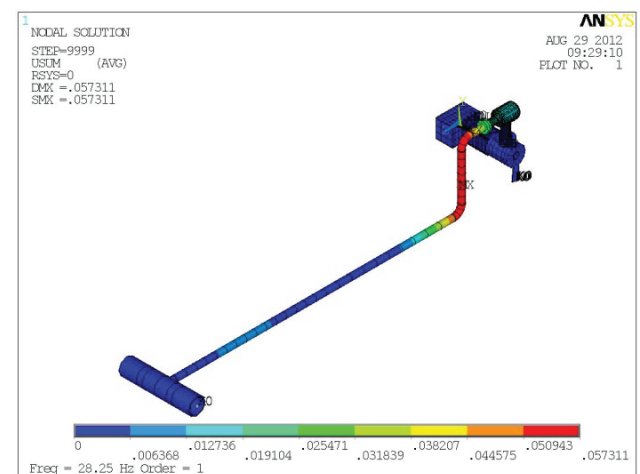


Figure 16. Peak Vibration Pattern with Potential Variation

Optimized Robust Compressor Station Design Methodology

by: Benjamin A. White, Barron J. Bichon, David L. Ransom, Eugene L. Broerman, Southwest Research Institute®

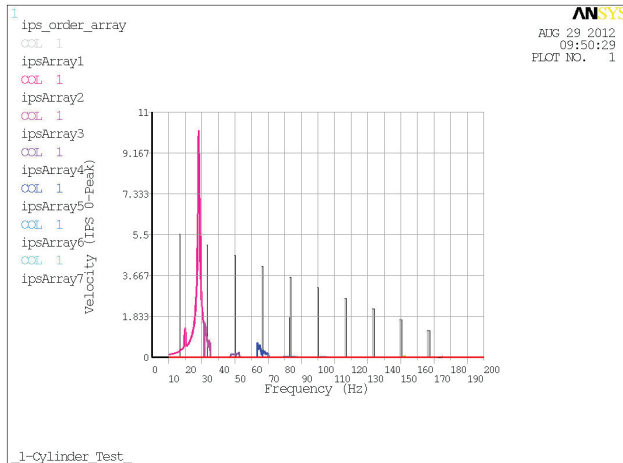


Figure 17. Vibration Plot with Potential Variation

2.11 Reliability-Based Design Optimization

Adding the reliability analysis computed in the previous section as a probabilistic constraint to the problem formulation, the system problem to be solved is now written as:

$$\begin{aligned} &\min \text{weight}(ID, Len) \\ &\text{s.t. } P[v_{\max}(ID, Len, \beta, Loc, c_1, c_2, \delta c, \delta k) > 1] < 1\% \\ &\quad P_{\text{drop}}(ID, Len, \beta, Loc) < 1\% \\ &\quad 18" < ID < 34" \text{ (in 2" increments)} \\ &\quad 20" < Len < 92" \text{ (in 2" increments)} \\ &\quad 0.5 < \beta < 0.7 \\ &\quad 90" < c_2 < 378" \end{aligned}$$

For this work, for any candidate design point, a full reliability analysis is performed to quantify the probability of failure given that design. EGO is used again as the design optimizer and EGRA is used in the reliability analysis. These are great options to reduce computational expense, but it is still time-consuming to perform a reliability analysis at every design point. To improve this, the optimization problem has been altered slightly to take advantage of knowledge gained on this problem thus far and to construct the problem in a way that is closer to how it might be approached in practice.

First, rather than allow the orifice β ratio to vary from 0 to 1 (all the way from fully closed to fully open), more realistic bounds are used and it is now restricted to be between 0.5 and 0.7. Next, it has been repeatedly observed that this system is relatively insensitive to the orifice location. For the RBDO problem, the value of Loc is fixed at a common value used in design (for this design, at 100%). The final modifications involve the clamp locations. It is unsurprising that the optimal location of the first clamp is as close to the bottle as

possible. If this system were designed manually, a clamp would certainly be placed in the same location. It therefore makes sense to remove this as a design variable and fix the location of the first clamp at 14 inches. This, in turn, increases the feasible region in which the second clamp could be placed, so its bounds have been increased (the lower bound has been reduced from 212 to 60 inches).

The optimal results from this RBDO study are shown in Table 8.

Table 8. Results of System Optimization with Reliability Included (RBDO)

Design Details		Output Details	
ID	20"	$weight$	464.7 lbs
Len	22"	$P[v_{\max} > 1]$	0.970%
b	0.56	P_{drop}	0.943%
c_2	99"		

At this design, the probability that the peak vibration exceeds 1 ips has been reduced from 52.9% to just 0.97%. To do this, the size of the bottle was increased; though the ID and Len are still very close their lower bound values. The orifice β ratio has been reduced slightly, causing the pressure drop to increase, but it still remains below the 1% allowable value. Interestingly, the second clamp has been placed at 99 inches, a value that was not possible given the previous problem formulation.

For comparison, the two-dimensional sensitivity study that was performed for the deterministic optimal design is repeated for this RBDO result. The contour map that results from this study is shown in Figure 18. This plot clearly shows a much larger region of the space that is in the success region (where $v_{\max} < 1$; shown in green).

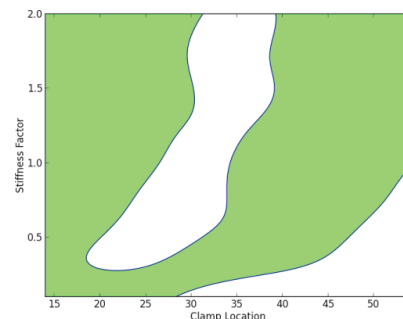


Figure 18. Filled Contour Plot Showing the Region Where, as the Location and Stiffness of Clamp 1 are Varied, the Peak Vibration Remains Below 1 ips (Shown in Green)

Optimized Robust Compressor Station Design Methodology

by: Benjamin A. White, Barron J. Bichon, David L. Ransom, Eugene L. Broerman, Southwest Research Institute®

2.12 Summary of All Bottle and System Optimization Results

Table 9 summarizes the results of the optimization runs discussed in this report.

Table 9. Summary of Optimization Results

System	Bottle Weight (lbs)	Vibration / 1.0 ips	Peak Stress / 3,000 psi	Probability of Vibration > 1.0 ips
Original Baseline	2,723	2.59	1.46	not calculated
Manual Bottle Design	723	0.703	0.243	not calculated
Two-Variable Optimization	658	0.638	0.250	not calculated
Six-Variable Optimization	356	0.531	not calculated	53%
Reliability Based Design Optimization	465	0.337	0.128	< 1%

From Table 9, it can be seen that an acceptable design (less than 1.0 inches per second of vibration and less than 3,000 psi stress) can be found using the traditional manual design methods. However, the two-variable optimization process is able to improve slightly on this design (lower weight/cost, lower vibration and similar stress). The six-variable optimization is able to improve significantly on this design (with lower weight/cost, lower vibration and lower stress), but can be subject to installation tolerances. Including reliability in the optimization process results in a design that is both optimized and robust.

3. CONCLUSIONS

As a result of this research project the feasibility of the optimization and robustness processes as applied to compressor design has been demonstrated.

Using a simple one-cylinder test model, this research project has developed computer coding that will automatically identify the worst load cases from the fluid system, optimize the full system to reduce vibration and bottle weight and recheck key parameters such as pressure drop and dynamic stress after the optimal solution is found. Additionally, the robustness of the design can be checked after an optimal design is found or the robustness can be included as part of the design optimization.

Ultimately, the results of the optimization process are similar to those achieved by typical experienced based design methods. However, the optimization process is able to provide improvements to the traditional design methods in several simultaneous areas (such as reducing bottle weight and vibration) by

evaluating many more potential design combinations. Additionally, the reliability based design optimization is able to successfully produce a design that is both optimized and robust to typical installation tolerances.

Moving forward, it is anticipated that these optimization methods can be applied to more complex designs. As the technologies described in this paper mature, there may come a time when a "Robustness Factor" can be developed as an additional means of quantifying the pulsation and vibration characteristics of a compressor system design during the analysis phase. Such a factor could be a numerical measure of the reliability of the system when subject to typical installation tolerances on items such as clamp locations, clamp stiffness values, etc.

4. REFERENCES

"Efficient Global Surrogate Modeling for Reliability-Based Design Optimization," Barron J. Bichon, Michael S. Eldred, Sankaran Mahadevan, and John M. McFarland, ASME Journal of Mechanical Design, Vol. 135, No. 1, January 2013, p. 011109 (13).

API Standard 618, 2007, "Reciprocating Compressors for Petroleum, Chemical, and Gas Industry Services," Fifth Edition, American Petroleum Institute, Washington, D.C.

White, B.A., "Mechanical Modeling of Compressor Manifold Systems," Compressor Tech^{Two}, Three-Part Series published, March 2006, April-May 2006, and June 2006.

Weilbacher, G.W., C.M. Gehri, R.E. Harris, B.A. White, C.R. Sparks, P.J. Pantermuehl, A.J. Smalley, and R. Goodenough, "Acoustic and Mechanical Dynamics Issues for High Horsepower, High-Speed Compressors in Gas Transmission Service," presented at the Gas Machinery Conference (GMC), October 7-9, 2002, Nashville, TN.

9th Conference of the EFRC
September 11th / 12th, 2014, Vienna

Systematic Calculation / Design of the Piston Rod Unit -143-
by: Vasillaq Kacani, LMF

An Advanced Model for Journal Paths in Reciprocating Compressors -150-
including Deformation, Cavitation and Crosshead Bearings
by: I.A.M. van der Kroon, P.N. Duineveld, Howden Thomassen Compressors BV

Thermodynamic Calculation of Reciprocating Compressor Plants -158-
by: Ullrich Hesse, Gotthard Will, Technische Universität Dresden



EUROPEAN FORUM
for RECIPROCATING
COMPRESSORS

SESSION CALCULATION 2



Systematic Calculation / Design of the Piston Rod Unit

by:

Vasillaq Kacani

Leobersdorfer Maschinenfabrik GmbH & Co. KG

Vienna, Austria

vasillaq.kacani@lmf.at

**9th Conference of the EFRC
September 11th / 12th, 2014, Vienna**

Abstract:

In this article a modern and economic method for the strength calculation of the piston rod unit and its components under different operating conditions will be presented. Herefore the commercial FEA - Software will be connected with the company-owned calculation tools. The parametric user input will be followed by an automatic Pre- and Postprocessing. Afterwards the strength calculation is processed on all critical points of the piston rod connection, assisted by an extra module, based on general standards and special codes for reciprocating compressors. In this process most arrangements of the piston rod unit as well as the special geometries of the single-components (piston, piston rod, piston nut,..) can be considered easily.

In this article the modeling of the notches, especially on the piston rod, piston as well as the piston nut will be covered in detail.

1 Introduction

The strength calculation of double acting standard piston for reciprocating compressors is described in ⁶. The presented paper investigates all components of piston rod unit considering the contact properties of all clamped parts and different piston design. The piston rod unit generally includes piston, piston nut, ring and piston rod. On crankcase side the piston rod is connected to the crosshead.

These components are under extremely high loads during the operation of the reciprocating compressor. The forces acting on the components are the pre-load force, the gas force, the temperature as well as the mass force. During one revolution of the crankshaft the gas and mass forces are changing their value and the direction. Further for each crankshaft angle the forces are different on different sections of piston rod unit. That means the strength calculation must be performed for each angle step with the actual pressure and acceleration at the local section and on each notch on all components of the piston rod unit.

Further the boundary conditions such as geometry, embedding of the contact surfaces, materials, strength grade, tight techniques as well as different operating cases of the reciprocating compressor are of importance.

In this paper a systematic design and calculation of the piston rod unit will be presented. This contains the three main steps: structure modelling, (preprocessing), definition of boundary condition, meshing, loads apply, calculation for each crank angle, post-processing (results). All steps are realized automatically using manufacturer calculation/design tools, commercial programming software VB6, C++, FEA-Software³, Scripting Language APDL³ (ANSYS Parametric Design Language) as well as guideline and standards.

The strength verification will be performed according the different guidelines^{1,2,4,5}.

A calculation software was developed to perform an automatic strength analysis of the components of the piston rod unit. The special features of the software are:

- Reduction of the simulation time
- Increasing the quality of calculation
- Calculation of stress curves at each notch along the notch angle α
- Systematic calculation/design and fault prevention through certified software.

2 Pre-processing

The software consists of several calculation modules and their interfaces between the components. The compressor data (like type, frame size, piston rod design, crosshead, connection rod, ..) material-data of the main components (modulus of elasticity, ultimate tensile strength, yield strength, Poisson ratio, fatigue stress values, thermal expansion coefficient ..) can be generated automatically internally from machine- and material databank.

The basic module is the manufacturer program for the design/calculation of the reciprocating compressors. The interface enables every user after the selection and design of a specific compressor, to call the software for the piston unit calculation.

The main data/parameters are a result of the previous compressor selection:

- Stroke, type of piston (one piece, two piece, welded piston..), compressor speed..
- Actual pressure curves over the crankshaft angle, in each cylinder compartments (HE, CE, idle or active compartment, SV-Unloader ..).
- Piston rod parameters: size, neck diameter, thread diameter, surface roughness, heat treatment..
- Piston nut data..

The further data can be input/edited interactively through the user. Fig. 1 shows a screen shot of the user input form with the sketch of the two pieces piston and various input parameters.

- Notch geometry, radius, element type, element size or number of elements. Distance Δs normal to the notch surface for the calculation of the stress gradient required for the fatigue analysis.
- Geometry of contact area between piston, piston rod and piston nut. Type and size of contact elements. Friction coefficient.
- Piston geometry (2D, 3D-modell)
- Welded piston with ribs
- Temperature distribution.
- The assembly preload force of the unit

So the geometry and the loads of the piston rod unit are determined. The data are written down in a temporary file. The next steps are the generating the FE-model, the definition of boundary condition,

Systematic Calculation / Design of the Piston Rod Unit

by: Vasillaq Kacani, LMF

applying of the loads, the calculation, as well as the stress evaluation. All this steps are effected automatically. A special interface for the FEA-simulation in the script language (APDL) was generated.

Fig. 1 User Input Form.

The screenshot shows a complex user input form for ANSYS simulation. It includes fields for material properties (e.g., Young's modulus, Poisson's ratio), dimensions (e.g., diameters, radii), and boundary conditions (e.g., fixed supports, applied forces). The form is organized into several columns, each representing a different part of the simulation setup. A 3D model of the piston rod is displayed on the right side of the form.

Fig. 2 shows the work process flowchart.

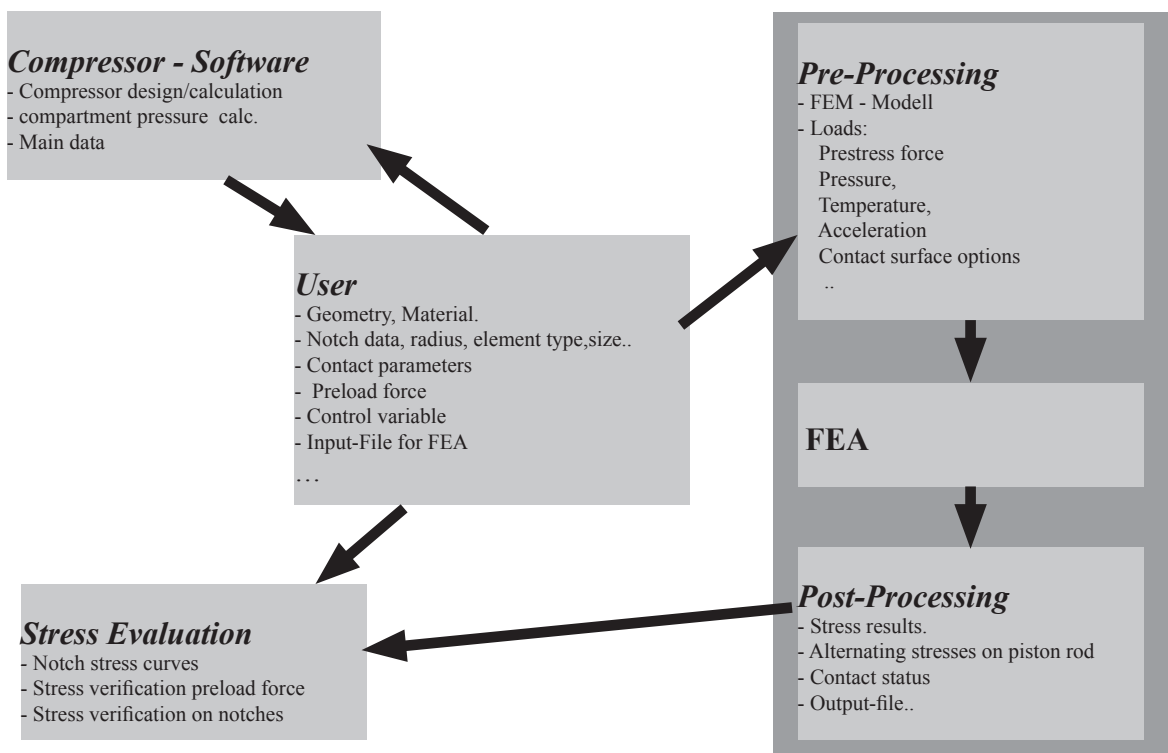


Fig. 2 Work process flowchart

3 Critical stress zones and contact areas.

Figure 3 shows the typical critical high stress zones 1 to 9 and the contact areas I, II, III,...VII.

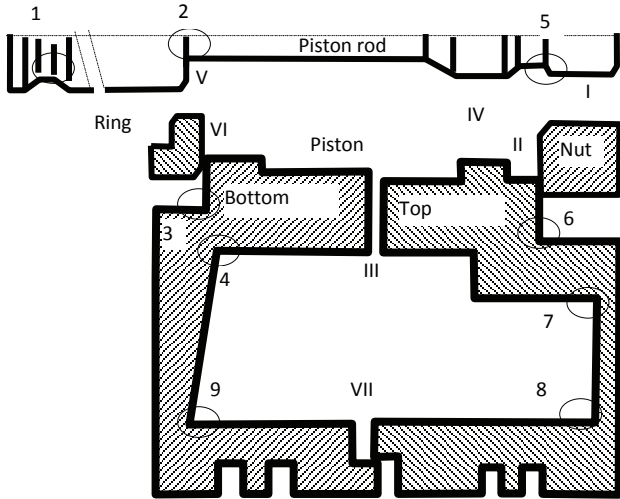


Fig. 3: Stress zones and contact areas.

The critical notches 1, 2 and 5 are in the piston rod. Notch 1 on crosshead side of piston rod is a conical shoulder with radius. Notch 2 is a square shoulder with fillet (radius) in circular shaft. 5 represents a V-notch in a circular shaft (thread). Notches 3, 4, 9 are located in bottom half of the piston 6, 7, 8 are in the top half of piston. These notches are representing changes on cross-section of piston with fillet of radius r . For welded piston the fillet radii shall be assumed to be 1mm (Radaj⁵).

4 Loads applied to the structure

The first load step is the preload force on the piston rod because of tightening of the piston nut. This load can be applying in ANSYS³ with pretension elements. This is the basic load. All other loads are superimposed on the basic load. When specifying the minimum axial assembly forces the loss of the preload force¹ due to the plastic deformation of the contact surfaces must be taken into consideration. In API 618 the recommendation for the minimum preload is 1.5 times the maximum allowable continuous piston rod load. The preload force must be checked for each application under the actual operating loads: pressure, acceleration and temperature. Often the

required preload force is much higher than the API recommendation. In The status of all contact areas, pressure and gap must be checked carefully for all operation condition. The prestress force has to prevent lifting or slide of all contact surfaces.

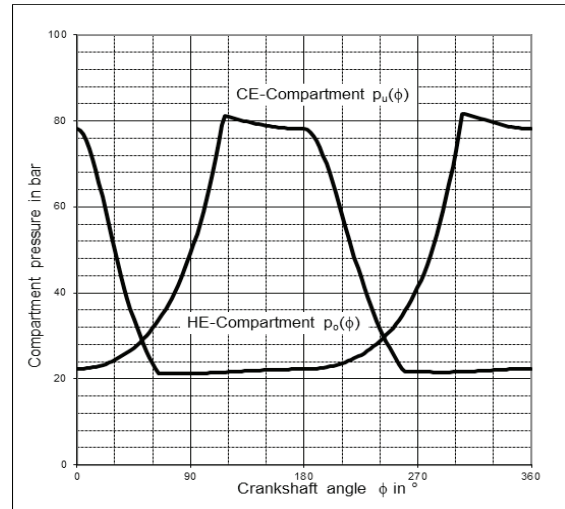


Fig. 3: Pressure versus crankshaft angle for double acting piston.

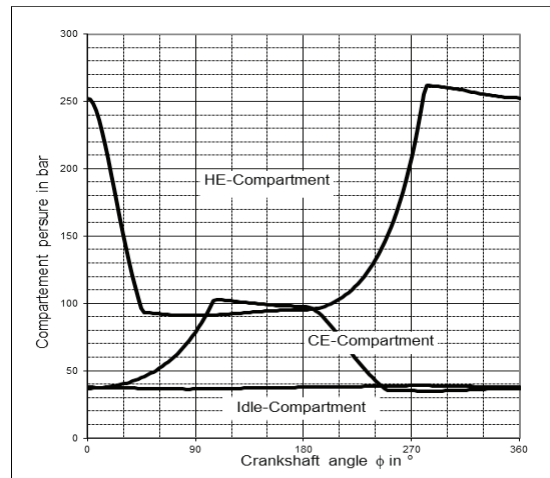


Fig. 4: Pressure versus crankshaft angle for stepped piston.

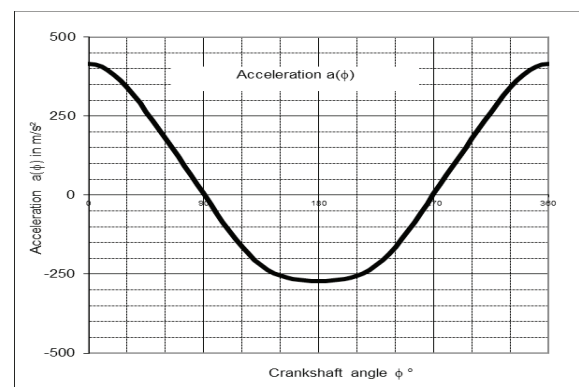


Fig. 5: Acceleration versus crankshaft angle.

Systematic Calculation / Design of the Piston Rod Unit

by: Vasillaq Kacani, LMF

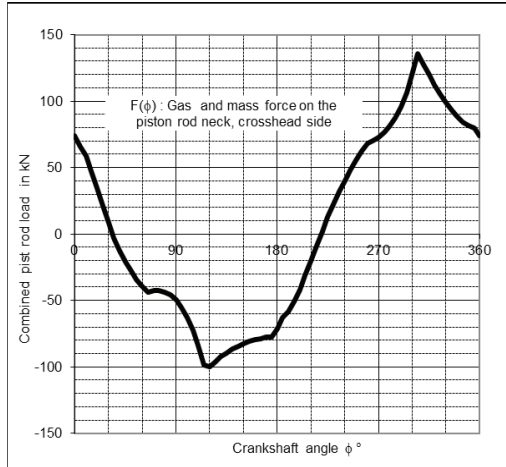


Fig. 6: Combined rod load at the piston rod neck, crosshead side versus crankshaft angle.

Figure 3 and 4 shows the typical pressure curves $p_o(\phi)$, $p_u(\phi)$ on CE-, HE- and idle-compartment for double acting and for stepped piston. These loads are applied on the corresponding areas of the structures (Fig. 7). Further the Figure 5 represents the acceleration and Figure 6 the resulting combined rod load at the piston rod neck crosshead side.

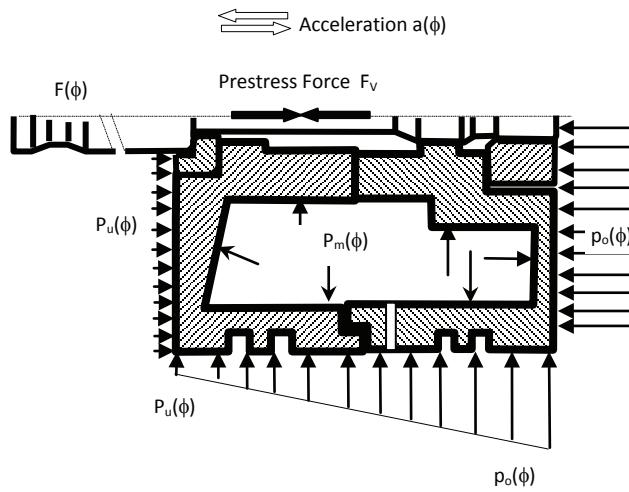


Fig. 7: Loads on the piston rod unit: Preload force F_v , pressure $p_u(\phi)$, $p_o(\phi)$ and acceleration $a(\phi)$.

5 Notch geometry, parameters and stress evaluation.

The main parameters of notches are (Fig.8):

- Shape of notch, local coordinate systems
- Geometry parameters: R, r, α, x, y

- Depth in vertical direction Δs
- Number of elements in circumferential direction 1
- Number of elements in radial direction 3

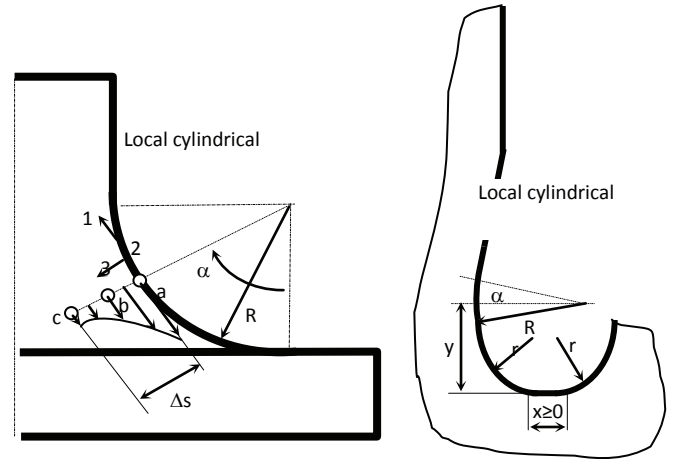


Fig. 8: Typical notch shape and required parameters.

The principal stresses in the local coordinate system are calculated in three directions 1, 2, and 3 along the path (angle α) and for each step of crankshaft ($\Delta\phi$ acc. 1 is 5°). The direction 1 and 2 are always parallel to the free surface. The third direction is perpendicular to free surface of the component.

The stresses are calculated on three points: position a on the free surface $\sigma_a(\alpha, \phi) = (\sigma_{1a}, \sigma_{2a}, \sigma_{3a})$, position b in a depth of $\Delta s/2$ $\sigma_b(\alpha, \phi) = (\sigma_{1b}, \sigma_{2b}, \sigma_{3b})$, as well as position c in a depth of Δs $\sigma_c(\alpha, \phi) = (\sigma_{1c}, \sigma_{2c}, \sigma_{3c})$, (Fig.8). The stress value for σ_1 in perpendicular direction (Δs) to the free surface can be approximated as a polynomial (second order): $\sigma_1 = A_0 + A_1 \cdot s + A_2 \cdot s^2$. The coefficients A_0, A_1 and A_2 can be calculated easy from the three stress values (position a,b,c) established by the FEA-Analysis. Finally the stress gradient can be determined, as required in ^{2,5}, for the strength verification. The equation for the gradient is:

$$\frac{d\sigma_1}{ds} = A_1 + 2 \cdot A_2 \cdot s$$

6 Meshing strategy of the structure

The meshing of the structure must be practice-oriented and the model should have a reasonable size. On the one hand the meshing of the components should be as course as possible to reduce the simulation time and on the other hand as fine as necessary with reference to the engineering tasks. For notches (Fig. 10) and the contact areas a fine controlled meshing is used to get the correct information for the required stresses,

contact status as well as the contact pressure. For other areas of the structure a free course mesh can be used. The element type and size can be adjusted by user. The following figure shows the different piston design (Fig.9): stepped piston 2D-model, two pieces double acting piston 2D and 3D- model, double acting welded piston with ribs 3D-model. All these models can be calculated automatically with the computer program.

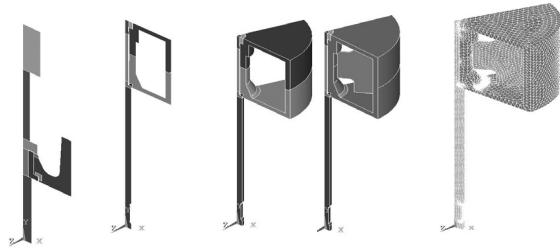


Fig. 9. Piston designs: Stepped piston 2D-Model, double acting piston 2D-Model, 3D-Model and 3D-model with ribs.

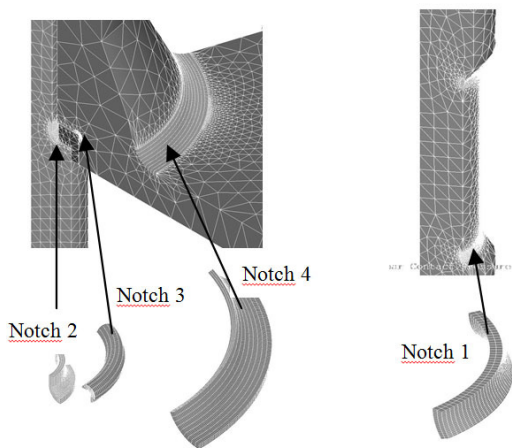


Fig. 10. Controlled fine mesh on notches, free course mesh on the other areas.

7 Finite Element Analysis and Results

The first simulation is the calculation of the prestressed structure under the preload force F_v . The next calculations are successively under operating condition: pressure, temperature as well as acceleration for each crankshaft angle.

The main results of the Finite Element Analysis are the forces / stresses at the piston rod neck, thread (piston side and crosshead side) and the stresses on all notches.

The strength verification of prestressed connection piston rod, ring, piston and piston nut is performed according ^{1,4} guideline. The reduction of preload

force of bolted joint due to the deformation of the contact surfaces is taken into consideration. From the FEA the actual preload force, the amplitude of the alternating force/stresses, maximum forces/stresses in the piston rod neck /thread as well as the resilience of the superimposed clamped parts and piston rod can be determined. From these values the safety factors are calculated. Further the status and the pressure on all contact areas is checked.

The next step is the stress evaluation on the notches. From the FEA results the distribution (stress curves) of stresses on the free surface, on the depth $\Delta s/2$ as well as on the depth Δs along the angle α for each notch and crankshaft angle ϕ are calculated. Further the required alternating stress amplitude σ_a , average stress σ_m as well the stress gradient $d\sigma/ds$ for the fatigue strength verification according ² are calculated.

Figure 11 to 14 shows the stress tangential to the free surface (direction 1) along the angle α in Notch 1, 2, 3 and 4 for two piston position: Bottom-Dead-Center BDC and Top-Dead-Center TDC.

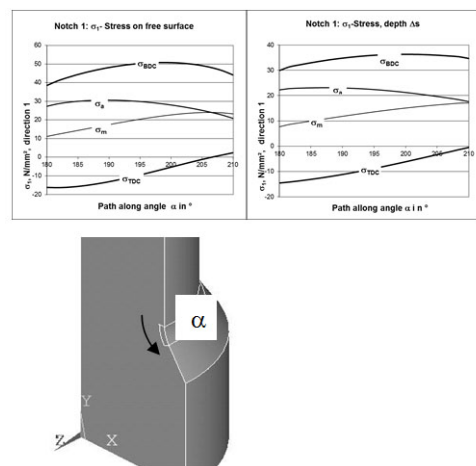


Fig. 11. Notch 1, Tangential stress curves at BDC, TDC, amplitude and average stress on free surface and in depth Δs .

Systematic Calculation / Design of the Piston Rod Unit

by: Vasillaq Kacani, LMF

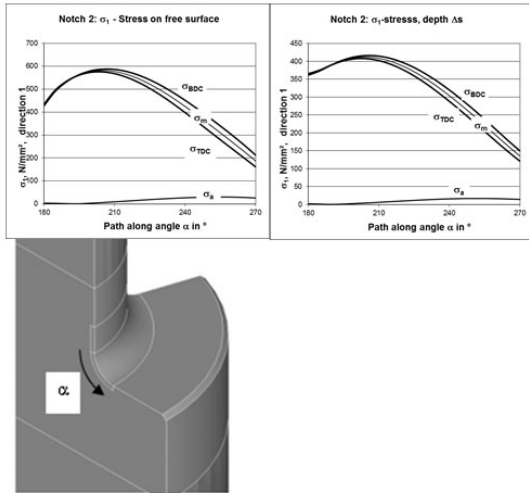


Fig. 12. Notch 2, Tangential stress curves at BDC, TDC, amplitude and average stress on free surface and in depth Δs.

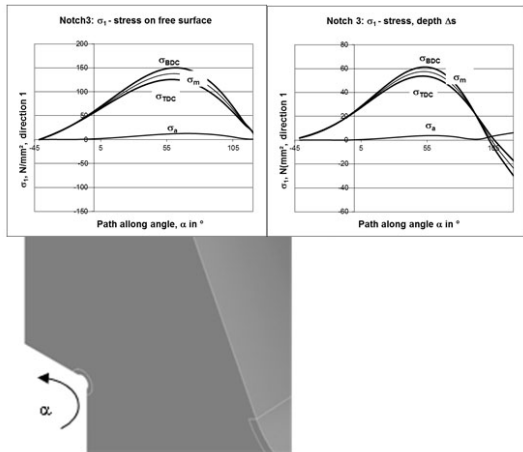


Fig. 13. Notch 3, Tangential stress curves at BDC, TDC, amplitude and average stress on free surface and in depth Δs

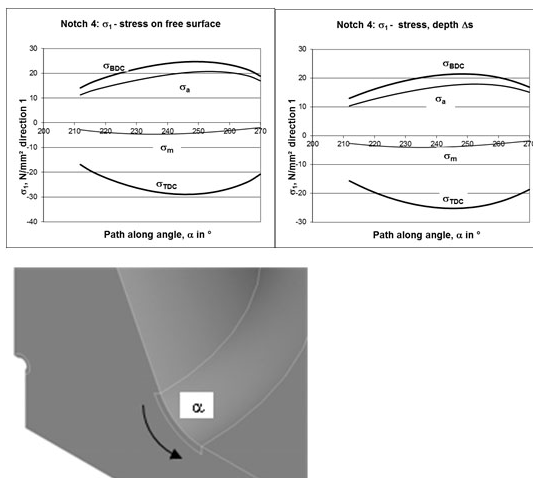


Fig. 14. Notch 4, Tangential stress curves at BDC, TDC, amplitude and average stress on free surface and in depth Δs

8 Summary

The components of the piston rod unit are under very high dynamic loads like: pressure, temperature and acceleration. Depending on the operation mode of the reciprocating compressor, normal operation, SV-Unloaders, VSD, variable operation conditions the load profile of piston rod unit changes. The individual single calculation for each load step requires an enormous effort. The traceability and documentation of analysis would be also a big effort. The method presents a so-called expert system connects different tested and proved modules like company tools, standards, company owned software as well as commercial software together. The calculation is carried out automatically. The main steps of the calculation are:

- Compressor calculation
- User input data
- Modelling of the structure
- Finite Element Analysis
- Verification of the preload force
- Status of the contact surfaces
- Stress verification on the relevant critical notches.

Instead of the suggested factor 1.5 in API 618 5th ed., para.6.10.1, a minimum factor of 1.75 is recommended.

References

- ¹ VDI 2230 Richtlinien. Systematic calculation of high duty bolted joints. Joints with one cylindrical bolt.
- ² FKM-Richtlinie. Rechnerischer Festigkeitsnachweis für Maschinenbauteile.
- ³ ANSYS , Simulation Software.
- ⁴ API Standard 618. Reciprocating Compressors for Petroleum, Chemical, and Gas Industry Services.
- ⁵ Hobbacher. Empfehlungen zur Schwingfestigkeit geschweißter Verbindungen und Bauteile.
- ⁶ Egidius Steinbusch, Gerhard Knop, Peter Houba, Frank Ohler, Klaus Hoff. Automatic Strength Calculation of pistons of Reciprocating Compressors. 4th Conference of the EFRC June 9th /10th, 2005, Antwerp



An Advanced Model for Journal Paths in Reciprocating Compressors including Deformation, Cavitation and Crosshead Bearings

by:

I.A.M. van der Kroon, P.N. Duineveld
Technology Department
Howden Thomassen Compressors BV
Rheden, The Netherlands
iak@thomassen.com

9th Conference of the EFRC
September 11th / 12th, 2014, Vienna

Abstract:

As the load capacity of reciprocating compressors continues to increase, it is increasingly important to be able to determine bearing performance in great detail. At the previous EFRC conference we presented an advanced model for journal bearings analysis with this purpose in mind, including the crosshead pin bearing. This model accounted for material deformation caused by the compressor loads and also showed that bearing design cannot always rely on commonly used models such as the Mobility method.

In this paper, an extended model is presented including the crosshead bearings and implemented with additional physical effects. Similar to the crosshead pin bearing, the crosshead bearings are much more challenging than the rotating bearings. Furthermore, the lateral crosshead load reversal often is marginal. Additional algorithms describe cavitation voids, oil supply and deformation caused by the pressure of the lubricant. The model has the option to consider an entire crank mechanism.

1 Introduction

The load capacity of reciprocating compressor is continuously becoming more challenging and demands for a better understanding of the performance of journal and plain bearings. Traditionally, the Mobility method [1,2] is utilized, which relates the lift to position and velocity of the journal through predefined functions based on the geometry. Although it is reliable in many applications, various physical effects cannot be taken into account.

At the 8th conference of the EFRC we presented an advanced model for the calculation of journal paths in bearings of reciprocating compressors [3]. The model was based on the unsteady two-dimensional Reynolds equations and accounted for arbitrary deformation due to compressor loads. Journal bearings have been the subject of other EFRC papers in the past [4]. In this paper the model is extended with two crucial elements: both plain crosshead shoe bearings.

Bearing performance is not solely characterized by the pressure distribution and the corresponding lift, but by failure potential as well, e.g. caused by cavitation and metallic contact. Force feed lubrication is widely applied as a counter measure, but pushes for a model to account for the dynamic interaction between the pressure in the supply line. Additional improvements are often required, e.g. correct design of grooved bearings constrains the growth of cavitation voids. It should also optimize lubricant consumption versus heat transfer. Another instance is to utilize deformation effects to relieve high loaded sections of the bearing.

However, the correct modelling of all phenomena is not straight-forward. Interaction between fluid and the bearing easily cause instabilities, even without the inclusion of deformation. Nevertheless, a computer application consisting of a model for bearing performance as described is a powerful analysis and design tool.

The paper's outline is as follows. First the relations for the pressure are derived for an unsteady, laminar flow field. Cavitation is included by allowing a two-phase flow and deformation by a mode-based elastohydrodynamic model. The results consist of a number of selected case studies.

2 Theoretical Aspects

2.1 Lubrication Equations

The geometrical arrangement of the crosshead and journal bearing are shown in figure 1. Their positions

are given by variables ϵ_1, ϵ_2 . The bearing and journal surfaces are separated by the film thickness h and one of the surfaces moves with entrainment velocity U . Squeeze velocity is denoted by \dot{h} , where a dot is the general notation for time differentiation. The liquid is incompressible and Newtonian, i.e. density ρ and viscosity μ are constant.

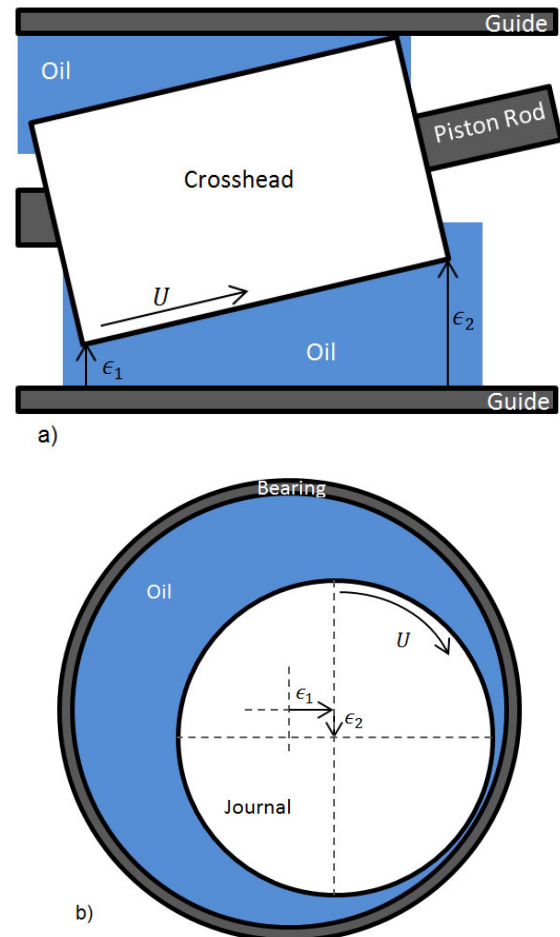


Figure 1: Bearing geometry for the crosshead (a) and journal bearing (b).

The Reynolds equation [4] is derived by assuming a very small film thickness compared to the bearing length ($h \ll L$) and a small Reynolds number (Re) throughout the film (actually $Re(h/L)^2 \ll 1$). Indeed, inertia may be neglected in many lubrication applications. The flux (or mass flow), ϕ , integrated over the entire film thickness is related to the pressure, p ,

$$\phi = \frac{\rho h U}{2} - \frac{\rho h^3}{12\mu} \nabla p. \quad (1)$$

SESSION CALCULATION 2

An Advanced Model for Journal Paths in Reciprocating Compressors including Deformation, Cavitation and Crosshead Bearings by: I.A.M. van der Kroon, P.N. Duineveld, Howden Thomassen Compressors BV

Continuity prescribes the local mass, ρh , to be conserved, which leads to the unsteady Reynolds equation [5]

$$\nabla \cdot \phi + \dot{\rho} h = 0. \quad (2)$$

For constant loaded bearings the film thickness will be stationary and the second term may be omitted.

Relevant boundary conditions are either on the pressure or the flux. At the edge of the film atmospheric pressure is assumed, but a constant supply pressure is an oversimplification. A one dimensional model of the supply line is coupled by adding its mass flow, ϕ_{in} , to the Reynolds equation. The details are not described here, but the dynamics depend on the header and inflow pressure and the dimensional characteristics of the supply line, among others.

The proposed model can be improved to include pressure-dependent density and viscosity. The latter can be obtained by means of a Kirchoff transform for arbitrary pressure-viscosity relations and also leaves the system intact. The first either leads to a non-linear system for p or a non-elliptical one after substituting a constant liquid bulk modulus $\beta = \rho \partial p / \partial \rho$.

2.2 Cavitation

Solutions of the Reynolds equation often exist of varying pressure profiles; pressure peaks generate lift, while very low pressures may incite cavitation, see figure 2. When the pressure drops below the vapour pressure, the large tensile stress in the fluid causes film rupture, i.e. a local phase change resulting in a mixture of vapour and liquid. The pressure inside the cavitation area is approximately at a constant value, p_{cav} , the cavitation pressure. The local density is the weighted sum of the liquid and vapour densities,

$$\rho = \theta \rho_l + (1 - \theta) \rho_v \approx \theta \rho_l, \quad (3)$$

with θ the liquid fraction. This relation is valid since the liquid is much denser than the vapour ($\rho_l \gg \rho_v$). Since the pressure is constant, the Reynolds equation in the cavitation zone reads as follows,

$$\rho_l \left(\nabla \cdot \frac{\theta h U}{2} + \dot{\theta} h \right) = 0, \quad (4)$$

which is similar to the model of Kumar and Booker [6]. They also note that mass conservation is not required to yield reasonable approximations for the film thickness and pressure. The main reason in this study to include continuity is to correctly predict the reformation of the liquid, such that potential cavitation damage may be predicted. In general, the groove design should be optimized to minimize lifetime of cavitation voids.

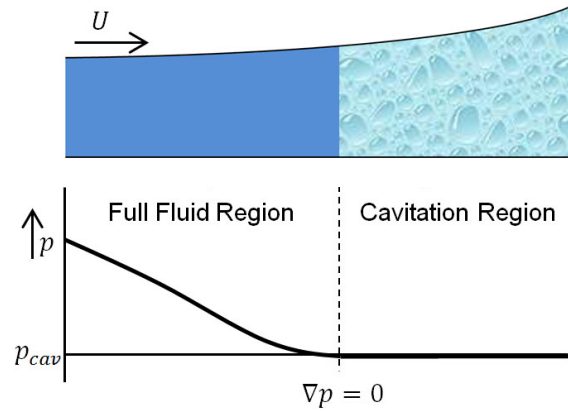


Figure 2: Schematic overview of cavitation: the fluid film ruptures when the pressure drops below the vapour pressure, creating a vapour void. In this divergent film, more fluid tends to flow to the right than is supplied from the left side due to the wall velocity. This effect is countered by a pressure gradient in the opposite direction. However, below the cavitation pressure, p_{cav} , vapor and fluid will coexist.

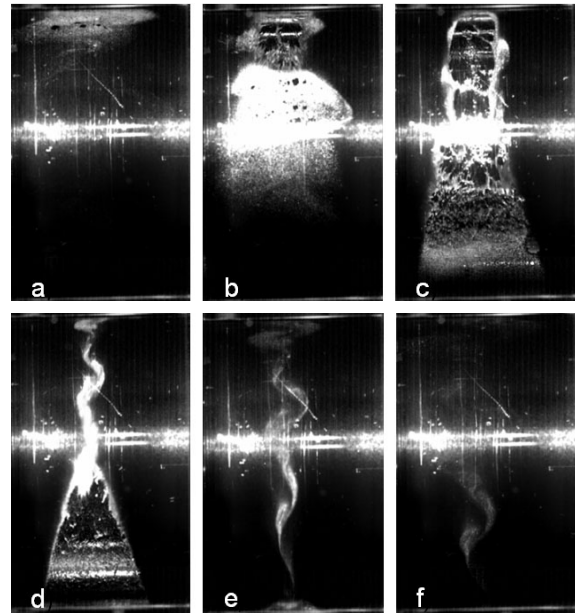


Figure 3: Experimental results of vaporous cavitation in a journal bearing rotating at 58.3Hz (3500rev/min) and recorded at 5000fps [9]. The images show one cycle and are approximately equi-spaced. a) is just after initial rupture, while b) and c) show growth of the void and its movement with the journal. Reformation begins at the top of the image as well and is visible in d) through f).

In practice a certain amount of air will always be dissolved in a lubricant. However, in virtual all circumstances the diffusion of air from the fluid into the cavity is a very slow process [7], such that cavitation is essentially vaporous in nature. In some cases, especially in stationary bearings, the cavity

An Advanced Model for Journal Paths in Reciprocating Compressors including Deformation, Cavitation and Crosshead Bearings by: I.A.M. van der Kroon, P.N. Duineveld, Howden Thomassen Compressors BV

is not destroyed and is gradually filled with air. The reverse is also true; the air bubbles do not dissolve easily in the lubricant once fully devolved. Although cavitation damage is unlikely in this case, the pressure inside the bubbles is complex to model. For an excellent overview of cavitation types and models please refer to [8] and references therein.

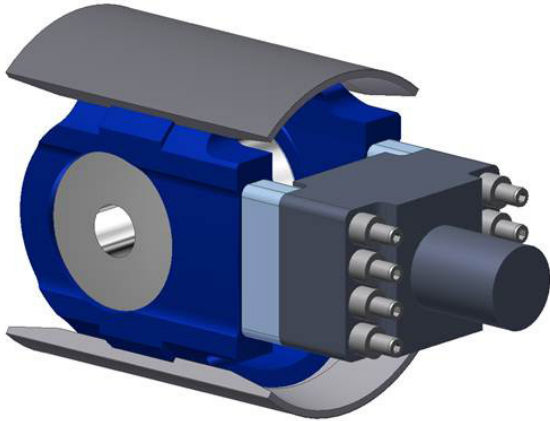


Figure 4: Schematic drawing of a flexible crosshead design. The crosshead (blue) with cylindrical small-end pin bearing and both shoes (grey) is connected to the flange and the piston rod (right). The shoes particularly deform at the unsupported flexible edges.

2.3 Bearing Deformation

In practice, the lubricant pressure will always deform the bearing. At high pressure locations the film thickness is enlarged, such that the pressure peak spreads out, i.e. the maximum pressure is lowered but the lift is hardly reduced. Of course, this effect is desired and may be enhanced by appropriate design of the bearing.

Many models exist describing elastohydrodynamic lubrication. Here, a modal decoupling model is implemented, i.e. the deformation is included as the sum of the eigenmodes of the bearing. Other mode-based elastohydrodynamic models can for instance be found in [10]. The main advantage is that the degrees of freedom of the system are relatively small, such that its dynamical evaluation is not too computationally expensive. Also, the squeeze velocity is well-defined in this model. Deformation is often treated as instantaneous, since its time scale is much smaller than that of the journal motion. However, this means that the velocity of the deformation is much larger, resulting in significant squeeze velocities. This demands for a model to include deformation dynamics accurately.

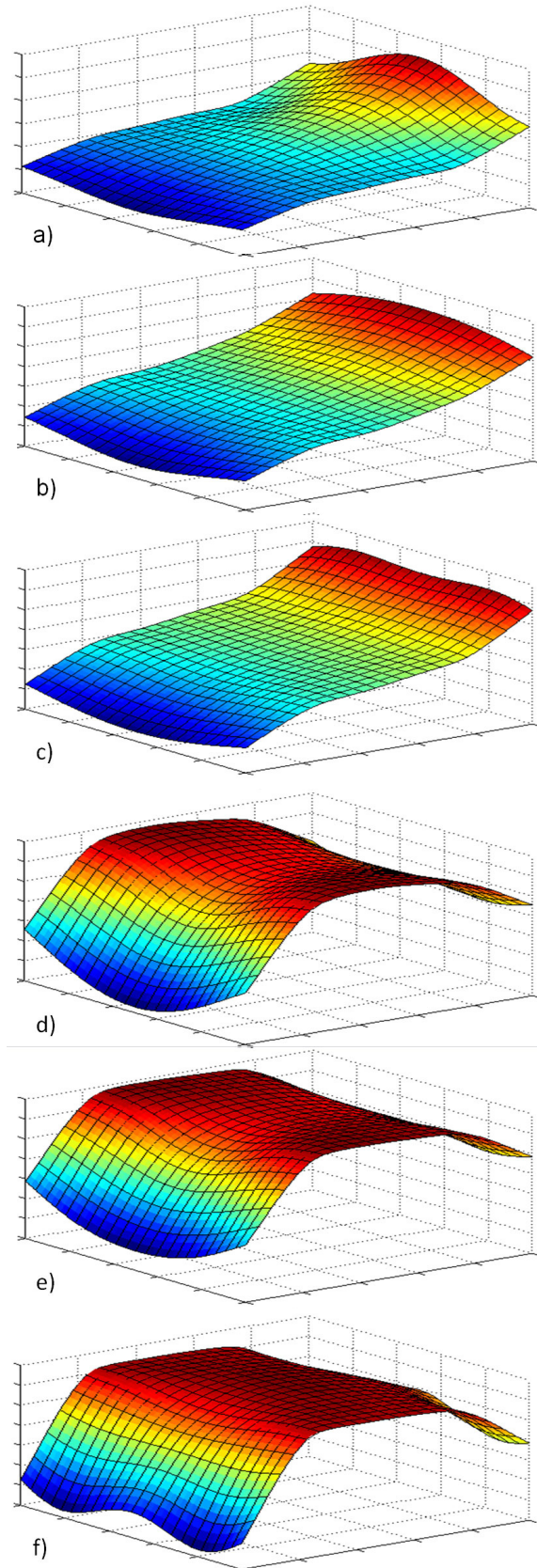


Figure 5: The deformation profiles (h_d) of a crosshead shoe for six modes of the flexible crosshead of figure 4. Especially, larger amplitudes are visible near the edges of the shoe. The configuration is such that the piston rod would be to the right of this shoe.

The deformation thickness, h_d , has to be added to the film thickness (and deformation squeeze, \dot{h}_d , to the squeeze velocity). In this model, deformation is decomposed in modal shapes,

$$h_d = \sum_j a_j d_j, \quad (5)$$

where a_j is the amplitude and the corresponding shape of the j -th mode. Figure 5 shows the deformation of a crosshead shoe for a number of modes.

A standard FEM package can be used to find the relevant mode shapes, as well as the mass and stiffness matrices, see for instance [11]. The deformation shapes of the material in direct contact with the film have to be stored. The interior can be omitted at the cost of modified matrices. The transformation to such a reduced system is outside the scope of this paper, but results in

$$\bar{\mathbf{M}}\ddot{\mathbf{a}} + \bar{\mathbf{K}}\mathbf{a} = f_d(p), \quad (6)$$

with $\bar{\mathbf{M}}$ and $\bar{\mathbf{K}}$ the reduced mass and stiffness matrices and $\mathbf{a} = [a_1, a_2, \dots]$ is the vector containing the amplitudes of the modes. Each mode is excited differently by the pressure field, which is represented by f_d , the mode-dependent force. The required number of modes used in simulation is often unknown. Therefore, modes should be added after every simulation until the change in results is negligible. Damping of 1% of the critical damping was included in order to prevent endless oscillations. To avoid instabilities and small step size selection, it is allowed to omit the inertia of a component, if the corresponding eigenfrequency is very high compared to the journal dynamics.

Naturally, any external load deforming the bearing, e.g. rod loads, has to be included as well. In many cases only the external forces cause significant deformation of the bearing. These loads may be included as a pressure at the corresponding surface, such that eq. 6 remains valid.

The journal and the crosshead guide are assumed rigid in the current analysis, since its stiffness is much larger than the bearing sleeve. However, an identical modal decomposition can be applied if the expected deformation is significant for the guide or journal as well.

2.4 Solution Strategy

Often the journal or crosshead position, ϵ , needs to be found as a function of a certain compressor loading, f_e ,

$$m\ddot{\epsilon} = f_e + f(p), \quad (7)$$

where m and $f_{(p)}$ are respectively the inertia and the corresponding lift force, as a function of the pressure. The unknowns are now the position *and* the deformation, i.e. ϵ and a . This requires simultaneous solutions of eq.6-7. The system is a coupled second order differential equation, which is solved by a variable step size Backward Differential Formula (BDF) for stability and speed, combined with a modified Newton-Krylov method and Richardson extrapolation.

The system is also implicit. The position and deformation variables are related to the pressure distribution (eq.6-7), which is related to the film thickness and its derivative (eq.1-2). The loop is closed by the relation for the total film thickness

$$h = h_g + h_r(\epsilon) + h_d(a), \quad (8)$$

which is the contribution from the grooves, journal position and the deformation respectively. The grooves are constant, but may lead to very steep profiles, since the minimal film thickness is of order 1-10 μ m while a groove may be a few millimetres deep. It was found that a 2nd order finite volume method with harmonic averaging resulted in good approximations, even for medium accurate grids.

3 Case Studies

Two case studies are presented in this section. Firstly, the performance for cavitation and refilling is shown for a rigid small-end bearing. Secondly, the results are presented for the flexible crosshead including deformation effects. For the latter case, a fixed number of modes is selected. The simulation is stopped when a stable periodic motion is obtained. Figure 6 shows the load curves used in the case studies. For simplicity, the supply pressure is held constant in all cases.

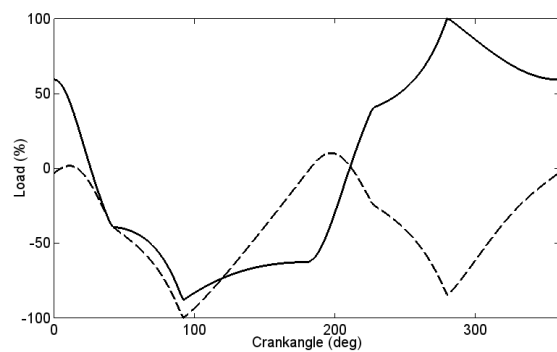


Figure 6: The load curves used in the case studies for the small-end bearing (solid) and the crosshead bearings (dashed). Load reversal occurs in both load cases.

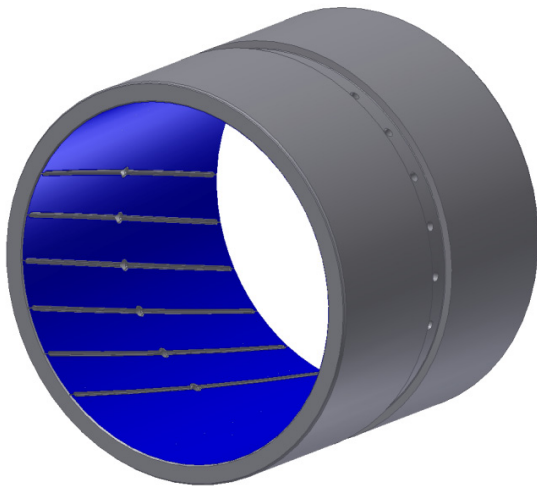
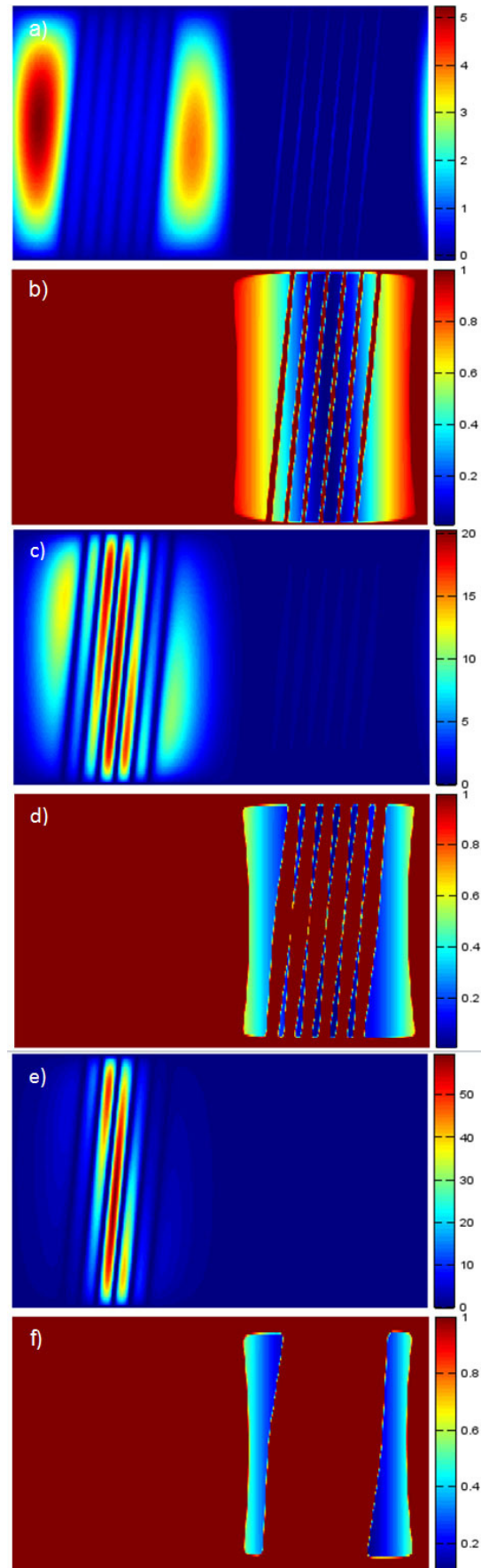


Figure 7: Groove pattern in the small-end bearing example. Both sides contain grooves in the same configuration. The small holes are oil supply holes and are held at constant pressure in this case.

3.1 Small-End Bearing

Figure 7 show the groove pattern in the small-end bearing. The pressure distribution and cavitation voids are plotted in figure 8. The grooves are able to refill the cavitation area between the grooves within 13.7 degrees crankangle after load reversal. This is an important observation when considering small and short load reversals. If the grooves are further apart, the larger areas allow for smaller maximum pressures while generating similar lift. However, the refilling properties will be worse, leading to cavitation damage in extreme cases. The simulation model allows for optimization of bearing and groove designs.

Figure 8: Presentation of the pressure (MPa(g)) distribution (a,c,e) and fluid fraction (b,d,f) for the converged cycle of the small-end bearing. The bearing circumference and width are on the horizontal and vertical axis respectively. At a crank angle of 26.4 degrees the external load is reversed (see figure 6), almost directly resulting in a large cavitation void. At 29.5 degrees (a,b) the void continues to grow and no film rupture is observed in the grooves. Out of the grooves, the fluid then refills the cavitation area. At 34.8 degrees (c,d) the void is separated at the center, while the pressure on the other side is steadily increasing. This is also visible at 40.1 degrees (e,f). At this instance the film between the grooves is completely refilled as well. The supply and cavitation pressures were 0.3MPa(g) and 0.2kPa(a).



The reformation of the fluid is very fast in the center, although the grooves are parallel. This should be expected since the supply line pressure is higher than atmospheric at the edges, such that the pressure in the grooves is highest in the center. However, this result is only obtained when the grooves are implemented accurately.

3.2 Crosshead

The grooves for the crosshead shoes are visible in figure 9. Figure 10 contains a comparison of the pressure distribution and film thicknesses for a flexible and rigid crosshead. For the latter, deformation is omitted, although all other properties, e.g. dimensions and mass, are identical.

Deformation effects will generally lower the overall pressure and increase the film thickness, as is the case for this simulation as well. This is understood as follows. For the rigid case the film profile is rather steep such that a pressure build-up is only locally possible. In the flexible case the pressure pushes the shoe upward resulting in a more straight film profile. The pressure is able to build up over this area resulting in a larger lift force and lower maximum pressures. In figure 10, a crank position is chosen where the maximum pressure is comparable, although the lift is clearly larger in the flexible case due to a better distribution of the pressure. In this instance, the deformation is small compared to the film thickness since the pressure is relatively small as well. However, for the resulting periodic motion, the minimum film thickness was 4.9 times larger for the flexible shoe while the maximum pressure was 2.8 times lower. Both cases experience the same characteristic motion, closely following the load curve.

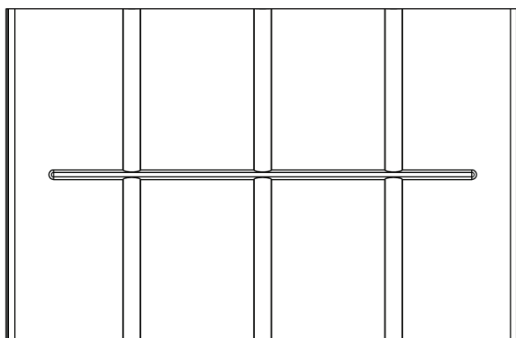


Figure 9: Groove pattern of the crosshead shoe example, identical for both shoes. A single lubricant line supplies the center groove, which is connected to three shallow transverse grooves.

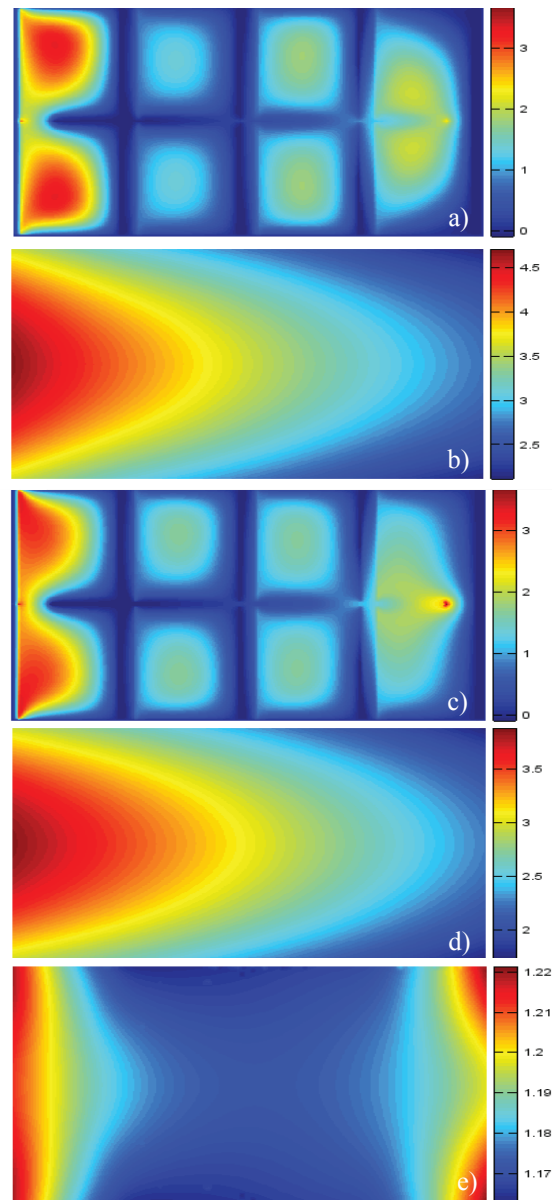


Figure 10: Presentation of the pressure (MPa(g)) distribution and film thickness (10-5m), for the crosshead at a crankangle of 108.3 degrees. The grooves are not shown in the film thickness plots. The fluid is moving to the right close to the maximum velocity. For the flexible crosshead the pressure (a) and the corresponding film thickness (b) are to be compared to the pressure (c) and thickness (d) in the rigid case. The rigid thickness is the distance between two unaligned cylindrical shells. The quotient of the thicknesses is plotted as well (e), to emphasize the function of the unsupported flexible edges. The local pressure maxima at the left and right of the center groove are caused by the fluid moving into or out of this very deep groove. The supply and cavitation pressures were 0.3MPa(g) and 0.2kPa(a).

4 Conclusion

A model is presented able to accurately simulate detailed effects in lubrication, e.g. grooves and deformation. The latter is included by a modal decomposition and coupled to FEM results, which streamlines design development in an engineering environment.

Cavitation and oil supply were included as well, which allows for in depth analysis of film reformation in combination with accurate groove modelling. (This gives this method a large advantage over other models such as the Mobility method.)

The difference between the rigid and flexible configuration is also clear. The larger deformation results in a better distribution of the pressure, resulting in smaller maximum pressures and larger film thicknesses. It is shown that bearing flexibility has advantages and should be exploited in bearing design as elastic deformation could be beneficial to bearing performance.

Although cavitation cannot be prevented, no indication of possible damage was found in the presented simulations. The design of groove profiles should be optimized for bearing performance. Generally, grooves placed closer to each other generate less lift but have better reformation properties, i.e. faster refill of cavitation voids. Supply line characteristics are important as well considering reformation, but is out of scope of this paper.

It is straight forward to consider the entire crank mechanism by expanding the deformation model accordingly and including all relevant bearings. Another logical extension would be to include heat transfer phenomena in the lubricant model. However, no large temperature fluctuations are expected, especially for stable periodic motion.

This model can easily be integrated in software packages. The limited calculation times of the method, accurately simulating the described physical effects, can straightforwardly be utilized for engineering purposes, ultimately resulting in optimized bearing performance. The model is a helpful tool to improve bearing performance to a large extent. It will be utilized in future designs and to improve the load capacity of existing bearings.

5 Acknowledgements

The authors would like thank Dr.Ir. C.H. Venner of the University of Twente for the many animated discussions and valuable advice.

Nomenclature

a	modal amplitudes (m)
d	modal shape
f, f_e, f_d	lift, external, modal lift force (N)
h	total film thickness (m)
h_r, h_g, h_d	rigid, grooved, deformed thickness (m)
\mathbf{K}	stiffness matrix (m^{-1})
\mathbf{K}	reduced stiffness matrix (Pa/m)
\mathbf{M}	mass matrix (kg)
\mathbf{M}	reduced mass matrix ($\text{Pa s}^2/\text{m}$)
m	inertia (kg)
p	pressure (Pa)
p_{cav}	cavitation pressure (Pa)
Re	Reynolds number
U	entrainment velocity (m/s)
β	liquid bulk modulus (Pa)
ϵ	journal/crosshead position (m)
ϕ	flux/mass flow (kg/ms)
ρ	density (kg/m^3)
ρ_f, ρ_v	liquid, vapour density (kg/m^3)
θ	liquid fraction

References

- Booker J. (1971): Dynamically loaded Journal Bearings: Numerical application of the mobility method. *J. Lubr. Tech.*, **93**, 168-176.
- Moes H. (2000): Lubrication and Beyond. Enschede : University of Twente.
- Duineveld P.N., Brogle B., Venner C.H., Van Loo S. (2012): Advanced multilevel solution of journal paths in reciprocating compressors including bearing deformation. *EFRC Conference*, 25-32.
- Hoff. K., Steinbusch E. (2008): Hydrodynamic calculation method for crosshead pin bearings especially under less rod load reversal loading. *EFRC Conference*.
- Reynolds, O. (1886): On the theory of lubrication and its application to Mr. Beauchamp Tower's experiments including an experimental determination of the viscosity of olive oil. *Philos. Trans. R. Soc. A*, **177**, 157-234.
- Kumar, A., Booker, J. F. (1991) A finite element cavitation algorithm. *J. Tribol.*, **113**(2), 276-286.
- Sun, D.C., Brewe, D.E. (1991): Two Reference Time Scales for Studying the Dynamic Cavitation of Liquid Films. *ASME/JSME Cavitation Symposium*.
- Braun, M.J., Hanon W.M. (2010): Cavitation formation and modelling for fluid film bearings; A review. *J. Eng. Tribol.*, **224**, 839-863.
- Xing, C. (2009): Analysis of the characteristics of a squeeze film damper by three-dimensional Navier-Stokes equations. University of Akron, Akron.
- Boedo S., Booker J.F. (2000): A Mode-Based Elastohydrodynamic Lubrication Model With Elastic Journal and Sleeve. *J. Tribol.*, **122**, 94-102.
- Krämer, E. (1984): Maschinendynamik, Springer-Verlag, Berlin.



**TECHNISCHE
UNIVERSITÄT
DRESDEN**

Thermodynamic Calculation of Reciprocating Compressor Plants

by:

Ullrich Hesse, Gotthard Will

Bitzer Chair of Refrigeration, Cryogenic and Compressor Technology

Technische Universität Dresden

Dresden, Germany

Ullrich.hesse@tu-dresden.de

**9th Conference of the EFRC
September 11th / 12th, 2014, Vienna**

Abstract:

The thermodynamic processes in the different gas chambers determine the volumetric capacity and the power consumption of a piston compressor. Methods for the prediction of these processes are used with varying degree of simplification. Motivation of the performed study was to gain information about the influence of the various simplifications and to test the concept of a comprehensive, but practical computation of these thermodynamic processes. Among others, the relationship between the behaviour of the valve and the processes in the valve chambers and pipes were investigated. An estimation of the kinetic energy improved the calculation of the time-dependent heat transfer coefficient in all the gas chambers.

The modelling of measured pressure gradients in the package chambers allowed conclusions about the effective gap areas of the individual sealing rings. For an approximation of the real gas behaviour the state-dependent change of the gas constant and of its relation to the specific heat was introduced into the calculations. The calculations were validated with measured results.

Thermodynamic Calculation of Reciprocating Compressor Plants

by: Ullrich Hesse, Gotthard Will, Technische Universität Dresden

1 Motivation and Goals

The volume flow and the power consumption of reciprocating compressor plants are especially defined by the thermodynamic processes inside the working chambers, which include mainly cylinders and valve chambers. These processes depend on the changes of state in all components of the plant where gas is passing through and their surroundings. Basically this leads to the necessity to have a look at the thermodynamic function of the complete plant during its design phase.

For the development of reciprocating compressor plants procedures are used that consider these complex relations more or less. Combined with the experience of the compressor manufacturers reciprocating compressor plants are designed that usually satisfy the demands of compressor operators.

So, what are the reasons to think again about the thermodynamic calculation of reciprocating compressor plants?

First and foremost for educational reasons it is unsatisfying to explain the thermodynamic relations to future mechanical engineers only with the help of empirical factors (e.g. temperature factor, leakage factor, medial polytropic exponent). Secondly it is difficult to generalize the perceptions that are based on experimental and theoretical investigations of specific reciprocating compressor problems if it is impossible to use a general and preferably realistic model for the thermodynamic processes in reciprocating compressor plants. The third reason is that the state of recent computer technology gives the opportunity to develop that kind of realistic and mostly generalized model of the thermodynamic processes.

For these reasons the development of a modular recalculation program for reciprocating compressor plants was started one year ago by the authors. This model functions as a support for compressor manufacturers and operators as well as for the education and research tasks at the university.

The thermodynamic program covers the calculation of the pressure variation in the valve chambers and reservoirs as well as speed variations inside the pipes. But it is not a substitute for specific calculation programs for pulsation in reciprocating compressor plants as e.g. PULSIM¹ does. It is also not an alternative for specific programs for the simulation of the valve behaviour like KV_DYN² even though it is grounded on the basic equations of valve dynamics of BÖSWIRTH². To consider the real gas behaviour some key data from an equation of state are needed (e.g. utilizing REFPROP³).

However, the developed program should run without the integration of any property tool in the calculation process.

The generalized calculation program should not be a substitute for specific design tools of compressor manufacturers, but it can support the analysis of differences between the layout and the measured results. It can also provide information on operation in partial load. To enable a practical use without any license costs the program should not draw on general programs for system simulation like MATLAB⁴.

Hereafter the following subjects will be discussed:

- the principle of a general modular simulation of a reciprocating compressor plant
- the thermodynamic basics of the calculation of the changes of state in the individual components of the plant
- discussion of specific examples of application

2 Structure of modelling the plant and the calculation program

The modelling of a reciprocating compressor plant is based on the assumption that it has a network structure. In that case the nodes of the network represent the chambers that are filled with gas. Here the thermodynamic state (p , T) is only a function of time and not a function of the location. This correlates to all working chamber, valve chambers and buffers. The boundary nodes are the chambers from which the gas is sucked in and discharged.

The links between the nodes of the network are all the elements wherein the fluid is passing from one node resp. chamber to another. This means every valve that is temporarily an open link between the working chambers and valve chambers and as well as the pipes between the valve chambers and buffers. Also the sealing elements have to be considered as links, as they minimize the unintended mass flow between chambers that are adjacent but still are connecting passes.

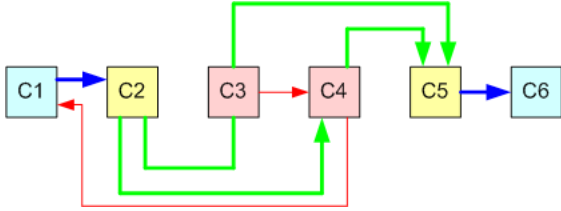
Additional types of links are the heat exchangers that are not primarily utilized for the fluid transport but for the heat rejection (re-cooling) of the gas before it enters the next stage or the pressure chamber. Other links are the wall elements which only transport the heat between different chambers respectively to the surrounding (including cooling medium and lubricant).

SESSION CALCULATION 2

Thermodynamic Calculation of Reciprocating Compressor Plants

by: Ullrich Hesse, Gotthard Will, Technische Universität Dresden

Figure 1 shows the model of the network as an example of a double-acting single stage reciprocating compressor.



List of chambers						
Logical	1	2	3	4	5	6
Technical	S	SC	WCT	WCB	DC	P

List of links								
Logical	LV11	LV2	LV3	LV4	LP1	LP2	S1	S2
Technical	SV TD	DV TD	SV BD	DV BD	SL	DL	Pack	PR
Inp. Ch.	2	3	2	4	1	5	4	3
Outp. Ch.	3	5	4	5	2	6	1	4

Figure 1: Network of double-acting single stage reciprocating compressor

The list of chambers and links contains the relation of the technical and the programs internal terms. Most notably the list of links describes the logical structure of the plant.

The time-depending gas state in all the chambers of the reciprocating compressor plant as well as the mass flows and heat flows in all links can numerically be calculated with the help of a time step method.

$$f(\tau + \Delta\tau) = f(\tau) + \frac{df}{d\tau}(\tau) \cdot \Delta\tau \quad (1)$$

Formula (1) describes the simplest pattern of the time step method. The time derivation of function f is defined by the conditions at the beginning of time step and is assumed to be constant during the complete time step.

The procedure is shown in figure 2. Figure 2a refers to the calculation of the state variables $SV(p, T)$ in chamber k and figure 2b correlates to the transport variables $TV(\dot{m}, \dot{H}, \dot{Q})$ in link l .

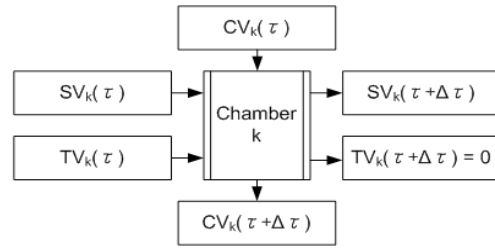


Figure 2a: Calculation of state variables in chamber k

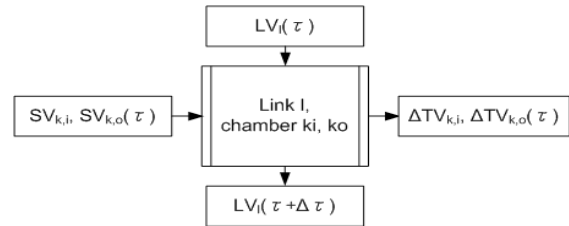


Figure 2b: Calculation of transport variables in link l

The schematic illustration displays that in case a) the state and transport variables in chamber k at the beginning of the time step as well as specific constant or time-depending chamber variable CV (e.g. volume, piston speed) form the input of the procedure *Chamber*. The output is the state of the gas and chamber at the end of the time step.

In case b) the procedure *Link* determines based on the state variables of the links inlet and outlet chamber (ki, ko) the contribution ΔTV to the summarized mass resp. enthalpy flow of the corresponding chambers.. A decisive part of the calculation is the state of the link whose changes during one time step are also determined. This state is described by the values LV (e.g. the current lift and the lifting speed of a valve respectively the pressure and speed distribution inside a pipe).

The summarized transport values have to be reset at the end of the procedure *Chamber* before the summation of the transport variables from all links of the chamber k can start for the next time step.

According to this the scheme in figure 3 shows a consistent set up of the specific procedures for the various types of links. It enables a very simple and clear calculation process.

Thermodynamic Calculation of Reciprocating Compressor Plants

by: Ullrich Hesse, Gotthard Will, Technische Universität Dresden

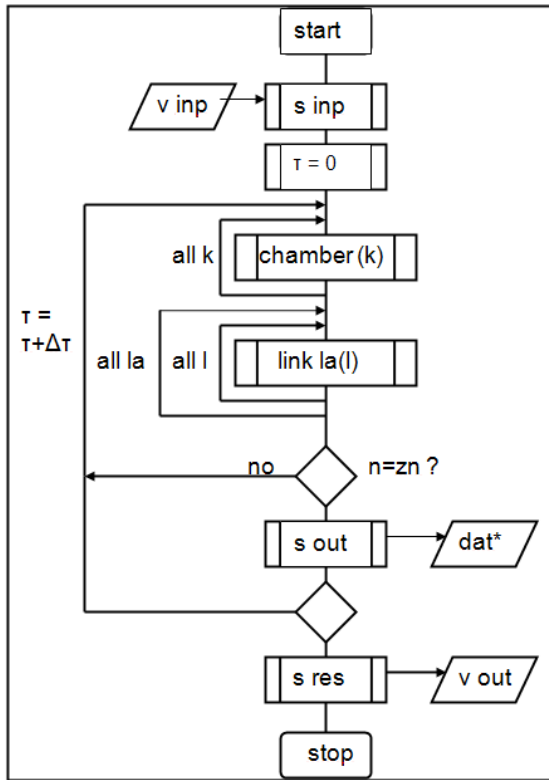


Figure 3: Structure of the recalculating program

The program requires an input file *v inp* that describes every chamber *k* and all links *l* of the reciprocating compressor plant. It provides an output file *v out* that contains the structure of the reciprocating compressor plant, mass and energy balances for every chamber and link, as well as for the entire compressor plant itself.

The calculation procedure takes place in a temporal loop with a given step range and step rate. In the loop of all chambers the changes of the state values are calculated. In another double loop for every type of link and for every link of one kind the transport values that correlate to the chambers are evaluated. The outer loop considers the type of the link while the inner loop deals with the number of links.

According to previous experiences the calculation of the state conditions of only a few working cycles is sufficient to find a stable solution, if the initial values have been set reasonably.

During the calculation of the last working cycle several selected files *dat** can be generated. They include the physical value * over time and can be used to visualize the thermodynamic processes (e.g. in terms of a *p,V*-diagram or a *T,s*-diagram).

3 Theoretical fundamentals of the thermodynamic calculation

3.1 Changes of state inside the chambers

Basis of the calculation are the general gas equation and the law of conservation of energy (1st law of thermodynamics). For the solution of the equation in a time step procedure both equations are used in a form that is derivated with respect to time (equation (2) and (3)).

$$\frac{1}{p} \frac{dp}{d\tau} = \frac{1}{T} \frac{dT}{d\tau} - \frac{1}{V} \frac{dV}{d\tau} + \frac{1}{m} \frac{dm}{d\tau} + \frac{1}{R} \frac{dR}{d\tau} \quad (2a)$$

$$R = R_0 \cdot Z \quad (2b)$$

$$\frac{1}{R} \frac{dR}{d\tau} = \frac{1}{Z} \frac{dZ}{d\tau} \quad (2c)$$

With transforming of equation (2) and (3) the explicit equations (4) and (5) for the temporal change of the state conditions *p* and *T* are obtained.

$$\frac{1}{p} \frac{dp}{d\tau} = \frac{K}{K-1} \left(\frac{p}{m \cdot K \cdot R \cdot T} \frac{dQ}{d\tau} - \frac{1}{V} \frac{dV}{d\tau} - \frac{1}{K} \frac{dK}{d\tau} \right) \quad (4)$$

$$\frac{1}{T} \frac{dT}{d\tau} = \frac{K}{K-1} \frac{1}{m \cdot K \cdot R \cdot T} \frac{dQ}{d\tau} - \frac{1}{K-1} \frac{1}{V} \frac{dV}{d\tau} - \frac{1}{m} \frac{dm}{d\tau} - \frac{K}{K-1} \frac{1}{K} \frac{dK}{d\tau} - \frac{1}{R} \frac{dR}{d\tau} \quad (5)$$

As each chamber of a compressor plant is an open system, the heat flow $dQ/d\tau$ in equations (3) to (5) represent the sum of the convective and substance-related heat input and output. Thus the evaluation of equation (4) and (5) requires besides the knowledge of the temporal alteration of the chambers volume also the provision of the mass, enthalpy and heat flows that enter respectively leaving the chamber.

If for the considered range of state an approximately ideal gas behaviour of the fluid can be assumed, than the following values are known:

$$\bullet \quad Z = 1 \quad (6a)$$

$$\bullet \quad R = R_0 \quad (6b)$$

$$\bullet \quad K = \frac{\kappa}{\kappa-1} \cdot R \quad (6c)$$

So, the terms with the derivations of R and K can be omitted.

The variance of the values R respectively Z and K have to be taken into account if the pressure inside the compressor is $p_{red} = p/p_{crit} \gg 1$ or the suction temperature is $T_{red} = T/T_{crit} < 1$.

3.2 Transport processes in the links

The calculation of the changes of state in every chamber of the reciprocating compressor plant takes place according to the same principle. Whereas the calculation of the transport processes for the different link types distinguish from each other.

Examples are the mass and enthalpy transport through the valves and pipes as well as the heat transport through the walls that enclose every chamber.

3.2.1 Mass flow through the valves

The assumption for the calculation of the mass flow through the valve is a nozzle flow through the valve gap. There is no heat input or dissipation and the kinetic energy inside the chamber after the valve (working chamber or discharge chamber) is completely converted into heat.

$$\dot{m} = h \cdot l_{gap} \cdot \alpha_{flow} \cdot \psi_m \sqrt{2 \cdot p \cdot \rho} \quad (7)$$

In equation (7) the variables h and l_{gap} represent the valve lift respectively the length of the valve gap. The flow coefficient α considers the irregularity of the speed in the cross section of the valve gap that is conditioned by the geometry and the friction. ψ_m is the flow coefficient that depends on the pressure ratio and has its maximum at the critical pressure ratio. The variables p and ρ define the state conditions in the chamber in front of the valve (suction chamber or working chamber).

For the determination of the time depending lift of a real valve the balance of forces needs to be considered.

$$\ddot{h} \cdot m_{pl} = F_{fluid} - F_C \quad (8)$$

The lift acceleration is a result of the difference of the fluid force and the spring force referred to the moving mass. The fluid force can be calculated with equation (9).

$$F_{fluid} = A_{seat} \cdot \psi_f \cdot \Delta p_{fluid} \quad (9)$$

The difficulty is not only to choose the correct force value ψ_f that depends on the design and the lift, but also that the pressure difference Δp_{fluid} that is not equal to the entire pressure difference Δp_{entire} between the chambers in front of and after the valve.

According to BÖSWIRTH² the energy balance for the valve flow reveals an expression for the pressure difference

$$\Delta p_{fluid} = \Delta p_{entire} - \Delta p_{pl} - \Delta p_{inertia} \quad (10)$$

wherein the last two terms express the pressure drop due to the work that is provided at the valve plate respectively due to the inertia of the gas. These terms can be calculated with the following equations.

$$\Delta p_{pl} = \rho \frac{F_{fluid} \cdot \dot{h}}{\dot{m}} \quad (11a)$$

$$\Delta p_{inertia} = \ddot{m} \cdot G \quad (11b)$$

The parameter of inertia G can be assumed according to BÖSWIRTH² depending on the valve geometry. Equation (11a, b) includes the mass flow with its temporal change. So the exact solution of the equation system (8 to 11) leads to a non-linear differential equation for the mass flow. This makes the use of the time step procedure for the calculation of the valve behaviour more difficult. As exemplary calculations revealed is the consideration of the terms in (11a, b) important especially at high rotational speeds and high pressure ratios.

3.2.2 Mass flow through the pipes

The gas flow inside the pipes of a reciprocating compressor plant is unsteady because the pressures inside the chambers are not constant. The compressibility and the inertia of the gas lead to the fact that the flow velocity c inside the pipes is also a function of the location.

Thermodynamic Calculation of Reciprocating Compressor Plants

by: Ullrich Hesse, Gotthard Will, Technische Universität Dresden

At constant cross-section of the pipe and isentropic gas flow the continuity equation and the impulse equation can be applied (12a, b).

$$\frac{\partial \rho}{\partial \tau} - \rho \frac{\partial c}{\partial x} = 0 \quad (12a)$$

$$\frac{\partial c}{\partial \tau} - \frac{1}{\rho} \frac{\partial p}{\partial x} = 0 \quad (12b)$$

For the solution of these equations the characteristic method can be used, which can be implemented in the time step procedure quite well. According to BRÜMMER⁵ a numeric procedure was developed that allows a predefinition of the time step and space step.

In that process the pressure p_x and the speed c_x at location x_i and time $\tau + \Delta\tau$ are determined of the pressure and speed values at the time τ at the locations A and B according to equations (13a, b). Here also the influence of friction is considered in the last term of equation (13b).

The position of A and B results from the slope of the characteristics that depend on the local values of the fluid speed and the speed of sound. For that reason the values p_A, p_B and c_A, c_B are defined by the interpolation of the values at the sampling points x_i .

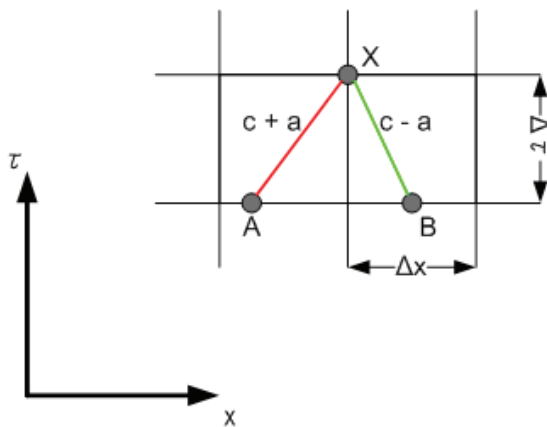


Figure 4: Solution domain of the characteristics method according to BRÜMMER⁵

$$p_x = \frac{1}{2} (\rho \cdot a \cdot (c_A - c_B) + (c_A + c_B)) \quad (13a)$$

$$c_x = \frac{1}{2} \left(\frac{1}{\rho \cdot a} \cdot (p_A - p_B) + (c_A + c_B) - 2 \cdot f_x \cdot \Delta\tau \right) \quad (13b)$$

The velocities c_i and c_{imax} are determinative of the mass flow at the beginning and the end of the pipe. But in both cases only on characteristic (X-B respectively X-A) is available. The pressures at the boundary points are identical to the pressures in the adjacent chambers.

3.2.3 Heat flow through the space restricting walls

Equation (14) is valid for the time depending convective heat flow through a wall of the area A_w and the temperature T_w into a chamber with the temperature T and the condition-based heat transfer coefficient α :

$$\dot{Q}_w = A_w \cdot \alpha \cdot (T_w - T) \quad (14)$$

If the following parameters are known only the heat transfer coefficient α is necessary for the solution of equation (14):

- Temperature T is defined by the calculation of the state conditions inside the chamber
- Temperature T_w can be calculated with the help of a heat flow balance at the wall element
- Area A_w of the wall element is known from the geometry of the observed chamber

As a general rule one takes the Nusselt equation for a turbulent flow along a plain panel as the starting point:

$$Nu = \alpha \cdot x / \lambda = 0.0325 \cdot Re^{0.8} \cdot Pr^{1/3} \quad (15a)$$

$$Re = \frac{x \cdot c}{\nu} \quad (15b)$$

For the creation of the Reynolds number the characteristic length and velocity must be used. These values have to correspond to the flow conditions in the observed chamber. Good experiences were found with the following assumptions:

The characteristic length x is set to

$$x = 4 \cdot V / A_w$$

For the characteristic velocity the approach

$$c = \sqrt{c_p^2 + c_{kin}^2} \quad \text{is used.}$$

SESSION CALCULATION 2

Thermodynamic Calculation of Reciprocating Compressor Plants

by: Ullrich Hesse, Gotthard Will, Technische Universität Dresden

Here c_p is the velocity of the piston and c_{kin} is defined by

$$c_{kin} = \sqrt{\frac{2 \cdot W_{kin}}{m}} \quad (16)$$

Here a velocity corresponds to a medial specific kinetic energy inside the chamber. This is not contrary to the assumption of the valve calculation that the kinetic energy is completely transformed into heat, but it only models the temporal procedure of the dissipation of kinetic energy.

The current kinetic energy at time $\tau + d\tau$ is a result from the following equation.

$$W_{kin}(\tau + d\tau) = W_{kin}(\tau) \cdot f_{dis} + dW_{kin} \quad (17)$$

Here $f_{dis} < 1$ is a factor that describes the dissipation of the kinetic energy and dW_{kin} is the kinetic input energy during the time frame $d\tau$.

The factor f_{dis} is defined by an assumed half-life $\tau_{0.5}$ for the kinetic energy. Due to considerations based on the theories of similarity this time should correspond to the Reynolds number, which is the ratio of the inertia and the friction force.

For that purpose the Reynolds number can be described by the following equation.

$$Re = \frac{x^2}{\tau \cdot \nu} \quad (18)$$

As a consequence the half-time is

$$\tau_{0.5} = C_{dis} \frac{16 \cdot V^2}{A_w^2 \cdot \nu} \quad (19)$$

and the factor of dissipation is defined by

$$f_{dis} = \exp\left(\frac{-\ln(2)}{\tau_{0.5}/d\tau}\right) \quad (20)$$

The increase of the kinetic energy inside the observed chamber during the time differential $d\tau$ can be deduced from the incoming and outgoing mass flow and its velocity:

$$dW_{kin} = \left(C_{kin,i} \cdot \dot{m}_i \frac{c_{gap,i}^2}{2} + C_{kin,o} \cdot \dot{m}_o \frac{c_{gap,o}^2}{2} \right) \cdot d\tau \quad (21)$$

Naturally the factors $C_{kin,i}$ and $C_{kin,o}$ are ≤ 1 .

A first benchmark for the coefficient C_{dis} was determined with the help of CFD simulations by LEHR⁸ for the fluid flow and the heat transport in valve chambers of an air brake compressor (see also chapter 4.2).

4 Examples of application

4.1 Single-stage double-acting balanced opposed compressor

In the context of an EFRC project about the internal cooling of a piston rod numerous investigations were made at a balanced opposed compressor⁷ that included unsteady pressure measurements in all working chambers, valve chambers and packing chambers. The measurement results provide good opportunity to compare the calculation program even if the compressor design differs from standard designs due to the specific goals of the tests.

The model of the reciprocating compressor plants structure corresponds to figure 1.

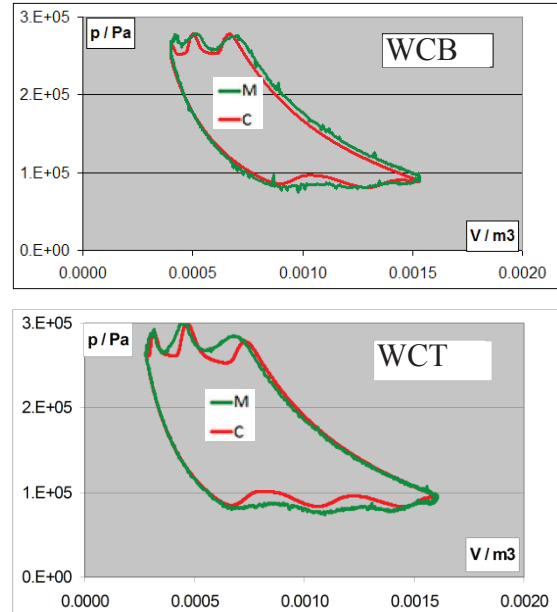


Figure 5: Comparison of calculated and measured indicator diagrams

The comparison of measurements (M) and Calculation (C) shows a satisfying accordance, especially at the behaviour of the compression and re-expansion line. The pressure oscillations during

Thermodynamic Calculation of Reciprocating Compressor Plants

by: Ullrich Hesse, Gotthard Will, Technische Universität Dresden

suction and discharge – which reflect the opening and closing of the valves – are a little bit exaggerated by the calculation but are qualitatively correct. So, the modelling of the valve is realistic despite of the only estimated valve parameters and the negligence of the gas inertia and work at the valve plates.

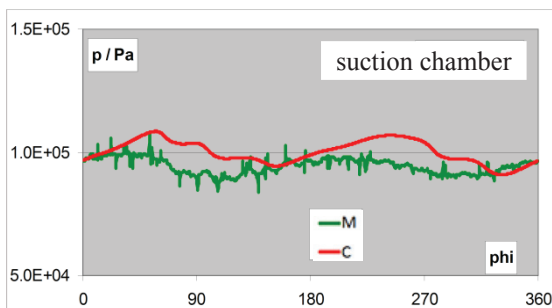
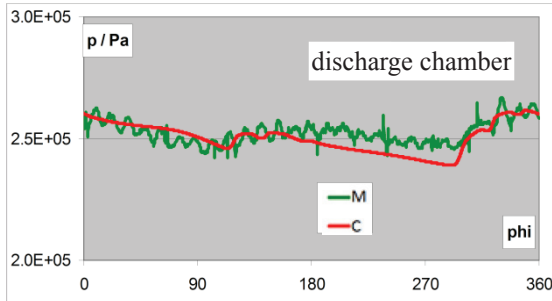


Figure 6: Comparison of calculated and measured pressure behaviour inside the valve chambers

Also the calculated amplitudes and phasing of the long-wave pressure oscillations inside the valve chambers have the correct magnitude. A reason for the differences can be the neglecting of the changes of diameters and branching of the pipes. Probably because of the relatively low number of steps in the calculation of the pipes, the higher frequency pressure oscillations are not reflected.

The measured pressure behaviour in the packing chambers can not only be used for the assumption of the frictional heat but it enables also statements to the effective gap sizes at the sealing elements (when they are described correctly in the calculation program). For that reason the estimated gap sizes were varied in the calculation program as long as the conformity of the pressure lines was achieved (see figure 7). Hence the effective gap sizes of the three packing rings are proportional to about 3:2:10.

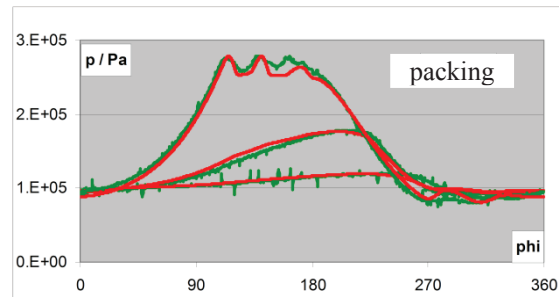
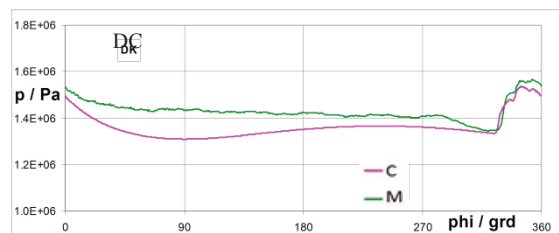
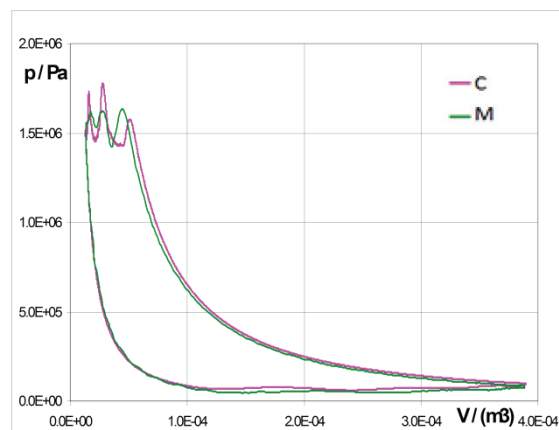


Figure 7: Comparison of calculated and measured pressure behaviour inside the packing chambers

4.2 Single stage air brake compressor

According to LEHR⁸ a single stage air brake compressor of a plunger piston design was investigated regarding the influence of different cooling conditions. Within the scope of these investigations the pressure behaviour inside the working chamber and the valve chambers were recorded. The time and location depending values of the heat transfer coefficients were determined by utilizing CFD simulations of the gas flow inside the chambers.

The high pressure ratio ($\pi=12.5$) and rotational speeds of the compressor of up to 2430 min⁻¹ complicate the reproduction of the valve behaviour.



— C
— M

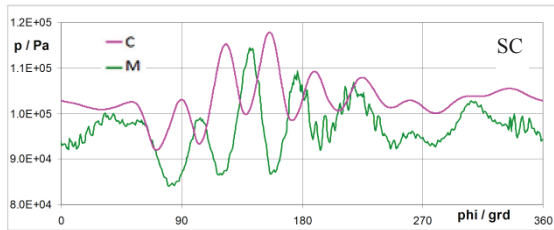


Figure 8: Comparison of calculated and measured pressure behaviour inside the working chamber and valve chambers

The comparison of measurement and calculation shows that especially the behaviour of the pressure valves (three single blades) can be reflected by the calculation only with larger discrepancies. On the other hand the pressure curves inside the valve chambers correspond qualitatively well.

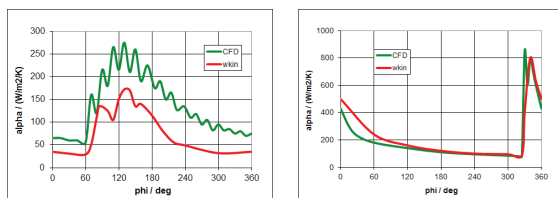


Figure 9: Temporal behaviour of the calculated heat transfer coefficient in the suction and discharge chamber at a rotational speed of 2430 min⁻¹ (left: with CFD simulation; right: from kinetic energy)

Figure 9 shows the – in a variety of ways – calculated heat transfer coefficients inside the valve chambers of the air brake compressor at the highest rotational speed as a function of the crank angle. The first diagram of figure 9 shows the area standardized values of the time-depending distribution of the heat transfer coefficients that were determined for a defined geometry of the chambers and three different given mass flow behaviours with the help of a CFD-simulation. The values in the diagram on the right of figure 9 were appointed with the estimation of the medial kinetic energy as it was described in chapter 3.2.3. Here the same set of values of the C-coefficients in equation 19 and 21 was used for both chambers and both investigated rotational speeds. But it can be seen that this simple way to reflect the tendencies of the detailed calculation has still the potential of improvement.

4.3 Double-stage double-acting balanced opposed compressor

For this example of application no measurements but only data of the design program were available. The structure of the plant could be described by the doubling of the structure in figure 1, where both structure parts are connected with each other by the cooler after the first stage. With the specified inter-cooling temperature of the design the pressure ratio of each stage was confirmed. Figure 10 shows the pressures in every working chamber and valve chamber as a function of the crank angle. No buffers in front of or after the valve chambers were provided in the structure of the plant in figure 1. This is the reason why the pressure curves in the upper part of figure 10 show relative high pressure oscillations inside the chambers and heat exchanger which affect the pressure behaviour in the working chambers during suction and discharge. When increasing the volumes of the chambers up to the values that are recommended in API 618 for buffers the lower diagram in figure 10 is the result.

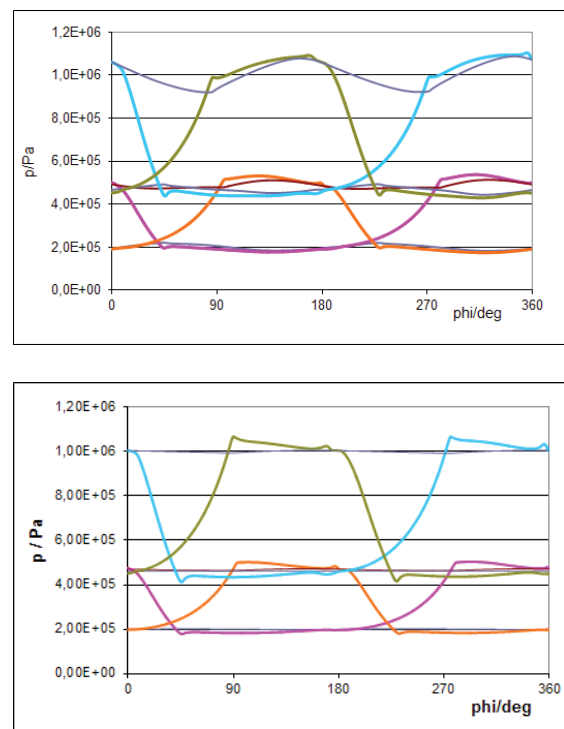


Figure 10: Pressure behaviour in every chamber of a double-stage compressor (top: w/o buffer, bottom with buffer)

Thermodynamic Calculation of Reciprocating Compressor Plants

by: Ullrich Hesse, Gotthard Will, Technische Universität Dresden

5 Conclusion

The examples prove the possibility of the thermodynamic calculation of different reciprocating compressor plants with a uniform algorithm.

The replication of the plant structure with a net model is simple and descriptive. Also the input of the parameters for the description of all plant components is not a problem if the design and the valve parameters are available.

The calculation enables the energetic evaluation of the compressor and its components with the help of energy balances of all plant components and the entire plant itself. Also the effects of parameter changes on the performance of the plant can be observed.

The calculation method provides the opportunity to extrapolate from measurements that can be achieved very easily to hardly measurable values (e.g. temperatures inside the working chamber or gap sizes of the sealing elements).

There is a close relation between the validation of this specific calculation method by application to well investigated compressor plants and the knowledge acquisition of the compressor plant developer. Thus the authors of this paper looking forward for a closer cooperation with a mutual benefit.


List of abbreviations

a	speed of sound
A_{seat}	area of valve seat
A_{w}	wall area
c	velocity of fluid inside pipe
C1-C6	chamber 1 to 6
$C_{\text{kin,i}}$	coefficient of partial consideration of kinetic input energy
$C_{\text{kin,o}}$	coefficient of partial consideration of kinetic output energy
c_p, c_{kin}	piston speed, equivalent speed of kinetic energy
CV	chamber variable
DC	discharge chamber
DVT,B	discharge valve, top dead side, bottom dead side
f	function
f_{dis}	dissipation factor of time step
$F_{\text{Fluid,C}}$	fluid force, spring force
f_x	coefficient of pipe friction
G	parameter of inertia
h, hp	valve lift, velocity of valve lift
H	enthalpy
K	factor of equation (3a)
LP1, LP2	pipes 1,2

LV	link variable
m	mass
\dot{m}	mass flow
\ddot{m}	time derivation of mass flow
m_{pl}	moving valve mass
n	number of working cycles
Nu	Nusselt number
P	pressure chamber
Pack	packing
PR	piston ring
Δp_{entire}	entire pressure difference at valve
Δp_{fluid}	fluid pressure difference at valve plate
$\Delta p_{\text{inertia}}$	pressure decrease caused by gas inertia
Δp_{pl}	pressure decrease caused by work of gas at moving valve pate
Q, \dot{Q}	heat, heat flow
R	general gas constant
R_0	specific gas constant
Re	Reynolds number
S	suction
S1, S2	sealings 1,2
SC	suction chamber
s inp	term of input procedure
s out	term of data output file
s result	term of result output file
SV	state variable
SVT,B	suction valve, top dead side, bottom dead side
TV	transport variable
ΔTV	increase of transport variable
T_w	wall temperature
V	Volume
V1-V4	valves 1 to 4
v inp	term of input file
v out	term of output file
WCT	working chamber top dead side
WCB	working chamber bottom dead side
W_{kin}	kinetic energy
x	coordinate along pipe axis
Z	compressibility factor
zn	maximum number of working cycles
α	heat transfer coefficient
κ	isentropic coefficient
λ	heat conduction coefficient
ρ	density
τ	time
$\tau_{0.5}$	half-time
ν	kinematic viscosity
Ψ_f	force coefficient of valve

References

- ¹ Egas, G.: PULSIM, a powerful tool for the control of vibrations in pipe Systems, G. Egas, TNO, CETIM 2001 Senlis, France
- ² Böswirth, L.: Strömung und Ventilplattenbewegung in Kolbenverdichterventilen, Wien, Eigenverlag 2002
- ³ REFPROP. NIST Standard Reference Database 23
- ⁴ MATLAB. Software des Unternehmens The MathWorks Inc.
- ⁵ Brümmer, A; Nadler, K: Simulation instationärer Strömungen mittels Charakteristikenverfahren, TU Dortmund, FG Fluidtechnik
- ⁶ Taschenbuch Maschinenbau 2, Verlag Technik, Berlin 1985, Abschnitt: Technische Thermodynamik, S. 557, Gl. 4.183
- ⁷ Thomas, C.: Innenkühlung der Kolbenstange von trockenlaufenden Kolbenverdichtern, TUDpress, 2014
- ⁸ Lehr, S.: Experimentelle und theoretische Untersuchungen zur Wärmeübertragung an einem kleinen Hubkolben-Luftverdichter. TUDpress, 2011
- ⁹ Flade, G.: Weiterentwicklung der Berechnungsmethoden für Kolbenverdichter auf der Basis zweidimensionaler. TUDpress, 2006
- ¹⁰ Huschenbett, M., Will, G.: Thermodynamic Simulation of Reciprocating Compressors to Enable Diagnostics Based on Measured Temperatures and Pressures. 4th EFRC-Conference, 2005, Antwerp



**Musicians set the tone.
HOERBIGER sets standards
for compressors.**

We make technology work.

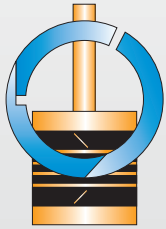
Like eHydroCOM, the energy saver for smaller compressors.

Like XperSEAL, the reliable rod sealing solution for zero gas leakage.

Like REE Assessments, which find solutions to optimize your machinery's reliability, efficiency and environmental soundness.

www.hoerbiger.com

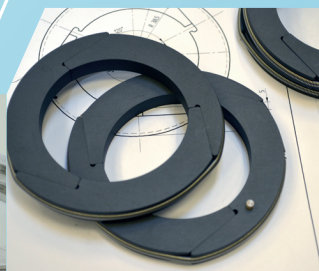
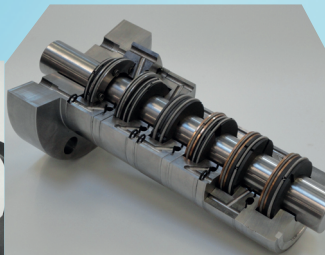
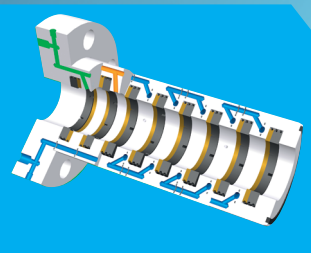

HOERBIGER
because performance counts



CASTANET. sa

Specialist in reciprocating compressor sealing technology

Experience and Quality at your service since 1978



Design, manufacture and reconditioning of sealing components for reciprocating compressors.

Piston rings
Rider rings
Rod pressure packings
Packing rings
Oil wiper packings
Oil scraper rings

Optimum material selection according to gas composition and operating conditions - Modification and improvement of sealing systems for longer service life (high performance materials, more efficient design to meet the demands of your service conditions) - Engineering studies to modify existing design and to upgrade your piston compressors - Conversion of lubricated compressors into oil-free compressors - Modification to API 618 standard.

CASTANET sa

2, rue de l'Industrie - B.P.N°10606 - 59164 Marpent - France

Tel : + 33.3.27.39.57.05 - Fax : + 33.3.27.67.18.75

contact@castanet-sa.fr - www.castanet-sa.fr

9th Conference of the EFRC September 11th / 12th, 2014, Vienna

Feasibility Investigation of Non-Metallic and Light Weight Metallic Materials for Light Weight Compressor Pistons by: *C.M. Wentzel & O.K. Bergsma, TU Delft NL, Faculty of Aerospace Engineering; A. Eijk, TNO;* -173-

EFRC Guidelines on how to avoid Liquid Problems in Reciprocating Compressor Systems by: *P. Shoeibi Omrani & A. Eijk, TNO* -187-

8th EFRC workshop for students “Reciprocating Compressors” by: *Gunther Machu, Chairman of the EFRC Student Excursion* -197-



EUROPEAN FORUM
for RECIPROCATING
COMPRESSORS

SESSION EFRC



Feasibility Investigation of Non-Metallic and Light Weight Metallic Materials for Light Weight Compressor Pistons

by:

C.M. Wentzel & O.K. Bergsma
TU Delft NL, Faculty of Aerospace Engineering
cyril@wentzeldynamics.com, O.K.Bergsma@tudelft.nl

A. Eijk
TNO, Delft, The Netherlands
andre.eijk@tno.nl

**9th Conference of the EFRC
September 11th / 12th, 2014, Vienna**

Abstract

Steel and aluminium have been the traditional materials of choice for pistons. In order to reduce moving mass-related vibrational problems, a feasibility assessment is made of the application of other materials in a project for the research group of the EFRC.

In particular, polymer and metal matrix composite as well as polymers as such were evaluated for this fatigue driven application. Since specific materials ideally require tailored designs, preliminary designs were conceived for all materials on the shortlist.

The work carried out up to now reports on progress made with the feasibility assessment of one particular mass saving application of solid polymer design for a piston. We applied a combined theoretical and experimental approach to assess applicability and do final material selection among the many possibilities. It was anticipated that very high cycle fatigue behaviour prediction at elevated temperature would be the most important aspect. As manufacturing quality is important, scaled demonstrator manufacturing trials are undertaken as well.

Fatigue behaviour of several polymer candidates such as high temperature grades epoxy (thermoset) and polysulfones (thermoplastic) was analysed in the light of more extensive characterisation of mechanical properties at different strain rates and creep and crack propagation behaviour. Such an analysis was explored to enable fatigue prediction at a scale which is normally beyond practical or financial restraints. The difficulties as well as a road ahead of this work in support of a dramatic mass reduction of compressor pistons will be highlighted.

1 Introduction

Up to now the applied materials for reciprocating compressors are made mainly of cast iron, cast steel, forged steel and aluminium due to the fact that these materials are cheap, strong, fit for purpose, and simply always used by default. In other parts of the industry e.g. automotive, aerospace, offshore (mainly pipes) etc., new materials such as composites have been developed and are used already for several years to overcome several disadvantages of the more conventional materials.

The materials which have been developed in the other industries include Metal Matrix Composites (MMC, metal with e.g. ceramic particulates) and fiber composite reinforced polymers (FRP).

As far as known, new materials have not been applied up to now for large parts of reciprocating compressors such as pistons and crosshead guides. It was not (yet) clear to the EFRC R&D group if and to which extent new materials had been applied for combustion engines and for other rotating equipment, e.g. pumps and turbo compressors.

The application of new materials for heavy parts of reciprocating compressors could have the following advantages:

- Lightweight, means lower unbalanced loads and lower total weight (mobile use).
- Lower mechanical vibrations due to lower masses.
- Increased stiffness¹.
- Reduced wear.
- Less thermal expansion.
- Higher shock load capacity (liquids, safety, external forces – i.e. submarine)
- Higher damping.

A trend in the reciprocating compressor industry is that the compressors become larger and have higher speeds. Some of them have speeds up to 1800 rpm. Especially the application of lightweight materials could have a great benefit due to the fact that the generated vibrations caused by the unbalanced forces and moments are a linear function of mass.

For that reason a precompetitive research project was started in 2013 by the R&D group of the EFRC to investigate the challenges of new lightweight materials for reciprocating compressors.

The final goal of the project was to find a suitable cost effective light weight material for those parts which have the largest contribution to the mechanical unbalanced vibrations: crossheads and pistons.

¹ stiffness, wear and expansion will appear as restraints, not as optimisation variables

The following was to be investigated as a minimum in the project:

- What are the most important characteristics of a good material?
- What are the total costs of each part (material, fabrication, machining etc.)?
- Testing: strength (static, fatigue), chemical resistance, wear resistance, temperature effects, etc.
- Fabrication verification.

The first phase of the project was as an extensive literature study and it was explicit in its conclusions about the potential benefits in weight reduction, while the materials which could be applied are many. Low density materials such as polymers applied to the piston will show already a mass reduction of approximately 40% even in its most simple embodiment. Due to the nature of polymers, fatigue performance at elevated temperature will always be critical. In addition, due to material damping, the generation of fatigue strength data in the gigacycle range through accelerated testing (increased frequency) becomes problematic. Experimental techniques hence become a major focus.

The application of polymers is now investigated in a demonstrator phase, i.e. phase 2 of the project. The scope of phase 2 was finally limited to the piston as it was shown in the preliminary study that this part gives the highest contribution to mass reduction while the initial complexity and risk can be relatively low.

In phase 2 the feasibility of the Solid Polymer Piston (SPP) concept is investigated in more detail, while simultaneously exploring even more low mass concepts, using a theoretical, design, analysis and experimental approach where necessary. Thus, to provide a good basis for the next test and verification level of this concept, confirming which mass reductions can be realistically expected.

This paper describes into some detail the results of the preliminary study. Phase 2 of the projects is not yet finished, and for that reason only some pertinent preliminary results will be discussed. It is expected that the results of the complete project will be presented on the next EFRC Conference in 2016.

2 Parts and design data definition

It was decided to start with one heavy part which is in direct contact with a gas and another part which is not. The crosshead and piston have been chosen for that purpose.

2.1 Piston

The piston has a heavy reciprocating weight, is in direct contact with the process gas and it can be lubricated or non-lubricated, see also Figure 1 for a generic design. Depending on the diameter of the piston and gas pressure in the cylinder, pistons can be made of cast iron, steel or aluminium and they can be hollow or solid. Hollow pistons are furnished with a gas vent hole in the head end face as required per API Standard 618¹.

The piston fits on the rod and rests against the piston rod shoulder. A ring (1) may be located between the piston crank end face and the shoulder. The piston sections are firmly clamped together on the rod by for example hydraulically tightening the piston nut.

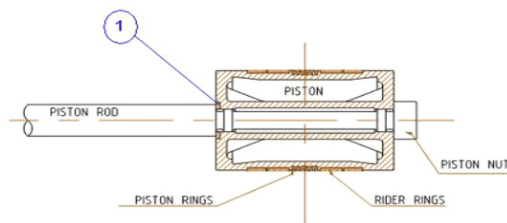


Figure 1 Example of a hollow piston

2.2. Crosshead

The crosshead has a heavy reciprocating weight, it is not in direct contact with the process gas, it is lubricated (motion work) and is highly dynamically loaded, see the example in Figure 2. The crosshead is provided with removable crosshead shoes (1) which are bolted to the crosshead body (3). All crossheads are made of cast steel. The crosshead shoes have white metal bearing surfaces. For proper lubrication, oil is provided from the main oil system between the crosshead shoes and the crosshead guide (2). For balancing reasons, if necessary, the crosshead can be equipped with balancing masses (4).

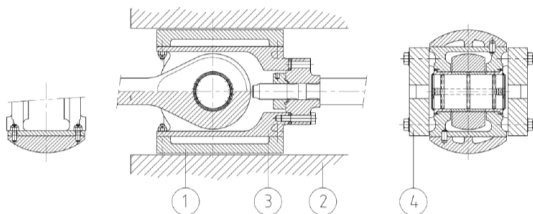


Figure 2 Example of a crosshead guide

2.3 Design data as used in the project

The design data of a typical, i.e. small to medium, reciprocating compressor, which is in the product line

of the EFRC R&D members, has been specified for this project and are as follows:

- Compressor rod load of 130 [kN], rod diameter 55 [mm];
- Compressor speed of 465 rpm ;
- Stroke of 260 [mm];
- Piston diameter of 410 [mm] with a length of 405 [mm];
- Piston pre-tension 215 [kN] (static load);
- Cylinder pressures: low 5.5 [bara], high 15 [bara] (dynamic load);
- Piston in following process gas: H₂, H₂S, CH₄, CO₂, H₂O mixes.

3 Phase 1 Preliminary study

3.1 Introduction

The preliminary study aims to identify the mass reduction potential for the several components and to make a broad assessment of the available materials and associated processing methods. This was done in an exploratory phase. Obviously, a literature study is a prominent part while also making an inventory of similar industrial products and analysing the requirements thoroughly.

3.2 Requirements analysis

In cases where an overall system is redefined by a full reconsideration of materials, it is important to scrutinise the functional and product requirements to guide the material and process selection and to identify any potential killer requirements.

Among the various requirement categories considered, stiffness, environment, loads and price require some discussion while it is obvious that mechanical fatigue strength is the single most important design driver, running at 8.5 Hz for twenty years into the Gigacycle domain (called Very High Cycle Fatigue, or VHCF for short). We then conclude with a mass overview of the preliminary baseline design which then defines the priorities.

Stiffness: the overall elongation between crosshead and piston faces determines the clearance volume. Given the piston rod length of 1.6 [m], a high rod modulus is required to achieve an elongation limited to 0.4 [mm], which is 10% of a typical clearance stroke of 4 [mm].

Environment: temperature is of utmost importance especially when polymers are considered. Two scenarios were specified with corresponding piston face temperature averaging 90°C with max. 150°C

gas temperature being relevant for chemical attack (120°C and 185°C for scenario 2). The typical crosshead temperature would be significantly lower at 60°C while the piston rod temperature itself would be a function of the heat transmitted from the piston and therefore its thermal conductivity. These temperatures were found to be crucial for the fatigue strength of polymers and also their long fiber composites.

The gaseous environment as specified in section 2.3 can be directly tested for mainly chemical resistance, but the trace gases could be more important. Water vapour content is a well known parameter which for example has a large influence on the equilibrium water content of nylons (PA6.6) and many of its properties. Next to this physical phenomenon, chemical resistance is to be checked towards the gases involved. Besides gases such as H₂S, CH₄, specific trace chlorides and other compounds should still be identified. Apart from the gases, also all compounds in the oils may play a role in corrosive attack under stress. Three mineral and synthetic oil grades were specified to evaluate physical absorption (swelling) mainly.

The corrosive environment effectively governs fatigue life of all-metal concepts as is illustrated in Figure 3. By careful material selection and possibly coating, such a dramatic reduction in allowable (surface-) stress levels may be avoided altogether.

It should be noted that in the present application, wear and fretting fatigue may play a role where significant tensile stresses occur in contact areas. The sealing ring grooves and piston nut areas are subject to such loading.

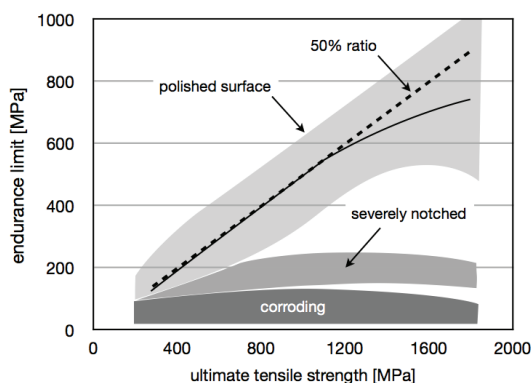


Figure 3 The effect of corrosion on fatigue strength of metals, based on [2].

An analysis of loads is based on the baseline transient gas pressure and mass loads as depicted in Figure 4. In terms of fatigue loading, the ratio of maximum and minimum load, R equals -1. The inertial unloading

appears to be less than 10% at the peaks, a fact that diminishes the benefit of moving mass reduction, albeit slightly. The prestress factor relative to the maximum rod load is 1.65.

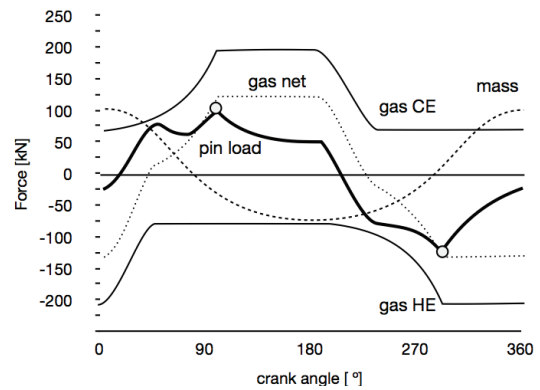


Figure 4 The loads acting on the system (HE = Head End, CE = Crank End).

The loads are cyclic at a frequency of 8.5 Hz, which may become critical for some polymers due to so-called hysteretic damping. Such self-heating leads to premature failure and should be included in the thermal analysis. In the trend towards faster compressors, the upper limit is roughly 20 or even 30 Hz, although the latter will be for small size designs.

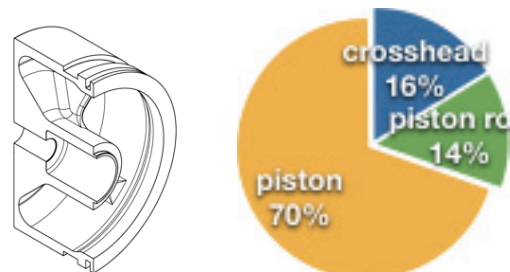


Figure 5 Mass breakdown of the baseline design in terms of structural mass (i.e. excluding the crosshead shoes); the piston mass is 150 [kg].

Finally, cost considerations must be taken into account at this early stage. A ballpark guideline was obtained based on typical cast nodular steel and machined aluminium fabrication of the baseline design. Somewhat higher cost could be acceptable, subject to trade-offs with lifetime cost and reduced vibration burden. For polymers, however, we may observe that when PEEK is applied, the materials bill only would already absorb the whole nominal budget.

Likewise, exotic materials such as Beryllium alloys can be excluded, noticing that even in Racing car formula F1 regulations such materials have been effectively banned on the basis of limitations of specific stiffness properties.

To conclude, we will look at the mass distribution of the baseline design and relate them to global stress levels. Figure 5 shows the relative distribution of structural mass. For maximum impact, the piston is tempting as a focus of the project. This however depends on the stress levels (Figure 6) for different design concepts and whether this offers room for improvement. This is the subject of the next paragraph.

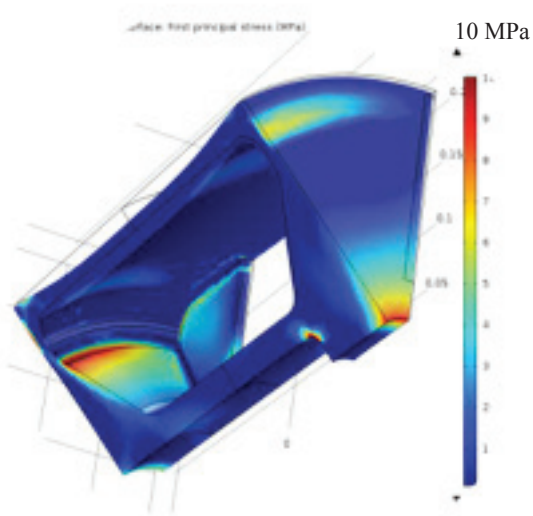


Figure 6 Plot of maximum principal stress in the baseline piston design shown in Figure 5.

3.3 Stress levels, design drivers and low density materials

A look at the stress analysis of the baseline design under an ultimate load case shows alternating principal (tensile) stress components up to 10 and locally 40 [MPa] (Figure 6). It is clear that such low stress levels must be due to the VHCF performance under a corrosive environment.

The stress amplitude in the piston rod on the other hand averages 55 [MPa], to be added to the prestress.

Now let us take a look at designs which are based on low density materials. The first thing that is clear is that the volume occupation can approach unity while still retaining a mass benefit. As a matter of fact, the baseline steel design occupies 36% of the available volume while the same mass of aluminium alloy would make a solid piston.

All densities lower than 2.8 [kg/l] would yield proportionally lower masses even for a solid piston. This idea is captured in Figure 7.

Let us look next at the stress levels that are associated with a solid piston (SP). These will be highest near the shaft, which is the part or area that takes the prestress and transmits the shear loads to the piston nut and shoulder.

Such shear loads scale with the average or nominal shear load to be transferred at a certain transition radius (from piston body to shaft). At both ends there will be somewhat higher stresses due to stress concentration effects, but the order of magnitude is 1 [MPa] when the 320 [N/mm] shear flow is transferred at a cylindrical (adhesively bonded) surface of 100 [mm] diameter. Such low stress levels could be feasible even for very low density materials. Allowable stress levels for new materials are the next subject to be discussed.

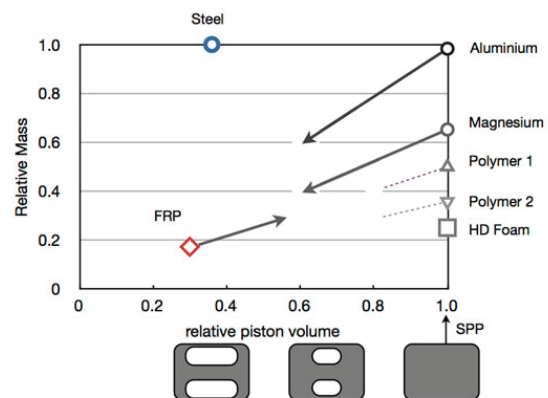


Figure 7 Piston mass for several lower density materials at variable piston volume fraction. SPP denotes Solid Polymer Piston and FRP Fiber Reinforced Polymer.

3.4 Materials inventory fatigue data

An extensive literature search was done to identify both relevant materials for the application and the corresponding fatigue strength performance.

The materials list that resulted is given in Table 1.

Table 1 Long list materials candidates overview.

class	grade / brand	remark
metals	Magnesium alloy	machined or cast; coating is mandatory
	Titanium CP or alloy	wrought alloy, semi-finished product is critical; processing expensive
	Aluminium AA2618-T4	automotive piston alloy
MMC	Ti-Boron	applied with long fibers
	Al-SiC	SiC as small particles <40%
polymers: thermo-plastics	PA6, PA6.6, PA4.6, PA12	nylons family; also cast or extruded
	POM	Often known under trade name Delrin
	PC	amorphous TP with good performance up to 120°C
	PSU, PES, (PEI)	high end engineering TP family; amorphous with very good properties up to 200°C
polymers: thermo-sets	epoxy	wide family with exceptionally good properties
	PU	polyurethane, a wide family, well known as casting polymers
	phenolic	A well established class of heat resistant thermosets (e.g. Bakelite)
	pdcpd	attractive RIM processing resulting in low moisture uptake, chemically resistant TS polymer (Telene and Metton)
fibers	metal	various options; also providing heat conductivity
	glass (basalt)	common high strength, low stiffness fiber
	carbon	stiff and strong, fatigue insensitive
	aramid	high tensile strength, lowest density

Now some examples will be given of fatigue behaviour. VHCF data typically exist in the wind energy discipline (often glass fiber based, so GFRP) and also where data is not very costly to generate (automotive, magnesium using high power ultrasonic test methods). Otherwise, available data often does not go beyond 10 million cycles, and does not address stress reversal (R= 0.1 is typical, though R= -1 is preferred).

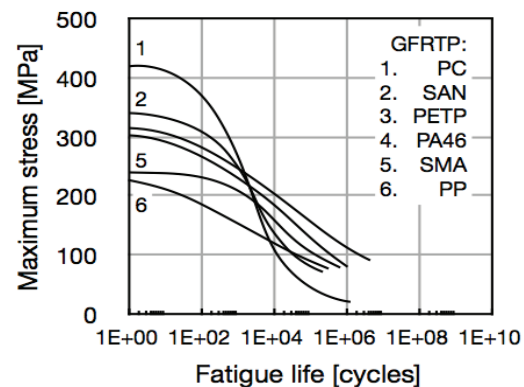


Figure 8 Fatigue curves for long glass fiber composites based on thermoplastic; at 20°C and R=0.1. Note the reversal of performance and steep deterioration.

An illustrative collection of data was taken from [6] as seen in Figure 8 where glass based thermoplastics show a strong in-plane strength decrease. At which level the strength would level-off is not clear. It is interesting to note that this particular PC grade, though listed as a candidate due to its thermal stability, performs worst in the high cycle domain.

Then if we look at short fiber based thermoplastics and the effect of temperature on a particular compound of PC/PET in Figure 9, we see that quite a significant strength is retained at our most stringent temperature of 120°C.

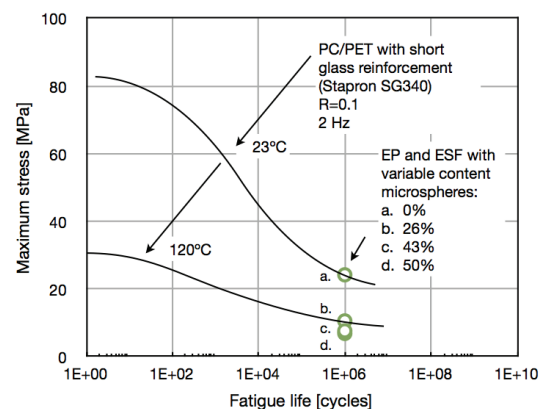


Figure 9 The effect of temperature on fatigue strength of a short fiber reinforced thermoplastic [6] and a comparison with epoxy (EP) with and without syntactic foam (ESF) structure [7].

Another type of composite is obtained when creating micro-cavities in a thermoset matrix by the addition of microspheres. The resulting ‘foam’ structure is called syntactic foam and its primary virtue is low

Feasibility Investigation of Non-Metallic and Light Weight Metallic Materials for Light Weight Compressor Pistons by: C.M. Wentzel & O.K. Bergsma, TU Delft NL, Faculty of Aerospace Engineering; A. Eijk, TNO;

density. The important point is then how much fatigue strength is retained relative to the virgin material (epoxy performs generally well). Indeed we see that this particular epoxy grade compares well with its glass fiber reinforced thermoplastic counterpart. The addition of microspheres caused the 20°C fatigue strength to decrease to well below 10 [MPa] in this investigation (the circular symbols b to d in Figure 9). Phase 2 re-addressed this class of materials, leading to much more favourable results for the commercially available grade (of Epoxy Syntactic Foam or ESF for short) investigated.

When confronted with the challenge of adopting a polymer with good VHCF properties, it is useful to bear in mind that small inclusions, even a second phase due to compounding, may act as a crack initiator. For this reason, one should be careful with short fibers as well and it also explains why addition of nano particles is generally unsuccessful. To visualise this aspect, Figure 10 is included, showing a scanning electron microscope (SEM) image of a blend polymer failed in fatigue, revealing the initiation sites within the many facets making up the fracture surface.

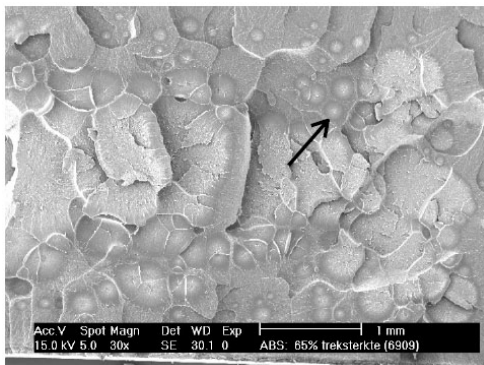


Figure 10 Fatigue failure initiation: multiple sites in a 'dirty' polymer compound (ABS), creating a faceted fracture surface visible in a SEM image [6].

As a last exploration of composite material fatigue performance, we see that the exceptional data in Figure 11 extends well into the gigacycle domain. There is a large database of similar data through the EU-sponsored research programme OPTIMAT [4]. The matrix here is a thermoset and the fibre is glass. It is important that the fit seems linear on a double logarithmic scale. This however is an empirical observation without necessary wider applicability.

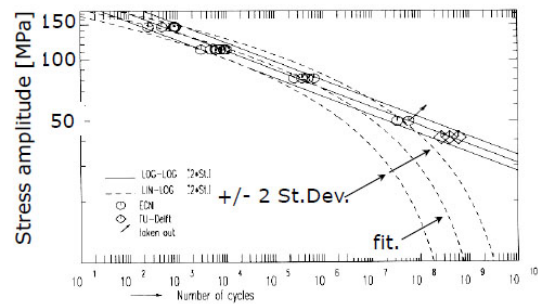


Figure 11 VHCF data from a wind energy research program [14]; the log-log fit describes the VHCF behaviour much better than the lin-log interpolation and extrapolation; $R = 0.1$.

It is good to set the fatigue data presented for polymers and composites into perspective. Light alloy (Aluminium and Magnesium) fatigue data are therefore presented with the addition of typical Metal Matrix Composites (MMC) data in Figure 12. Besides a comparison between different material types across the light alloys, also some effects of corrosion and elevated temperatures are shown. Similar effects were found due to an environment of mineral or synthetic lubrication oils [11].

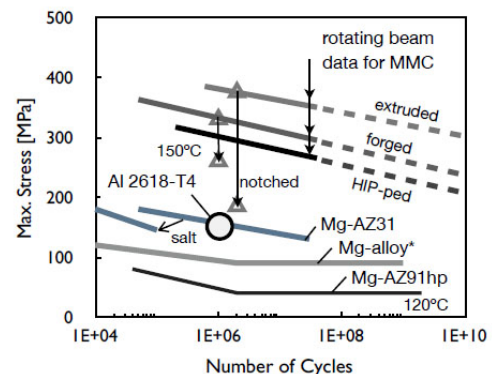


Figure 12 Fatigue trends for a MMC grade (AMC225XE-T4) with temperature and notch effects [13]; compared to a popular aluminium piston alloy and curves for both wrought* [8] and cast (AZ91) magnesium alloys [9], also including a salt corroding effect for wrought AZ31 [15].

What we may conclude from the compilation in Figure 12 is that indeed MMC can offer a significant advantage over other light alloys when design stress levels become high (and the volume factor correspondingly low). However, if the properties of alloys such as the 'piston-alloy' Al2618 or AZ31 could be maintained in the corrosive environment, then already allowable stress levels are significantly

high, approaching 80 [MPa]. Due to an intrinsic presence of microporosities, cast Magnesium alloys should be considered unsuitable even in this case of a high pressure casting process.

3.5 SPP (solid piston) manufacturing concepts

Given the concept of a solid polymer piston in combination with the many material and manufacturing options, a wealth of options exists to achieve a piston with low mass and adequate fatigue life. It was considered crucial to allow an affordable and well-controlled processing method. The options schematic in Figure 13 was conceived from the idea that bonded thick plates of prefabricated polymer could be used for the bulk of the volume for economic processing (13b and 13c). Problems with exotherm control, residual stress and processed mass limitations that would exist for cast or compression moulded (COM) or reaction injection moulded (RIM) materials would hence be mitigated. Extrusion (EXT) is an economical TP manufacturing method up to intermediate sizes. Another feature in some of the concepts in Figure 13 addresses the additional functionality which can be added in the outer layers. The thermal barrier in 13d would make it possible that maximum cooling from the piston would be obtained; this is beneficial for improved fatigue strength but obviously depends on the conductivity of the piston.



Figure 13 Different piston variations defined for the SPP-concept.

The sleeve option as depicted in Figure 13e could be a simple measure to circumvent unknown or inadequate wear and robustness properties of low density materials which are considered for the piston body. The sleeve could be metal and would have the necessary cut-outs for sealing and rider rings. Finally, the gradient core concept 13f involves the gradual decrease of the core mass density at greater radii where the required strength would be significantly lower.

Such a decrease could be stepwise or even gradual, although the latter may be very challenging in terms of manufacturing technology (the distribution would be ‘antacentrifugal’).

3.6 Phase 1 conclusion

After the preliminary study it became clear that the piston is the most logical component to focus on in the next project phase. The largest mass reduction can be achieved for this relatively simple structure with low stress levels for low density materials. Though the piston rod is equally simple, stiffness and joining requirements make steel a logical choice while the crosshead is a truly complex part with multi-axis loads, requiring much more effort for a small potential benefit.

We may then distinguish between two classes of materials with their corresponding structural concept.

The first is that of low density materials with low but adequate fatigue strength at elevated temperatures up to 120°C, which can be applied in a solid piston. This offers already a mass reduction in the order of 50% of the piston proper.

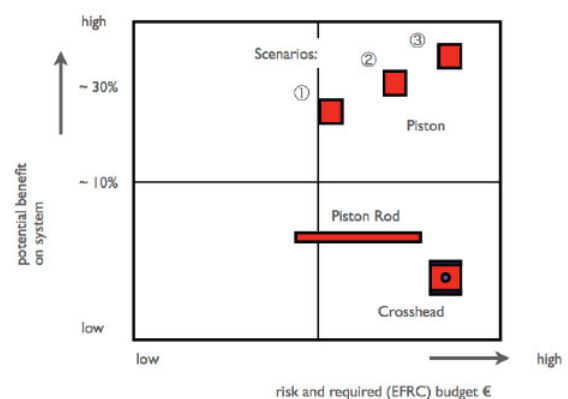


Figure 14 Summary of mass reduction potential findings for the three compressor components. Scenario 1 is associated with the SPP concept while scenario 2 would be an advanced (non-solid) concept in this study; scenario 3 would be a near-optimised fiber reinforced composite (FRP) solution.

The second is focused on materials with relatively high fatigue strength which can be applied in a hollow cylinder design where adequate protection against corrosion is either offered or not additionally needed. MMC materials show strengths up to 200 [MPa] with as yet unidentified corrosion issues. Magnesium and aluminium alloys could approach 100 [MPa] if protected well.

Carbon fiber composites are virtually insensitive to fatigue, but the design and manufacturing process should be flawless to avoid non-fiber dominated behaviour. If a unidirectional lay-up can be achieved through design, then also glass fiber can be considered with the promise of economy such as found in GFRP automotive leaf springs. This class of possibilities, aiming for the highest mass reduction, is designated ‘scenario 2’ in Figure 14 which schematically puts the system mass reduction in perspective of the effort and risk involved.

4 Phase 2 Demonstrator Solid Polymer Piston (SPP)

4.1 Introduction

A part of the phase 1 result is the specification of an overall master plan covering development in the pre-competitive stages and indicating the opportunities for competitive branches of development. Its application is currently investigated in a demonstrator phase, i.e. phase 2 of the project. The scope of phase 2 was limited to the piston as it was shown from the literature study that this part gives the highest benefit in mass reduction while the initial complexity and risk can be relatively low. The chart describing such a master plan, leading to a demonstrator is given in Figure 15.

The final results are expected at the end of 2014 and for that reason only the preliminary results are presented here.

4.2 Some results of Phase 2

4.2.1 Introduction

The work plan is outlined in Figure 16. This phase can be split up into the following three main activities, the results of which are summarized in the next chapters:

- Activity 1: Demonstrator activities (SPP concept)
- Activity 2: Common technology issues investigation
- Activity 3: Advanced concepts study

4.2.2 Activity 1: Demonstrator activities (SPP concept)

Based on the SPP concept, the purpose of this work package is to obtain a hardware demonstrator, either full scale or scaled to 1:2. Critical concept features are being designed and investigated, such as the integration with a compatible shaft structure. The shaft shall absorb the preload without excessive stress relaxation and be designed to provide a low stress concentration over the bond line to the piston body. It is interesting to observe that the thermal stress due to mismatch in CTE² can be tailored by careful choice of the stress free curing temperature of the adhesive.

Based on the findings of phase 1, thermal analysis plays an important role. Both thermal stress (from the generally bigger thermal expansion for polymers) and hysteretic heat generated during fast cycles result in a stress and temperature field which are decisive

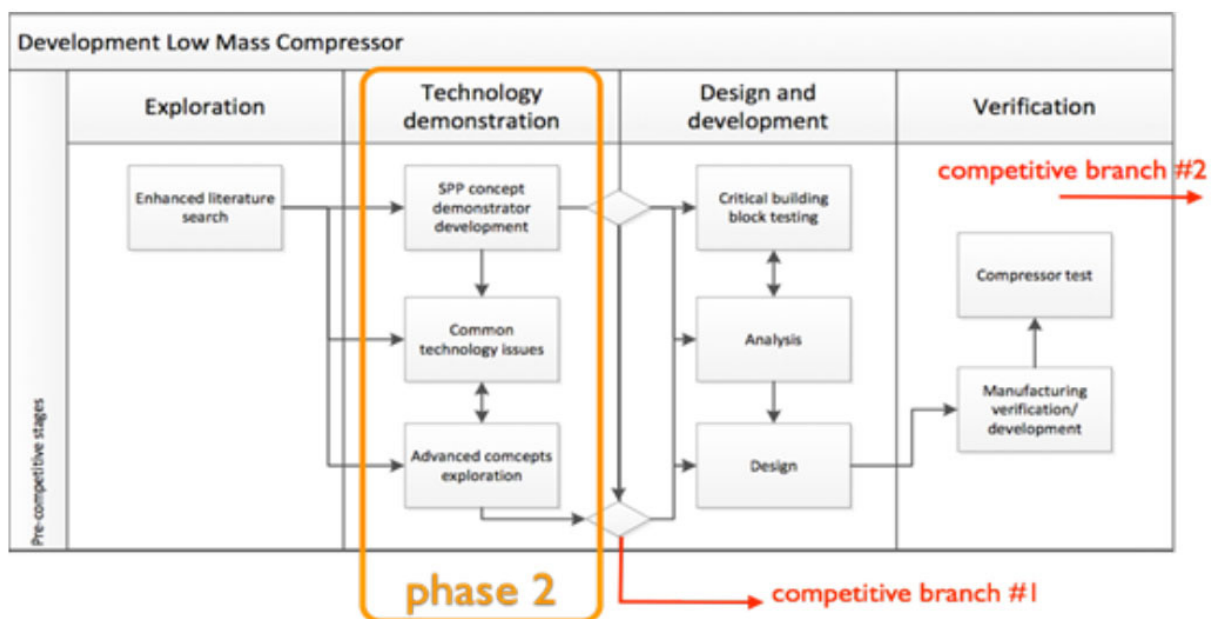


Figure 15 Master plan Phase 2 “Demonstrator”

² CTE: Coefficient of Thermal Expansion; approx. 12 [$\mu\text{strain/K}$] for steel, 23 for aluminium, 50 and up to 80 for polymers.

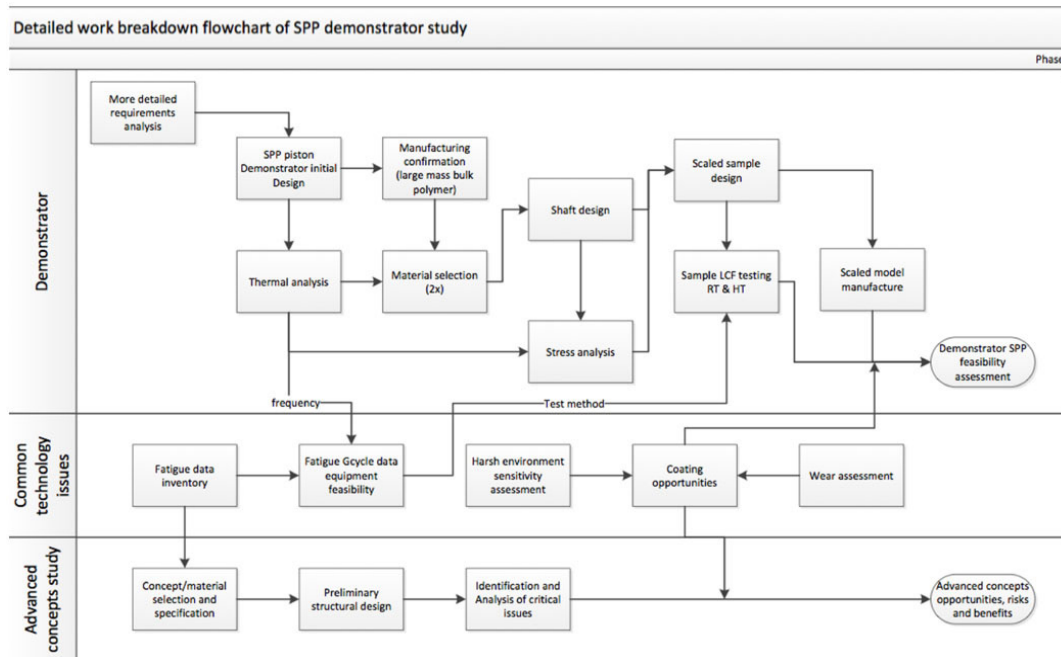


Figure 16 Schematic chart of phase 2 of the overall project, detailing three main activities.

for expected fatigue life, while also the conductivity parameter should be considered. Materials selection has resulted in a maximum of 4 materials which are studied in parallel in the subsequent manufacturing trials and experimental fatigue investigation. This choice could for example be made to include a thermoset and a thermoplastic option, or based on size or an oil/gas resistance criterion. The testing should reveal or confirm the sensitivity to elevated temperature as obtained from the thermal analysis. Although data in the Giga-cycle domain is required, this is beyond the project scope. Nevertheless, an effort has been made to rank materials on the basis of available and expected performance.

The critical strength issue concentrates around the interface between the piston body and the shaft component. This is an adhesively bonded joint the strength of which should be higher than the two adherends.

The computed stress concentration and reversal in fatigue are shown in Figure 17. A circumferential groove was applied in order to reduce the stress concentration and to move it away from the outer surface. Such detail design is essential to make the SPP concept feasible.

Two materials have been screen-tested in order to establish an order of magnitude fatigue strength. The first is a thermoplastic, PPES. The second is an epoxy based syntactic foam (ESF). Elevated temperature testing was considered crucial for both materials.

Figure 18 summarizes the findings for PPES which was subjected to tensile testing and creep rupture testing with alternating stress.

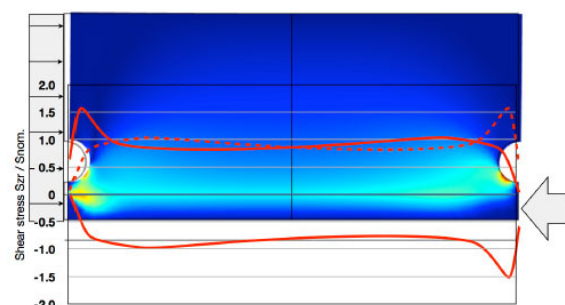


Figure 17 Shear stress concentration over the shaft to piston body interface with stress reduction groove feature; the shaft is aluminium (without pre-stress). The dashed line indicates load reversal.

The constant tensile stress has an obvious creep effect, but on a long timescale (towards 1 Gs) the extrapolation of the static curves still retains maximum stress levels above 20 [MPa]. If however the stress is cycled (slowly at 0.1 Hz and at R=0.1 in this case), the extrapolated curves fall short of what is required even at 90°C with a life in order of 105 [s].

Although the test does not fully reflect the desired conditions (R= -1, biaxial stress), the results are not encouraging. The performance of PPSU seems to be better, but further analysis should reveal how much better the fatigue behaviour could be.

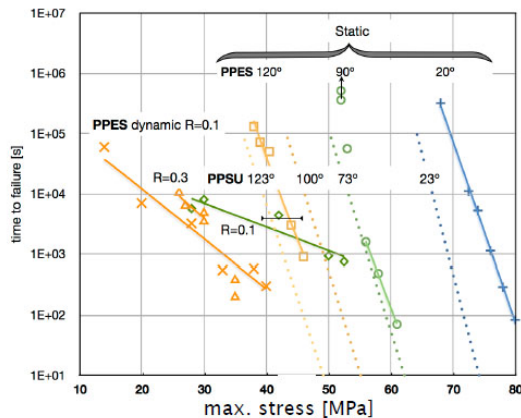


Figure 18 Time to failure (creep rupture) versus maximum tensile stress; static and cyclic for PPES (solid lines) and PPSU (dotted lines) polymers at different temperatures.

PPES and PPSU are both high grade engineering thermoplastics with high glass transition temperatures ($>200^{\circ}\text{C}$), but we tentatively conclude that they seem to be inadequate for our application.

Turning now to the class of thermosets, Figure 19 shows measured fatigue behaviour in three-point bending of ESF material. When comparing with results from literature as given in Figure 9, it is seen that the improvement brings the performance in a useful range, although extrapolation on a double log scale is tentative as yet. It is seen that temperature increase towards 100°C does not noticeably deteriorate the strength while 120°C is only slightly worse.

4.2.3 Activity 2: Common technology issues investigation

Issues which are common to all concepts, including the advanced light weight concepts of activity 3, are investigated here. Obviously fatigue data inventory of all involved materials is a key task. Ultimately, it could even be that the existence of VHCF data for a specific material qualifies it for end selection. Due to low material damping, Magnesium alloys are at an advantage here, because due to low material damping, ultrasonic test techniques can be economically applied.

The economical generation of data requires smart low-budget test equipment solutions addressing an increase of test frequency at low stress and multiplication of samples (simultaneous testing).

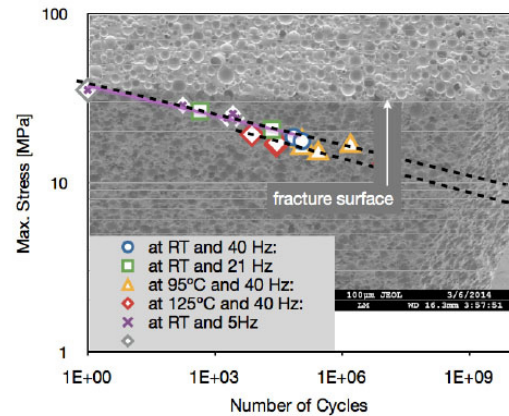


Figure 19 Fatigue behaviour from screening test in 3P-bending of industrially available high temperature ESF with elevated test frequency and temperature. Dashed line represent tentative pseudo-extrapolations for 20°C (RT) and 100°C .

A new 'lean' test configuration is under study, based on a rotation oscillating equipment. For materials with low damping this could enable a test frequency of 300 Hz in shear (i.e. $R = -1$). Obviously, polymers to be tested in this machine should have exceptionally low damping and have forced cooling.

Another development is the fusion of material test and component test in a scaled sample. The 'scaled sample' test set-up of Figure 20 allows the $R = -1$ fatigue shear strength to be tested in conjunction with the bonding to the shaft, the pre-stress and stress concentrations.

One primary concern is the sensitivity of the shortlist materials to the hot gas environment. This has been covered by comparing against known performance of these materials. One particular aspect of concern is hydrogen ingress and either degradation of performance or susceptibility to harmful effects during decompression after high pressure saturation. A worst-case screening test is foreseen in the remainder of the project.

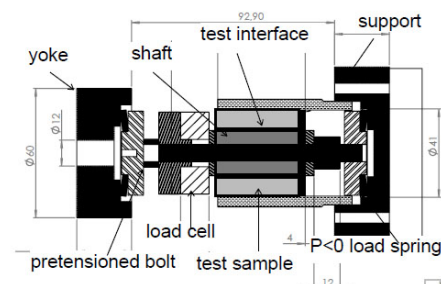


Figure 20 Cylinder test adapter for converting simple compression machine to $R = -1$ biaxial shear test machine.

Coating technology has been addressed to some extent to assess the potential application of high resilience polymers such as LCP's3 to otherwise environmentally susceptible materials [5]. For the assessment of wear, a load case has been defined (e.g. involving the sealing rings) and a relative comparison has been aimed at. An experimental scratch test has shown to be a good indicator for this.

A relevant coating technology for light metal alloys is plasma electrolytic oxidation (e.g. Keronite®). Robustness of the coating is of primary concern.

Next to coating, cladding could also be considered. Corrosion resistant layers such as pure aluminium and e.g. tantalum can be applied by explosive cladding to create a very strong metallic bond. Although this is most easily done on flat plates, also cladding on a (curved) product level is possible in principle [16]. From aerospace grade clad sheet, it is however known that the pure aluminium cladding layer has a detrimental effect up to 50% in fatigue strength. Then the obvious question would be to which degree exactly such a reduction would be worse or better than the effect of corrosion on the bare metal. The surfaces to be cladded should be designed with the explosive cladding in mind. This possibility will be explored further in the remainder of the project.

4.2.4 Activity 3: Advanced concepts study

Although the SPP concept already will provide a significant mass reduction in the order of 50%, a higher mass reduction of for example 70% could be achieved where the additional effort seems justified. Also, an improved metallic baseline might be attractive for certain markets. At least two other concepts will therefore be synthesised for feasibility assessment purposes. As a starting point, a Magnesium or metal matrix option has been chosen, along with a long fibre polymer composite.

While the structure concept for a (hollow) metal design will be more or less conventional, long fibre composite material could be applied in several concepts which reflect different manufacturing methods. One such a concept is shown in Figure 21.

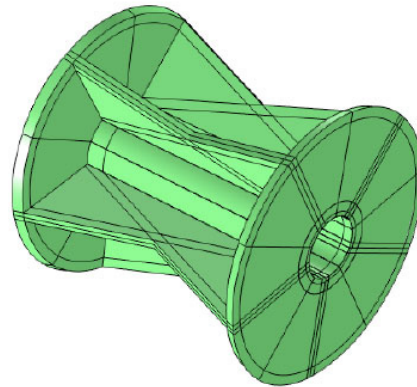


Figure 21 One possible fiber based solution consisting of ribbed compression member units which can be displaced relative to each other (aligned version is shown); structural decoupling from the cylindrical shell (omitted for clarity) in axial direction is essential.

One variation of this concept intends to keep the material stressed in compression, thereby alleviating the fatigue problem. An obvious issue here is the pressure that has to be assumed to act from within the cavity. The API standard 618 [1] requires the cavity to be vented from considerations of hazard during maintenance. This requirement would preclude this kind of solution.

A third advanced concept is effectively being investigated already by considering the ESF material for the SPP, as this introduces porosity on a material level. The addition of roughly 50% microspheres brings the density already down to 0.7 [kg/l] which would result in a mass reduction significantly beyond the target.

5 Conclusions

A project is in progress to address the potential for a significant mass reduction for moving parts of reciprocating compressors.

From the results to date it seems that up to 50% mass reduction can be achieved with a limited effort using polymers and/or long fiber composites. A current major focus is to obtain or generate fatigue data in the Gigacycle domain under representative elevated temperatures and environmental conditions.

Although several thermoplastic material candidates appeared to be disappointing in their strength retention, a promising low density material, epoxy syntactic foam (EFS) was identified and tested. The positive results give rise to further activities in the

Feasibility Investigation of Non-Metallic and Light Weight Metallic Materials for Light Weight Compressor Pistons by: C.M. Wentzel & O.K. Bergsma, TU Delft NL, Faculty of Aerospace Engineering; A. Eijk, TNO;

area of design, biaxial testing and the development of proper dedicated test methods.

The performance and potential of light metal alloys (including MMC's) could be significantly improved if suitable coating or cladding systems can be found. Several candidates exist.

Acknowledgements

The authors would like to thank the R&D sponsors of the EFRC for their permission to publish the results of this project.

Furthermore the authors like to thank the members of the EFRC R&D steering committee to their active contribution in the project.

References

- ¹ API Standard 618 "Reciprocating Compressors for Petroleum, Chemical, and Gas Industry Services", 5th edition 2007
- ² Design for fatigue resistance. Chapter from ASM Handbook Volume 20, Materials Selection and Design.
- ³ Bryan Harris (editor) (2003). Fatigue in Composites. Woodward Publishing Ltd.
- ⁴ R.P.L. Nijssen (2006). Fatigue Life Prediction and Strength Degradation of Wind Turbine Rotor Blade Composites. PhD thesis Delft University of Technology.
- ⁵ G.L. Gurriero (2012). Liquid Crystalline Thermosetting Polymers as Protective Coatings for Aerospace. PhD thesis, Delft University of Technology, 2012
- ⁶ private communication with Prof. Dr. R. Marissen, DSM company. R. Marissen (2013), Lecture notes on fracture mechanics and composites. Delft University of Technology.
- ⁷ Ferreira, J.A.M.; Salviano, K.; Costa, J.D.; Capela, C.. (2010): Fatigue behaviour in hybrid hollow microspheres/ fibre reinforced composites. *J. Mater. Sci.* 45:3547-3553.
- ⁸ D.K. Xu, L. Liu, Y.B. Xu, E.H. Han. (2007): The micromechanism of fatigue crack propagation for a forged Mg–Zn–Y–Zr alloy in the gigacycle fatigue regime. *Journal of Alloys and Compounds* 454, 123–128.
- ⁹ Mayera, H.; Papakyriacoub, M; Zettla, B; Vacica, S. (2005): Endurance limit and threshold stress intensity of die cast magnesium and aluminium alloys at elevated temperatures. *International Journal of Fatigue* 27, 1076–1088.
- ¹⁰ Zeng, Rong-chang; Zhang, Jin; Huang, Wei-jiu; Dietzel, W.; Kainer, K.U.; Blawert, C.; Ke, Wei. (2006): Review of studies on corrosion of magnesium alloys. *Trans.Nonferrous Met. SOC.China* 16. s763-s771.
- ¹¹ Eliezer, A.; Medlinsky, O.; Haddad, K.; Ben-Hamu, G.. (2008): Corrosion fatigue behavior of magnesium alloys under oil environments. *Materials Science and Engineering A* 477, 129–136
- ¹² Bathias, C. (1999): There is no infinite fatigue life in metallic materials. *Fatigue Fract. Engng. Mater. Struct.* Vol. 22, Nr. 7, 559-565
- ¹³ Anon. (2013): AMC225XE brochure, Particle Reinforced Aluminium alloy. Materion Company.
- ¹⁴ van Delft, D.R.V.; Rink, H.D.; Joosse, P.A.; Bach, P.W.. (1994): Fatigue behaviour of fibreglass wind turbine blade material at the very high cycle range. EWEC'94 conf. Thessaloniki, Vol. 1, 379-384.
- ¹⁵ Unigovski, Y; Eliezer, A.; Abramov, E; Snir, Y.; Gutman, G.M.. (2003): Corrosion fatigue of extruded magnesium alloys. *Materials and Engineering A360* 132–139.
- ¹⁶ Meuken, D.; Carton, E. P. (2004): Explosive Welding and Cladding. SHOCK COMPRESSION OF CONDENSED MATTER - 2003: Proceedings of the Conference of the American Physical Society Topical Group on Shock Compression of Condensed Matter. AIP Conference Proceedings, Volume 706, pp. 1110- 1113 (2004)



EFRC Guidelines on how to avoid Liquid Problems in Reciprocating Compressor Systems

by:

P. Shoeibi Omrani & A. Eijk
TNO, Delft, The Netherlands

pejman.shoeibiomrani@tno.nl , andre.eijk@tno.nl

9th Conference of the EFRC
September 11th / 12th, 2014, Vienna

Abstract:

Reciprocating compressors are widely used in a variety of industries. Issues with using reciprocating compressors are reliability concerns, especially system failures due to the presence of liquids. The working principle of reciprocating compressors are based on the gas compression of a closed volume and due to incompressibility of the liquid phase, the compressor is incapable of handling the liquid carryover inside the compressor cylinder. Additionally, as the liquid is being carried over into the compressor cylinder, it is too late for taking actions to avoid failures. Thus, it is desired to design and operate a reciprocating compressor system to prevent liquids from entering and accumulating in the system.

This paper focuses on the liquid carryover problems in reciprocating compressor systems: how they occur, what are the consequences and what are the measures in the design and operation of the system to prevent liquid carryover problems. Since the liquid carryover can be initiated at each component of the system, every component in the system is studied individually for its contribution to the liquid accumulation and carryover. This paper is a summary of the research project funded by the R&D group of EFRC and performed by TNO. The paper describes the results of the different steps carried out in the project which are as follows:

- Literature survey.
- Face-to-face meetings with a number of operators, equipment OEM's etc.
- Internet survey.
- Setting up the guidelines.
- International workshop.

The final result of the project is a document named "EFRC Guidelines on how to avoid liquid problems in reciprocating compressors systems". This document consists of engineering guidelines on the design of different components and on the operation of reciprocating compressor systems on how to avoid liquid problems. The guidelines can be downloaded from the EFRC website www.recip.org

EFRC Guidelines on how to avoid Liquid Problems in Reciprocating Compressor Systems

by: P. Shoeibi Omrani & A. Eijk, TNO

1 Introduction

Reciprocating compressors are widely used in a variety of industries. Issues with using reciprocating compressors are reliability concerns, especially system failures due to the presence of liquid. The working principle of reciprocating compressors are based on the gas compression and due to incompressibility of the liquid phase, the compressor is incapable of handling the liquid carryover inside the compressor cylinder. Liquid is harmful to a compressor not only because it imposes significant hydraulic forces, which may result in loss of containment (typically head cover dislodged) but it also imparts an effect of literally “washing away” any protective and lubricating effects of compressor oil and rider materials. For instance, internal bearings suffer due to the type of liquid contaminant entering the machine¹. Different components of a reciprocating compressor system which can be impacted by the presence of liquid includes pistons, piston rods, piston rings, packings, bearings, valves, O-rings, bolts and the driver.

Additionally, as the liquid is being carried over into the compressor cylinder, there are no means of taking actions to avoid catastrophic failures. Thus, it is desired to design and operate a reciprocating compressor system to prevent liquid problems in the system.

This was also concluded from a reliability survey as carried out by the R&D group of the EFRC⁹.

For these reasons it was decided by EFRC to start an R&D project on the development of EFRC guidelines how to avoid liquid problems in reciprocating compressor systems.

Different steps of the project are as follows:

Phase 1: Literature survey

Study and evaluation of the liquid carryover problems; how they occur, what are the consequences and what are the measures in the design and operation of the system to prevent the liquid carryover problem.

Phase 2: Interviews

Face-to-face meetings with several OEM's, packagers and operators to get insight into the liquid carryover problem in practice and internal/international guidelines used to prevent it.

Phase 3: Internet survey

An internet survey was setup to get statistical information from the participants on the liquid carryover problem. The survey was setup based on the outcome of the literature survey and interviews.

Phase 4: Setting up guidelines

Based on the results of the previous phases, guidelines on the design and operation of reciprocating compressor systems in order to avoid liquid problems were set up.

Phase 5: International workshop

Organising an international workshop to reach consensus on the EFRC guidelines developed for preventing liquid carryover in reciprocating compressor systems.

This paper will give an overview of results of the different steps in the EFRC project.

2 Literature survey

Literature relevant to the liquid carryover problems in reciprocating compressor systems has been found from universities, OEM's and operators articles in the related conferences and API guidelines. In general compressor failures due to fluid components can be caused by²:

- Liquid carryover (slugs from separator or low points in piping, from interstage coolers, flow transients). This will lead to high forces which can damage parts of the system e.g. piston, bearings and crack shaft.
- Wet gas; This can cause a decrease in the efficiency and can also damage the compressor valves. It can also lead to corrosion problems and complex failure modes.
- Gas containing liquids could wash away the oil film from the compressor cylinder leading to a higher wear and a decrease in efficiency and life time.
- Carbon formation: high temperatures, oils, and gases make carbonaceous debris.

This literature survey focusses on liquid carryover initiation, development and methods to mitigate it. The liquid can enter the compressor by three major mechanisms: liquid carry over from the upstream separator, condensation of the gas flow in the components upstream of the compressor inlet (e.g. suction line) and excessive pre-lubrication in lubricated machines.

Liquid content flowing from the upstream separator can be transported directly to the compressor cylinder or accumulate in low spots of the piping or in the suction damper. In case of accumulation, sudden flow changes can cause a large amount of

accumulated liquid be transported which can finally enter the compressor cylinder.

Different studies were performed in an attempt to quantify the effect of liquid carryover in the reciprocating compressor cylinder. It was found that the presence of liquid significantly increases the cylinder pressure³ (Figure 1), discharge pressure⁴, load on valve and crosshead pin⁵ and compressor power (electrical current)⁶.

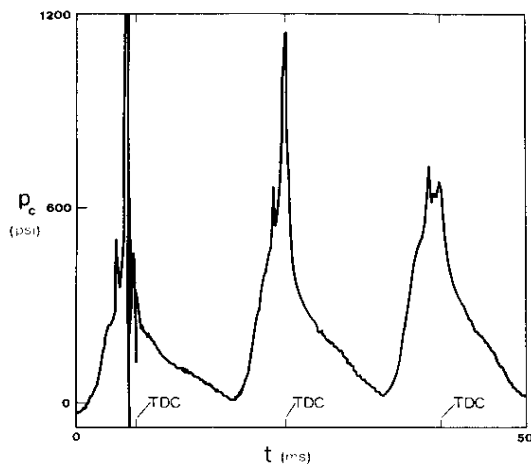


Figure 1: Measured cylinder pressure during slugging, the compressor was started at $t=0$ ³

The amount and the form of liquid entering the compressor cylinder have an effect on the extent of the damage, which can ultimately be a catastrophic failure and loss of process containment. Liquid can enter the compressor cylinder in three forms: droplets, slugs or films. Slugs and liquid film can directly lead to a complete failure of the compressor cylinder valve and bearings, even if the liquid volume is less than approximately 50% of the clearance volume⁵. Droplets with a low volume fraction will not lead to an instantaneous failure. However, they stimulate long-term failures, such as valve sticking, which can decrease the compressor efficiency and reliability. An approximated curve is given in Figure 2 to show the relation between the compressor life-time and the droplet size injected in the compressor cylinder.

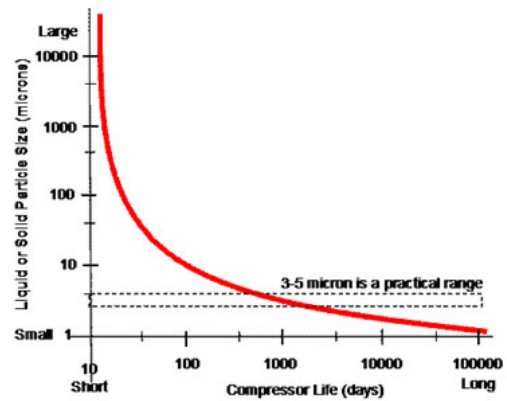


Figure 2: Compressor life versus the injected droplet size⁷

Despite the fact that liquid carryover problems can cause damage on internal parts of the compressor cylinder (e.g. valves, bearings, etc.), the problem is initiated in other components upstream the compressor cylinder, such as separator, suction line and suction damper. Thus, the design and operation of these components is of great importance. Up to now, there are no standard and detailed guidelines on how to prevent liquid problems in compressor systems, especially for reciprocating compressors. There are some design rules indicated in section 7.7.1.4. of the API Standard 618, 5th edition which are summarized as follows⁸:

- Liquid separator shall be as close as possible to the compressor suction side.
- Separator efficiency over the operating flow rates shall be maintained.
- Sufficient separator volume to handle incoming slugs.
- Sufficient gas velocity in the line from the separator to the cylinder to minimize liquid dropout.
- Elimination of the low points between the separator and cylinder;
- Sloping of the piping system.
- Insulation to minimize heat losses.
- Heat tracing to maintain the gas temperature at or above the dew point.

It is of general opinion that the API 618 guidelines on preventing liquid carryover problems, give too little information and guidance for this specific problem. Additionally, the general remarks as given in the literature, do not give quantitative values or specific engineering standards how to avoid liquid carryover problems. The guideline which is intended to be developed shall as a minimum indicate the type and volume of the separator, how much the operating gas temperature shall be above the dew point, etc. For that reason, interviews with several operators and

EFRC Guidelines on how to avoid Liquid Problems in Reciprocating Compressor Systems

by: P. Shoeibi Omrani & A. Eijk, TNO

OEM's were setup to get more insight in the practical problems and proven engineering solutions.

3 Interviews

As discussed, there are no detailed guidelines or standards on how to prevent liquid carryover problems in reciprocating compressor systems. There is also a lack of knowledge in some specific areas on how to avoid liquid problems. For instance, which type of gasses leads to more liquid problems? Which type of compressor cylinder valves has higher resistance against liquid forces? When is heat tracing and insulation of the piping important and required? Which type of separators are more suitable in reciprocating compressors applications?

Additionally, there is an inconsistency between some items of the available guidelines and literature in this field. For that reason, face-to-face meetings were arranged with different compressor OEM's, engineering companies, packagers and end users. A short summary of the results is as follows:

- Wet gasses, heavy hydrocarbons, saturated gas, natural gas and flare gas have higher chance of liquid carryover (bone-dry gasses barely exist in practice).
- In general, inadequate separation, process offset and transients, changing the gas composition, incorrect restarting, cold start or start during the commissioning phase and operating the system outside its operational envelope increase the chance of liquid carryover.
- Regarding the pulsation dampers, the suction dampers seem to be more crucial for liquid carryover.
- Liquid carryover problems are often not considered in the design of pulsation dampers.
- Separators which are designed for a specific condition, are sometimes used outside their operating envelope which can enhance the liquid carryover.
- In multistage compressors with intercoolers, separators shall be used downstream each intercooler.
- Suction and interstage lines are more critical for liquid carryover and they have to be sloped towards the separator.
- There are different types of level gauges, alarms and sensors connected to the system, which do not directly monitor liquid accumulation and carryover (no preventive monitoring).
- Root-cause analysis are performed after each compressor trip to assess whether the problem was caused by liquid carryover or other problems.
- As it was mentioned, incorrect restart, cold start or start during the commissioning phase (due to possible liquids and condensates and also excessive lubrication) could lead to liquid carryover problems. For that purpose, internal procedures are developed in some companies to restart their compressor system with respect to liquid carryover prevention.
- Communications and collaborations are viewed as not sufficient between the different parties involved in the design and operation of the compressor systems.
- Cylinder lubrication shall be regularly monitored to prevent excessive lubrication (liquid carryover).
- Process gas sampling and analysis is very crucial. Most of the time sampling is not representative and adequate safety margins are not taken into account.
- The currently available guidelines are not developed specifically to avoid liquid carryover problems and they do not give quantitative rules. For this purpose, some companies adapted guidelines which are based on their experiences and the lessons learned database.
- Engineering guidelines for placing drains, heat tracing, insulation and sloping is required.
- It is required to mention in the guidelines that good communication is necessary between different parties which are involved in the design of the compressor system e.g. compressor and separator OEM, engineering company and end user.

From the interviews, it was concluded that only the API Standard 618 together with some developed internal guidelines of the interviewed companies are used to prevent liquid carryover problems. It was also concluded that during the design of a complete compressor system, the components such as dampers and piping are not designed with respect to avoiding liquid problems. For that reason more detailed and quantitative rules and guidelines are required for the basic design and operation of reciprocating compressor systems to ensure a safe, reliable and efficient operation of the complete systems for the long term with respect to liquid carryover. For instance, guidelines in choosing an appropriate type of a separator, pipe layout with an adequate sloping, etc. shall be addressed and explained in the guidelines. Thus, developing guidelines on how to prevent liquid carryover is essential.

4 Internet survey

The information obtained from the interviews gave insight in the practical aspects of the problem. However, the information was too limited due to a relative small number of interviews. In order to get better statistical data from a broader range of participants, an internet survey was setup.

The survey consisted of 11 sections: general information of the participants, liquid problems experiences, design of different components in the system, condition monitoring, type of performed calculations, restart procedure and the available guidelines. This survey was sent to 500 participants of which 102 participants have partially filled-out the survey and 65 have finished the complete survey. A short summary of the internet survey results are given as follows:

- Most of the participants, around 45%, have indicated that changes in the process and ambient conditions are the main cause for liquid carryover. Another main cause was indicated to be the restart of an existing compressor (13%).
- 89% of the participants have indicated that liquid problems were observed only in case of accidents, during start-up or transients conditions such as switching to part load of a cylinder.
- Liquid carryover problems were detected in most of the cases when the compressor had failed or when the liquid level of the separator was increased, see also Figure 3.
- Approximately 29% of the participants do not calculate liquid formation during the design phase, see also Figure 4.
- 95% of the participants use a separator upstream of the compressor cylinder. The reason that 5% of the participants do not use a separator is due to costs and design limitations.
- Approximately 90% of the participants uses interstage separators in multistage compressors with or without intercooler.
- Approximately 59% of the participants use drains on both the suction and discharge dampers. Approximately 19% do not install drains on pulsation dampers.
- Most of the participants indicated that the pipe routing is based on keeping the vibration levels to acceptable levels and by keeping the thermal stresses to allowable code limits. They do not design the pipe routing with respect to liquid carryover.

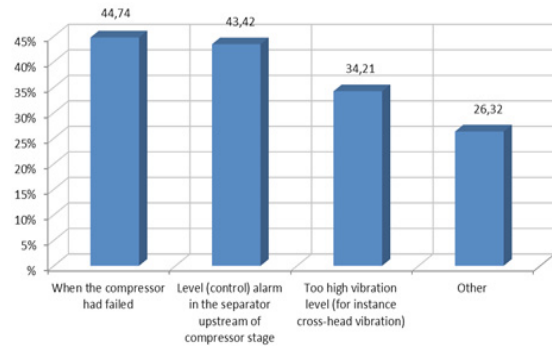


Figure 3: The first sign indicating the liquid carryover; the percentages were calculated based on the number of participants and multiple answers were permitted

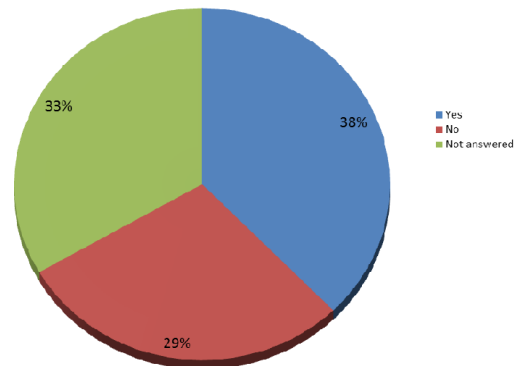


Figure 4: Pie chart indicating which of the participants calculate liquid formation during the design.

- The suction piping is in most of the cases sloped towards the separator.
- Approximately 29% of the participants do not use heat tracing on the suction line. 50% of the participants insulate the piping system.
- It was indicated that none of the monitoring systems can predict and prevent liquid carryover. Amongst the available monitoring methods, measuring the liquid level of a separator combined with an automatic drain had the highest level of satisfactory.
- 74% of the participants use or have used the API Standard 618 to design and operate their compressor with respect to avoiding liquid carry over.
- More than 60% has the opinion that the available guidelines are not sufficient to avoid liquid carryover in reciprocating compressor systems.
- Participants have ranked a sequence of steps for restarting a compressor. Their rankings were averaged and used as a basis for the restart procedure to be included in the guidelines and will be discussed in the next section.

EFRC Guidelines on how to avoid Liquid Problems in Reciprocating Compressor Systems

by: P. Shoeibi Omrani & A. Eijk, TNO

- Participants have also indicated a number of points which shall be included in the EFRC guidelines on how to prevent liquid carryover. For instance, possible configurations for pipe routing, choosing the optimum layout and volume of a separator, pulsation damper design, start-up procedure and heat tracing of different components e.g. piping and dampers shall be included in the guidelines.

5 Setting up the guidelines

The results of the literature survey, face-to-face meetings and internet survey were gathered and have been used to develop the EFRC guidelines. In this section, the scope of the guidelines document and different chapters will be summarized. The document "EFRC Guidelines on how to avoid liquid problems in reciprocating compressor systems" can be downloaded from the EFRC website: www.recip.org.

5.1 Scope of guidelines

The EFRC guidelines are divided into two main parts. The first part is focusing on the design of compressor components with respect to liquid carryover prevention and the second part is focusing on the operation of the reciprocating compressor system. In these guidelines each component in the system is being discussed in order to decrease the chance of liquid related problems. Engineering rules are given to increase the awareness on the design and operation of different compressor system's components. It is recommended to use the EFRC guidelines in conjunction with the more detailed guidelines which are specifically developed for each component of the reciprocating compressor systems, such as separator, pulsation damper, etc.

The system components which are covered by these guidelines are:

- Separators and their auxiliaries, such as demisters, level control, etc.
- Pulsation dampers.
- Upstream, downstream and interstage piping.
- Drains.
- Miscellaneous.

In the section of separators, engineering rules on the pre-selection, design check and operation of separators are given. The rules on how to check the separator as designed by the vendor are valid for pressures up to 105 barg. For pressure above 105 barg, the capacity of separators will be further de-rated and the design procedure shall be done in consultation with a separator expert.

The various types of reciprocating compressor systems for which the guidelines can be used are given here:

- Horizontal, vertical, V-, W- and L-type compressor systems.
- Constant and variable speed compressors.
- Compressors driven by electric motors, gas and diesel engines, steam turbines, with or without a gearbox, flexible or rigid coupling.
- Dry running and lubricated reciprocating compressors.
- Compressor systems for all types of gases.
- Diaphragm compressors.
- Labyrinth compressors.

Further on it shall be noted that the guidelines can only be used for the booster compressors parts of a hyper compressor system but not for the hyper compressor part itself.

5.2 Separator

This section of the guidelines focuses on the design check and operation of separators with respect to liquid carryover prevention. The following topics are discussed in the separator section:

- Engineering guidelines for pre-selection of separators and demisters.
- Rules on how to check the vendor's design of a separator and its auxiliaries.
- Additional engineering rules for the design and operation of separators.

A summary of important points on separators are given as follows:

- According to API 618, 99% of droplets above 10 μm shall be removed by the liquid separation device. In practice these values are not achievable, due to the fact that the cut-off diameter (droplet diameter corresponding to the separation efficiency) of separators is dependent on the process conditions. Field experiences have shown that with a well-designed separator with proper auxiliaries and a large enough operating envelope, liquid related problems can be mitigated.

- The aim for choosing a separator shall be to achieve the highest possible efficiency for all process (temperature, pressure, molecular weight, density etc.) and flow conditions (full load, part load, compressor speed range, etc.) as indicated on the compressor data sheets.
- Transient conditions such as start-up and shut down, appeared to be very critical parameter on the separator efficiency and shall be considered in the design phase.
- There might be situations where systems can operate safe and reliable with a lower efficiency separator. Decisions on the acceptance of a lower efficiency (<95% for all specified conditions by the purchaser) shall preferably be based on proven designs and relevant experiences in similar applications.

The separator efficiency and final separator design shall be agreed upon between the vendor and the purchaser.

- A summary of different types of gas-liquid separators are given in Table 1. Each type of separators is ranked for different capabilities, such as slug handling, droplet handling, turn-down ratio (ratio of the maximum and minimum flow rate inside the separator), pressure drop and fouling tolerance.
- The minimum requirement of the separator vessel diameter can be checked using equation (1);

$$D_{\min} = \sqrt{\frac{4Q_{\text{gas,max,operation}}}{\pi K}} \sqrt{\frac{\rho_G}{\rho_L - \rho_G}} \quad (1)$$

In which:

ID_{\min}	Vessel inner diameter [m]
$Q_{\text{gas,max, operation}}$	Maximum operating gas volumetric flow rate at the inlet nozzle of the separator [m^3/s]
$\rho_{G,L}$	Gas and liquid density [kg/m^3]
K	Souders-Brown velocity [m/s]

- Values for Souders-Brown velocity¹⁰ for different type of separators at different operating pressures are given in the guidelines.
- The maximum gas velocity $U_{G,\max}$ shall be considered as given in equation (2) instead of the average velocity¹¹. These velocities are defined at the inlet of the separator, see also Figure 5.

$$U_{G,\max} = \bar{U}_G + U'_G \quad (2)$$

In which:

$U_{G,\max}$	Maximum gas velocity [m/s]
\bar{U}_G	Average gas velocity based on the average actual flow rate [m/s]
U'_G	Fluctuating gas velocity [m/s]

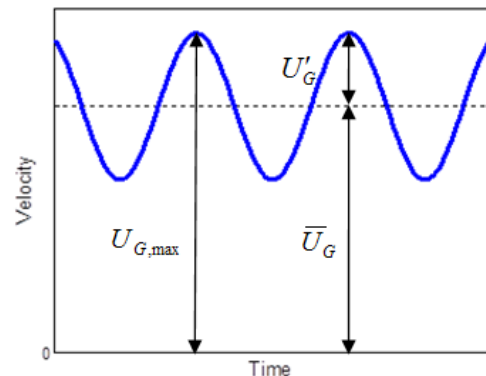


Figure 5: Definition of mean, fluctuating and maximum velocity

- In order to calculate the fluctuating gas velocity in an accurate way, it is necessary to perform a pulsation analysis according to the API Standard 618⁸. However, an approximation of the fluctuating gas velocity can be calculated with the maximum allowable pressure pulsation levels, equation (3). The maximum allowable pressure pulsations could be calculated from the API Standard 618.

$$U'_G = 0.5 \cdot \sqrt[5]{\frac{P'}{\rho_G c}} \quad (3)$$

In which:

U'_G	Fluctuating gas velocity (m/s)
P'	Maximum allowable peak-to-peak level of pressure pulsations [bara]
c	Gas sound speed [m/s]
ρ_G	Gas density [kg/m^3]

- The length to diameter ratio for horizontal separators and height to diameter ratio for vertical separators, called aspect ratio, shall properly be designed and chosen. Low aspect ratios can lead to low separation efficiency.
- Sufficient spacing between the inlet and outlet of the separator is required to ensure the separation efficiency. Additionally, the distance between the separator inlet and internal devices, such as

EFRC Guidelines on how to avoid Liquid Problems in Reciprocating Compressor Systems

by: P. Shoeibi Omrani & A. Eijk, TNO

- demisters, is of great importance, the smaller the distance, the lower the separation efficiency.
- Each compressor unit must be equipped with an individual separator unit if more than one compressor is mounted in the compressor system unless the separator is designed for the maximum flow of all possible combinations of running compressors.
 - For lubricated compressors, a separator must be installed at the suction side (separating lube oil transported via bypass lines), at each interstage and if specified at the final discharge (e.g. if dry gases are required).
 - Each separator shall be located upstream of the compressor and as close as possible to the compressor.
 - For interstages, a separator must be located downstream of each intercooler and as close as possible to the compressor. According to the API Standard 618, the capacity of the lower part of the separator shall be sufficient to contain the maximum expected liquid flow from any specified operating condition for not less than 15 minutes, without activating any alarm. This

criterion can be used if an incoming slug into the separator is not expected.

- If an incoming slug is expected, the volume of the lower part of separator shall be able to handle the liquid hold-up of the expected liquid flow for 5 minutes plus the slug volume. If the incoming slug volume is not known, the volume shall be approximated as a minimum of 2-5 seconds of the maximum feed flow rate of the mixture (gas and liquid) based on the density of the liquid (100% liquid pipe hold-up). This means that a liquid column is entering the separator for 2-5 seconds with the maximum feed flow rate.

5.3 Pulsation dampers

This section of the guidelines focuses on the design considerations of pulsation dampers with respect to liquid carryover prevention.

The main function of pulsation dampers is to reduce the pulsations in the system to acceptable levels. Thus, the pulsation dampers are not

Table 1. Comparison between different characteristics of Gas/Liquid separators

Type of separators	Slug handling***	Droplet handling	Turndown ratio****	Pressure drop****	Fouling tolerance
Vertical Knockout-drums	+	-	++	--	++
Horizontal knockout-drums	++	-	++	--	++
Cyclone with tangential inlet	+	+	0	+	++
Cyclone with straight line and swirler	++	+	0	+	0
Horizontal vane-type*	+	+	0	-	-/---*****
Vertical vane-type (in-line)*	--	0	0	-	-/---*****
Vertical vane-type (vertical)*	+	+	0	-	-/---*****
Horizontal wire mesh*	++	++	-	-	-/---*****
Vertical wire mesh*	0	++	-	-	-/---*****
Cyclone packs with wire mesh*	++	++	+	0	0/-
Cyclone packs with vane pack*	++	++	0	0	0/-
Coalescers	--	++	++**	++	--

Explanation of used symbols:

--: very low, -: low, 0: moderate, +: high, ++: very high

* These demisters are combined with a knock-out drum

** Limited by droplet size and entrainment onset

*** Slug handling of each device can be improved with a suitable inlet device

**** See Annex A for values of turn down ratio and approximated pressure drop

***** Depends on the type of wire mesh or vane pack

designed to work as a separator. However, these devices are ideal spots for liquid to accumulate and lead to liquid carryover. Even if a separator has a proper design for all defined operating conditions, it is always possible that liquid can enter the pulsation damper during offset conditions or that condensates will be formed or accumulated inside the damper. For this purpose, several design criteria for pulsation dampers are given as follows:

- For suction dampers without internals, such as baffle plates or half pipes, drains are not necessary to be installed.
- For lubricated machines, each discharge damper shall be equipped with a manual drain.
- For a damper with baffle plates, the drain shall be mounted in the first compartment downstream the cylinder nozzle.
- More detailed guidelines on the location of drain valves for horizontal and vertical pulsation dampers with different type of internals, such as half pipe and baffle plates are given in the EFRC guidelines.
- Bootlegs shall be avoided.
- Drain holes shall be drilled on the internals to avoid liquid accumulation, see examples in Figure 6 and Figure 7. The drain holes shall have a minimum diameter of 10 mm and a maximum diameter of 15 mm or 2% of the internal area in which the hole is drilled.
- The purpose of heat tracing of a suction pulsation damper is to keep the process gas temperature constant and above its dew point. Insulation shall always be installed if heat tracing is installed.
- Insulation is always preferred to be installed for the suction damper. For the discharge damper insulation or other protection may be required for temperature safety reasons (personnel protection).

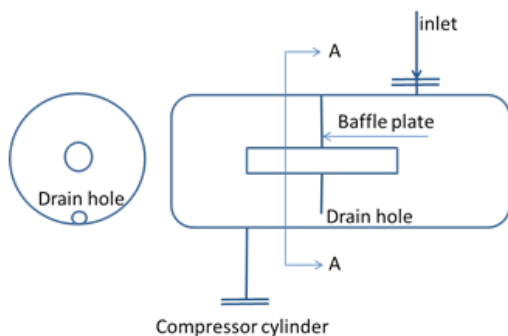


Figure 6: Example of a suction damper with baffle plate and drain hole

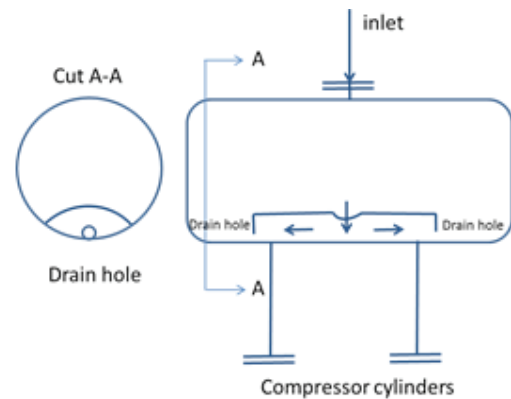


Figure 7: Example of a suction damper with a half-pipe with drain holes

5.4 Piping

- The design of the discharge piping with respect to liquid problems is less crucial but it is also necessary to be considered. In general, the pipe configuration shall be designed in such a way to avoid liquid accumulation in low points and blocked points (dead-end).
- The suction piping upstream and downstream the inlet separator shall always be sloped towards the separator. The minimum slope shall always be 1:100.
- Flare lines shall also be sloped with a minimum slope of 1:100. The sloping shall be towards the main header piping to avoid a collection of liquid upstream the valve.
- Low points and pockets shall be avoided.
- In case pockets cannot be avoided, they have to be equipped with a drain valve, see Figure 8. Opening of these valves needs to be part of the start-up procedure and periodic inspection.

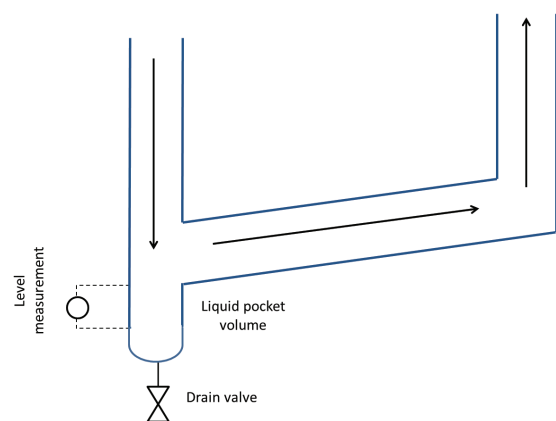


Figure 8: Example of a pocket with bootleg, level measurement device and a drain valve

EFRC Guidelines on how to avoid Liquid Problems in Reciprocating Compressor Systems

by: P. Shoeibi Omrani & A. Eijk, TNO

- Process gas dew point shall be calculated in an accurate way at each compression stage. A dew point margin of 10 °C shall be considered due to possible uncertainties in the models and process gas sampling accuracies.
- Heat tracing of the suction piping shall be considered to ensure that the process gas temperature will always be above the dew point.
- Insulation shall always be installed if heat tracing is installed.
- It is recommended to use an individual separator for each compressor unit. However, if one separator is used for multiple compressors as shown in Figure 9, each suction line shall be equipped with a block valve and an individual drain system.

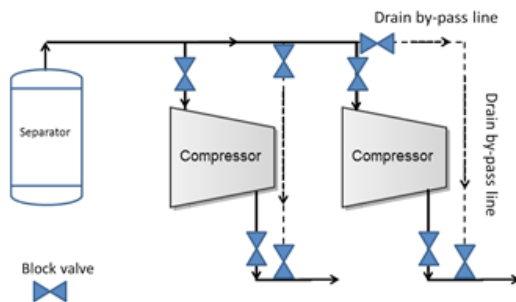


Figure 9: Example of the drain by-pass line and block valve configuration for a multiple compressor system with one common separator.

5.5 Miscellaneous

In this part, some design and operational guidelines on other system's components are given to mitigate liquid carryover problems. Different topics such as compressor valves, cylinder lubrication, valve unloaders, coolers and compressor recycle operation are discussed.

- Compressor cylinder lubrication shall only be started shortly prior to start-up in order to avoid lubricating oil to flood the compressor cylinder.
- Condensation of the process gas can lead to lubricating oil dissolution. For this purpose a heavier-bodied oil or synthetic oil shall be used.
- In case of changing the process gas or process conditions, the system will operate at off-design conditions. For these conditions, the system shall be checked again under the new conditions and required modifications shall be implemented if necessary. The modifications shall be performed in consultation with compressor and equipment OEM's, separation

specialist, process and pipe engineer and end-user.

- During the compressor recycle operation, the process gas will experience the Joule-Thompson cooling effect caused by the pressure loss over the recycle valve. This cooling can increase the condensation rate and the chance of liquid carryover. In the design of separators these effects shall also be included.

5.6 Operations

Since most of the liquid carryover problems are initiated during the start-up or cold restart of the compressor, a procedure was developed to give a step-by-step approach to prevent liquid carryover problems during these conditions. A summary of the procedures is as follows:

- Cooling water temperature at the cylinder inlet shall be at least 5°C above the gas inlet temperature (in all conditions). Preferably temperature control is automatic.
- Adequate time must be allowed prior to start-up for the heater and cooling water flow and heat tracing to warm up the compressor cylinders.
- Pre-lubrication of cylinders and packings shall be kept to a minimum and shall be advised by the OEM or based on experiences with a specific compressor or lubrication systems.
- Before start-up all process equipment such as coolers, pulsation dampers, piping (especially pockets) and separators shall be drained. Discharge pulsation dampers shall also be drained due to the fact that liquid condensates and lube oil can be accumulated and may cause problems in the downstream compressors and process equipment or may be fed back into the suction piping via the by-pass lines.
- If the process allows for it, the compressor loading shall be achieved by small increments instead of by a sudden large step.

6 International workshop

On 18 March 2013 an international workshop was held. Several equipment and compressor OEM's, and engineering companies attended the workshop. The target of the workshop was to achieve a consensus on the proposed guidelines which was finally reached after ample discussions on different topics.

7 Conclusions

Up to 2014 there were no engineering guidelines and standards on how to prevent liquid carryover problems in reciprocating compressor systems. Such guidelines were necessary to ensure the reliability, safety and efficiency for the long term operation of the reciprocating compressor system. The R&D group of the EFRC has started a project for that reason to develop guidelines for the design and operation of reciprocating compressor systems with respect to liquid carryover prevention.

The project consisted of different phases, literature survey, interviews, internet survey, setting up guidelines and international workshop. The results of the literature survey gave an overview of the mechanisms leading to the presence of liquids in the compressor. Additionally, the effect of each component in the compressor system on the liquid problem was reviewed.

Interviews gave more insight into the practical issues on liquid carryover problems and methods that each party is performing to mitigate the problem. The internet survey was setup to get more information and knowledge from the participants distributed all around the world.

The results of a literature survey, interviews and an internet survey were used as a basis for developing the guidelines. The guidelines were reviewed by experts in this field and presented in an international workshop to get consensus on the complete document.

The guidelines are focussing on the pre-selection, the design check and on the operation of different components as installed normally in reciprocating compressor systems. Most of the components, such as piping and pulsation dampers are normally not designed to mitigate liquid carryover problems. Normative and quantitative guidelines are given in the EFRC guidelines for various design parameters of system components.

It is believed that the chance on having liquid problems in reciprocating compressor systems is reduced considerably by applying the recommendations as given in the EFRC guidelines.

8 Acknowledgements

The authors would like to thank the R&D sponsors of the EFRC for their permission for publishing the results of this project and all participants of the workshop for their active contribution. We are thankful to Jeroen van Koperen (Shell Projects and Technology), for his active contribution as EFRC project coordinator. We would also like to thank Stefan Belfroid for his contribution and helpful comments during the project.

References

- ¹ M. I. Comyn, F. Boer, R. Garza, J. S. Hansen, I. Bjorkevol, G. Wiken, "Reliability experienced with offshore reinjection compressors", Proceeding of the 3rd EFRC conference, Vienna, 2003.
- ² H. P. Bloch, J. J. Hoefner, "Reciprocating Compressors, Operation and Maintenance", Gulf Professional Publishing, 996.
- ³ R. Singh, J. Nieter, G. Jr. Prater, "An investigation of the compressor slugging phenomenon", ASHRAE Transactions, 92(4):250-258. 1986.
- ⁴ C. R. Laughman, R. R. Lal Foy, W. Wichakool, P. R. Armstrong, S. B. Leeb, L.K. Norford, J. Rodriguez, K. Goebel, A. Patterson-Hine, E. C. Lupton, "Electrical and Mechanical Methods for Detecting Liquid Slugging in Reciprocating Compressors", Proceeding of International Compressor Engineering Conference at Purdue, July 14-17, 2008.
- ⁵ B. G. Shiva Parsad, "Effect of Liquid on a Reciprocating Compressor", Journal of Energy Resources Technology, Vol. 124, 2002.
- ⁶ C. R. Laughman, P. R. Armstrong, L. K. Norford, S. B. Leeb, "The Detection of Liquid Slugging Phenomena in Reciprocating Compressors via Power Measurements", Proceeding of International Compressor Engineering Conference at Purdue, July 17-20, 2006.
- ⁷ Barringer & Associates, Inc. website (2012): <http://www.barringer1.com/dec08prb.htm>
- ⁸ Reciprocating Compressors for Petroleum, Chemical, and Gas Industry services, API standard 618, 5th edition, December 2007.
- ⁹ A. Eijk & L. van Lier, "Compressor Reliability Survey", 7th Conference of the EFRC, October 21st - 22nd, 2010.
- ¹⁰ M. Souders, G. G. Brown, "Design of fractionating columns, entrainment and capacity, Industrial and Engineering chemistry", 38(1): 98-103, 1934.
- ¹¹ S. P. C. Belfroid, G. J. N. Alberts, "Effect of pulsations on separator efficiency", 4th Conference of the EFRC, June 9th-10th, 2005.



8th EFRC workshop for students “Reciprocating compressors”

June 10th to June 13th 2014
Czech Republic and Austria

by
Gunther Machu
Chairman of the EFRC Student Excursion
gunther.machu@hoerbiger.com

9th Conference of the EFRC September 11th / 12th, 2014, Vienna

The EFRC Student’s Excursion takes place every second year and has been initiated in the year 2000. The clear goal is to introduce students from all over Europe to the reciprocating compressor industry and gain their interest to start a career in this business area. In order to provide a good overview the intention is to visit endusers, compressor manufacturers and component suppliers in the natural gas and process gas industry. As education is also part EFRC’s mission, lectures about various topics around the reciprocating compressor are also given during the course of the excursion.

In 2014 the excursion took place in the Czech Republic and Austria, and we (me and former chairman Siegmund Cierniak) had the opportunity to visit HOERBIGER Vienna, Leobersdorfer Maschinenfabrik (LMF), an underground natural gas storage plant of RWE in the Czech Republic, a chemical plant of BOREALIS in Schwechat, Austria and finally the Vienna University of Technology. We selected 26 students (based on their application letter and curriculum vita) out of a pool of 35 applicants from Italy, Austria, Germany, Spain, the Netherlands, Poland, Russia, Slovakia, Swiss, Lebanese and Egypt.

SESSION EFRC

8th EFRC workshop for students “Reciprocating compressors”

by: Gunther Machu, Chairman of the EFRC Student Excursion

Day 1

Day 1 started at HOERBIGER Compression Technology in Vienna with an introduction to the EFRC, a lecture on “The reciprocating compressor and its performance determining components“ (valves and rings and packings) by G. Machu and finally a museum and factory tour (by Mr. Christian Leitner and Helmut Lang).



Fig. 1: At the HOERBIGER museum and factory

Then we continued to the Leobersdorfer Maschinenfabrik (LMF) with lectures given by Thomas Heumesser on

- The reciprocating compressor – design basics
- Compressor applications

Later we had the opportunity to visit the LMF factory, where we were able to see a large API 618 process gas compressor, natural gas compressors and also seismic packages.



Fig. 2: Thomas Heumesser explaining compressor design details at LMF



Fig. 3: The 2014 EFRC Students in front of an API618 process gas compressor at LMF

8th EFRC workshop for students “Reciprocating Compressors”*by: Gunther Machu, Chairman of the EFRC Student Excursion*

We ended a very interesting day at a local restaurant with a dinner sponsored by LMF.

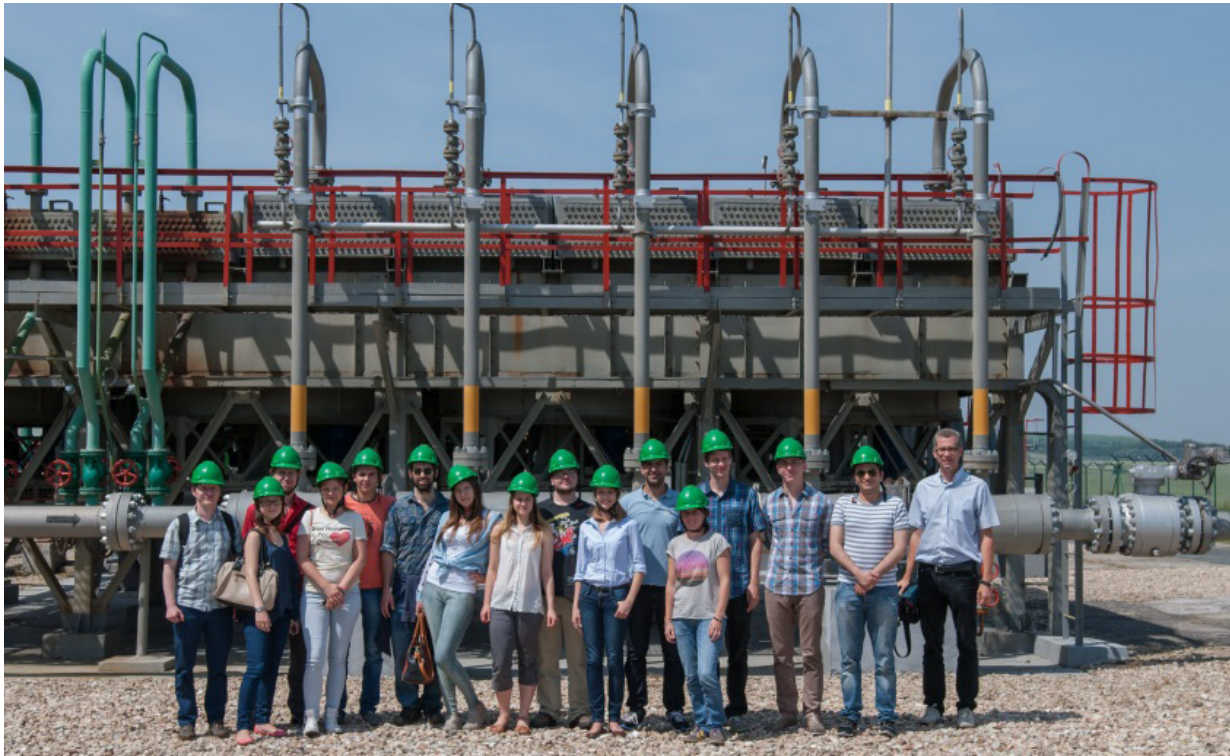
Day 2

Fig. 4: Group 2 at UGS Dolni Dunajovice

The next day we visited an underground natural gas storage plant of RWE in the Czech Republic.

Mr. Jiri Kafka (RWE) gave an introduction to “UGS Dolní Dunajovice and the role of the reciprocating compressor in the gas storage business”.

Later we were split in two groups and visited the plant and learned a lot about the geology, the technology and process steps in dealing with the natural gas in underground storage facilities.

We ended the day at Cesky Krumlov with a nice walk through the old town.



Fig. 5: at Cesky Krumlov enjoying the evening

8th EFRC workshop for students “Reciprocating Compressors”

by: Gunther Machu, Chairman of the EFRC Student Excursion

Day 3

We headed back to Schwechat (Austria) to visit the chemical plant of BOREALIS. Mr. Wolfgang Stagl gave an introduction to BOREALIS and explained the role of reciprocating compressors in the chemical industry, as well as explained the specific recip's BOREALIS has in use.



Fig. 6: At the BOREALIS chemical plant, changing clothes to tour the facility.

In the afternoon we had the fantastic chance to visit the various types of compression equipment at the plant.

Day 4

This day was dedicated to the educational part – Prof. Herbert Steinrück was hosting us at the Vienna University of Technology and gave a lecture about the “Basics of gas dynamics and flow in reciprocating compressors”. André Eijk from TNO (who joined us in the evening of Day 3) was rounding off the day with a presentation on “Pulsations and Vibrations on reciprocating compressors”.

Last but not least Mr. Konrad Klotsche (TU Dresden) presented the homework task for the students. Completing this task within the deadline of two weeks is accompanied by attractive prizes for the students, as the top three finishers are invited to the 2014 EFRC conference.

The winner additionally gets invited to a special, one week compressor training by GE Oil & Gas in Florence, Italy. Second place gets 500 € in cash.

And here are the 2014 winners of the student's homework:

1st place goes to Mr. Christoph Buchner, Austria

2nd place goes to Mr. Arrigo Battistelli, Italy

3rd place goes to Mr. Jan Tuhovcak, Slovenia



Fig. 7: In front of the BOREALIS training center

8th EFRC workshop for students “Reciprocating Compressors”

by: *Gunther Machu, Chairman of the EFRC Student Excursion*



Fig. 8: 1st place winner C. Buchner,
2nd place A. Battistelli and
3rd place J. Tuhovcak

9th Conference of the EFRC September 11th / 12th, 2014, Vienna

Capacity Control System Applications and Developments -205-
by: A. Raggi, A. Giampà, COZZANI; M. Grassi, INEOS

Revamp of an Existing Reciprocating-Compressor Unit -217-
by: Andreas Hahn, Klaus Hoff and Gerhard Knop, NEUMAN & ESSER

Challenges of Oxygen Reciprocating Piston Compressors -227-
by: Wolfgang Grillhofer, Air Liquide



EUROPEAN FORUM
for RECIPROCATING
COMPRESSORS

SESSION DESIGN



Capacity Control System Applications and Developments

by:

A.Raggi, A.Giampà

Dott.Ing.Mario COZZANI S.r.l.

Arcola (SP), Italy

info@cozzani.com

M.Grassi

INEOS Manufacturing Italia SpA

Rosignano (LI), Italy

manrico.grassi@ineos.com

**9th Conference of the EFRC
September 11th / 12th, 2014, Hofburg, Vienna**

Abstract:

The completely electronic reverse flow capacity control system has been object of detailed studies to reach the required targets of performance and reliability.

This paper describes the development, installation, set up phase and improvements of the control system in the production site of INEOS Polyolefins in Rosignano (LI), Italy.

A first measurement campaign has been carried out on an existing compression unit before the installation of the system. Appropriated valve covers have been used to acquire the indicated cycles, in order to define the initial state of the plant.

After the control system installation, some measurements have been carried out analysing its behaviour at the different capacities required by the production plant. Significant parameters, such as pressure trends, PV diagrams, regulation range, repetitiveness of the actuator positions, etc, have been kept under control over the time.

New plant investments enabled the installation of two new compressor units equipped with two different capacity control systems: the inverter and the reverse flow system. The paper shows also a direct comparison between the two systems.

1 Introduction¹

Increasing attention to energy saving and to performance optimization, combined with the evolution of technologies, achieved higher reliability targets developing increasingly performing and complex equipments for the production of new machines.

New technologies and cost reduction of electronic components enabled the development and spreading of capacity regulation devices, which allow optimizing both energy consumption and the global control of the machines. The stepless capacity control of reciprocating compressors is generally achieved by systems based on VSD (variable speed driver), that changes the compressor rotation speed, or based on reverse flow regulation, which acts on the suction valve opening timing.^{2,3}

During these last years, Cozzani has developed, a capacity control system, which allows adjusting the capacity through the reverse flow method.⁴

The system is completely innovative because it is absolutely the first operated only by electric current in order to control the closing of the compressor suction valves at each compression cycle. Thanks to this strategy the compressor processes the exact capacity required by the end user.

Since the first phases of the project development, performance has been constantly evaluated, in terms of efficiency and reliability targets.

Several tests have been carried out on the first prototype to optimize the performances with particular attention to the flexibility of the product in order to simplify all interfacing aspects between the system and the compressor plant. Starting from 2012, the system has been installed on a compressor at INEOS Manufacturing Plant in Rosignano Solvay (LI). To comply to the best with the plant requirements, dedicated measurements have been carried out on the existing machine in order to acquire the operating conditions and to analyse several control strategies which have been implemented and tested directly on the compressor after the start-up.

The good results allowed the installation of the system on a new machine of the same plant in August 2013.

The configuration of the plant, where the new machine is presently installed, has enabled further performance evaluations and direct comparison with other capacity control methods.

2 Capacity control system development^{5, 6, 7}

The capacity control system based on the reverse flow method enables a stepless adjustment of the reciprocating compressor capacity.

Operating principle is based on a forced delay in the suction valve closure compared to its natural closing instant. The valve is kept open even after the end of the suction phase (BDC); this produces a compression delay and part of the gas flows back from the cylinder into the suction volume. The amount of reversed gas is proportional to the time that the suction valve is kept open.

The compressor capacity can be controlled acting on the suction valve closure delay. This kind of control method allows acting on the suction valve sealing element positions. Due to the particular complexity of the task it is essential to introduce electronic control devices in order to control the valve actuators assuring the necessary accuracy and repeatability.

The system is characterized by a set of electromechanical actuators, each one connected to an electronic control device. Starting from the prototype development phase, the use of electronic systems has enabled to perform advanced control techniques necessary to achieve the performances required by the application.

The capacity control system consists of the following main components (*Figure 1*):

1. Electric actuators installed on suction valve covers, controlling the valve sealing element positions;
2. System Control Unit (SCU);
3. Actuator Control Units (ACUs);
4. Sensors for the measurements required by the system;

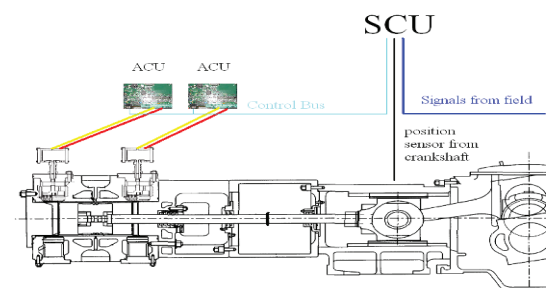


Figure 1: Electronic control system scheme

Capacity Control System Applications and Developments

by: A.Raggi, A.Giampà, COZZANI; M.Grassi, INEOS

The control structure for the suction valves actuators is showed in *Figure 2*:

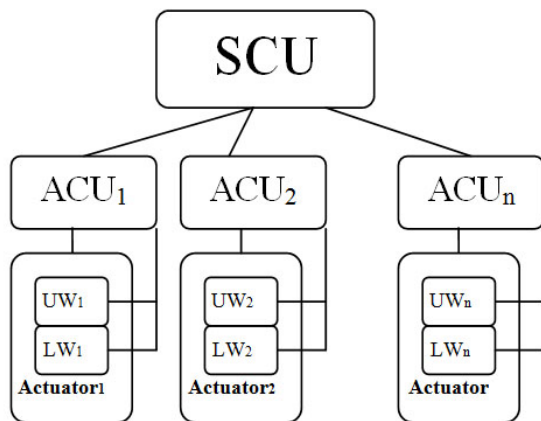


Figure 2: Capacity control system structure

The SCU receives digital signals from the compressor system (mainly the crankshaft position signals), in order to acquire the exact piston position during each cycle and the input signal used for the capacity control. This information is used to set the actuator control parameters. The aim of SCU is to coordinate the control of each suction valve and consequently of the entire compressor working cycle.

ACUs are the actuator control units. They receive information from the SCU regarding valve opening moment and its holding time and convert the above information in voltages across the magnetic windings which determine the movement of the actuators. Consequently the actuators can act on the valve sealing elements.

The actuator consists of a central sliding part, called “armature”, two electromagnets, placed at the opposite sides of the armature, which purpose is to move the armature linearly (and consequently the lower rod which acts on the valve finger type unloader) and two springs located at the opposite sides of the armature in order to accelerate and to decelerate the actuator moving parts (*Figure 3*).

In the actuator lower part there are gaskets and recycle gas connections, whereas the connectors and the sensor used to acquire the rod position are located in the upper part.

This device has been designed to have a high dynamic performance able to respond positively to the strict times required by the various phases of the compressor cycle.

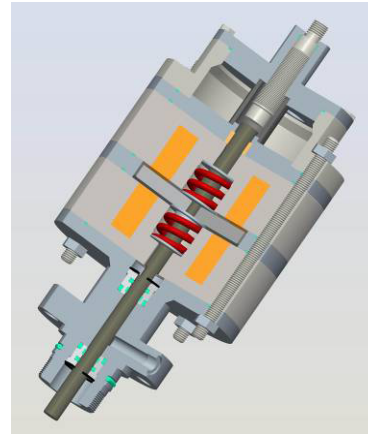


Figure 3: Actuator CAD model

The characteristics of the force generated by the two electromagnets (proportional to the square of current and decreasing with the increase of the gap between the electromagnet and the armature) allow to use limited currents to hold the valve open (armature in contact with the magnet). At the same time the intrinsic characteristics of the actuator will ensure the required dynamic performance.

In fact the two springs have the double function of accelerating the armature during the separation phase from the magnets and of decelerating it during the approaching phase. In this way, the speed during the impacts between armature and magnets is limited.

This double action of the springs allows a regenerative action avoiding unnecessary energy dissipation. At the same time, the springs contribute to the armature movement when the gap is at its maximum value, thus limiting the generation of high currents to move the armature.

In order to ensure the correct operation of the system, Cozzani has developed and patented a highly sophisticated control algorithm which achieves the following objectives:

- to limit the armature impact velocity during the approaching phase. High velocities would produce unacceptable noise level.
- to ensure a transition time between the upper and the lower position compatible with the performance demands.
- to guarantee a high holding force when the air gap is equal to zero (forces necessary to keep the suction valve open during the reverse flow phase).

The development of the control algorithm has been performed considering the non-linearity issues of

Capacity Control System Applications and Developments

by: A.Raggi, A.Giampà, COZZANI; M.Grassi, INEOS

the magnetic characteristic, and the variation of the gas force which depends on the different running condition of the reciprocating compressor.

Dedicated tests have been carried out in order to define the force generated by the electromagnets as a function of the geometrical characteristics of the windings and of the magnetic characteristics of the used ferromagnetic materials. Electromagnets with different geometric characteristics have been tested changing gap and current in order to define their relation with the force.

The results have been particularly useful in the development of the control algorithm in order to identify the optimal parameters to reduce the impact speed and to optimize the performance in terms of repeatability and synchronization of the motion with the reference trajectory.

Several tests have been carried out, at the beginning in the Cozzani facility and then at the end user site, in order to verify the system functionality.

The first installation has been on a single-stage single effect air compressor. This testing phase has allowed to obtain the first results on the capacity control and on power consumption.

Afterwards the capacity control system has been installed on a two stage double acting reciprocating air compressor with suction at atmospheric pressure and discharge at 10 bar.

The machine has been equipped with an actuator for each suction valve and the whole set of actuators has been used to control the compressor capacity.

The tests have been performed at several compressor speeds in order to verify the behavior of the system at the different operative conditions (Figure 4 and Figure 5).



Figure 4: Compressor with capacity control system

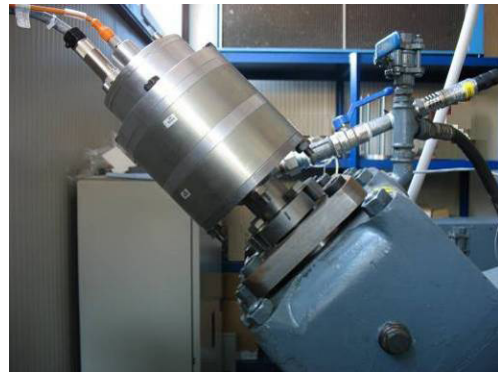


Figure 5: 2nd stage actuator

The compressor has been equipped with a monitoring system used to acquire the pressures in suction/discharge plena and in the two cylinders. The detected power and pressure trends had shown the efficiency of the system in controlling the suction valve closing instant, adapting perfectly the flow generated by the compressor to the demands of the plant.

Afterwards the system has been installed on a three-stage oil-free high speed compressor (1000 rpm) used to compress air up to 40 bar (Figure 6).

The machine was characterized by a double acting first stage with two suction and two discharge valves for each cylinder end, whereas the second and third stages were single-acting with one suction and one discharge valve for each cylinder end. The compressor has been equipped installing one actuator on each effect (therefore in the first stage only one of the two suction valves of each effect was controlled). The system has been set up to control the flow rate in order to make the compressor capacity equal to the one required by the plant, keeping the final pressure constant. This has been achieved keeping the interstage pressures constant too. In this way, the system could work correctly even if the flows in each stage were different (eg. introducing an amount of recovered gas in the interstage piping).

This was possible as each actuator works independently from each other in order to make the control of the different interstage pressure independent.

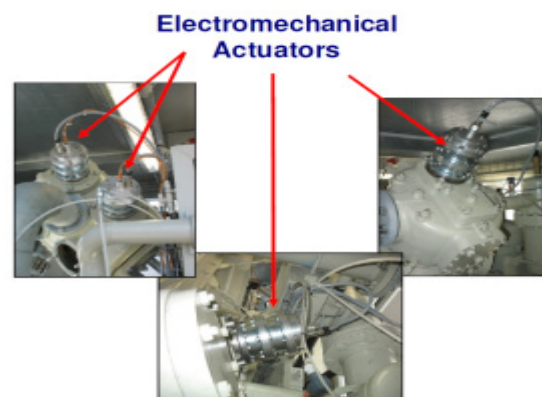


Figure 6: Details of the installed actuator

Capacity Control System Applications and Developments

by: A.Raggi, A.Giampà, COZZANI; M.Grassi, INEOS

Also in this case, the results obtained analysing the acquired compressor characteristics have confirmed that the system can efficiently adapt the capacity to the one required.

3 INEOS Manufacturing Plant in Rosignano Solvay (LI) - Italy

INEOS Manufacturing plant is in Rosignano Solvay (LI) - Italy and produces high-density polyethylene (HDPE) through hexane slurry process since the 1960s. The production capacity is about 200ktonn/year with approx. 180 employees. Ethylene is supplied by ships and through a dedicated dock stored in a cryogenic tank of 5ktonn. The suitably gasified ethylene is then conveyed to the polymerization reactors where it reacts with other raw materials and catalysts produced by INEOS and is converted to HDPE fluff. The fluff is moved to the final extrusion treatment plant through pneumatic conveying systems and intermediate storage silos and there it is extruded and transformed into granular form. The finished product is loaded and shipped directly to the customers. Currently, about thirty different resins are made for applications ranging from Blow Molding to the injection through mono and bimodal technology. INEOS plant works 24/7 on three shifts.

Recently with an investment of nearly two million euros the ethylene recovery plant has been revamped. The surplus of ethylene that doesn't react with other raw materials in the polymerization reactors has to be recovered and properly treated to be used again, so as to reduce the polymer production costs. The recovery plant is therefore essential to assure the minimization of production costs which would become unbearable in case of its malfunctioning. In fact the cost of ethylene represents more than the 80% of the final sale value of the product and the efficiency of the recovery system is fundamental to ensure competitiveness.

The unreacted gas coming from the reactors are conveyed at a pressure of about 0.3 bar to a group of reciprocating compressors which, in three subsequent compression and cooling phases, allow the recovery of hexane and butene in liquid form. The ethylene compressed to about 30 bar is then delivered to other final treatment columns to obtain a gas that can be used again in the reaction.

Object of the revamping is the compression and inter-stage condensing plant consisting of three Termomeccanica horizontal compressors working in parallel, with a capacity of 900Nm³/h each. Two of these compressors allowed to compress a variable gas flow rate from zero to approx. 1400Nm³/h, while the third one was in stand-by as back up. All compressors run at a constant speed and are equipped with a stepless pneumatic capacity control system, controlled by DCS on the basis of the suction pressure setpoint that must be

kept constant. In addition the system is equipped with a bypass between the third and the first stage with a manual valve used only during the plant start-up, before the treated gas reaches the minimum flow rate for the activation of the capacity control system.

The low reliability of the plant was mainly due to the unreliability of the three installed compressors. Also their position (very close to the control room) was an element of risk to be solved.

From the reliability point of view, the main troubles were related to the compressor valve breaking on suction and discharge side. The frequent valve plate (metallic type) failures were probably caused by the old control system which stressed the sealing element through the unloader at each compression cycle. Additional problems were related to the corrosion of the interstage elements such as heat exchangers, piping and check valves. A brief investigation on the costs for the revamping of the existing plant compared to the building up of a new one, showed that the two solutions were quite similar regarding the costs, but not to be compared as regards the results. For this reason INEOS Manufacturing decided to build up a completely new recovery plant.

4 Experiences on Termomeccanica Compressor

In the first half of 2012 the Cozzani capacity control system was chosen to meet the needs of capacity controlling of a compressor for high-density polyethylene production at the INEOS Manufacturing plant in Rosignano Solvay (LI).

The three stage machine consists of four double acting cylinders, two in the first stage, one in the second stage and one in the third stage. It works 24/7 at 460 rpm. The compressor, manufactured by Termomeccanica, runs since the 1960s, compressing ethylene with a capacity of 900Nm³/h at approximately 3.0MPa. The actual capacity depends on the changing operating conditions of the whole production plant (Figure 7).



Figure 7: Compressor with the installed capacity control system

Capacity Control System Applications and Developments

by: A.Raggi, A.Giampà, COZZANI; M.Grassi, INEOS

Prior to the capacity control system installation and during the normal operation, dedicated measurements have been carried out on the compressor. Specific pressure and temperature transmitters have been installed on the machine (Figure 8). The transmitters, connected to the data acquisition system, have allowed monitoring the main variable trends including cylinder pressures and discharge temperatures of each stage.



Figure 8: Compressor with the Cozzani portable acquisition system installed

The analysis of the operating conditions of the machine has enabled the determination of some parameters useful to optimize the capacity control system working for this specific application.

The installation, which has been completed in just two days, has required only the placement of the electrical panel, the connection of power and control signal cables to and from the plant control room, the installation of the crankshaft position sensor to detect the exact position of the pistons and the installation of the actuators on the suction valve covers.

Several tests have been carried out on the machine in order to improve the behaviour of the system in accordance with the plant needs.

The machine has been checked according to different compressor control strategies which had been evaluated during the preliminary phase of the system development. Each solution has been implemented and verified by monitoring the trend of the characteristic parameters of the machine for different plant operating conditions through the installed acquisition system.

One of the analysed capacity control methods consists in acting on the suction valve closing time only for the valves of one of the two ends of each cylinder (the opposite ends run at full load or idle condition without any modification on the valve timing).

This technique has been tested by commuting the ends controlled to the ones kept at idle or full load (Figure 9).

In this way it is possible to reduce the number of working cycles of each actuator ensuring the same efficacy in capacity controlling and improving the system reliability.

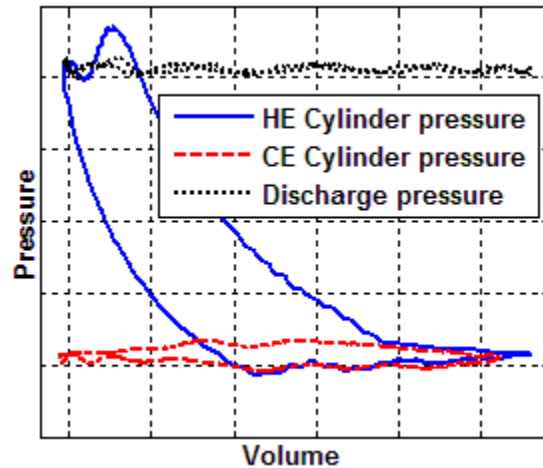


Figure 9: Pressure trends with HE controlled and CE at idle.

The same compressor has then been used to carry out further tests controlling simultaneously the suction valve closing time of all the cylinder ends (Figure 10).

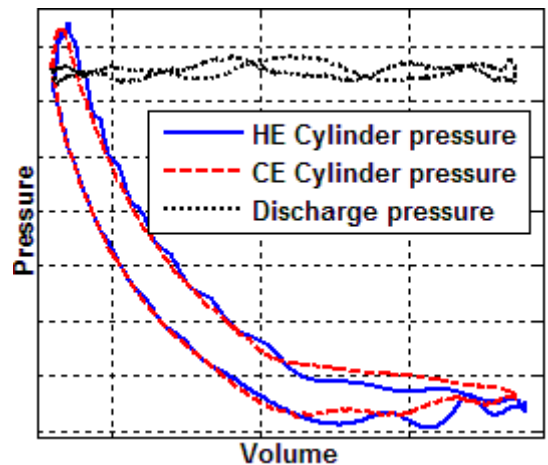


Figure 10: Pressure trends with both the ends controlled.

No modification to the system is required in order to switch from one control way to the other. The change can be operated by software without any action on the hardware.

The acquisitions of the discharge valve cover temperatures have shown that there is no dependence of the discharge temperatures from the compressor control rate (Figure 11).

Capacity Control System Applications and Developments

by: A.Raggi, A.Giampà, COZZANI; M.Grassi, INEOS

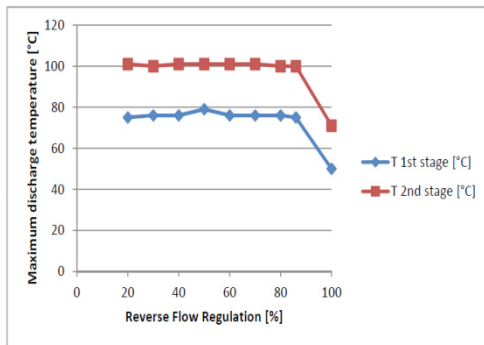


Figure 11: Discharge temperatures vs reverse flow regulation.

The system has then been refined by implementing some features permitted by the specific application and designed to improve the reliability and management of the possible faults.

During the preliminary phase, the operating conditions and the actuator configuration on the compressor have been analysed and a control strategy for every possible case of anomaly has been identified, which, thanks to the use of the actuators, allows to control the capacity correctly.

The system continuously performs diagnostic functions on each actuator. If a fault is detected, the actuator is disabled and the system keeps on operating with the other actuators. The end user can also disable an actuator by software. If in a system, for whatever reason, there are disabled actuators, the system adopts the strategies studied for that specific compressor and makes it possible to control anyway the capacity through the available actuators.

The system has been running for one year properly, controlling the compressor capacity required by the plant. After about 8000 running hours (equivalent to 235,200,000 cycles of actuations on the suction valves and consequently actuator rod displacements), valves and actuators have been inspected. All inspected parts showed very slight wear and before the compressor shut down the system was controlling correctly (Figure 12, Figure 13 and Figure 14).



Figure 12: No wear on the fingers after 8000 running hours.



Figure 13: No wear on the actuator rod after 8000 running hours.



Figure 14: Slight signs on the plate produced by the fingers which didn't have any effect on regulation.

5 New compression and interstage condensing plant

After one year of continuous running, INEOS Manufacturing plant has installed two new compressors (Figure 15). The three stage compressors have three double acting cylinders and compress ethylene up to a pressure of 3.0 MPa. Each compressor has a nominal power of 355 kW and a capacity of 1800 Nm³/h.



Figure 15: New compression and interstage condensing plant after the revamp of August 2013

Capacity Control System Applications and Developments

by: A.Raggi, A.Giampà, COZZANI; M.Grassi, INEOS

Both machines need a capacity control system. INEOS chose the Cozzani capacity control system for one compressor and the VSD method for the other. The two compressors have been equipped with taps for cylinder pressure acquisition in order to allow the installation of a data acquisition system used to analyse and to optimize the behaviour of the system and to evaluate the global behaviour of the compressors.

Both machines are monitored by the control room, which generates outputs for each of the two capacity control systems, in order to keep the first stage suction pressure constant. The compressors are equipped with bypass valves: one is automatic and can be controlled from the control room either with the inverter or with reverse flow capacity control system and the other is manhandled locally by the staff.

6 Experiences on the new controlled compressor

The Cozzani control system exchanges some signals for management and monitoring with the control room and receives the reference signal to control the capacity. The compressor (Figure 16) is controlled from the control room () by implementing a logic that generates the reference signal for the reverse flow capacity control system and for the bypass valve.



Figure 16: Compressor controlled by Cozzani control system

INEOS has developed its own logic for the plant start-up: the compressor is started when the bypass valve is closed and the capacity control system switches between the minimum capacity and the idle condition, as long as the discharge pressure reaches 10 bar. After that, the control logic changes and the stepless capacity control regulation drives the process up to the steady working condition of 3.0 MPa.

The compressor is controlled, to keep the suction pressure constant, through a PI controller, which set point is set manually from the control room.

If the suction pressure drops down under the reference value, the regulation system reacts by increasing the delay in suction valve closing (this reduces the capacity).

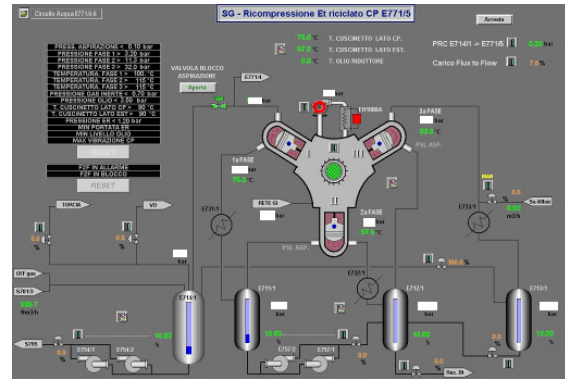


Figure 17: Control room screenshot of the compressor with reverse flow capacity control system

If, on the other hand, the suction pressure increases, the regulation system reacts by decreasing the suction valve closing delay (this increases the capacity).

The control logic (Figure 18) manages both reverse flow capacity system and automatic bypass valve: in order to guarantee minimum energy consumption, the bypass is closed from the rated capacity up to the lowest one allowed by reverse flow control system; only if the required capacity is lower than this value, the control logic starts to open the automatic bypass.

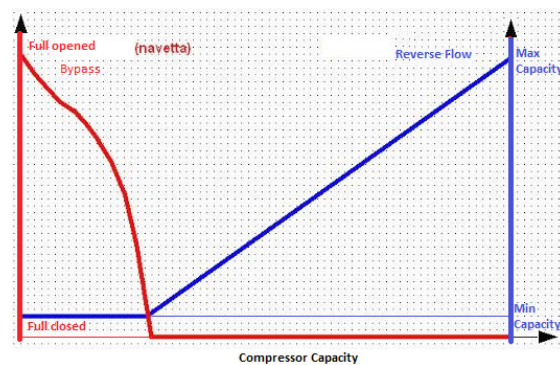


Figure 18: Compressor control logic

The compressor has been analysed to verify the correct capacity control system functionality at the different plant working conditions. The effected checks have shown the capability of efficiently controlling the suction pressure in the different plant working conditions.

Capacity Control System Applications and Developments

by: A.Raggi, A.Giampà, COZZANI; M.Grassi, INEOS

The control system effectiveness has also been verified by acquiring and observing the cylinder pressure and discharge temperature trends. The graphs confirm the correct pressure (Figure 19) and temperature (Figure 20) trends, typical of a compressor equipped with a reverse flow system.

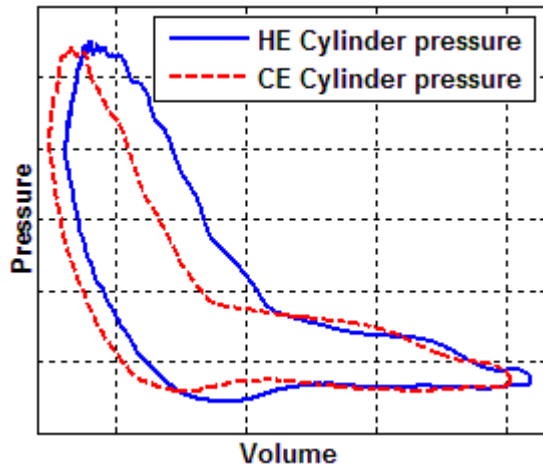


Figure 19: Cylinder pressures with reverse flow system.

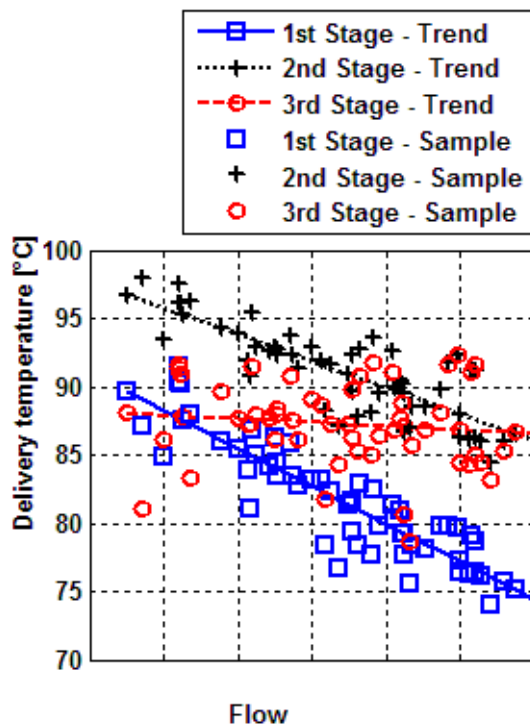


Figure 20: Discharge temperatures vs flow.

7 Experience on a new VSD controlled compressor

The control room regulates the compressor (Figure 21) flow rate:

- by means of a reference signal for the VSD to change the compressor speed
- by means of the actuators which command the unloading of part of the cylinders
- acting on the automatic bypass valve.



Figure 21: Compressor controlled by VSD

The compressor is started running at 50% of its maximum speed with the bypass valve kept close and only one cylinder end loaded for each stage. In this condition, if the first stage suction pressure decreases, the bypass valve is opened. On the contrary, if the pressure increases, the bypass valve is kept close and the compressor speed is increased.

When the speed reaches a defined threshold, the control room sets the compressor to work with both ends of each stage loaded. This produces an instantaneous gas flow doubling which introduces a discontinuity in the compressor capacity.

The non-linearity is managed controlling the first stage suction pressure. If the pressure increases, the speed is reduced and the bypass valve opened (all cylinder ends are still loaded). The control for the unloading of one cylinder end per stage is generated only if the pressure reaches a second threshold (different from the one defined before).

It is important to notice that the switching between single and double acting operation generates a discontinuity in the flow which can cause an imbalance in the plant.

Two different threshold values have been defined in order to have a minimum time interval between the two commutations. In this way, a hysteresis is created and the stability is granted during operation.

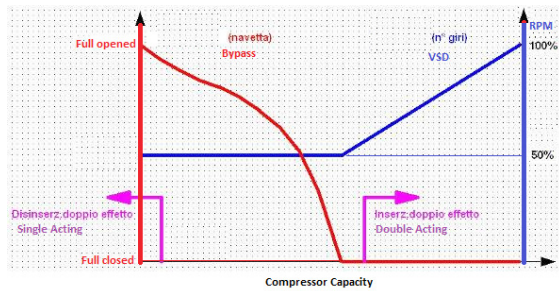


Figure 22: VSD compressor control logic

When the compressor runs as single acting, the loaded/unloaded ends are commuted every 30 running minutes in order to balance the loading time of each end.

The evolution of the main compressor parameters have been studied measuring and analyzing the machine working conditions in the different operating conditions.

The compressor working cycles have been evaluated acquiring cylinder pressures of each stage. As flow rate is controlled changing the compressor speed, the pressure has the typical trend of a full load running machine.

The pressure trend analysis (Figure 23) at several speeds allows observing the presence of pulsation during the suction or the discharge phase. This phenomenon is emphasized in particular at low speeds.

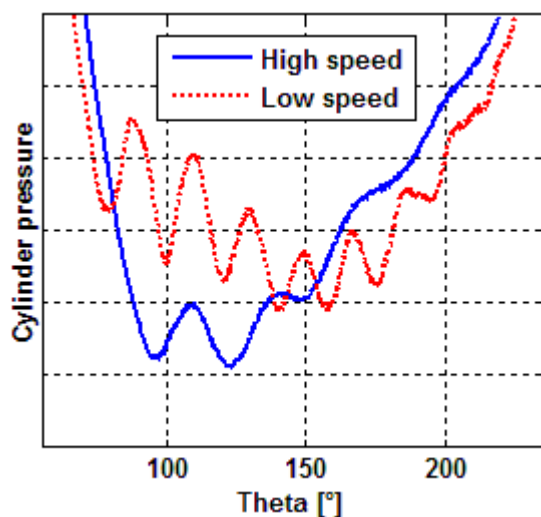


Figure 23: Pressures for different speeds.

These pressure fluctuations are typically due to valve plate (or ring) fluttering phenomena and can negatively influence valve life especially if the compressor often run at low speeds due to plant requirements.

8 Comparison between the compressor controlled by reverse flow system and the compressor controlled by VSD

Data acquisition results of both machines have been analyzed in order to compare the operating conditions, at the same flow rate, set by the two capacity control systems.

The two studied machines are identical, therefore the detected differences in power consumption and valve behavior depend on the system adopted to adjust the flow rate.

The power comparison between the two systems has been done neglecting the contribute of inverter.

The discharge temperature trends detected in the two compressors for different flow rates have been compared. The temperatures of the reverse flow system controlled compressor are higher than those of the VSD controlled machine and decrease with the flow.

This phenomenon is typical in capacity control systems based on the reverse flow method. In fact, the gas flows back from the cylinder into the suction piping with a temperature that is higher in comparison to the temperature of the gas coming from the process. This produces an increase of the average suction temperature and consequently of the discharge temperature.

The graph in Figure 24 shows the temperature trends measured on the two compressors. The temperature increase in the case of reverse flow system is anyway minimal and doesn't affect the process.

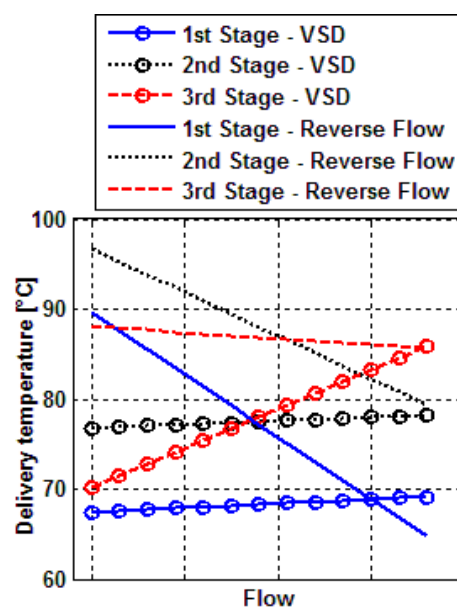


Figure 24: Temperature vs flow

Capacity Control System Applications and Developments

by: A.Raggi, A.Giampà, COZZANI; M.Grassi, INEOS

The analysis of the cylinder pressure trends (Figure 25) highlights that, at the same flow rate, the pressure fluctuations during the suction phase are significantly higher in the compressor equipped with the VSD system compared to the one equipped with the reverse flow system.

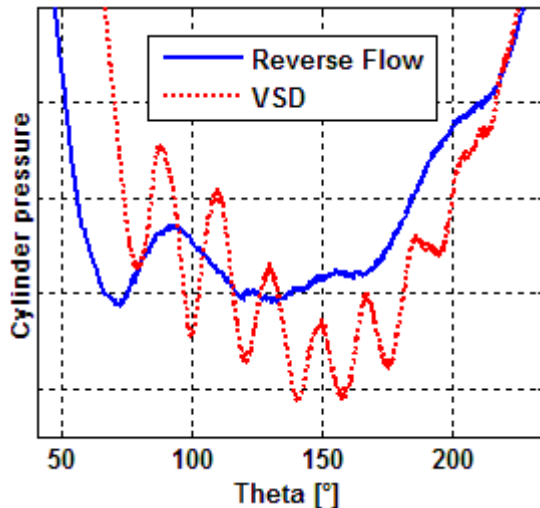


Figure 25: Cylinder pressures during suction phase

The difference is related to the control strategy types. The reverse flow system performs a flow regulation by controlling the closing instant of the suction valves. To perform this function, the valve finger is actuated in order to keep the sealing element in open position starting from the first instant of the suction phase up to the one defined by the control system. Suction occurs with the valve is forced in open condition, thus fluttering phenomena are not possible. This reduces the wear on springs and plate/rings, ensuring better reliability and longer valve life.

It must be considered that oscillations are generally emphasized when compressor speed is lower than the asynchronous motor nominal speed. The compressor set with the reverse flow system works always at the nominal speed, whereas the one controlled by an inverter generally operates at a lower speed.

In addition, the valve closure control limits the maximum sealing element speed to velocities lower than 1 m/s (Figure 26). Such values are much lower than those obtained when the suction valve is not controlled. Finally, the action of the finger type unloader during the valve closing phase assures a fully axial sealing element motion, minimizing the impact stresses (usually high when pitch and roll movements are present) and this ensures an increase of the suction valve life.

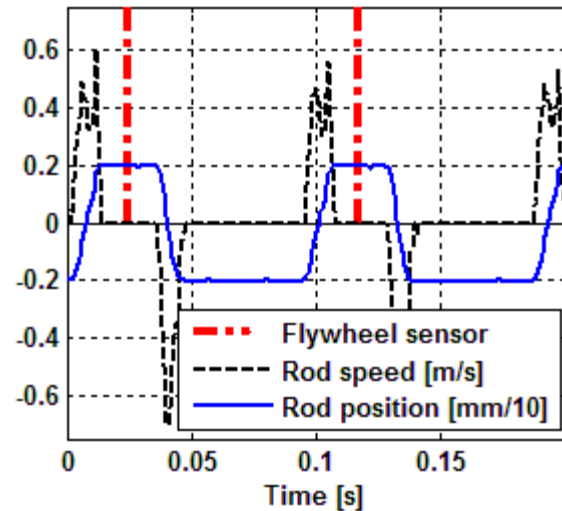


Figure 26: Actuator position and speed

Position and speed of the actuator are controlled by an algorithm implemented by an electronic board. The controller drives the actuator compensating the gas force in order to reduce the rod speed in correspondence with the passage through the middle of the stroke.

When the compressor runs at full load, the suction valve is not controlled and fluttering phenomena may occur. These phenomena are sensibly reduced when valve plate/ring position is driven by the valve capacity control system.

The behavior of the two compressors has been monitored and analyzed starting from August 2013 and the reverse flow system has shown a higher capability in capacity control (up to 15% of the nominal flow rate) in comparison to VSD (up to 50% the nominal flow rate) (Figure 27). For this reason at the operating range required by the plant the use of the bypass was not necessary for the compressor with the reverse flow system. On the contrary, the compressor with VSD was mainly run with the bypass open. The use of reverse flow system system has contributed to a decrease of power consumption.

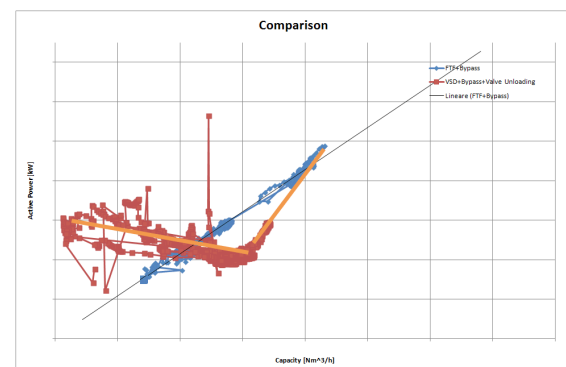


Figure 27: Power vs Capacity for both compressors (inverter power consumption is not considered)

Capacity Control System Applications and Developments

by: A.Raggi, A.Giampà, COZZANI; M.Grassi, INEOS

In the following table (Figure 28) the main characteristics of the two systems installed in the INEOS Manufacturing plant in Rosignano Solvay (LI) are summarized.

	Reverse flow system + Bypass	VSD+Bypass+ Valve Unloading
Power consumption	++	+
Temperature	-	=
Suction valve reliability	+++	--
Discharge valve reliability	=	--

+++Excellent; ++Very good; +Good; =Equal; -Bad; --Very bad

Figure 28: Comparison between the compressor controlled by reverse flow system and the compressor controlled by VSD

9 Conclusions

The capacity control in reciprocating compressors required to adapt compressor flow to process demands can be performed through different devices.

The paper shows some applications of the reverse flow capacity control system developed and patented by Dott. Ing. Mario Cozzani srl.

After several experimental tests carried out in Cozzani facility and at some of its customers, the control system has been installed on two different reciprocating compressors operating in INEOS Manufacturing plant in Rosignano Solvay (LI) – Italy used for HDPE production and running in ATEX zone.

The system has been running for one year on the first of these two compressors, properly controlling the capacity at the values required by the plant. After nearly 8000 hours of capacity controlling, valves and actuators have been inspected. All components showed very moderate wear and the system regulation capability before inspection was correctly assured.

The good results obtained by the first compressor convinced INEOS Manufacturing plant to install the system on a new machine of the same plant in August 2013. A direct comparison between two different capacity control methods has been possible thanks to a second compressor controlled through VSD and bypass. Temperatures, cylinder pressures and power consumptions in both cases have been acquired for

the same capacity and advantages/disadvantages have been evaluated.

The reverse flow system has proved a better capacity control capability (up to 15% of nominal flow rate) in comparison to VSD (up to 50% of nominal flow rate). For this reason, in the operating range required by the plant, the compressor with reverse flow system has mainly run with closed bypass while the machine with VSD has mainly run with open bypass.

This capability of the system is an important feature for plants where a wide capacity range is required because it allows power consumption saving.

In addition, the analyses on valve behaviour have confirmed that the system can reduce valve plate impact stresses and can assure its fully axial motion. This grants a better valve reliability. On the contrary, VSD system does not offer the same advantage and contributes to an increase of stress on the valves.

The expected temperature increase, typical of reverse the flow systems, was not relevant.

References

- 1 – API Standard 618 “Reciprocating Compressors for Petroleum, Chemical and Gas Industry Services”
- 2 – Workshop “ Compressor Control“, 5th EFRC-Conference 2007 Prague
- 3 –M.Schiavone, „New rotary valve Actuated by Electronic Control“, 2nd EFRC-Conference 2001 Den Haag.
- 4 – M.Schiavone, A.Raggi, “Electromechanical Actuator for Reciprocating Compressor Stepless Control”, 6th EFRC-Conference 2008, Düsseldorf.
- 5 – Matlab User’s Guide
- 6 – A. Isidori, Nonlinear Control Systems, Third Edition, Springer Verlag
- 7 – H. K. Khalil, Nonlinear Systems, Third Edition, Pearson Education International Inc.



Revamp of an Existing Reciprocating- Compressor Unit

by:

Andreas Hahn

Head of Revamp & Modernisation

NEUMAN & ESSER Deutschland GmbH & Co KG

Übach - Palenberg, Germany

andreas.hahn@neuman-esser.de

Co-author

Klaus Hoff & Gerhard Knop

**9th Conference of the EFRC
September 11th / 12th, 2014, Vienna**

Evaluation for capacity increase of an existing reciprocating compressor unit and consideration of machine directive / ATEX:

Due to new or expanded process requirements, customers are requesting compressor adaptations. Reciprocating Compressors are always “tailor made design” exactly for the described original operating conditions and capacity. Since processes and/ or product specifications demands for changed operating conditions due to new developments and requirements, it makes sense to verify the producer’s durable good, the existing compressor equipment in order to see, if it is possible to modify or revamp to make the new process conditions or capacity feasible.

A reciprocating compressor is “heavy machinery” and designed for long lifetime. Revamping offers the possibilities to use the investment of compressor even for changed requirements. Based on a case story the procedure to handle the revamp business is presented.

According to the actual legal situation in Europe, for significant compressor modifications it is necessary to follow the regulations by machine directive and ATEX (for hazardous installations). Also the procedures for an ATEX declaration are presented, to demonstrate the necessary investigations for compressor and accessories. Depending on the kind of modification, the installation of a revamp and the operation of such modified equipment is allowed only with valid original equipment manufacturer (OEM) declaration according to machine directive (CE) and ATEX!

Revamp of an Existing Reciprocating-Compressor Unit

by: *Andreas Hahn, Klaus Hoff and Gerhard Knop, NEUMAN & ESSER*

1 Introduction

In 2003 NEA Group delivered a reciprocating compressor unit size 2 SZL 320H to a refinery in East-Europe for a desulphurisation process, compressing hydrogen from 28 bar suction- up to 85 bar discharge pressure. The reciprocating compressor is a 2-crank, horizontal, 2 cylinder stages, double acting, lubricated service machine as principally shown at Figure No. 1. with a nominal rod force of 530 kN allowable rod load.

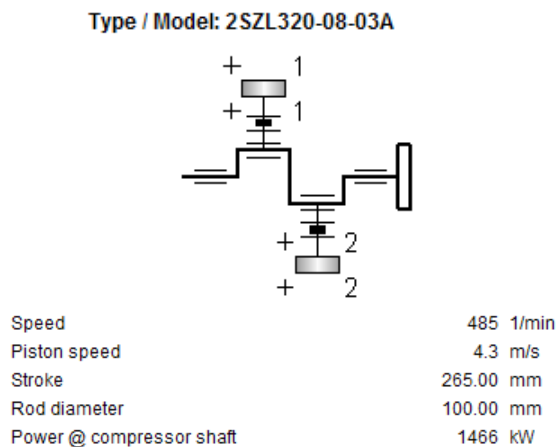


Figure No. 1

Figure 1: 2- crank compressor with 2 stages and flywheel, base data for the original supplied compressor unit

The compressor is direct driven by an electric motor rigidly coupled, nominal driver power of 1.700 kW. The capacity at original design was approx. 33.000 Nm³/h at a suction temperature of -5 °C.

The NEA scope for the whole compressor unit was inclusive the pulsation vessels (suction- and discharge side each stage) interstage cooler, interstage separator up to check valve last stage.

After only 5 years of successful operation, the demand on hydrogen gas increased due to clean fuels requirements and the refinery management had to react on the market requirements.

An engineering contractor was assigned by customer to prepare detailed specifications based on the new required operating conditions and to find the best solution to fulfil the new requirement. The job definition was to reach the required capacities even at worst operating conditions.

2 Verification of Compressor feasibility

2.1 As-built situation and pre-check

First of all the existing reciprocating compressor is re-calculated according to the original- / as built situation with the compressor design tool according to the actual state-of-the-art. It is mandatory to match the measured operating data. That way it is verified that the compressor fulfils the designated process conditions without deviations to avoid general mechanical or performance problems. The main compressor characteristics in dimensions, materials weights and loads must be checked to have the basis for further calculations.

After that a calculation is made with new operating conditions, based on the existing compressor design.

For this case story the new required capacity at new defined operating conditions could not be reached with the existing compressor.

In a first step there is a pre-check in order to see if an adaptation of the compressor for the new operating conditions is principally possible!

Not only the compressor itself has to be modified, but also the accessories around need to be considered for a modification.

With a positive pre-check result meaning there are one or more technically feasible possibilities to reach the requirements, the possibility of a revamp project is given.

There are different possibilities to increase the capacity e.g. by compressor speed, by compressor stroke, by cylinder bore. These have to be checked to optimise the revamp measures to a minimum.

2.2 Preparation of an engineer bid

The detailed verification for a compressor revamp is done in form of an engineering study. In addition to the job specifications the compressor characteristics and details have to be checked based on existing documentation. The accessories also need to be checked for the new application. To optimise the revamp solution and to prepare a revamp proposal, different possibilities have to be evaluated that will finally result in a tailor made technically safe and economically responsible solution.

Revamp of an Existing Reciprocating-Compressor Unit

by: Andreas Hahn, Klaus Hoff and Gerhard Knop, NEUMAN & ESSER

2.3 Feasibility study and revamp possibilities

2.3.1 Evaluation Matrix

To fulfill the customer’s requirements the best option of compressor modification has to be evaluated. Therefore all sorts of technically feasible possibilities are selected and prepared in an “Evaluation – Matrix”, see Figure No. 2. The “Evaluation – Matrix” shows on the one side the different technical solutions for the compressor revamp and on the other side different project features. According to the customer’s ideas the project features are benchmarked with different quantifiers on a scale 1 - 10. Position by position the different technical revamp possibilities get evaluated by multiplying the quantifier of each project feature by the evaluation factor (ok-better-best) of the technical revamp possibility. So in the end by scoring the points, the best solution for the revamp is evaluated.

Quantifier	Project features	Revamp possib. 1	Revamp possib. 2
(1 ---- 10)	Costs	(...)	(...)
(1 ---- 10)	Efficiency	(ok-	(...)
(1 ---- 10)	Reliability	better-	(times
(1 ---- 10)	Availability	best)	quantifier)
(1 ---- 10)	Safety	(...)	(...)
(1 ---- 10)	Vibrations	(...)	(...)
(1 ---- 10)	Emissions	(...)	(...)
(1 ---- 10)	...	(...)	(...)
	SCORE		

Figure No. 2

Figure 2: NEA Revamp Evaluation Matrix

According to the scoring the optimum revamp solution can be selected and used for the following detail verification.

2.3.2 Thermodynamics and compressor calculation

The detailed verification starts by implementing the specific compressor details regarding the loads, dimensions, weights into the NEA compressor design tool KO³ (Kompressor-Optimierung Version 3). Figure No. 3 represents the general input mask for reciprocating compressors base data. There the current and the old NEA compressor sizes are installed. According to internal up-upgrades to different compressors, the year of construction is essential for the lay out and the allowable loads. For non-NEA Compressors a similar NEA compressor size is selected according to analogies in the main compressor characters. The load limits according to

the existing compressor have to be adjusted and the main characters for the existing compressor have to be cross-checked and adapted.

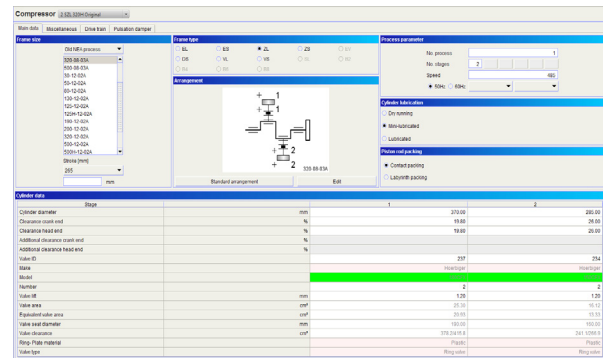


Figure No. 3

Figure 3: Input mask for compressor data NEA KO³

The new case data for future operation have to be added to the calculation software. To run the thermodynamic calculation the gas analysis, suction pressure, suction temperature, discharge pressure and required capacity must be known for each process or case. Figure No. 4 represents the input mask for operating data.

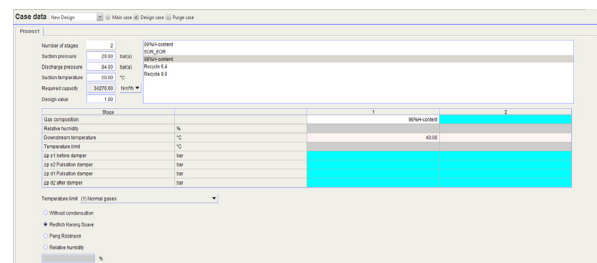


Figure No. 4

Figure 4: Input mask for case data NEA KO³

To match the required capacity, it is necessary to vary the compressor design figures according to the selected revamp possibility.

To increase the capacity of a reciprocating compressor in principle the following possibilities in general are possible, but have to be evaluated according to the actual compressor feasibilities.

- Possibility 1: Increase of suction pressure
- Suction pressure could not be increased due to process conditions

Revamp of an Existing Reciprocating-Compressor Unit

by: *Andreas Hahn, Klaus Hoff and Gerhard Knop, NEUMAN & ESSER*

- Possibility 2: Speed increase
 - Because of the direct coupled drive the next asynchronous motor speed is not feasible, since the allowable medium piston speed is exceeded! Also a speed increase always means a certain risk to vibrations and additional loads for foundation
- Possibility 3: increase of cylinder diameter
 - Due to the operating conditions and allowable rod loads, it is not possible to only increase cylinder \varnothing due to exceeded rod loads.
- Possibility 4: increase of compressor stroke
 - + Stroke increase was possible due to the design of driving mechanism, also without modifying the actual cylinder – \varnothing 's!
- Possibility 5: a combination of the different alternatives
 - Due to the required capacity, it is sufficient to realize by new stroke only. A combination of different alternatives just would increase costs.
- Possibility 6: Installation of an additional compressor in parallel
 - There is no additional space to install another compressor.

So for this case story the conclusion was to install a new compressor crankshaft with enlarged stroke to fulfill customer requirements within the allowable compressor limits. The piston rods and piston had to be replaced due the running length at existing cylinders. The advantage is that the cylinders do not change; the general compressor arrangement can remain.

2.3.3 Verification of compressor valves

Each variation in process condition or compressor characters has an impact on compressor valves, also here! After having the detail calculation for compressor layout the valve design needs to be confirmed. Since the valve dynamics have a major influence on compressor performance, the valve check is mandatory to confirm the compressor lay out.

Typically, a slight change in the stroke of the compressor doesn't influence the valve dynamics drastically. However, it was reported that the compressor suffered from valve problems and lack of delivery rate. The assumption was that oil sticking effects could be responsible for this problem. Therefore, a valve dynamics calculation was done. The valve dynamics tool can also be responsible for oil sticking effects. Figure 5 shows the result of this calculation for the original spring design of the valve.

It is immediately visible that a late closing of the suction valve due to sticking at the valve guard takes place. This effect leads to a reduction of flow and to higher impact velocities. The effect can be remedied by stronger spring design of the existing valve.

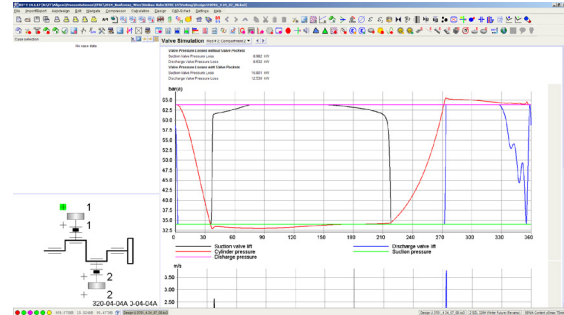


Figure No. 5

Figure 5: Valve dynamics of 1st stage with original valve spring design

A new spring design was done together with the valve manufacturer. Figure 6 shows the valve dynamics with the new, stronger valve spring design. The suction valve starts to close earlier due to the stronger springs. The valve is close at bottom dead centre. The delivery rate is correct.

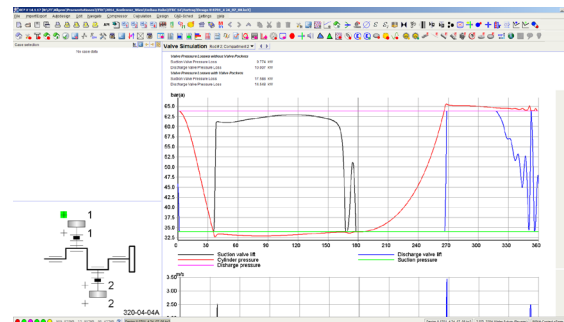


Figure No. 6

Figure 6: Valve dynamics of 1st stage with modified valve spring design

In the end the valve size could remain only the internals had to be adapted according to the new required operating conditions.

2.3.4 Mechanical properties, rod loads, bearing calculation

After the thermodynamics and valves are confirmed, the mechanical properties for compressor must be verified. For verification of the mechanical properties the safety relief valve settings of each stage are an important fact for compressor lay out, because the set pressures determine the max. rod forces and static design pressures!

Revamp of an Existing Reciprocating-Compressor Unit

by: *Andreas Hahn, Klaus Hoff and Gerhard Knop, NEUMAN & ESSER*

For compressor lay-out/ verification the mass- and gas forces and the combined forces (= rod forces) have to be considered. All kind of forces have to be verified to be inside the allowable loading limits.

Typically, this kind of revamp increases the rod loading of the compressor given. Therefore, the standard procedure is to examine the compressor by means of the compressor design program. All compressor parts loaded by the rod load need to be reviewed in terms of possible overloading.

All critical design cases planned to be used after the revamp must be considered and examined carefully. The design program KO³ used for that examining gives a direct impression of the load situation for the given case by a bar chart diagram per rod.

For reciprocating compressors there are sensitive construction groups that have to be checked separately according to the operating conditions.

The most sensitive compressor construction groups are listed at the bar chart diagram for each rod as shown in the following figures. Figure No. 7. indicates the different loads in bar-charts for each calculation for rod no. 1 and Figure No. 8 accordingly for rod no.2.

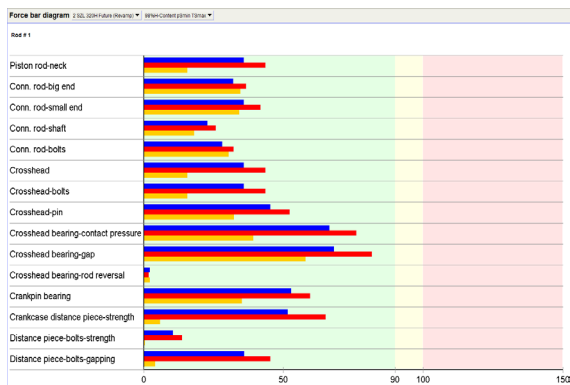


Figure No. 7

Figure 7: Bar-chart for loads on sensitive compressor construction groups "Rod 1"

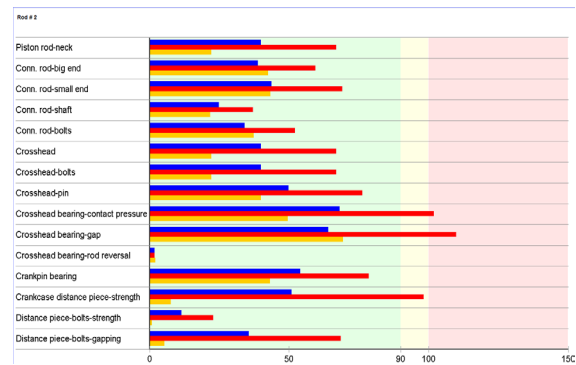


Figure No. 8

Figure 8: Bar-chart for loads on sensitive compressor construction groups "Rod 2"

At the KO³ calculation the max allowable loads (100%) are already given for NEA compressors. To find a reliable result even for non-NEA compressors, the analogies and the specific values for dimensions, weights and materials need to be checked and the rod load limits need to be adapted.

The yellow bars represent the load utilization of the individual components in terms of the loading at idle run, meaning the compression chambers are just loaded by the suction pressure of the stage. This is more or less the inertia load acting on the components. Typically, this load is not critical for low to mean speed compressors.

The blue bars represent the load utilization of the individual components in terms of the loading at design condition. The compressor parts are loaded by the gas load due to design suction and discharge pressure and by the inertia load.

The red bars represent the load utilization of the individual components in terms of the loading at pressure safety valve (PSV) condition on discharge side.

Another aspect are the different situations for crosshead-pin bearings at full load and part load operation. It is required that there is always sufficient rod reversal available.

Typically, the crosshead bearing is one of the most critical components in a reciprocating compressor. This bearing can fail due to too high hydrodynamic oil pressure, too small minimum oil film thickness or too less rod load reversal. The design program accommodates this fact by checking these three failure scenarios individually. As one can see, the crosshead bearing seems to be slightly overloaded at PSV-condition in terms of the minimum oil film thickness for this revamp. The equations behind the load utilization of the crosshead bearing are derived

Revamp of an Existing Reciprocating-Compressor Unit

by: *Andreas Hahn, Klaus Hoff and Gerhard Knop, NEUMAN & ESSER*

from a parameter study done with the hydrodynamic bearing calculation tool developed some years ago¹. The safety margins included in these equations are conservatively chosen. As long as the load utilization of the crosshead bearing is below 100% the design is definitely on the safe side. On the other side, this doesn't mean that the bearing is overloaded when the load utilization is above 100%. It just requires a more detailed investigation.

For this, an EHD-tool (Elasto-Hydrodynamic) developed by K. Hoff and E. Steinbusch is available to assess the bearing hydrodynamics. This EHD-tool is an integral part of the compressor design program and can be applied by all trained users. The EHD calculation time for the bearing takes only a few seconds on a typical notebook. The assessment of the results is also very simple since one just has to compare the max hydrodynamic pressure and the min hydrodynamic film thickness with the critical reference values.

Figure No. 9 shows a cross sectional view of the crosshead bearing's elasto-hydrodynamic load situation under max connecting rod tension load. Both the small end eye bearing and the banjo crosshead pin are strongly deformed under the hydrodynamic pressure. The deformation is so strong that the real hydrodynamic pressure needs to be applied for its calculation.

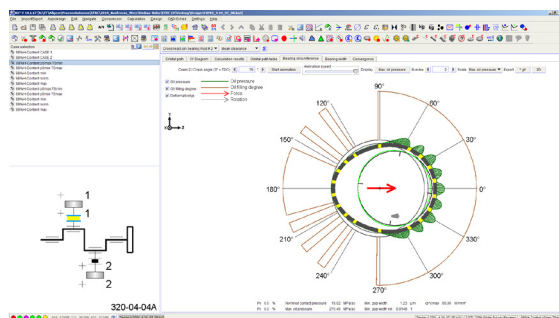


Figure No. 9

Figure 9: View of the elasto-hydrodynamic load situation under max tension load

A simple representation of the rod loading by a single load would simplify the calculation process extremely since the deformation would become independent from the hydrodynamic pressure. Unfortunately, this simple representation is not possible because it would yield such a dramatic deformation that interference between bearing and pin would occur. The mathematical calculation process becomes therefore more complex since the resilience of the structure needs to be implicitly introduced in the hydrodynamic solver.

As one can easily see from figure 9, the deformation reduces the hydrodynamic peak pressure compared to a rigid structure since a more equally distributed hydrodynamic pressure takes place along the loaded side of the bearing. Consequently, the min oil film thickness also becomes less critical.

The analogous elasto-hydrodynamic load situation under max connecting rod compression load is given in figure 10.

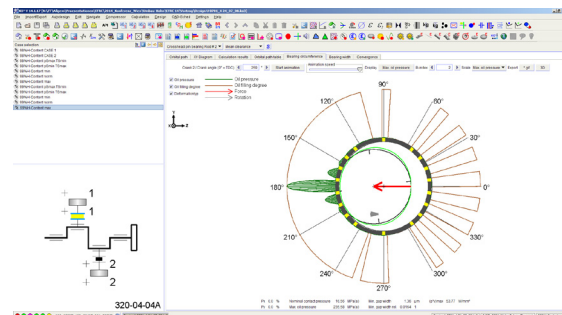


Figure Nr. 10

Figure 10: View of the elasto-hydrodynamic load situation under max compression load

Only a slight deformation of the bearing takes place. Consequently, the hydrodynamic pressure build-up is concentrated on the central load area between the corresponding oil supply grooves. This is the reason why, even under the condition of identical compression and tension rod load, the compression side of the crosshead pin bearing is much more critical than the tension side. Unfortunately, the compression load of a reciprocating compressor is typically higher than the tension load.

The EHD-analysis of the crosshead bearing in terms of hydrodynamic pressure and min oil film thickness revealed no critical bearing load for this revamp.

2.3.5 Crankshaft Strength

Increasing the stroke of a crankshaft apparently produces higher stress levels which need to be checked in terms of fatigue strength.

The crankshaft load is generally dominated by bending and/or torsion. Their quantification can be carried out by making use of analytical bar models yielding nominal stress levels. Prospective critical locations are the fillets at the crank webs. The evaluation of the stress concentration there is the decisive task in this context. Due to the permanently varying rod load during a crank shaft revolution, the maximum stress in these fillets changes its circumferential position and magnitude all the time.

This effect can be best quantified by utilizing finite element analysis (FEA) models. They are used to

Revamp of an Existing Reciprocating-Compressor Unit

by: *Andreas Hahn, Klaus Hoff and Gerhard Knop, NEUMAN & ESSER*

adjust the local stress situation of the FEA with the analytical bar model by means of stress concentration factors (SCF). Fig. 11 shows an example of such a model.

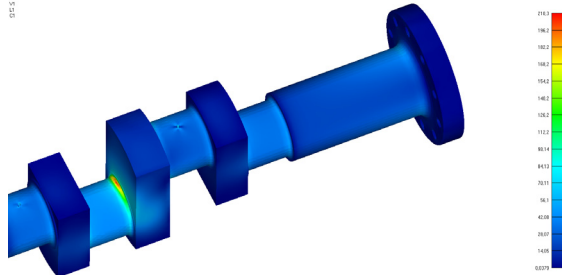


Figure Nr. 11

Figure 11: FEA Stress plot of the crankshaft

Once a sufficient amount of FEA simulations has been performed, their results can be used to identify and adjust analytical approaches which produce approximately the same results as the FEA. That way, the individual crankshaft strength for a given job can be verified most accurately and quickly in the compressor design program without the need for intensive FEA studies. Fig. 12 shows the model of the revamped compressor.

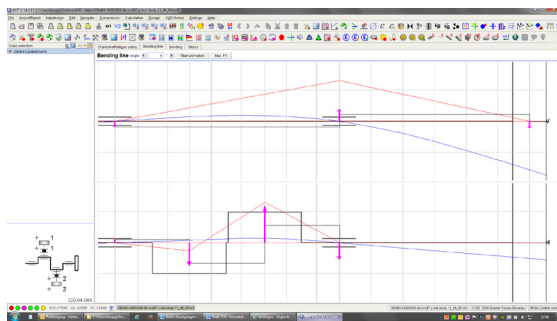


Figure Nr. 12

Figure 12: Bar model of the crankshaft

The compressor crankshaft in question was modified with an increased stroke. The torsional load at the most critical location had been very low before the revamp and hardly increased afterwards. The bending load on the other hand is more dominant in this application and rose approximately proportional with the stroke increase. Nevertheless, it remained still moderate and left a robust shaft that raised no necessities for any further design adjustment like using a higher grade material, increasing the fillet radii or even the pin diameter.

3 Verification of Accessories

3.1 Main motor

Each compressor upgrade also effects a verification of the accessories. The new required compressor power must be covered by the existing motor power, or the existing motor must be increased, too. The nowadays actual API 618 Rev.5 requires to have sufficient motor power for cases each stage against the safety relief valve set pressure + 5% safety margin.

3.2 Torsion analysis

For direct coupled compressors it is mandatory to run a new torsion analysis. Only by the new torsion analysis the components of the drive train can be verified and avoid torsion vibrations and compressor damage.

At the looked-at-case, because of its short length, the compressor crankshaft is only very little sensitive to torsional vibrations. This does not significantly change after increasing the stroke.

Between compressor and induction motor however, a rather large flywheel is clamped with two rigid flanges which makes the drive train susceptible to torsional vibrations. The large flywheel had to be installed with the original machinery in order to protect the electric power supply grid against the current fluctuations which are inherent in every motor driving a reciprocating compressor. So the system we have is basically a two-mass oscillator capable of torsion within the motor shaft section between flywheel and rotor core. The natural frequency of this is not affected by a changed crank shaft stroke. It is only the torsional excitation that rises to some extent.

Therefore the torsional vibration simulation had to be rechecked for the revamp and everything had been found to be within acceptable levels.

3.3 Gascoolers, Vessels, Piping

Is there an increase in capacity and power, the coolers have to be verified for the new operating conditions. These detail checks need to be done by the Original-Equipment-Manufacturer (OEM) for the heat exchangers. Based on utilities and design limits the equipment is re-calculated for the new operating conditions.

Further there is an effect for the piping and vessels. For a new flow or new operating conditions the sizing and ratings need to be confirmed. To avoid unallowable high pulsation there is a damper check performed based on the existing vessel design and

Revamp of an Existing Reciprocating-Compressor Unit

by: *Andreas Hahn, Klaus Hoff and Gerhard Knop, NEUMAN & ESSER*

according to the limits of API 618. The damper check can be run with the NEA KO³ calculation also and considers the new compressor layout overall processes and operating cases. The result allows a first information as to whether the existing vessels are still sufficient, critical or too small. Figure No. 13 shows the KO³ print for visual results of damper check 1st stage suction.

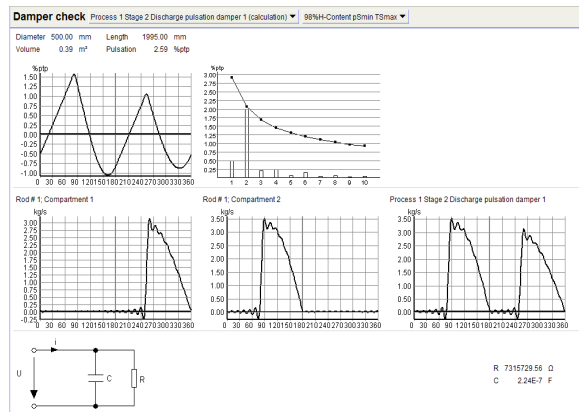


Figure No. 13

Figure 13: Damper check data by KO³

The NEA damper check by KO³ software just gives preliminary results for the expected pulsations after the revamp. The KO³ software gives a proposal for pulsation damper design as indicated in Figure No. 14 for pulsation damper 1st stage suction. The main dimensions (\varnothing x length), the volume, the nozzles size and rating, expected pulsation; gas and process data and expected pressure losses are informed..

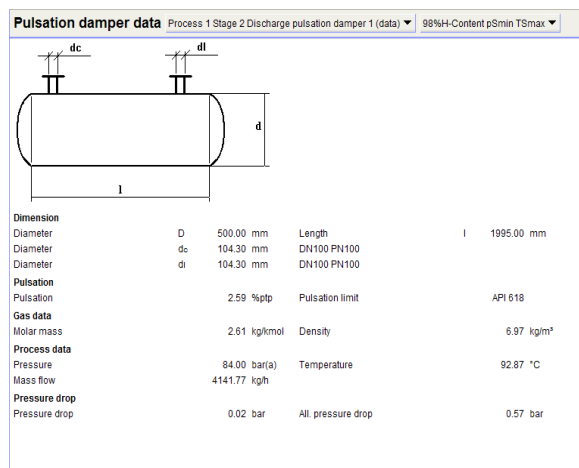


Figure No. 14

Figure 14: Pulsation damper data by KO³

Finally for a detailed verification and for giving a warranty for vibrations according to the API 618 regulation and NEA workshop standards, it is necessary to run a pulsation study and mechanical response study additionally

3.4 Pulsation study

A pulsation and mechanical study has been carried out also for the original compressor design in our case. The modifications on compressor design and thermodynamic operating conditions were communicated to the supplier to re-investigate and validate the system.

For the pulsation study the cases to be investigated are single- and parallel operation, the different operating conditions at normal situation (100%) capacity and also for the capacity control range between 100 – 15% by stepless suction valve unloading. According to experiences with synchronized suction valve unloading, the critical point for pulsation volume design is at approx. 70% capacity.

In case the study requires doing it, the modifications to be applied to the system to satisfy acceptable operations by order of preference are the following:

- Modification of restriction orifices
- Modification of existing piping supports
- Modification of pulsation dampers

In our case story the calculation results showed up with too high pulsation levels as well as unbalanced forces at pulsation vessel suction side 1st stage for the existing vessel volume. Therefore a new acoustic filter has to be considered with increased volume and dimensions. Also the steel construction to support the new vessel and new orifices for the line side have to be considered.

Due to CAD tools according to new machine business the verification for general arrangement of the new equipment, preparation of P&ID, list of instruments and creation of a logic plan could be handled and a solution out of one hand could be presented.

4 Machine Directive / ATEX

According to the actual effective machine directive 2006/42/EC and directive 94/9/EC (ATEX) it is essential in case of a substantial modification, that there is a manufacturer declaration for the modified equipment.

The operating company has to ensure a conformity according to machine directive and ATEX for the whole operation time. This is also mandatory for used machines which are substantially modified in case of a Revamp.

Revamp of an Existing Reciprocating-Compressor Unit

by: *Andreas Hahn, Klaus Hoff and Gerhard Knop, NEUMAN & ESSER*

ATEX does not apply for repairs without new features or other modifications or for spare parts intended to replace a defective or worn out part.

In our case story there is a capacity increase within the original operating conditions by installation of a new crankshaft with an enlarged stroke. The crankcase and the other internals of the driving mechanism remain. Also the cylinders 1st and 2nd stages of the compressor remain. To realise the enlarged stroke there are new piston and piston rods designed. The other compressor characters as there are speed and cylinder bore remain identical as at original design.

To run the compressor under high suction pressure and low suction temperature the driver has to be renewed.

The oil system, the control system and the other equipment was certified already according to ATEX when the compressor unit was installed in year 2004 and did not need to be modified.

The distributed control system (DCS) and the compressor instrumentation for safety control could remain, only set points at the instrument list have to be adapted.

To reflect if a substantial modification need to be considered, the following questions have to be checked carefully:

- Are there changes in function or operating conditions for the compressor unit?
- Are all the hazards covered by actual risk analysis?
- Or do new risks or new hazardous events exist after the revamp?
- What about effects or incidence rate due to existing hazards?

The process presented in Figure No. 15 also shows the evaluation for OEM and operating company to check if a substantial modification is on hand.

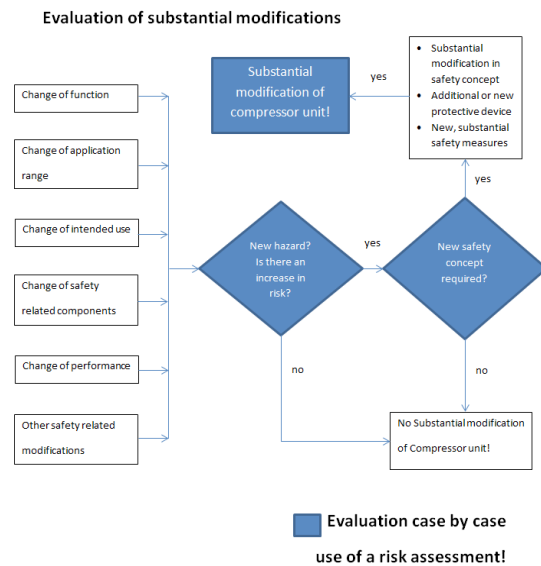


Figure No. 15

Figure 15: Evaluation process of substantial modifications

4.1 Evaluation by risk analysis

For reciprocating compressor units NEA Group has generated a spark hazard analysis and risk assessment. If there is a substantial modification on hand by a revamp, the assessment is performed and measures are indicated. When there is a full documentation for compressor data, materials and design available, it is possible to prepare a declaration according to machine directive and ATEX. The reciprocating compressors can be confirmed for CE Ex II 2G T3.

4.2 Results of analysis

For the described revamp there are

- no new hazardous events versus the previous situation
- none of the existing hazardous events increased, the new stroke is re-calculated and loads are checked by OEM. This means the existing safety protections would have been sufficient even after the revamp
- beside compressor lay – out all existing hazardous events covered by the existing risk – analysis e.g.:
 - incident rates and effects of pressure and temperature shift
 - valve failures
 - pressure packings
 - rod-reversals
 - crosshead and bearings
 - drive components
 - oil pump / oil system
 - compressor function and safety system is identical

Revamp of an Existing Reciprocating-Compressor Unit

by: *Andreas Hahn, Klaus Hoff and Gerhard Knop, NEUMAN & ESSER*

as before the revamp

- boundaries and interaction with bordering systems
- compressors remains within the same operational environment, that means classification and configuration of hazardous areas do not change

This risk evaluation is mandatory for each revamp project and ***must be performed*** during the revamp project phase! The results of the evaluation must be documented, for a proof.

5 Management of Product Safety

For Revamp and modernisation a special management for product safety is necessary. It must be assured by OEM or an expert authority that the considered revamp measures are a safe solution and the way how the revamp is selected and designed as well as the risk analysis must be documented in detail.

For major revamp job or modification, the advised product process just as for new compressor design need to be followed. This means procedure of all scheduled quality control instructions for feasibility study, risk assessment design engineering, and fabrication.

For smaller jobs or refurbishments technical job description, risk assessment (in case of substantial modifications), technical reports, and 4-eyes-principle are necessary.

In both cases a systematic and controlled preparation of technical documentation is mandatory.

At the end of a revamp job it is necessary:

- to receive a manufacturer declaration of conformity for substantial modifications as defined by machine directive 2006/42/EC and directive 94/9/EC (ATEX).
- or to have a detailed technical report giving the reason if there is no substantial modification on hand.

6 Conclusion

Revamp and modernisation is a special product that needs special handling. Due to the fact that there are a lot of reciprocating compressors running for decades and even can run for decades more, it is a good opportunity to make them fit for the nowadays technical specifications and process conditions by revamping. With the right technical support by a compressor OEM, the reciprocating compressor can be prepared for long term operation and matching the demands of the operator company.

From the inquiry followed by a feasibility study, the possibilities to modify reciprocating compressors are evaluated. The revamp proposal will show up a technically safe and economically reasonable solution to use a high part of the existing resources. Beside the compressor and the compressor equipment itself, also the operator infrastructure like foundation, compressor house, cable routing, pipe racks, etc. can be further used.

According to the nowadays law regulations of machine directive 2006/42/EC and directive 94/9/EC (ATEX) the handling for new machine business and for revamps is strictly advised. A substantial modification does not automatically exist for major revamps, but can arise on the other hand even at smaller revamps if the revamp will guide to changed risk assessments. Only an OEM or an expert authority with sophisticated engineering knowledge for reciprocating compressors can provide the necessary manufacturer declaration or documentation to bring the operator company in the position to receive a permission to start the revamped unit into operation.

References

Hydrodynamic calculation method for crosshead pin bearings especially under less rod load reversal loading,
by Klaus Hoff and Egidius Steinbusch
6th Conference of the EFRC, October 28th/29th, 2008
Düsseldorf, Germany



Challenges of Oxygen Reciprocating Piston Compressors

by:

Wolfgang Grillhofer

Rotating Machinery Expert

Large Industries European Platform

Air Liquide, Austria

Wolfgang.grillhofer@airliquide.com

**9th Conference of the EFRC
September 11th / 12th, 2014, Vienna**

Abstract:

Special concern must be taken for oxygen compressors from safety point of view. Besides the use of materials with proven high oxygen compatibility it is necessary to avoid possible sources for ignition as heat and friction for example. This concerns the part design as well as the correct planning and performance of maintenance activities.

In practice part failures or malfunctions were observed on different machine types. The concerned parts were pistons, piston rods and packings. All these parts are critical parts as they are in contact with oxygen or could be in contact with oxygen and thus part failures can easily result in heat production due to e.g. broken parts. However, re-design is not the answer to each damage as the Air Liquide experience has shown. There is also a high impact of the compressor operation and the applied maintenance strategy. It must be understood what are the consequences of auxiliary system malfunctions and not reliable performed maintenance.

Challenges of Oxygen Reciprocating Piston Compressors

by: Wolfgang Grillhofer, Air Liquide

1 Introduction

Air Liquide is operating oxygen plants which do deliver the product at a lower pressure than required by the customer or the pipeline network. In such cases compressors are used in order to boost the oxygen pressure to the required level.

Depending on the specified volume flow and the discharge pressure centrifugal turbo compressors or reciprocating piston compressors are in use. As the risk for a fire with compressed oxygen is evident, such machines must be designed according agreed standards and also the installation must fulfil some special requirements.

Air Liquides experience in operating oxygen reciprocating piston and turbo compressors is more than 50 years and always safety was the biggest concern. Today around 220 oxygen compressors are installed and used for production all over the world. State of the art protection installation as e.g. safety barriers and safety procedures are in place in order to ensure best protection for the operating personal.

This paper summarizes some selected experiences Air Liquide has done in the past with oxygen reciprocating piston compressors concerning part damages and wear. The consequences will be described and respective conclusions and improvement actions will be summarized.

Only in one of the following cases the damage was linked to a fire. But because of the risk of safety issues with machines compressing oxygen it is of high importance to analyze every damage experienced in the past. Target of such assessments of cases without fires is to evaluate if respective failure modes could have the potential for developing an oxygen fire. If yes, it would be necessary to agree on additional actions in order to exclude or minimize the risk of repeating such damages also again to lower the failure rate.

2 Pistons

The oxygen reciprocating piston compressors which are installed in Air Liquide plants can be categorized in two groups from piston design point of view. The first group of compressors has vertical cylinders and is using pistons without piston rings i.e. labyrinth type with cylinder liner integral to the cylinder. The other group summarizes all compressors equipped with pistons which have piston rings.

In this section two cases are documented which describe piston damages of both design. Most probable causes are summarized and identified possible improvement actions are discussed.

2.1 Pistons without Piston Rings

The first case concerns a piston of a three stage compressor with four vertical cylinders and which has pistons without piston rings. The pistons have some grooves on the circumference which are creating small vortexes during the piston reciprocating movement. The effect of these vortexes is strong enough to maintain certain tightness between the moving piston and the cylinder wall, refer also to figure 1.

An advantage from this design is that during normal operating conditions there is no contact between the moving piston and the cylinder wall. Thus no additional heat due to friction is created. On the other hand the internal leakage over the piston is higher compared to the design using piston rings.

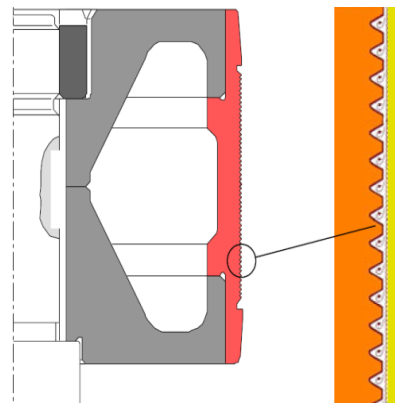


Figure 1: Principle Design of used Piston without Piston Rings

What can be also seen in figure 1 is that pistons of this design are made of three main parts. One disc at the head end and one disc at the crank end are clamping the circumference part with the grooves. All three parts are fixed on the piston rod by applying a piston nut at the end.

During a major overhaul the pistons of all cylinders were disassembled and checked. It was found that one first stage piston had two big cracks on the circumference part of the piston with the second crack on the opposite side of the first one. Both cracks showed a development parallel to the piston rod axes. As can be seen also in figure 2 there were signs that the piston touched the cylinder wall at the crack sections.

Challenges of Oxygen Reciprocating Piston Compressors

by: Wolfgang Grillhofer, Air Liquide



Figure 2: Damaged Labyrinth Piston

It is difficult to say if the cracks developed because the piston touched the cylinder or if the contact between the piston and cylinder wall was a consequence of the crack development.

As most probable causes two possibilities were identified:

- The clamping forces necessary for reliable fixing of the piston parts during all operation conditions were too low.
- Insufficient cooling, overheating.

There is no ranking between the above mentioned possibilities. Each of these possible causes can be the root cause of the experienced piston damage.

In order to maintain respective force to clamp all the three parts together it is necessary to realize a defined head end to crank end piston disc distance. Before piston re-assembly the two discs are put together on the piston rod without the circumferential piston part. Then this distance is measured at different points, refer to figure 3. It is necessary that this distance is shorter in each point compared to the circumferential piston inner part length and thus not exceeds the specified maximum value. When now this distance is within the specified range a certain pre-tension is maintained when the discs are clamped together by respective piston nut. For this discussed case it cannot be excluded that this pre-tension was relaxed or was not enough for the bigger first stage piston which has the larger diameter.



Figure 3: Piston Pre-Tension Measurement

Another impact to be considered in this case is possible overheating. A too high gas temperature due to insufficient gas cooling in respective inter stage cooling could be the reason for a clearance reduction. This can happen also for the first stage as there is a recycle line after the first stage discharge and inter stage cooler back to the suction side. A second bypass line is foreseen after the last stage and the third stage cooler. It is common to use especially the bypass line after the first stage for volume flow regulation.

After checking the cooling water circuit it turned out that there was mud in the cylinder cooling duct. For this design the cylinder cooling is mainly to maintain a certain cylinder wall temperature which is essential to keep the inner diameter change within specified limits. When there is insufficient cylinder cooling it is thinkable that the clearance between the piston and the cylinder wall changed. In case of an increased piston to cylinder clearance the internal gas recycling between the piston crank end and the piston head end will further increase the cylinder temperature.

In this case the described piston damage did not result in an oxygen fire. The piston parts are made of materials complying with EIGA rules, i.e. they have high oxygen compatibility. However, it is important to mention that broken parts of this material could come between the moving piston and the cylinder inner surface. Due to friction high temperatures could be developed which would increase the risk of a fire with the cylinder material. So the development of a fire cannot be excluded in case of such piston damage.

2.2 Pistons with Piston Rings

The following presented case of experienced piston damage concerns a one stage booster compressor with two vertical cylinders. The crankshaft turns with 585 rpm and the design volume flow is given

Challenges of Oxygen Reciprocating Piston Compressors

by: Wolfgang Grillhofer, Air Liquide

with 21000 Nm³/hr. The oxygen is delivered from the air separation unit with 26,4 barg and needs to be compressed to the pipeline pressure of 64 barg by this reciprocating piston compressor.

In 2011 the compressor tripped as the vibrations on the drive end cylinder exceeding the trip value. It was possible to safely shut down the compressor. As there was no indication for a possible failure during the first visual compressor check it was decided to open the concerned cylinder. Inside the cylinder parts of the piston bolts and some debris were found. Figure 4 below shows that the broken parts came between the moving piston and the cylinder head thus damaging the piston surface. A lot of hammering marks were identified on the piston top surface.

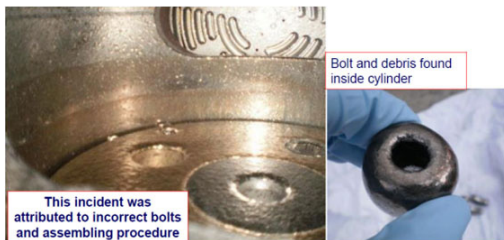


Figure 4: Piston Damage

In order to understand the most possible cause in this case it is necessary to have a look to the sectional drawing of the concerned piston as shown in figure 5. The piston body was made of three parts and the non metallic piston rings were situated in respective chambers. The crank end piston body was clamped together with the centre piston body on the piston rod by four bolts. The head end piston body then was clamping together all the piston ring chambers with the piston rings by using four long bolts.

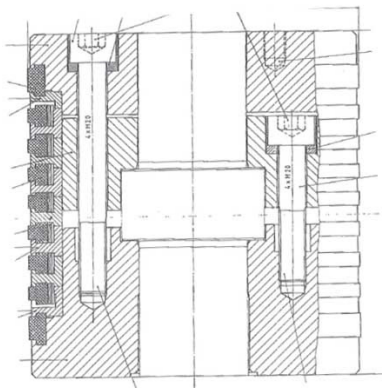


Figure 5: Three Piece Piston with Piston Rings

It was now evident that one of the bolts failed. A possible reason for that could be that the bolts were

not assembled correctly. Especially for this design it is very important to follow strictly the defined installation procedure.

A new piston of same design was installed on this cylinder and the compressor was put into operation after the repair.

It turned out that in this case the replacement of the damaged drive end cylinder piston was not enough in order to operate the compressor reliably until the next major overhaul.

About one year after this incident a fire occurred on the other cylinder, the non drive end cylinder. Most probable cause was again linked to a weakness in the piston bolt connections. Investigations resulted in wear marks on the inner surface of the crank end piston part. It seemed that due to loosen piston bolts the piston parts could slightly move up and down relative to the piston rod. Such a movement would create high temperature because of the friction between the piston parts and the piston rod.

Because of compressor history it was decided to re-design the piston. A suggestion was made to manufacture two piece pistons. The two parts shall be fixed on the piston rod by using one nut on the piston rod thread. Furthermore the materials were changed in order to increase the margin in terms of fire resistance.

2.3 Conclusion of Piston Damages

One general conclusion is that materials for piston parts shall be used that have good oxygen compatibility as described in the actual EIGA document IGC Doc 10/09/E.

Furthermore it was shown with the described cases that also the piston design has a big influence on the reliability and safe compressor operation.

Also extraordinary temperature increase due to friction or not sufficient cooling must be avoided in any case. As it was shown in this section this can be the reason for high temperature increase causing parts damage or even an oxygen fire.

3 Piston Rod and Piston Rod Packing

The challenge of piston rods used in oxygen compressors is not only to withstand the mechanical forces but also to be oxygen compliant from material point of view. Especially when coated rods are used only proven technology in terms of oxygen compatibility for the coating shall be applied.

Challenges of Oxygen Reciprocating Piston Compressors

by: Wolfgang Grillhofer, Air Liquide

Piston rod packings are made of several parts including non metallic piston rings. A reliable design and the use of oxygen compatible materials are essential for a safe compressor operation.

In the following sections some experienced piston rod and packing issues will be summarized in order to show the importance of reliable design, manufacturing and of choosing the correct material.

3.1 Piston Rod Damage

During a major overhaul of a three stage compressor with four vertical cylinders also the pistons with the piston rods were pulled for a detailed check. In this case the oxygen was compressed from 1,02 bara to 25 bara with double acting pistons.

It was found that the piston rod lost already some parts of the coating in the oil scraper section. The concerned rod was in operation for about 54000 hrs. As can be seen in the figure 6 a lot of cracks were visible in the section where the parts were broken out. It is interesting that the crack pattern developed regularly into small hexagonal fragments.



Figure 6: Damaged Piston Rod

The root cause analysis in this case is not finished yet. Some of the possible causes which are still under investigation are failure in the coating process, use of not sufficient coating materials and overheating in the oil scraper section for example.

As a rod with such damage would cause increased wear on respective oil scraper rings and thus resulting in a not reliable oil removal performance it was decided to go with a new piston rod.

3.2 Piston Rod Packing

Regular maintenance was applied to a multistage pis-

ton compressor with double acting pistons and vertical cylinders. Pulling the pistons with respective piston rods was included in the maintenance plan and also the disassembly and inspection of the packings.

The non contact labyrinth rings made of non metallic material showed wear marks on the inner surface. More concern was caused by the damaged springs which are used to axially clamp respective rings in their metallic containers. In figure 7 it can be seen that the last windings were worn.



Figure 7: Labyrinth Packing Ring and Damaged Spring

As it was necessary to complete the maintenance in respective time schedule new rings and springs were installed. A discussion with the OEM for possible improvement is outstanding. However, this example has shown the importance of an agreed maintenance plan based on a combination of predictable and time based actions as Air Liquide has implemented.

In the next case which is described in the following extraordinary piston rod packing leakage was observed several times. The concerned packing is installed in a double acting piston compressor with two vertical cylinders. Two leakage lines do collect respective oxygen leakage at defined lines at the packing and in one of these lines the leakage is measured. In this case the challenge from piston rod packing point of view is the high discharge pressure of 64 barg.

Figure 8 below shows the packing in upside down position and respective sectional drawing. Nine non contact and non metallic labyrinth rings have the task to reduce the pressure from the cylinder pressure down to the ambient pressure. One pair of contact rings also made of non metallic material at the end shall ensure tightness to the distance piece.

Challenges of Oxygen Reciprocating Piston Compressors

by: Wolfgang Grillhofer, Air Liquide

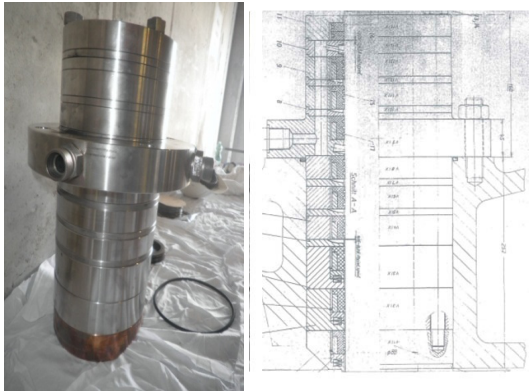


Figure 8: High Pressure Piston Rod Packing

After pulling the piston rod and visual investigation black deposit was observed on the piston rod in the packing area. It shall be pointed out that the deposit was not only in the contact ring section but also in the section of the non contact rings as can be seen in figure 9.



Figure 9: Piston Rod Wear Pattern

The observed wear pattern in the non contact ring section could be explained only by radial movement of the rings. This was also supported by signs of such movement on some of the metallic containers.

During the investigation of this issue also non permanent vibration measurement and diagnostic was performed by doing a nitrogen test run. As a result all RMS values were below the EFRC recommended values. However, there were some higher order peaks in the vibration spectrum detected which could have such an influence on the rings to cause radial movement. Possible causes for such high order peaks are structural vibration caused by e.g. valve motion, leakage flow induced vibrations or some influences from noise effects.

As a first step a leakage recovery line back to the cylinder suction line which was originally foreseen but did not exist anymore will now be re-assembled. This shall exclude possible leakage flow induced vibrations as then there is a point in the packing with

defined pressure. Further actions will be defined depending on the results of this first correction action.

3.3 Piston Rod and Packing Conclusions

As piston rods and packings are also in contact with oxygen it is important that for these parts only materials with good oxygen compatibility are used and reliable manufacturing processes are applied. In case of part damage broken pieces can come between moving and non moving parts thus creating high temperatures. On the other hand damages were observed which have the potential of eliminating the oil film removal along the piston rod.

Furthermore it is of same importance to have a maintenance strategy in place which ensures detecting possible problems before a big damage.

4 Inspection and Maintenance

Besides the need of reliable design and the use of only proven materials with high oxygen compatibility it is necessary to agree on inspection techniques and intervals as well as maintenance plans.

Air Liquide is following the reliability centred maintenance philosophy, i.e. to get the best combination of e.g. time based and condition based maintenance actions.

In the following one example of improved procedure for piston rod oil detection is presented as well as a short summary of most important maintenance related issues affecting the compressor reliability and safety will be given.

4.1 Piston Rod Oil Detection

For safety reasons it is essential for oxygen reciprocating piston compressors that there is absolutely no oil or grease on the piston rod in the gas packing section. Grease or oil in this area can come into contact with oxygen which would increase the risk of a fire.

From design point of view the vertical piston rods mainly have non metallic oil shield rings installed. Such rings are installed above the piston rod bearing when there is one or simply before the gas packing area, refer also to the figure below. In normal cases oil on the piston rod shall be already removed by the oil scraper rings which are installed in the piston rod bearing casing for this compressor type. The oil shield rings are the last barrier before the packing section.

Challenges of Oxygen Reciprocating Piston Compressors

by: Wolfgang Grillhofer, Air Liquide



Figure 10: Piston Rod Oil Shield Ring

A wide known safety procedure is to check the piston rod for oil and grease regularly. This can be done only when the compressor is shut down. The major reason therefore is that the oxygen compressors have to be operated within a closed barrier which must not be entered during compressor operation. The other reason is that it would not be possible to do a reliable observation of the piston rod for oil films when the compressor is in operation.

For continuous monitoring Air Liquide has installed cameras close to each piston rod in some plants to test this technique. Figure 11 is showing such an installation as an example.



Figure 11: Camera Installation for Continuous Piston Rod Observation Concerning Oil Film Development

Pictures from the piston rod are thus transferred to the operating room and are displayed on a separate screen, refer also to figure 12.

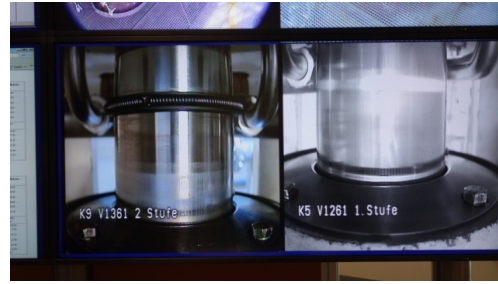


Figure 12: Screens Displaying Piston Rod Surface

Cameras are already used within the safety barrier in order to watch the oxygen compressor during operation. So this was a logical expansion of this procedure in order to improve the safety.

Practice has shown that such camera installations are useful to identify oil on the oil scraper ring casing cover disc, the black ring in figure 12.

4.2 Maintenance

It is obvious that regular maintenance is necessary in order to keep oxygen compressors in reliable operating condition. Wear parts have to be inspected and the overall condition of the compressor must be assessed regularly.

The parameters available from continuous monitoring as e.g. oxygen temperatures measured close to respective cylinder valves are taken as an input for deciding if the compressor shall be shut down for maintenance. However, as oxygen compressors must be handled with care from safety point of view Air Liquide has also defined maximum operating hours. When such limits are reached maintenance has to be scheduled without delay also when the trends of the operating parameters are still normal.

Experience has shown that during the maintenance mistakes can occur which can have catastrophic consequences during operation when they are not detected. In the following two examples to this topic shall be presented.

The first example concerned the exchange of worn oil scraper rings. During a major overhaul of a multi-stage compressor with vertical cylinders also the oil scraper rings were changed. These rings are installed right above the piston rod bearing and have the task to remove reliably excessive oil from the piston rod. In the section before it was already pointed out that this is an important safety feature.

After the overhaul was finished the compressor was put under nitrogen for a test run. During this test run it was then observed that the oil was not removed

Challenges of Oxygen Reciprocating Piston Compressors

by: Wolfgang Grillhofer, Air Liquide

reliably from one piston rod. The compressor was stopped and it was decided to disassemble the oil scraper rings. One of the three installed rings was installed in the wrong direction. It must be understood that these oil scraper rings are uni-directional from oil removal point of view.

Figure 13 shows one of the concerned oil scraper rings. It is a slotted ring made of a copper alloy and pressed onto the rod by a spring. The inner geometry is like that there are one sharp edge and a phase. The ring must be installed with the sharp edge to the crankshaft end, only then the oil scraper performance is ensured.



Figure 13: Oil Scraper Rings

In the second case also a major overhaul was performed on a multistage compressor with vertical cylinders. During the test run increased packing leakage was observed and therefore the decision was to shut down the compressor and to re-open concerned packings. The investigations resulted in dust particles which came between the moving piston rod and respective static piston rings. It must be understood that the vertical compressor is from open distance piece design which means that the distance piece openings are closed only with windows made by acryl glass during compressor operation. When maintenance is performed also on the packings, piston rods, etc. these windows are removed.

In this case there was no platform around the compressor which could be used also for maintenance. Temporary scaffolding had to be installed which was disassembled right before the compressor was started for the nitrogen test run. It turned out that during the scaffolding disassembly the distance piece windows were not yet installed. So most probably dust particles from the scaffolding were introduced into the distance piece and were not removed before the compressor start. These particles then caused the immediate wear on respective non metallic packing rings which resulted in increased leakage already during the test run.

4.3 Inspection and Maintenance Conclusions

Experience has shown that it is important to have a reliable inspection and maintenance philosophy in place. But this is not enough for ensuring a good compressor operation. It is also essential to implement a procedure for checking respective maintenance task for completion and correctness. The basis for that is an agreed machine specific action plan. By using such a plan holding points can be defined in order to check especially critical actions together.

5 Conclusion

Because of increased safety risk oxygen compressors need a special treatment. This concerns the design including used materials as well as the inspection and maintenance philosophy.

Although the rate of failures with fires as consequences experienced in Air Liquide plants is already low, Air Liquides ambition is always to improve respective safety conditions. That's why it is important for Air Liquide to investigate every case of damages and to identify possible improvements.

In the past Air Liquide has experienced part damages and malfunctions of oxygen compressors from different manufacturers and types. The cases presented in this paper concerned pistons, piston rods, packings and oil scraper rings. Some of these cases were linked to the design and thus improvement was only possible by a re-design. Also the compressor operation and the condition of the auxiliary systems as for example the cooling water system had an important influence on the parts reliability. It is necessary to operate the oxygen compressors in a clean environment and to maintain the auxiliary systems in good condition.

It was also summarized in this paper that the way how inspection and maintenance is realized has a big impact on the compressor reliability. Also during this period failures cannot be excluded which can have an enormous impact on the compressor operation. The risk for such failures can be reduced by following some best practices based on Air Liquide experiences. For example it is necessary to communicate to maintenance personal to have always an agreed action plan in place. Another best practice is to define some holding points during the maintenance for checking the actions already done and to briefly discuss the next steps.

Challenges of Oxygen Reciprocating Piston Compressors

by: *Wolfgang Grillhofer, Air Liquide*

6 Acknowledgements

Herewith I want to thank all colleagues from Air Liquide who have supported this paper. In particular for this topic I had fruitful discussions with our oxygen experts Alain Colson from SIS department, Jean-Francois Rauch from LI-WIM organisation and Daniel Machon Diez de Baldeon from engineering.

9th Conference of the EFRC September 11th / 12th, 2014, Vienna

**Performance Improvement of Dry-Running Sealing Systems by
Optimization of Wear Compensation,** -239-
by: Norbert Feistel, Burckhardt Compression AG

**Scientific Research Methods to analyse Compressor Wear Parts and
Lubricants** -248-
by: Thomas Heumesser, LMF



SESSION SEALING / WEAR 2

**EUROPEAN FORUM
for RECIPROCATING
COMPRESSORS**



Performance Improvement of Dry-Running Sealing Systems by Optimization of Wear Compensation

by:

Norbert Feistel

Research and Development

Burckhardt Compression AG

CH-8404 Winterthur, Switzerland

norbert.feistel@burckhardtcompression.com

**9th Conference of the EFRC
September 11th / 12th, 2014, Vienna**

Abstract:

Wear compensation serves to maintain frictional contact despite progressive loss of material, and is ideally characterized by maximum utilization of the radial ring dimension as wear, given a constant sealing effect. In practice, however, this can only be achieved to a limited extent because ring materials suitable for dry running often exhibit pronounced cold-flow properties or low elongation at break, so that optimal wear compensation for the sealing element is not always possible. New approaches to wear compensation for piston and packing rings allow better utilization of the theoretically available wear as well as use of a wider spectrum of material. Proper combination of these parameters results in a more consistent sealing efficiency, better stability in the run-in state of the sealing elements and a prolonged service life of the sealing system.

1 Introduction

The performance of dry-running friction systems is limited mainly by a friction coefficient which is significantly higher compared to oil lubrication, and a wear rate which increases rapidly with load. Despite all the progress made in recent years in the field of tribology, the material loss of dry-running sealing and rider rings is therefore much more pronounced compared with oil-lubricated compressors, especially if high demands are placed in terms of load parameters. Accordingly, dry-running sealing elements are often in an extreme state of wear before the end of the aspired service life, only remnants of their original structure being recognizable in some cases.

But the reverse phenomenon is also observed, especially during compression of gases with a low molecular mass. Poor sealing efficiency might necessitate replacement of the sealing elements here even though they are visually still in good condition. Discussions of sealing element state become irrelevant if a declining sealing function degrades the compressor's capacity and efficiency due to high gas losses, or even impairs its functionality through an overshoot of permissible process parameters in the form of a high compression temperature, for instance.

Even the most favourable dry-running characteristics are of little use if the sealing efficiency is lost prematurely. For sealing elements to have a long service life, optimization of their design is therefore useful in addition to minimizing the wear rate. In addition to known measures for reducing contact pressure, the quality of wear compensation is also of importance here. The benefits of a sealing element that offers a greater proportion of the radial ring dimension as wear given a constant sealing efficiency are obvious. This not only extends service life significantly, but also reduces the gas losses and, thus, improves the compression efficiency.

2 Various concepts of wear compensation

Oil-free piston compressors employ sealing elements capable of wear compensation in the form of common friction rings, as well as elements without wear compensation such as labyrinth and gap seals. Also available are sealing elements which transition to contactless sealing after an initial period of friction. The various versions of these designs differ mainly in the dimensioning of the permissible wear path intended for the duration of the friction phase.

Because labyrinth and gap seals cannot compensate material loss, wear here inevitably increases the flow area for the leakage mass flow, and consequently

degrades the sealing efficiency. In such cases, the sealing efficiency can be stabilized, in particular, through proper guidance to avoid frictional contact, and high wear resistance to gas contamination. In contrast, friction rings have the objective of preferably long and full contact to the counter body in order to minimize the flow area. The various sealing element designs can therefore be categorized as follows:

- Frictionless labyrinth and gap seals without wear compensation
- Sealing elements that transition from a frictional state to a contactless state
- Friction sealing elements with unlimited wear

Friction contact is maintained through elastic / plastic deformation of a curved beam in the case of one-piece sealing rings, and through radial / tangential shifting of individual segments in the case of segmented sealing rings. Although segmentation of the sealing rings avoids the high bending load arising during wear compensation for one-piece rings, not all materials are feasible for every ring style. Early designs of dry-running piston rod sealing systems were often based on carbon materials. Favoured here due to these materials' low breaking elongation were designs with the simplest possible segment geometry, even if this did not always achieve an optimal sealing efficiency. This still applies to some modern dry-running materials.

Popular notions about the function of friction rings often assume a proportional relationship between wear and leakage, for instance, as in the case of a simple piston ring without a joint sealing. For sealing elements with a joint sealing, however, the relationship between wear and leakage is much more complex.

2.1 Wear compensation of packing rings

Because leakage gas from a piston-rod sealing system (packing) escapes from the cylinder, the sealing efficiency here must usually meet higher demands than those placed on a piston sealing system. The high demands on sealing function are met by more elaborate design and more complex sealing element style. The packing sealing elements usually have a segmented design. These multi-part rings have the advantage that they can also be mounted on a built-in piston rod, regardless of the ring material. But one-piece designs similar to piston rings are also sometimes used as packing rings.

In the case of common packing ring designs, wear increases the circumference of the ring sections making friction contact. To prevent the individual segments from obstructing each other in this process,

Performance Improvement of Dry-Running Sealing Systems by Optimization of Wear Compensation

by: Norbert Feistel, Burckhardt Compression AG

the following wear compensation methods are commonly employed:

- Gaps between individual segments allow limited wear (Figures 1a, 1b)
- The segments are partly moved away from the piston rod during operation (Figure 1c)
- The segments move over each other during operation (Figure 1d)

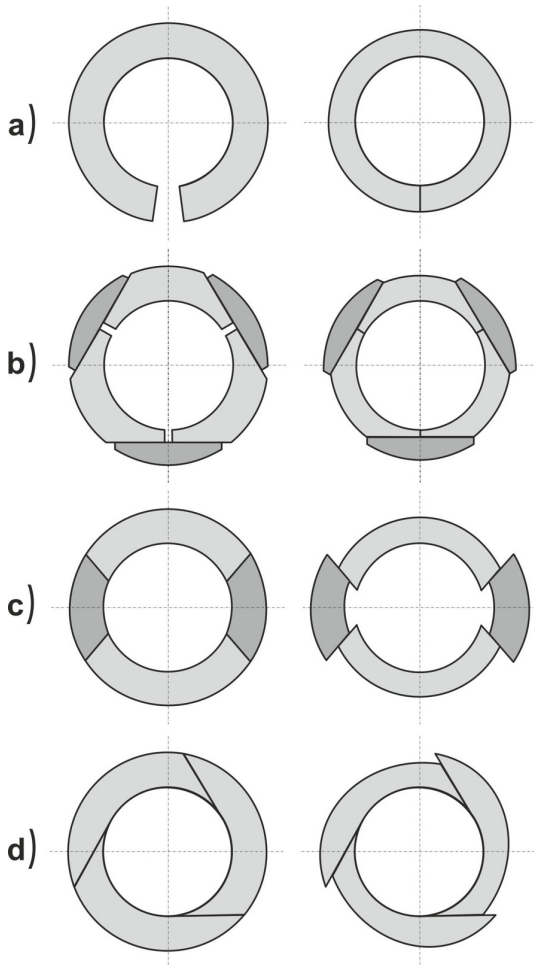


Figure 1: Different wear compensation methods for packing rings (new condition on the left in each case): a) One-piece ring. b) Six-piece ring. c) Four-piece ring with unequal segments. d) TID ring

The gaps existent in the new state or arising during operation between the individual ring parts are either covered by additional radial and / or axial segments, or they remain open and thereby reduce the sealing efficiency.

An important distinction criterion for packing rings in whose case wear causes individual joint ends to approach each other in the circumferential direction is the presence or absence of design limits on wear compensation. Packing rings with limited wear

include all designs with a butt joint, for example, in the form of a one-piece ring (Figure 1a) or segmented designs such as the six-piece ring (Figure 1b) as well as the widely used three-piece, radially cut cover ring. Designs which can wear out indefinitely include the four-piece ring with unequal segments (Figure 1c) or the packing ring cut tangentially with respect to the piston rod (TID ring, Figure 1d).

In the case of packing rings with limited wear, the sealing function changes from a frictional seal to a contactless labyrinth or gap seal after compensation of the set wear path. This procedure is generally used for throttle rings to achieve a frictionless seal with a minimal flow area through low running-in wear. However, because material loss along the individual segments is not even, therefore increasing the flow area with progressive wear, the running-in wear for throttle rings is usually limited to low values less than one millimetre of the radial ring dimension.

By contrast, increasing the permissible wear path to several millimetres of the radial ring dimension, as is usually the case with the actual packing rings, can have the following disadvantages:

- On transition to the frictionless state, the sealing efficiency is already so bad that the sealing element is useless.
- The remaining radial ring dimension is insufficient for the applied pressure difference, and the sealing element fails due to fracture or elastic / plastic deformation (Figure 2).



Figure 2: Failure by fracture near the joint of a packing ring with limited wear

But even if the sealing element achieves a frictionless state with a good sealing efficiency, this does not necessarily remain stable. The change in a packing ring's sealing efficiency on transition to the frictionless state can be clearly demonstrated in a test: Three packing rings of the step bridge design (penguin ring) made of carbon / graphite filled PTFE were designed with a joint clearance of just one millimetre between any two segments. The small joint clearance here was intended to ensure the best possible sealing

efficiency in the run-in state. The three packing rings for a piston rod diameter of 50 mm were subjected to a constant pressure of 24 barg in the tailrod packing of a nitrogen compressor¹.

For a test duration of 530 hours, Figure 3 provides a dimensionless representation of the pressure difference over sealing element number 3 located furthest away from the compression chamber, as well as the entire sealing system's leakage and the temperature measured inside the piston rod. During the first approximately 150 hours, the sealing element worked as a friction ring and was subjected to 70 % to 80 % of the total pressure difference. Within the next 50 hours, the pressure difference over the sealing element rose to about 100 %, while the leakage and piston rod temperature decreased. In this phase, the entire joint clearance was already used up and the sealing element transitioned to the contactless state. During continued operation, the leakage began to increase again until the diminishing sealing efficiency suddenly caused a shift in pressure difference to the two remaining sealing elements after approximately 520 hours.

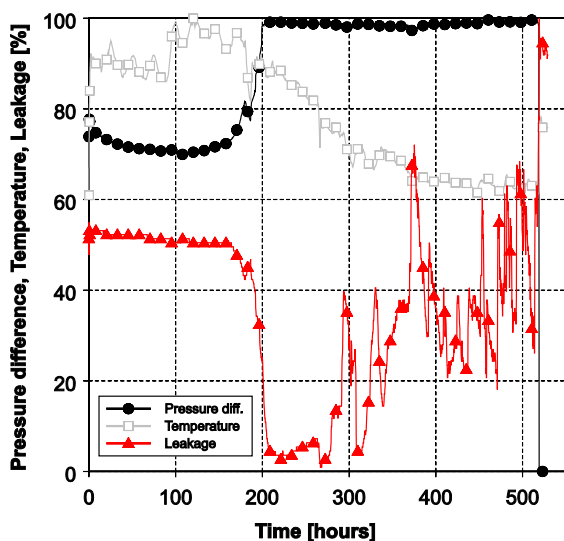


Figure 3: Characteristics of pressure difference, leakage and piston rod temperature on transition of a packing ring from frictional to contactless sealing function

Although the disadvantages mentioned above can be avoided through the use of packing rings without limited wear, the sealing efficiency of these variants also declines slightly with progressive wear. In addition, the installation of packing rings without limited wear requires special measures. For instance, a mounting sleeve is often used to secure the packing rings against the garter springs' forces so that protruding segments are not damaged during

installation of the piston rod. Packing rings of the step bridge design (penguin ring) offer a special feature here. Appropriate joint geometry can be used to regulate whether the sealing element is to transition to a frictionless state, or whether it can wear indefinitely, similarly to the TID ring (Figure 1d). Figure 4 shows the special design of a penguin ring without a wear limit; this design can be easily installed while nonetheless permitting full wear.



Figure 4: Penguin ring version with unlimited wear compared to a segment in the new state (top)

2.2 Wear compensation of piston rings

A piston ring is usually designed as a one-piece ring with a butt or scarf joint. In contrast to a packing ring, the two joints move away from each other during wear compensation of a piston ring, thereby increasing the joint clearance. Depending on the desired utilization of the available radial ring dimension as a wear path, the increase in joint clearance can achieve significant values (Figure 5). If half the radial ring dimension of 16 mm is to serve as a wear path in the case of a piston ring for a cylinder diameter of 250 mm, for example, the distance between the two joint ends increases by 50.27 mm. Without a joint sealing, this leads to an increased flow area and thus to a deterioration of the sealing efficiency. Especially in the case of dry-running compression of hydrogen, such piston rings made of an expensive material like polymer blend or high-temperature polymer do not permit economical use, and the achievable lifetime remains considerably shorter than the theoretically attainable value.

Performance Improvement of Dry-Running Sealing Systems by Optimization of Wear Compensation

by: Norbert Feistel, Burckhardt Compression AG

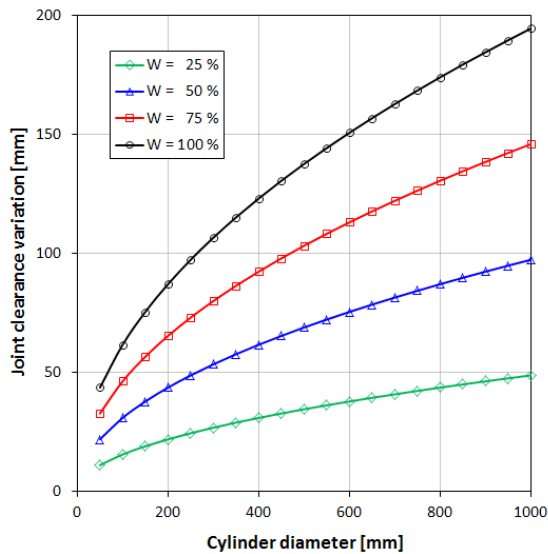


Figure 5: Variation of a piston ring's joint clearance depending on the wear W of the radial ring dimension

Piston rings with a joint sealing offer an advantage here, although it is still rather insignificant in the new state, and is brought to bear only with progressive wear². Common types of piston rings with a joint sealing incorporate a step-cut or gas-tight joint. This method of joint sealing is produced for a given cylinder diameter by using piston rings with a diameter which is roughly 3% - 5% larger, the resultant difference in circumference being available for limited joint coverage. Often, however, the special properties of dry-running materials do not allow realization of such a joint sealing. Known, for instance, are highly filled polymers possessing a matrix of PTFE or resin and exhibiting superb wear resistance in several very dry gases, but whose elongation-at-break of less than 2% only makes them suitable for simple joint geometries, usually comprising just two-piece variants, in fact.

An alternative technique of producing a joint sealing is to use two or more one-piece piston rings, combined and secured against twisting such that they mutually seal the joints. In this high-cost variant, joint sealing is guaranteed as far as theoretically complete wear of the actual sealing ring. A well-known example of this is the twin ring².

The wear path of the piston rings is usually unlimited, i.e. they can wear out completely. There is also a design comprising a retained piston ring which transitions from a frictional seal to a contactless labyrinth or gap seal after a given wear path has been completed⁴.

3 Piston ring with joint lock

If a piston ring is to allow use of the greatest possible portion of the radial ring dimension as a wear path without a significant decline in the sealing efficiency, a joint sealing becomes inevitable. However, common designs of such joint sealings have a variety of disadvantages which become apparent particularly in applications involving high pressure difference. The high forces and torques present here require a robust design for the piston rings, mostly on the basis of a high temperature polymer such as modified PEEK. The problems observed in practice range from difficulty in assembly due to high rigidity and incomplete contact with the cylinder wall to frequently observed plastic deformation and / or failure by fracture in the region of the joint sealing during operation.

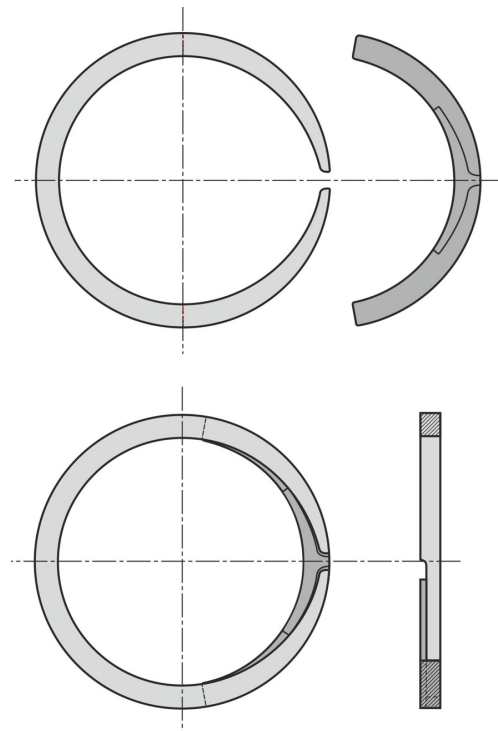


Figure 6: Sealing of a piston ring joint using a joint lock

The joint coverage of nearly 360 degrees offered by a combination of two one-piece piston rings is not needed for theoretically complete wear of the radial ring dimension (Figure 5). The cover ring's circumference can therefore be reduced significantly without a loss in functionality. A version with a circumference of less than 180 degrees is advantageous here, so that one ring can be used to economically manufacture several cover rings. However, the main advantage of such a shortened cover ring, referred to as joint lock, is that it is not bent for the purpose of installation, instead merely being slid into the piston groove.

Furthermore, wear compensation for the joint lock is performed through radial shifting toward the cylinder wall instead of elastic / plastic deformation. This allows a robust design of the joint lock, for example, using a high-temperature polymer with good strength properties to better withstand high pressures.

The lock is designed to seal the piston ring's joint in the radial and axial directions. Accordingly, the piston ring has appropriate recesses for the integration of the joint lock (Figure 6). Especially in the case of a horizontal compression stage, radial shifts in the joint lock in the de-pressurized state can open the joint sealing. When the compressor is started, however, the joint lock is pressed back toward cylinder wall by the pressure difference, thereby fully covering the piston ring's joint (Figure 7). Tests in a horizontal hydrogen compressor showed that the joint lock can be activated reliably both with single-acting and double-acting compression, and the sealing efficiency of these piston rings is comparable to that of twin rings². Figure 8 shows the arrangement of the joint lock near a piston ring's joint.

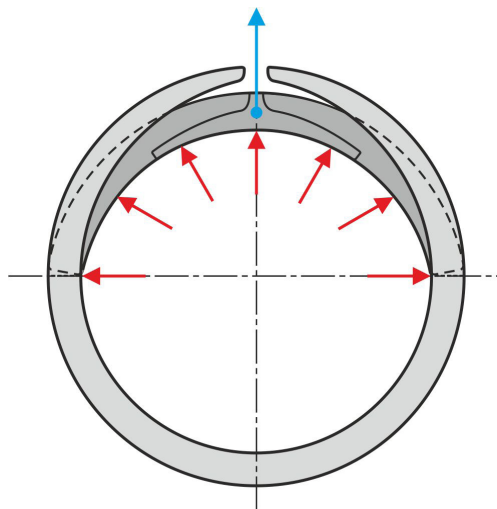


Figure 7: Activation of the joint lock by gas pressure



Figure 8: Piston ring with joint lock

4 Packing ring with a maximum radial wear path

Maximum utilization of the radial ring dimension as a wear path requires a method of wear compensation which avoids increases in existent flow area, or additional formations thereof, as material is removed progressively. This can be achieved by segments whose width at the inner diameter is equal to that at the outer diameter. This geometric design allows unimpeded wear compensation without the need for gaps between the individual segments. This permits full coverage of the piston rod's circumference. However, the special segment shape requires a base ring which ensures that all segments are arranged in the correct position with respect to the piston rod, and are only capable of radial shifts (Figure 9).

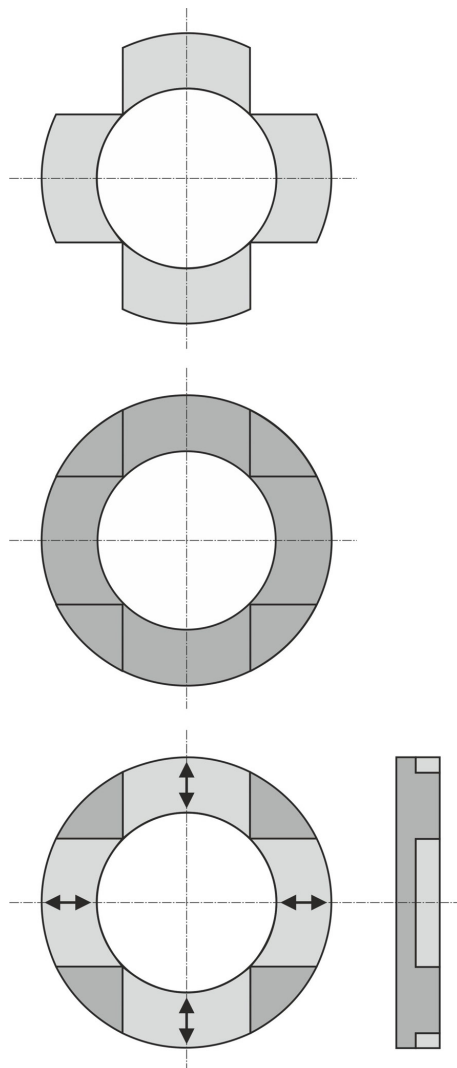


Figure 9: Schematic representation of wear compensation for an MP ring (MP-4P) with four segments (above) in a special base ring (centre)

Performance Improvement of Dry-Running Sealing Systems by Optimization of Wear Compensation

by: Norbert Feistel, Burckhardt Compression AG

Due to manufacturing tolerances, it is not possible to avoid small gaps between the segments and their guides, as well as between individual segments on the piston rod's circumference. These gaps define the sealing ring's maximum leakage. Progressive wear during operation leads to a formation of ridges at either end of each segment. These segment peaks are pushed into the gaps between the segments, thus reducing the flow area and improving the sealing efficiency. Optimizing this effect makes it possible to achieve leakage values which can even be lower than those of a TID ring in the new state. Figure 10 shows the average leakage over an operating period of 100 hours in each case. Tested from each of the different versions was only a single ring at a suction pressure of 16 barg and final pressure of 40 barg.

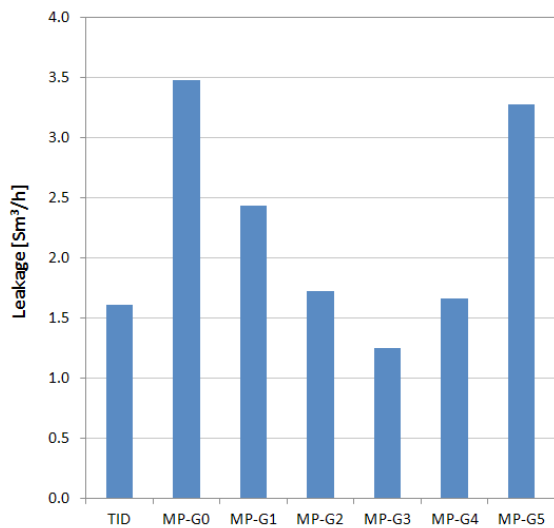


Figure 10: Average leakage values from single-ring tests with nitrogen ($P_s = 16$ barg, $P_d = 40$ barg) for several geometric versions of the MP ring (MP-4P) compared to a TID packing ring

The effect of ridge formation can be further intensified if the segments are arranged at a 45-degree angle instead of a 90-degree angle with respect to each other. The number of segments of this multi-piece ring (MP ring) is limited only by the boundary conditions for minimum segment width. Figure 11 shows an MP ring with eight segments. Figure 12 shows average leakage values in a hydrogen compressor over an operating period of 500 hours for three different dry-running packings each comprising six penguin rings, six MP rings with four segments (MP-4P) and six MP rings with eight segments (MP-8P). The tests were conducted at a suction pressure of 40 barg and a final pressure of 100 barg (piston rod diameter = 50 mm). Under these conditions, the leakage of the MP version with eight segments was lower by more than half compared to the version with four segments and achieved the level of the penguin design.

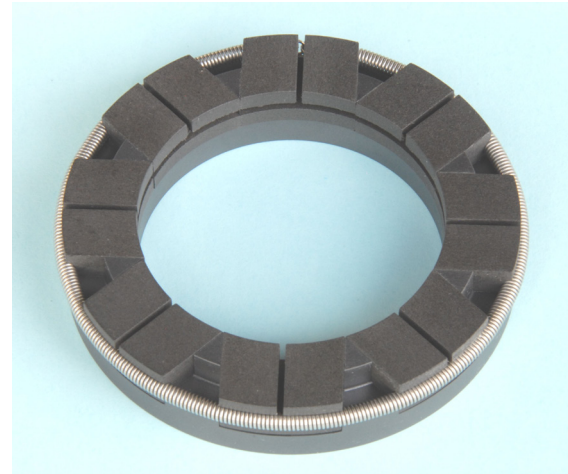


Figure 11: MP ring with eight pressure-relieved segments (MP-8P)

The MP ring makes it possible to use and completely wear out materials not suitable for normal designs due to the bending stresses prevailing in such cases. The simple segment contour also allows easy implementation of a pressure relief groove³. This measure achieves amazingly low wear rates even at a challenging final pressure of 100 bar for dry-running packings. All sealing elements of the three test packings were made of the same PTFE / PPS polymer blend. However, the two MP variants exhibited significantly lower wear rates compared to the conventional penguin packing, the version with four segments having a slight advantage (Figure 12). In terms of a combination of sealing efficiency and wear characteristics, however, the version with eight segments is the better compromise.

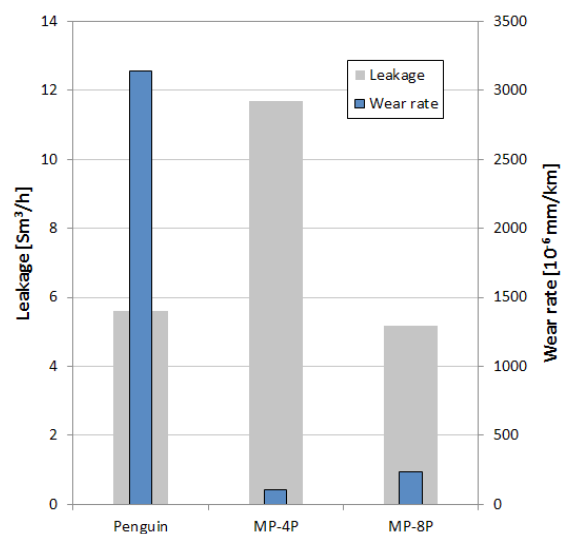


Figure 12: Comparison of average leakage and wear rate for packings each comprising of six penguin, MP-4P and MP-8P packing rings in hydrogen ($P_s = 40$ barg, $P_d = 100$ barg, $C_m = 3.4$ m/s)

5 Stabilization of a packing ring's run-in state

Often arranged in addition to the frictional packing rings are one or more contactless sealing rings right at the packing inlet, near the compression chamber. Known as throttle rings or pressure breaker rings, these packing rings are intended to bear the dynamic component of the pressure difference, which they throttle without any wear in the ideal case. Usually, a low degree of running-in wear is planned to minimize the flow area. As described in section 2.1, however, a sealing element's operational reliability and sealing efficiency are not necessarily retained following transition to the contactless state. Especially for segmented packing rings, exposure to the dynamic pressure component leads to failure by fracture and / or plastic deformation³. By contrast, a highly stable sealing efficiency during frictionless operation is exhibited by one-piece, endless sealing rings, though these do not permit minimization of flow area through running-in wear.

A new approach to stabilizing a packing ring's run-in state combines an endless ring's stability with a segmented packing ring's capability for running-in wear. The principle is based on two serially arranged endless rings moving from opposite directions toward the piston rod. One half of either ring can thus wear, both rings mutually covering the crescent-shaped gap arising between the other ring half and piston rod.

The two endless rings are made to shift by a spring-loaded actuator ring comprising dry-running plastic with a butt joint (Figure 13). The sealing rings are housed in eccentric grooves in the actuator ring, the eccentricity defining the maximum possible radial wear. Each sealing element is furnished with a fixation tappet placed in the actuator ring's joint. This anti-twist mechanism ensures that material removal takes place only in the region of a defined semi-circle. Once the radial clearance has been compensated, the friction rings transition to a contactless sealing function. Figure 14 shows such a sealing element in a particularly heavy-duty design comprising two endless sealing rings made of a special bronze modified with solid lubricant for dry-running.

Tests with a nitrogen compressor's tailrod packing demonstrated the high load capacity of such sealing elements when used as throttle rings. In this context, a sealing system consisting of four throttle rings and three penguin rings was subjected to a suction pressure of 40 barg and a final pressure of 100 barg. Figure 15 shows the related pressure characteristics measured in the cylinder and the individual sealing element chambers. Clearly visible is how the four

throttle rings fully eradicate the high dynamic pressure difference of up to 60 bar, therefore constituting excellent protection for the subsequent, segmented packing rings.

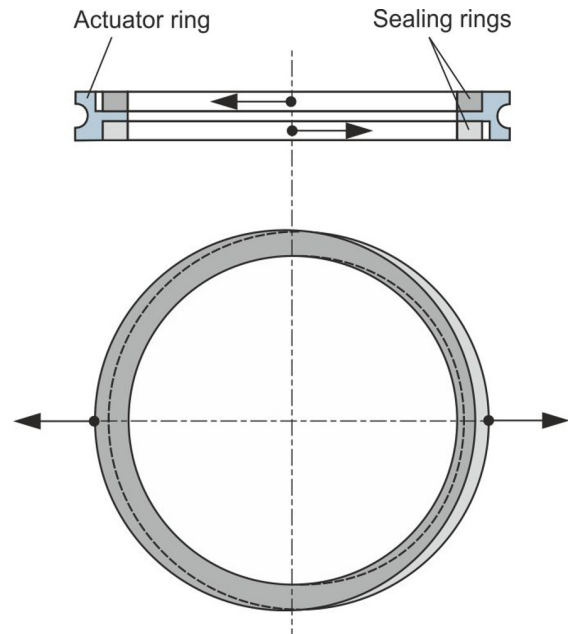


Figure 13: Schematic representation of wear compensation for two endless rings through opposite shifts



Figure 14: Robust design of a throttle ring comprising two endless sealing rings in an actuator ring

Performance Improvement of Dry-Running Sealing Systems by Optimization of Wear Compensation

by: Norbert Feistel, Burckhardt Compression AG

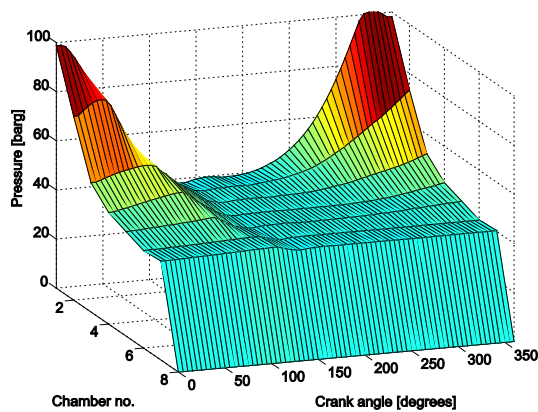


Figure 15: Pressure distribution of a packing comprising four throttle rings (chambers 1 - 4) and three penguin rings (chambers 5 - 7), nitrogen, $P_s = 40$ barg, $P_d = 100$ barg, $C_m = 3.2$ m/s

6 Summary

Maximum utilization of the radial ring dimension as a wear path requires a method of wear compensation which avoids increases in existent flow area, or additional formations thereof, as material is removed progressively. With regard to piston rod sealing, this is achieved by a special segment geometry, the segment width at the inner diameter being equal to that at the outer diameter. This design enables theoretically complete coverage of the piston rod's circumference, while allowing full and unimpeded wear of the segments.

In the cylinder, too, use of the greatest possible portion of the radial piston ring dimension without a significant decline in the sealing efficiency is associated with effective and robust joint sealing. Here, a piston ring with a special joint lock constitutes an effective alternative to familiar methods such as joint overlapping or combination of several one-piece rings. For installation, the expedient variant with a circumference of less than 180 degrees need not be bent, but is instead simply slid into the piston groove.

Sealing elements that transition from a frictional state to a frictionless require, in particular, high stability in the run-in state, even with a high pressure load. A new approach to stabilizing a packing ring's run-in state combines an endless ring's stability with a segmented sealing ring's capability for running-in wear. The principle is based on two serially arranged endless rings moving from opposite directions toward the piston rod.

A common feature of all three new concepts is that wear compensation is based on shifts in ring components, rather than their elastic / plastic deformation. This also allows the use of materials not suitable for a high bending stresses, thus expanding the choice of dry-running materials.

Notations

PTFE	Polytetrafluorethylene
PPS	Polyphenylsulfide
PEEK	Polyetheretherketone
P_s	Suction pressure
P_d	Discharge pressure
C_m	Average piston velocity
W	Wear
MP-4P	MP-packing ring with four segments
MP-8P	MP-packing ring with eight segments

References

- Vetter, G.; Feistel, N.: Behavior of dry-running piston rod sealing systems in crosshead compressors Hydrocarbon Processing, Sept. 2004, 99 – 107
- Feistel, N.: Influence of piston-ring design on the capacity of a dry-running hydrogen compressor 3rd EFRC-Conference, Vienna, Austria, 2003, S. 141 – 149
- Feistel, N.: Service life improvement of piston-rod sealing systems by means of pressure-relieved sealing elements 4th EFRC-Conference, Antwerp, Belgium, 2005, 23 – 30
- Feistel, N.: Zehn Jahre erfolgreicher Einsatz von TID-Kolbenringen bei hohen Druckdifferenzen Industripumpen + Kompressoren 2, 2010, S. 75 – 82



Scientific Research Methods to Analyse Compressor Wear Parts and Lubricants

by:

Thomas Heumesser

Vice President Sales

Leobersdorfer Maschinenfabrik GmbH & Co KG (LMF)

Leobersdorf, Austria

thomas.heumesser@LMF.at

**9th Conference of the EFRC
September 11th / 12th, 2014, Vienna**

Abstract:

Design, layout and material selection of piston compressors and respective parts for various and complex gases need a deep understanding and knowledge in materials, rings, packings, valves and lubricants. Compressor OEMs have certain experience, but today scientific methods may help to solve the root cause of operational and wear problems in piston compressors. Chemical research, material analyses and analyse of compression lubricants may help to detect failure and wear mechanism. Cooperations with scientific research institutes opens a lot of analysing methods to get deeper knowledge in parts, materials and operational behaviour in piston machines. Examples show this new setup and prove a different way to solve running problems like extensive wears or chemical reaction between parts or lubricants. This applies not only to parts of the compressor OEM, but includes parts of sub suppliers in the compressor business.

1 Introduction

It is commonly understood, that reciprocating piston compressor machines need extensive service and maintenance work and cause costs during continuous operation. Operators and manufacturers struggle to get better service intervals and longer lifetime of lubrication fluids in compressors. All these values may normally be extended only, if the operator and the manufacturer cooperate to find a good solution between the compressed gases, the material, the environment and the lubrication fluids of a machine. The reality is sometimes very different, failures and bad operation of parts are not explored and the parts are only changed to shorten any stop of the compressor. As a consequence of this wrong process, failures will happen again and may sometimes lead to series faults of some parts.

The cooperation between the wear part manufacturers and the compressor equipment manufacturer is often not constructive. The lack of any examination, only the easy change of the parts, will not help the operators to find the reason for the damage of the part. Today research work may help to investigate materials, operation values, the lubrication situation and the tribology process of moving parts inside the compressor.

The root cause of a failure can be analysed from various sides. The chemical composition of the material may give information as well as any solvable parts in the lubrication oil. A case to case decision has to be taken to find the right way and process to meet the target. Sometimes test series may help not to get misled.

The following chapters will firstly deal with common compressor parts and then focus on the relevant wear parts afterwards. Specifications of these parts and the specific operational situation may be compared and possible failure causes analysed. Practical examples will explain the chemical, operational and technical processes to find a satisfactory explanation and analysis.

2 Relevant parts of a reciprocating compressor

A balanced opposed two cylinder compressor and a vertical compressor block are used as examples. Both blocks have distance pieces, main packings, intermediate packings, oil wipers and piston rings. Cylinder diameters, stages and stroke are not relevant for this investigation. Rotational speed will be considered for the practical examples, if any influence is necessary to explain a failure. For all examples it is supposed, that the compressor is calculated conservatively and that there is no failure influence in power or piston rod force. Any overload in design is not part of this analysis.

The following cross section drawings (Fig. 2.1 and Fig. 2.2) show relevant compressor parts which have an impact on the tribology process between moving parts. Several parameters are described to show the influences:

1. Crankshaft, main bearings, connection rod bearings, temperature, lube oil, particles, pollutants
2. Crosshead, crosshead pin, crosshead bearing, temperature, lube oil, particles, pollutants, additional forces initiated via the piston rod in case of failure conditions
3. Oil wiper and piston rod, ring material, ring contact pressure, temperature, lube oil
4. Intermediate packing, if separated distance pieces are used, ring material, ring contact pressure, temperature
5. Main packing with elements and rings, gas pressure, temperature, ring material, chemical durability, mechanical stiffness, gliding abilities, gas composition, lube oil in lubricated version, cooling water and seal- or vent gas, depending on the design.

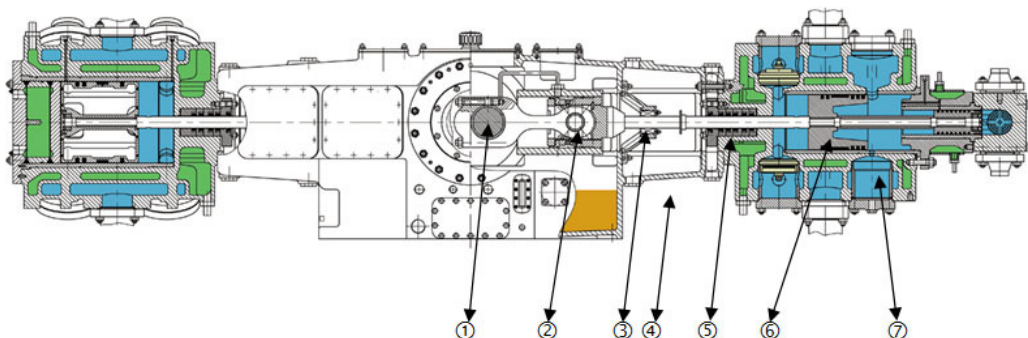


Figure 2.1: Cross section of a balanced opposed piston compressor

6. Piston rings, gas pressure, temperature, ring material, chemical durability, mechanical stiffness, gliding abilities, gas composition, lubricated or dry running, particles
7. Suction- and discharge compressor valves, plate material, design, gas composition, chemical durability, temperature, particles and pollutants
8. Lube oil in compressor crank case, because of its importance the lube oil will be examined separately. Parameters like temperature, particles, pollutants, durability, aging, chemical reactions, gas solubility, viscosity and miscibility have a great influence on lifetime and changing intervals.
9. Cylinder lubrication oil, gas pressure, temperature, gas solubility, particles and all oil parameters as described before.

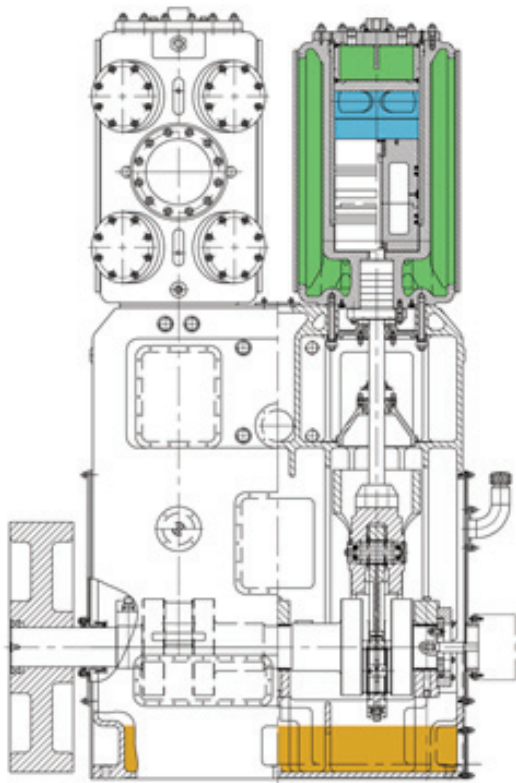


Figure 2.2: Cross section of a vertical compressor block

The parameters described show a great variety of influences on wear of compressor parts and on the compressor lifetime calculation. Certainly this list is not complete and a lot of possible parameters and factors may be added. The following chapters will concentrate on some detailed wear and failure processes and show some relevant examples.

3 Compressor engineering

A lot of all the reasons of unpleasant compressor operation (Fig. 3.1) originate in the basic engineering phase of the compressor design. Not only the compressor design engineer is responsible, but also the compressor part sub-suppliers sometimes cannot find the best solution for their customer.

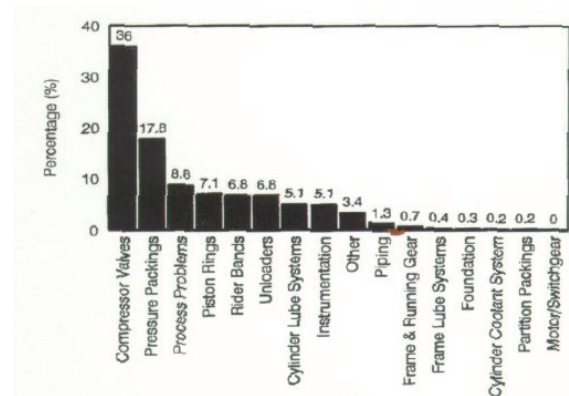


Figure 3.1: Causes of unscheduled compressor shutdowns [1]

Let us have a deeper look on the normal purchasing process of valves, packings, rings or other compressor parts. During the phase of a machine quotation all these parts have to be priced urgently and the technical offer is normally not as deeply specified as it should. If the compressor order is placed by the customer and the engineering starts, a correct specification is issued, and all customer data, like gas composition, operational situation, temperatures and pressures are the basis for a new inquiry. Engineering is late, sub-suppliers think they have already done their engineering in the project phase, and following this opinion the sub-suppliers often take their first offers, sometimes despite the updated technical requisition from the engineering department. This incomplete and wrong process nearly always leads to a later failure situation.

Sometimes also process data is missing from the customer side. Especially data like the humidity in gas compositions lead to wrong design of parts. The design engineer has to prepare carefully to ask for all these values during the design process. In some process situations, customers stick to their gas composition calculation, as real and measured data is not available. This situation may also lead to wrong material design and unnecessary operational faults after start-up.

The importance of this design phase is often not taken seriously. Parameters like temperature, lubrication oil or the gas composition lead to extensive wear in parts

Scientific Research Methods to Analyse Compressor Wear Parts and Lubricants

by: Thomas Heumesser, LMF

and operational misbehaviour of the compressor. Normally these causes for failures are very difficult to detect. Engineers and service staff do not take into account, that there might be wrong materials or incorrect parts in the machine. Reduced lifetime and service intervals show that something is wrong and the customer normally forces the supplier to find the reason.

4 Case studies of incidents in customer compressor units

The following practical examples show failure histories and explanations of chemical and mechanical root causes.

4.1 Extensive wear of piston rings in a non-lubricated gas compressor

At the customer site two non lubricated natural gas compressors work as pre-compression stage for a gas turbine power plant. Both machines are situated inside the power plant building and run under constant environmental conditions. (Fig. 4.1.1) Both are equipped with variable speed drive control and a rather sophisticated valve unloading logic to maintain a constant gas pressure for the gas turbine. The compressed gas is natural gas with a high methane content – Russian natural gas. The API618 compressors are horizontal with only one cylinder each.



Figure. 4.1.1: Natural gas compressor according API618

During the design phase no outstanding problems happened, the compressor wear parts were ordered from a well know manufacturer and the selection was done according to the technical and commercial view. Testrun, installation and commission needed a lot of time, as the adaption of the control philosophy had to be performed and tested to maintain the necessary parameters of the gas turbine. After the commissioning phase the compressors operated 4000h satisfactorily.

The first incident was detected shortly afterwards, much too early for any normal lifetime of internal compressor parts. Particles were observed in the discharge gas, but the gas at the suction side was clean and dry. The cylinder was disassembled and the view was very bad - markings in the cylinder liner (Fig. 4.1.2.), worn piston rings and a damaged piston rod packing. As there was no time at all to investigate any reason, the damaged parts were changed, the liner was grinded and the cylinder was re-assembled to maintain the operation shortly. Everybody knew that this was not the final solution and the technical reason had to be found urgently.

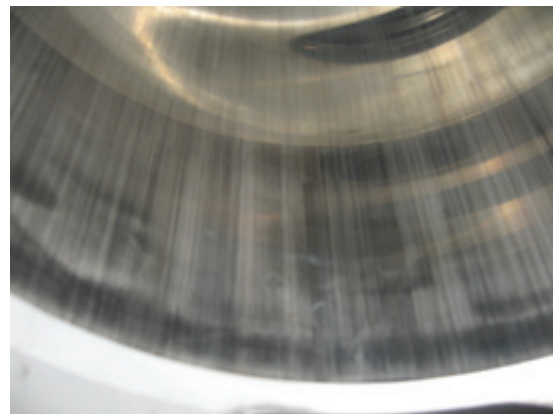


Figure. 4.1.2: Damaged cylinder liner with marks and scoring

A long discussion with the ring sub-supplier started. The normal “repair” strategy was to exchange the parts without any change and without any investigation of the root cause. Neither the end customer nor the manufacturer were satisfied with this proposal and an independent, profound technical study was agreed on. A material analysis with the RFA / XRF (X-ray fluorescence spectroscopy) method was performed. (Fig 4.1.3.)

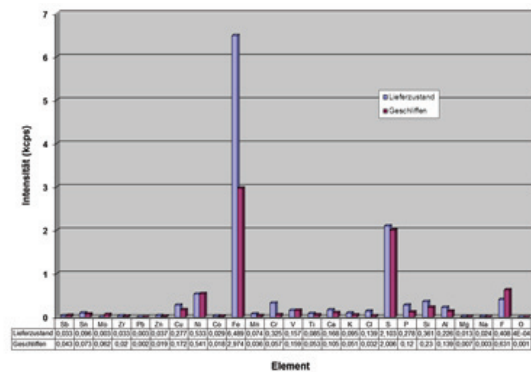


Figure. 4.1.3: RFA/XRF analysis of piston ring material

The result was some surprise – an excerpt of the test report showed the following: ... *the first test of the ring was done without cleaning in the delivered status. For the second test the surface was grinded to avoid any pollutants on the material. Iron, sulphur and flour were detected, the iron concentration was lower in the grinded sample, therefore surface pollution with iron may be expected. The ring material was explicitly confirmed as Teflon. Anorganic filling materials like MoS₂ as lubricant or calcium-aluminium-silicon oxide for better wear resistance or copper and bronze for better thermal conductivity were not found. The conclusion shows, that such a material was not appropriate for the use with high mechanical and thermal load of the ring. The delivered parts were the wrong ones for this use.*

The very bad performance was explained – the supplier did not believe, that such an investigation was done by the compressor manufacturer. He needed some time, but finally he confirmed our view and the customer got new and revised parts. Until now both compressors have been running without any further problems and have a better service interval than before. A real explanation for such a bad performance in design and execution of the rings could not be given by the sub-supplier.

4.2 Packing rings in extreme environmental conditions

Not only piston ring wear may create root cause histories, also packing rings may have similar problems. The described incident was even worse as a number of serial machines were affected and all the efforts to solve the problem had to be achieved in a non European country. (Fig. 4.2.1.)



Figure. 4.2.1: natural gas compressor station

To start at the beginning – suppliers were compared, technical data was checked, parameters were revised. The commercial decision overruled anything else, as a series of machines had to be equipped. The first set of the piston rod packing had excellent performance. The compressor is a three stage machine with two

cylinders, balanced opposed, high speed, lubricated and for natural gas. The guaranteed lifetime of the packings was one year permanent operation (8800h). The customer used wrong and not specified oil brands and extended the service interval until gas was smelled in the compressor building because of bigger leakage of the packings. Total service intervals reached up to 16000h. The customer was happy and the performance of these packings was really outstanding.

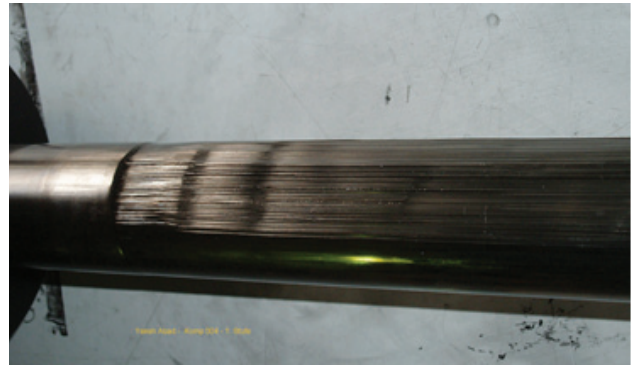


Figure. 4.2.2: damaged piston rod

How did all the trouble start? The packings had to be changed, even though the lifetime had been so good before. The “new” set of packings had a lifetime of 1000h until the first leakage and the gas smell were detected. The compressor had to be dismantled and the damage was bad. Not only the packing rings were worn and had to be changed, also the piston rod was “grinded” by the packing elements and had a smaller diameter. (Fig. 4.2.2) Any change of elements did not improve the situation. A long process of investigation started. Parameters like gas composition, oil quality, humidity, material use and technical changes were parts of this discussion. The packing supplier confirmed, that he had not changed anything, but severe doubts arose. Alternative methods were compared and a measurement and analysis program started. The following methods were used:

- FTIR (*Fourier transform infrared spectroscopy*) to analyse the base material
- RFA/XRF (*X-ray fluorescence spectroscopy*) and EDX (*energy dispersive X-ray spectroscopy*) to detect the elements in the material
- TGA (*thermogravimetric analysis*) of the quantitative content of the anorganic filling materials
- DSC (*differential scanning calorimetry*) to detect the thermal melting process of the material
- REM/SEM (*scanning electron microscope*) for the analysis of surface elements.

Scientific Research Methods to Analyse Compressor Wear Parts and Lubricants

by: Thomas Heumesser, LMF

The analysis was difficult to interpret as the individual result did not match completely and a chemical model followed as the next and final step:the damaged packing rings contain copper, tin and lead, all parts of the bronze inside the ring material. The main non metallic part is sulphur, also as PbS and CuS, (Fig. 4.2.3) sulphates do not exist as oxygen is missing inside the packing. The rings lost their outer shape and were attacked from the inner diameter side in such a way, that the metal structure disappeared and the open silicate fibres (Fig. 4.2.4) could grind the piston rod surface. The chemical mechanism is sulphur corrosion with humidity. The corrosion product is stored in the distances between the rings and glues the system together.

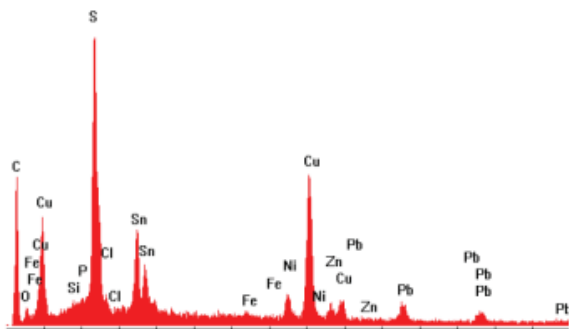


Figure. 4.2.3: EDX spectrum of the ring material to show all elements and their concentration

The packing design was changed and it was not visible, why the first set of packings had such a good performance. The claim was not ended and the discussions followed until the supplier admitted that there had been a change in the production location and apparently not all the information necessary had been transferred.

4.3 Compressor oil research

Research concerning compressor oils and the oil changing process during operation are a wide range for further investigations. Not only the lifetime of oil is relevant, also failure analysis of parts and particles in the lube oil may help and bring further knowledge. A public founded research project was started some years ago. In this project the analysis of new and used compressor oil was done for a lot of different brands. Frequent contaminations were studied as follows:

- Water in oil – measurement is very difficult, free water is mostly not dissolved and the sample is therefore not correct. Water is developed as condensate in interrupted compressor operation or due to extreme climate conditions.
- Oil mixture with wrong oil or old used oil, which is not cleaned before changing. Fast reaction and wrong operation.
- Coking – high temperature and failures in other parts (rings, valves, etc.) in lubricated services. Measurement methods to be adapted according the composition
- Particles, metal parts in oil – analysis of the particles and search for the origin of the particle to detect failures
- Solubility of compressed gas in oil. Probing and development of trends to find a theoretical basis and the prediction for new design.

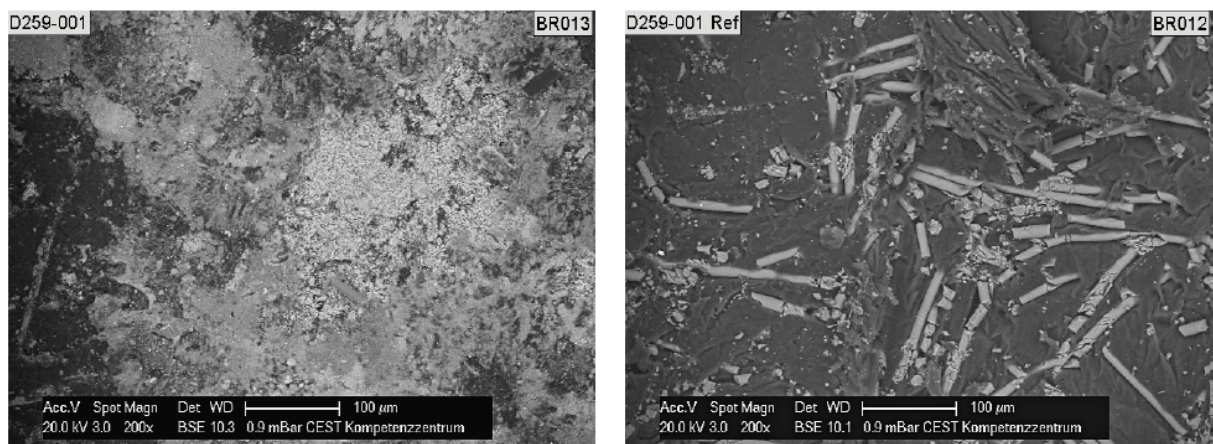


Figure. 4.2.4: Electronic microscope pictures following EDX spectrum, left: polymer with metal particles - right: polymer with filled fibres

4.4 Compressor oil measurement

The composition of lubrication oil may be analysed easily by the FTIR (*Fourier transform infrared spectroscopy*) method. The resulting diagrams are compared to find the differences in the measured oil composition.

The normal procedure for the analysis of used compressor lubrication oils includes the following values and methods:

- Viscosity
- Density
- Visual look, smell
- Water contents
- Acid contents / neutralisation value
- Wear, particles, additives,
- Infrared spectroscopy, oil aging, contamination

4.4.1 Oil contamination and wrong oil

During service of a three stage, two cylinder, V-shape compressor a bad oil condition was detected in the crankcase after 700h of operation after the last oil change. An oil sample was taken and the analysis started with normal methods, followed by an infrared spectroscopy. The correct oil filling is Rarus 827 synthetic oil, the spectrum showed no correct match. The first estimation was that maybe a mineral oil Rarus 429 was used, but the sample had a higher viscosity. (Fig. 4.4.1.) Finally the test result proved the use of a “wrong” and inappropriate oil brand.

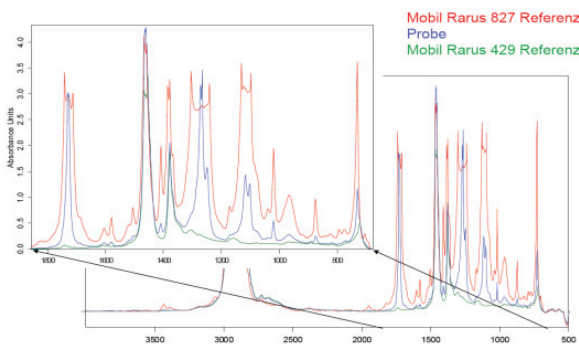


Figure. 4.4.1: FTIR spectroscopy with 3 different oils

4.4.2 Wrong oil mixture

Oil problems may happen at any customer’s. This time it was another customer with a similar

compressor unit. The compressor had already 44545h of operation at the customer site and the oil sample was taken at 4700h after the last oil change. The first analysis showed high water content and apparently some mixed oil composition. First estimation was a mixture of the original oil brand with an ester oil. The following FTIR spectroscopy proved the same result. (Fig. 4.4.2.) Ester peaks in the spectrum are clearly visible.

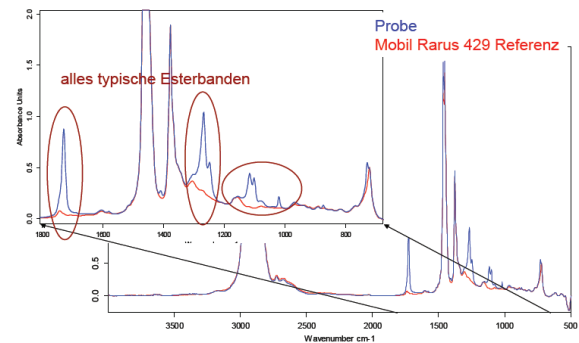


Figure. 4.4.2: FTIR spectroscopy with Ester peaks because of mixture with wrong oils

4.4.3 Use of wrong oil

This customer has two similar units in his production line. Both machines approximately had 5000h after the last oil change. The customer had claimed operational problems before and there was a permanent discussion about the oil quality. Bad oil quality is a risk for the machine operation and may influence any damage of other parts. To satisfy both the customer and the compressor manufacturer, a sample was analysed. (Fig. 4.4.3.) The result was not the one the customer expected, in the FTIR spectroscopy both oil fillings were found to be inappropriate.

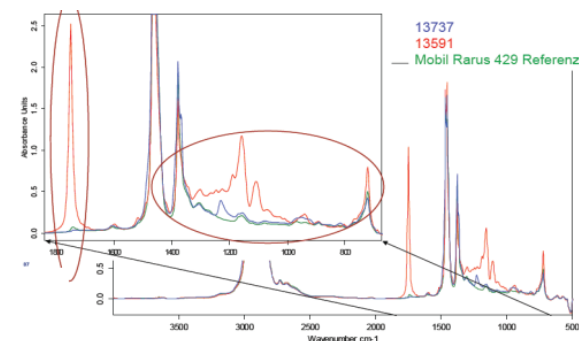


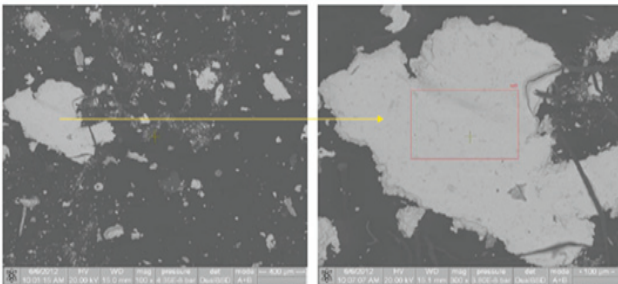
Figure. 4.4.3: FTIR spectroscopy with wrong oil brands on two similar machines

Scientific Research Methods to Analyse Compressor Wear Parts and Lubricants

by: Thomas Heumesser, LMF

4.4.4 Particle analysis in the oil filter

Particles in the oil flow are always a good possibility to detect wear and failure of compressor parts like bearings or the crosshead guiding. The correct point to analyse particles is the oil filter as all abrasion will be collected there. Both element- analysis and electro-microscopic investigation show metal particles. (Fig. 4.4.4.) Part size and number normally give an indication, if normal wear or any failure have to be examined. Interpretation is not easy, but the first indication is normally very important to trace any malfunction of a compressor. Each incident has to be decided case by case.



spt1: 92% Sn, 8% Cu

→ Weißmetall

Figure. 4.4.4: REM/SEM surface investigation together with EDX material analysis

5 Conclusion

As compressor manufacturer we have learned a lot. Evidently all these examples show positive conclusions, but during the fact finding process the situation was sometimes critical, the customer got angry, the solution lasted longer than expected and our claim management needed nerves. In the end, if an explanation is shown and a solution is near, the unit is running again and the lifetime of wear parts is in the range of a good and reliable compressor unit, the customer is satisfied and sometimes thanks the manufacturer for his effort.

All the described methods cannot be performed by the compressor manufacturer alone. Deep and detailed knowledge is necessary and scientific institutes and universities were involved in some of these conclusions and measurement cycles. In funded research projects European scientific cooperation helped to find better and easier ways to do the jobs. Also limited financial and technical resources were supported to help the compressor manufacturer in research and development.

The insufficient work and design for quotations at our sub-suppliers for compressor wear parts was also visible. More accurate and technically better offers

will help in the design process. All discussions during the design phase will never cost as much as any claim will do afterwards. Last but not least – a better acceptance and understanding of failures is preferred.

6 Acknowledgements

As already explained, scientific help was necessary in most solutions. The base research work for compressor oils, their use and their acceptance was mainly developed in a cooperation with the AC²T research institute in Austria and within the European COMET K2 project Xtribology.

References

- 1 S. Foreman, Compressor valves and unloaders for reciprocating compressors, DR, 2002
- 2 T. Heumesser, Fehler- und Schadensanalyse an Kolbenkompressoren mit Hilfe wissenschaftlicher Analysen von Materialien und Betriebsstoffen, 17. Workshop Kolbenverdichter, 2013, Kötter Consulting Engineers
- 3 T. Heumesser, M. Hauptkorn, Forschung Kompressoröle, Conference of the Austrian Tribologic Association (ÖTG), 2013
- 4 A. Grafl, M. Hauptkorn, Approval of the spare part lubricants - Selection process for oils, COMET K2 Project, Xtribology, 2012
- 5 OFI Technologie & Innovation, research and test project 310.108, 2008
- 6 J. Zbiral, TU Vienna, Institute of Chemical Technologies and Analytics, material test project, 2008

9th Conference of the EFRC September 11th / 12th, 2014, Vienna

Eliminating Excessive Lubrication

by: Alexander, Lee, CPI

-259-

Case Study: Community Noise Annoyance Mitigation with Intake / Exhaust Silencer Redesign *by: Broerman, Eugene L., Durke, Ray G., Baldwin, Richard M. Southwest Research Institute®*

-265-



EUROPEAN FORUM
for RECIPROCATING
COMPRESSORS

SESSION LUBRICATION



Eliminating Excessive Lubrication

by:

Alexander, Lee

Director of Technology, Technology Group

CPI

Houston, USA

lee.alexander@c-p-i.com

**9th Conference of the EFRC
September 11th / 12th, 2014, Vienna**

Abstract:

Under and over lubrication is quite often a result of improper manual adjustment of lubricator pumps. It is common practice to run “break in” lubrication rates for new or overhauled compressors. It is very often the case that the lubrication rates are not scaled back to normal levels, especially in remote locations.

CPI has developed a product that solves all of these problems by optimizing the amount of oil that is injected into a reciprocating compressor. A Smart Controller replaces the manual adjuster on a conventional lubrication pump and has the ability to automatically adjust the stroke length and hence the output of the pump.

The Smart Controller constantly monitors the quantity of oil cycling through the divider block via the signal from a no-flow shutdown device. When the quantity of oil delivered to the compressor unexpectedly changes the Smart Controller compensates for this, always ensuring an optimum lubrication level.

Eliminating Excessive Lubrication

by: Alexander, Lee, CPI

1. Introduction

There has been much improvement in the field of materials technology specifically with PolyTetraFluoroEthylene (PTFE) and PolyEtherEtherKetone (PEEK) mixed with various fillers. These advanced PTFE and PEEK based products have extended the wear characteristics and hence reliability of piston, rider, and packing rings.

Through improved modeling simulation we have a better understanding of the flow characteristics of reciprocating compressor valves and hence their life. All of these advancements can easily be diminished when one important aspect of the total reciprocating compressor operation is over looked; the lubrication system.

In many instances of poor reliability, reciprocating compressor wear components and valves are first looked at the root cause of the reduced life. In many situations the lubrication system and ultimately the amount of lubrication oil is not optimal for the application and run time is not optimized. The compressor needs to be viewed as a complete system and the interaction between all components is essential.

Compounding this fact is that oil is one of the highest costs associated with the operation of lubricated compressors. For the average compressor operator oil usage can average 25-30% of running costs.

Managing these costs in today's economic environment is more important as excessive lubrication erodes operator's profitability as well as impact the reliability of critical sealing components.

It is common practice to run "break in" lubrication rates for new or overhauled compressors for a period of around 200 hours after start up. This "break in" period prevents excessive temperature at start up, allows conformity of piston and packing rings to mating surfaces and allows debris to be carried away.

It is very often the case that the lubrication rates are not scaled back to normal levels, especially in remote locations. When operating a large fleet of compressors there is significant profit that can be gained through an optimum lubrication system.

There is also an added cost of having this additional lubrication oil in the gas stream; the longevity of coalescing filters can be greatly improved when lubrication oil rates are set to the correct levels preserving the life of the filters, again increasing the probability of an operation.

2. The Lubrication System

The compressor lubrication system has four (4) basic functions;

- Serves as a coolant
- Washes away particle matter and helps sealing
- Prevents corrosion
- Reduces friction

The importance of a correctly engineered lubrication system depends upon the following aspects;

- Compressor specification
- Gas application
- Type of oil

Each of these factors effects the lubrication oil requirements for a specific compressor application.

For reciprocating compressors two basic types of lubrication systems are employed to deliver correct levels of lubrication oil to the injection points, pump to point lubrication systems and divider block systems.

Either of these lubrication systems can be direct drive where lubrication gearbox crank rotation is driven by the compressor. This is advantageous for variable speed compressors as the quantity of oil automatically adjusts to the compressor speed. Alternatively the lubrication system can be independently driven from a motor; this is advantageous for pre-lubrication before compressor start up.

Figures 1 & 2 illustrates pump to point systems in which a lubricator gearbox holds individual pumps which are responsible for delivery of oil to each injection point of the compressor. As a result these lubricators are much larger to hold a higher number of pumps.

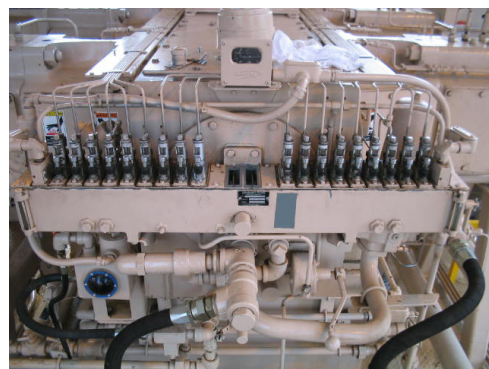


Figure 1: Center drive Pump to Point lubrication system

Eliminating Excessive Lubrication

by: Alexander, Lee, CPI

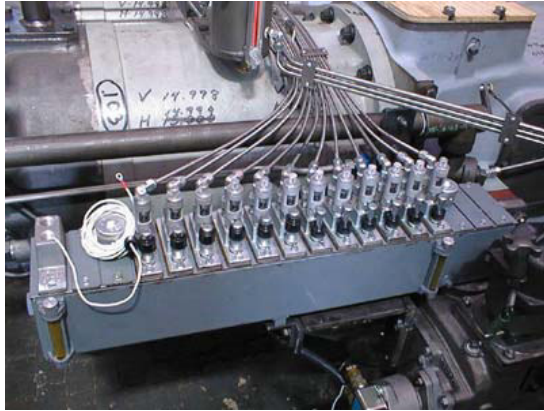


Figure 2: Right-hand drive Pump to Point lubrication system

The advantages of a pump to point system are summarized below;

- Gearbox cam speeds are much slower resulting in less wear.
- Individual flow rates are easily adjustable without affecting other pump outputs.
- Individual pump unit failures do not affect other pump units.

The disadvantages of a pump to point system are summarized below;

- Difficult and costly to monitor each individual pump output accurately.
- Difficult to shut down the compressor
- Difficult and costly to add pressure gauges on the outlet of each pump assembly.
- Sight glass drip rates are not a perfect measurement of actual pump output.

Figure 3 illustrates a divider block lubrication system which consists of a single block or multiple divider blocks which are each a single line hydraulic circuit.

Each block has a minimum of three elements with a total of six (6) outputs. The block receives the lubricant at the inlet and divides it between the individual lube injection points on the compressor or engine.

Secondary divider blocks, located on or near the compressor cylinders, can be supplied with lubricant from a master divider block to further divide the lubricant between the various lube points.

Precise delivery rates to each cylinder and packing lube point are achieved by the use of various sized pistons in the differing divider block elements.

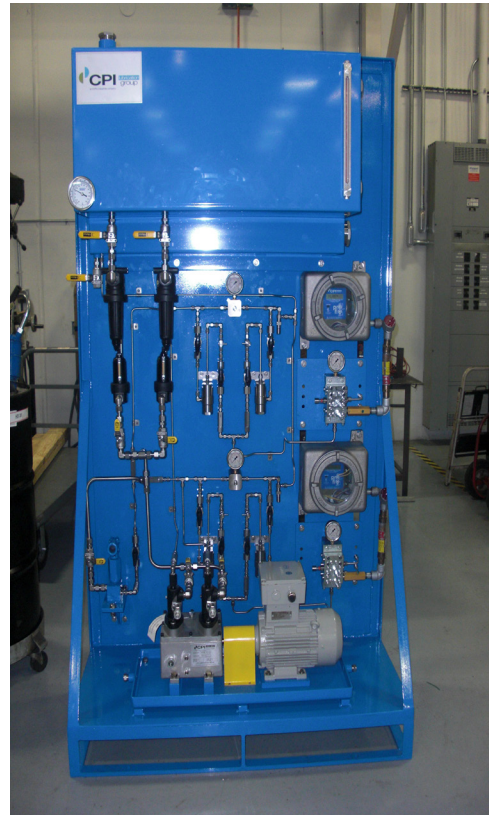


Figure 3: Complete Divider Block lubrication system



Figure 4: Divider Block component with lubrication monitor and shut down device

The advantages of a divider block lubrication system are summarized below:

- Only one divider block element needs to be monitored to assure proper operation of the entire lubrication system. A no-flow device can monitor the supply of compressor lubrication oil and shut the compressor down if insufficient oil is delivered to the compressor as illustrated in Figure 4 above.

Eliminating Excessive Lubrication

by: Alexander, Lee, CPI

- Output monitored at the divider block is a true measurement of the quantity of lubricant delivered to each point on the compressor.
- Only one or two pumps are responsible for the pressure and output of every lube point.

The disadvantages of a divider block system are summarized below:

- Camshaft speeds are higher with less gearing resulting in more potential wear and tear on drive train components.
- Balancing valves must be used when pressure differentials between lube points exceed 55 to 83 bar (800 to 1200 psi).
- Individual divider blocks must be reconfigured in order to change individual flow rates.

Although both systems have their respective advantages and disadvantages, the most critical aspect of their design is controlling the quantity of oil that is delivered to both the running surfaces of the piston rod and the cylinder liner.

3. Compressor Lubrication Rates

Under normal circumstances oil should be evenly applied to a film thickness of about 0.002 inches on the surfaces that will see a mating counter surface. Lubrication rates are required to be calculated for both the cylinder and piston rod independently. Lubrication rate formulas for both the cylinder and rod have the same structure but with differing constants.

At the simplest level, the base quantities of oil are calculated based on the following compressor parameters;

- Cylinder Diameter (D_{cyl})
- Stroke (S)
- Speed (RPM)
- Cylinder Rate Constant (C_1)

Cylinder Lubrication Feed Rate

$$= D_{cyl} \times S \times RPM \times C_1$$

Additional factors need to be applied to these base rate calculations depending on the compressor application;

- Cylinder discharge pressure factor (F_p)
- Molecular Weight of Gas factor (F_s)
- Particulate in the Gas factor (F_l)
- Lubrication Oil grade factor (F_o)

Cylinder Lubrication Feed Rate =

$$D_{cyl} \times S \times RPM \times C_1 \times F_p \times F_s \times F_l \times F_o$$

All of these factors have an effect on the viscosity of the oil and the ability to be able to lubricate effectively. Once the total amount of oil has been calculated this needs to be split between the number of injection points.

For a long period of time the quantity of oil was split equally between the multiple injection points of the cylinder or packing case. More recently there has been an adoption of providing an increased amount of oil to the upper or top cylinder lubrication point and the higher pressure end of the packing case. If this methodology is applied, typically two thirds of the total quantity is applied to the top of the cylinder and to the high pressure end of the packing case.

4. Effects of Over and Under Lubrication

Delivering the correct amount and grade of oil to the proper points for rod packing and piston & rider rings is a prerequisite for compressor reliability. If too little oil is applied this can result in increased temperature and accelerated wear of seal and wear rings. If excessive wear occurs, this can lead to secondary damage including scuffing or scoring to more expensive cylinder components such as the piston rod and cylinder liner.

Excessive lubrication is equally if not more damaging to reciprocating compressor sealing component reliability. Too much lubrication oil in the cylinders can lead to valve sticktion. The oil between the valve sealing elements and the seat can lead to delayed opening of the valves. The delay in the opening allows the pressure to increase within the cylinder which causes the valve to open with a higher than normal impact velocity and increased stress to all the sealing elements.

Eliminating Excessive Lubrication

by: Alexander, Lee, CPI



Figure 5: Reciprocating compressor valve with signs of excessive cylinder lubrication.

Hydraulic locking is caused when there is excessive lubrication oil in the packing case and the packing ring sets do not have enough side clearance in the cups. This in turn causes increased heat and the packing rings to extrude and fail.



Figure 6: Reciprocating compressor packing case rings with signs of excessive lubrication.

5. The Importance of Maintaining Consistent Lubrication Rates

The lubrication system itself has moving components that can see wear and lead to under lubrication of the compressor. The two major sources of wear in the lubrication system are the lubricator positive displacement pump and divider block element piston. When the pump starts to wear its output decreases and the quantity of oil delivered into the system reduces. For a pump to point system this decreases the quantity of oil for a single injection point. In the case of a divider block system it decreases all the injection points associated with that pump but to each to a lesser extent. When a divider block element wears the oil will be distributed to the point of least

resistance. This can cause a lubrication injection point of a higher pressure to be under lubricated and a lower pressure injection point to be over lubricated¹.

6. Solving the Excessive Lubrication Problem

The manual adjuster on a conventional lubrication pump is replaced with a Smart Controller, it has the ability to automatically increase or decrease the output of the pump by adjusting the stroke length of the pump. Traditionally operators have to remove the rubber boot and screw the manual adjustment in or out adjusting the stroke of the pump while watching the changes in cycle time.

The Smart Controller is installed in a CPI pump and monitors the amount of oil injected into the compressor through the use of a signal feedback loop from a No Flow device or Captured Proximity Switch that is installed on the lubrication system divider block. The frequency of the pulses from the No Flow device or captured proximity switches informs the Smart Controller as to the change in quantity of oil.

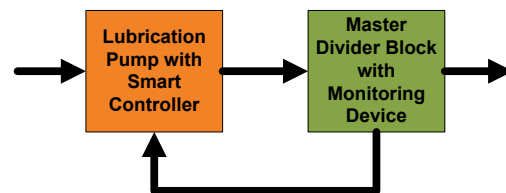


Figure 7: Illustrating the feedback to the Smart Controller from a master divider block with a monitoring device.

The Smart Controller is setup quickly through the configuration of the following four key parameters;

1. The divider block cycle time set point; this is the ideal number of seconds that it takes a divider block to cycle with the optimum level of lubrication being delivered to the compressor.
2. The lubrication break in hours; this is the number of hours that typically an increased amount of lubrication oil is delivered to the compressor. This ensures at start up that excessive heat is not generated and material from conformity of sealing rings.
3. The lubrication break in factor; this is the level at which the lubrication oil is increased during break in.
4. The divider block element total; this allows the quantity of oil consumed to be calculated.

Eliminating Excessive Lubrication

by: Alexander, Lee, CPI



Figure 8: Illustrating an example Smart Controller which replaces a traditional pump flushing unit.

After the initial flow optimization is made the Smart Controller continually monitors the cycle time and makes appropriate adjustments. If debris or foreign material is introduced into the lubrication system which causes wear to the pump and the output decreases the Smart Controller can make adjustments to maintain the cycle time. If significant adjustments have to be made signaling severe damage to the lubrication a warning can be generated to notify the operator.

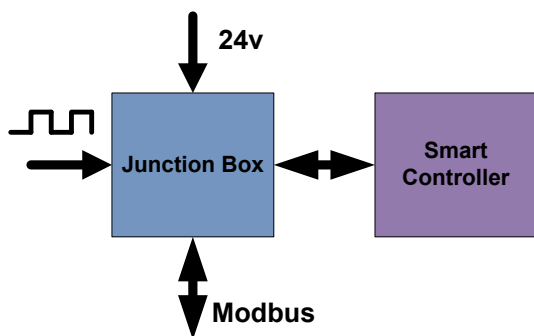


Figure 9: Illustrating the connectivity of a Smart Controller unit.

The Smart Controller presents status and alarm information via the Modbus 485 protocol that can be fed into an existing compressor panel or SCADA system to provide compressor operators real time lubrication data.

The Smart Controller has the option to shut down a compressor in a complete no flow condition ².

7. Conclusion

Ensuring the correct level of lubrication oil is supplied to a reciprocating compressor is key to achieving the maximum possible life of critical sealing parts including packing rings, piston & rider rings and valves. Both under and over lubrication can degrade the overall reliability of the reciprocating compressor.

Lubrication systems are typically passive and they only have the ability to provide the status of the system at a given point in time. Pumps with Smart Controllers have extended the capability of lubrication systems making them active. It provides the ability to decrease the level of lubrication oil when transitioning from break in rates to normal rates. In addition it increases lubrication oil levels if the flow is compromised, so the reliability of critical sealing parts is not compromised.

8. Acknowledgements

Robin Wilson – CPI Global Technical Advisor

References

¹ Alexander, Lee (2013): Eliminating Excessive Compressor Lubrication; CompressorTech 2, November 2013.

² Alexander, Lee (2012): Reciprocating Compressor Lubrication Systems need fine tuning; CompressorTech 2, June 2012



New Approach for a Smart Compressor Lubrication System

by:

Matthias Kornfeld, Bernhard Spiegl, Bernhard Fritz
Research & Development
HOERBIGER Ventilwerke GmbH & Co KG
Vienna, Austria
matthias.kornfeld@hoerbiger.com

9th Conference of the EFRC
September 11th / 12th, 2014, Vienna

Abstract:

Awareness of the deficiencies of today's cylinder lubrication systems has been growing in recent times. Economic as well as environmental concerns call for the lubrication rate to be kept as low as possible while not sacrificing compressor reliability. However, common lubrication systems are lacking in accuracy and versatility.

This paper describes the development of a new "smart" lubrication system based on single-point electromagnetically actuated oil injectors fed from a pressurised manifold and controlled by a central unit.

With built-in flow monitoring and temperature control, the new injectors deliver oil accurately and repeatably. A two-way link to a central control unit provides excellent diagnostics, fault tolerance, and the ability to adjust lubrication rates automatically as required, for instance an increase when "running in" or a reduction when operating at part load. The result promises to be more reliable and flexible lubrication, yet with lower oil consumption. The new system has been tested successfully on a real compressor.

We also briefly discuss research into understanding the fundamentals of compressor lubrication. Replacing the current empirical approach with sound theory, perhaps coupled with the new system's ability to inject oil at a precise crank angle, may further reduce oil consumption without compromising reliability.

New Approach for a Smart Compressor Lubrication System*by: Matthias Kornfeld, Bernhard Spiegl and Bernhard Fritz, HOERBIGER***1 Introduction**

Compressor lubrication is a vital yet neglected area. Recent research and development has yielded rings, packing and valves with greatly improved performance and durability. Lubrication systems for cylinders and packings, meanwhile, have not kept pace.

Every operator knows that proper lubrication of cylinders and packings is essential to the reliable operation of the great majority of reciprocating compressors. Despite this, however, over- and under-lubrication remain common. It has been said that 80% of all compressor failures are caused by improper lubrication [1]; field reports indicate that this is an exaggeration, but lube issues are certainly frequent.

There are plenty of reasons not to over-lubricate. With a typical consumption of 5–8 l/day, oil can account for 25–30% of the running costs of a compressor in terms of spares and consumables [2]. Excess oil can cause valves to stick, and oil carryover may damage catalysts and other sensitive processes downstream. Where oil is removed from the gas stream, disposal of used filters has both financial and environmental costs.

Yet the serious consequences of under-lubrication, coupled with the variability and unreliability of current lubrication systems, provide a strong incentive to over-lubricate. It is probably fair to say that most compressors today run over-lubricated.

This is often down to the lack of flexibility available from current lubrication systems. For instance, when a compressor is new or has been recently overhauled it is common practice to double the lubrication rate during the “running-in” period. Once running-in is complete, the lube rate should be reduced to its normal value. Unfortunately this is often not done, especially for compressors in remote areas or large fleets, because of the complexity of adjusting oil flowrates with conventional lube systems. As a result, the compressor spends most of its life running over-lubricated.

Another example is that a compressor running at part load need less oil. Conventional lube systems are not good at adjusting oil flow to suit the operating conditions, so again over-lubrication is the result.

This paper describes the development of a lubrication system that can reduce oil use, control it accurately, and provide monitoring, flexibility, and confidence over a wide range of operating conditions and oil types.

2 Old and new approaches to lubrication**2.1 Current lubrication systems**

For decades, every reciprocating compressor has used one of two basic lubrication system types [3]:

- pump-to-point;
- divider block.

Both are driven either directly from the compressor or by an independent electric motor.

The pump-to-point system consists of a set of metering pump modules, each feeding a single lubrication point. The pump modules come in different sizes and pressure ratings. A sight glass is usually the only method of adjusting the oil drip rate.

The divider block systems uses a single adjustable pump with one or more divider blocks, each of which diverts oil in turn to a single lubrication point for a preset period. Volumetric accuracy tends to be poor.

Both systems are purely mechanical. They must be fitted with no-flow devices to shut down the compressor in the event of lubrication failure, and they are difficult to adjust for changes in operating conditions.

2.2 Common-rail systems

If the oil injection point could be made “smarter”, it would be possible to separate the two functions of pressure generation and metering. This would bring many advantages in terms of metering accuracy, flexibility and reliability.

The idea is nothing new: it is standard technology in the fuel systems of modern car engines. In a typical engine injection system, a high-pressure pump feeds a number of injectors via a so-called “common rail”, a manifold which also acts as a reservoir of high-pressure fuel.

New Approach for a Smart Compressor Lubrication System

by: Matthias Kornfeld, Bernhard Spiegl and Bernhard Fritz, HOERBIGER

Conventional diesel injectors are designed for tens of millions of injection cycles at pressures up to 1,800 bar. They are therefore an obvious starting point for the development of a common rail system for compressor cylinder lubrication.

A first demonstrator design consisted of two standard automotive injectors embedded in a carrier block. This was tested on the second stage of an atmospheric air compressor (Figure 1).



Figure 1: Demonstrator for a common rail injector system (left) and compressor installation (right).

With this rig we were able to prove the basic workability of common-rail injection for compressor lubrication. However, we identified several problems with the use of automotive injectors:

- standard diesel injectors are too large for convenient use as oil injectors;
- the necessary independent safety features cannot be retrofitted;
- use in explosive atmospheres is not possible;
- the cost of extensive modification would not be economically justifiable.

It was therefore clear that we would have to develop a purpose-designed injector.

3. Requirements for injectors

3.1 Comparison of electric actuators

For compactness and low cost, the actuator needs to be fully electric. Hydraulic systems would be too bulky and complex for this duty.

Many operating principles are available for electric actuators [4], including:

- piezoelectric actuators;
- solenoids;
- linear motors;
- Lorentz force actuators.

The requirements for a practical cylinder lubrication injector are:

- maximum injection frequency 1 Hz;
- minimum injection timing 1 ms;
- must withstand typical compressor vibration levels;
- suitable for explosive atmospheres;
- able to handle different grades of oil;
- leak-free up to 300 bar;
- maintenance intervals of 48,000 hours;
- high reliability.

It soon became clear that only two operating principles – piezoelectric actuators and solenoids – would be suitable for this duty.

3.2 Piezoelectric actuators

Over the last 10 years actuators based on piezo ceramic stacks have become widely used in the automotive industry for high-pressure fuel injection. They exhibit inherently high actuation speeds, good energy efficiency and high accuracy. A typical piezo stack 30 mm long can achieve stroke lengths of about 50 μm . To reach a few tenths of a millimetre – the stroke length needed for a compressor lubrication injector – would accordingly require taller stacks or the use of hydraulic amplifiers [5].

However, standard automotive piezo actuators have two drawbacks. First, they are comparatively expensive.

Second, they have a characteristically tall, narrow shape which is not ideal for use in a compressor environment. This shape derives from both the height of the piezo stack and the need to compensate for thermal expansion. Instead of coupling the actuator directly to the injection needle, the design includes two separate circuits for high and low pressures, respectively. This compensates for thermal expansion, as well as amplifying the stroke, but at the cost of extra height.

New Approach for a Smart Compressor Lubrication System

by: Matthias Kornfeld, Bernhard Spiegl and Bernhard Fritz, HOERBIGER

3.3 Solenoids

Solenoids are characterised by simple design and low costs. Over short distances they can achieve high forces, and their dynamic behaviour is adequate for lube injectors.

In many applications the use of solenoids is restricted by heat generated as a result of eddy currents and ohmic losses. Since the solenoids needed for lube injectors are small and do not have to operate at high frequencies, eddy currents and hence heat generation are not a significant problem.

Even though piezo actuators are technically superior to solenoids, the latter can meet all the design requirements at much lower costs than those of piezo actuators. Solenoids were therefore chosen as the basis for the new smart cylinder lubrication system.

4. The new system in detail

4.1 System overview

The new compressor-specific cylinder lubrication system is based on a smart combination of a solenoid-powered injector with embedded flow metering and 2-wire digital communications, a central control system, a reliable oil pump and a high-pressure common rail (Figure 2).

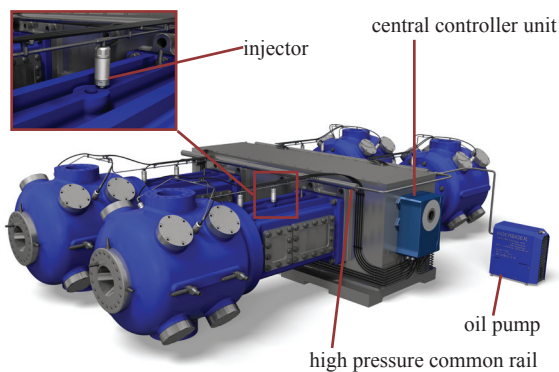


Figure 2: Schematic of an electromagnetically actuated common rail lubrication system.

The oil pump is the simplest of these components. Hydraulic lube pumps are standardized units used in many industrial applications; the only particular requirements for our application are high reliability and a relatively high operating pressure (300 bar). Accordingly, the new system can use either the compressor’s existing crankshaft-driven lube pump or an external pump. The latter has the advantage that lubrication can begin before the compressor is started.

The injector and control system, which are much more demanding, are discussed in detail in the following sections.

4.2 Injector solenoid

The injector is at the heart of the new lubrication system. In designing a reliable actuator for the injector, the challenge is to minimise both magnetic losses and damping – the latter caused by the presence of oil between the solenoid and the corresponding anchor plate.

Since these two objectives influence the design in opposite directions, careful optimisation that also takes costs into account is the key to a suitable commercial design (Figure 3).



Figure 3: Injector design: prototype (left) and serial version (right).

The solenoid has to be designed for use in a range of different oil types, and to provide sufficient force for injection pressures up to 300 bar.

4.3 Embedded flow sensor

Accurate flow monitoring at every lube point is key not only to minimising oil use but also to increasing the reliability and safety of the whole lubrication system.

The injector therefore contains an integrated flow sensor capable of detecting lube rates down to 0.5 drops (0.025 ml) per injection, independent of oil viscosity, temperature and injection pressure. Linked to the main controller via an embedded signal processing module in the injector, with real-time feedback, this allows sophisticated control and safety strategies to be applied.

New Approach for a Smart Compressor Lubrication System

by: Matthias Kornfeld, Bernhard Spiegl and Bernhard Fritz, HOERBIGER

4.4 Integrated check valve

A necessary component in any type of compressor lubrication system is a check valve to ensure that no process gas is pushed back into the supply line. Without a check valve, gas can collect in the pump and cause it to fail.

The check valve used in the new lubrication system is of the soft-seat type, integrated into the injector and mounted so that it is permanently filled with oil to guarantee proper sealing.

With pressurised oil in the supply line right up to the injector needle, the injector delivers maximum reliability regardless of mounting position by preventing gas aggregation in the injector and dry running of the check valve seal.

4.5 Temperature management

Once the oil has been injected, its effectiveness as a lubricant depends to a considerable extent on its viscosity. Especially during startup, high oil viscosity due to low ambient temperatures can hinder good lubrication.

To counteract this, a small current can be passed through the solenoid to warm the oil before injection. Obviously the current has to be low enough not to actuate the injector.

A temperature sensor with close thermal coupling to the oil reservoir in the injector provides feedback to the main controller unit, allowing the system to optimise the temperature and thus the oil viscosity.

4.6 Two-wire installation

The key to simple installation is to keep the number of wires as low as possible. Conventional wiring for the injector's power supply, flow sensor and temperature sensor would require at least six wires.

Using embedded electronics for signal processing and communicating with the main control unit, we can reduce the number of wires to just two. The resulting 8-bit digital signal (Figure 4) not only lowers cabling costs but also reduces the risk of electromagnetic interference, which is a common problem in the vicinity of compressors and their drivers.

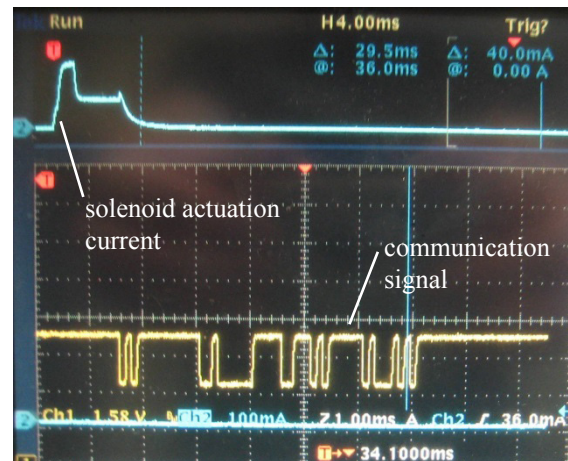


Figure 4: 8-bit communication signal between injector and main control unit.

4.7 Control philosophy

The main control unit is the “brain” of the lubrication system, actuating the injectors mounted at each lube point and processing the feedback signals from the sensors.

The use of microprocessor-controlled injectors, a freely programmable controller and a bus interface for status and data communication offers new flexibility in changing lube rates during operation – something that is hard to realise with existing mechanical systems.

The controller also has a couple of external signal inputs that could be used to monitor temperatures or pressures elsewhere on the machine, or even the crank angle. These allow sophisticated control and safety strategies to be implemented, and even equip the new lube system with the basic functions of a compressor monitoring system. In conjunction with an optional wireless interface and modern remote access applications this offers new opportunities in controlling and monitoring whole fleets of compressors.

The use of a TDC sensor would also allow oil to be injected at a precise point in the cycle. So far we have not shown any advantage in doing this, but it is an interesting possibility for the future (see below).

New Approach for a Smart Compressor Lubrication System

by: Matthias Kornfeld, Bernhard Spiegl and Bernhard Fritz, HOERBIGER

5. Ensuring reliability

Failsafe operation is the most important prerequisite for any lubrication system.

Lubrication failure will result in increased surface temperatures, massive wear and immediately secondary damage such as scuffing or scoring of expensive piston rods and cylinder liners. Excessive lubrication can be equally damaging, leading to oil stiction of the valves and hydraulic locking in the packings.

Reliable monitoring of the lube system, preferably on the basis of more than one independent feedback signal, is therefore essential.

The injector itself directly provides two important monitoring functions: detection of injector needle motion via solenoid coil current feedback, and oil flowrate from the built-in sensor.

An additional pressure sensor can be installed in the oil supply rail and connected to the control unit via one of the additional signal channels. This allows monitoring of the oil supply pressure, while analysis of pressure spikes in the supply rail can confirm that the injectors are opening and closing correctly.

Smart combination and processing of these different feedback signals maximises safety while simplifying the process of detecting and identifying failures. The control unit can thus distinguish several failure modes:

- lube pump failure;
- injector solenoid failure;
- blockage of supply line or injector;
- leaking injector; and
- leaking supply line.

This in turn offers the possibility of adaptive behaviour in the event of a partial system failure. On a large compressor with more than one lube point per cylinder, for example, the failure of a single injector need not trigger an immediate shutdown. Instead, the remaining injectors could increase their oil flowrates automatically to make up for the loss.

6. Testing

6.1 Workshop tests

While it is of course essential to test the system on a real compressor, this is of limited value when it comes to emulating the failure modes of the various components and testing different designs (such as varying the number of injectors or experimenting with different oil types and pressures).

We therefore developed a test rig (Figure 5) that works with a variety of injector designs and operating conditions, and can emulate various component failures. This proved to be a valuable tool during the development phase, allowing us to carry out the first functional tests of the injector and the controller electronics, vary the parameters, optimise the injector mechanics and electronics, and run endurance tests.

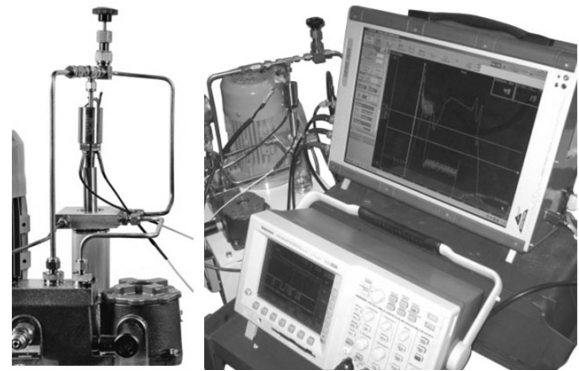


Figure 5: Lube system test rig.

6.2 Compressor tests

The first test on a real compressor was done on our in-house test compressor. The new system was installed to provide cylinder and packing lubrication for the second stage (Figure 6).

The existing crankshaft-driven lube pump was used to feed the common rail. The injectors were controlled by a prototype of the main controller electronics, which at this stage was already capable of communicating with the injectors and modulating the amount of oil injected according to an external load signal.

New Approach for a Smart Compressor Lubrication System

by: Matthias Kornfeld, Bernhard Spiegl and Bernhard Fritz, HOERBIGER

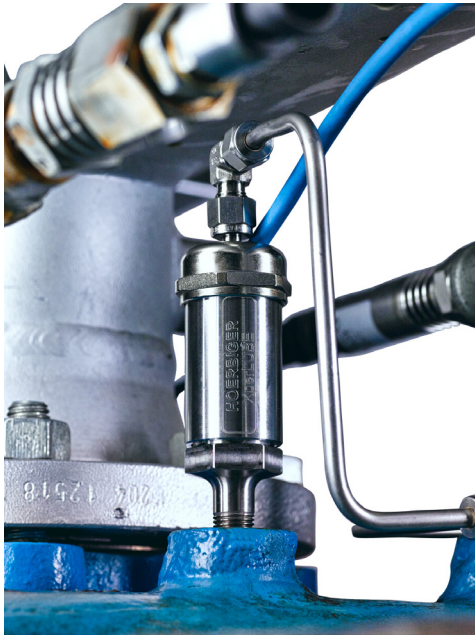


Figure 6: Compressor installation: lube point 1 on the second-stage cylinder.

So far this first test has proven the practicability and reliability of the new system.

7. Systems comparison

Obviously no field reports are yet available for injector-based lubrication systems, and there are only a few reliable datasets comparing the performance of different existing lubrication systems. The following comparison is therefore based on datasheet values and technical features. Due to the variety of possible lubrication system configurations, we do not claim that this comparison is complete; it is intended simply as an overview.

Table 1 compares the features of two typical current lubrication systems against the injector system. The “standard” conventional system is based on a divider block equipped with a no-flow device, but without any monitoring capabilities. The “high-end” version is a pump-to-point system in which each line is equipped with an automatic pump adjuster and lube rate monitoring device; its functionality approaches that of the injector system.

The flexibility to change lube rates independently for each lube point is an advantage. The injection system can do this at much higher frequency than is possible with the high-end conventional system. With a standard conventional system it is only possible to change individual lube rates by adjusting the divider block setting, which entails a lot of work and is only

possible during compressor shutdowns; at other times it is limited to changes in lube rate for all the lube points at once.

When it comes to metering accuracy, the injector system benefits from embedded flow sensors with a resolution of a few tens of microliters (around 0.5 drops), compared to standard flow monitoring devices with a resolution of around 10 mL (200 drops).

This inherent gain in accuracy is reinforced by the ability of the injector system to provide closed-loop control of flowrate for each lube point. The position of the injector close to the lube point brings a further advantage with respect to matching the injection timing precisely to the crank angle.

In the case of the injector system, more responsive and more accurate flow monitoring ultimately yields much better ability to detect lubrication failures.

	Standard system	High-end system	Injector system
Flexibility of changing lube rates	–	+	+
Injection accuracy	○	○	+
Accuracy monitoring	--	○	+
Response time of the flow sensor	--	○	+
Failsafe operation	○	+	+
Failure detection	–	○	+

Table 1: Comparison of different lubrication systems.

8. Summary and outlook

As the new lubrication system enters field testing and approaches commercial production, progress to date has been very promising.

At last, compressors have lubrication technology whose sophistication matches that of modern valves, packings and monitoring systems. The new system is more accurate, and above all more reliable, than current all-mechanical systems based on divider blocks or individual metering pumps. It is also much more flexible in terms of adapting to changes in compressor operating conditions, diagnosing faults and mitigating the consequences of partial failures.

New Approach for a Smart Compressor Lubrication System

by: Matthias Kornfeld, Bernhard Spiegl and Bernhard Fritz, HOERBIGER

Looking further ahead, another way to reduce oil consumption may result from a better understanding of compressor lubrication. Up to now, very little is actually known about the transport mechanisms in the cylinder and packings that control oil consumption. The formulas currently used are semi-empirical, with the typical form:

$$Q = D n s K$$

where the lube rate Q in principle only depends on the bore diameter D , the speed n , the stroke s and an empirical constant K which varies significantly between compressor manufacturers.

A theory of compressor lubrication based on first principles might allow us to minimise the lubrication rate without sacrificing reliability.

Such a theory would have to take into account effects like evaporation as well as the complex elasto-hydrodynamic interaction between the thin oil film itself and the cylinder liner, rider rings and piston rings (Figure 7).

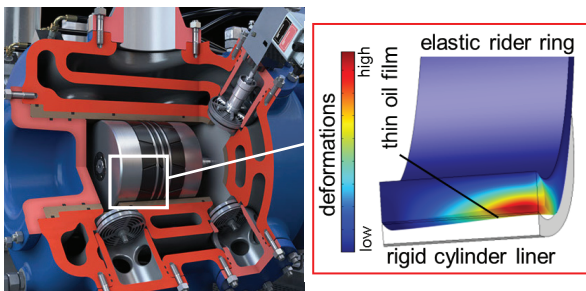


Figure 7: Deformed rider ring due to elasto-hydrodynamic interaction with the oil film

Our first simulations of the oil transport mechanism, based on the motion of the piston and the elasto-hydrodynamic interaction between the rings and the oil film, have yielded promising results that form a first step towards a new understanding of compressor lubrication theory. In further work we plan to consider the effects of oil evaporation, surface roughness, and oil transport driven by the gas flow during suction and discharge, and to validate our models on a test rig.

The ability of the new system to inject oil at a precise point during the stroke is an interesting possibility here.

References

[1] Antwerp Lion Oil Works N.V., *Compressor lubrication products – up to 525bar*; www.lionoil.be, 20.02.2014

[2] Lee, A., *Reciprocating compressor oil systems need fine tuning*, *CompressorTech Two*, June 2012, 32–36

[3] Hanlon, P. C., *Compressor Handbook*, McGraw-Hill, 2001

[4] Spiegl, B., Dolovai, P., Lindner-Silwester, T., *New concept for electrical stepless compressor capacity-control system*, 2012, 8th EFRC conference, 192–201

[5] Heywang, W., Lubitz, K., Wersing, W., *Piezoelectricity – Evolution and Future of a Technology*, Springer-Verlag, Heidelberg, 2008



Maximize Reliability, Availability & Profitability with Ariel API 618 Process Compressors



**WORLD STANDARD
COMPRESSORS**

With more than 19,000 possible frame and cylinder configurations for API 618 process service, Ariel compressors can be designed and built to maximize your unique process operation. Ariel has been producing durable, low-maintenance reciprocating compressors since 1966 and API 618 compressors since 1999. Ariel offers high quality compressors that ensure long continuous run-times.

Visit www.arielcorp.com to find an Ariel Process distributor in your region.

9th Conference of the EFRC September 11th / 12th, 2014, Vienna

Case Study: Community Noise Annoyance Mitigation with Intake / Exhaust Silencer Redesign by: *Eugene L. Broerman, Ray G. Durke, Richard M. Baldwin; Southwest Research Institute®* -277-

Integrity Evaluation of Small Bore Connections (Branch Connections) by: *Chris B. Harper, Beta Machinery Analysis* -284-



EUROPEAN FORUM
for RECIPROCATING
COMPRESSORS

SESSION PULSATION 2

SOUTHWEST RESEARCH INSTITUTE®

Case Study: Community Noise Annoyance Mitigation with Intake / Exhaust Silencer Redesign

by:

Broerman, Eugene L., Durke, Ray G., Baldwin, Richard M.
Southwest Research Institute®
San Antonio, USA
EBroerman@swri.org

9th Conference of the EFRC
September 11th / 12th, 2014, Vienna

Abstract

An evaluation of community noise/vibration annoyance was commissioned to identify the causes of complaints from residents living near a compressor station and to develop potential modifications for mitigation. Rather than process piping pulsations causing the problem, a less common problem source was identified. Elevated pulsation levels from both the intake and exhaust manifolds coupled into the atmosphere and were present at frequencies below the range of human hearing, but were determined to be the most likely cause of rattling window panes, doors, cabinets, etc. The pressure pulsations originated inside both the inlet and exhaust manifolds of one particular type of engine at the nearby compressor station. Field measurements identified the pulsation characteristics at the residences, identified the pulsation characteristics within the engine manifolds, and provided data for correlation with acoustic models. The models of both the inlet and exhaust piping systems predicted that the existing silencers allowed unfiltered low frequency pulsation (pressure fluctuations) to pass into the atmosphere at the same frequencies as the elevated sound pulsation frequencies measured at the residences. New silencers were designed that reduced the coupling of the engine manifold pulsations to the atmosphere at both the intake and exhaust. This paper will describe the field measurements used to diagnose the problem and identify the source; a pulsation analysis and silencer redesign; and follow up field measurements to assess the quality of the redesign.

INTRODUCTION

Southwest Research Institute® was contracted to investigate complaints of rattling and shaking of windows, doors, cabinets, etc., from residents living near a gas transmission station. Compression at the station was provided by two models of integral compressors: Ingersoll Rand KVG (10-cylinder) and KVS (12-cylinder) units and by two gas turbine-driven centrifugal compressors. Field tests were conducted to identify the sources of the neighbors’ complaints and to aid in development of modifications to reduce complaints.

This article presents field testing activities to verify the excitation sources, a pulsation analysis to develop modifications for reducing offending pulsations, and follow-up field tests for verification. The subject problem is somewhat unique in that the complaints of rattling are vibration-related, but the primary driving source is inaudible pulsations produced in the engine intake and exhaust manifold piping.

1 FIELD TESTING TO IDENTIFY PROBLEM SOURCES

In an effort to characterize the local complaints, sound pressures and vibration measurements were recorded at nearby home sites and outside the compressor building as the operating conditions of each type of compressor was varied. Vibration measurements were recorded on the foundation of the residences as well as in the ground near each home to assess the potential of ground borne vibration transmitted from the compressor station. In summary, it was found that ground-borne vibration was not present.

Air-borne sound pressure measurements identified a peak occurring near 12.5 to 13 Hz at the residences and near the compressor building as seen in Figure 2. This frequency is below the range of human hearing, but was considered a likely source of rattling. The noise measurements were made in engineering units of Pascals due to the low pressure levels. One Pascal (Pa) is equal to 0.000145 psi.

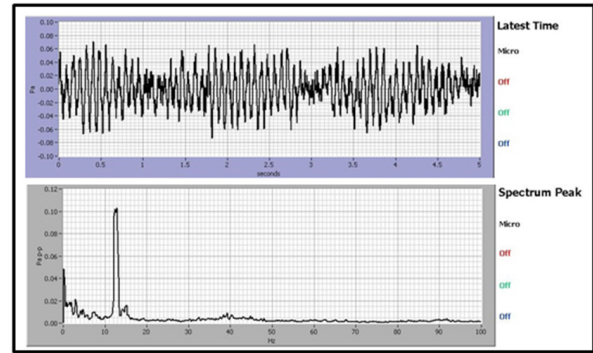


Figure 1. Sound Pressure Data Recorded at Residence – with 4 KVG, 2 KVS, and Turbine Operating

In order to identify the sources of the air-borne pulsations, testing was conducted with various units operating over a range of conditions to track the pulsations near 12.5 Hz. Field measurements showed that the elevated pulsations near 12.5 Hz corresponded to 2.5 times (2.5x) the running speed of the KVG units. When the engine running speed was varied over the operating range of 300 to 330 rpm, the 2.5x component in the sound and pulsation data tracked speed and varied from about 12.5 to 13.75 Hz. A summary of those pulsation measurements near 2.5x is presented in Table 1. The testing effort identified the KVG units as the primary source of the elevated 2.5x energy and eliminated the KVS units and the turbine-driven units as potential sources.

Table 1. Noise Pressures (Pascals, pk-pk) Detected near 2.5x at Various Test Locations

Units Operating	Compressor Station	Home 1	Home 2	Home 3	Home 4	Home 5
All Off	0.06	0.00	0.02	0.01	0.05	0.00
Gas Turbine & KVS Units	0.03	0.02	0.02	0.06	0.06	0.05
4 KVG Units & Turbine	0.96	0.09	0.25	0.20	0.18	0.14

Air-borne sound pressure measurements near the inlet duct to the engines could not distinguish whether the source was from the intake or the exhaust. A pressure measurement taken inside the inlet duct shows high pulsation at 2.5x the running speed and much lower amplitudes at several harmonics of running speed as displayed in Figure 2 below. The indication is that at least a portion of the noise at the residences originates from the inlet duct.

Case Study: Community Noise Annoyance Mitigation with Intake / Exhaust Silencer Redesign

by: Eugene L. Broerman, Ray G. Durke, Richard M. Baldwin; Southwest Research Institute®

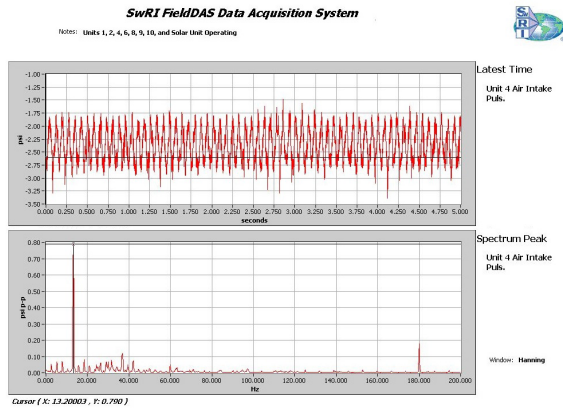


Figure 2. Pulsation Data Recorded in Unit 4 Intake Duct Showing 2.5 Multiple Pulsations

2 FIELD TESTING TO MAP AIR INTAKE AND EXHAUST PULSATIONS

A separate testing effort was conducted utilizing high temperature transducers to measure pulsations in the engine inlet and exhaust manifolds in order to define pulsation characteristics contributing to the high 2.5x pulsations and to provide data for correlation with an acoustic model of the intake/exhaust manifolds. A schematic of the exhaust system is provided in Figure 3.

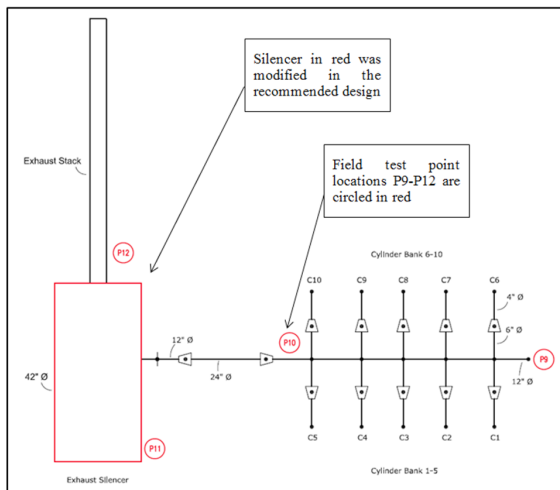


Figure 3. Engine Exhaust Manifold Schematic

The pulsations at 2.5x the running speed dominated the spectrum and reached a maximum at the capped end of the manifold, location P9, as seen from the data in Figure 4.

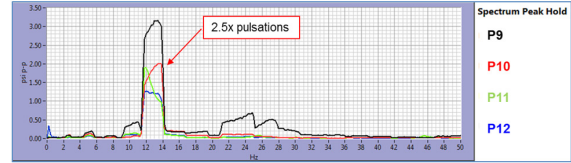


Figure 4. Pulsation Spectra Recorded in Exhaust Manifold

From the summary of pulsation amplitudes in Table 2, note that the 2.5x pulsation amplitudes measured in the exhaust piping are thousands of times more than those measured at the residences.

Table 2. Summary of Maximum 2.5x Pulsations Measured in the Exhaust Manifold

Test Point	Maximum Pulsation (psi pk-pk)	Maximum Pulsation (Pascals pk-pk)
P9	3.2	22,000
P10	2.0	13,800
P11	1.9	13,100
P12	1.3	8,900

The inlet manifold is represented in Figure 5 and is a somewhat more complex piping system. The field measurements identified a strong acoustic response at 2.5x running speed that contains a pulsation maximum at the capped end of each cylinder bank (test locations P5 and P8), and a minimum near the header between the cylinder banks (between test points P3 and P6).

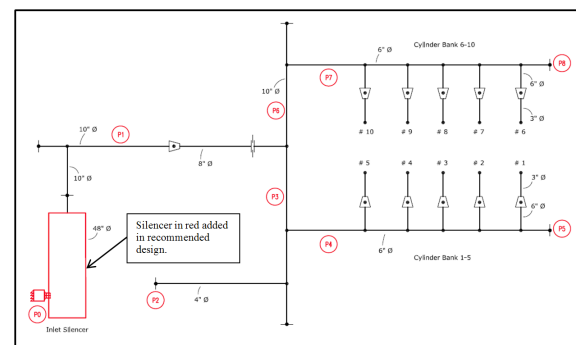


Figure 5. Engine Intake Manifold Schematic

Spectral pulsation plots of data recorded inside the intake manifold show the 2.5x pulsations present over the speed range, which is similar to the pulsation data measured in the exhaust system. A summary of the maximum pulsation amplitudes near 2.5x is provided in Table 3. The pulsation amplitudes in the intake manifold are lower than those in the exhaust by about

SESSION PULSATION 2

Case Study: Community Noise Annoyance Mitigation with Intake / Exhaust Silencer Redesign

by: Eugene L. Broerman, Ray G. Durke, Richard M. Baldwin; Southwest Research Institute®

a factor of 3. Data from the field studies was used for calibration of an acoustic model of the manifold systems. Comparisons of the field measurements with the model predictions are included in subsequent sections.

Table 3. Summary of Maximum 2.5x Pulsations Measured in the Inlet Air Manifold

Test Point	Maximum Pulsation (psi pk-pk @2.5x)	Maximum Pulsation (Pascal pk-pk @2.5x)
P1	0.2	1,400
P2	0.8	5,500
P3	0.47	3,200
P4	0.65	4,500
P5	0.86	5,900
P6	0.39	2,700
P7	0.17	1,200
P8	1.13	7,800

Figure 6 shows an example installation of a pressure transducer in the intake manifold at the capped end of the cylinder bank near cylinder 1, test point P5.



Figure 6. Pressure Transducer Installed at End of Manifold – Test Point P5

3 PULSATION MODEL

An acoustic model of both the inlet and exhaust manifolds was developed to explore the sources of the energy near 2.5x running speed and to investigate potential modifications for pulsation mitigation. The extent of the piping included in the modeling is summarized in Figure 3 and Figure 5. A summary of model results are presented in the following sections.

4 EXHAUST MANIFOLD MODEL

The pulsation model of the exhaust piping indicated that an acoustic response was present in the system near 12.5 Hz. A pulsation maximum was predicted at the capped end of the header and lower amplitudes near the stack. The red plot in Figure 7 shows model predictions of the pulsation in the stack for the existing piping system. The spectrum is dominated by the response peak near 12.5 Hz

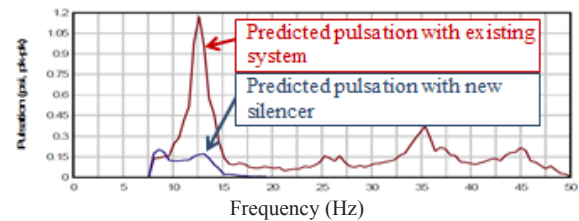


Figure 7. Predicted Pulsations in Exhaust Stack

Modifications to reduce pulsations by changing the manifold length, adding orifice plates, and providing an acoustic filter installed as part of the silencer were investigated. The operating company desired the most reliable solution, which was an acoustic filter designed into the silencer to attenuate pulsations associated with 2.5x engine running speed and higher harmonics.

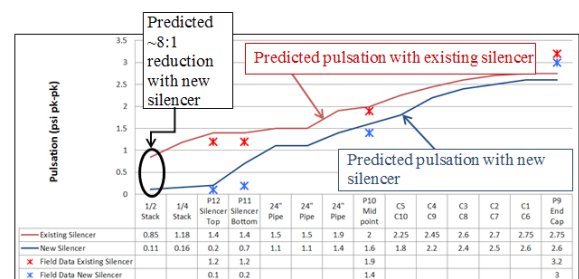


Figure 8. Exhaust Manifold and Piping Pulsation Summary – Predictions and Field Data (reference Figure 3 for test point locations)

Figure 8 shows pulsation amplitudes near 12.5 Hz predicted by the model in red for the existing manifold and in blue with the new silencer installed. Field measurements acquired at four locations in the manifold piping, indicated by stars, show good correlation with the model and field data. The important aspect of the design is the predicted amplitudes in the exhaust stack are reduced by a factor of about 8 with the new silencer installed. It was assumed that the primary coupling of the excitation energy near 2.5x running speed to the atmosphere occurs at the exhaust stack outlet. A spectral plot of pulsation predicted in the stack is shown in Figure 7, where the red line is the model prediction of pulsations with the original silencer and the blue line is the predicted amplitude

Case Study: Community Noise Annoyance Mitigation with Intake / Exhaust Silencer Redesign

by: Eugene L. Broerman, Ray G. Durke, Richard M. Baldwin; Southwest Research Institute®

with the new silencer installed.

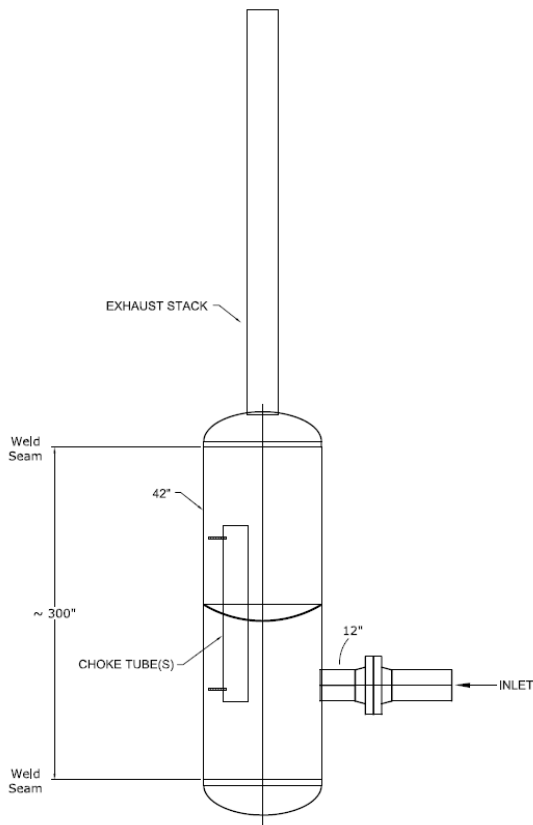


Figure 9. New Exhaust Silencer to Attenuate 2.5x Pulsations

Replacing the existing silencer with the silencer presented in Figure 9, results in predictions of significant reduction of 2.5x running speed pulsations in the piping downstream of the filter; therefore, installation of the new silencer should reduce the pulsations that couple into the atmosphere at the end of the stack.

5 INLET MANIFOLD PIPING

The pulsation analysis of the engine inlet air piping indicated that an acoustic response should be expected in the system near the top range of 2.5x running speed. The acoustic resonance is associated with the length of piping from the capped end of the cylinder 6-10 bank to the capped end of the cylinder 1-5 bank. The response predicted at the inlet to the original intake system is given in red in Figure 10. As shown, the response amplitude is significant from approximately 11 Hz to 15.5 Hz. Field data matches relatively well with the model predictions, showing higher 2.5x pulsations at higher running speeds.

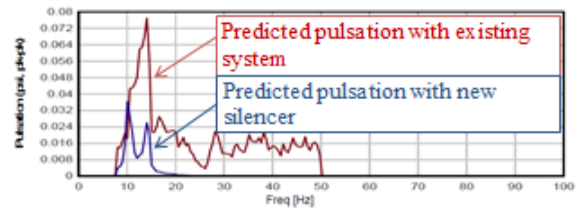


Figure 10. Predicted Pulsations at Intake Manifold

The acoustic mode shape of the pulsation response in the inlet manifold model is provided in Figure 11 for the cylinder bank of cylinders 6 through 10. The model predictions (shown as a red line) match the field data (plotted as red stars) fairly closely and show a pulsation maximum at the closed end of the cylinder bank and a minimum near the inlet.

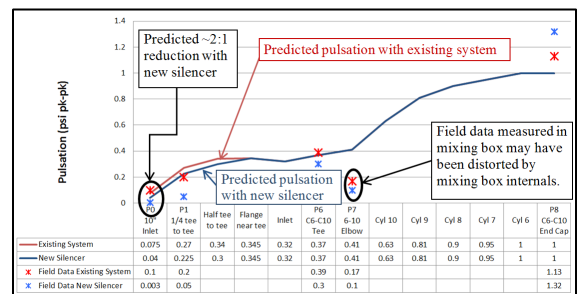


Figure 11. Intake Manifold and Piping Pulsation Summary – Predictions and Field Data (reference Figure 5 for test point locations)

Acoustic modifications were investigated to mitigate the 2.5x pulsations which included orifices to damp the resonance, a piping length change to shift the frequency of the response, and the addition of side branch resonators to absorb the pulsations. A more reliable modification to provide pulsation attenuation for airborne pulsations from the inlet piping was developed. The design utilized an acoustic filter with an inlet silencer similar to that developed for the exhaust system. The acoustic filter was designed to attenuate the 2.5x engine pulsations upstream of the silencer that would pass into the atmosphere. A drawing of the new inlet silencer design is provided in Figure 12.

Pulsation predictions within the intake piping with the silencer installed, the blue line in Figure 11, do not vary significantly from pulsations in the original manifold model (the red line in Figure 11). However, the objective of the new inlet silencer is to attenuate the pulsations near 2.5x that pass into the atmosphere. Therefore, the key pulsation data is at the inlet to the intake system. The predicted pulsation spectra at the 10-inch inlet piping can best be seen in Figure 10 for both the original piping (in red) and with the new

SESSION PULSATION 2

Case Study: Community Noise Annoyance Mitigation with Intake / Exhaust Silencer Redesign

by: Eugene L. Broerman, Ray G. Durke, Richard M. Baldwin; Southwest Research Institute®

silencer installed (in blue). Adding the new silencer to the acoustic model results in a reduction of the 2.5x pulsations by approximately 2:1 at the inlet to the intake system. These predictions are an indication that the pulsations transmitted into the atmosphere at the engine intake will be significantly reduced.

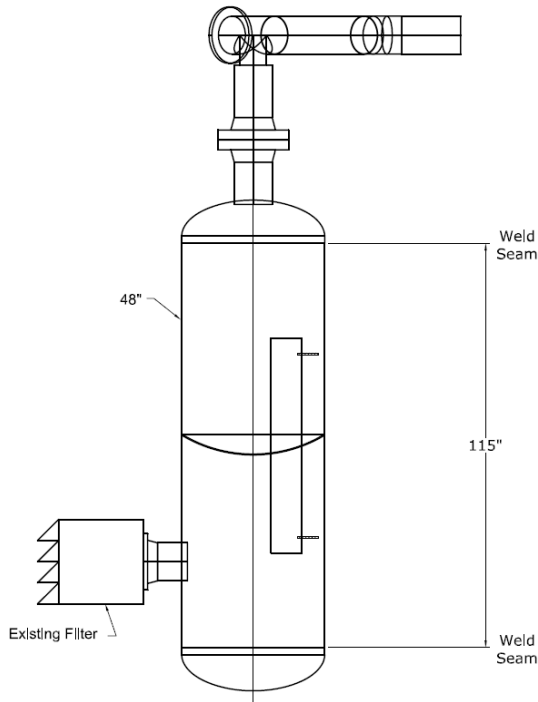


Figure 12. New Inlet Silencer

6 FIELD TEST TO VERIFY MODEL PREDICTION

Field measurements were recorded with the recommended inlet and exhaust silencers installed on one unit to verify performance prior to installation on all six units. Field measured pulsations in the intake and exhaust piping systems are summarized by the blue stars in Figures 8 and 11. Pulsation amplitudes at the inlet and outlet of the intake and exhaust systems, respectively, were significantly reduced after the new silencers were installed, as predicted in the pulsation modeling. Field sound measurements were recorded at locations similar to those recorded in the previous field tests with microphones located outside the compressor building and at Home 2 and Home 3 to assess the effects of the new silencers. Table 4 provides a summary of the measurements and shows a significant decrease in the 2.5x pulsations with the silencers installed.

Table 4. Sound Pressures at 2.5x at Noted Test Locations

Units Operating	Sound Pressures (Pascals pk-pk)		
	Compressor Station	Home 2	Home 3
All KVG Units Off	0.07	0.04	0.06
1 KVG Unit with Existing System	1.6	0.15	0.12
1 KVG Unit with New Silencers	0.47	0.07	0.02

The test results indicate that the sound pressures at 2.5x are lower with the new silencers by factors of about 3:1 near the compressor building, 2:1 at Home 2, and about 6:1 at Home 3. With the lower levels present, the sound pressure measurements are more erratic and can be affected by local noises. Figure 13 shows spectral plots recorded at Home 2, while Figure 14 shows sound pressure measured in the compressor station. The data distinctly indicates that the new silencers attenuate the 2.5x sound component, and also show the presence of more random low-level sound pressures present over the lower frequency band.

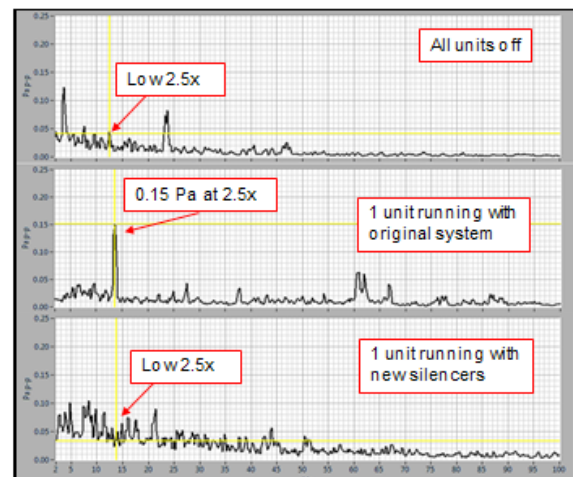


Figure 13. Sound Pressure Spectra at Home 2

Case Study: Community Noise Annoyance Mitigation with Intake / Exhaust Silencer Redesign

by: Eugene L. Broerman, Ray G. Durke, Richard M. Baldwin; Southwest Research Institute®

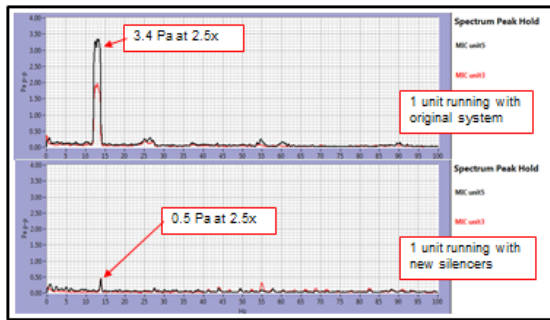


Figure 14. Sound Pressure Spectra at Compressor Station

Based on the results of the tests, the decision was made to install the silencers on the remaining units. A follow-up field study was performed to evaluate the system when all six units were fitted with the new silencers. Sound data was measured at the station and at two home sites. A reduction of at least 2:1 was measured at the compressor station, a reduction of more than 6:1 at one home site, and a reduction of approximately 5 to 30% at the second residence. It is not yet clear why the noise measured at one of the nearby home sites was not significantly reduced by the installation of the new silencers. Possible explanations include phased coupling of the residual pulsations when operating all six units, or a secondary transmission path radiating from the intake or exhaust manifold, or pulsations from the gas process piping. However, it is clear that the 2.5x pulsations transmitted into the atmosphere were reduced significantly by the installation of the newly designed silencers.

7 CONCLUSION

Key points of the field investigation, pulsation analysis, and follow-up testing are provided below:

- Pulsations inside process piping are a common source of noise and vibration at compressor installations. In this case, pulsations from engine intake and exhaust piping networks were identified as sources of vibration complaints from local residences.
- Initial field tests to address community annoyance complaints identified airborne sound pressure peaks occurring at homes near the compressor station that corresponded to 2.5x running speed of one type of compressor unit. Although the 12.5 to 14 Hz frequency was well below the range of human hearing, this lone peak in the sound spectrum was considered the most likely cause of the rattling and shaking complaints.

- Field measured pulsations inside the engine intake and exhaust manifold piping revealed strong pulsations at 2.5x running speed and were shown to be the source of the elevated sound pressure energy detected at the local houses.
- An acoustic model of the exhaust gas manifold identified a quarter wave pulsation response in the piping system. Of several potential design modifications, the most reliable option for reducing the pulsations transmitted into the atmosphere was replacement of the existing silencer with a low-pass acoustic filter type silencer designed to attenuate the 2.5x running speed pulsations (and higher frequency pulsations). This design was predicted to provide a reduction of about 8:1 in the 2.5x pulsations as measured in the exhaust stack.
- Acoustic modeling of the engine intake manifold indicated that a half-wave acoustic resonance existed in the system near the 2.5x frequency. A low-pass silencer was designed to attenuate the 2.5x pulsations similar to that of the exhaust system. A maximum reduction of about 2:1 in the 2.5x pulsations was predicted at the inlet.
- Field measurements conducted with the new silencers on one unit revealed that the sound pressure spike near 2.5x was eliminated.
- Field tests conducted with the new silencers installed on all six units revealed that the sound pressure spike near 2.5x was eliminated at the compressor station and one of the home sites, but remained at a second home site. It is possible that a second transmission path or a different sound source is contributing to the sound at the second home. Sound reductions at the compressor station and home sites were considered sufficient by the client; therefore, no further investigation was pursued.

8 REFERENCES

- K. Brun, E. Bowles and D. Deffenbaugh (2008): Development of a Transient Fluid Dynamic Solver for Compression System Pulsation Analysis. 6th European Forum for Reciprocating Compressors, Dusseldorf, Germany.
- Pierce, Allan D. (1981): Acoustics – An Introduction to Its Physical Principles and Application. McGraw-Hill.



Integrity Evaluation of Small Bore Connections (Branch Connections)

by:

Chris B. Harper
Principal Engineer
Beta Machinery Analysis
Calgary, Canada
charper@betamachinery.com

9th Conference of the EFRC
September 10th - 12th, 2014, Vienna

Abstract:

Evidence shows that vibration induced failure of small bore connections (SBC), also called branch connections or small bore piping, is an ongoing challenge during both the design phase and field testing. Failure of small bore piping on reciprocating compressor systems is a common industry problem. In fact, many industry experts believe that these failures represent the highest integrity risk and more attention is needed during the design and when conducting vibration surveys.

The Energy Institute and Gas Machinery Research Council provide recommendations and screening guidelines for the evaluation of SBCs in vibratory service. There are other screening guidelines available for vibration-induced fatigue failure that contain stress calculations.

These guidelines and approaches are useful for screening SBCs but they are not as useful for advanced analysis and field vibration surveys. A more comprehensive approach is needed to help industry with this question, "what to do if a SBC fails the EI or GMRC guideline?"

This technical paper will:

- Summarize existing approaches, recommendations and guidelines for SBC;
- Identify gaps and challenges in applying the existing approaches;
- Recommend an approach to address these gaps, and proposed guidelines for new designs; and
- Provide a proposed methodology for evaluating SBC vibration in the field.

SBC vibration guidelines are not currently included in the upcoming EFRC/ISO vibration guidelines. The results and findings from this paper could be a valuable input to addressing SBC integrity risks in this ISO (or other) standards.

Integrity Evaluation of Small Bore Connections (Branch Connections)

by: Chris B. Harper, Beta Machinery Analysis

1 Introduction

Small bore connections (SBCs) are a major source of failure on piping systems but are infrequently evaluated during the design phase of a project or during the field commissioning phase. Piping vibration and fatigue can account for up to 20% of hydrocarbon releases, and a large portion of those are due to failure of small bore connections [1]. Hydrocarbon emissions can lead to fire, explosions, injuries, property and environmental damage.

The following paper outlines different approaches, standards and guidelines that relate to SBC, both in the design phase, and during field testing.

To address the existing industry challenges, a practical approach is provided to improve the design and integrity of SBCs. The following recommendations are based on years of field testing, research, involvement with API 688/618 and GMRC committees, and involvement with a number of original equipment manufacturers (OEMs) of rotating machinery, packagers of rotating machinery, and end-users/owners.

While the following examples and discussion focus on reciprocating compressor applications, the approaches and recommendations apply to SBC located near reciprocating pumps, as well as centrifugal machines, or nearby piping system.

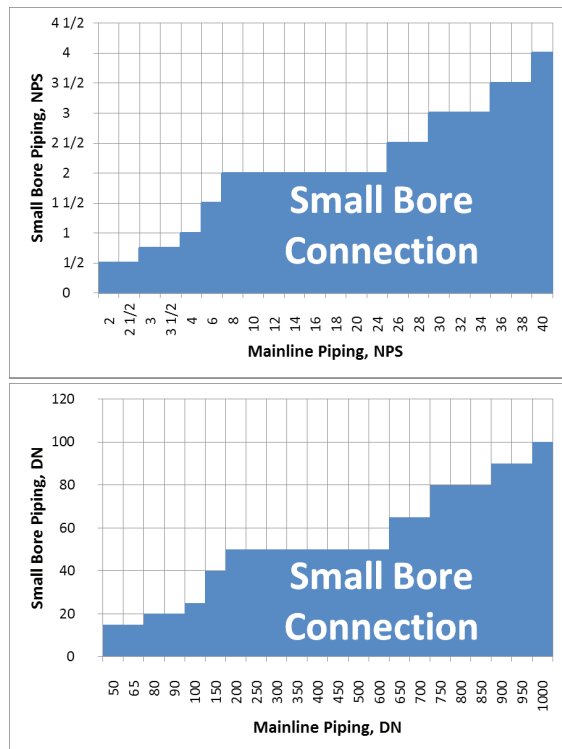


Figure 1. Small bore connection definition chart

1.1 Definitions

A small bore connection (SBC) is defined as a branched connection on mainline piping that is NPS 2” (DN 50) and smaller, including connections that have a branch pipe to mainline pipe ratio (“branch ratio”) of less than 10%, and excluding connections that have a branch ratio greater than 25%. Note that “mainline piping” could also describe equipment like a vessel or cooler to which the SBC is attached. A chart showing the SBC size definition is shown in Figure 1 above.

Small bore piping (SBP) is defined as the piping that is attached to the small bore connection, extending until the effect of the mainline piping vibration is negligible (typically, the nearest support or brace). Refer to Figure 2 for an illustration.

The small bore piping that is of most concern is that which contains production fluid at operating pressure. Auxiliary lines, like pneumatic air, crankcase vents, etc., are not as critical.

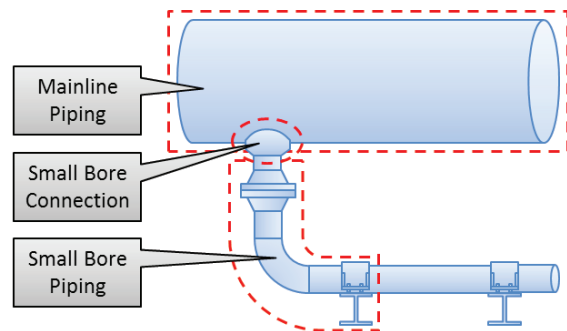


Figure 2. Small bore and mainline piping definitions

1.2 Acronyms

ID	One dimensional
ANSI	American National Standards Institute
DN	Diamètre nominal
EDI	Engineering Dynamics Incorporated
EI	Energy Institute
EPC	Engineering, procurement and construction
ESD	Emergency shutdown
FEA	Finite element analysis
GMRC	Gas Machinery Research Council
LOF	Likelihood of failure
MNF	Mechanical natural frequency
ODS	Operating deflected shape
PSV	Pressure safety (or relief) valve
RFLWN	Raised face long weld neck (flanges)
SBC	Small bore connection
SBP	Small bore piping

2 Challenges and Gaps with Current Practices

A large number of compressor/pump systems are fabricated and installed without a detailed design of SBP weight, geometry, or location, including the SBCs located off-skid or away from the compressor or pump frame.

It is rare that a specification will require a SBP audit at the design stage or during field commissioning. The lack of detailed analysis is due to these reasons:

- The design and layout of small bore piping is not known during the design stage. It is either shop-run or field-run, and there may not be drawings available.
- Even if the drawings are available at the design stage, the mass of non-standard components may be unknown because they have not been selected by the purchasing department, or they will be specified by the EPC. SBP mechanical natural frequencies (MNFs) are more sensitive to uncertainties in concentrated masses because they represent a higher percentage of the total mass of the SBP.
- Field audits may not be specified because of confusion about what piping is classified as SBP, and what vibration guidelines should be used.
- A thorough evaluation of small bore piping requires a shop test or a field evaluation. Different companies (and departments within companies) are involved at different stages, like front-end engineers, design, procurement, testing, commissioning, and operations. Therefore, a complete SBC evaluation involves coordination with many companies and departments.

These practical issues and limitations at the design stage, and during compressor start-up, are significant barriers to resolving SBC integrity risks.

3 Current Design Evaluation Methodology

There are various articles and guidelines on suggested approaches to review SBCs during the design stage of a project. This section briefly outlines these approaches and summarizes their advantages and disadvantages.

At the design stage, there are basically two evaluation methodologies: robustness and mechanical natural

frequency (MNF).

- The robustness of a SBC can be judged based on characteristics like piping diameter, thickness, flange rating, and location on the mainline piping. These can be compared to the characteristics of well-designed SBC. This methodology is limited to SBCs that fall into certain predefined groups. Also, there is some risk remaining because of the statistical nature of this method.
- The SBP MNF can be estimated (using empirical calculations or finite element analysis) and compared to industry guidelines. Currently, there is not industry-wide consensus on the MNF guidelines to use.

3.1 Best Practices

Many owners, EPCs, and machinery packagers have best practices on SBC design. These include guidelines on what type of connection to use (e.g., weldolet, sweepolet, or welded tee), welding procedures on SBCs, whether bracing is required, where small bore connections should be located, etc. In many cases, these are specified due to pressure requirements, and not specifically for reducing vibration-induced fatigue failure, but are useful nonetheless in avoiding some problems.

Below is a list of good practices in SBC design [2]:

1. Avoid locating SBCs near within about 20' (6m) of rotating machinery, including pulsation bottles and scrubbers on reciprocating compressor manifolds.
2. Avoid mounting SBCs within 10 mainline pipe diameters of pressure reducing devices (e.g., recycle valves, control valves, relief valves, or tight orifice plates) and fittings (e.g., elbows, tees, and reducers).
3. SBCs should be located within 2 mainline pipe diameters of pipe clamps and not on long unsupported piping spans. SBCs should be schedule 80 thickness, as a minimum.
4. Heavy valves (including isolation valves, double block and bleed, and gate valves) should not be used on SBCs. Use low profile valves instead, like monoflange valves. If large valves are required, use gussets on the SBC or brace the valve back to the mainline pipe. Other alternatives are to use robust connections like RFLWN or stud-ding outlet connections.

Integrity Evaluation of Small Bore Connections (Branch Connections)by: *Chris B. Harper, Beta Machinery Analysis*

5. Cantilever-type SBP should be as short as possible, and should avoid heavy valves, elbows, and tees.

Best practices are useful in reducing poor SBC design, but still leave some risk of vibration and fatigue failure.

3.2 Energy Institute Guideline

The Energy Institute (EI) has published a guideline for evaluating the failure risk of mainline and SBP [1]. The SBP can be evaluated either in conjunction with a mainline piping evaluation, or separately.

The EI assessment of SBP is a robustness methodology that calculates a likelihood of failure (LOF) for the connection. The SBP LOF calculation is based on the mainline dynamic forces (optional), the SBP geometry, and the location of the SBC on the mainline piping. If the LOF is greater than 0.7, then the SBP should be redesigned or braced.

The EI guideline considers the SBC fitting type (e.g., weldolet, threadolet, sockolet), SBP length and thickness, and presence of heavy valves. However, it does not estimate the SBP MNF.

3.3 GMRC Design Guideline

The Gas Machinery Research Council (GMRC) assessment of SBP is based on simple finite element analysis (FEA) models, which estimate the MNF and quasi-static stress (due to horizontal 1.5 G load) [3]. The MNF is compared to the appropriate MNF guideline (Table 1), and the maximum predicted stress is compared to a 3000 psi (20.7 MPa) 0-peak (“peak”) stress guideline. From this, a chart of SBP lengths versus weights can be referenced for guidance on selecting and designing SBP. The three main variables used for evaluation are the SBP configuration, length, and mass.

In the chart (Table 1), “Near” means within 20-25 feet (6.1-7.6 m) of the machinery and “N” means number of plungers.

While the GMRC assessment is more accurate than the EI assessment, it is still deficient in some respects. Although many layouts are covered by the GMRC guideline, the list is not exhaustive. The recommended simple 1D FEA method does not predict the stress and flexibility at the connection accurately. In some cases, the highest stress in a SBC is not in the SBP but in the mainline pipe (which is not modelled).

Table 1: GMRC Natural Frequency Guideline

Machinery	Natural Frequency Guideline	
	(Near)	(Far)
Reciprocating Compressor	> 4.8 * maximum runspeed	> 2.4 * maximum runspeed
Centrifugal Compressor	Detailed analysis recommended	> 15 Hz
Reciprocating Pump	> N * 2.4 * maximum runspeed	> N * 1.2 * maximum runspeed
Centrifugal Pump	> 2.4 * maximum runspeed	> 15 Hz

4 Current Field Evaluation Methodology

Currently, most companies treat SBP the same as mainline piping, when screening vibrations. Some companies will use more accurate vibration guidelines, which consider the small bore geometry, like those described in ASME OM-S/G-2003 [4], by Woodside Energy [5], or by EDI [6]. A few companies also use finite element analysis (FEA) to determine an allowable vibration guideline; a detailed discussion of FEA strategies will be presented in Section 5.1.

4.1 Screening Vibration Guideline

1.0 inch/sec peak (25.4 mm/sec peak) is a good screening guideline for SBP vibration. This guideline can be compared to spectrum (frequency domain) or, if base motion is subtracted out, to time domain waveforms.

To evaluate this screening guideline, a simple one dimensional (1D) FEA model was created (similar to the procedure described in Ref. [3]) to test different cantilevered SBP configurations. (Cantilever SBP is very common on mainline piping and vessels, as shown in Figure 3.) The SBP ranged from NPS 0.5” to 2” (DN 15 to 50), the flange ratings varied from ANSI 150 to 600, and some included gate valves. The stresses were compared to a 3000 psi (20.7 MPa) peak-to-peak allowable stress range. While there was no clear trend, the results do show that cantilevered SBP has an allowable vibration that varies between about 1.0 in/s peak to 3 in/s peak (25 mm/s peak to 76 mm/s peak) (Figure 3). This suggests that a vibration screening guideline of 1.0 inch/sec peak (25.4 mm/sec peak) is reasonable.

Vibration guidelines can be in displacement, velocity or acceleration. Velocity is a good screening guideline because for pipe with no concentrated mass, the peak stress at resonance is related to velocity only, not geometry. Vibration guidelines will be discussed in more detail in section 4.4.

Integrity Evaluation of Small Bore Connections (Branch Connections)

by: Chris B. Harper, Beta Machinery Analysis

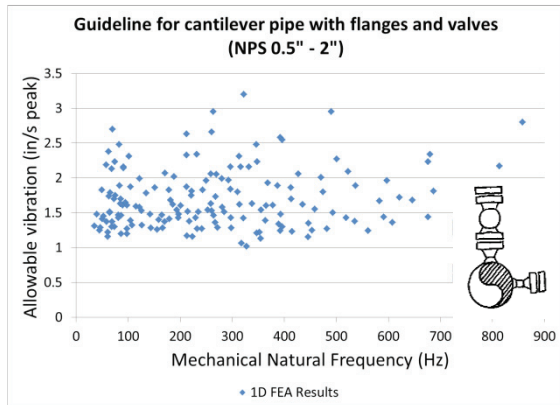


Figure 3. Allowable vibration for cantilever-type SBP

4.2 Woodside Energy Guideline

A paper by Woodside Energy describes a procedure to calculate stress due to measured acceleration in cantilevered SBP with concentrated masses [5]. A vibration velocity screening guideline is also provided, along with a robustness classification (Table 2).

Table 2. Woodside Energy vibration screening guideline

Small Bore Piping Type	Robustness Classification	Screening Velocity	
		mm/s peak	in/s peak
Cantilevered	Weak	15	0.6
	Moderate	30	1.2
	Robust	50	2.0
Continuous or supported	Weak	40	1.6
	Robust	60	2.4

While this method is more accurate than other methods, it has some limitations:

- It is more common to measure piping vibration in velocity or displacement, not acceleration.
- The method is applicable to the first mode of vibration of cantilevered SBP only. Therefore the acceleration measurements must be filtered in a band around the first MNF.
- The vibration measurement must be taken at the center of mass of the concentrated mass.

4.3 ASME OM-S/G-2003 Guideline

This standard for nuclear power plants describes a

method for determining an allowable displacement limit, for steady-state vibrations, based on SBP configuration, length, and diameter [4]. It also has a non-mandatory Appendices for determining allowable velocity levels, and describes a method for determining an allowable acceleration limit for cantilevered small bore piping, which is similar to the method described by Woodside Energy.

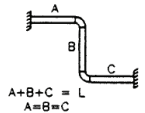
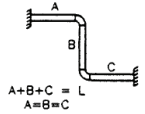
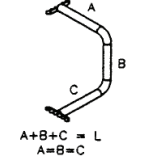
While this standard does go into some detail about how to calculate the allowable displacement limit, the paper “Displacement Method for Determining Acceptable Piping Vibration Amplitudes” [6] presents a simpler and more comprehensive method for determining an acceptable vibration limit, based on ASME OM-S/G-1991. This older version of the standard is still substantially the same, for the purpose of calculating an allowable displacement limit.

Table 3: Allowable vibration factor

Configuration	Diagram	K_a
Fixed-Free		0.0569
Simply Supported		0.0203
Fixed-Supported		0.00979
Fixed-Fixed		0.00710
L-Bend, Out-of-Plane, Equal Leg Length		0.0110
L-Bend, In-Plane, Equal Leg Length		0.00267
U-Bend, Out-of-Plane, Equal Leg Length		0.00746
U-Bend, In-Plane, Equal Leg Length		0.00555

Integrity Evaluation of Small Bore Connections (Branch Connections)

by: Chris B. Harper, Beta Machinery Analysis

Z-Bend, Out-of-Plane, Equal Leg Length		0.00592
Z-Bend, In-Plane, Equal Leg Length		0.00591
3D-Bend, Equal Leg Length		0.00523

4.4 ASME OM-S/G-1991 (EDI Paper)

This method [6] is recommended by the author for calculating an allowable displacement limit for piping, including SBP. The allowable vibration amplitude, Y_{all} (mil peak-to-peak or micron peak-to-peak), for different configurations of pipe is defined by:

$$Y_{all} = K_a \frac{L^2}{D}$$

L is the pipe length (in or mm), D is the pipe actual outer diameter (in or mm), and K_a is a factor based on the pipe configuration for the first vibration mode shape (Table 3 above). K_a is calculated by dividing the maximum allowable un-intensified dynamic stress range of 3000 psi peak-to-peak (20.7 MPa peak-to-peak) by the deflection stress factor, K_p , found in Ref. [6]. Y_{all} can be compared to vibration measurements, presented as either spectrum or time domain waveforms (the latter, as long as relative motion is measured; refer to section 6.3).

To convert this allowable deflection limit into an allowable velocity limit, V_{all} (in/s peak or mm/s peak), use the following formula:

$$V_{all} = Y_{all} \frac{f_{meas}}{318.31}$$

f_{meas} is the measured MNF of the first vibration mode shape of the small bore piping (Hz).

4.5 Multiple Vibration Modes

In the case where multiple mode shapes are excited by the mainline piping (i.e., the operating deflected shape (ODS) is a combination of k different modes), the allowable vibration is defined by:

$$\sum_{i=1}^k \frac{Y_i}{Y_{i,all}} \leq 1$$

Y_i is the measured vibration amplitude for mode i , and $Y_{i,all}$ is the allowable vibration amplitude for mode i (mil peak-to-peak or mm peak-to-peak). This assumes:

- The frequency of vibration of a mode is not an integer multiple of any another mode.
- The location of highest vibration amplitude occurs at the same point for all modes.
- The location of highest stress occurs at the same point for all modes.

The example of two modes being excited is shown in Figure 4. In this example, there is low frequency vibration that is in-phase with the mainline piping and has the same amplitude. This vibration can be ignored, because it does not cause significant stress.

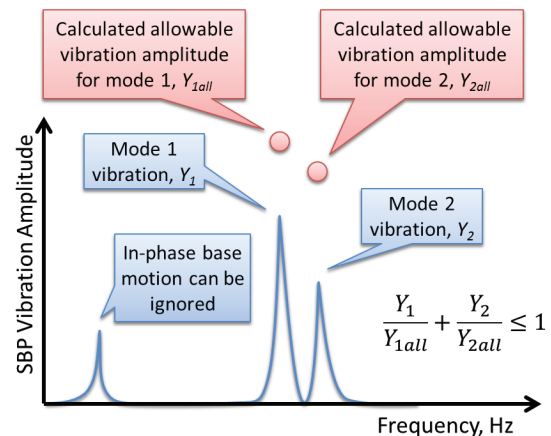


Figure 4. Multiple vibration mode example

5 Recommended Design Approach

The recommended design approach for evaluating SBP is to use one of the design guidelines described by the EI (section 3.2) or GMRC (section 3.3). For small bore connections that appear high risk, a detailed FEA can be conducted.

5.1 Finite Element Analysis

The goal of a detailed FEA at the design stage is to estimate the MNF of the SBP and calculate an allowable deflection limit, for use during field evaluations. Note that it is not possible to estimate the stress in the small bore piping at the design stage because the base

Integrity Evaluation of Small Bore Connections (Branch Connections)

by: Chris B. Harper, Beta Machinery Analysis

motion of the mainline piping is typically not known. However, the stress (at the connection) per deflection (on the SBP) can be calculated.

5.1.1. Scope of Model

Some of the mainline piping is required to accurately model the SBC. As a start, at least one diameter of mainline piping should be used, upstream and downstream of the connection. In some cases, significant shell vibration occurs with the small bore vibration, especially for thin-walled mainline piping.

The FEA model must be accurate enough to calculate the MNF of the SBP (typically within +/-10%) and to estimate the stress near the SBC. There are several methods available for estimating the stress near a weld using the hot spot stress technique; one is described in Ref. [7].

5.1.2. Damping

The damping on SBP is typically only material damping. The critical damping ratio is usually between 0.5% and 2%, and can be measured during an impact (bump) test.

Damping is an important consideration because most SBP are excited at their resonant frequencies.

5.1.3. Stress per Deflection Evaluation

Most failures on SBP occur near the connection point to the mainline piping. The crack can occur in the mainline piping or in the SBP, but typically the latter. Estimating the stress at the connection is required to calculate the allowable deflection limit.

The relationship between the deflection of the SBP and the stress at the connection depends on the actual field-measured operating deflected shape (ODS). While the actual ODS can be simulated using FEA (using base excitation), there are some alternative methods for determining a relationship between deflection and stress:

1. **Base excitation.** This is when the mainline piping in the FEA model is excited at a certain frequency or with broadband vibration. This method most closely resembles the ODS of the SBP, but it is also the most computationally intensive. Additionally, base motion of the mainline piping is rarely known at the design stage.
2. **Mode shape.** This method makes the assumption that the ODS resembles the vibration mode

shape (eigenvector) of the SBP. It is the method used in Ref. [4], [5] and [6]. This method is very quick and accurate, except in the case where multiple SBP modes are excited by the mainline piping vibration. In that case, the procedure described in section 4.5 can be used.

3. **Acceleration load.** This method applies an acceleration load (e.g., gravity) to the SBP to get a deflected shape. This method is not recommended, except when considering vibration due to transient motion of the mainline piping, or deflection due to quasi-static loads like seismic.
4. **Point load.** This method applies a load or deflection at a location (typically at the anti-node, or point of highest deflection) to get a deflected shape. This method is not recommended (because it can be non-conservative when compared to base excitation). It can be used to model static loads due to thermal expansion, for example.

5.1.4. Allowable Deflection Calculation

Once the stress per deflection is calculated, the allowable deflection can be calculated by using an allowable stress (typically the endurance strength which is based on weld type). The MNF of SBP is high enough that failure usually occurs in hours or days. Therefore, the SBC must be designed for infinite life, except in the case of transient vibrations (section 6.6).

6 Recommended Field Approach

The recommended field approach for evaluating SBP is the following:

1. Take velocity measurement on SBP at the anti-node location (i.e., location of highest vibration) and compare it to a screening guideline. Use relative vibrations (Section 6.3), if possible, or else simply add the SBP vibration and mainline piping vibration. If under guideline, the vibration is acceptable. If over guideline, go to step 2.
2. Compare vibration measurement to a geometry-based guideline, like ASME OM-S/G. This will require either converting vibration measurements to displacement or measuring the MNF of the SBP (to convert the guideline to velocity). If under guideline, the vibration is acceptable. If over guideline, go to step 3.
3. Compare vibration measurement to a guideline based on FEA using either the base excitation or mode shape method. If under guideline, the

Integrity Evaluation of Small Bore Connections (Branch Connections)

by: Chris B. Harper, Beta Machinery Analysis

vibration is acceptable. If over guideline, go to step 4. If the transient vibration is over guideline and the steady-state vibration is under guideline, then do a fatigue life calculation (Section 6.6).

4. Modify the SBP by either bracing, reinforcing the connection (e.g., gusseting), removing or moving the SBP, or replacing concentrated masses like valves with shorter and lighter styles.

6.1 Impact Test

If the vibrations cannot be measured because the unit is not running (e.g., during a shop inspection), then the MNF can be measured using an impact (bump) test, and compared to the GMRC guideline (Table 1). The SBP MNFs should be kept at least 10% away from known significant excitation forces. Additionally, it is recommended that the MNF of SBP that can be excited by horizontal vibrations of the reciprocating compressor cylinders (or pump plungers) are above the horizontal natural frequency of the cylinders, which is typically 300 Hz and below.

6.2 Worst Case Operating Conditions

It is unlikely that the operating conditions present during the vibration audit are the worst case the piping system will see. To compensate for this, take measurements at several operating conditions (e.g., rotating machinery speed, loading, pressure, flow rates). If this is not possible, then pro-rate the vibration measurements based on the expected worst case operating conditions. This can be done by calculating the ratio of pulsation-induced shaking forces at the as-found condition and the worst case condition, for example.

6.3 Relative Vibration

The vibration of the SBP relative to the mainline piping is the only vibration of interest, as it is the vibration that causes stress. In most cases, this relative vibration is highest at the SBP MNF. If the SBP is moving at the same amplitude and in-phase with the mainline piping, then the stress on the connection will be very low. The mainline piping vibration can be subtracted out from the vibration of the small bore piping (either using software or hardware). In some cases, the effect of the rotational vibration of the mainline piping must be subtracted out, also.

If the mainline piping vibration is low compared to the SBP vibration (i.e., 10% of the SBP vibration, or 0.1 in/s peak, whichever is lower) then it can be ignored. If the phase between the SBP and mainline

piping vibration cannot be determined, they can be added together, as a conservative estimation of the SBP vibration. (At resonance, the phase between the mainline piping and the SBP vibration is 90°).

6.4 Coordinate Systems

The naming convention for SBP coordinate systems is a smaller issue, but can be important when many connections are being audited. One useful system is shown in Figure 5, which references SBP directions relative to the mainline piping it is connected to. These direction names (T/R/P) are different from the standard Horizontal/Vertical/Axial or X/Y/Z, and therefore help reduce confusion.

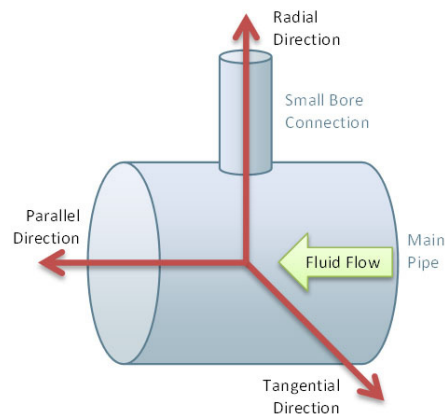


Figure 5. Small bore connection coordinate system

6.5 Pipe Strain

Pipe strain is strain introduced into piping systems due to misalignment and static deflections. It can be seen when pipe clamps are loosened and piping moves away from the clamped position, revealing gaps. It cannot be totally eliminated because piping is deflected during normal operation due to temperature and pressure. However, it is recommended that all pipe strain be removed at the installation (ambient) temperature by shimming with metal (or compliant) shims and comparing flange misalignment to standards such as ASME B31.3.

Pipe strain affects piping in several ways. It increases the MNF of the piping. It increases the vibration response of the SBP (speculated due to a reduction in damping). It also introduces mean stresses into the SBC which lowers the remaining allowable endurance strength. This can be quantified using a Goodman or Soderberg diagram.

Integrity Evaluation of Small Bore Connections (Branch Connections)

by: *Chris B. Harper, Beta Machinery Analysis*

It is recommended to post-weld heat treat critical SBCs to reduce the residual weld stress. This will tend to increase the allowable vibration of the SBP before fatigue failure occurs.

6.6 Transient Vibrations

Transient vibrations on SBP typically occur during events like changing operating conditions, other units coming online, normal start-up and shutdown, emergency shutdown, and valve operation (e.g., control valves or pressure relief valves). It is challenging to measure vibrations during these events without specialized equipment and using many vibration sensors. However, these short term events are important since they can affect the fatigue life of the SPC. If transient vibrations are significant, compared to steady-state vibrations, it is recommended fatigue life calculations be done, using Miner's rule.

7 Mitigation

The simplest method for dealing with high risk SBCs is to remove the connection altogether. Redundant connections and connections that can be isolated (e.g., double block and bleed valves) are typically installed to increase the reliability of a piping system, but can actually decrease the reliability if they become a high fatigue-failure risk.

High risk SBP can be moved to a location with lower base excitation. An example would be to move a pressure safety valve (PSV) from the top of a suction pulsation bottle to the shell of the scrubber (and brace the PSV back to the scrubber shell) or on to the piping upstream of the scrubber.

If detailed information is known about the small bore connection MNF and the excitation frequency, the SBP can be detuned by adding mass. This will lower vibrations of the SBP by separating the SBP MNF from the excitation frequency by at least 10%.

High risk SBP that cannot be removed, moved, or redesigned can be braced. A brace is most effective when the brace is parallel to the direction of vibration. The brace stiffness is significantly affected by the stiffness of the weakest (i.e., most flexible) part, therefore, good connection and fit is required for a brace.

8 Summary

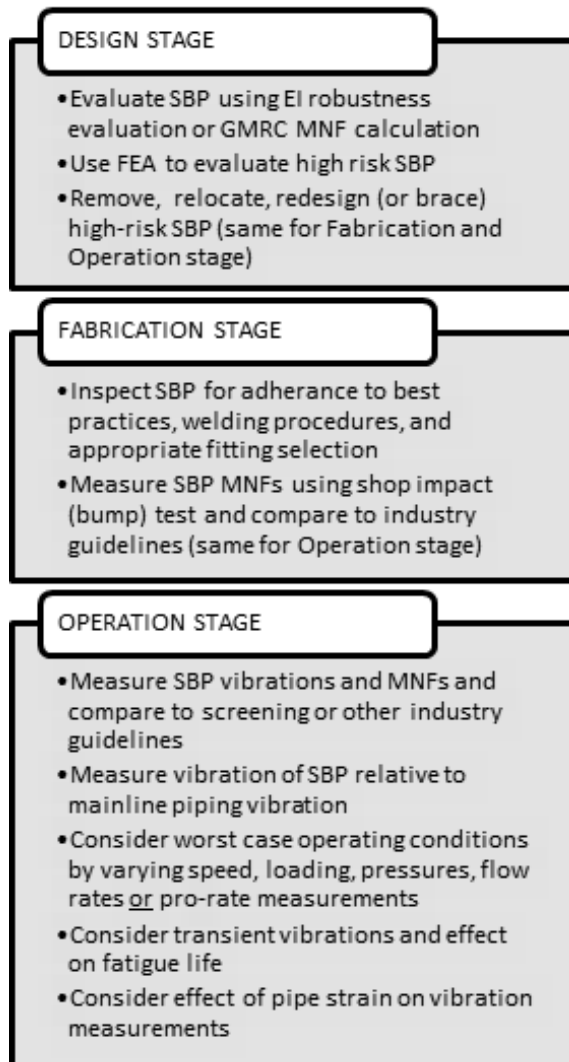
SBP can be a significant integrity risk on a piping system. A methodology is required to evaluate SBP during the design, fabrication, and commissioning of machinery and piping systems. The recommended evaluation procedure, outlined in this paper, is shown in Table 4.

9 References

1. Guidelines for the Avoidance of Vibration Induced Fatigue Failure in Process Pipework, 2nd Edition, Energy Institute, January 2008.
2. Vibration Related Failures of Small-Bore Attachments, B. C. Howes & C. B. Harper, Gas Machinery Conference, October 2003.
3. Design Guideline for Small Diameter Branch Connections, Releases 1.0, Gas Machinery Research Council, March 2011.
4. Standards and Guides for Operation and Maintenance of Nuclear Power Plants, ASME OM-S/G-2003, January 2004.
5. Fatigue of Cantilevered Pipe Fittings Subjected to Vibration, M. Hamblin, Woodside Energy, April 2003.
6. Displacement Method for Determining Acceptable Piping Vibration Amplitudes, J. C. Wachel, Engineering Dynamics Incorporated, 1995.
7. Unfired Pressure Vessels - Part 3: Design, BS EN 13445-3:2009, July 2009.

Integrity Evaluation of Small Bore Connections (Branch Connections)*by: Chris B. Harper, Beta Machinery Analysis*

Table 4. Small bore piping evaluation procedure



COMMITMENT FOR LIFE

BORSIG ZM COMPRESSION ZM

BORSIG ZM Compression GmbH, a member of the BORSIG Group, offers flexible, innovative and high-quality solutions for compressors. Our products stand for high quality, competence and reliability. We develop and manufacture modular machine concepts to meet each individual customer's requirements. Entire concepts from planning and design to manufacturing and assembly are our philosophy.

Reciprocating Compressors for Process Gases, API 618

Our modular designed compressor series for process gases comprises machines with both vertical and horizontal cylinder arrangements with up to a maximum of 6 axes. The series has been developed for the heaviest continuous operation.

Discharge pressure: ... 1,000 bara
Capacity/flow: ... 115,000 m³/h
Power: ... 16,000 kW

Centrifugal Compressors for Process Gases, API 617

up to 80 bara, 100,000 m³/h and 12,000 kW

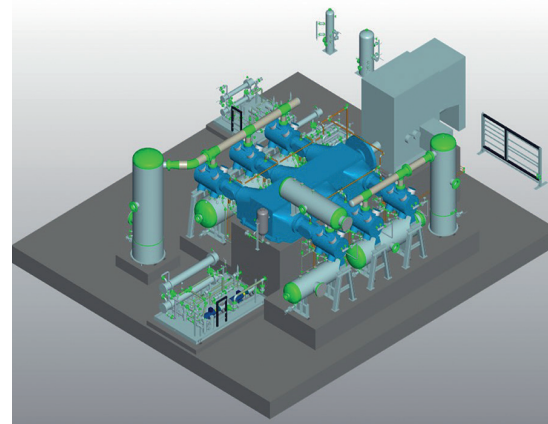
Compressor Valves

BORSIG BlueLine

combines control system, machine protection and condition monitoring for reciprocating and centrifugal compressor units

Services

Installation, overhauling, engineering, maintenance, spare parts management, training



BORSIG ZM Compression GmbH

Seiferitzer Allee 26
D-08393 Meerane / Germany

Phone: +49 (0) 3764 / 5390-0
E-mail: info@zm.borsig.de

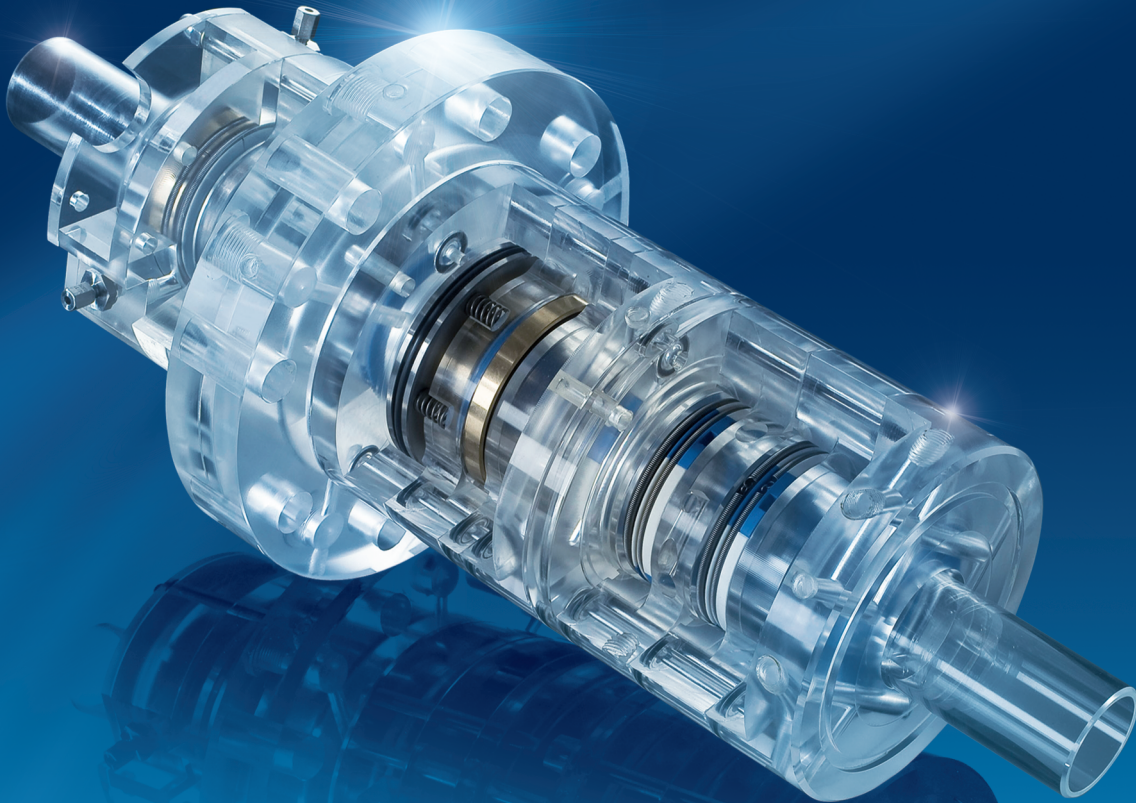
Fax: +49 (0) 3764 / 5390-5092

www.borsig.de/zm



STASSKOL

SEALING EXPERTS SINCE 1920



- Customized sealing systems for your challenging application in compressor engineering
- Test bed that is unique in the world with tribological test equipment
- Own material production in the field of plastics
- Clear OEM strategy
- Global expansion



+49 (0) 3925 288 100
info@staskol.de
www.staskol.de

9th Conference of the EFRC September 11th / 12th, 2014, Vienna

Gas-to-Liquids Technology and the Use of Reciprocating Compressors

-299-

by: Benjamin F. Williams, Ariel Corporation

Managing Start-Up Conditions of Hyper Compressors

-305-

*by: Marcello Agostini, Cosimo Carcasci, Alessio Cristofani,
Compression Service Technology*



EUROPEAN FORUM
for RECIPROCATING
COMPRESSORS

SESSION APPLICATION



Gas-to-Liquids Technology and the Use of Reciprocating Compressors

by:

Benjamin F. Williams

Process Application and Account Manager

Ariel Corporation

Mount Vernon, Ohio, USA

bwilliams@arielcorp.com

**9th Conference of the EFRC
September 11th / 12th, 2014, Vienna**

Abstract:

Due to the current abundance of natural gas and the resultant impact on its price; gas-to-liquids (GTL) facilities are being considered throughout the world. This emerging GTL market will provide new opportunities for the use of reciprocating compressors. The purpose of this paper is to provide a brief history of GTL technology and to describe how reciprocating compressors would be used in these facilities.

1 Introduction

GTL technology has existed for almost 100 years. The technology is very important since it is much less expensive to transport liquids than gases. Until recently, the consensus has been that only large (Mega) GTL facilities are economically feasible. However, for a number of reasons that opinion is changing and a number of smaller scale (Mini) GTL facilities are being considered, primarily in the U.S.

A large number of companies are currently considering GTL facilities of 5,000 barrels per day (bpd) or less. Although centrifugal compressors are the normal type of equipment used in large-scale GTL facilities, small-scale GTL facilities will provide a number of opportunities for the use of reciprocating compressors. These opportunities will be discussed along with a brief history of the gas to liquid market and what drives it.

2 Gas to Liquid Technology

2.1 History

Gas-to-liquids, as the name implies, is a means to convert gas to hydrocarbon liquids. Today, there are a number of GTL technologies, however for the purposes of this paper the focus will be on the Fischer-Tropsch process.

One of the most significant events in the history of GTL was the development of the Fischer-Tropsch reactor. In 1925, Mr Franz Fischer and Mr Hans Tropsch (F-T) developed a chemical process that converted syn-gas (a mixture of hydrogen and carbon monoxide) to liquid hydrocarbons.

The source of syn-gas will identify the type of F-T technology being applied. As noted above these are:

- GTL – Natural gas to liquids
- CTL – Coal to liquids
- BTL – Biomass to liquids

As each of these ultimately involves the conversion of syn-gas to liquids; we are including each technology under the term "GTL".

Here is a very simplified schematic of the F-T process.

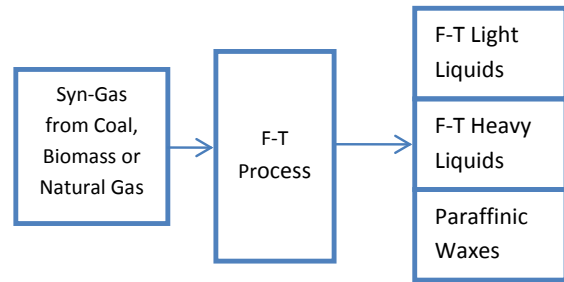


Figure 1: Simplified F-T Process

The F-T liquids and paraffinic waxes produced in the reactor are further processed, either by isomerization or hydrocracking. The end result products include diesel, naphtha or light gasoline.

During World War 2, the F-T process was used by Germany to produce over 600,000 barrels of vehicle fuel per year from coal. This accounted for almost 75% of the liquid fuel used in Germany at that time.

In the late 1940's, the F-T process was used to produce liquid fuel from natural gas at the Carthage Hydrocol facility in Brownsville, TX. This facility produced approximately 350,000 barrels of fuel per year. This lasted until 1953 when a huge increase in the price of natural gas made the facility uneconomical and it was shutdown.

The F-T process was later used by Sasol when they constructed a facility in Sasolburg to convert coal to liquid fuel in 1955. With the exception of this facility, the GTL industry was relatively quiet until the OPEC Oil Embargo in the early 1970's.

In the 1990's due to significant natural gas supplies, Shell built a large-scale GTL facility in Bintulu, Malaysia. This facility converted natural gas to liquids. The plant produced approximately 15,000 barrels of light diesel per day.

In addition to the tremendous amount of oil available in Qatar, there is also a huge amount of natural gas. The North Field in Qatar is the largest natural gas field in the world. Very large LNG (liquefied natural gas) terminals operate in the Ras Laffan Industrial City along with two of the world's largest GTL facilities; Oryx and Pearl.

The Oryx facility, a partnership between Sasol and Qatar Petroleum, has been in operation since 2007. The facility produces approximately 32,000 barrels per day of diesel fuel, naphtha and LPG from natural gas.

The Shell Pearl GTL facility, a Production Sharing

Gas-to-Liquids Technology and the Use of Reciprocating Compressors

by: Benjamin F. Williams, Ariel Corporation

Agreement (PSA) between Shell and Qatar Petroleum, is the largest GTL facility in the world. The Pearl GTL facility processes approximately 1.6 BCFD (1.8 million Nm³/hr) of wellhead gas. The facility produces 140,000 barrels of GTL per day and an additional 120,000 barrels per day of natural gas liquids. The facility, which is now fully on-line, cost between \$18-19 billion USD.



Figure 2: Shell Pearl GTL¹

GTL facilities are very expensive and the facilities mentioned above were only considered viable due to an abundance of feedstock at very low cost and a strong desire or need to become energy independent. Because of the high cost and delivery time of the components required for an F-T GTL facility, the consensus has been that only very large facilities like those above would be considered economically feasible.

Recently, there has been a change and there is a growing movement toward smaller facilities. This is primarily in the United States. Other areas where numerous small-scale GTL facilities are being considered are Uzbekistan and Brazil.

2.2 Why Now

2.2.1. Abundance of Natural Gas

In the United States, shale gas has led to an abundance of natural gas and natural gas liquids (NGL). The NGL is transported to refineries and petrochemical plants for use as feed stock. (Note – NGL processes are not considered GTL processes.)

The abundance of natural gas has had a huge impact on the price of natural gas. The price of oil is still relatively high, so the difference between the price of natural gas and oil (also known as “the spread”), make the economics of small to moderate size GTL facilities quite attractive. The consensus seems to be that as long as the spread is close to \$100.00 USD (73.00 Euro), GTL makes sense and can be profitable.

2.2.2. Demand for Clean Fuels

Increased global demand for cleaner burning fuels, such as clean diesel, and the current premium price of diesel fuel are other reasons these smaller GTL facilities are under consideration. One of the largest of these is to be located in Northeast Ohio which is considered one of the most prolific areas in the U.S. for the sale of diesel fuel.

2.2.3. Reduce Flaring

Much of the gas found in shale areas is considered “stranded”. This means there is insufficient gas processing capacity or available pipeline capacity to transport this gas. Currently, excess gas is being flared. The reduction in the flaring of natural gas is another reason that GTL facilities are being considered.

In the United States, two very large shale gas areas are the Bakken area in North Dakota and the Eagle Ford area in Texas. Both areas are flaring significant amounts of gas.

The photo below was taken from the International Space Station. It shows the United States at night and the flaring of gas in the Bakken and Eagle Ford areas is clearly visible from space.

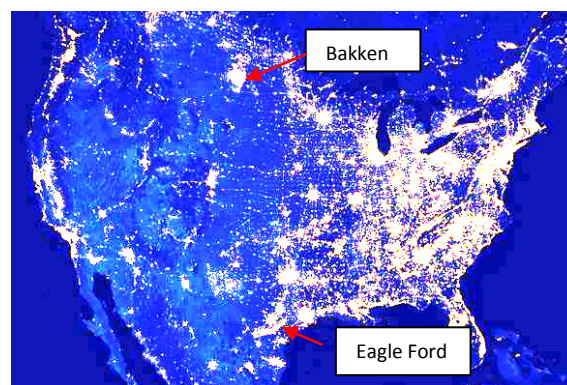


Figure 3: Photo of U.S. at night highlighting the Bakken and Eagle Ford areas.²

2.2.4. Technological Advancements

As mentioned previously, due to the high cost of equipment associated with GTL facilities, only large scale plants have been considered economical. However, smaller equipment and new technologies have been proven by small pilot plants that have been in operation for a number of years. The smaller, less expensive equipment and new technologies are the basis for the small-scale GTL plants being considered.

Gas-to-Liquids Technology and the Use of Reciprocating Compressors

by: Benjamin F. Williams, Ariel Corporation

Although the cost associated with GTL is being significantly reduced by these equipment and technological advancements; these small-scale GTL facilities are not inexpensive.

In discussions with a number of companies involved in the industry, it seems that a good rule of thumb is that these facilities cost approximately \$100,000.00 USD (currently equal to 73,000.00 Euro) per barrel per day of GTL produced. For example, a 3,500 barrels per day facility would cost \$350,000,000.00 USD (255,500,000 Euro) to build.

3 The Gas to Liquids Process

3.1 Process Description

A GTL facility is almost like three types of facilities in one. These are:

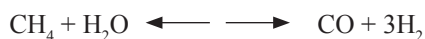
- A gas processing plant
- A synthesis gas plant
- A refinery

The GTL process begins with the feedstock. The source of the feedstock could be coal, biomass or natural gas.

If coal or biomass is the feedstock, a gasification unit will be required. The gasification unit will require oxygen which typically is supplied from an air separation unit (ASU). The gasification process produces syn-gas. The syn-gas will require additional processing and cleaning to remove particulates, sulfur and other impurities that will be harmful to the F-T process.

If the feedstock is natural gas, it will be processed to remove sulfur and other impurities (if required) and then mixed with steam in a steam methane reformer (SMR) or in an auto thermal reformer (ATR). The SMR process uses natural gas and steam to produce hydrogen and carbon monoxide.

The basic equation for the SMR process is:



After gasification or reforming, the “clean” syn-gas then enters the F-T reactor. The reactor contains cobalt-based or iron-based catalyst. The syn-gas is converted into long chain hydrocarbon liquids and wax.

The long chain hydrocarbons and waxes may require additional processing or refining. This may include

isomerization and hydro-cracking. The end products produced include LPGs (liquefied petroleum gases), naphtha, diesel fuel and lubricants.

3.2 Compression Requirements

As described above, there are a number of different applications / services required in the GTL process, depending on the design of the facility. A typical GTL facility would require compression for the following applications:

- Oxygen
- Feed Gas
- Syn-Gas
- Fuel Gas
- Hydrogen Make-up and Recycle
- Tail Gas
- Off-gas

Please note that the compressor recommendations are based on smaller sized GTL facilities and not the large commercial scale plants described above.

3.2.1. Oxygen

Oxygen is typically supplied from an ASU. Oxygen is required for the gasification of coal or biomass and can also be used as part of the natural gas reforming process.

3.2.2. Feed Gas

The Feed gas is natural gas that is mixed with steam in the steam methane reformer to form syn-gas. Feed gas compression may be either a rotary screw, centrifugal or reciprocating compressor. Special attention must be paid to gas composition in order to select proper materials of construction for the compressor.

3.2.3. Syn-Gas

Syn-gas compression can be by either rotary screw, centrifugal or reciprocating compressor. This is very dependent on the hydrogen content of the gas stream; the more hydrogen, the lighter the gas. Although rotary screw and centrifugal compressors are capable of compressing lighter gases; they are very susceptible to internal leakage. This internal leakage decreases the efficiency of the rotary screw and centrifugal compressors. They must account for the leakage by increasing in size. Reciprocating compressors are better suited for lighter gases.

Gas-to-Liquids Technology and the Use of Reciprocating Compressors

by: Benjamin F. Williams, Ariel Corporation

3.2.4. Hydrogen and Hydrogen Recycle

Hydrogen is required in a number of processes associated with GTL facilities. It is required for desulfurization prior to the F-T reactor and during the “product improvement” or upgrading process after the F-T reactor. There may also be a hydrogen recycle service required. Reciprocating compressors are better suited for these light gas applications. Additionally, the volume of gas required better suits a reciprocating compressor rather than a centrifugal.

3.2.5. Tail Gas

Tail Gas is the gas remaining after the F-T reactor has processed the syn-gas into the longer chain hydrocarbons and waxes. Tail gas is typically comprised of hydrogen, carbon monoxide and lighter hydrocarbons. Tail gas may be sent to flare or recycled. In a tail gas recycle system, it is sent back to the process inlet to mix with the incoming syn-gas or used as fuel gas. Once again, this tends to be a light gas, so reciprocating compressors are the better option.

3.2.6. Off-gas

Depending on the design of the plant, there may be an off-gas stream. The off-gas stream may be used in the hydrogen recovery unit (HRU) or mixed with syn-gas for fuel.

Many of the gasses, applications and processes associated with a GTL facility are the same as would be found in a refinery or petrochemical plant. Reliability requirements would also be the same as required in the downstream industry. This means low discharge temperatures and reduced piston speeds are very important. Lubricated and non-lubricated cylinders can be used, depending on the gas composition.

3.3 GTL Modularization

A common design theme for the small-scale GTL facilities is modularization. Each section of the plant is fabricated in a shop on portable steel structures. The individual modules are then assembled together at site.

This approach has huge economic advantages; the fabrication of each module takes place in a shop rather than in the field. Simply put, this makes it much easier to fabricate and assemble the modules. Working in a shop removes the weather element and provides a much cleaner environment to work in. This will reduce the time required to build the modules and will also improve the quality of construction. Shipment

of the modules is much easier and more cost effective than shipping individual components to site. Once in the field, installation time is greatly reduced.

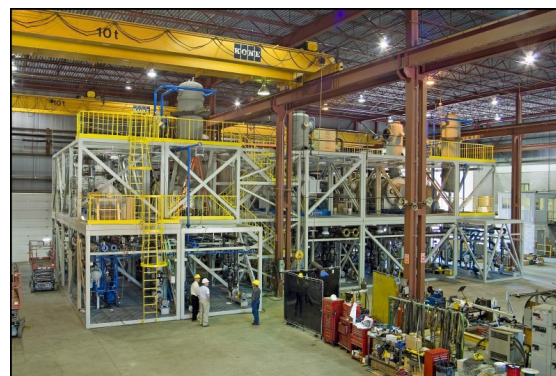


Figure 4: Modular plant construction in a shop³.

Modularized GTL facilities present unique challenges due to their size. Equipment and components must fit inside a specific envelope. Approximate dimensions for these modules are 4 meters (W) x 4 meters (H) x 14 meters (L). If the modules were to be installed in shipping containers, they would need to be even smaller.

Due to the size restrictions associated with modular GTL facilities, the reciprocating compressors used in these facilities would typically need to be shorter stroke types. This type of reciprocating compressor has been packaged (modularized) on structural steel skids for decades and lends itself very well to the modular GTL concept

The reciprocating compressor module will typically include the compressor, electric motor driver, piping, pulsation dampeners, moisture separators (with associated level controls and instrumentation), process gas cooling, associated instrumentation and controls along with the frame and cylinder lubrication systems; assembled and installed on a structural steel skid. Local control panels may or may not be required; dependent on site requirements.



Figure 5: Reciprocating compressor package⁴

4 Possible Complications for the Small-Scale GTL Market

Although the concept of small-scale GTL facilities is becoming more widely accepted, there are still hurdles that must be overcome. As previously noted, although smaller, these facilities are not inexpensive and require significant financial backing.

Any fluctuation in the prices of natural gas and oil can give pause to those who are considering investing in this technology. With the amount of natural gas currently available, those who are in the GTL industry say this concern is minimal. If the spread between oil and natural gas remains high, small-scale GTL can be profitable.

Almost all of these small-scale GTL facilities will require some type of environmental / political permit prior to construction. This permitting process can be very arduous and time consuming. How smoothly this process goes will influence subsequent permitting applications.

Other technologies are being tested in pilot plants that may be less expensive than GTL. These include gas to methanol (GTM) and methanol to gasoline (MTG). LNG is also deemed to be less expensive than GTL. However, LNG requires very large volumes of natural gas to be economically feasible.

These possible complications have led to a bit of a “wait and see” attitude regarding the construction of additional small-scale GTL facilities.

5 Conclusion

Gas-to-liquids technology has existed for almost 100 years. Although some smaller-scale GTL facilities do exist, the consensus has been that only large scale GTL plants are economically feasible. Technological advancements along with an abundance of natural gas, increased demand for cleaner burning fuels and a desire to reduce the flaring of stranded natural gas has changed that viewpoint.

Small-scale modular GTL facilities are being planned for a number of locations. These smaller scale GTL facilities offer multiple applications requiring reciprocating compressors. These include feed gas, syn-gas, hydrogen make-up and recycle and tail gas services. Short stroke compressor packages can be incorporated into the modular plant design.

Economics will eventually decide whether small-scale GTL facilities make sense. Industry

experts state that the current spread between natural gas and oil should remain in place due to the abundance of natural gas. For this reason, they believe small-scale GTL will be successful. This offers great potential for the use of reciprocating compressors.

6 References

- 1 **Pearl GTL - <http://www.shell.com/global/aboutshell/major-projects-2/pearl/overview.html>**
- 2 Photo – NASA
- 3 Modular Plant Design – www.zeton.com
- 4 Photo-Lone Star Compressor Corporation

Reference Article - “Smaller-scale GTL enters the mainstream” – R. Lipski – Velocys

www.fischer-tropsch.org

Gas-to-Liquids Technology Forum 2013 -
Personal notes



Managing Start-Up Conditions of Hyper Compressors

by:

Marcello Agostini, Cosimo Carcasci, Alessio Cristofani

Senior Engineering Consultant, Technical Assistance Manager, Rotating Machinery Manager

Compression Service Technology S.r.l.

Florence, Italy

marcello.agostini@cstfirenze.com

**9th Conference of the EFRC
September 11th / 12th, 2014, Vienna**

ABSTRACT

The heart of LDPE plants is considered to be the high pressure vessel where the chemical reactions of polymerization, that transform Ethylene into Low Density Polyethylene, take place. This is then the basic material for the construction of many plastic objects used in our everyday life.

These reactors can generally work with pressures up to 350 MPa and special high-tech reciprocating compressors are the machines commonly used to reach these extreme operating conditions.

Performance and safety are key considerations and operator experience is essential for optimal and safe plant operation. Plant automation also contributes significantly to safety and to optimizing process conditions.

The compressor start-up and shut-down procedures, typically described in maintenance manuals, do not always give a complete overview of the phenomena involved inside the compressor cylinders during start-up transients. These procedures are therefore analysed, in order to draw up guidelines to prevent damages to plunger seals and to keep loads within design limits, without compromising the design performance. The multiple gas compositions of co-polymers and the fact that gas expansion can cause a reduction in temperature, also require attention, to avoid damage due to polymer deposits inside the compressor cylinders.

After a brief description of these machines and the actual polymerization process practical recommendations are provided on the necessary procedures to reach the operating pressures with correct distribution of the pressure ratio between the two stages, as well as the implementation of a combined control link in the system architecture. Recommendations will also be given concerning the minimum pressure to be maintained on the plunger head, in order both to keep the contact with the crosshead and minimize the risk of failure of such a brittle component.

NOMENCLATURE

LDPE = Low Density Polyethylene
 HPLLDPE = High Pressure Linear Low Density Polyethylene
 FDA= Food and Drug Administration
 CLA=Center Line Average

1 INTRODUCTION

The polymerization of Ethylene to produce Low Density Polyethylene requires compressors capable of bringing the gas to pressures in the range of 160 to 350 Mpa, depending on the type of process utilized [1]. The compression of the gas at these extreme pressures is achieved by dividing the overall compression ratio into two steps: a first step from the Ethylene production pressure ranging from 2 to 5 Mpa to about 30 Mpa and a second step from 30 Mpa to the final pressure of 160 to 350 Mpa (23,000 to 50,000 psi). The first step is normally done with a heavy-duty reciprocating compressor of the balanced-opposed type which is called the Primary compressor, while the second step is done in two compression stages with very special compressors, still reciprocating type but employing many high-tech features to withstand the extreme working conditions, which are widely called Hyper compressors or Secondary compressors.

even high pressure linear low-density polyethylene (HPLLDPE) with the addition of Butylene [2]. Also the final application of the polymer influences the production process; for instance, if the polymer has to be employed to produce film to protect food, all the substances utilized for the production of that particular LDPE must be compatible with food and approved by the FDA.

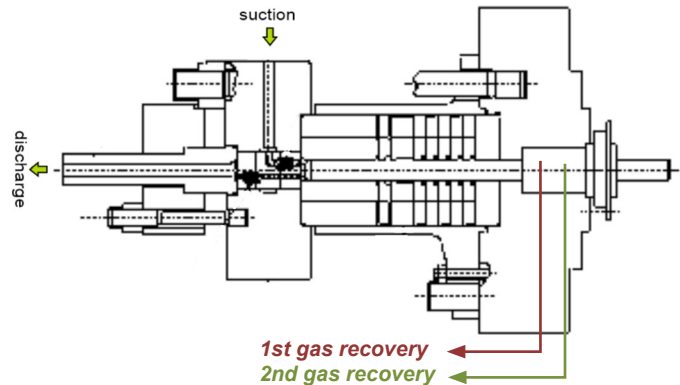


Fig. 1 Sketch of an High-pressure cylinder [2]

The main challenges for the safety and reliability of operation of Hyper compressors are the following:

- | | | | |
|-----------------|--------------------------|---------------------------|--------------------|
| 1. Crude Oil | 6. Cat. cracking | 11. Steam cracking | 15. Cononomers: |
| 2. Natural gas | 7. Refinery gas recovery | 12. C3 gas | Butene |
| 3. Refinery | 8. Gas Oil | 13. Ethylene purification | Hexene |
| 4. Distillation | 9. Naphtha | 14. Ethylene | Vinyl Acetate |
| 5. Powerformers | 10. Ethane | | Acrylic Acid |
| | | | 16. Plastics plant |
| | | | 17. Polyethylene |

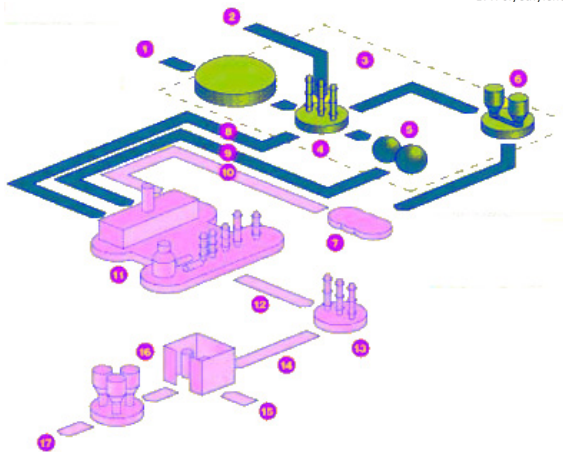


Fig. 2: Typical Polyethylene production process

Basically, LDPE is not a single product but is a variety of products which are produced either with dedicated production lines or, even in the same line, during different production campaigns. For example, simple LDPE can be produced without additives and copolymers with Vinyl Acetate or with Acrylates or

- The sliding parts and particularly the pistons, which are plunger type and are made of sintered tungsten carbide, which is a very hard but brittle material, and the seals, which are mainly packing type and made of a special bronze alloy. A typical cylinder arrangement is shown in Fig. 1.
- The crank mechanism that must withstand extremely high loads but, at the same time, assure a very precise movement of the thrust piece driving the plunger in order to avoid misalignment between the two parts and bending stresses on the plunger in both cold and warm conditions. Several different crank mechanism designs have been utilized by the various manufacturers since this technology was developed in the forties but only two are currently available on the market: one that has a special self-aligned crosshead and a second one with a crosshead driven by two connecting rods and an auxiliary crosshead [2].
- The fatigue resistance of the pressure components, which are subject to the fluctuating pressure between the suction and discharge and which are shaped in such a way as to favour stress concentration such as cross-bored thick-walled cylinders [3], [4] which require, in certain cases, to utilize the technique of the “autofrettage” [5] to generate pre-compressive stresses in the most critical points.

Managing Start-Up Conditions of Hyper Compressors

by: Marcello Agostini, Cosimo Carcasci, Alessio Cristofani, Compression Service Technology

- The risks related to the gas in the polymerization of Ethylene, which in certain conditions can decompose creating very large overpressure waves.

2 MAIN OPERATING PROBLEMS CONNECTED WITH SECONDARY COMPRESSORS

2.1 Cylinder packing pressure distribution

The cylinder packing, is generally composed of one pressure-breaker ring and five sealing elements. The pressure-breaker is designed to assure a gradual flow of gas through the main packing rings and facilitate gas backflow into the cylinder during the expansion/suction stroke to remove, as much as possible, the friction heat from the packing. In addition, it is designed to assure a smooth depressurization of the gas trapped in the small housing chambers between the packing cups and the packing seals, which could “explode” and damage sealing ring elements such as the tangential lips, garter spring and reference pin. The design and material of the sealing elements are very important for their performance, not only because of the very high pressure but also in consideration of the fact that the lubricating oils employed must be a compromise between the tribological properties and the acceptability for the final product to be in contact with food.

When the running-in of the cylinder packing seals is done properly and the surface finish of the plunger is in the correct range within $Ra=0,05$ micron ($2 \mu\text{m}$ CLA), seal life can reach up to 60,000 hours on the first stage at about 150 Mpa and up to 40,000 hours on the second stage with a discharge pressure of 300 Mpa. Nevertheless good design and correct operation in steady conditions are not sufficient to ensure acceptable performance of the cylinder seals in the field. Also the way the running-in of the cylinders is performed and how the transient conditions are managed are of great importance for their behaviour and lifetime.

Understanding the pressure distribution the packing in operation is of key importance in knowing how to proceed in utilization of the hyper compressor cylinders. This is also due to the fact that sometimes the instruction manuals of these machines are rather vague about this point.

The pressure distribution along the cylinder packings of Hyper compressors, when compressing Ethylene with a normal compression ratio, is in fact rather special. In general, the first sealing elements are affected by the pressure fluctuation occurring in the compression chamber, while the last elements are subject to a near steady pressure [6].

When a compression stage is not producing any compression ratio, i.e. the discharge pressure of the relevant cylinders is almost the same as the suction, the packing is subject to a near steady pressure. In this condition, the pressure distribution along the packing is generally similar to that in a labyrinth; so that the velocity of gas escaping through the packing reaches

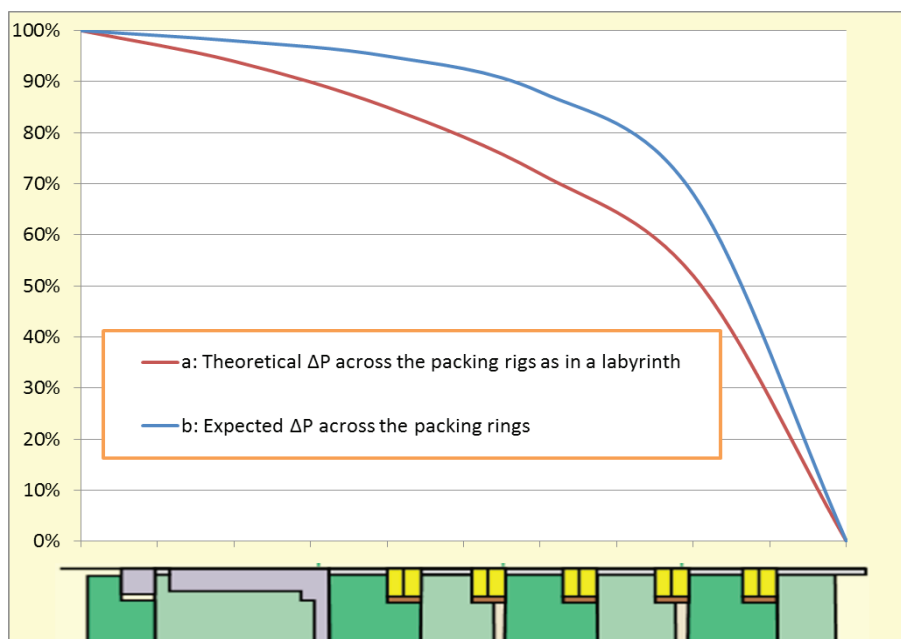


Fig. 3. Differential pressures across the packing rings [9]

Managing Start-Up Conditions of Hyper Compressors

by: *Marcello Agostini, Cosimo Carcasci, Alessio Cristofani, Compression Service Technology*

the maximum value at the last sealing ring where the gas volume is highest due to the density being at minimum level. The differential pressure across this ring is therefore the greatest of all the packing rings. This situation causes the last ring to be more forced against the plunger with the result that the gas leakage area becomes smaller and the escaping gas is reduced in quantity; consequently, the other packing rings become relaxed and the theoretical ΔP can be even worse than in a labyrinth. Fig. 3 shows a calculation of the pressure distribution across the packing rings according to the theoretical “labyrinth model” and an average “expected” real distribution according to the measurements reported in [2] and [8].

In these conditions the force pushing the last packing ring against the plunger can reach too high a value because it has to support more than 50% of the total steady pressure inside the cylinder.

If the steady pressure reaches too high values during the running-in period, it can cause abnormal wear, deformation and breakage of the last ring, and sometimes also that of the adjacent ring; thus the lifetime of the whole packing can be compromised with early replacement of the cylinder. For this reason, high steady pressure values must be avoided both when the Hyper compressors are started-up and when they are stopped to be depressurized.

2.2 Plunger-to-thrust piece connection

The connection between the plungers and the crosshead or thrust piece is also another important part of the hyper compressor.

The problem here is that the plunger, which is strongly pushed against the thrust piece by the gas pressure when the compressor is in normal operation, is under much less pressure during the start-up and decompression period but, nevertheless must, even in this condition, be kept positively in contact with the thrust piece in order to avoid detachment of the two parts.

There are two possible solutions: one is to have a rigid flanged connection between the two parts (Fig. 4) and the other is to rely on the force due to the gas pressure and have a safety device to keep the plunger connected even in the event of insufficient gas pressure (Fig. 5).

The red lines show the surfaces where the pressure forces, caused the tightening between bolt and thrust piece, are acting.

In both cases the effect is to keep the plunger pressed against the thrust piece but the rigid connection in Fig. 4 increase the risk of over-constraining because gas loads acts as a second constrain of the plunger and the thrust piece itself.

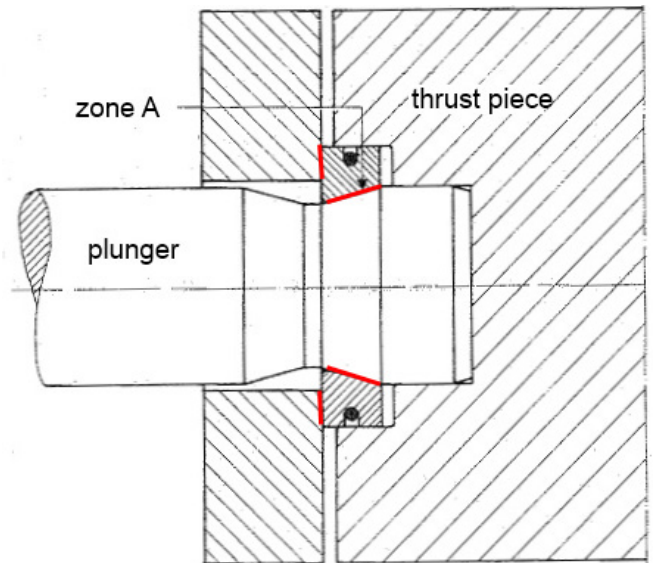


Fig. 4. Typical rigid connection between plunger and thrust piece [7]

This solution has the advantage of not strictly needing any pressure in the cylinder to keep the contact but has the risk that, if the plunger and thrust piece are misaligned, fretting might occur in zone A and this could initiate a fatigue fracture [4].

Conversely the solution in the Fig. 5 requires the compressor to be operated with a gas pressure inside the cylinder of at least 10 Mpa to ensure contact between the plunger and thrust piece. In authors’ opinion, this condition of start-up with pressurized cylinders is helpful also with the solution of Fig. 4 as it gives a better positioning of the plungers and helps minimize the risk of fretting and for this reason, it will here below be considered as a necessary condition for a good hyper compressor start-up.

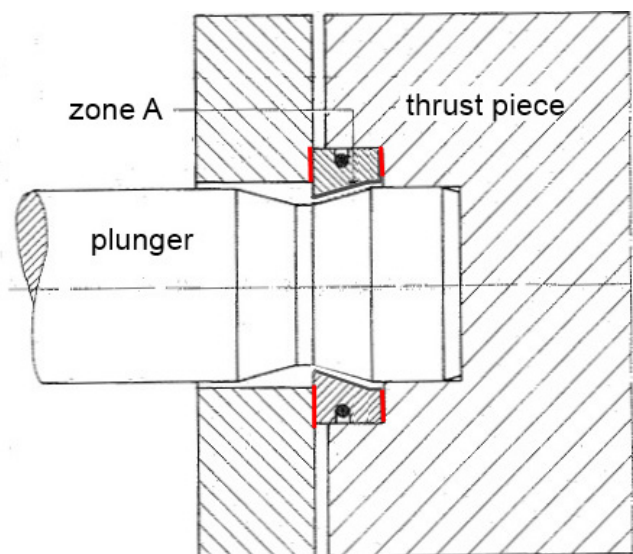


Fig. 5. Plunger-crosshead special connection

Managing Start-Up Conditions of Hyper Compressors

by: *Marcello Agostini, Cosimo Carcasci, Alessio Cristofani, Compression Service Technology*

2.3 Cylinder packing temperature distribution

When hyper compressor cylinders are working the packing temperature is largely related to the friction of the sealing rings against the plunger and is kept at acceptable levels by:

- the oil cooling the packing cups and the plunger
- the compressed gas which is flowing back into the cylinder during expansion/suction strokes

In contrast, when these compressors run with steady pressure, the gas back flow into the cylinder during the suction stroke is practically zero, and as a result the heat removal by the gas trapped in the small chambers between the sealing rings and their cups is difficult. In addition, the fact that, for the reasons explained above in connection with the pressure distribution, almost all the friction heat is generated in the area where the last sealing rings are located makes heat removal more problematic. Therefore, the combination of high static differential pressure and the consequent concentrated high thermal level have to be avoided as they are responsible for the premature damage of the sealing rings. In order to avoid this critical situation it is necessary to follow a special procedure that is reported in the following para "Critical transients".

2.4 Compression ratio sharing between the 1st and 2nd stage

Due to the low compressibility of Ethylene at high pressure, the generated volumes of the 1st and 2nd stage cylinders are not much different so that, to have a compression ratio greater than one on the 2nd stage, it is necessary that the final pressure is higher than a certain value, otherwise the 2nd stage cylinders would be in the condition of steady pressure considered at the previous para. "Cylinder packing temperature distribution" with the related problems. Also for this reason it is necessary to follow the above mentioned procedure.

3 SUGGESTIONS FOR A CORRECT OPERATION OF HYPER COMPRESSORS IN TRANSIENT CONDITIONS

3.1 Lessons learned from the field

A hyper compressor operating at 260 Mpa experienced

some premature damaging of the 2nd stage cylinder packings, all of which occurred with high gas leakage and plunger overheating. On dismantling the cylinders it was observed that the last two sealing elements of the packing were completely worn-out while the first sealing elements were in good condition. The plunger surface showed a bronze coloration which was more evident on the rear part of the plunger where the last sealing elements work.

The analysis of the events showed that the start-up and the following running-in of the compressor were done keeping the 2nd stage cylinders operating at rather high pressure for a long time, without producing any compression ratio.

By the light of the knowledge reported in the previous para. "Main operating problems connected with secondary compressors", there was evidently a correlation between the way the running-in was made and the failure.

This led us to think that it was necessary to establish a kind of procedure to run the Hyper compressors correctly even in transient conditions.

3.2 Critical transients

Two typical situations are considered during which the secondary compressor is subject to transient conditions:

- the plant production is stopped for a short period and it remains under pressure. Under this condition the procedure followed to restart the primary and secondary compressors does not present particular problems and is generally specified in the instruction manuals
- the plant is empty as the first start-up or follows a cylinder substitution for maintenance

In this situations, the primary compressor is put in operation and is kept running for a relatively long time to fill the plant before starting the secondary compressor. Under this transient condition the secondary compressor remains idle and is crossed by the gas coming from the primary compressor. As we have seen before, it must be avoided that the secondary compressor is started when the suction pressure reaches too high a level with the reported negative consequences. On the other hand, we have seen that there is a minimum pressure level to be observed to avoid possible problems to the plungers.

3.3 Procedure for a correct compressor start-up or stop

As we have seen in the previous para "Main operating problems connected with secondary compressors",

Managing Start-Up Conditions of Hyper Compressors

by: *Marcello Agostini, Cosimo Carcasi, Alessio Cristofani, Compression Service Technology*

the described critical conditions must be avoided, during transient conditions such as start-ups and stops. Although the availability of Hyper compressors has reached extremely good values, the way normally followed to carryout maintenance on to the cylinders by changing one at a time when necessary, plus the fact that most compressors have multiple cylinders, causes a substantial number of stoppages and start-ups every year, so it is very important to treat these transients carefully.

This objective can be reached by adopting the specific procedure described below. For a better understanding of the following description, refer to Annex A where a typical LDPE loop is outlined.

3.3.1 Minimum secondary compressor suction pressure

First one must start-up the primary compressor and close its overall bypass in order to raise the delivery pressure in the range of 10 to 12 Mpa. At this point, the compression load on the joint between the plunger and the thrust piece is enough to win the friction forces between the plunger itself and the packing rings plus the inertia forces of the plunger masses, so that one can start-up the secondary compressor safely, being sure that there will not be any detachment and hammering between the two pieces, thus fulfilling the condition indicated at para. "Cylinder packing pressure distribution".

3.3.2 Relationship between primary compressor discharge and hyper compressor final pressures to avoid cylinder damage

One could think it advantageous to delay the hyper compressors starting until the full nominal suction pressure is reached: generally in the range 23÷30 Mpa. On the contrary, this pressure range is not ideal when the secondary compressor is standing but crossed through by the gas, because the gas escaping and expanding through the cylinder packing sealing elements, can excessively cool the cylinders which are not heated by compression and friction. This cooling, can lead to liquefying the gas (see Fig. 10) thus generating the conditions for damaging the main packing rings and the seal rings of the plunger cooling chamber.

This over cooling is always critical, even more so when secondary compressors have to feed autoclave reactors which require even longer time to be filled than the tubular ones.

For this reason, when secondary compressors are idle, it is advisable to keep the oil of the plunger and cylinder cooling circuit temporarily heated until the hyper compressor is started, in order to supply, instead of removing, heat to the cylinders and plungers in order to counteract the temperature reduction caused by the expanding gas.

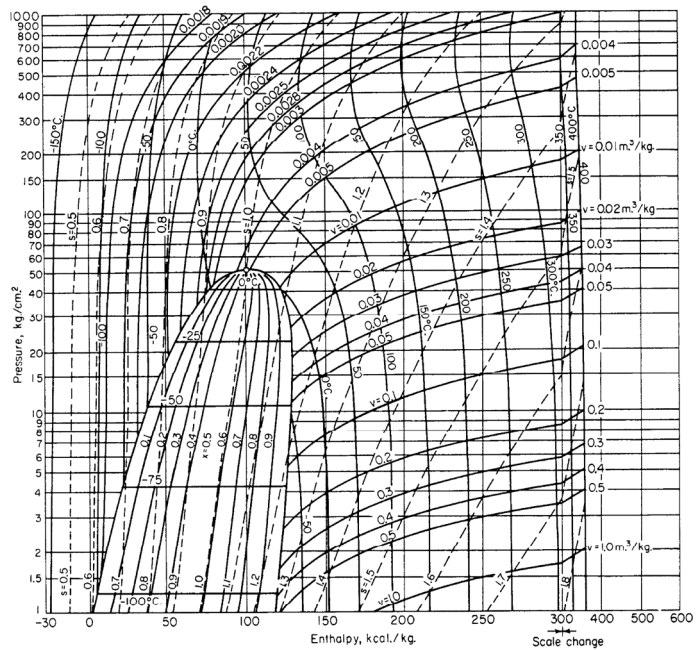


Fig. 6. Enthalpy-Pressure for Ethylene

When the primary compressor has filled the secondary compressor loop with a pressure of about 12 Mpa, the secondary compressor is started-up. The pressure in the loop tends to increase due to the pumping effect of the secondary compressor which in turn is fed with fresh Ethylene by the primary compressor and by the gas recycling from the high pressure plant. One continues to raise the pressure on the delivery of the hyper compressor keeping suction pressure at about 12 Mpa by gradually closing the overall bypass of the high pressure loop.

An example of a procedure to correctly manage the relationship between the primary and secondary delivery pressures in order to avoid all the aforementioned problems, is reported in Fig. 7 which has been elaborated for the case of the start-up of a secondary compressor with the following characteristics:

1st stage bore:	101 mm
2nd stage bore:	86 mm
Compressor speed:	214 RPM
Stroke:	400 mm
Suction pressure:	25 Mpa
Discharge pressure:	270 Mpa

Fig. 7 shows the 2nd stage secondary compressor discharge pressure versus the primary compressor discharge pressure. In detail it prescribes that one must increase the hyper compressor delivery pressure up to about 40 Mpa keeping the primary compressor delivery pressure constant at about 12 Mpa and then follow the line "Advisable 2nd stage discharge pressure" when the primary compressor discharge pressure increases.

Managing Start-Up Conditions of Hyper Compressors

by: *Marcello Agostini, Cosimo Carcasci, Alessio Cristofani, Compression Service Technology*

By following this curve one gets the following results:

- no plunger hammering because the 1st stage suction pressure is higher than 10 Mpa;
- good distribution of differential pressure among all the packing sealing rings before reaching too high a 2nd stage discharge pressure, obtained by the gradual increase of differential pressure across the 2nd stage;
- operating conditions which result in a good 2nd stage compression ratio at relatively low pressure which avoids too high steady pressure in the cylinder and makes it possible to achieve the beneficial cooling inside the 2nd stage packings with the gas back flow.

Fig. 7 also reports the curve for “No 2nd stage pumping”, which is the value of the 2nd stage discharge pressure that should, in any case, be exceeded to avoid the aforesaid problems as is the locus where the 2nd stage cylinder does not produce any compression ratio and is subject to a constant pressure, which we have seen to be negative.

The same considerations have to be made also for plant depressurization. In addition, during the discharge pressure reduction, before reaching steady

pressure in the 2nd stage, it is advisable to stop the catalyst injection to avoid low polymer formation in the packing seal ring area and to permit the removal of the polymer, already present, by the gas back flow. In this way the polymer is drawn back into the cylinder to be dragged away by the gas main stream, letting the packing be as clean as possible, thus avoiding the problem of polymer sticking on the sealing rings and plunger when the compressor is restarted.

3.3.3 Parameters to keep under control

To be sure that the above mentioned functional sequence is followed one must have a control system for the machine and the process that ensures that the parameters affecting the machine behaviour are properly controlled. The parameters to be controlled are the following:

- Primary compressor discharge pressure
- Secondary compressor discharge pressure
- Secondary compressor interstage pressure
- Cooling oil differential temperature
- Plunger surface temperature
- Leak gas temperature and throughput

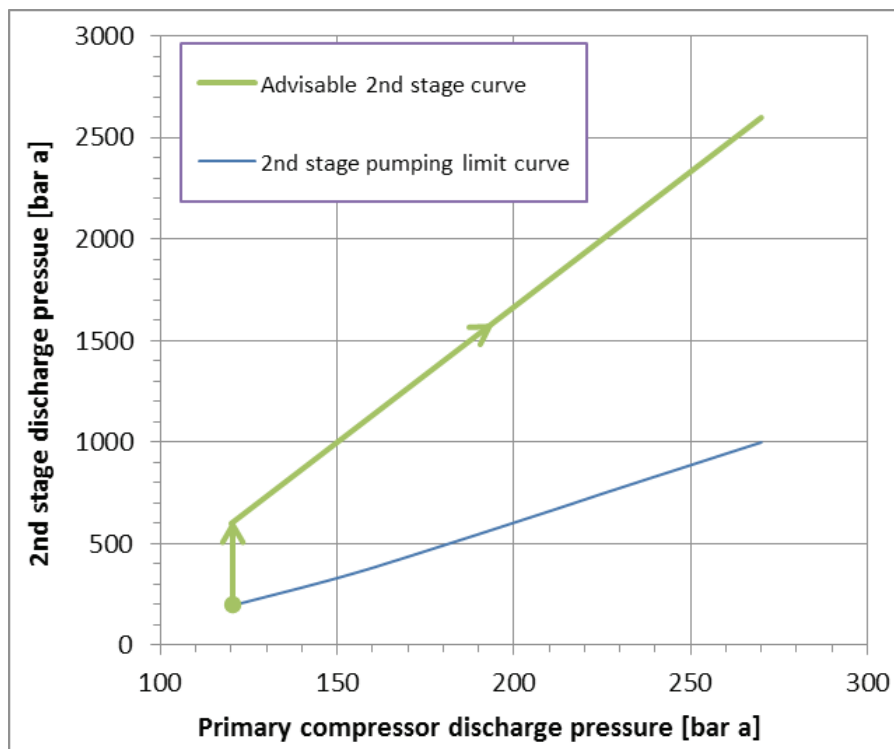


Fig. 7. Minimum secondary compressor final pressure to permit 2nd stage pumping during start-up

4 AUTOMATION, MONITORING AND MAINTENANCE

4.1 Automation to avoid critical conditions

Secondary compressors have reached very high availability and reliability factors (>99.5%). This achievement, which reduces the cost of the product, is obtained by improved design of the compressors, plant automation, careful operator monitoring, with knowledge and experience of plant and compressors operation.

Centralized control and operation of the plant allows optimization of the process parameters and shorter periods of transient operation, with even more outstanding performance of the whole plant.

In a typical LDPE plant, pressures are generally controlled according to the diagram shown in Fig. 8:

- A throttling valve controls the Ethylene pressure upstream of the primary compressor.
- Pressure between the primary and secondary compressor is controlled acting on the primary compressor recycle, or by another capacity control system (if any).
- Secondary compressor discharge pressure, which is also the reactor pressure, is commonly controlled by a throttling valve installed downstream of the reactor.

Once the importance of the relationship between the inlet and outlet pressure from the secondary compressor recognized, in order to avoid the critical situation of the secondary compressor described in para. “Procedure for a correct compressor start-up or stop”, the load operation can be guided by plant personnel or carried out automatically according to the mentioned ramp.

Using the above instrumentation a specific control philosophy for the operating pressures can be achieved during start-up. The recommended pressure ratio that has to be trailed for the hyper compressor can be automatically controlled, until normal operating conditions are reached and the reaction can be started. The clouded logic signal that links the pressure controller of primary and secondary final pressures can be implemented into the plant logic control system; in this way the suggested ramp shown in para. “Procedure for a correct compressor start-up or stop”, could be automatically followed during start-up transients.

Since the diagram shown in Fig. 7 was designed considering a particular compressor geometry, the curve can be slightly different on other Hyper compressors or with other process pressures. A detail analysis needs to be performed before implementing such a philosophy in the control system.

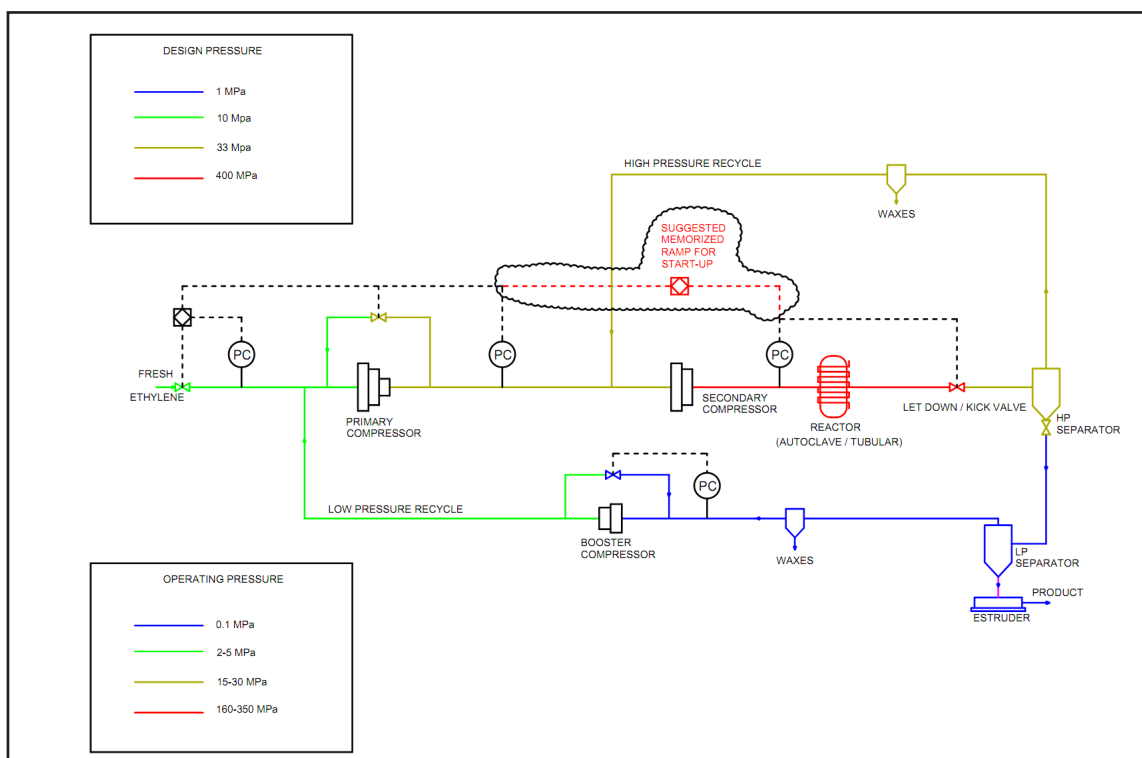


Fig. 8: Simplified LDPE process flow diagram

Managing Start-Up Conditions of Hyper Compressors

by: Marcello Agostini, Cosimo Carcasci, Alessio Cristofani, Compression Service Technology

4.2 Monitoring gas meaningful parameters

Monitoring systems help to keep the plant under control and to carry out compressor predictive and proactive maintenance. Special transmitters combined with a diagnostic system can highlight any deviation of some parameters to take early action, if necessary, to maintain safe operating conditions or to signal the need to schedule a maintenance service.

Packing usually has two recovery lines, see Fig. 1: a first, or high pressure one, (at maximum 1 Mpa, depending on the application) and a second, or low pressure one, recovery (~0.15 Mpa).

The measurement of the gas leakage, especially from the high pressure line, through the packing gives an indication of the condition of the packing :

- a high gas leakage rate at low temperature with ice formation on the outer surface of recovery pipes during the running, excluding the first hours of compression with new packing rings, can point to abnormal wear of these items. Progressive gas leakage and gas temperature reduction are generally connected with progressive wear of packing rings. Sometimes also abnormal plunger run-out can highlight high gas quantity escaping through the packing.
- hot gas passing through the recovery pipes can indicate a very small leakage. These leakages can be due to packing rings fitting the plunger surface too throughly, but could also be caused by hard polymer clogging on one or more rings.

Gas leakage measurements are useful not only during normal operating conditions but can also be used to monitor the correct behavior of the start-up transients, to avoid the occurrence of the problems described above.

A special piece of equipment designed specifically for hyper compressor gas leakage measurement is shown in Fig. 10.

The arrangement was studied specifically for Ethylene compression systems, to avoid the risk of wax clogging of the measurement device.

The purpose of this system is to continuously monitor and store the mass flow and temperature measurements taken from each high pressure packing recovery line.

Many other monitoring devices are normally installed on the machine, to control also mechanical parameters, such as these briefly described below.

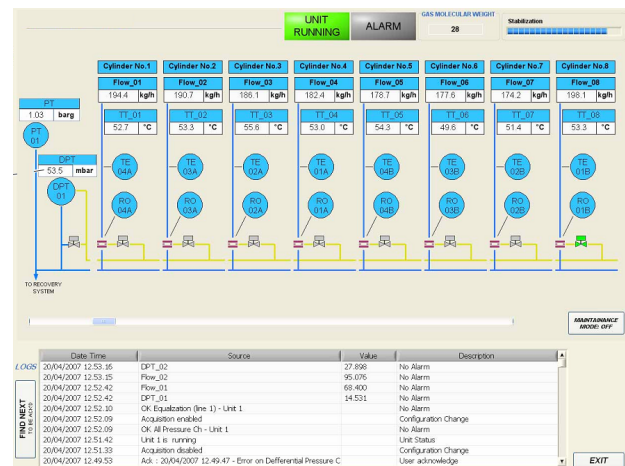


Fig. 9. Packing leakage monitoring system control panel



Fig. 10. Packing leakage monitoring system

Vertical and horizontal probes are installed to measure plunger run-out which in general results around a value of 0.075 mm peak to peak. An alarm is usually set at around 0.20 mm (8mils) and trip at 0.25 mm (10mils). Deviations of plunger run-out from normal values can indicate a modification of the plunger arrangement, for example, due to damage to the guide or to abnormal behavior of the thrust piece and bearings [8]. A thermocouple with a special adapter can be put in contact with the plunger to measure its surface temperature which, in the case of a peak, gives an indication of abnormal packing operation, to be further investigated to avoid premature wear.

Managing Start-Up Conditions of Hyper Compressors

by: *Marcello Agostini, Cosimo Carcasci, Alessio Cristofani, Compression Service Technology*

Vibration instruments are almost always installed on the crankcase to give alarms or shutdown the compressor before reaching failure, which could be catastrophic.

Other vibration sensors can be located in such a way to measure the vibration in three directions (cylinder axis, crankshaft axis and vertical), to have an indication concerning the behavior of the complete machine; these readings must always be performed taking into account the operating conditions and relevant vibration history. The velocity of vibration can indicate some impending problem when out of the pattern model previously experienced, and can help to establish a maintenance schedule [9].

4.3 Maintenance

A continuous monitoring and diagnostic activity, such as the one described in para "Monitoring gas meaningful parameters", can be very useful to schedule compressor maintenance in a predictive more than a preventive way. In consideration of the fact that LDPE is, at least partially, a seasonal production, predictive maintenance can be of great help in planning plant outages in order to avoid, within the safety constraints, the periods of major demand for this commodity.

Generally an LDPE plant has a single flow measurement of the whole packing recovery lines, which means that it is impossible to locate the origin of a leakage, in the case of excessive flow.

On the contrary, the system shown in Fig. 9 and Fig. 10, providing a measurement for each recovery line, gives the possibility to immediately discover the leakage source and schedule the maintenance directly addressing the problem.

5 CONCLUSIONS

Secondary compressors for LDPE production are nowadays designed and manufactured following the most advanced methods and technologies which are necessary to assure safety and reliability under the extreme pressure levels at which they operate.

Operation and maintenance must be the same level design and manufacturing and therefore all the lessons learned on the field shall be introduced in the day-to-day operation of the machines. In particular, in order to avoid the problems reported it is necessary to perform the thermodynamic analysis of the machine not only at full load but also for operation during transients.

If this stage is performed in a non-correct way, serious damage to the packing, and consequently to the plunger, can occur. A lesson learned case was

presented, in order to focus the attention on the correct compression ratio that should be maintained across each stage of the Hyper compressor. Implementation of control systems could also be of great help to avoid the start-up and depressurization sequence being simply left to human intervention action. However training on these issues for the operating people should not be underestimated. Finally, one must stress the importance of providing the strategic machinery, such as the Hyper compressors, with adequate monitoring and diagnostic systems to detect the emergence of critical situations as soon as possible.

6 REFERENCES

- [1] B. Crossland, K.E. Bett, Sir H. Ford, "Review of Some of the Major Engineering Developments in the High-Pressure Polyethylene Process", 1933-1933, Institute of Mechanical Engineering, 1986, Vol. 200, Ne A4
- [2] P. C. Hanlon (Editor), "Compressor Handbook", Chapter 7 – Very High Pressure Compressors, E. Giacomelli & A. Traversari, pag 7.44, McGraw-Hill, 2001
- [3] J.L. Morrison, B. Crossland, J.S. Parry, "Fatigue strength of Cylinders with Cross Bores", Journal of Mech. Eng. Sci, 1959
- [4] A. Chaaban, N. Baraké, "Elasto-Plastic Analysis of High Pressure Vessels with Radial Cross Bores", P.V.P., Vol. 263, High Pressure Codes, Analysis and Applications – ASME, 1993
- [5] D.W. Rees, "The Fatigue Life of Thick-Walled Autofrettaged Cylinders with Closed Ends, Fatigue Fracture" Eng. Mater. Struct., Vol. 14, pp 51-68, 1991
- [6] A. Traversari, E. Giacomelli, "Some Investigation on the Behaviour of High Pressure Packing Used in Secondary Compressors For LDPE Production", 2nd int. Conf. on High Pressure Engineering, University of Sussex, Brighton, England, July 8-10, 1975, pp 57-58
- [7] A. Traversari, P. Beni, "Design of a Safe Secondary Compressor, Chemical Engineering Progress", Vol. 70, No. 9, pp 56-59, 1974

Managing Start-Up Conditions of Hyper Compressors

by: Marcello Agostini, Cosimo Carcasci, Alessio Cristofani, Compression Service Technology

- [8] E. Giacomelli, M. Agostini, "Safety, operation and maintenance of LDPE secondary compressors", P.V.P., Vol. 238, Codes and Standards and Applications for High Pressure Equipment – ASME, 1992

- [9] M. Spagno, B. Spagno, "Sviluppo delle tenute per compressori alternativi ad alte pressioni", Manutenzione, Tecnica e Management, January 2003



THREE CONFERENCES UNDER ONE ROOF

The third „International Rotating Equipment Conference - Pumps and Compressors“ will take place again in Düsseldorf with three forums united under one roof:

- 10th EFRC Conference
- 11th Pump Users International Forum
- 4th Compressor Users International Forum

Be part of it: Almost 1000 participants from over 40 countries will attend this event.

10th EFRC Conference
September 14th / 15th, 2016
Düsseldorf, Germany

www.recip.org



EFRC
EUROPEAN FORUM
for RECIPROCATING
COMPRESSORS

SAVE THE DATE

Promoter

EFRC

European Forum for Reciprocating Compressors e.V.
c/o Technische Universität Dresden
01062 Dresden
Germany

Phone: +49 351 463 3449 1
Fax: +49 351 463 37759
E-mail: contact@recip.org

EFRC Board

René Peters (Chairman)
Peter Steinrück
Matthias Tanner

Editor

Herbert Steinrück
Vienna University of Technology
Institute of Fluid Mechanics and Heat Transfer

Conference Committee

Christian Prinz, HOERBIGER
Anja Parnigoni, HOERBIGER
Martina Frenz, NEUMAN & ESSER
Daniela Daron, BURCKHARDT
Tanja Scheidegger, BURCKHARDT
Noëlle Kotter, HOWDEN THOMASSEN
André Eijk, TNO

Advisory Board

H. Steinrück, B. Streibl - TU VIENNA
P. Duineveld - HOWDEN THOMASSEN
E. Drewes - PROGNOSTGÖ XYUZ
A. Allenspach - BURCKHARDT
K. Hoff, G. Knop - NEUMAN & ESSER
T. Heumesser - LMF
A. Eijk, R. Peters - TNO
Ch. Prinz - HOERBIGER
M. Langelà - STASSKOL

Layout

Anja Parnigoni, HOERBIGER